

PWR FLECHT-SET PHASE A REPORT

J. A. Blaisdell
L. E. Hochreiter
J. P. Waring

December 1973

APPROVED:



C. L. Caso, Manager
Safeguards Engineering

APPROVED:



A. P. Suda
Project Engineer

Program Jointly Funded by Westinghouse, USAEC, Electric
Power Research Institute under Contract AT(11-1)-2279

WESTINGHOUSE ELECTRIC CORPORATION
Nuclear Energy Systems
P. O. Box 355
Pittsburgh, Pennsylvania 15230

1

2

3

LEGAL NOTICE

This report was prepared as an account of Government-sponsored work. Neither the United States, nor the Commission, nor any person acting on behalf of the Commission:

- A. Makes any warranty or representation, expressed or implied, with respect to the accuracy, completeness, or usefulness of the information contained in this report, or that the use of any information, apparatus, method, or process disclosed in this report may not infringe privately owned rights; or
- B. Assumes any liabilities with respect to the use of, or for damages resulting from the use of any information, apparatus, method, or process disclosed in this report.

As used in the above, "person acting on behalf of the Commission" includes any employe or contractor of the Commission, or employe of such contractor, to the extent that such employe or contractor of the Commission, or employe of such contractor prepares, disseminates, or provides access to, any information pursuant to his employment or contract with the Commission, or his employment with such contractor.

1

2

3

4

TABLE OF CONTENTS

Section	Title	Page
1	INTRODUCTION	1-1
	1.1 OBJECTIVES	1-1
2	TEST DESCRIPTION	2-1
	2.1 FACILITY DESCRIPTION	2-1
	2.2 INSTRUMENTATION	2-7
	2.3 TEST PROCEDURES	2-12
	2.4 INITIAL HOUSING TEMPERATURE DISTRIBUTION	2-15
3	DISCUSSION OF TEST RESULTS	3-1
	3.1 GENERAL RESULTS	3-1
	3.1.1 Summary of Run Conditions and Test Results	3-2
	3.2 DISCUSSION OF CALCULATION METHODS	3-5
	3.3 PRESENTATION AND ANALYSIS OF SELECTED RUNS	3-9
	3.3.1 Data Analysis for Run 4923	3-9
	3.3.1.1 General Observations	3-10
	3.3.1.2 Mass Balance	3-10
	3.3.1.3 Flooding Rate	3-12
	3.3.1.4 Entrainment	3-17
	3.3.1.5 Quench Front and Test Section Axial Pressure Drop Data	3-20
	3.3.1.6 Rod Temperature and Heat Transfer Coefficient Behavior	3-23
	3.3.1.7 Fluid Temperature at Various Points in the System	3-29
	3.3.1.8 Housing Behavior	3-29
	3.3.1.9 Energy Balance	3-33

TABLE OF CONTENTS (Cont)

Section	Title	Page
3.3.2	Data Analysis for Run 2919	3-35
3.3.2.1	General Observations	3-36
3.3.2.2	Mass Balance	3-36
3.3.2.3	Flooding Rate	3-38
3.3.2.4	Entrainment	3-45
3.3.2.5	Quench Front and Test Section Axial Pressure Drop Data	3-48
3.3.2.6	Rod Temperature and Heat Transfer Coefficient Behavior	3-51
3.3.2.7	Fluid Temperatures at Various Points in the System	3-55
3.3.2.8	Housing Behavior	3-55
3.3.2.9	Energy Balance	3-61
3.4	HOUSING EFFECTS IN FLECHT-SET TESTS	3-63
3.5	PARAMETER EFFECTS	3-99
3.5.1	Inlet Coolant Subcooling	3-99
3.5.2	Initial Clad Temperature	3-105
3.5.3	Peak Power Generation	3-116
3.5.4	Containment Pressure	3-123
3.5.5	Injection Rate	3-131
4	SUMMARY AND CONCLUSIONS	4-1
4.1	FLECHT-SET PHASE A CONCLUSIONS	4-1
4.2	LOW CLAD TEMPERATURE FLECHT TESTS	4-4
4.3	TOP SPRAY TESTS	4-5
5	REFERENCES	5-1
APPENDIX A	FLECHT-SET DATA SHEETS	A-1
APPENDIX B	LOW CLAD TEMPERATURE FLECHT TESTS	B-1
B.1	INTRODUCTION	B-1
B.1.1	Rationale for Tests	B-1
B.1.2	Objective	B-1

TABLE OF CONTENTS (Cont)

Section	Title	Page
B.2	TEST DESCRIPTION	B-2
B.2.1	Facility Layout	B-2
B.2.2	Instrumentation and Data Acquisition	B-2
B.2.3	Test Procedure	
B.3	CALCULATION AND DATA REDUCTION	B-5
B.4	DISCUSSION OF TEST RESULTS	B-6
B.4.1	Run Summary	B-6
B.4.2	Typical Test Results	B-10
B.4.3	Housing Axial Pressure Data	B-15
B.5	PARAMETER EFFECTS	B-24
B.5.1	Initial Clad Temperature	B-24
B.5.2	Coolant Subcooling	B-28
B.5.3	Pressure	B-28
B.5.4	Flooding Rate	B-35
B.5.5	Peak Power	B-35
B.6	CONCLUSIONS	B-38
APPENDIX B-1	LOW CLAD TEMPERATURE FLECHT RUN SUMMARY SHEETS	B-39
APPENDIX C	TOP INJECTION TESTS	C-1
C.1	INTRODUCTION	C-3
C.1.1	Purpose of Tests	C-3
C.2	TEST DESCRIPTION	C-3
C.2.1	Facility Layout	C-3
C.2.2	Instrumentation and Data Acquisition	C-6
C.2.3	Test Procedure	C-6
C.3	CALCULATIONS AND DATA REDUCTION	C-8
C.4	DISCUSSION OF TEST RESULTS	C-8
C.4.1	Run Summary Sheets	C-8
C.4.2	General Observations	C-8
C.4.3	Parameter Effects on Top Injection Performance	C-15

TABLE OF CONTENTS (Cont)

Section	Title	Page
	C.4.3.1 Peak Power Effects	C-15
	C.4.3.2 Initial Temperature Effects	C-21
	C.4.3.3 Injection Water Temperature	C-21
	C.4.3.4 Injection Flow Effects	C-29
	C.4.3.5 Examination of the Bundle Venting Effect	C-32
C.5	CONCLUSIONS	C-38
APPENDIX C-1	TOP INJECTION TEST RUN SUMMARY SHEETS	C-45

LIST OF ILLUSTRATIONS

Figure	Title	Page
2-1	Schematic of Phase A Facility	2-2
2-2	Schematic of Phase A Test Section	2-3
2-3	Schematic of Phase A Separator Tank	2-4
2-4	Double Ended Cold Leg Break (Guillotine) Accumulators and Pump Injection Flow Rates versus Time	2-8
2-5	Measured Power Decay Used in FLECHTSET (Phase A)	2-9
2-6	Comparison of FLECHTSET Power Decay to ANS Standard	2-10
2-7	Cross Section of 10 x 10 Bundle Showing Instrument Locations	2-11
2-8	Thermocouple Locations	2-13
2-9	Pressure and Differential Pressure Transducer Locations	2-14
3-1	Schematic of Downcomer "Level" Transducer	3-6
3-2	Mass Balance for Run 4923	3-11
3-3	Downcomer Head vs. Time - Run 4923	3-13
3-4	Flooding Rate vs. Time - Run 4923	3-14
3-5	Pressure Drops for Run 4923	3-15
3-6	Mass Flow Rates - Run 4923	3-18
3-7	Mass Effluent Rate Fraction - Run 4923	3-19
3-8	Total Mass Effluent Fraction - Run 4923	3-21
3-9	Rod Temperature Quench Front Envelope - Run 4923	3-22
3-10	Downcomer and Test Section Pressure Drop Data - Run 4923	3-24

LIST OF ILLUSTRATIONS (cont)

Figure	Title	Page
3-11	Quench Front Envelope and Void Fraction Profiles - Run 4923	3-25
3-12	Clad Temperature History - Run 4923	3-26
3-13	Rod Heat Transfer Coefficients - Run 4923	3-27
3-14	Comparison of Predicted and Measured Midplane Heat Transfer Coefficients - Run 4923	3-28
3-15	Test Section Inlet and Outlet Fluid Temperature - Run 4923	3-30
3-16	Fluid Temperature Upstream of Loop Orifice - Run 4923	3-31
3-17	Housing Temperature Data - Run 4923	3-32
3-18	Mass Balance - Run 2919	3-37
3-19	Downcomer Head vs. Time - Run 2919	3-39
3-20	Downcomer Fluid Overflow Rate - Run 2910	3-40
3-21	Flooding Rate vs. Time - Run 2919	3-41
3-22	Pressure Drop Data - Run 2919	3-42
3-23	Housing Axial Pressure Drop Data - 2919	3-44
3-24	Mass Flow Rates - Run 2919	3-46
3-25	Mass Effluent Rate Fraction - Run 2919	3-47
3-26	Total Mass Effluent Fraction - Run 2919	3-49
3-27	Temperature Quench Front Envelope - Run 2919	3-50
3-28	Temperature Quench Front Envelope and Average Void Fraction Profiles - Run 2919	3-52
3-29	Clad Temperature and Heat Transfer Coefficient vs. Time - Run 2919	3-53
3-30	Comparison of Predicted and Measured Midplane Heat Transfer Coefficient - Run 2919	3-54

LIST OF ILLUSTRATIONS (cont)

Figure	Title	Page
3-31	Test Section Inlet and Outlet Fluid Temperature - Run 2919	3-56
3-32	Fluid Temperature Upstream of Loop Orifice - Run 2919	3-57
3-33	Housing Temperature Data - Run 2919	3-58
3-34	Midplane Clad Temperatures at Different Radial Distances from the Test Section Housing Wall - Run 2919	3-60
3-35	Heater Rod Hookup for Housing Effects Tests	3-66
3-36	Midplane Quench Time vs. Heat Input Below 6' up to 6' Quench Time per Unit Volume of Fluid Below 6'	3-68
3-37	Midplane Quench Time vs. Heat Input by Housing and Outer Row of Rods Below 6' Quench Time per Unit Volume of Fluid in Periphery Channel	3-71
3-38	Comparison of Quench Front Envelope vs. Time for Runs 5115 and 5316	3-72
3-39	Downcomer Pressure Drop vs. Time for Different Housing Temperatures	3-73
3-40	Comparison of Loop Pressure Drops for Runs 5115 and 5316	3-74
3-41	Comparison of Mass Put Into Bundle and Mass Remaining in Bundle for Runs 5115 and 5316	3-76
3-42	Comparison of Flooding Rates for Runs 5316 and 5115	3-77
3-43	Comparison of Vapor Flow Rates for Runs 5316 and 5115	3-78
3-44	Comparison of Bundle Axial Pressure Drops for Runs 5115 and 5316	3-79
3-45	Comparison of Total Mass Effluent Fractions for Runs 5115 and 5316	3-80
3-46	Comparison of Mass Stored in Upper Plenum Extension for Runs 5115 and 5316	3-82
3-47	Comparison of Midplane Clad Temperature and Heat Transfer Coefficient for Runs 5115 and 5316	3-83

LIST OF ILLUSTRATIONS (cont)

Figure	Title	Page
3-48	Effect of the Number of Heated Rods on Midplane Clad Temperature and Heat Transfer Coefficient	3-85
3-49	Effect of the Number of Heated Rods on the Flooding Rate and Vapor Effluent Mass Flow Rate	3-86
3-50	Effect of the Number of Heated Rods on the Test Section Mass Input and Storage	3-87
3-51	Effect of the Number of Heated Rods on Downcomer and Test Section Pressure Drop	3-88
3-52	Effect of Peak Power on Midplane Clad Temperature and Heat Transfer Coefficient	3-89
3-53	Effect of Peak Power on Flooding Rate and Vapor Mass Flow Rate	3-90
3-54	Effect of Peak Power on Test Section Mass Input and Storage	3-91
3-55	Effect of Peak Power on Downcomer and Test Section Pressure Drop	3-92
3-56	Effect of Housing Temperature on Test Section Flooding Rate and Vapor Mass Flow Rate	3-94
3-57	Effect of Housing Temperature on Test Section Mass Input and Storage	3-95
3-58	Effect of Housing Temperature on Downcomer and Test Section Pressure Drops	3-96
3-59	Effect of Housing Temperature on Midplane Clad Temperature and Heat Transfer Coefficient	3-97
3-60	Effect of Inlet Subcooling on Flooding Rate at 20 Psia Containment Pressure	3-101
3-61	Effect of Inlet Subcooling on Mass Stored in the Bundle and Liquid Collected in Separator Tank at 20 Psia Containment Pressure	3-102
3-62	Effect of Inlet Subcooling on the Rod Quench Front Envelope at 20 Psia Containment Pressure	3-103

LIST OF ILLUSTRATIONS (cont)

Figure	Title	Page
3-63	Effect of Inlet Subcooling on Midplane Heat Transfer Coefficient at 20 Psia Containment Pressure	3-104
3-64	Effect of Inlet Subcooling on the Vapor Generated and Mass Stored in the Bundle at 60 Psia Containment Pressure	3-106
3-65	Effect of Inlet Subcooling on the Midplane Heat Transfer Coefficient at 60 Psia Containment Pressure	3-107
3-66	Effect of Initial Clad Temperature on 6' Temperature Rise, Turnaround Time, and Quench Time at 20 Psia Containment Pressure	3-108
3-67	Effect of Initial Clad Temperature on the Mass Remaining in the Bundle and the Mass of Liquid Collected in the Separator Tank at 20 Psia Containment Pressure	3-110
3-68	Effect of Initial Clad Temperature on Flooding Rate at 20 Psia Containment Pressure	3-111
3-69	Effect of Initial Clad Temperature on Rod Quench Front Behavior at 20 Psia Containment Pressure	3-112
3-70	Effect of Initial Clad Temperature on Midplane Heat Transfer Coefficient at 20 Psia Containment Pressure	3-113
3-71	Effect of Initial Clad Temperature on Midplane Temperature Rise, Turnaround Time, and Quench Time at 60 Psia Containment Pressure	3-114
3-72	Effect of Initial Clad Temperature on the Mass Put into the Bundle, Mass Remaining in the Bundle, and Liquid Collected in the Separator Tank at 60 Psia Containment Pressure	3-115
3-73	Effect of Initial Clad Temperature on Flooding Rate at 60 Psia Containment Pressure	3-117
3-74	Effect of Initial Clad Temperature on Rod Quench Front Behavior at 60 Psia Containment Pressure	3-118
3-75	Effect of Initial Clad Temperature on Midplane Heat Transfer Coefficient at 60 Psia Containment Pressure	3-119

LIST OF ILLUSTRATIONS (cont)

Figure	Title	Page
3-76	Effect of Peak Power on 6' Quench Time, Turnaround Time, and Temperature Rise at 20 Psia Containment Pressure	3-120
3-77	Effect of Peak Power on the Mass Remaining in the Bundle and the Liquid Collected in the Separator Tank at 20 Psia Containment Pressure	3-121
3-78	Effect of Peak Power on the Flooding Rate at 20 Psia Containment Pressure	3-122
3-79	Effect of Peak Power on Rod and Housing Quench Front Behavior at 20 Psia Containment Pressure	3-124
3-80	Effect of Peak Power on Midplane Heat Transfer Coefficient at 20 Psia Containment Pressure	3-125
3-81	Effect of Containment Pressure on Midplane Quench Time, Turnaround Time, and Temperature Rise	3-127
3-82	Effect of Containment Pressure on the Vapor Mass Flow Rate	3-128
3-83	Effect of Containment Pressure on the Rod Quench Front Envelope	3-129
3-84	Effect of Containment Pressure on Mass Remaining in Bundle and Liquid Collected in Separator Tank	3-130
3-85	Effect of Containment Pressure on Flooding Rate	3-132
3-86	Effect of Containment Pressure on Midplane Heat Transfer Coefficient	3-133
3-87	Injection Flood Rates at 20 Psia	3-134
3-88	Flooding Rates for Runs 3117, 3006, and 2605	3-135
3-89	Downcomer Elevation for Runs 2605, 3006, and 3117	3-136
3-90	Midplane Heat Transient Coefficient for Runs 2605, 3006, and 3117	3-138
3-91	Rod Quench Envelope and Housing Quench Front for Runs 3117, 2605, and 3006	3-139
3-92	Midplane Heat Transfer Coefficient for Runs 1709 and 2023, Rod 7D	3-140

LIST OF ILLUSTRATIONS (cont)

Figure	Title	Page
3-93	Downcomer Elevations and Flooding Rate, Runs 1709 and 2023	3-141
B-1	Low Initial Temperature Series Test Section Configuration	B-3
B-2	Flooding Rate Profiles	B-9
B-3	Envelope of Temperature Quench Front - Run 2420	B-11
B-4	Housing Axial Pressure Data - Run 2420	B-12
B-5	Mass Calculation - Run 2420	B-13
B-6	Mass Effluent Fraction - Run 2420	B-14
B-7	Initial Clad Temperature vs. Elevation	B-16
B-8	Comparison of Quench Front and Differential Pressure Data	B-17
B-9	Comparison of Quench Front and Differential Pressure Data	B-18
B-10	Comparison of Quench Front and Differential Pressure Data	B-19
B-11	Comparison of Quench Front and Differential Pressure Data	B-20
B-12	Comparison of Quench Front and Differential Pressure Data	B-21
B-13	Comparison of Quench Front and Differential Pressure Data	B-22
B-14	Comparison of Quench Front and Differential Pressure Data	B-23
B-15	Comparison of FLECHT Temperature Quench Fronts with Low Clad Temperature FLECHT	B-25
B-16	Effect of Initial Temperature on Quench Front	B-26
B-17	Effect of Initial Clad Temperature on Maximum Clad Temperature	B-27

LIST OF ILLUSTRATIONS (cont)

Figure	Title	Page
B-18	Effect of Initial Clad Temperature on Entrainment	B-29
B-19	Effect of Initial Clad Temperature on Quench Front	B-30
B-20	Effect of Initial Clad Temperature on Maximum Clad Temperature	B-31
B-21	Effect of Initial Clad Temperature on Entrainment	B-32
B-22	Effect of Inlet Water Subcooling	B-33
B-23	Effect of Pressure	B-34
B-24	Effect of Flooding Rate	B-36
B-25	Effect of Peak Power	B-37
C-1	FLECHT-SET Configuration for Top Injection Tests	C-4
C-2	Top Injection Position	C-5
C-3	Run 5703, Ten-foot Cross-Sectional Bundle Maximum Temperatures, Turnaround Times, and Quench Times	C-11
C-4	Run 5703, Six-foot Cross-Sectional Bundle Maximum Temperatures, Turnaround Times, and Quench Times	C-12
C-5	Run 5703, Four-foot Cross-Sectional Bundle Maximum Temperatures, Turnaround Times, and Quench Times	C-13
C-6	Run 5703, Two-foot Cross-Sectional Bundle Maximum Temperatures, Turnaround Times, and Quench Times	C-14
C-7	Effect of Peak Power on Maximum Temperature Envelope	C-17
C-8	Effect of Power on Rod 5G, Six-Foot Heat Transfer and Temperature	C-18
C-9	Run 5501, Six-foot Cross-Sectional Bundle Maximum Temperatures, Turnaround Times, and Quench Times	C-19
C-10	Run 5602, Six-foot Cross-Sectional Bundle Maximum Temperatures, Turnaround Times, and Quench Times	C-20
C-11	Effect of Initial Temperature on Maximum Temperature Envelope	C-22

LIST OF ILLUSTRATIONS (cont)

Figure	Title	Page
C-12	Effect of Initial Temperature on Rod 5G, Six-foot Heat Transfer	C-23
C-13	Effect of Initial Temperature on Rod 5G Transient	C-24
C-14	Run 5904, Six-foot Cross-Sectional Bundle Maximum Temperatures, Turnaround Times, and Quench Times	C-25
C-15	Effect of Injection Water Temperature on Maximum Temperature Envelope	C-26
C-16	Effect of Injection Water Temperature on Rod 5G Rod Heat Transfer	C-27
C-17	Effect of Injection Water Temperature on Rod 5G Temperature	C-28
C-18	Run 6106, Six-foot Cross-Sectional Bundle Maximum Temperatures, Turnaround Times, and Quench Times	C-30
C-19	Run 6408, Six-foot Cross-Sectional Bundle Maximum Temperatures, Turnaround Times, and Quench Times	C-31
C-20	Effect of Injection Water Flow Rate on Maximum Temperature Envelope	C-33
C-21	Effect of Injection Water Flow Rate on Rod 5G Heat Transfer	C-34
C-22	Effect of Injection Water Flow Rate on Rod 5G Temperature Transient	C-35
C-23	Run 6205, Six-foot Cross-Sectional Bundle Maximum Temperatures, Turnaround Times, and Quench Times	C-36
C-24	Effect of Bundle Venting on Maximum Temperature Envelope	C-37
C-25	Effect of Bundle Venting on Rod 5G, Six-foot Heat Transfer	C-39
C-26	Effect of Bundle Venting on Rod 5G, Six-foot Temperature	C-40
C-27	Effect of Bundle Venting on Rod 5G Heat Transfer at All Elevations	C-41
C-28	Run 6007, Six-foot Cross-Sectional Bundle Maximum Temperatures, Turnaround Times, and Quench Times	C-42

—

—

—

LIST OF TABLES

Section	Title	Page
2-1	FLECHT-SET Phase A Dimensions	2-5
2-2	Comparison of Test and PWR Flow Areas	2-6
3-1	Nominal Run Conditions and Parameter Variations	3-3
3-2	FLECHT-SET Phase A Data Summary	3-4
3-3	Test Conditions for Housing Effects Tests	3-65
3-4	Total Heat Input to Fluid Below Midplane Up to Midplane Quench Time	3-67
3-5	Heat Input to Periphery Channel Below Midplane Up to Midplane Quench Time	3-70
B-1	Low Initial Clad Temperature FLECHT Tests - Run Conditions and Results	B-7
C-1	Top Injection Test Matrix	C-7
C-2	Top Injection Tests Mass Collected	C-10
C-3	Top Injection Test Results	C-16

—

—

—

SECTION 1

INTRODUCTION

1.1 OBJECTIVES

This report describes the results of three test series:

1. Phase A FLECHT-SET tests are presented in Sections 1 through 5 and Appendix A.
2. Low clad temperature FLECHT tests are presented in Appendix B.
3. Top Injection cooling tests are presented in Appendix C.

This program is a continuation of the FLECHT Program. Reports previously published on the FLECHT Program are as follows:

1. WCAP-7200
2. WCAP-7288
3. WCAP-7435
4. WCAP-7544
5. WCAP-7665
6. WCAP-7931
7. WCAP-7906

The overall objective of the FLECHT-SET program is to provide experimental data on the influence of system effects on emergency core cooling (ECC) behavior during the reflood phase of a loss-of-coolant accident (LOCA). Ultimately, the test data obtained will be used to verify existing analytical techniques or serve as the basis for the development of new ones. However, improvement of codes was not included in the scope of this program. It is expected that all interested groups will pursue analytical model development and code improvement independently since each has a different code.

Based on the previous FLECHT programmed flooding rate tests and preliminary scoping test experience, the facility behavior was sufficiently understood to enable the selection of test conditions necessary to ensure valid data and the measurement of all parameters important to code development. As in most programs, certain experimental limitations existed. To fulfill the objective of providing experimental data for the development of analytical techniques, the system response need only be similar (as realistic as practical), and not necessarily identical to that of a PWR. Thus, this test program was not intended to be classified in the demonstration test category.

FLECHT-SET Phases B and C will be performed after the completion of Phase A. Phase B is intended to more nearly simulate the reflood phase of a PWR LOCA with broken and unbroken loops, including steam generator heat addition, elevation rate and particularly test section effluent two-phase flow rate.

Phases B and C will be performed after the completion of Phase A. Phase B is intended to more nearly simulate the reflood phase of a PWR LOCA with broken and unbroken loops, including steam generator head addition, elevation effects, and the feedback of the unbroken loop discharge on the fluid in the downcomer. Phase B will be done in two parts. Phase B1 will utilize the same type of heater rods used in previous FLECHT series which had a symmetrical axial power distribution. Phase B2 will utilize heater rods with a skewed axial power distribution. Phase C is included in the program scope to incorporate those features into the system simulation which may not be readily accomplished in Phase B.

SECTION 2

TEST DESCRIPTION

2.1 FACILITY DESCRIPTION

The PWR FLECHT test facility was modified so that its response more nearly simulated the reflood phase of a LOCA. A downcomer, an upper plenum extension, and an exhaust loop were added to the existing FLECHT 10 x 10 test section as described in Figures 2-1, 2-2, 2-3, and Table 2-1. The exhaust loop included a liquid separator (see Figure 2-3) in the position normally occupied by the steam generator. Downstream of the separator, the piping was heated well above saturation temperature to ensure single-phase steam flow through the orifice which provided additional flow resistance and a means for measuring the vapor flow rate. The steam discharged to a large tank which was maintained at constant pressure by an exhaust control valve.

The primary facility design requirements were to maintain typical PWR loop flow resistances, elevations, lengths and to scale the flow areas by the ratio of a typical four-loop PWR core flow area to the flow area of the FLECHT 10 x 10 rod bundle, and to utilize as much as possible of the existing FLECHT facility. Thus, the downcomer fill-up rate, exhaust velocities, transport times, and delays caused by mass storage and venting flow resistance should be similar to those expected in a four-loop PWR during a portion of the reflood phase of a LOCA. In this program the test bundle simulated a portion of an average power fuel assembly and the loop resistance was set to that of a pipe flow area consistent with the bundle flow area

A comparison of the various PWR flow areas to the flow areas used in the test facility is shown in Table 2-2. The scaling factor used was the ratio of a four-loop PWR core flow area to the FLECHT bundle flow area (370). Pipe sizes were chosen so that this ratio was maintained as closely as possible. The FLECHT upper plenum could not be changed practically because the heater

NOTES

1. DRAWING NOT TO SCALE
2. ALL ELEVATIONS ARE GIVEN IN REFERENCE TO BOTTOM OF HEATED LENGTH
3. VOLUME BELOW HEATED LENGTH = 2.516 FT³
4. NUMBERS REFER TO ITEMS IN TABLE 2-1

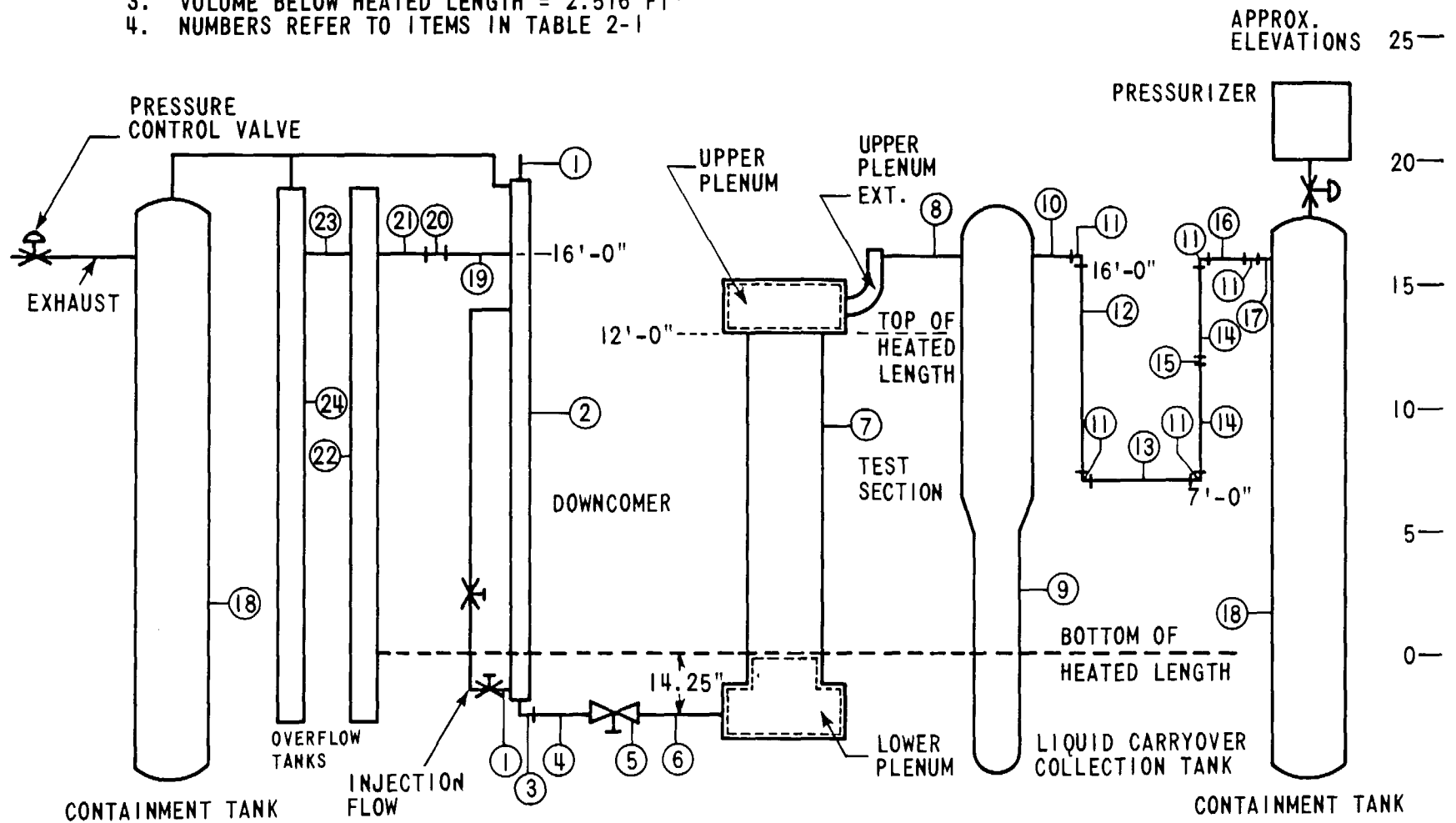


Figure 2-1. Schematic of Phase A Facility

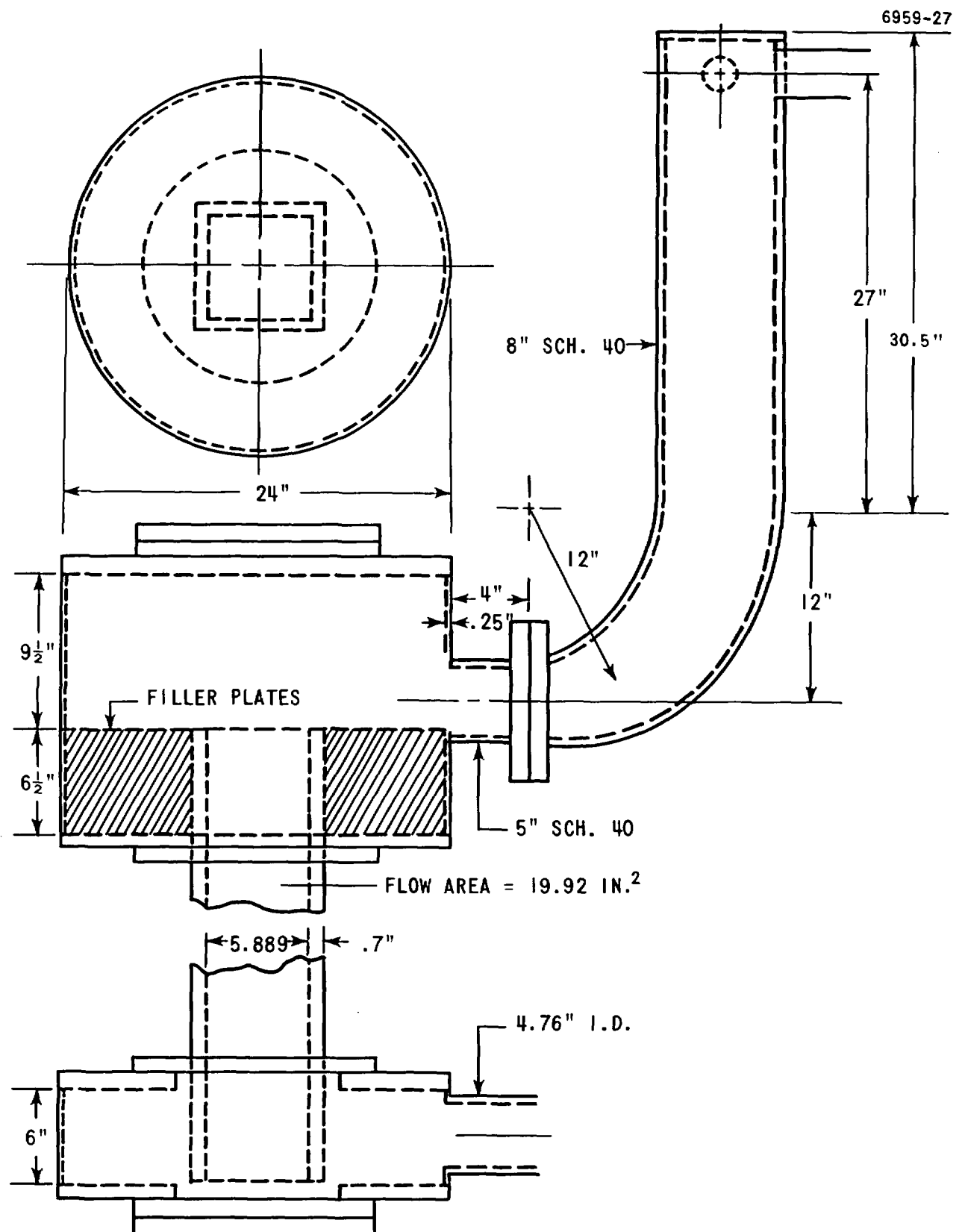


Figure 2-2. Schematic of Phase A Test Section

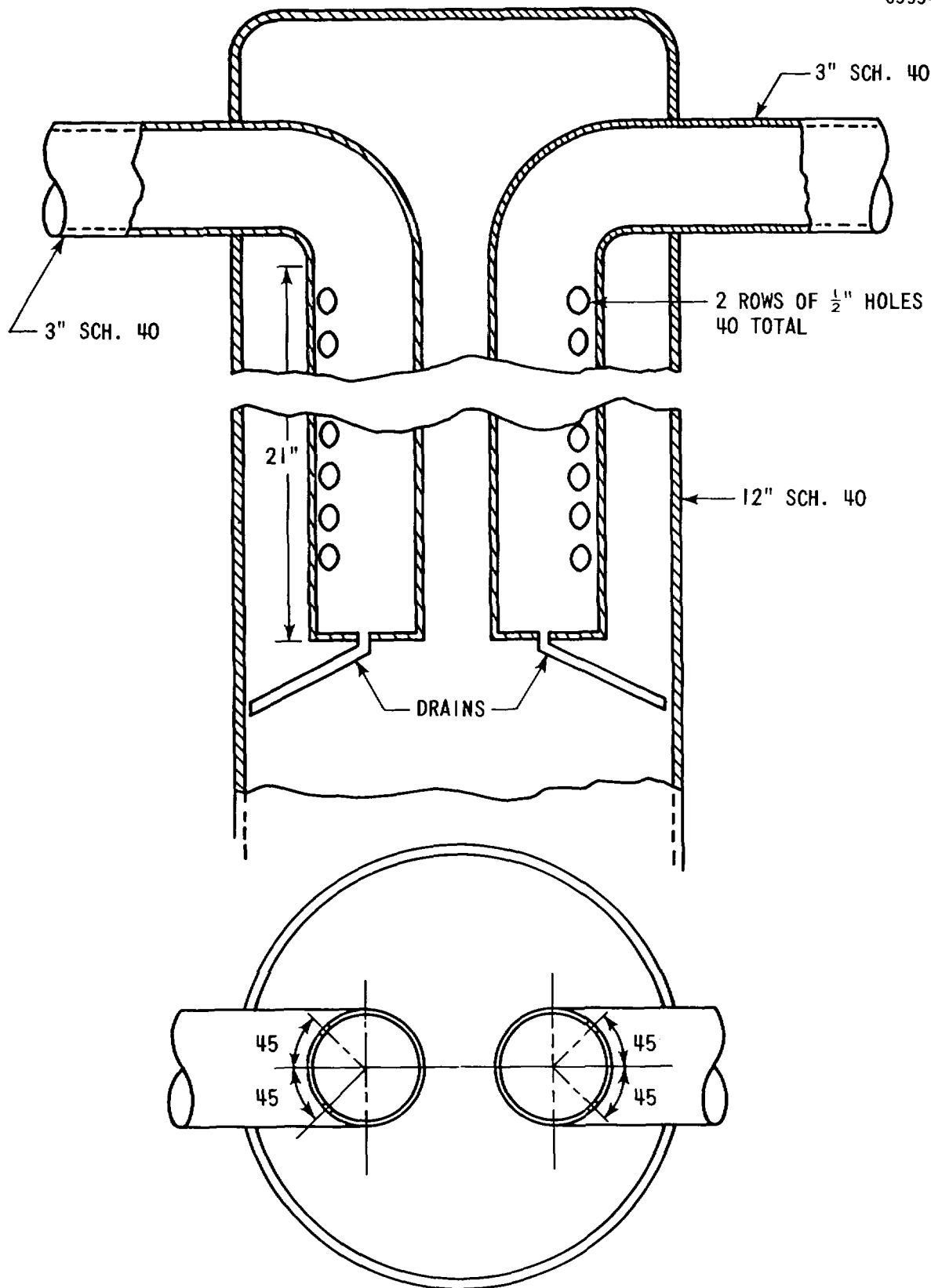


Figure 2-3. Schematic of Phase A Separator Tank

TABLE 2-1
FLECHT-SET PHASE A DIMENSIONS

Item	Description	Centerline Length (ft)	ID (in.)	Flow Area (ft ²)	Volume (ft ³)
1	Pipe, 1-1/2 in. Sch. 40	--	1.61	.01414	--
2	Downcomer	19.77 (to elbow)	4.760	.1235	2.44
3	90° Elbow (L/R) 5 in. Sch. 40	--	5.047	.1390	--
4	Pipe, 5 in.	3.21	4.760	.1235	.40
5	Valve	.833	5.047	.1363	.11
6	Pipe, 5 in.	3.21	4.760	.1235	.40
7	Test Section				
	Lower Plenum	--	--	--	1.50
	Heated Length	12.0		.1383	1.66
	Upper Plenum	--	--	2.91	2.38
	Upper Plenum Ext	--	7.981	.3474	1.28
8	Pipe, 3 in. Sch. 40	18.5	3.068	.05130	.95
9	Carryover Tank	19.50 top bot	11.938 7.981	-- --	11.11
10	Pipe, 3 in. Sch. 40	.63	3.068	.05130	.03
11	90° Elbow (L/R) 3 in. Sch. 40	--	3.068	.05130	--
12	Pipe, 3 in. Sch. 40	9.0	3.068	.05130	.46
13	Pipe, 3 in. Sch. 40	10.0	3.068	.05130	.51
14	Pipe, 3 in. Sch. 40	4.5	3.068	.05130	.23
15	Orifice (sq. cut) 20 psia	--	1.76	.01689	--
	60 psia	--	2.025	.02237	--
16	Pipe, 3 in. Sch. 40	10.0	3.068	.05130	.51
17	Pipe, 3 in. Sch. 40	.54	3.068	.05130	.03
18	Containment Tank	20	23.250	--	59.85
19	Pipe, 1-1/2 in. Sch. 40	2.17	1.61	.01414	.03
20	90° Elbow (L/R) 1-1/2 in. Sch. 40	--	1.61	.01414	--
21	Pipe, 1-1/2 in. Sch. 40	2.85	1.61	.01414	.04
22	Overflow Tank	20.75	6.065	--	4.094
23	Pipe, 1-1/2 in. ID Tubing	.92	1.500	.01225	.01
24	Overflow Tank	20.75	6.065	--	4.094

TABLE 2-2

COMPARISON OF TEST AND PWR FLOW AREAS

Component	Flow Area (ft ²)		Ratio
	PWR	FLECHT-SET	
Downcomer	45.8*	0.124	369
Core	51.2	0.138	370
Upper Plenum	95.	2.91	32
Upper Plenum Extension	--	0.347	274
Hot Leg	4.58 x 4	0.051	357
Cold Leg	4.12 x 4	0.051	320

*Includes core baffle region.

rods were of fixed length and penetrated the top of the upper plenum. The upper plenum volume was scaled to a PWR upper plenum by adding on an extension which also allowed the upper plenum discharge to be 4 ft above the top of the heated length. The loop resistance coefficient was determined experimentally so that the loop pressure drop per pound of saturated steam flowing in the loop was similar to that of a typical PWR unbroken loop under locked rotor conditions with superheated steam flowing from the steam generator inlet to the break location. This resulted in a loop resistance coefficient, defined as $K \approx 2\rho_{\text{sat}} \Delta P_{\text{loop}} / G_{\text{hot leg}}^2$, on the order of 30.

The absence of a loop steam generator simulation means that the results are typical of a PWR up to the time water is collected in the separator. The effect of the storage of water in the steam generator inlet piping and lower plenum and the possible vaporization of water in the steam generator tubes were not simulated in this series of tests.

The coolant was injected directly into the top of the downcomer in the first five 20 psia tests. It was found that the injection water condensed the steam in the downcomer, dropping the downcomer pressure. Since the lower plenum had been prefilled, the resulting pressure imbalance pushed the prefill water into the downcomer, causing approximately 10 seconds delay in the start of reflood. This particular phenomenon is a consequence of the testing method and geometry and is not characteristic of a PWR. During a PWR blowdown, the accumulator

water will flow around the barrel-vessel annulus, condensing some of the steam generated by the core and begin to fill the reactor lower plenum. The accumulator injection during the later stages of blowdown condenses much of the residual steam remaining in the annulus. At the same time, the pressure in the annulus drops to approximately containment pressure due to the close proximity of the break. Thus, it was felt that the condensation effect observed in the test, which resulted in a pressure above the downcomer fluid approximately 1 psi lower than containment pressure, was not typical of a PWR during reflood. The condensation phenomenon was partially eliminated by moving the injection point below the level of the prefill water in the downcomer. The injecting angle was perpendicular to the direction of flow so that the effect of the injection water momentum was negligible. This phenomenon will be studied further in Phase B tests where more than one injection location will be tested.

The nominal injection rates were determined from Figure 2-4 which shows typical accumulator and pump injection rates for three loops of a four-loop PWR, consistent with the assumed loss of broken loop ECC injection and minimum safeguards flow rate. The high injection rate and its duration were varied parametrically in the test series.

The power decay used in this series of tests, shown in Figure 2-5, is a result of normalizing the curve shown in Figure 2-6 to the value at 30 seconds after shutdown. The excellent agreement between the FLECHT-SET power decay and the ANS standard including 20 percent uncertainty is also shown in Figure 2-6.

2.2 INSTRUMENTATION

Test section instrumentation used in these experiments was nearly identical to that of the 10 x 10 FLECHT test section described in Reference 1. The heater rod thermocouple locations are shown in Figure 2-7. It should be noted that the heater rods used in this series of tests had extensive use in previous tests. As a result some of the thermocouples failed as testing proceeded.

In Phase A the calculation of flooding rate, heat release, and effluent flow rates (both liquid and vapor phases) were of primary importance. In addition, it was desirable to obtain knowledge of the mechanisms causing any oscillations

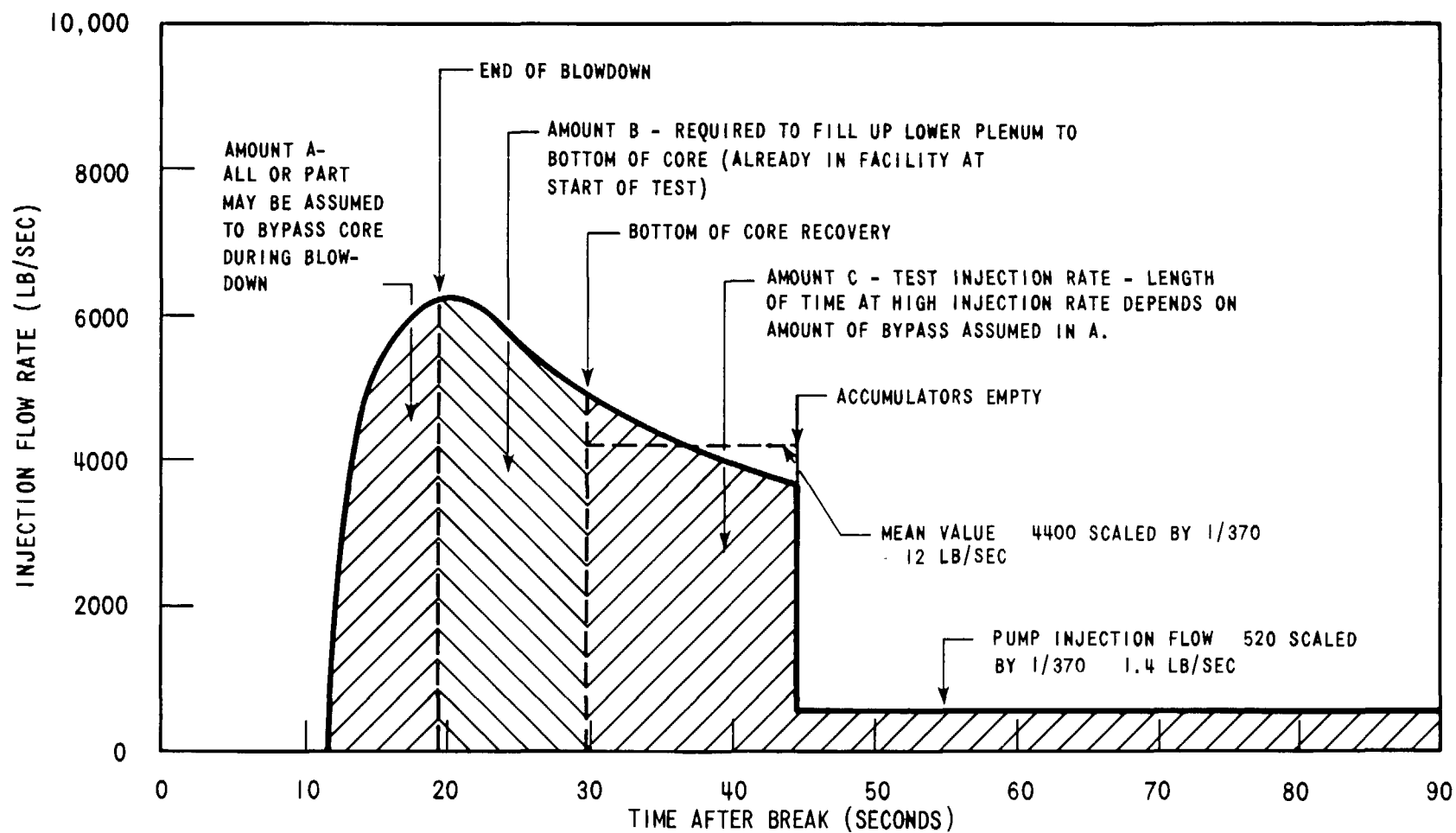


Figure 2-4. Double Ended Cold Leg Break (Guillotine) Accumulators and Pump Injection Flow Rates versus Time

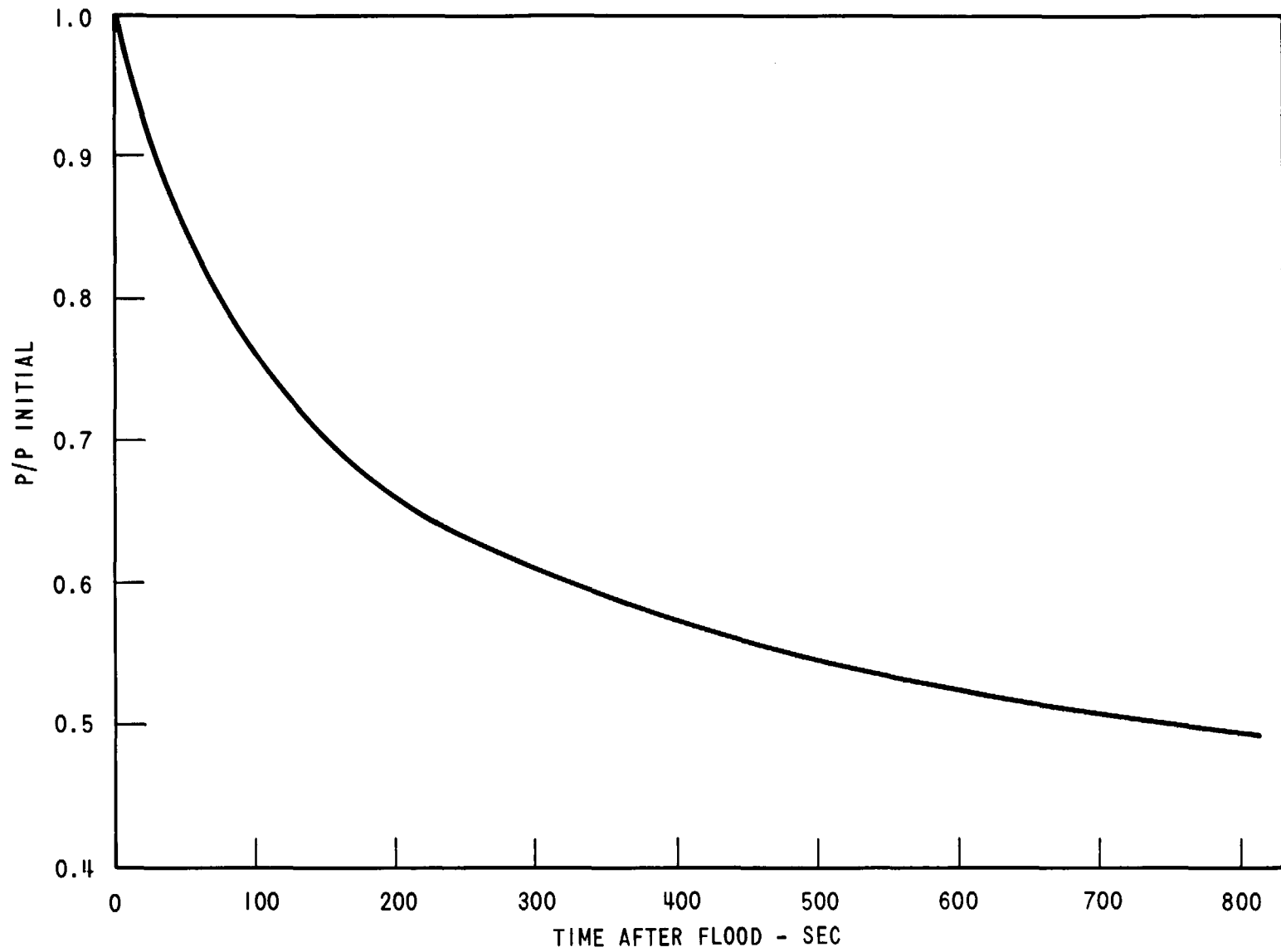


Figure 2-5. Measured Power Decay Used in FLECHTSET (Phase A)

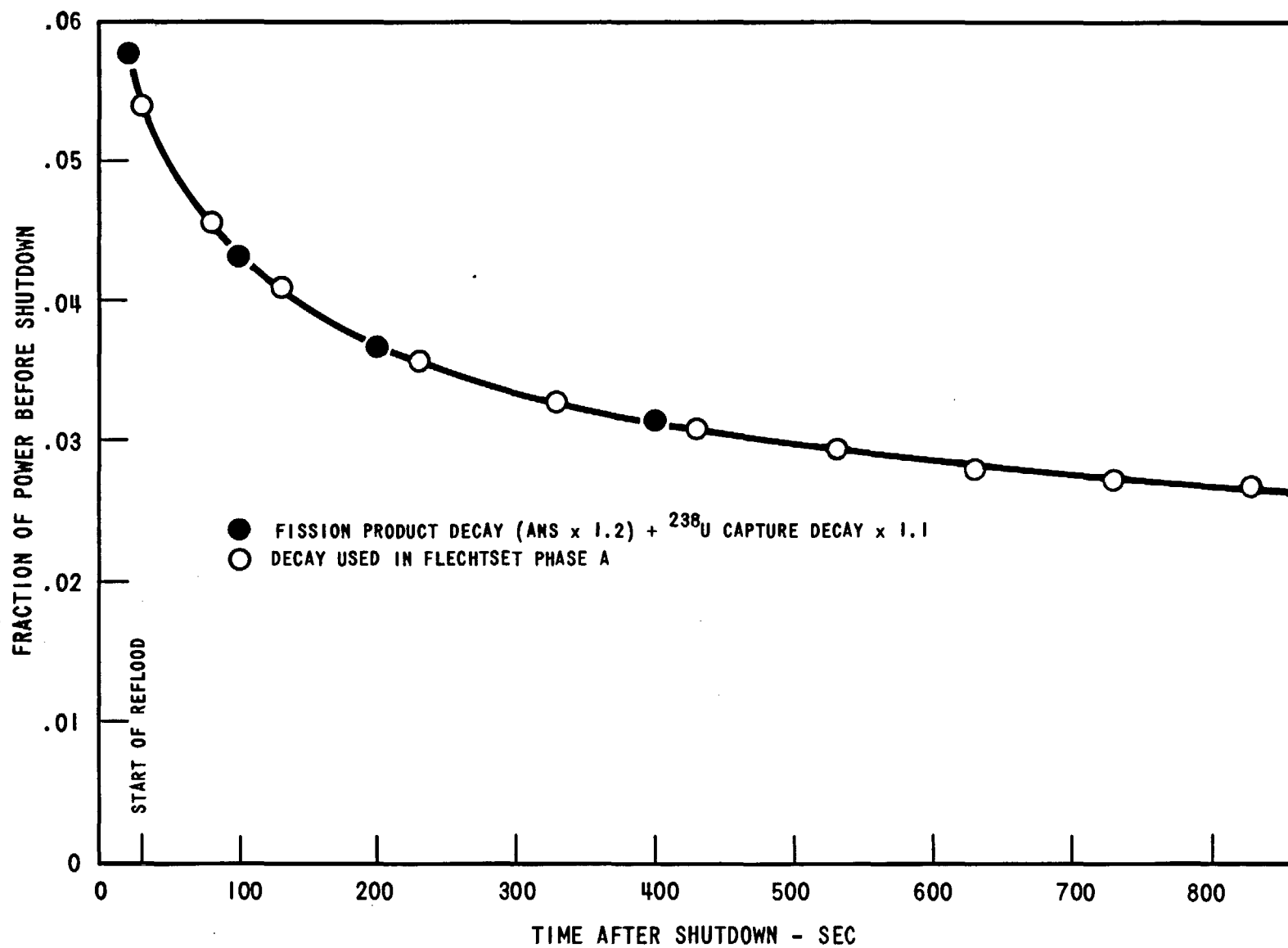
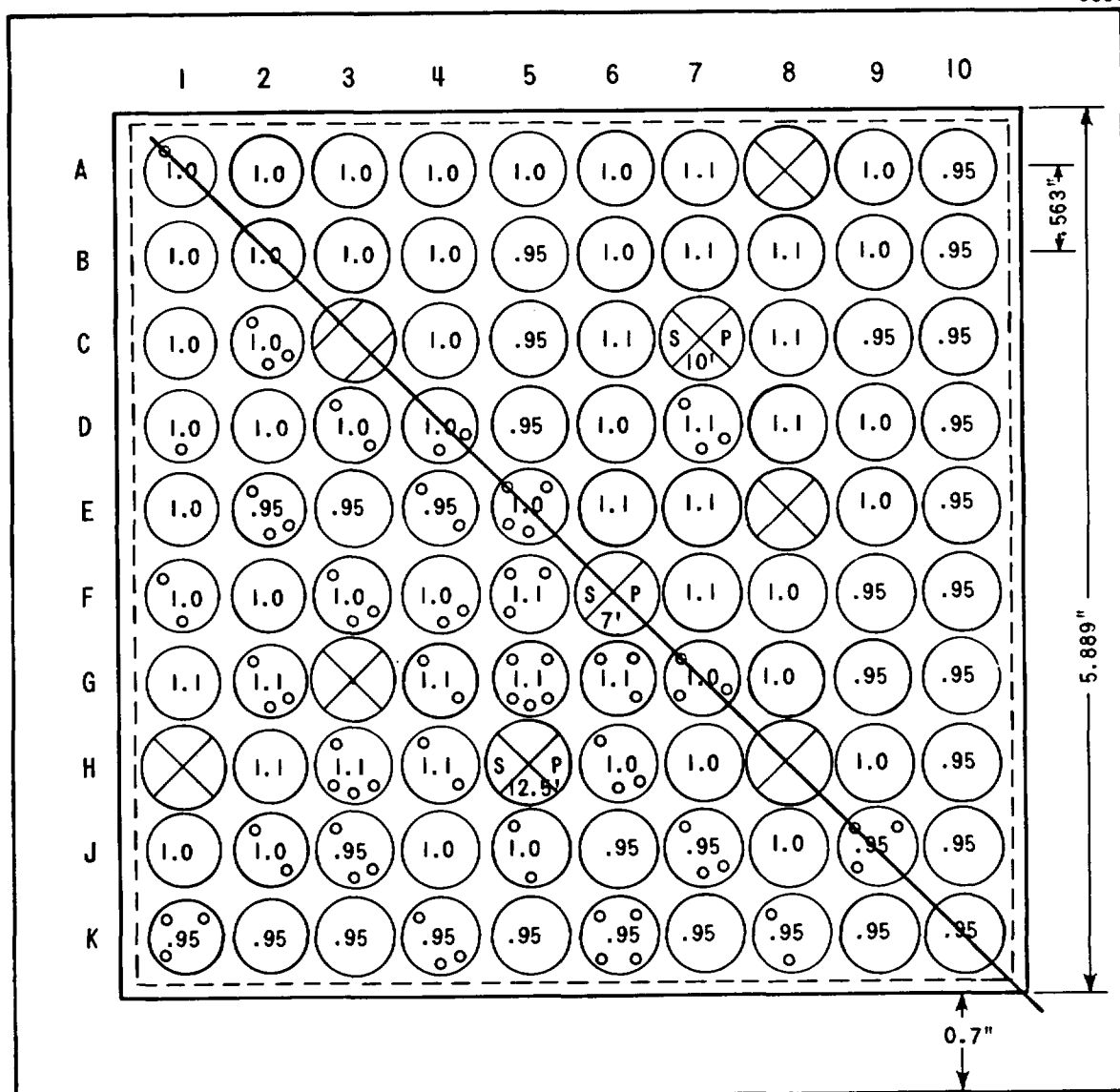


Figure 2-6. Comparison of FLECHTSET Power Decay to ANS Standard



- 10' 2' 8' 4' 6'
- INSTRUMENTED HEATER ROD SHOWING ELEVATION OF THERMOCOUPLES - DIAMETER .422 INCH
- UNINSTRUMENTED THIMBLE - DIAMETER .545 INCH
- THIMBLE CONTAINING STEAM PROBE - DIAMETER .545 INCH
- INSTRUMENT TUBE - DIAMETER .463 INCH

Figure 2-7. Cross Section of 10 x 10 Bundle Showing Instrument Locations

that occurred. The placement of instrumentation was designed to provide the required data. Figures 2-8 and 2-9 show the placement of the loop thermocouples and pressure transducers, respectively. Four additional differential pressure transducers were added for runs with prefix numbers greater than or equal to 39 when it became obvious that water was being stored in the upper plenum extension. These transducers, shown as dashed lines in Figure 2-9, were installed at the 10 ft and 11 ft-9 in. elevations on the test section and at the 12 ft-7 in. and 15 ft elevations on the upper plenum extension. The reference leg connection was moved from the 13 ft-6 in. location in the upper plenum to the top of the upper plenum extension. The injection flow rates were measured using two Brooks recording rotameters. The power supplied to the bundle was measured by three Hall-Effect watt transducers.

2.3 TEST PROCEDURES

The coolant supply tanks were filled with demineralized water, and the water was circulated as it was heated to the specified inlet conditions in order to prevent stratification. The flow housing was heated to the initial temperature profile as defined in Section 2.4. The downcomer and lower plenum were heated to the specified coolant inlet temperature so that the coolant would not pick up heat from pipe walls before entering the test section. The upper plenum, hot leg, liquid separator, and containment tanks were heated to 20 degrees above the saturation temperature in order to minimize heat transfer between the fluid and the pipe walls. The 9 ft U-bend between the separator and containment tanks was heated to 500°F so that any unseparated droplets would be vaporized before passing through the loop orifice.

When all temperatures were within preset tolerances ($\pm 20^\circ\text{F}$ for wall temperature and $\pm 10^\circ\text{F}$ for fluid temperature), the heaters (except those on the 9-ft U-bend) were turned off and the coolant injection tanks were pressurized with nitrogen. The loop was then pressurized with steam to the desired pressure. While maintaining the loop pressure constant, the lower plenum and downcomer were filled with water to the bottom of the heated length. Power was then supplied to the rods, and the rods were allowed to heat up until the desired initial temperature was reached. At this time coolant injection and the decay of rod power were initiated automatically. The coolant injection rate was normally stepped down

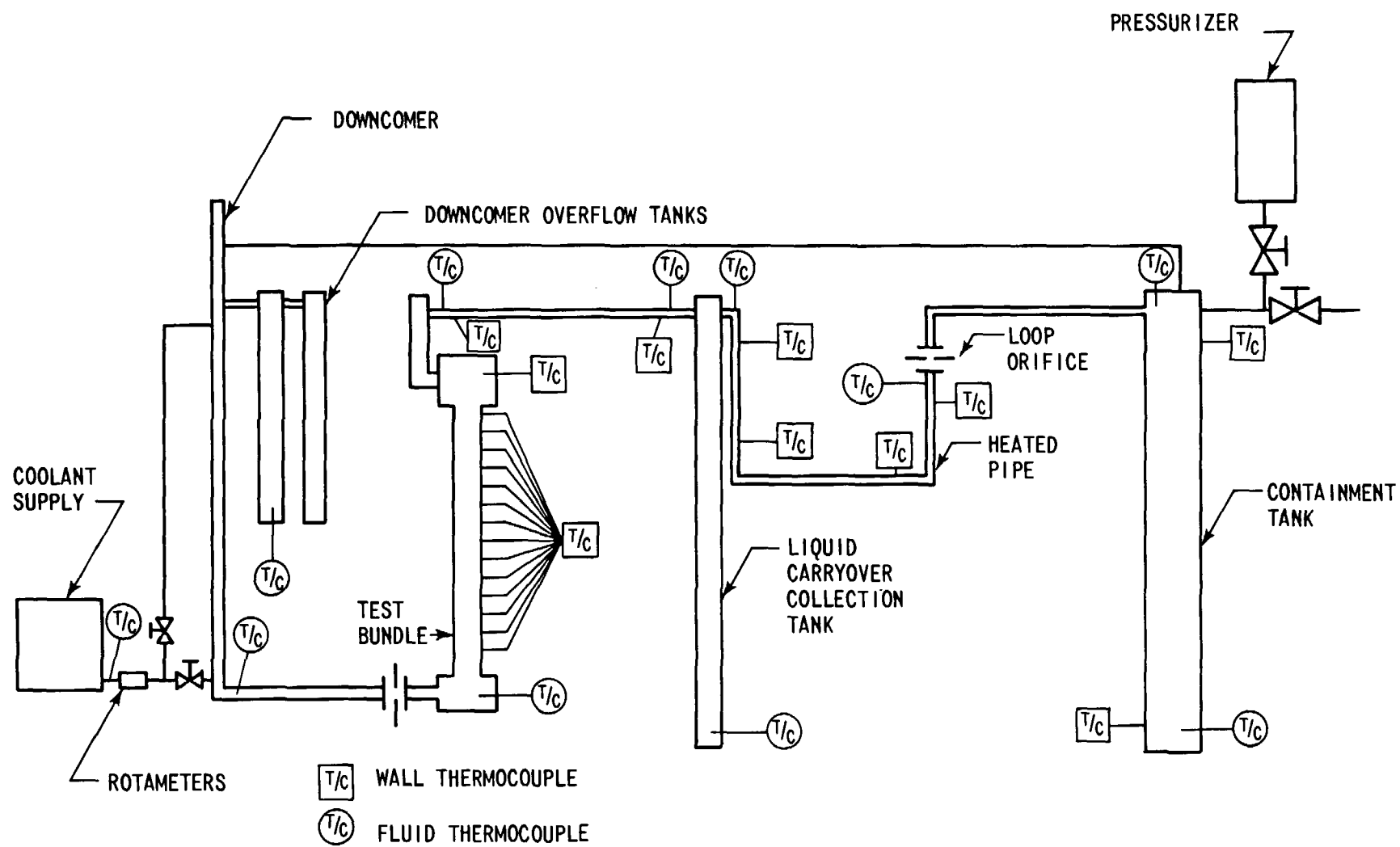


Figure 2-8. Thermocouple Locations

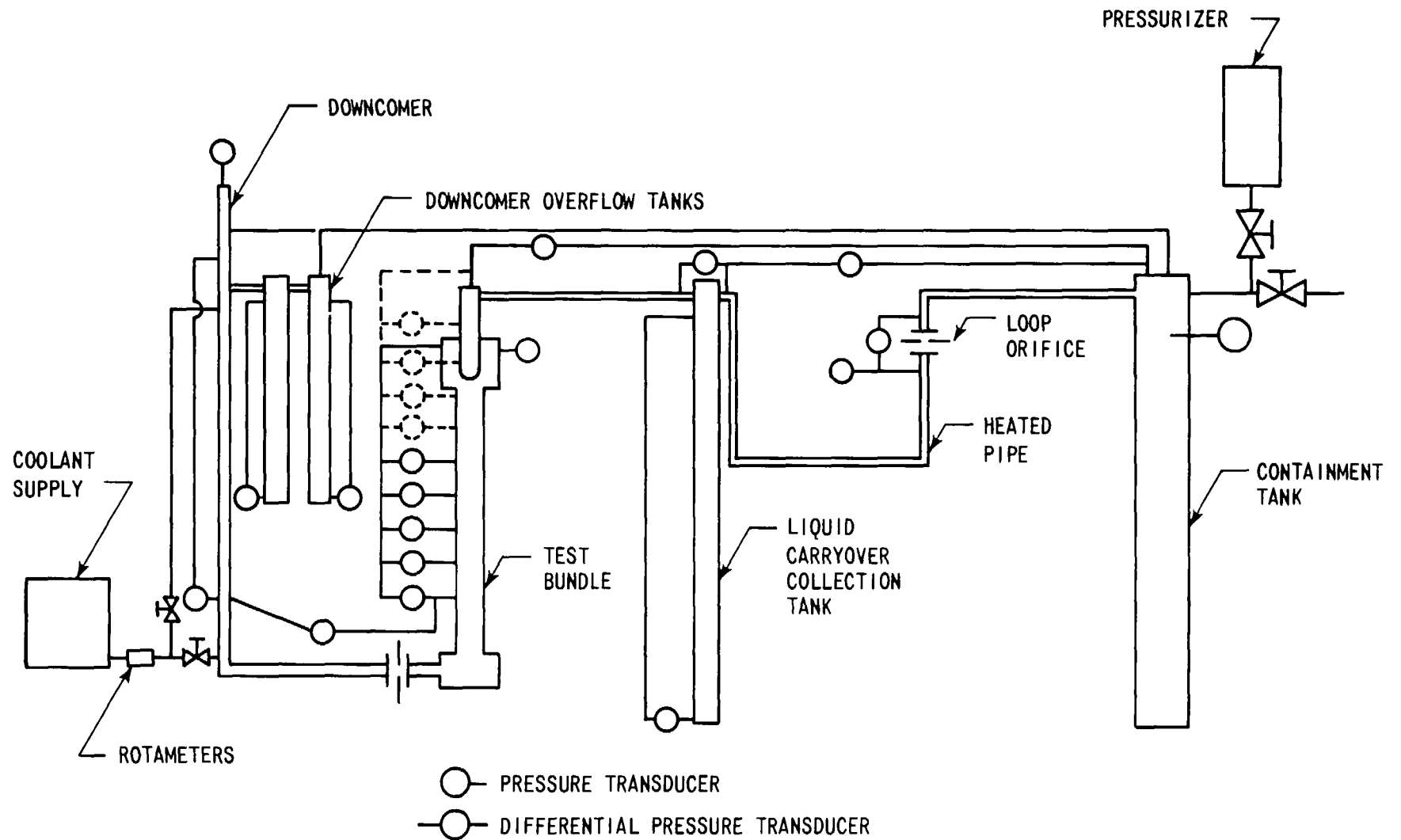


Figure 2-9. Pressure and Differential Pressure Transducer Locations

after a preset time from a high injection rate to the lower injection rate. The step in flow rate was accomplished by switching solenoid valves so that a high head centrifugal pump, which supplied the difference between the high and low flow rates, went into a bypass mode.

The tests were terminated using one of the following procedures:

1. By turning off power and the injection water immediately after quenching of the upper elevations of the test section, as indicated by the pen recorders.
2. By leaving the power and coolant injection flow on until the water supply was depleted.
3. By turning off the injection flow several seconds after quenching the test section and leaving the power on until the rod thermocouples indicated rising temperatures in the upper elevations.

A VIDAR digital data acquisition system scanned heater rod and housing wall thermocouple signals every 5.5 seconds during the test and stored the information on magnetic tape. This was the only information which did not require manual processing. Various pipe wall and fluid temperatures were recorded on paper tape by a small Hewlett-Packard data acquisition system. Pressure and pressure drop data were continuously recorded using two VISICORDERS and two Texas Instrument pen recorders. The coolant injection rates, several critical heater rod temperatures, and the power input to the three radial power zones were also recorded on Texas Instrument pen recorders.

2.4 INITIAL HOUSING TEMPERATURE DISTRIBUTION

The same criterion was used to determine the initial housing temperature profiles as in the FLECHT experiments described in Reference 2.

The situation is repeated here for completeness.

One can consider a unit cell around each heater rod having the dimensions of the heater rod pitch (.563 in.). When this is done for all rods, the result is a large 5.63 in. x 5.63 in. square. However, the test section inside dimension is 5.889 in. and is the result of a design which made the hydraulic radius of the flow channel near the wall equal to that of an interior flow

channel. The result is an additional flow channel near the wall having the same flow area as ~16.8 heater rod unit cells. In order to supply heat to fluid in this channel, the housing was heated to a specified initial temperature distribution. The housing temperature was chosen so that the housing releases the same heat as an equivalent row of rods from the inlet elevation to the midplane elevation over the time from the start of flooding to the quench of the midplane. This criterion stated mathematically is:

$$(\rho CA)_{\text{housing}} \int_0^6 (T_h - T_{\text{sat}}) dz = 16.8 \left\{ \sum_i (\rho_i C_i A_i)_{\text{rod}} \int_0^6 (T_r - T_{\text{sat}})_{\text{initial}} dz \right. \\ \left. + \int_0^{6'} \int_0^{t_{6'}^{\text{quench}}} q'_{\text{generated}} dt dz \right\}$$

The above equation results in an average housing temperature. The axial housing temperature distribution was chosen to be the same as the heater rod axial power distribution.

It was impossible to accurately predict the midplane quench time since the variable flooding rate was not known before the test. Thus, an average flooding rate was estimated and the midplane quench time was determined from the correlation (TQGFT) in Reference 1.

More will be said about the effects of the flow housing on the test results in later sections.

SECTION 3

DISCUSSION OF TEST RESULTS

3.1 GENERAL RESULTS

In the FLECHT-SET tests there was a dynamic coupling between flooding rate, downcomer and test section heads, release rate, steam generation rate, and loop pressure drop. In addition, the outlet flow rate did not change significantly when the flooding rate changed rapidly, implying that there is a time delay before the outlet flow rate is affected by a change in flooding rate.

The core and downcomer levels oscillated with a period of approximately 3 seconds during the initial portion of the reflood transient. As flooding continued, the observed oscillations became smaller and ended before the midplane quenched. The calculated time-averaged flooding rate showed that a large surge of coolant entered the test section during the first 10 seconds. The calculated average flooding rate then decreased to approximately 1 in./sec for 60 psia tests.

The midplane heat transfer coefficients obtained in the tests were generally higher than would be predicted by using the averaged flooding rate values and the FLECHT correlations as given in Reference 1. The procedure used to predict the heat transfer coefficient was to input the calculated instantaneous flooding rate into the FLECHT correlation at a time determined by dividing the total mass put into the bundle by the calculated inlet mass flow rate.

The entrained water did not appear in the separator tank (location of the steam generator) until 100 to 200 seconds after the start of reflood. In some cases the entire test section had quenched before any water collected in the separator. Movies taken at the 9-foot elevation of the test section show a large number of droplets moving upward ~ 5 seconds after the start of injection and onward. Although the view through the window is restricted to a small portion of the bundle cross section, droplets could not be observed

falling back into the bundle. The delay was caused by the storage of entrained water in the upper plenum and upper plenum extension. The power and flow were left on in several runs after the bundle had quenched, and it was found that overflow from the test section continued as long as power was on. Movies taken during such a run indicate the existence of a relatively high void fraction (.6 to .8) in the bundle at the 9 ft elevation, which was substantiated by axial pressure drop measurements.

3.1.1 Summary of Run Conditions and Test Results

Twenty-five tests were run during the FLECHT-SET Phase A series. The nominal conditions and the parameter variations are shown in Table 3-1. Table 3-2 summarizes the exact run conditions, measured temperature behavior of the hottest midplane rod, and measured loop resistance coefficient for each valid run performed in this test series. Additional data for the runs are included in Appendix A of this report. The parameters used to characterize the test behavior are as follows:

1. Maximum Midplane Temperature. Defined as the maximum midplane temperature recorded during the test.
2. Turnaround Time. Defined as the time after the start of flooding at which the maximum midplane temperature was recorded.
3. Midplane Quench Time. Defined as the time after the start of flooding at which the temperature of the hottest midplane rod starts to drop very rapidly.
4. Loop Resistance Coefficient. Defined as the nondimensional number obtained by dividing the loop pressure drop by the dynamic head of saturated steam flowing through the hot leg at a time before a two-phase mixture flow through the hot leg, i.e.,

$$K = \left[\frac{\Delta p_{\text{loop}}}{(1/2 \rho V^2)_{\text{hot leg(sat)}}} \right]_{\text{test}} = \left[K_{\text{hot leg}} + \frac{\rho_{\text{sat}}}{\rho_{\text{cold leg}}} \left(K_{\text{cold leg}} + K_{\text{pump}} + 9K_{\text{downcomer-break}} \right) \right]_{\text{PWR}}$$

TABLE 3-1

NOMINAL RUN CONDITIONS AND PARAMETER VARIATIONS

	<u>Nominal</u>	<u>Variation</u>
Containment Pressure (psia)	20 and 60	40
Peak Power (kw/ft)	0.7	0.4, 1.0
Initial Peak Clad Temp (°F)	1100	700, 900, 1400
Coolant Injection Temp (°F)	150	200
Injection Rate (lb/sec)	12 for first 14 sec and 1.4 after 14 sec	6 for first 28 sec, 1.4 after 28 sec, and 1.4 continuous

TABLE 3-2

FLECHT-SET PHASE A DATA SUMMARY

Run No.	Containment Pressure (psia)	Peak Power (kw/ft)	Initial Peak Clad Temp (°F)	Coolant Inj. Temp (°F)	Average Housing Temp (°F)	Injection Rate (lb/sec)	Max. Midplane Temp. (°F)	Turnaround Time (sec)	Midplane Quench Time (sec)	Loop Resis. Coef. $\frac{1}{P/(1/2 cu)}$	Remarks
1510 ⁽¹⁾	55	0.7	1112	164	454	10.44 first 14 sec 1.37 after 14 sec	1279 (4G)	41	115	30	
1709 ⁽¹⁾	60	0.7	1106	168	443	1.32 continuous	1581 (4G)	83	188	29	
1827 ⁽¹⁾	60	0.4	1112	161	399	9.63 first 14 sec 1.36 after 14 sec	1150 (5G)	12	93	28	
1926 ⁽¹⁾	59	1.0	1120	163	567	12.91 first 14 sec 1.65 after 14 sec	1580 (4G)	104	202	27	
2023 ⁽¹⁾	59	0.7	1112	161	441	10.4 first 14 sec 1.38 after 14 sec	1278 (4G)	41	111	30	
2207	22	0.7	1100	160	470	12.12 first 14 sec 1.19 after 14 sec	1489 (4G)	107	270	31	
2605	20	0.7	1104	157	482	5.7 first 28 sec 1.23 after 28 sec	1551 (4G)	136	322	30	
2718	20	0.7	1399	156	499	9.83 first 14 sec 1.23 after 28 sec	1769 (4G)	120	373	31	
2822 ⁽²⁾	19	0.4	1092	163	396	11.0 first 14 sec 1.16 after 14 sec	1170 (4G)	40	155	33	
2919	20	0.7	912	153	458	10.10 first 14 sec 1.2 after 14 sec	1476 (4G)	122	285	33	Rod 2G burned out
3006 ⁽²⁾	20	0.7	1115	162	488	1.17 continuous	1816 (4G)	139	439	32	
3117 ⁽²⁾	20	0.7	1113	159	474	11.22 first 14 sec 1.10 after 14 sec	1437 (5G)	133	281	35	
3339 ⁽²⁾	20	0.7	1073	195	435	11.50 first 14 sec 1.17 after 14 sec	1451 (5G)	116	308	31	
3421 ⁽²⁾	20	1.0	1098	161	612	11.78 first 14 sec 1.20 after 14 sec	1857 (5G)	149	627	31	Max Bundle temp at 8' = 1913° at 339 sec. Ran out of water at 775 sec
3928 ⁽²⁾	62	0.7	1102	201	431	12.0 first 14 sec 1.3 after 14 sec	1167 (5G)	20	96	32	
4024 ⁽²⁾	59	0.7	1402	155	509	10.99 first 14 sec 1.4 after 14 sec	1433 (5G)	7	133	28	
4313	60	0.646	1105	154	299	9.70 first 14 sec 1.2 after 14 sec	1163 (5G)	9	83	32	90 heated rods. No radial power variation
4412	61	0.646	1107	159	297	10.9 first 14 sec 1.2 after 14 sec	1164 (5G)	9	77	30	82 heated rods. No radial power variation
4530 ⁽²⁾	40	0.7	1115	161	436	8.8 first 14 sec 1.2 after 14 sec	1224 (5G)	36	129	31	
4825 ⁽²⁾	60	0.7	712	156	395	10.7 first 14 sec 1.2 after 14 sec	877 (5G)	27	66	31	
4923 ⁽²⁾	61	0.7	1111	158	449	10.52 first 14 sec 1.19 after 14 sec	1167 (5G)	19	97	31	
5115	61	0.759	1110	154	294	9.0 first 14 sec 1.2 after 14 sec	1172 (5G)	10	90	31	90 heated rods. No radial power variation
5214	61	0.646	1103	159	301	10.2 first 14 sec 1.19 after 14 sec	1156 (5G)	8	66	29	70 heated rods. No radial power variation
5316	61	0.646	1107	159	424	10.1 first 14 sec 1.18 after 14 sec	1160 (5G)	12	89	32	90 heated rods. No radial power variation
5413	61	0.646	1125	155	614	10.8 first 14 sec 1.25 after 14 sec	1159 (5G)	7	118	31	90 heated rods. No radial power variation

⁽¹⁾ Coolant injected at top of downcomer⁽²⁾ Rod 2G burned out. Changed radial power from (1.1, 1.0, .95) to (1.1, 1.0, .98%). Maintained same total power

3.2 DISCUSSION OF CALCULATION METHODS

The local heat flux from the heater rods was calculated from the heater rod thermocouple data using the DATAR code. DATAR is the inverse heat conduction code which has been used satisfactorily throughout the FLECHT program.

A complete description of DATAR can be found in Reference 3.

The varying flooding rate into the test section was calculated from a mass balance on the downcomer and downcomer overflow tanks. This can be written as:

$$M_{\text{input}} = \int_0^t \dot{m}_{\text{input}} dt = \int_0^t \dot{m}_{\text{inj}} dt - M_D(t) - M_O(t)$$

where \dot{m}_{inj} is the injection mass flow rate to the downcomer and M_D and M_O are the masses of water stored in the downcomer and downcomer overflow tanks, respectively. The flooding rate was obtained from the time rate of change of the mass put into the test section (M_{input}). The injection mass flow rates were determined from the pen recorder trace of the output of the two Brooks Rotameters. Water in the downcomer overflowed into a small diameter tank when the water level reached 16 feet above the elevation of the bottom of the heated length. The mass in the tank was determined as a function of time from the output of a differential pressure transducer installed for this purpose. The mass in the downcomer was calculated using the output of a differential pressure transducer which measured the pressure difference between the bottom (elevation of the bottom of the heated length) and top of the downcomer. It should be noted that the pressure difference cannot be related exactly to the mass of water in the downcomer if the water level is oscillating. This dilemma was caused by the fluid acceleration during the oscillations and can be illustrated using a simple example. Consider the column of water shown in Figure 3-1. The pressure drop measured by the transducer (ignoring friction) is

$$\Delta p = \rho g h_a + \rho h_a \frac{du}{dt}$$

where h_a is the actual water level and u is the upward velocity of the fluid in the downcomer.

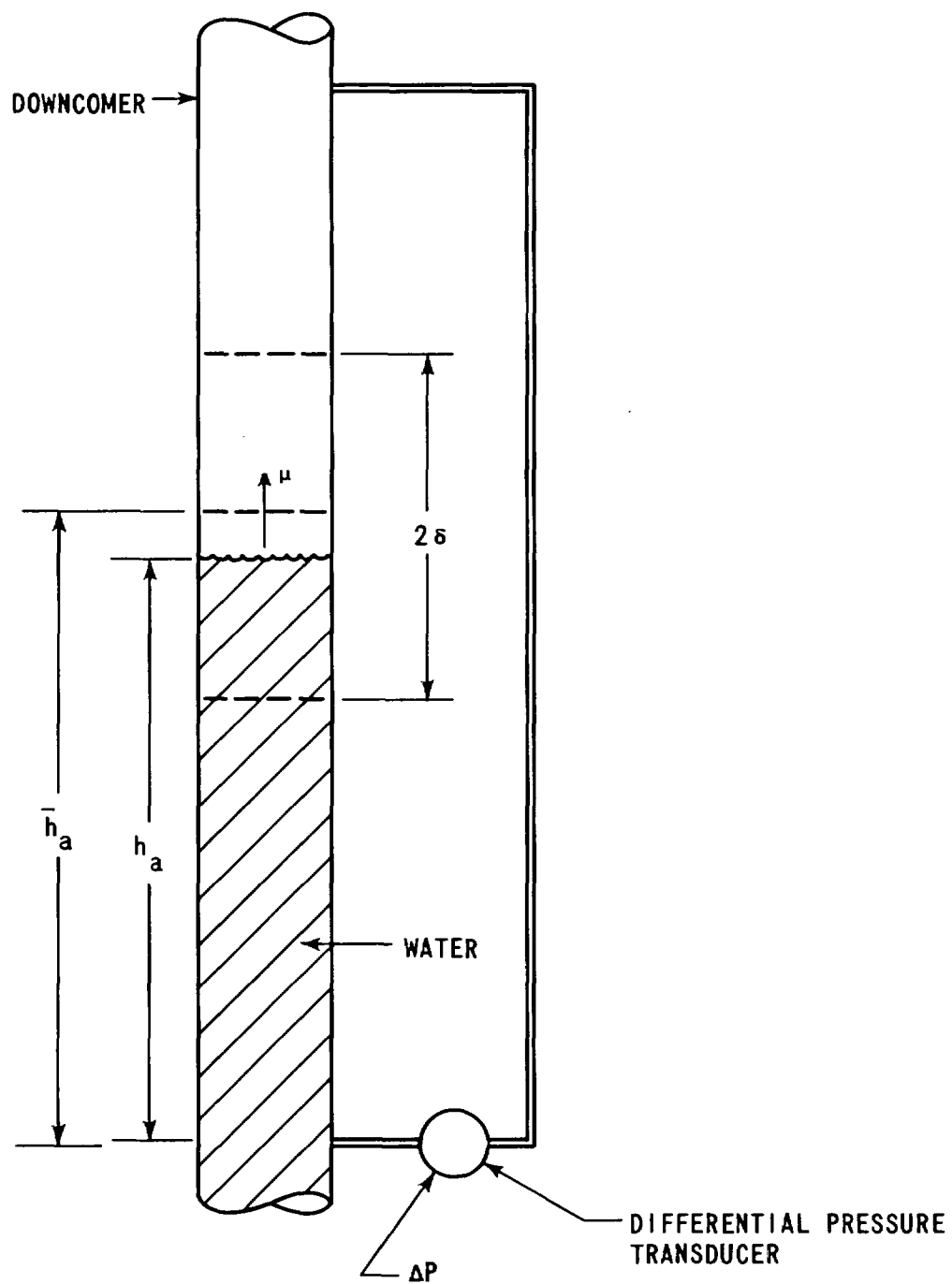


Figure 3-1. Schematic of Downcomer "Level" Transducer

Suppose the actual oscillating water level (h_a) can be represented by

$$h_a = \bar{h}_a + \delta \sin \omega t$$

where δ and ω are the amplitude and frequency of the oscillating water level.

It can be shown that the pressure transducer would indicate a height of water (h_I) given by

$$h_I = \frac{\Delta P}{\rho g} = h_a \left(1 - \frac{\delta \omega^2}{g} \sin \omega t\right)$$

Thus, in order to determine the water level one must measure the time varying fluid acceleration as well as the pressure drop.

The quantity $\delta \omega^2/g$ is on the order of 0.2 and is the ratio of the maximum fluid acceleration to gravitational acceleration. The above equation shows that a rising pressure difference may be caused by a falling water level. It was for this reason that the instantaneous flooding rate could not be calculated using this technique during the period of the oscillations. The flooding rates presented were obtained by estimating the mean downcomer elevation (\bar{h}_a) during the period of the oscillations. There is a small error involved in determining the mean downcomer elevation from the mean of the downcomer head measurement. Depending on how one determines the mean downcomer head, the error is on the order of 0.15 ft to 0.3 ft of water.

The varying steam flow rate out of the test section was measured from the pressure drop across a calibrated orifice downstream of the liquid separator. The piping downstream of the separator was heated to $\sim 500^\circ\text{F}$ before the test, and the heaters were left on during the test to ensure single-phase flow through the orifice. The pressure and temperature of the steam were measured upstream of the orifice in order to determine the steam density. Although the flow was pulsating through the orifice during the period of the oscillations, steady-state methods could be used to measure the mass flow rate because the Strouhal number based on orifice diameter was on the order of 0.0003, which is small enough so that the effect of fluid unsteadiness through the

orifice could be ignored. The mean mass flow rates presented were determined using the mean pressure drop across the orifice, resulting in an insignificant error (less than 1 percent) during the period of the oscillations.

The mass stored in the test section was calculated using the test section axial pressure drop data. The pressure drop was assumed to consist only of static head. This implies that friction and acceleration effects were negligible. The error resulting from this assumption can be estimated by considering the pressure drop across a typical 2 ft section:

$$\Delta p = \Delta p_{\text{liquid}} + \Delta p_{\text{vapor}} + \Delta p_{\text{mom}} + \Delta p_{\text{fric}}$$

The first two terms can be no bigger than their single-phase values, or

$$\Delta p_{\text{liquid}} \leq 0.83 \text{ psi}$$

$$\Delta p_{\text{vapor}} \leq 0.002 \text{ psi}$$

The third term can be estimated from the change in quality in the section due to heat release, or

$$\Delta p_{\text{mom}} \approx G^2 \Delta v = \frac{\dot{m}}{A^2} \dot{Q} \frac{v_{fg}}{h_{fg}} \approx 0.002 \text{ psi}$$

when $\dot{Q} = 100 \text{ Btu/sec}$, and $\dot{m} = 1.5 \text{ lb/sec}$, which are typical maximum values. The fourth term can be estimated assuming that all of the generated steam passes through the bundle at some point. This results in

$$\Delta p_{\text{fric}} = 2 C_f \rho v^2 L/D \approx 0.02 \text{ psi}$$

where it was assumed that:

$$\dot{m}_{\text{vapor}} \approx 0.4 \text{ lb/sec}$$

$$\rho \approx 0.05 \text{ lb/ft}^3$$

$$D \approx 0.54 \text{ in. (hydraulic diameter of a unit cell)}$$

which are typical values for a 20 psia run. Since the data could not be read closer than ~ 0.1 psia, which is greater than all the above terms except the liquid static head, it was felt that the remaining terms could be neglected.

3.3 PRESENTATION AND ANALYSIS OF SELECTED RUNS

The data from two of the twenty-five runs presented in Appendix A are examined in detail in this section. The two runs selected were chosen on the basis of having conditions as close to the nominal conditions as possible and having the least instrumentation difficulties.

It was evident from the data that there is a strong coupling between flooding rate, downcomer head, heat release, steam generation, and loop pressure drop. The change in downcomer liquid level, along with injection rate, determines the flooding rate. The bundle flooding rate, in a complex way, determines the heat release and the steam generation rate. The downcomer head, in turn, is determined by the loop pressure drop caused by the venting of the generated steam through the loop flow resistance, the static head of fluid stored in the test section, and the injection rate. The rate at which steam is generated early in the reflood of the bundle is sufficient to drive liquid level oscillations in the core and downcomer. Thus, during this period the flooding rate into the bundle oscillates on the order of ± 40 inches per second (peak to peak) while the time average flooding rate first increases to 5 or 6 in./sec and then, after ~ 10 seconds, decreases to 1 or 2 in./sec. The oscillations diminish with time and generally stop by the time the midplane has quenched.

3.3.1 Data Analysis for Run 4923

The following conditions pertain to Run 4923:

Containment Pressure = 61 psia

Initial Clad Temperature = 1111°F (5G)

Peak Power = 0.7 kw/ft

Coolant Injection Temperature = 158°F

Injection Flow Rate = 10.52 lb/sec, first 14 sec
1.19 lb/sec, after 14 sec

This run was conducted at the "nominal" conditions with a 60 psia containment pressure. The loop resistance coefficient based on saturated vapor following in the hot leg was ~ 31 , which is typical of a PWR under locked rotor conditions.

3.3.1.1 General Observations

Visicorder traces of the test section pressure drop indicated that at ~ 2 seconds after flooding the core level reached ~ 1.2 ft and then dropped slightly, indicating that steam generation had started. Large oscillations in core and downcomer liquid levels started shortly afterward. Movies taken at the 9 ft elevation show sheets of water droplets passing the window with a period of ~ 3 seconds. Visicorder traces of the upper plenum extension pressure drop indicate that the entrained water reached that elevation during the period of the high injection rate and that entrained water started collecting in the upper plenum extension after the first 20 seconds. Visicorder traces of the test section pressure drop and the movie indicate that the oscillations ended 50 seconds after the start of flood. Shortly after the oscillations ended the flow regime at the 9 ft window appeared to change from dispersed droplet flow to a churn-like flow. The flow regime remained churn-like until the end of the test.

3.3.1.2 Mass Balance

The mass balance for Run 4923 is shown in Figure 3-2. It shows the time-varying mass storage in the bundle, upper plenum extension, and separator tanks. The upper plenum was not sufficiently instrumented to determine the time-varying mass storage in the upper plenum, but it was found that 11 pounds of water were required to fill the spaces between the filler plate in the upper plenum annulus, and it was assumed that these spaces were filled by the time water started accumulating in the upper plenum extension. Also shown in Figure 3-2 is the time integral of the vapor mass flow rate as calculated from the orifice pressure drop, pressure, and temperature data.

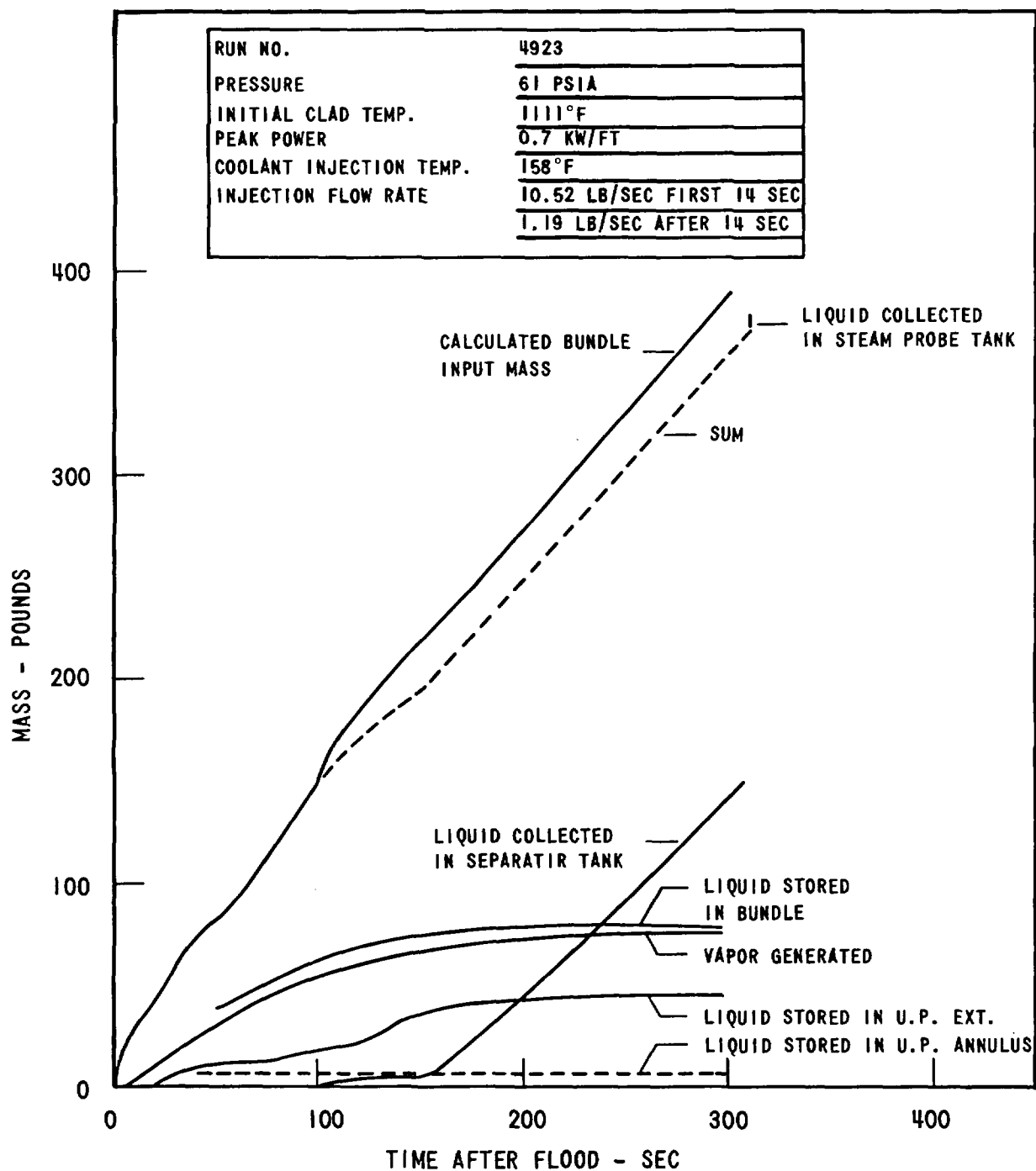


Figure 3-2. Mass Balance for Run 4923

These five quantities were added together and compared to the calculated bundle input mass which was obtained from a mass balance on the downcomer and downcomer overflow tanks. At the end of the test it was found that 5 pounds of water had collected in the steam probe tank. This quantity was added to the mass balance at the end of the test. When the power and flow were turned off at the end of the test, the steam flow stopped, the voids collapsed, and the water held up in the upper plenum extension and upper plenum drained down into the bundle. The bundle overflowed into the upper plenum. Within experimental accuracy, the total mass in the bundle and upper plenum after the test was nearly the same as the mass in the bundle and upper plenum extension just before the end of the test. This indicates that there was very little mass accumulation, except for the 11 pounds between the filter plates, in the upper plenum during the test. This was not expected and is not completely understood. An effort will be made in Phase B to better understand this behavior.

3.3.1.3 Flooding Rate

The flooding rate was determined from a mass balance on the downcomer as described in Section 3.2. Thus, when the downcomer water level rises, remains unchanged, or falls, the flooding rate into the bundle is less than, equal to, or greater than the injection flow rate, respectively. The mass stored in the downcomer was determined from the pressure drop measurement shown in Figure 3-3 which is a reduced tracing of the pen recorder data. During the oscillations the mean downcomer head, indicated by a dashed line in Figure 3-3, was used to determine the average flooding rate. The oscillations can be seen to grow in amplitude to $\sim \pm 1$ psi and then decay slowly to zero at ~ 55 seconds after flood. The period of the oscillation was ~ 3 seconds. The calculated average flooding rate is shown in Figure 3-4. To better understand the fluctuating flooding rate, refer to the pressure drop data shown in Figure 3-5. It is the pressure drop from the bottom of the downcomer to the containment which determines the downcomer level and, in turn, the flooding rate.

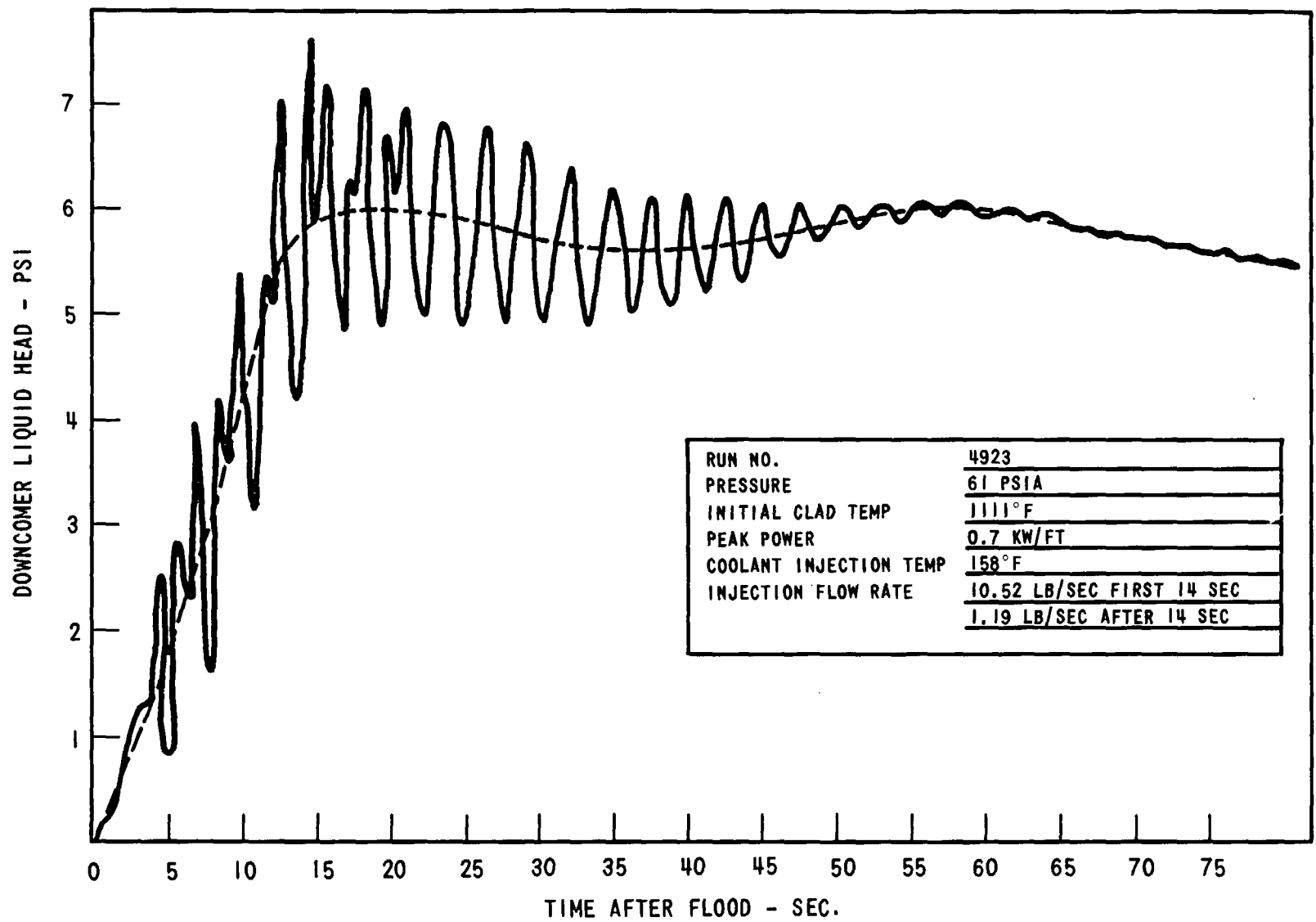


Figure 3-3. Downcomer Head vs. Time - Run 4923

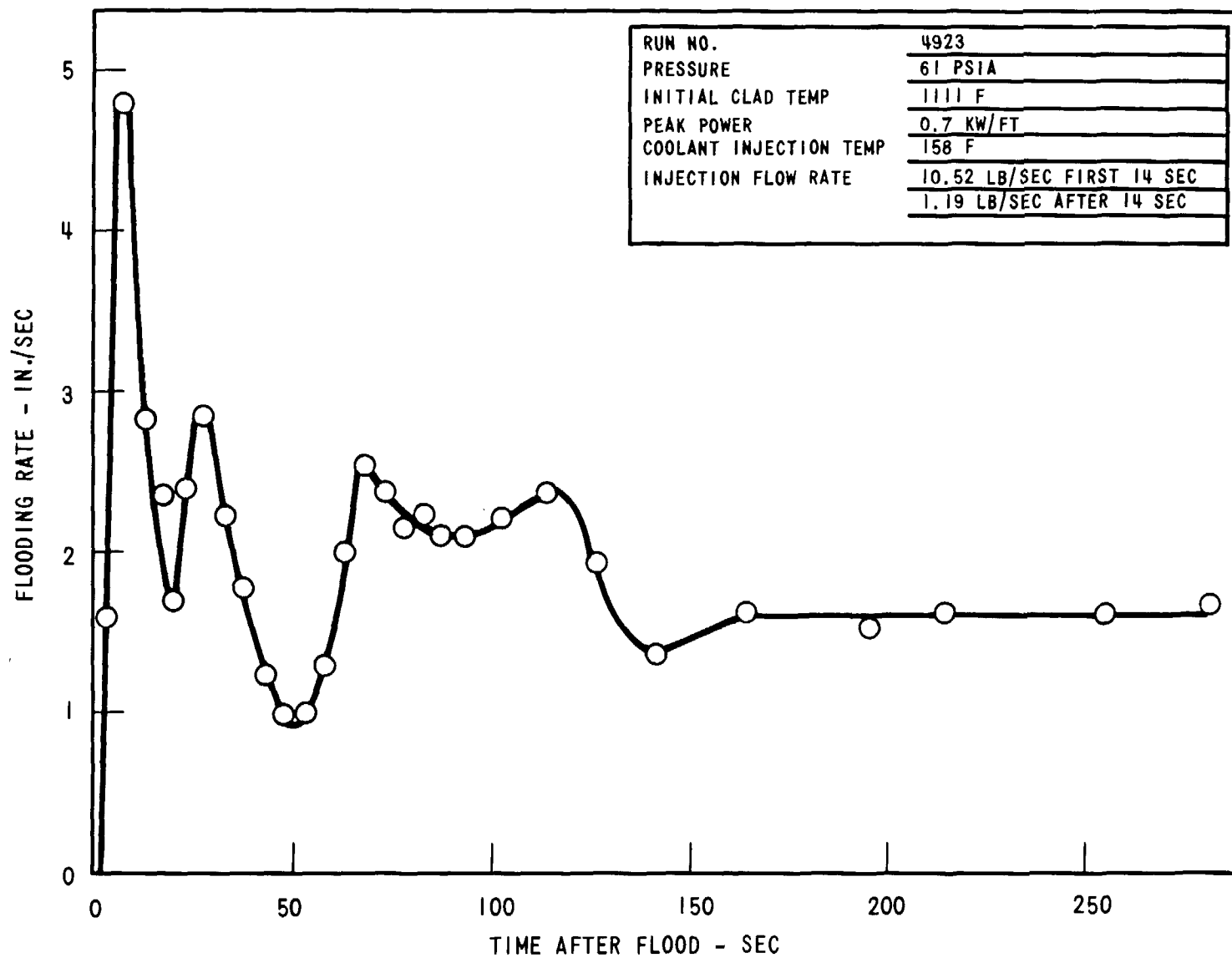


Figure 3-4. Flooding Rate vs. Time - Run 4923

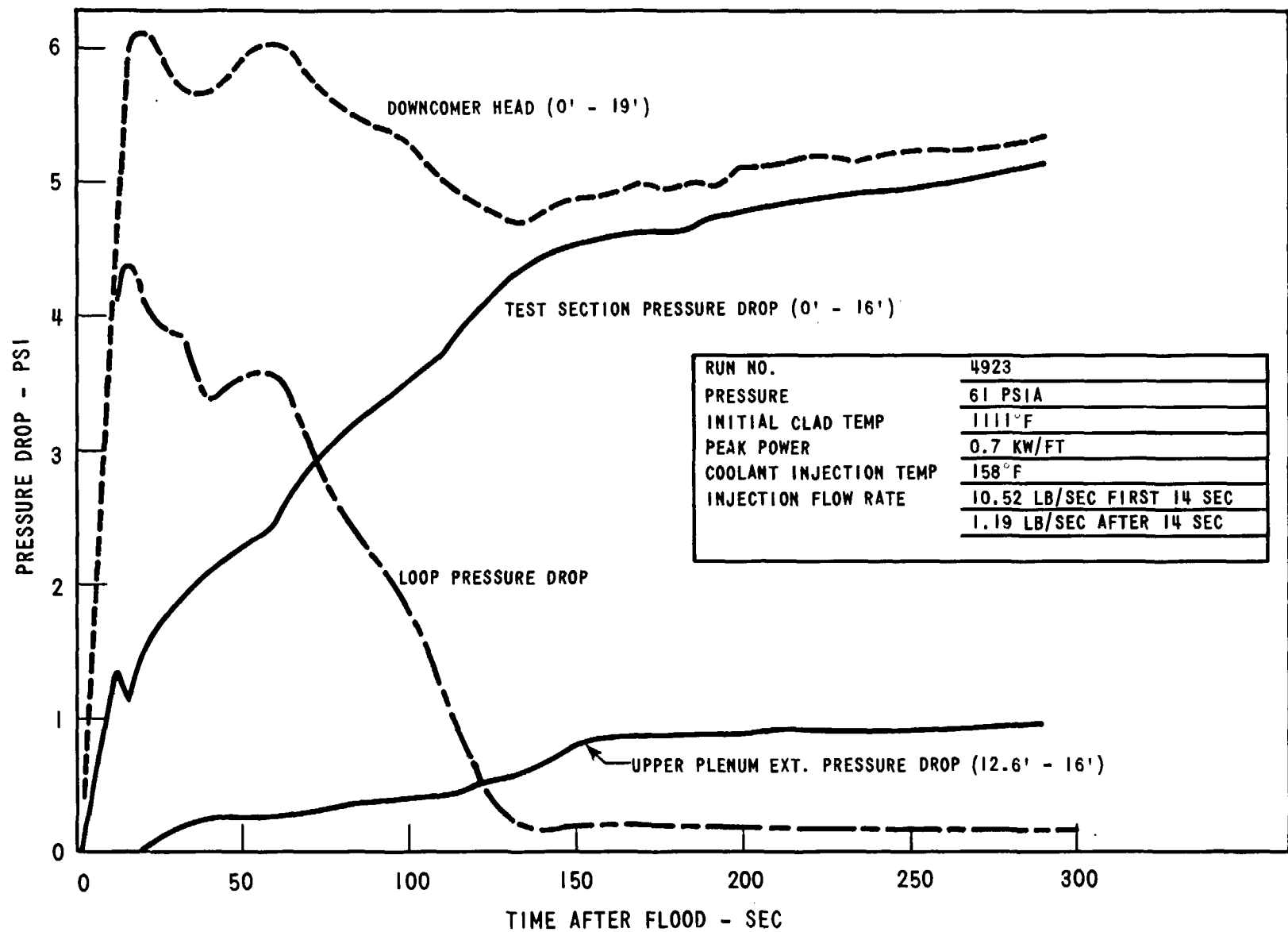


Figure 3-5. Pressure Drops for Run 4923

Figure 3-5 shows that the downcomer and the test section filled at a fairly rapid rate initially resulting in a flooding rate of ~ 4.8 in./sec. The loop pressure drop, which is proportional to the square of the steam flow rate, increased rapidly after the first 2 seconds, reaching a maximum at ~ 14 seconds when the high injection rate ended. Prior to the termination of the high injection rate the calculated flooding rate began decreasing because of the rising loop pressure drop. When the high injection rate ended, the loop pressure drop was sufficient to limit the flooding rate to a value lower than the injection rate and the downcomer level continued to rise slightly. Figure 3-5 further shows that the water inventory in the bundle began to decrease when the flooding rate decreased, and some of the water was either vaporized or entrained and carried out of the bundle. This combination of events yielded a higher ΔH (downcomer head - bundle head) and therefore a higher flooding rate which stopped the downcomer level increase. The increased flooding rate introduced colder water in the bundle and reduced steam generation. Thus, the loop pressure drop decreased and the water inventory in the bundle increased again as the flooding rate increased to ~ 3 in./sec. During this time the entrained water carried out of the bundle began to collect in the upper plenum extension and the downcomer water level dropped. The increasing test section pressure drop and decreasing downcomer driving force eventually reduced the flooding rate. During the same time period the vapor flow rate increased as noted by the rise in loop pressure drop at 40 seconds, and the accumulation rate of water in the upper plenum extension decreased. A possible reason for this is that during a transient when the flooding rate decreases voids may form below the quench as the saturation point moves down resulting in more steam generation between the quench front and the saturation point. Thus, for a time the steam flow rate would increase. However, the quench front velocity would eventually slow down and rod-stored energy would be removed at a slower rate, reducing the steam flow rate. When the transient resulted in an increasing flooding rate, the voids below the quench front would collapse resulting in less steam generation.

In addition, subcooled droplets could be entrained resulting in less steam generation above the quench front. Eventually, however, the quench front velocity would increase, resulting in an increased heat release rate, and the steam flow rate would increase. Thus, during a transient in flooding rate, the steam generation rate first tends to drive the transient in the same direction and then opposes it. This model explains the oscillating behavior of the flooding rate in this and other gravity feed tests.

3.3.1.4 Entrainment

The liquid and vapor mass flow rates out of the test section were measured from the fill-up rate of the liquid separator tank and the pressure drop across the loop orifice. It was not possible to measure the instantaneous liquid flow rate leaving the test section because of the location and geometry of the collection tank. It was also noted previously that during a flooding rate transient the vapor flow rate generally decreased as the flooding rate increased, as shown in Figure 3-6. The bundle mass accumulation rate is also shown in Figure 3-6 and was determined from the bundle pressure drop measurements. It can be seen that the bundle mass accumulation rate generally follows the same trends as the flooding rate.

The mass effluent rate fraction was determined using two methods and the results are shown in Figure 3-7. The first method used was to determine the ratio of the instantaneous test section effluent mass flow rate (liquid plus vapor) to the instantaneous calculated test section inlet mass flow rate. The second method used was to determine the ratio of the bundle effluent mass flow rate, as determined from a mass balance on the bundle, to the instantaneous test section inlet mass flow rate. Within experimental accuracy the results of the two methods differ by the ratio of the mass accumulation rate in the upper plenum and upper plenum extension to the test section inlet mass flow rate. It can be seen in Figure 3-7 that results of both methods fluctuate considerably as the flooding rate fluctuates. The results of the two methods are also seen to be quite different from 50 to 150 seconds, which is the time period during which mass is accumulating in the upper plenum extension, as shown in Figure 3-5. It can be seen that the average mass effluent rate fraction, calculated from the test section

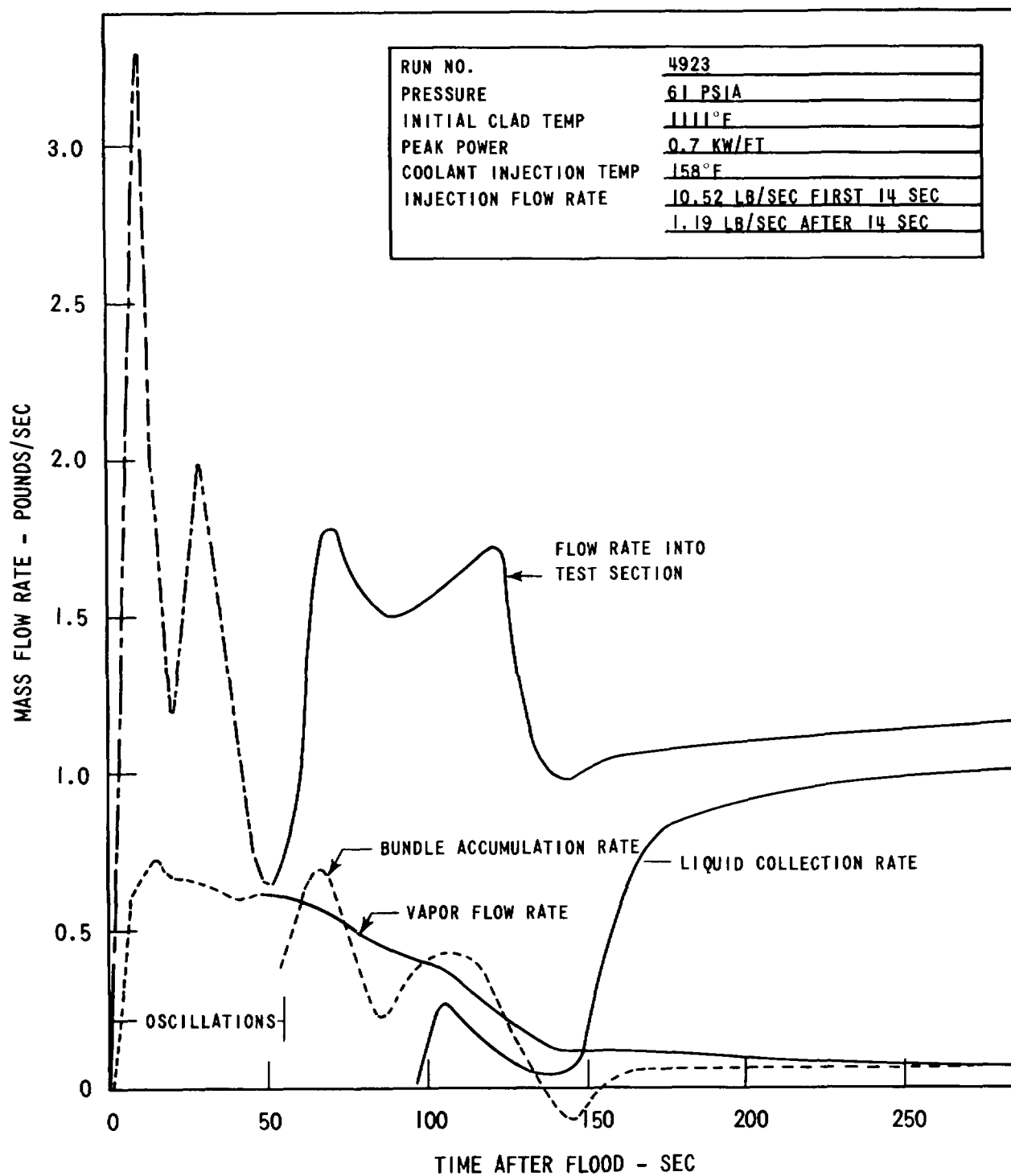


Figure 3-6. Mass Flow Rates - Run 4923

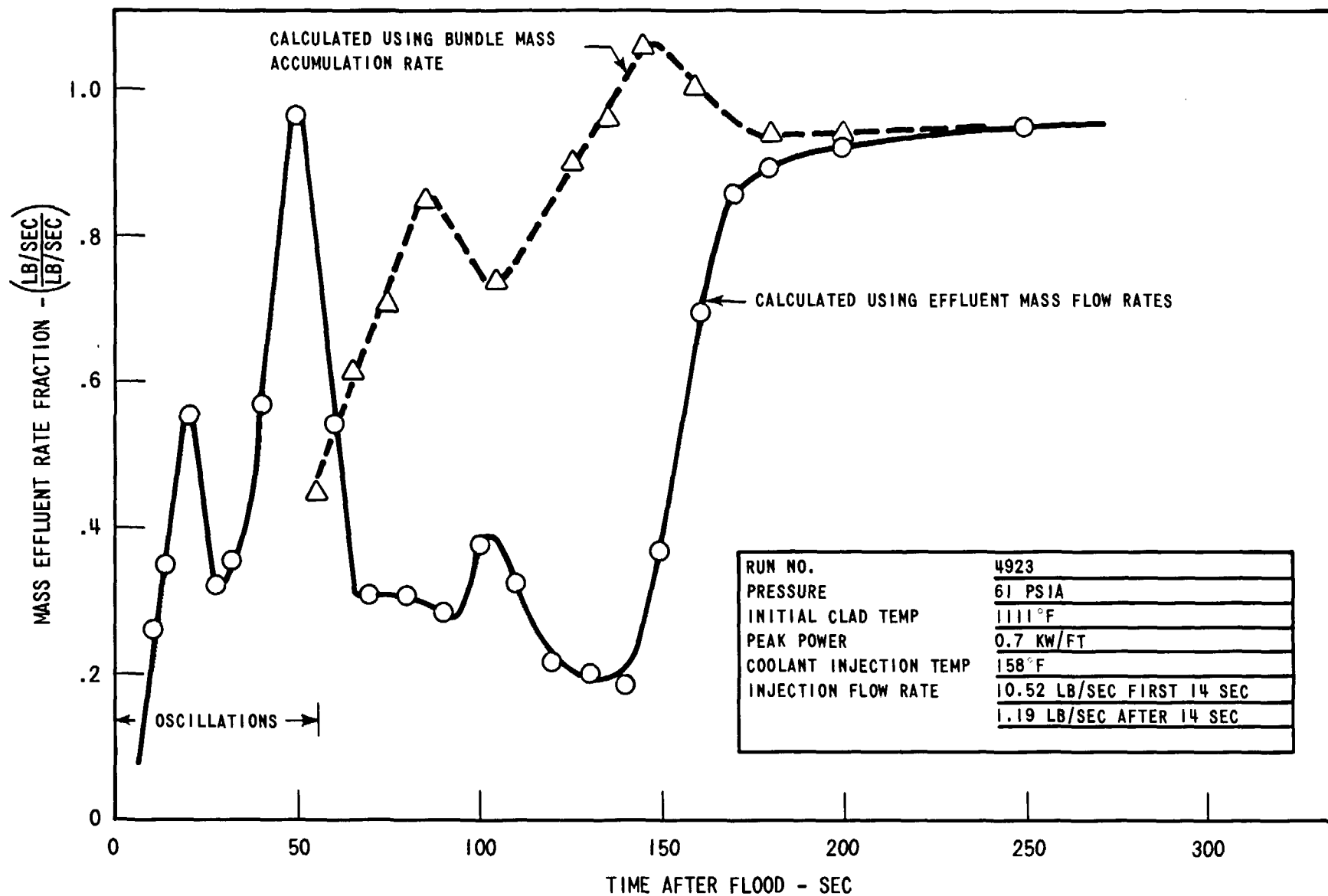


Figure 3-7. Mass Effluent Rate Fraction - Run 4923

effluent mass flow rate, up to the time of the midplane quench (~ 100 sec) is quite low ($\sim .5$) as compared to FLECHT results. This difference was primarily caused by the fact that no liquid effluent was collected until after the midplane quench. The mass effluent fraction calculated using the bundle effluent flow rate could not be determined accurately during the period of the oscillations.

Since the ratio of mass effluent flow rate to inlet flow rate is difficult to interpret when the inlet flow rate varies as much as shown in Figure 3-6, the mass effluent fraction is also presented as the ratio of total mass effluent to total test section mass input, i.e.,

$$F = \frac{\int_0^t \dot{m}_{\text{effluent}} dt}{\int_0^t \dot{m}_{\text{flood}} dt}$$

There are two ways to define this fraction, depending on whether one is interested in the flow out of the test section or out of the bundle, the difference being the mass stored in the upper plenum and upper plenum extension. The total mass effluent fraction is shown in Figure 3-8 calculated both ways. The fraction of the input flow which passed out of the bundle was calculated from a mass balance on the bundle, i.e.,

$$\left(\frac{m_{\text{out}}}{m_{\text{input}}}\right)_{\text{bundle}} = \frac{m_{\text{input}} - m_{\text{remaining in bundle}}}{m_{\text{input}}}$$

The fraction which passed through the loop was calculated from the sum of the mass collected in the separator tank and the integral of the vapor flow rate, i.e.,

$$\left(\frac{m_{\text{out}}}{m_{\text{input}}}\right)_{\text{loop}} = \frac{m_{\text{liquid collected}} + \int_0^t \dot{m}_{\text{vapor}} dt}{m_{\text{input}}}$$

3.3.1.5 Quench Front and Test Section Axial Pressure Drop Data

The heater rod temperature quench front envelope is shown in Figure 3-9. The midplane quenched at ~ 100 seconds after flood. The quench "fronts" moved toward the center of the bundle from the top and bottom. The lower

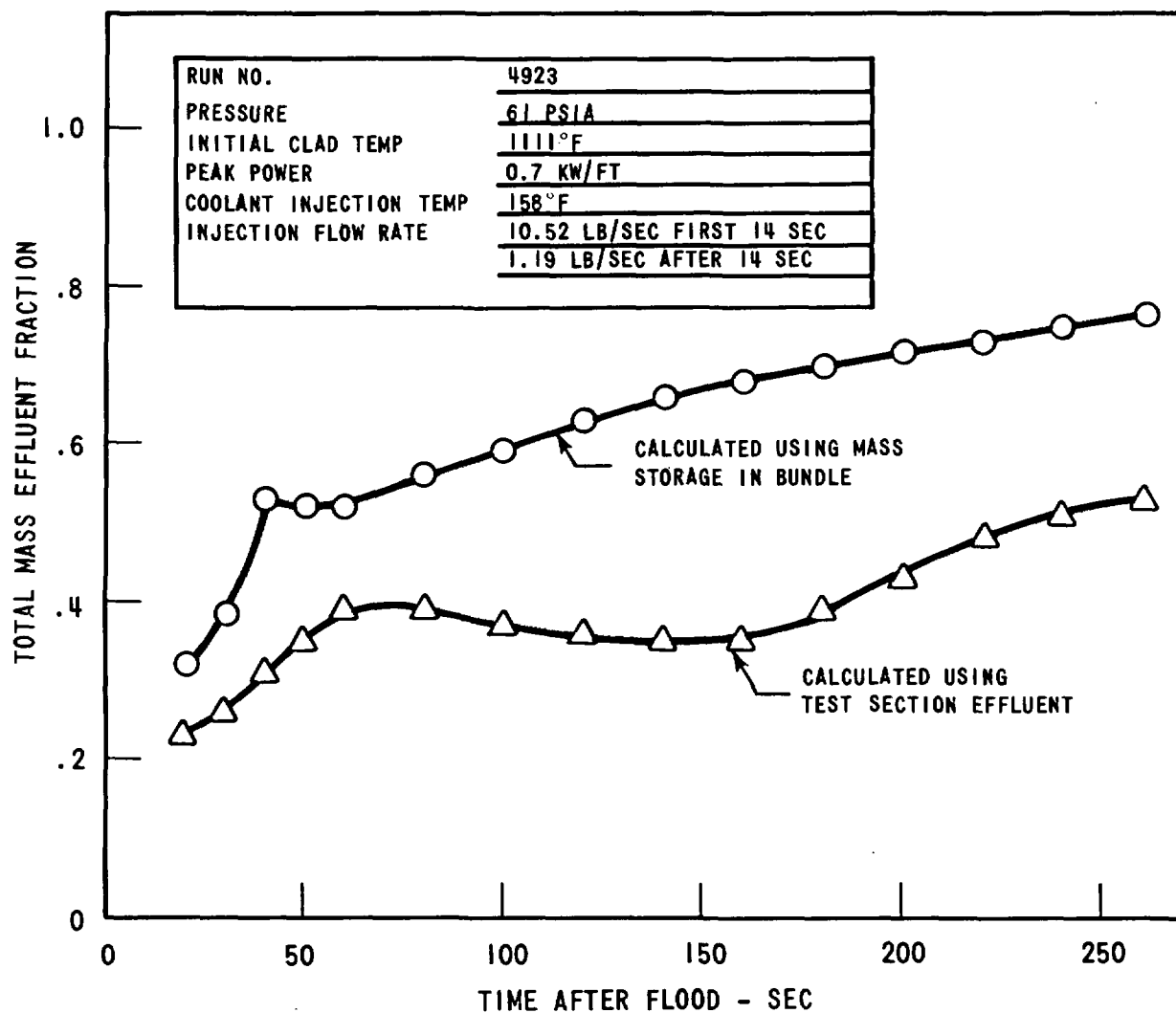


Figure 3-8. Total Mass Effluent Fraction - Run 4923

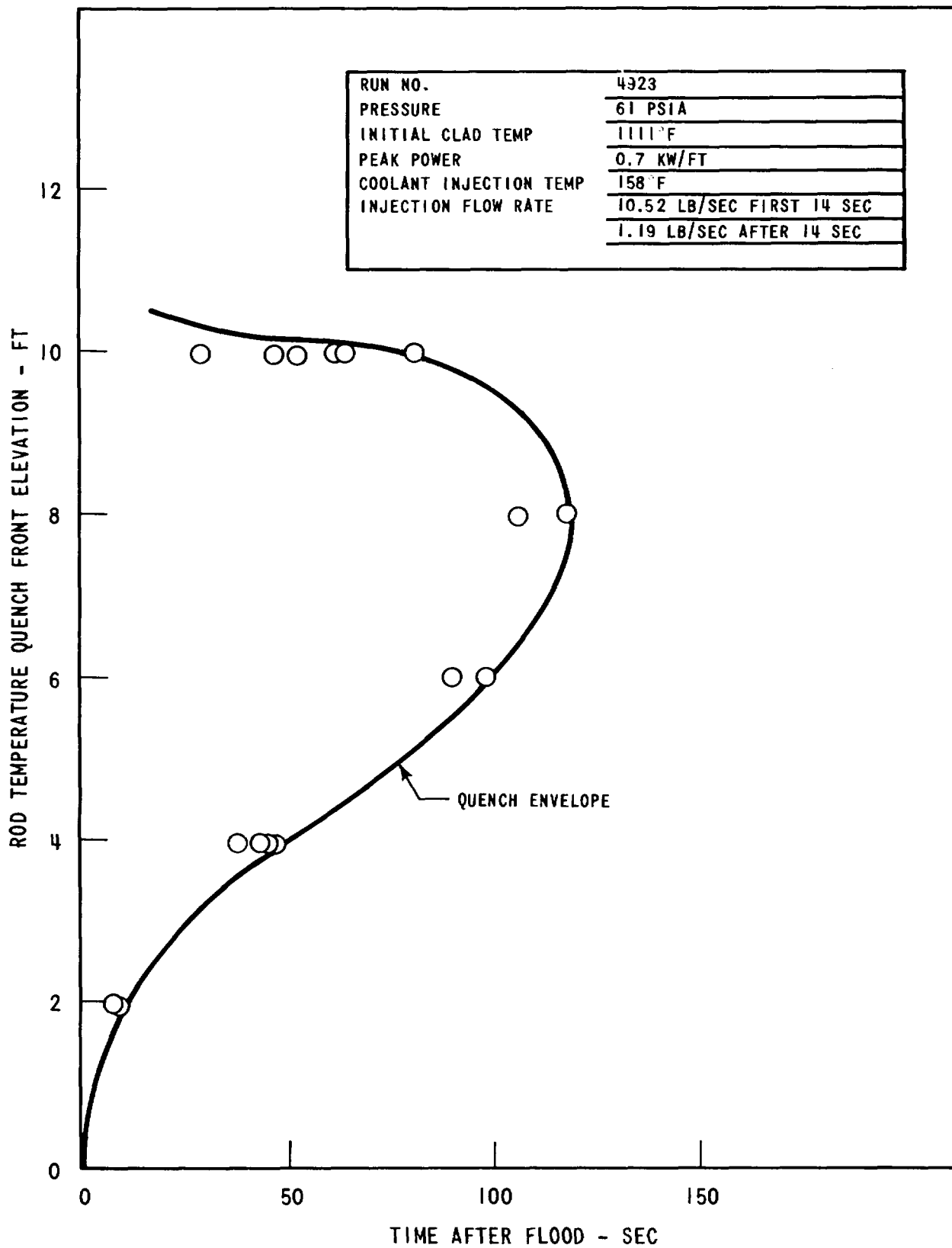


Figure 3-9. Rod Temperature Quench Front Envelope - Run 4923

quench front moved up rapidly, quenching the 2-foot elevation by 7 seconds after flood, when it slowed to $\sim .4$ in./sec. The upper quench "front" moved down to the 10 ft elevation very quickly, but the scatter in 10-ft quench times indicates quenching over a 50-second interval. The upper elevations of the bundle are cooled by the steam flow and entrained droplets generated at the lower elevation of the bundle. It is also possible that the upper elevations of the rods are quenched by a falling film of water, making the term sputtering front perhaps more descriptive than quench front at the upper elevations of the bundle.

The test section axial pressure drop data are shown in Figure 3-10. The average void fraction between two axial pressure taps was determined from the pressure drop between those two points as shown in Figure 3-11. The quench front elevation is shown on the same plot and one can get an idea of the void fraction at the quench elevation. After the oscillations ended the quench front below 6 ft nearly coincided with the .25 void fraction curve. The void fraction at higher elevations at the time of quench increased with elevation as shown in Figure 3-11. It can also be seen that the zero void fraction elevation did not advance beyond the midplane of the bundle even after the bundle had completely quenched. This is to be expected because the decay heat being removed by the subcooled inlet water raises the temperature of the coolant as it proceeds up the bundle. The flooding rate, inlet subcooling, and decay heat are sufficient to cause boiling to occur near the midplane.

3.3.1.6 Rod Temperature and Heat Transfer Coefficient Behavior

The clad temperature and heat transfer coefficients for the 2, 4, 6, 8 and 10 ft elevations of typical high-power heater rods are shown in Figures 3-12 and 3-13. The FLECHT correlation described in Reference 1 was used to predict the midplane heat transfer coefficient using the technique described in Section 3.1. As can be seen in Figure 3-14 the predicted heat transfer coefficient is generally lower than the measured data.

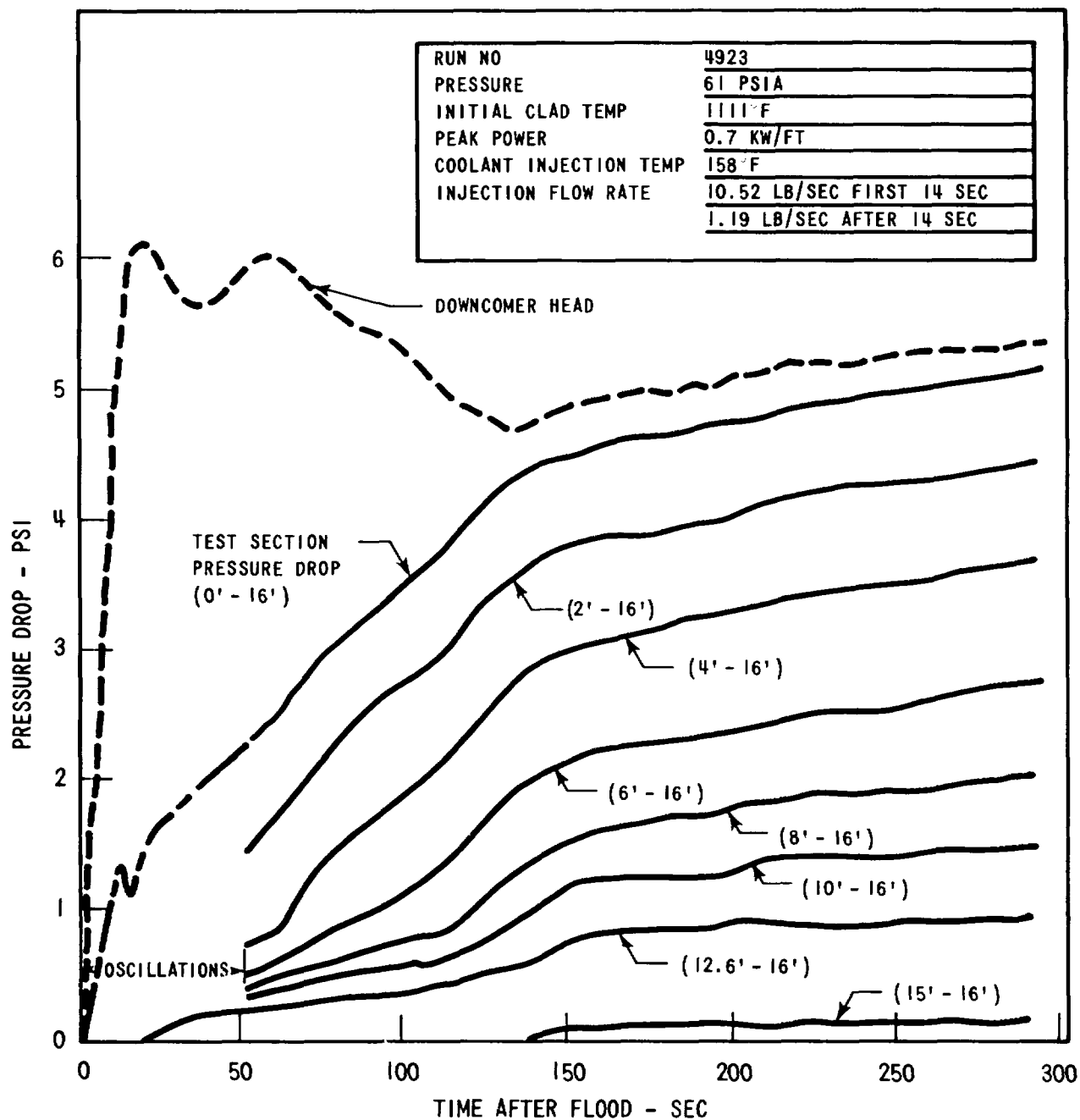


Figure 3-10. Downcomer and Test Section Pressure Drop Data - Run 4923

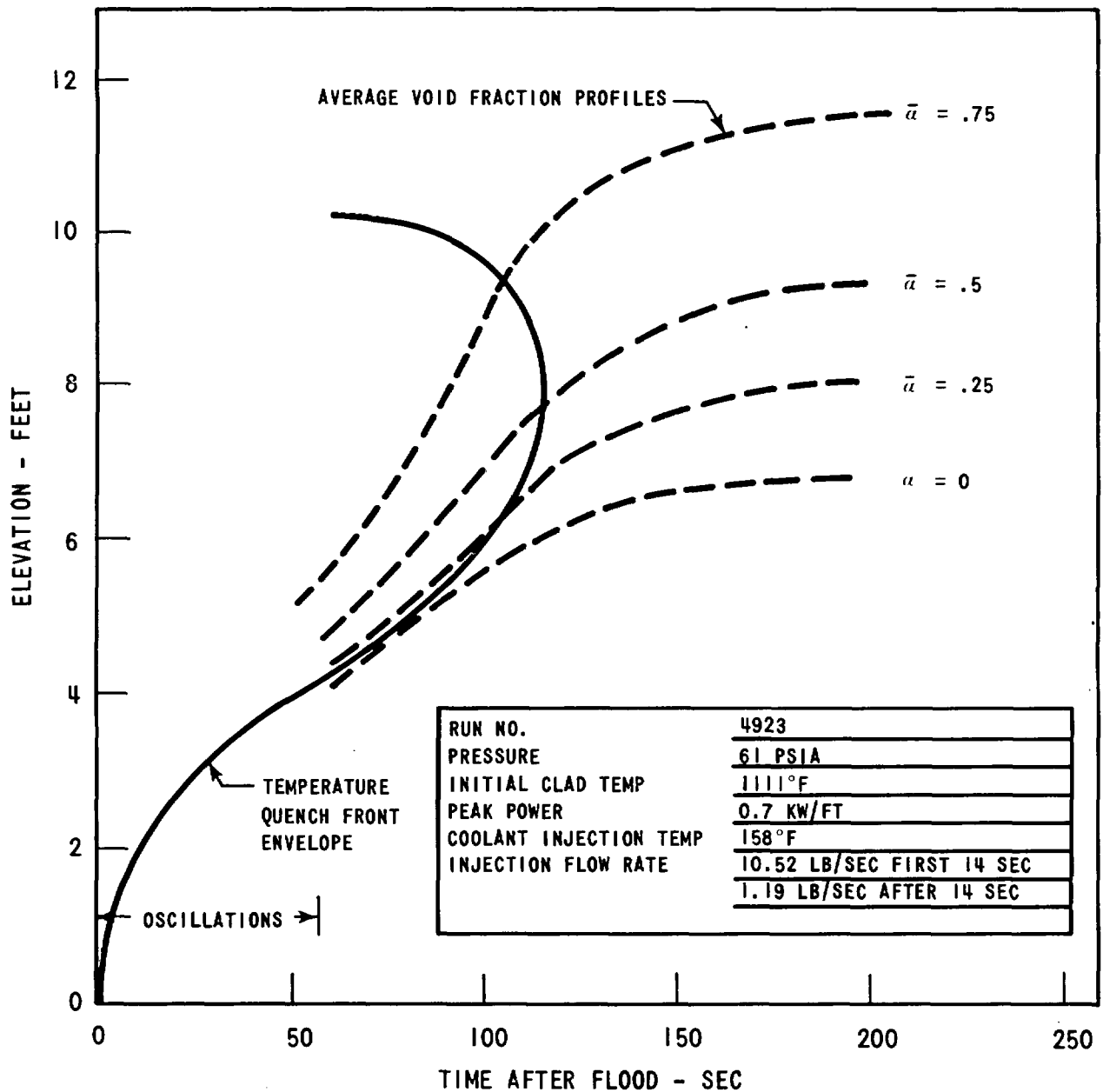


Figure 3-11. Quench Front Envelope and Void Fraction Profiles - Run 4923

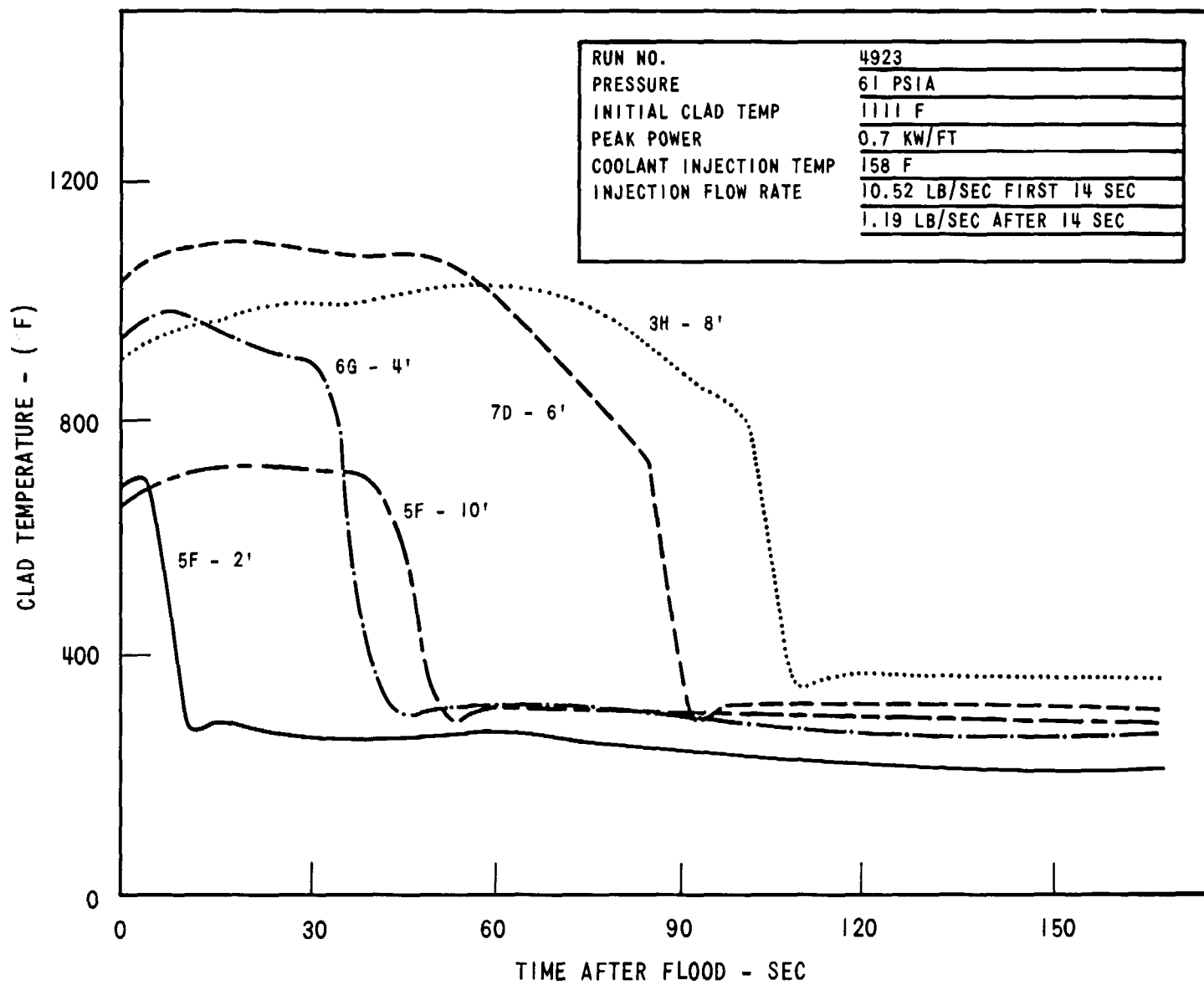


Figure 3-12. Clad Temperature History - Run 4923

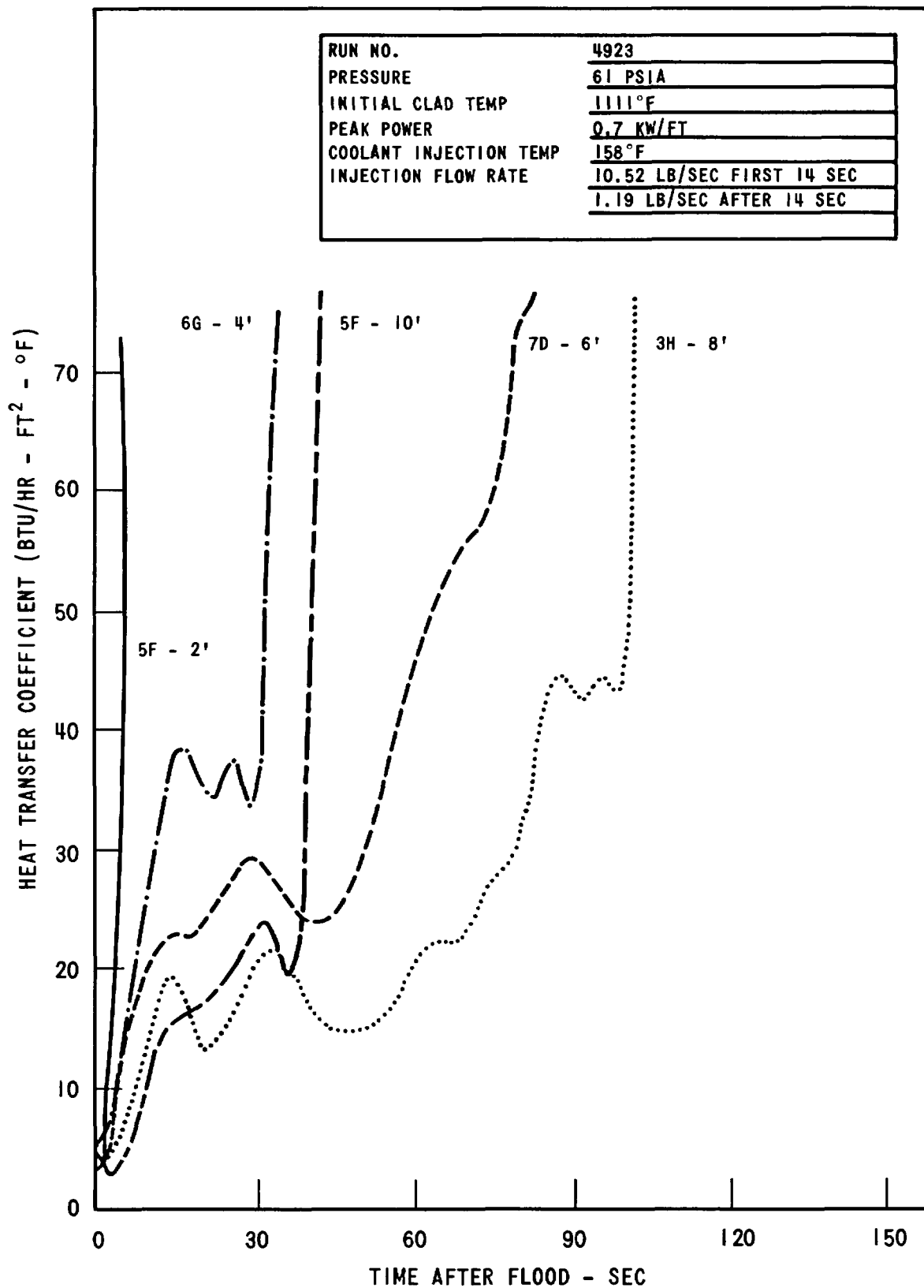


Figure 3-13. Rod Heat Transfer Coefficients - Run 4923

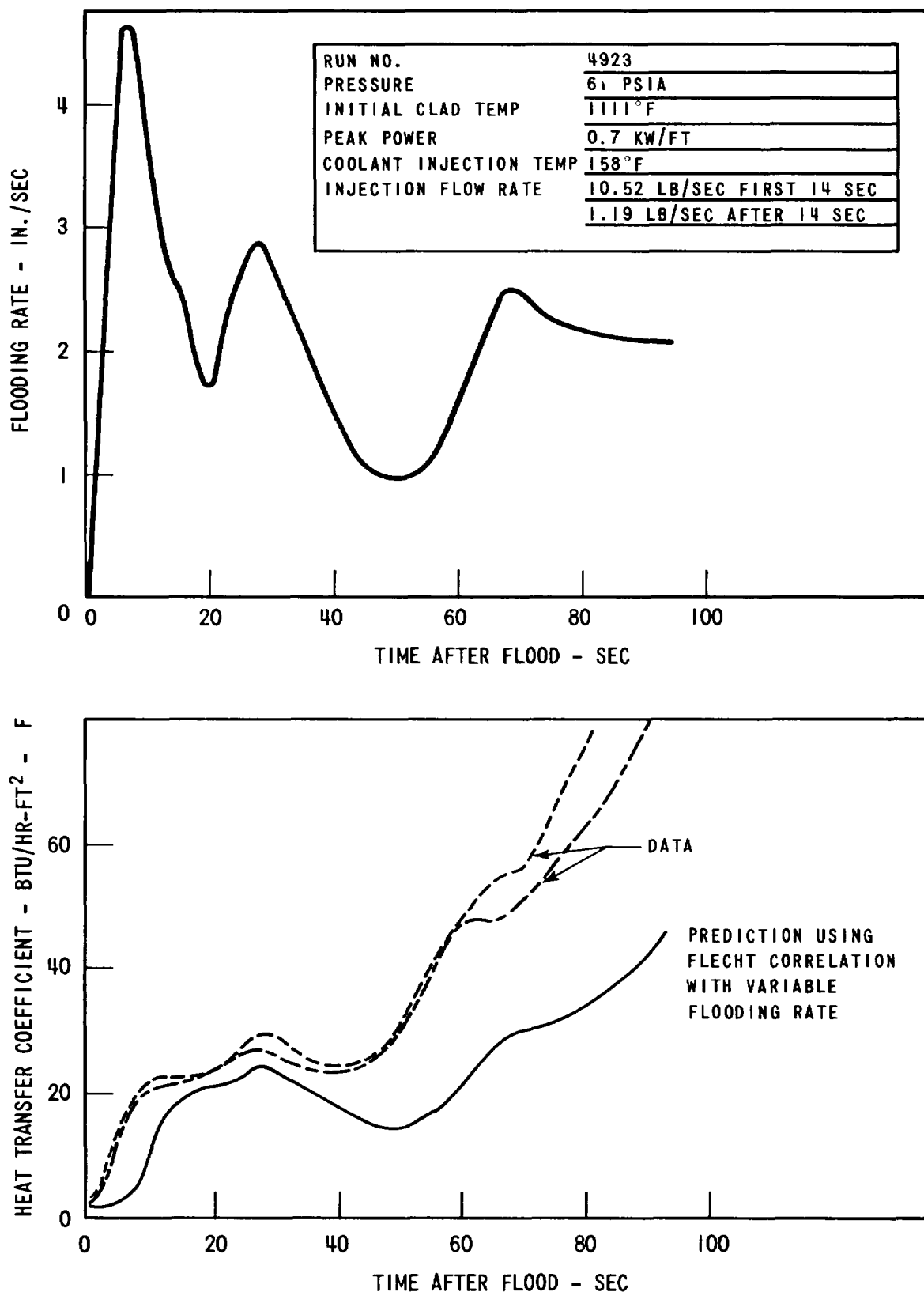


Figure 3-14. Comparison of Predicted and Measured Midplane Heat Transfer Coefficients - Run 4923

3.3.1.7 Fluid Temperatures at Various Points in the System

The test section inlet and outlet fluid temperature measurements are shown in Figure 3-15. It can be seen that the coolant supply temperature was relatively constant at 158°F. The fluid in the lower plenum flowed in and out of the bundle during the oscillations, which account for the high measured lower plenum fluid temperature during the first 60 seconds. As soon as the oscillations stopped, the hot water was displaced by the colder water in the downcomer, and the lower plenum fluid temperature dropped steadily to the temperature of the injection water.

The fluid temperature at the hot leg inlet is also shown in Figure 3-15. The initially high fluid temperature measurement was due to the discharge of the superheated steam which filled the bundle prior to the start of flood. Ten seconds after the start of flood the exhaust fluid temperature started dropping. After 50 seconds the exhaust fluid temperature was nearly equal to the local saturation temperature indicated as a broken line in Figure 3-15.

The fluid temperature upstream of the loop orifice is shown in Figure 3-16. The piping between the liquid separator tank and the loop orifice was heated to a high temperature before the test. In addition, the heaters were left on during the test so that any unseparated droplets would be vaporized before flowing through the orifice and a meaningful mass flow rate could be obtained from the pressure drop across the orifice. It can be seen in Figure 3-16 that the measured fluid temperature upstream of the orifice did indicate superheated steam flowing through the orifice.

3.3.1.8 Housing Behavior

The housing temperature data are shown in Figure 3-17. The initial housing temperature profile was chosen assuming that the midplane would quench at ~ 120 sec. Since the midplane quenched at 100 sec, the initial average housing temperature was ~ 20°F too high using the criterion described in Section 2.4. As can be seen in Figure 3-17, the lower elevations of the housing cooled very quickly during the oscillations. This was a result of the housing temperature being below the wetting temperature. During the oscillations the water level rose quite high into the test section, resulting

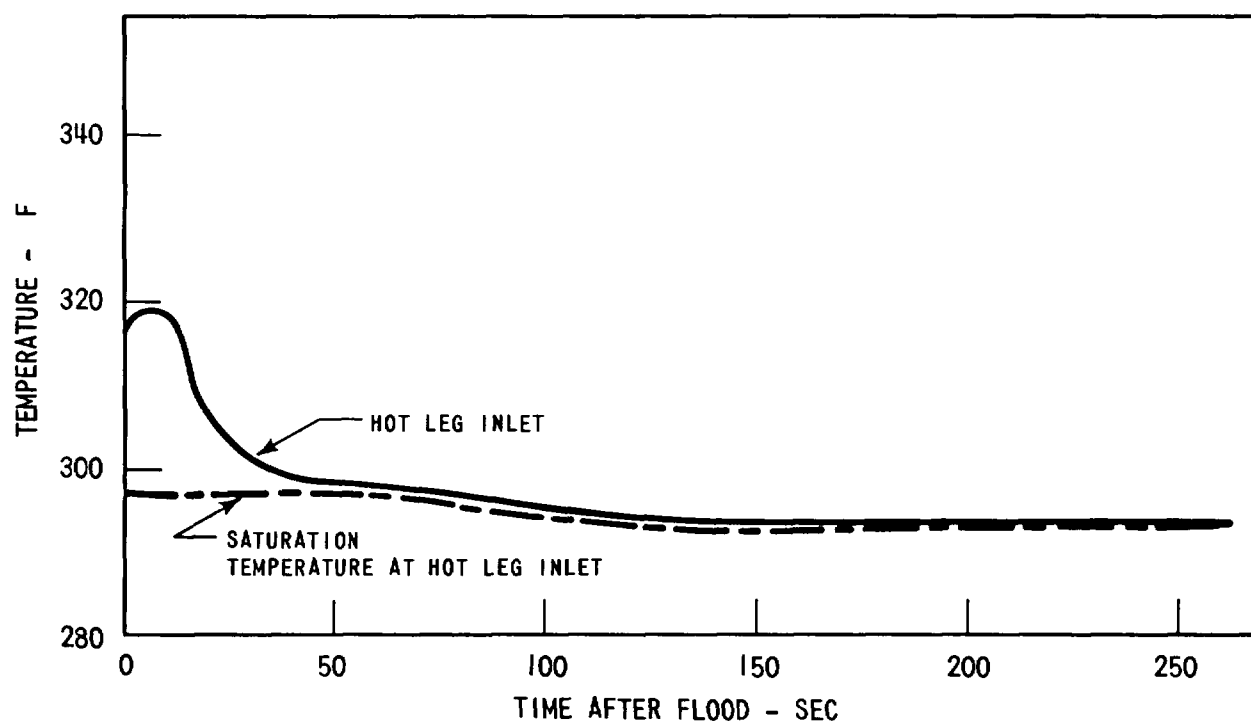
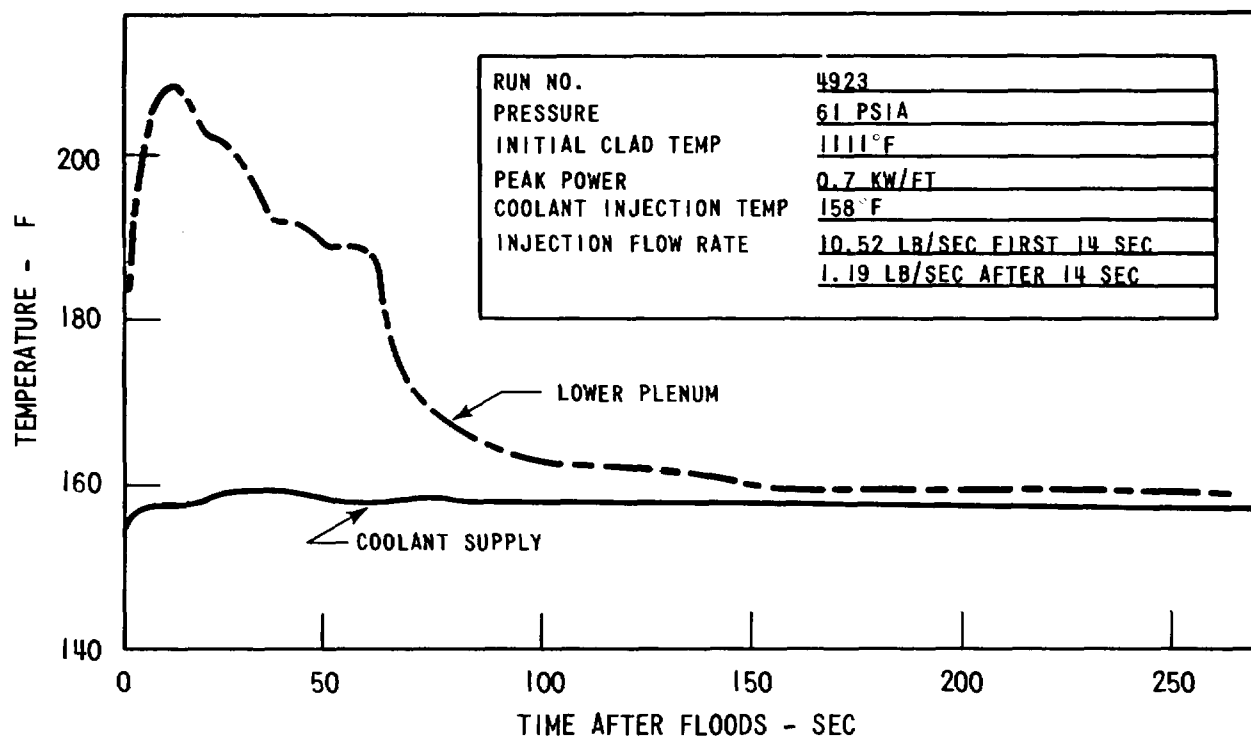


Figure 3-15. Test Section Inlet and Outlet Fluid Temperature - Run 4923

3-31

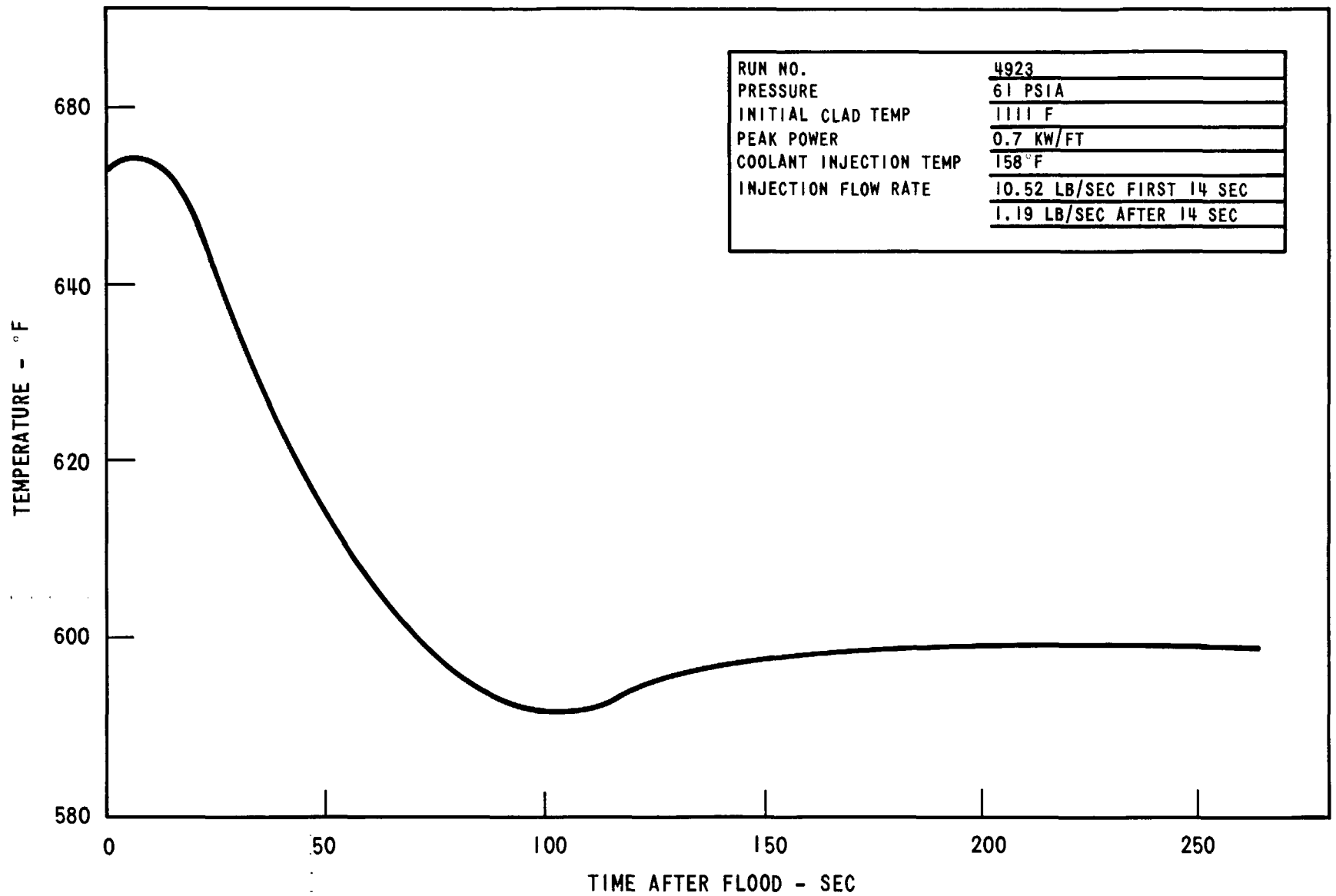


Figure 3-16. Fluid Temperature Upstream of Loop Orifice - Run 4923

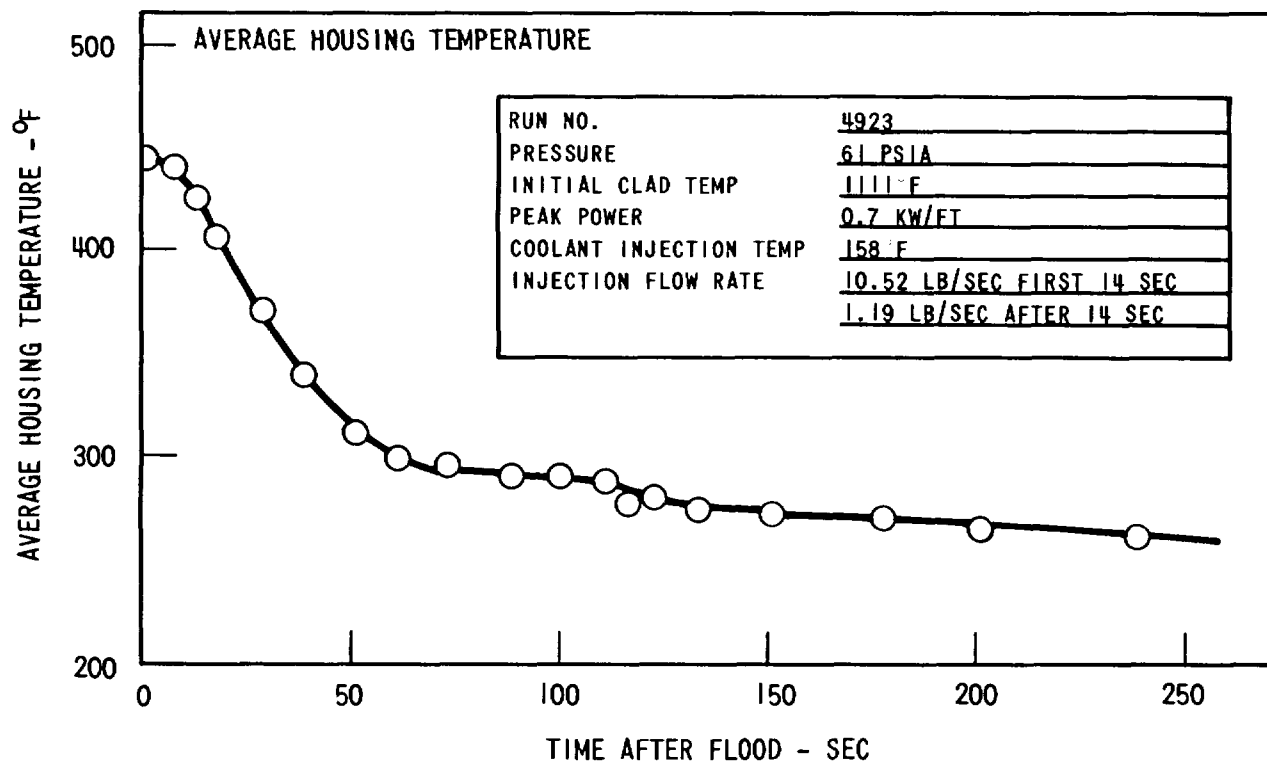
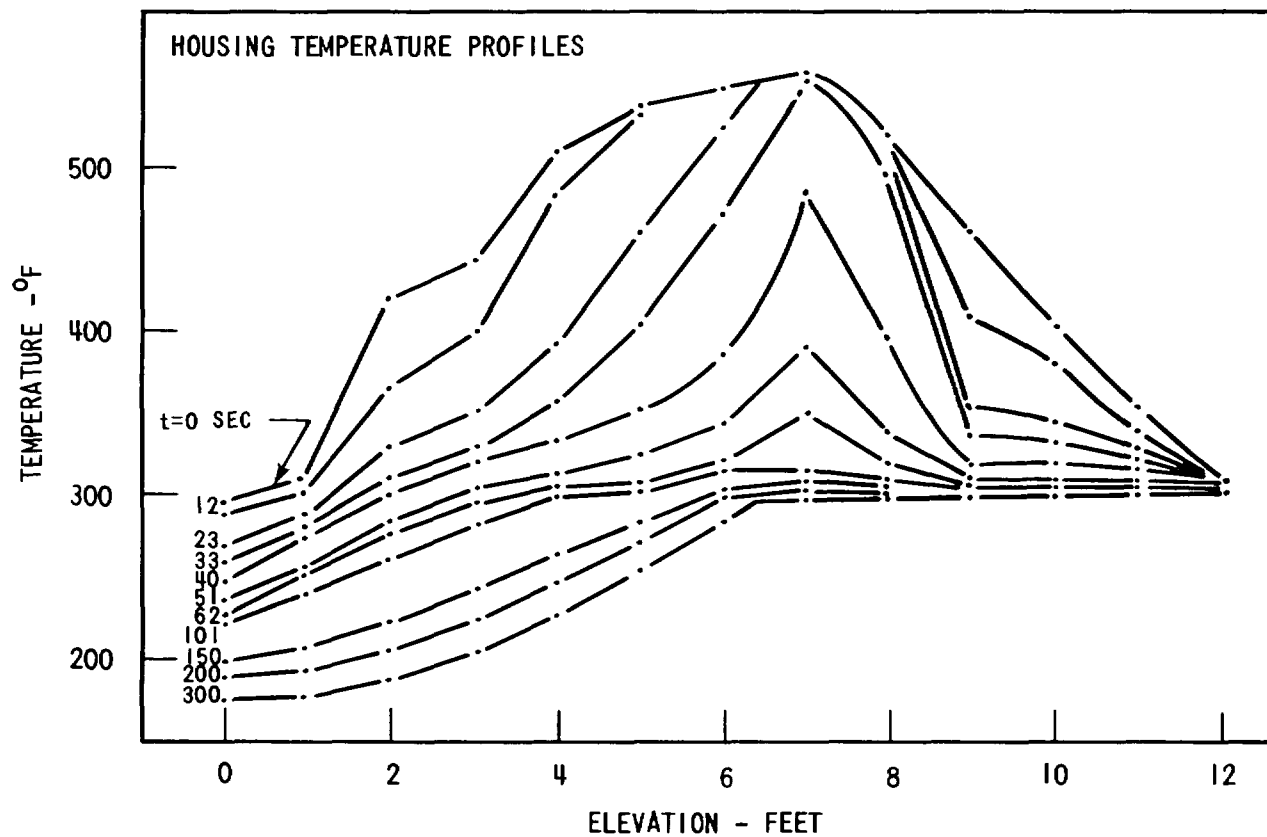


Figure 3-17. Housing Temperature Data - Run 4923

in very high heat transfer rates at the housing walls and subsequent rapid cooling of the housing. It can also be seen in Figure 3-17 that the lower 6 feet of the housing shows the effect of the subcooled inlet water. At ~ 300 seconds after flood the housing temperature is a few degrees above the temperature of the inlet water at the inlet and rises to the saturation temperature just above the midplane of the bundle.

3.3.1.9 Energy Balance

An overall energy balance was performed using the measured mass flow rates and mass storage, the energy inputs from the stored energy in the heater rods and housing walls, and the input electrical energy from the heater rods for the duration of the test (300 sec). The result of the overall energy balance was quite good, being off by only 2 percent, verifying the accuracy of the data.

The results of the energy balance are summarized as follows:

1. Stored Energy Released by Heater Rods

$$n \sum_i \rho_i C_i A_i \int_0^{12} (T_i - T_f)_r dz = 2.3 \times 10^4 \text{ Btu}$$

where n is the number of heater rods, $\rho_i C_i A_i$ is the product of the density, specific heat, and cross-sectional area of a portion of the heater rod and $(T_i - T_f)_r$ is the difference between the initial and final rod temperatures.

2. Stored Energy Released by the Housing

$$\rho_h C_h A_h \int_0^{12} (T_i - T_f)_h dz = 1.5 \times 10^4 \text{ Btu}$$

where $\rho_h C_h A_h$ is the product of the density, specific heat, and cross-sectional area of the housing and $(T_i - T_f)_h$ is the difference between the initial and final housing temperatures.

3. Energy Input from Decay Heat

$$\frac{n Q'_{\max}}{1.1 \times 1.66} \times L \times I(t) = 8.5 \times 10^4 \text{ Btu at 300 sec}$$

where n is the number of heater rods, Q'_{\max} is the initial peak heat flux, L is the heater rod length, $I(t)$ is the integral of the power decay curve, and 1.1×1.66 is the product of the radial and axial power factors.

4. Energy Input from Coolant

$$m_{\text{input}} \times h_{\text{coolant}} = 4.9 \times 10^4 \text{ Btu at 300 sec}$$

where m_{input} is the total mass put into the test section over the duration of the test and h_{coolant} is the enthalpy of the injected coolant.

5. Energy Carried Away by Steam

$$m_{\text{vapor}} \times h_g = 9.0 \times 10^4 \text{ Btu}$$

where m_{vapor} is the total mass of vapor discharged from the bundle and h_g is the enthalpy of saturated vapor.

6. Energy Carried Away by the Liquid

$$m_{\text{liquid collected}} \times h_f = 4.0 \times 10^4 \text{ Btu}$$

where $m_{\text{liquid collected}}$ is the mass of liquid collected in the separator tanks at the end of the test and h_f is the enthalpy of saturated liquid.

7. Stored Energy of Fluid Remaining in the Test Section

$$m_{\text{liquid stored}} \times h_f \approx 3.8 \times 10^4 \text{ Btu}$$

where $m_{\text{liquid stored}}$ is the water stored in the test section, upper

plenum, and steam probe tank at the end of the test and h_f is the enthalpy of saturated liquid.

8. Energy Balance

Total energy input	17.2×10^4 Btu
Total energy stored or carried away	16.8×10^4 Btu
Percent error	+2%

3.3.2 Data Analysis for Run 2919

The following conditions pertain to Run 2919:

Containment Pressure	20 psia
Initial Clad Temperature	912°F
Peak Power	0.7 kw/ft
Coolant Injection Temperature	153°F
Injection Flow Rate	10.1 lb/sec, first 14 sec 1.2 lb/sec, after 14 sec

Run 2919 was chosen for presentation in lieu of the nominal 20 psia run (2207) since two of the housing differential pressure transducers were not functioning properly during Run 2207. There was little difference between the two runs other than a 200°F lower initial clad temperature for Run 2919. The maximum clad temperatures reached during both runs were nearly the same. This is to be expected because the heat transfer coefficients were about the same and the required temperature difference to get the heat removal rate equal to the heat generation rate is about the same.

The calculated loop resistance coefficient based on saturated steam flowing in the hot leg was ~ 33 which is typical of a PWR during reflood, assuming the pump rotor was locked.

3.3.2.1 General Observations

Visicorder traces of the bundle pressure drop indicated that the bundle filled to ~ 0.9 ft. before the bundle level dropped slightly, indicating that steam generation had started. Large oscillations in the core and downcomer liquid levels started shortly afterward with a period of ~ 3 seconds. The water in the downcomer started overflowing during the oscillations after ~ 40 seconds. Water in the downcomer continued to overflow for the first 320 seconds although the overflow rate decreased after ~ 230 seconds. After 320 seconds the downcomer water level decreased since the flooding rate was generally greater than the injection rate into the downcomer. This was caused by a reduction in steam generation rate because the test section housing had quenched.

3.3.2.2 Mass Balance

The result of a mass balance on the test section is shown in Figure 3-18, which consists of 5 curves. The excellent agreement between the calculated mass put into the test section and the sum of the masses of fluid either stored in or discharged from the system confirms the accuracy of the measurements. The mass put into the system was calculated from a mass balance on the fluid in the downcomer and downcomer overflow tanks. The mass discharged from the system was obtained from the integral of the measured vapor mass flow rate and the measured accumulation of water in the separator tank. The mass stored in the bundle was determined from the housing axial pressure drop measurement. Since there were no test section pressure drops measured above the 8 ft. elevation, the mass stored in the upper plenum and upper plenum extension was determined after the end of the test when the water, which had been held up by the steam flow, drained back into the bundle. This amount of water (~ 34 lb) was accounted for at the end of the test. Similarly, the mass stored between the plate filling the upper plenum annulus (11 lb) and that extracted and stored in the steam probe tanks (~ 7 lb) were accounted for at the end of the test. Figure 3-18 also shows that no water was collected in the separator tank until ~ 250 seconds after flood.

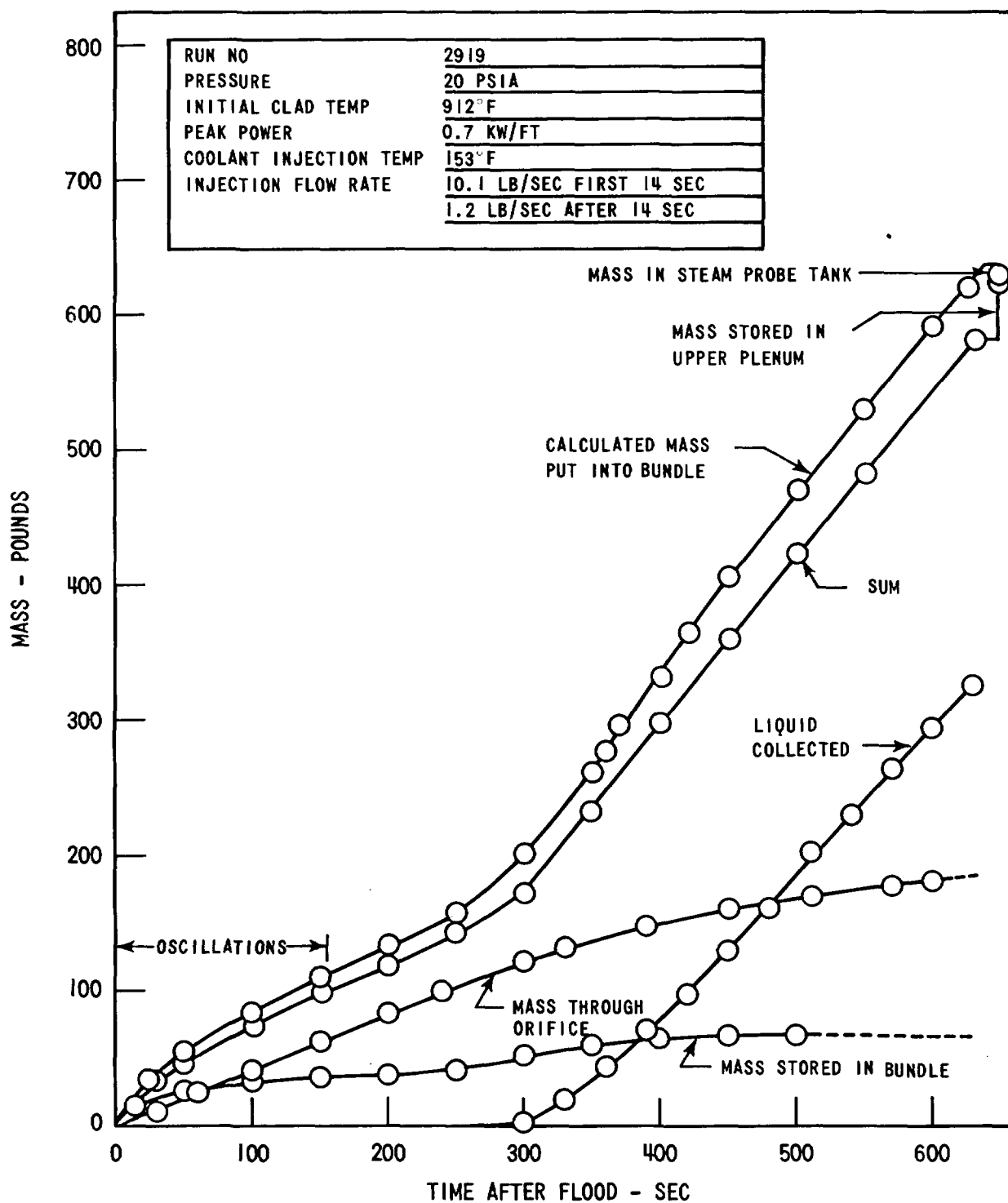


Figure 3-18. Mass Balance - Run 2919

3.3.2.3 Flooding Rate

The flooding rate was determined from a mass balance on the fluid in the downcomer and downcomer overflow tank as described in Section 3.2. Thus, when the storage of water in the downcomer and downcomer overflow tank increases, decreases, or remains unchanged, the flooding rate is less than, greater than, or equal to the injection rate into the downcomer, respectively. The mass stored in the downcomer was determined from the downcomer pressure drop measurement shown in Figure 3-19, which is a reduced tracing of a portion of the pen recorder data. During the oscillations, which had a period of ~ 3 seconds and lasted until ~ 155 seconds after flood, the mean downcomer head, indicated by a dashed line in Figure 3-19, was used to determine the average flooding rate. When water was overflowing the downcomer, the overflow rate was determined from the accumulation rate of water in the overflow tank shown in Figure 3-20. The calculated average flooding rate is shown in Figure 3-21. The flooding rate increased to almost 3 in./sec during the period of the high injection rate, after which it decreased to ~ 0.7 in./sec. The flooding rate increased again at ~ 220 seconds to ~ 2 in./sec and then began fluctuating between 2.7 in./sec and 1.7 in./sec. To understand the flooding rate behavior, refer to the pressure drop data shown in Figure 3-22. If the bundle and loop pressure drops are subtracted from the downcomer pressure drop, the result is a pressure drop equal to the sum of the pressure drop across the upper plenum extension and the pressure drop from the top of the downcomer to the containment tank. As can be seen in Figure 3-22, the resulting pressure drop is approximately 1.4 psi initially, but after 230 sec reduced to ~ 0.65 psi and remained relatively constant for the remainder of the test. A possible cause of the large initial pressure drop is the condensation of steam in the downcomer overflow tank which is vented to the containment tank, as shown in Figure 2-1, by a 1 inch pipe. When the water in the downcomer overflowed into the overflow tank, a large surface area of subcooled water was exposed to the steam in the tank. The steam apparently condensed, causing a local decrease in pressure and a flow of steam from the containment tank to the overflow tank. The flow resistance in the small vent pipe was sufficient to result in the large pressure drop shown in Figure 3-22. As shown in Figure 3-20, the overflow rate decreased

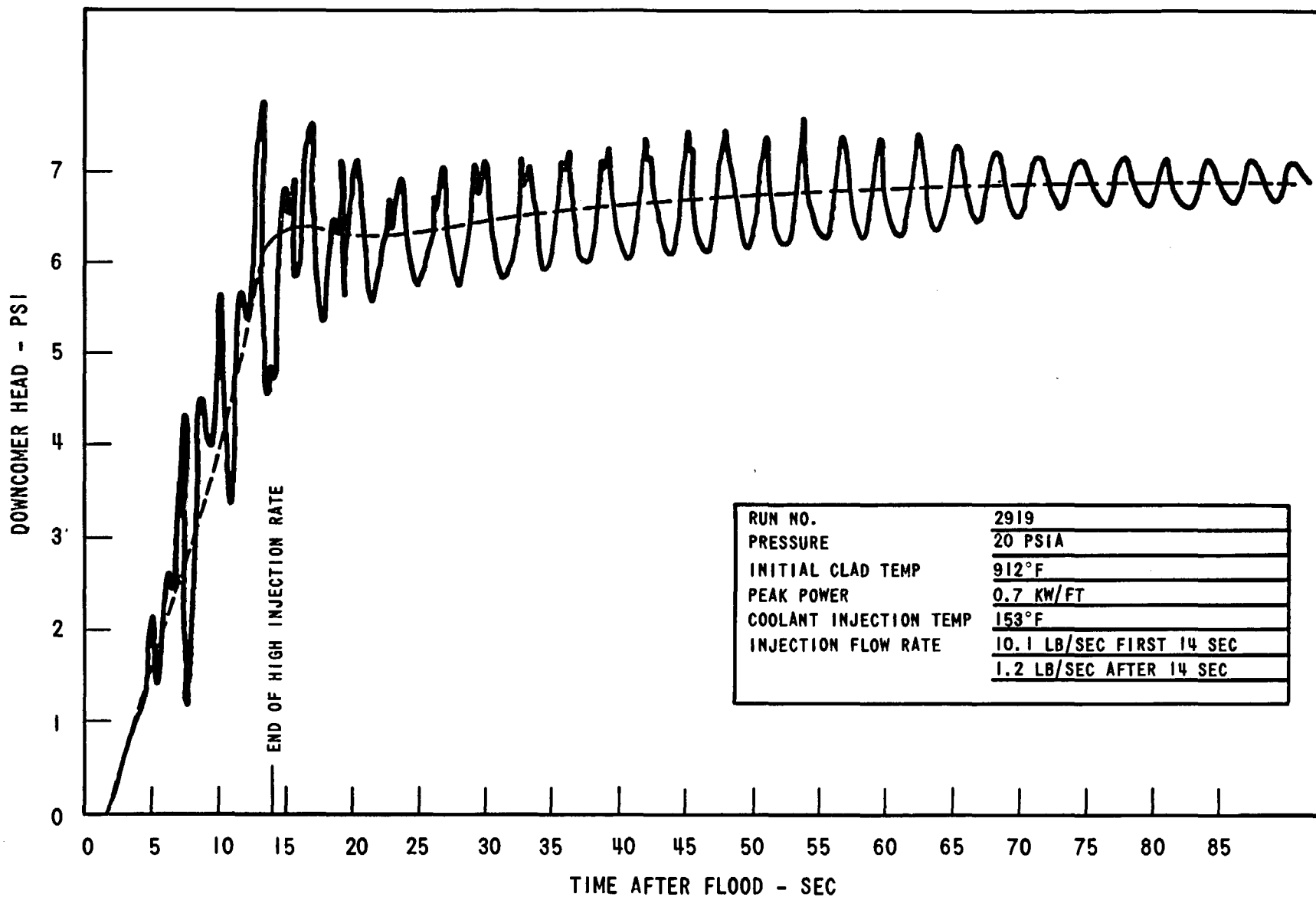


Figure 3-19. Downcomer Head vs. Time - Run 2919

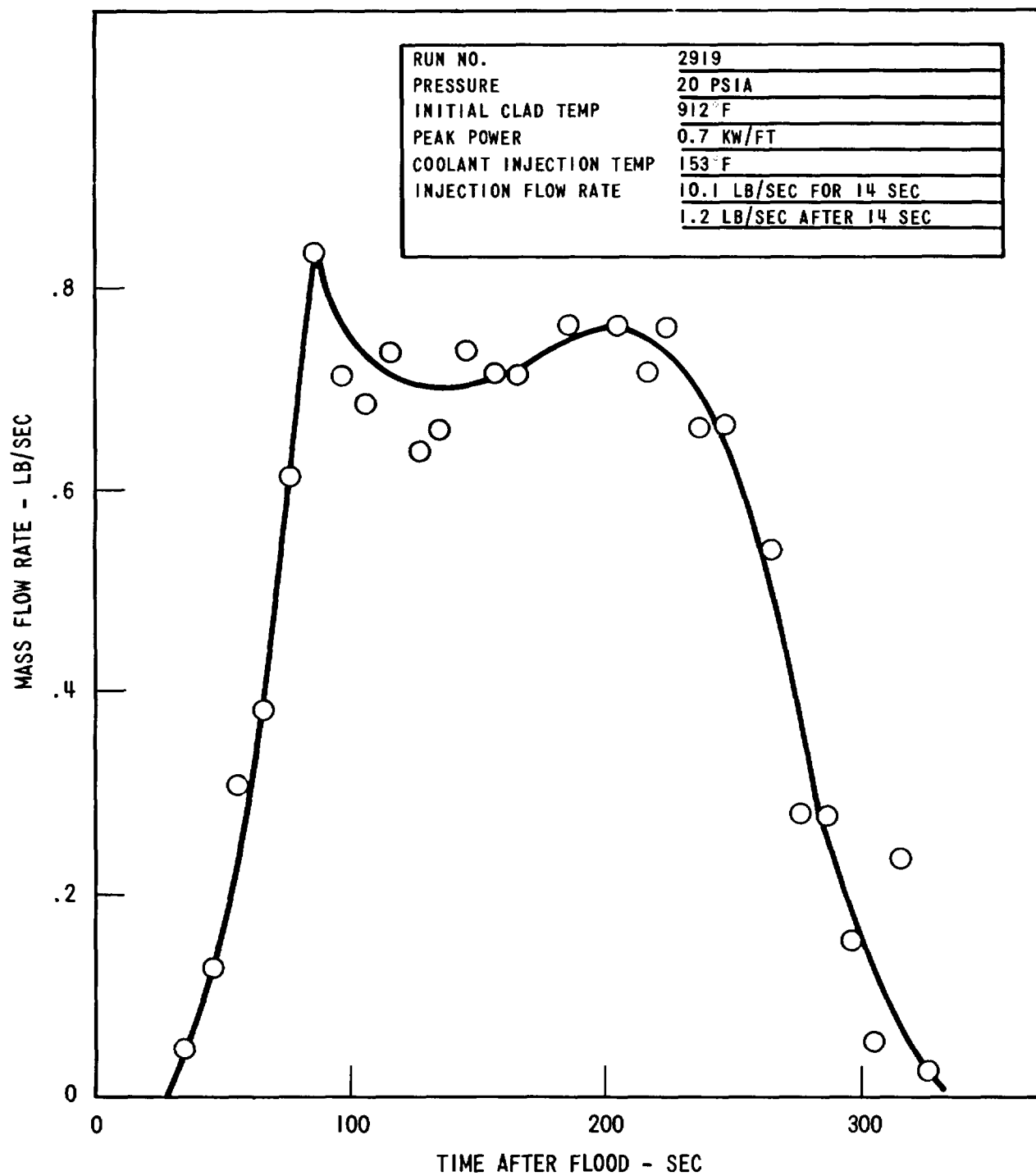


Figure 3-20 Downcomer Fluid Overflow Rate - Run 2919

3-41

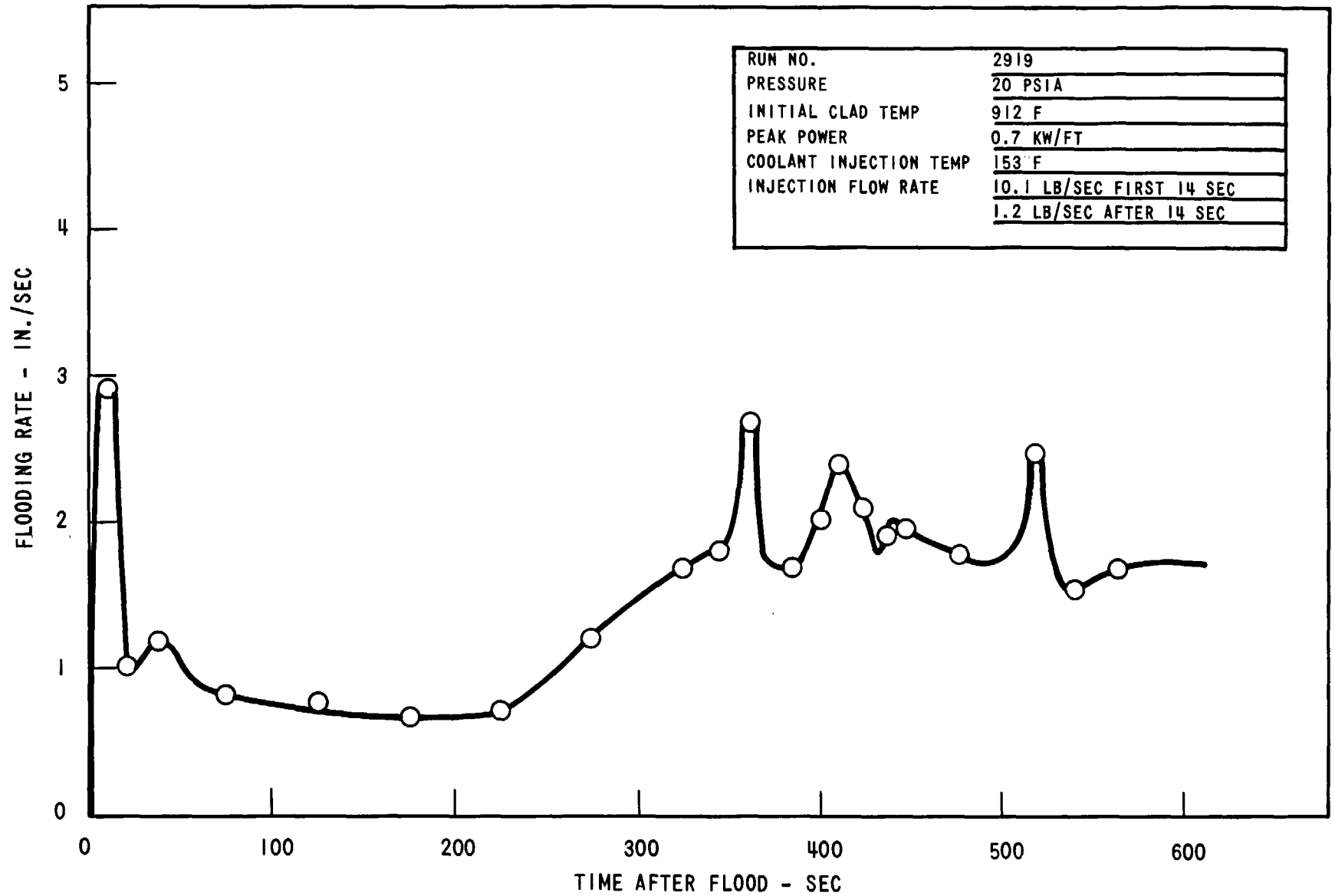


Figure 3-21. Flooding Rate vs. Time - Run 2919

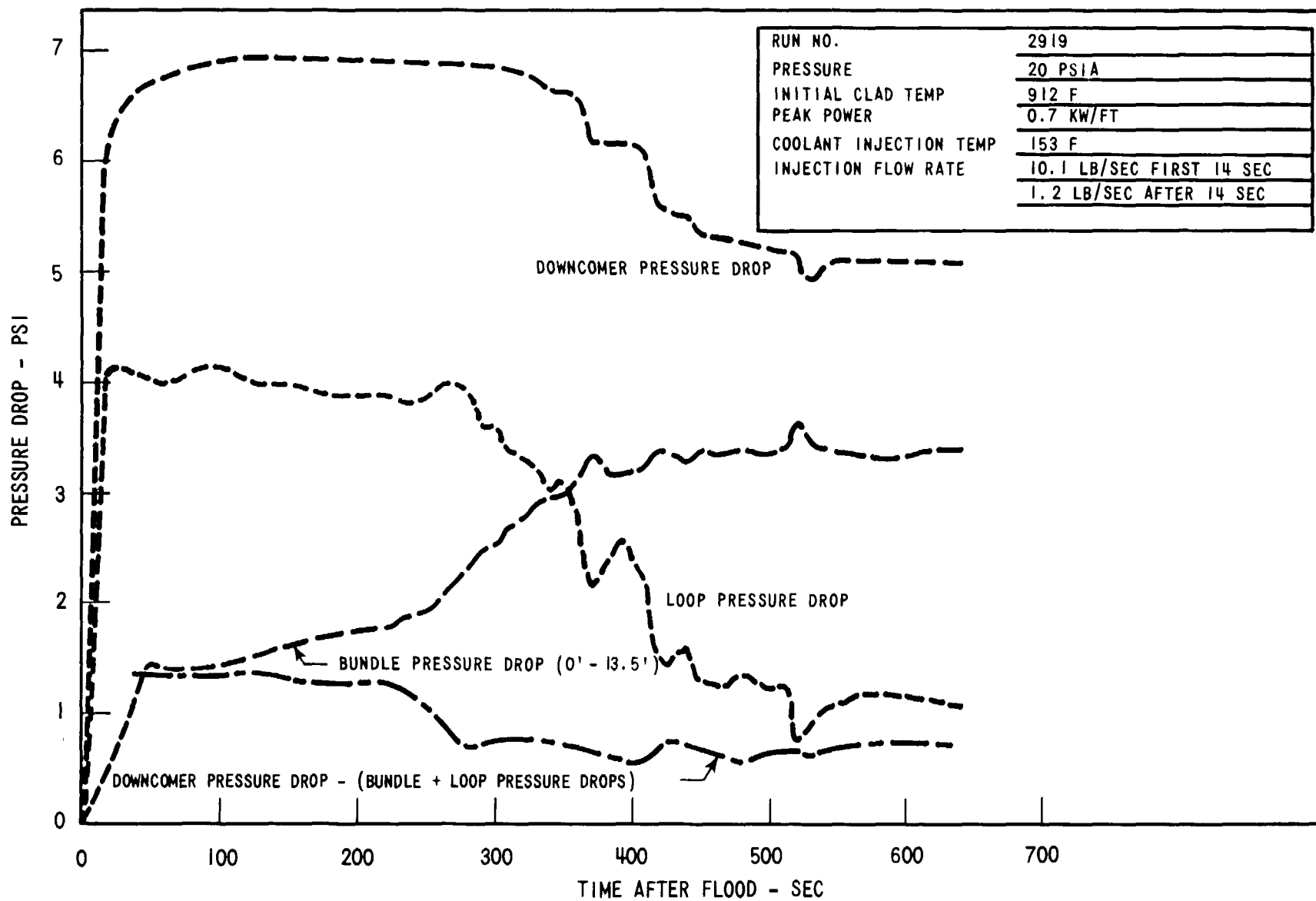


Figure 3-22. Pressure Drop Data Run 2919

after ~ 230 seconds, which was the same time that the condensation rate and the pressure drop between the downcomer and containment tank decreased. Since the pressure drop between the bottom of the downcomer and the containment tank increased, the flooding rate increased rapidly as shown in Figure 3-21. This phenomenon is certainly not typical of a PWR since the unbroken loops in a PWR discharge through the downcomer to the containment, resulting in a small positive pressure drop from the downcomer to the containment. Since the driving force during reflood is the pressure drop from the bottom of the downcomer to the containment, the 1.4 psi pressure drop from the containment to the top of the downcomer caused by the condensation resulted in a 20 percent decrease in driving head. The reduction in driving head certainly reduced the flooding rate and slowed the rise of the quench front. It is estimated that the flooding rate would have been ~ 15 percent higher if the condensation had not occurred.

The pressure drop discussed above decreased to ~ 0.65 psi after 230 sec and remained relatively constant throughout the remainder of the run. This pressure drop was caused by the pressure drop across the upper plenum extension and is consistent with results obtained after additional differential pressure transducers were installed on the upper plenum extension. The pressure difference at the end of the run corresponds to ~ 33 pounds of water being stored in the upper plenum extension. This is nearly the same amount which drained back into the bundle after the power was turned off and indicates that very little water collected in the upper plenum during the run except for the 11 pounds of water which filled the spaces between the filler plate in the upper plenum annulus. This is consistent with results discussed in Section 3.3.1.

As shown in Figure 3-21, the flooding rate fluctuated between 1.7 in./sec and 2.7 in./sec from 350 seconds to the end of the test. The fluctuations can be explained by referring to the pressure drop data shown in Figures 3-22 and 3-23. At 370 seconds after flood the temperature quench front is estimated to be near the 7 ft elevation. An energy balance on the lower part of the bundle indicates that at this time the inlet water reaches the saturation temperature approximately 2 feet below the quench front. Thus, steam was being generated from the 5 foot elevation to the top of the bundle. A

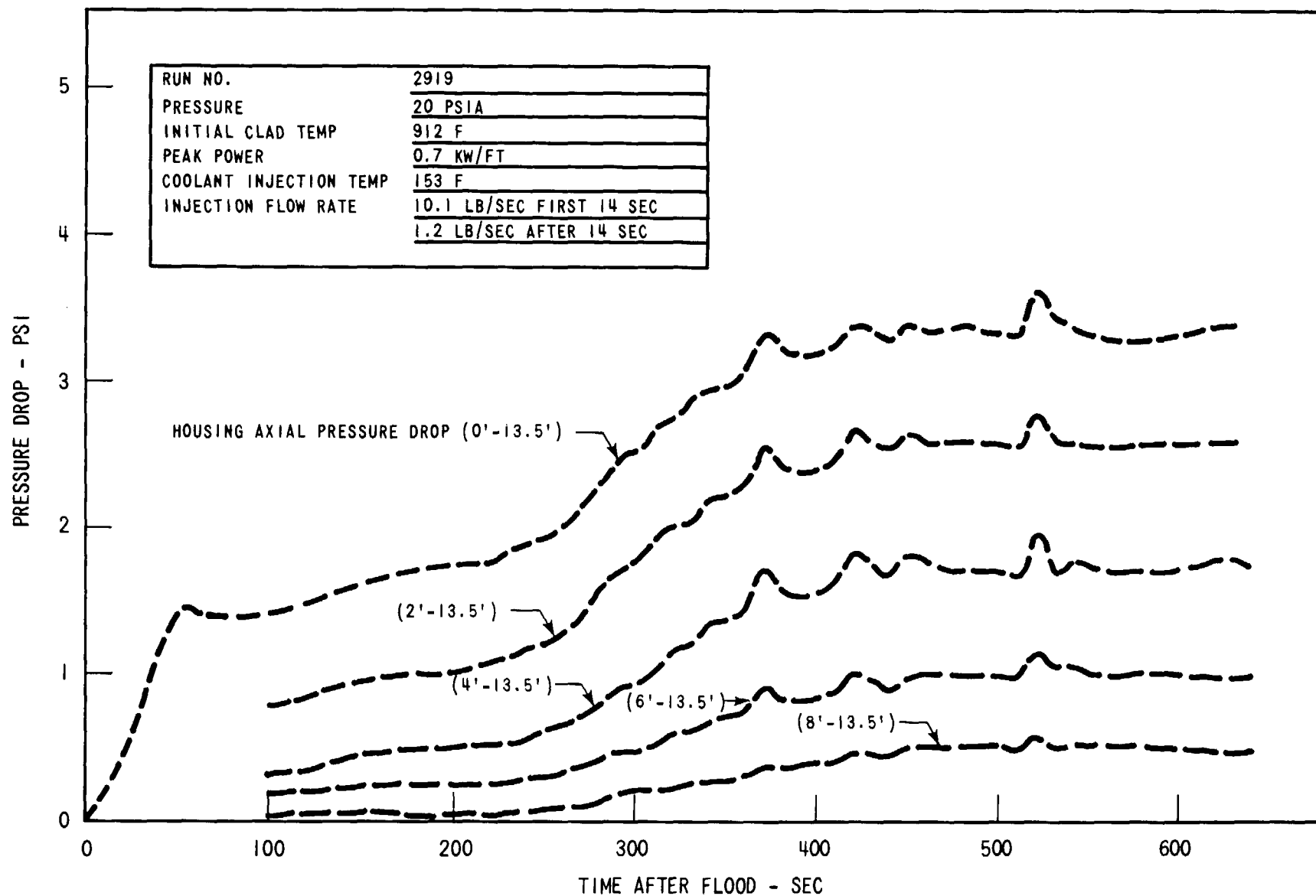


Figure 3-23. Housing Axial Pressure Drop Data - Run 2919

perturbation resulting in an increase in flooding rate collapses the voids at the boiling front and the boiling front moves upward. Thus, less of the energy removed from the core results in steam generation. Since the steam generation rate decreases, the loop pressure drop decreases as can be seen in Figure 3-22 at ~370 sec. As the driving head (the downcomer pressure drop minus the test section pressure drop) decreases, the flooding rate decreases and the boiling front moves down in the bundle. The mass of water in the bundle decreases as some of it is vaporized and some is entrained and carried out of the test section. This phenomenon has been observed in many two-phase flow systems and is commonly called a density wave oscillation.

3.3.2.4 Entrainment

The liquid and vapor mass flow rates out of the test section were measured from the fill up rate of the liquid separator tank and the pressure drop across the loop orifice, respectively. It was not possible to measure the instantaneous liquid flow rate from the test section because of the geometry of the separator tank. Thus, the measured liquid flow rate does not reflect the instantaneous flooding rate when the flooding rate fluctuates as shown in Figure 3-24. In addition, the vapor flow rate is rather insensitive to the flooding rate changes; in fact it decreases slightly as the flooding rate increases as discussed previously.

The mass effluent rate fraction was determined using two different methods; the results are shown in Figure 3-25. The first method used was to determine the ratio of total measured test section effluent mass flow rate (liquid plus vapor) to the test section inlet mass flow rate. The second method used was to perform a mass balance on the bundle to determine the mass flow rate out of the bundle from the difference between the inlet flow rate and the bundle

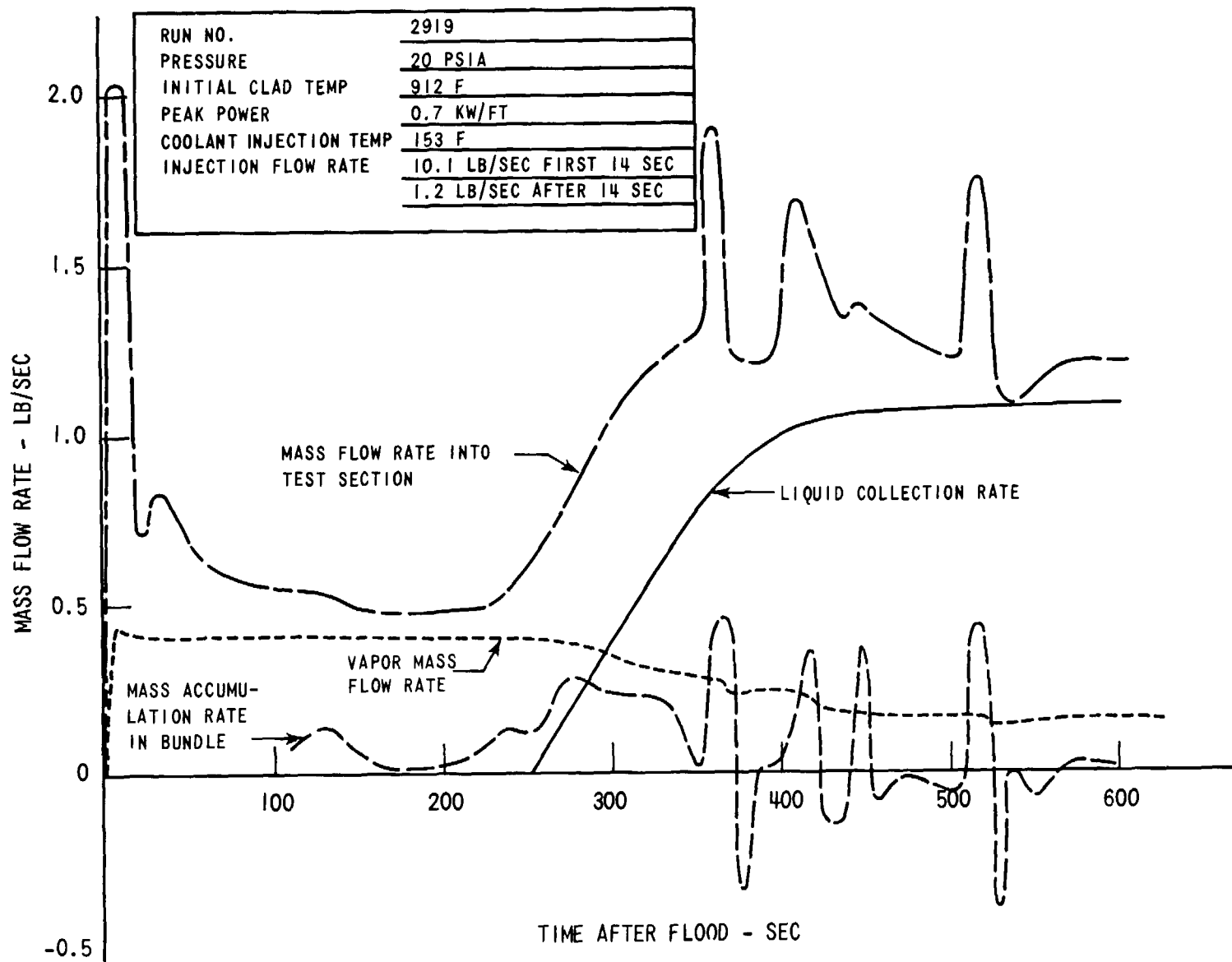


Figure 3-24. Mass Flow Rates - Run 2919

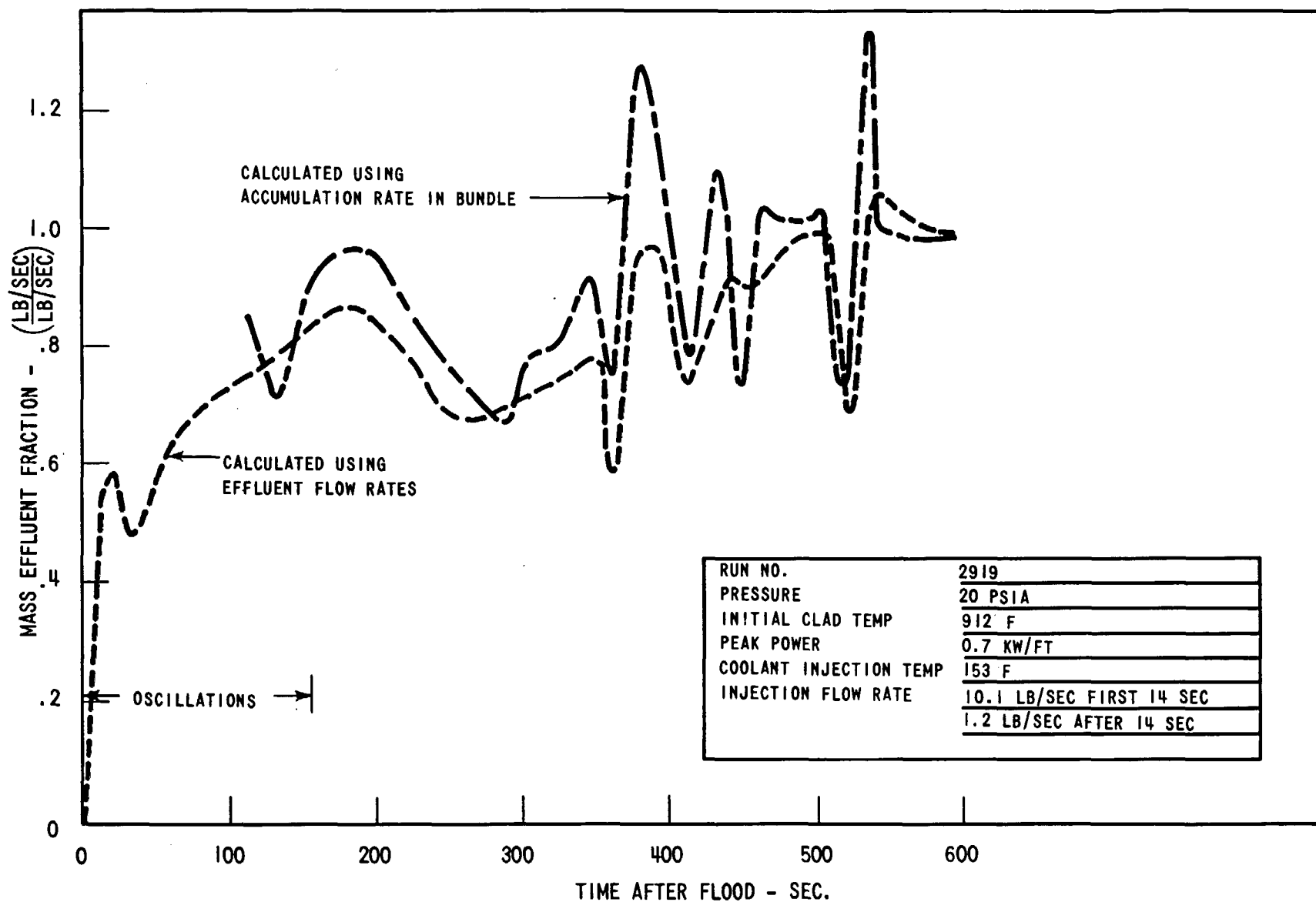


Figure 3-25. Mass Effluent Rate Fraction - Run 2919

mass accumulation rate as calculated from the bundle pressure drop measurements. Within experimental accuracy, the two methods differ only by the mass accumulation rate in the upper plenum and upper plenum extension to the test section inlet mass flow rate. As shown in Figure 3-25 the two methods reveal the same trends. Generally, the second method results in higher mass effluent fractions, indicating a predominantly positive accumulation rate in the upper plenum and upper plenum extension. It is also noted that late in the transient the second method indicates mass effluent fractions greater than one. This occurs after 350 seconds when the test section mass decreases during the flooding rate fluctuations.

The average mass effluent fraction obtained by the second method prior to the midplane quench is typical of results obtained in the FLECHT experiments. The average effluent fraction obtained by the first method prior to the midplane quench is considerably lower (~ 10 percent) than the FLECHT results and reflects the mass storage in the upper plenum volume.

Since the mass effluent fraction based on flow rates fluctuates as shown in Figure 3-25, the data are also presented in Figure 3-26 as the ratio of the total mass effluent to the total test section mass input. The total mass effluent fraction was also calculated using two methods. The first method was to determine the ratio of the total test section mass effluent (liquid and vapor) to the total test section mass input. The second method was to determine the ratio of the total bundle mass effluent from a mass balance on the bundle, to the total test section mass input. Within experimental accuracy, the difference between the two methods is the ratio of the mass stored in the upper plenum and upper plenum extension to the total test section mass input.

3.3.2.5 Quench Front and Test Section Axial Pressure Drop Data

The heater rod temperature quench front envelope is shown in Figure 3-27. The midplane quenched at ~ 385 seconds after flood and the quench "fronts" moved toward the center of the bundle from the top and bottom. The lower quench front moved up rapidly quenching the 2 ft elevation by 11 seconds after flood when it slowed to ~ 0.14 in./sec. The quench front velocity remained

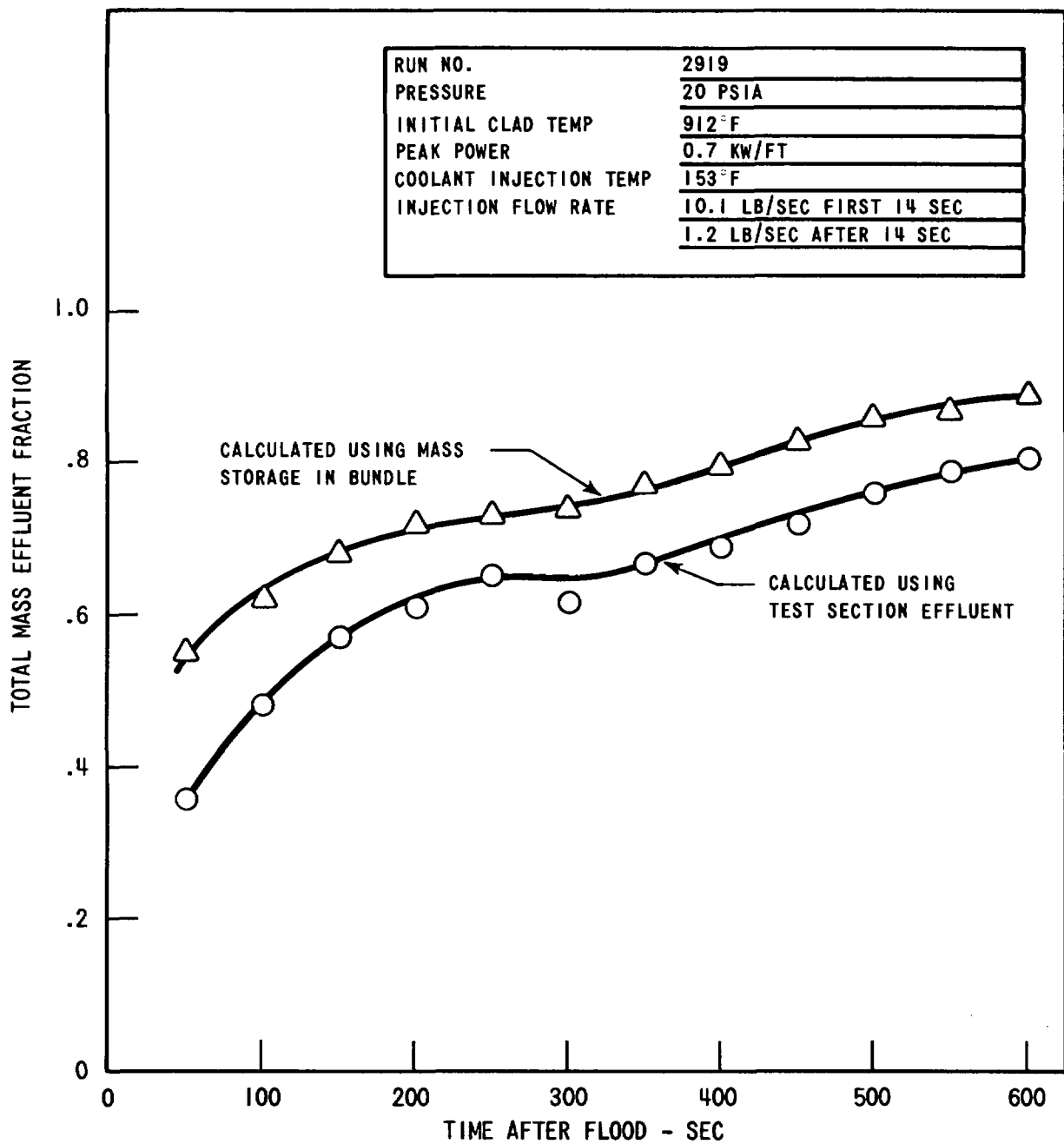


Figure 3-26. Total Mass Effluent Fraction - Run 2919

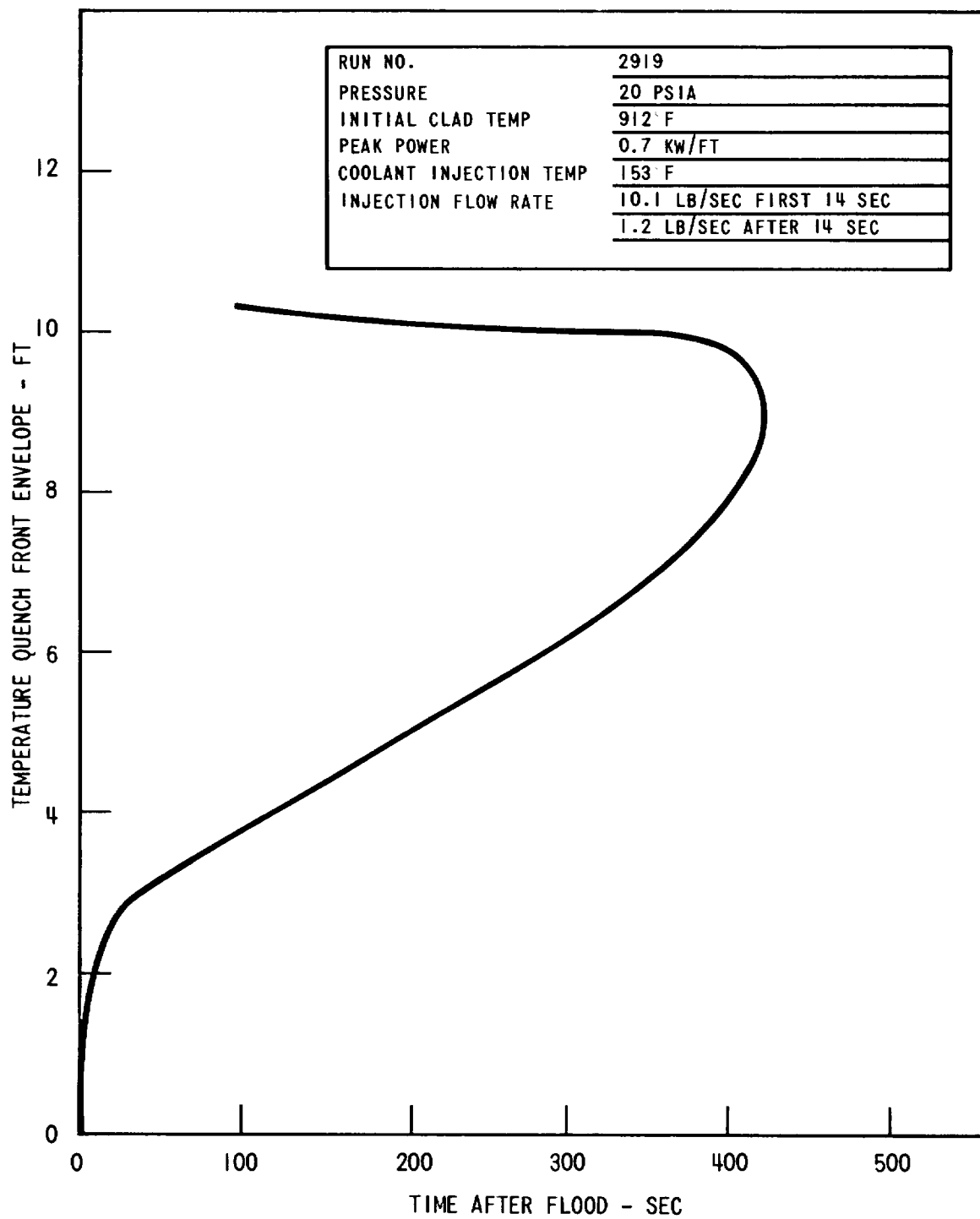


Figure 3-27. Temperature Quench Front Envelope - Run 2919

relatively constant until the midplane quenched, after which it increased slightly to ~ 0.2 in./sec. Thermocouples at the 8 ft elevation were the last to quench. The upper quench front, or sputtering front, moved down to the 10 ft elevation very quickly for some rods, but the 10 ft quench times were scattered over a 300 second time interval. A possible cause of this is that the upper elevations of the rods are quenched by steam and randomly dispersed droplets, resulting in considerable rod to rod variation in heat transfer coefficient.

The bundle axial pressure drop data, shown in Figure 3-23, were used to calculate the average void fraction between two axial pressure taps. The results are shown in Figure 3-28, along with the quench front elevation and the void fraction distribution relative to the quench front position. It can be seen that the void fraction at the quench front elevation was on the order of 0.7 for approximately the first 230 seconds. These results are similar to the FLECHT constant flooding rate tests described in Reference 2 for similar conditions. When the flooding rate increased after ~ 230 seconds, the void fraction at the quench front decreased to ~ 0.5 as shown. It can be seen that the zero void fraction elevation never advanced past the 6 ft elevation and moved up and down during the period the flooding rate fluctuated, causing the fluctuation in the boiling front elevation. An energy balance on the coolant flowing into the bundle also predicts that the coolant will be heated to the saturation temperature just below the midplane of the bundle.

3.3.2.6 Rod Temperature and Heat Transfer Coefficient Behavior

The clad temperature and heat transfer coefficients for the 2 ft, 4 ft, 6 ft, 8 ft, and 10 ft elevations of typical high power heater rods are shown in Figure 3-29. The FLECHT correlation described in Reference 1 was used to predict the midplane heat transfer coefficient by the technique described in Section 3.1. As can be seen in Figure 3-30, the data show significant

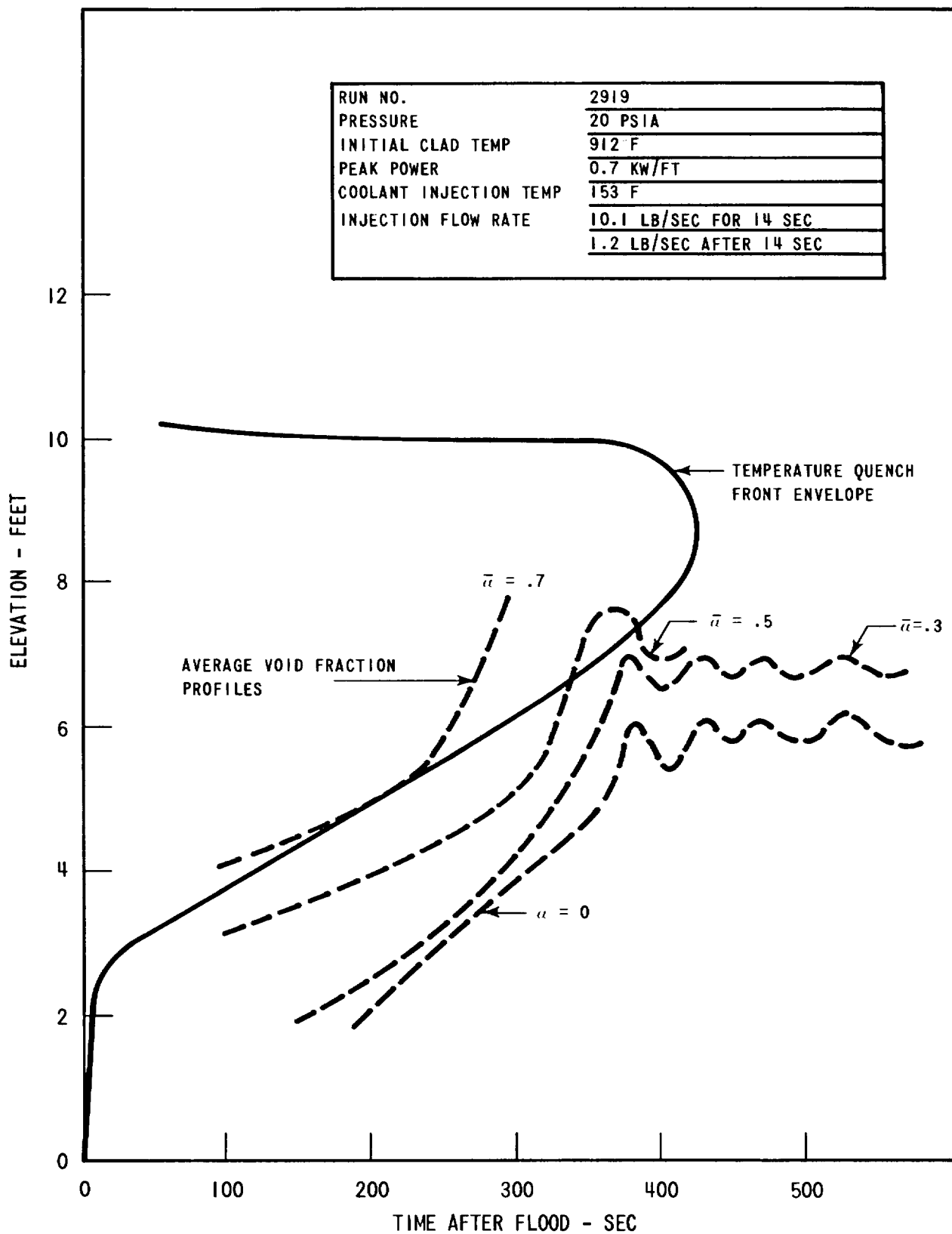


Figure 3-28. Temperature Quench Front Envelope and Average Void Fraction Profiles - Run 2919

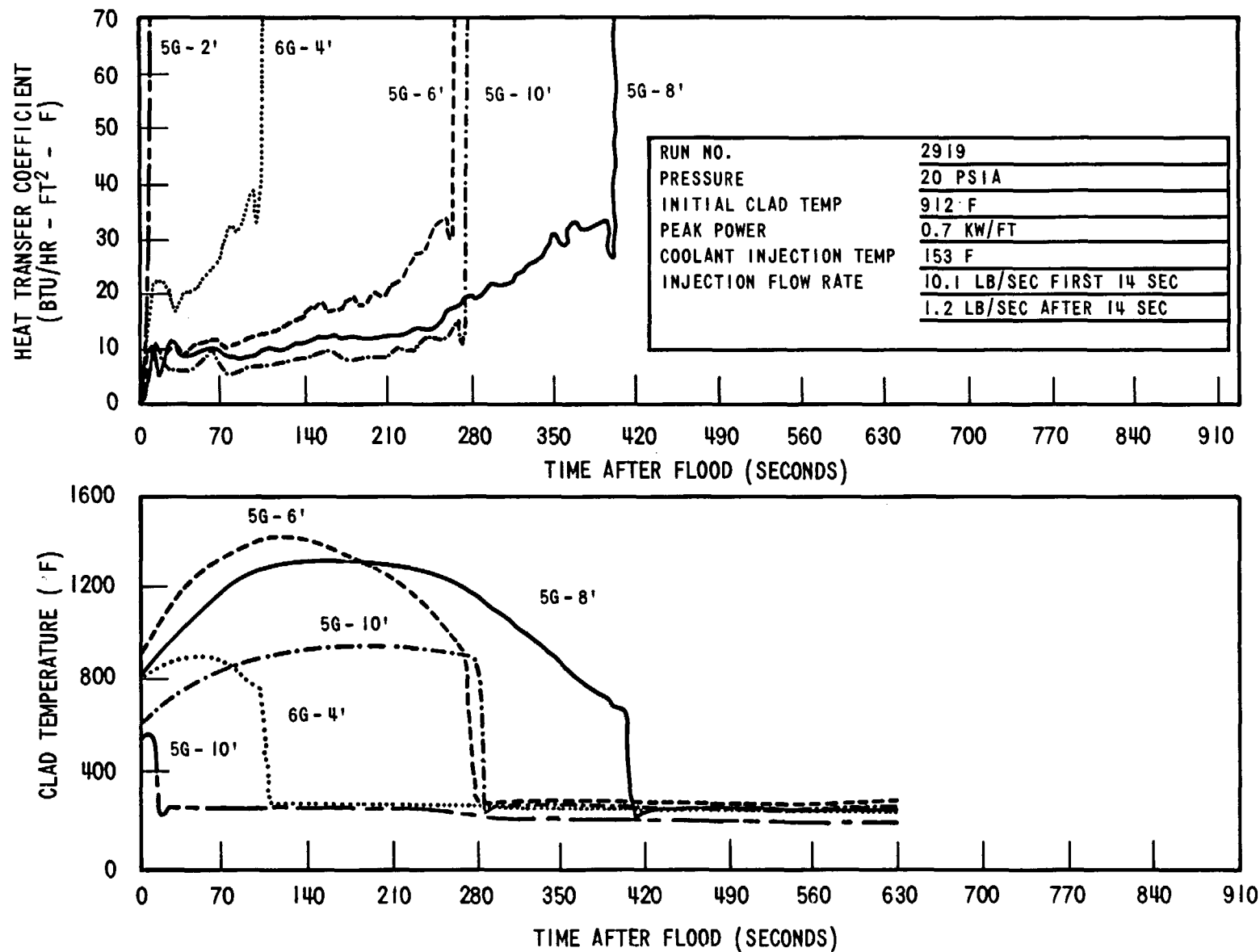


Figure 3-29. Clad Temperature and Heat Transfer Coefficient vs. Time Run 2919

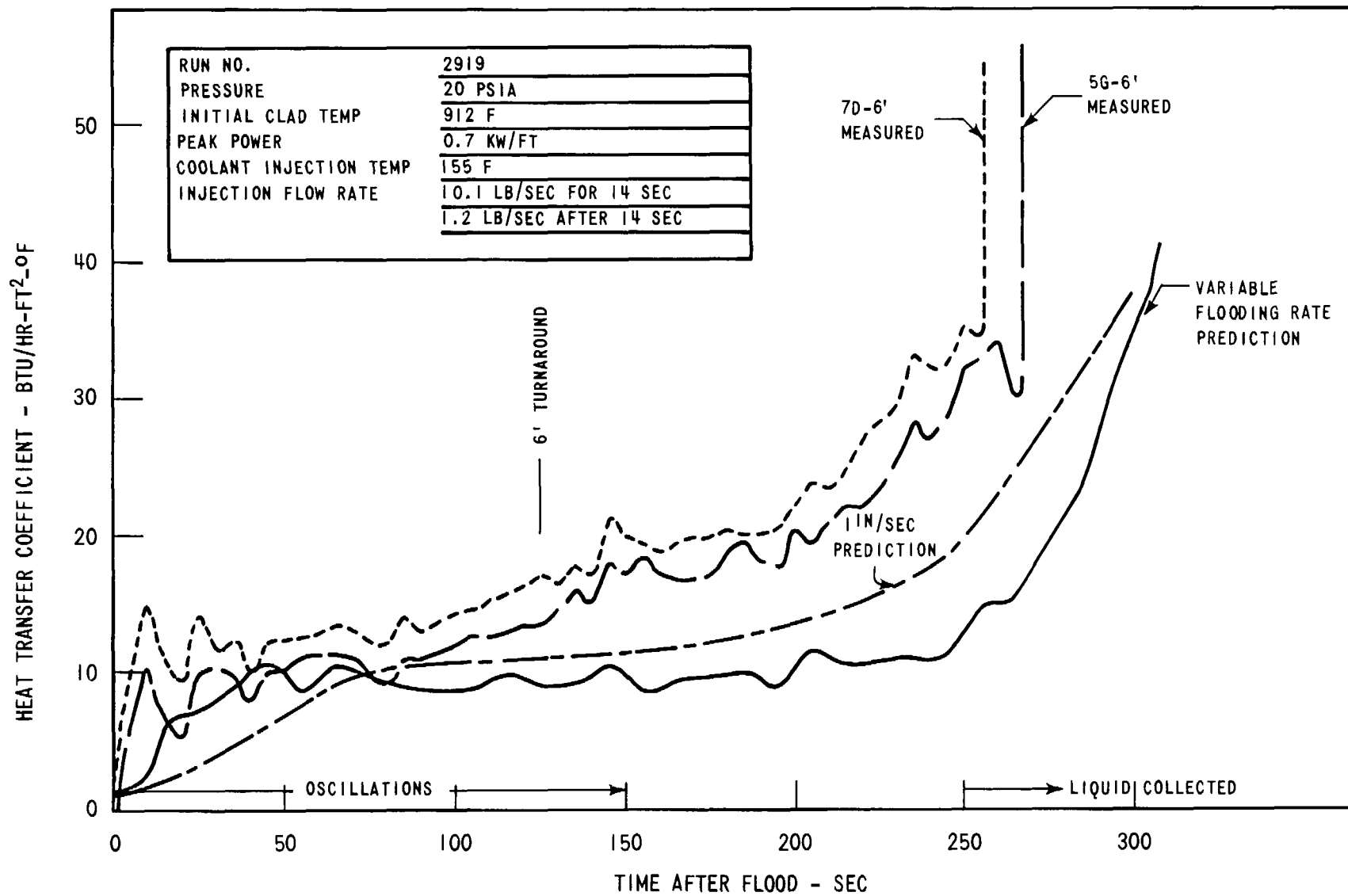


Figure 3-30. Comparison of Predicted and Measured Midplane Heat Transfer Coefficient - Run 2919

margin over the predicted heat transfer coefficient. At the time of the 6 ft turnaround the measured heat transfer coefficient is ~ 50 percent higher than the predicted heat transfer coefficient.

3.3.2.7 Fluid Temperatures at Various Points in the System

The test section inlet and outlet fluid temperatures are shown in Figure 3-31. The coolant supply temperature was relatively constant at 153°F. The fluid in the lower plenum flowed in and out of the bundle during the oscillations, which accounts for the high measured fluid temperature during this period. As the amplitude of the oscillations decreased, the lower plenum fluid temperature decreased and eventually became equal to the coolant injection temperature.

The fluid temperature at the hot leg inlet is also shown in Figure 3-31. The initially high fluid temperature measurement was due to the discharge of the stagnant steam filling the bundle prior to the start of flood. After ~ 60 seconds the hot leg inlet temperature decreased to the local saturation temperature indicated by the dashed line in Figure 3-31.

The fluid temperature upstream of the loop orifice is shown in Figure 3-32. The piping between the liquid separator tank and the orifice was heated to a high temperature before the test. In addition, the heaters were left on during the test so that any unseparated droplets would be vaporized before flowing through the orifice and a meaningful mass flow rate could be obtained from the pressure drop across the orifice. Figure 3-32 shows that the measured fluid temperature upstream of the orifice did indicate superheated steam flowing through the orifice.

3.3.2.8 Housing Behavior

The housing temperature data are shown in Figure 3-33. The initial housing temperature profile was chosen assuming that the midplane would quench at ~ 275 seconds, which was within the scatter of the 6 ft quench time. As shown in Figure 3-32, the housing walls below 5 ft and above 9 ft were quenched by ~ 160 seconds after flood, leaving the 4 ft midsection unquenched.

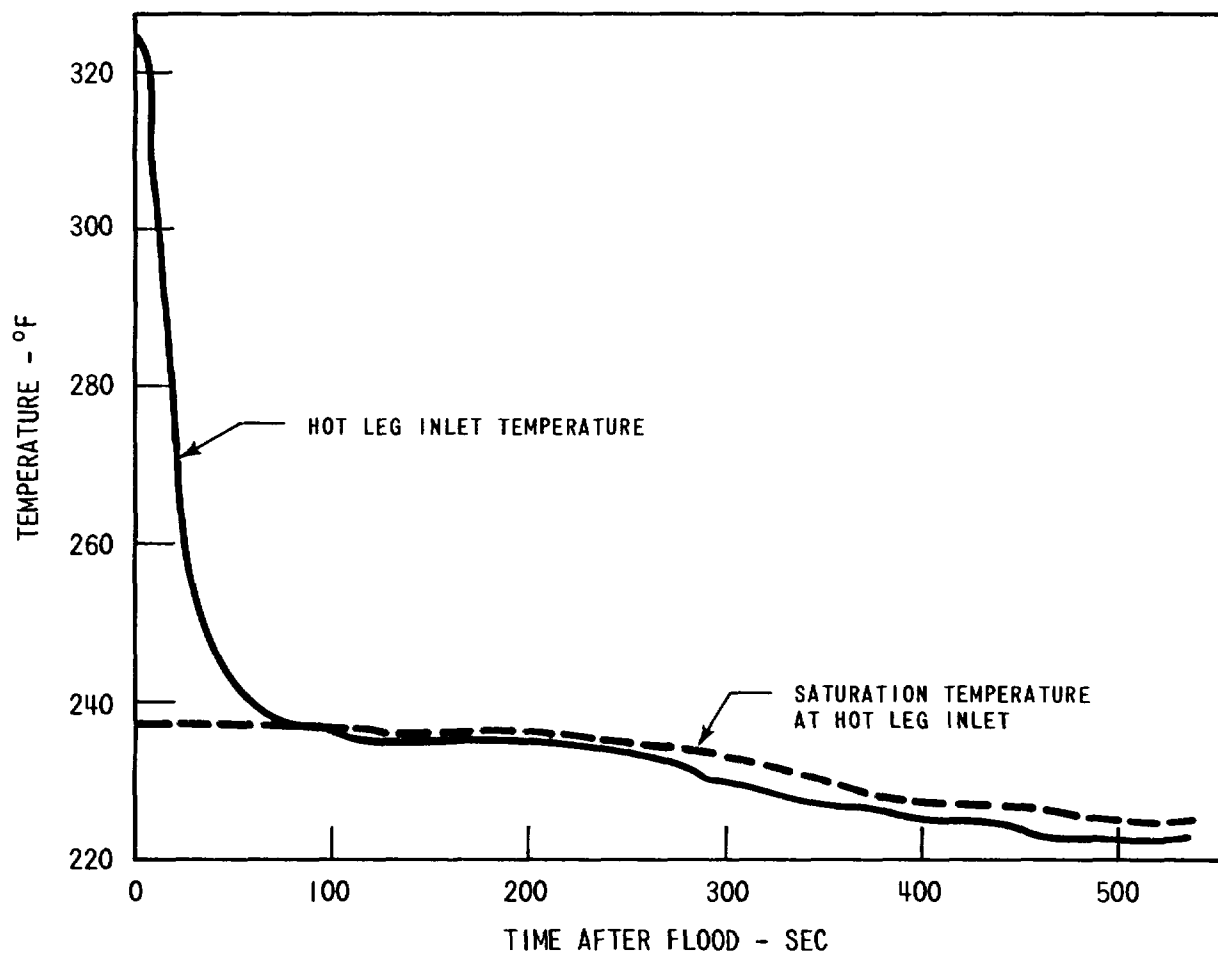
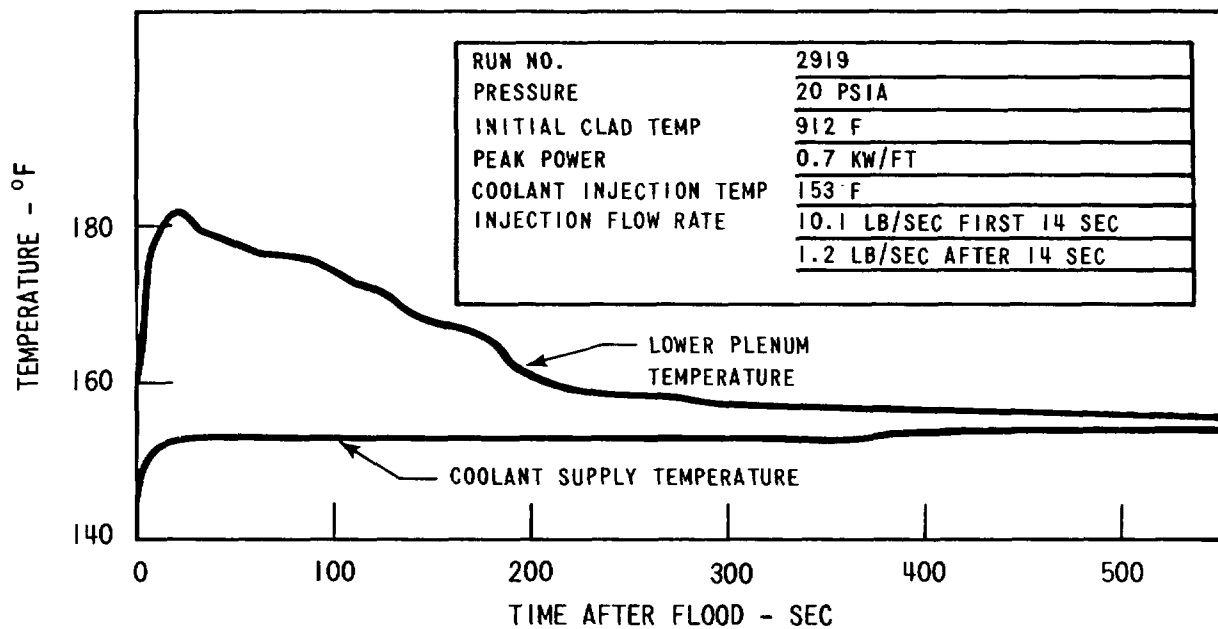


Figure 3-31. Test Section Inlet and Outlet Fluid Temperatures - Run 2919

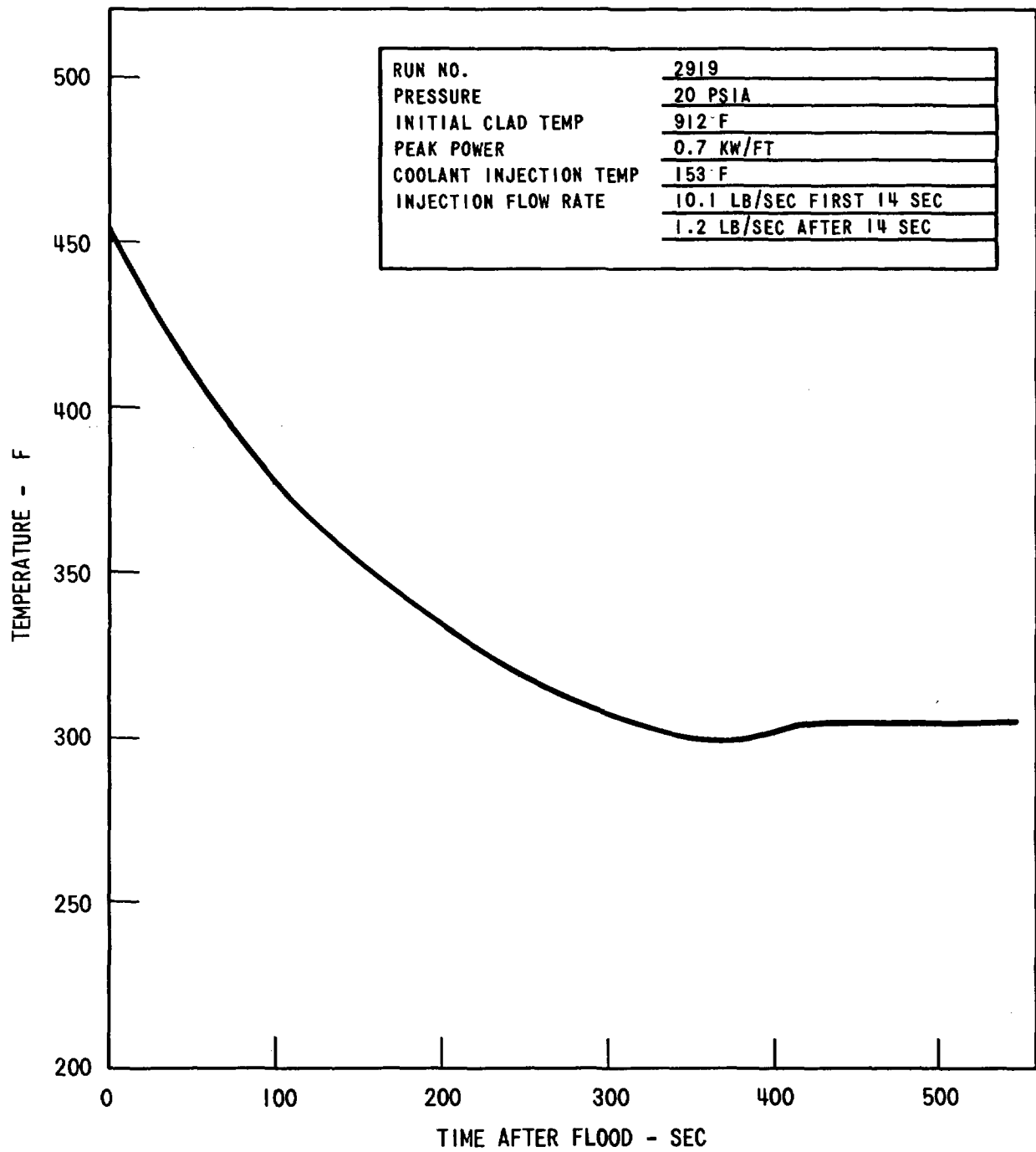


Figure 3-32. Fluid Temperature Upstream of Loop Orifice - Run 2919

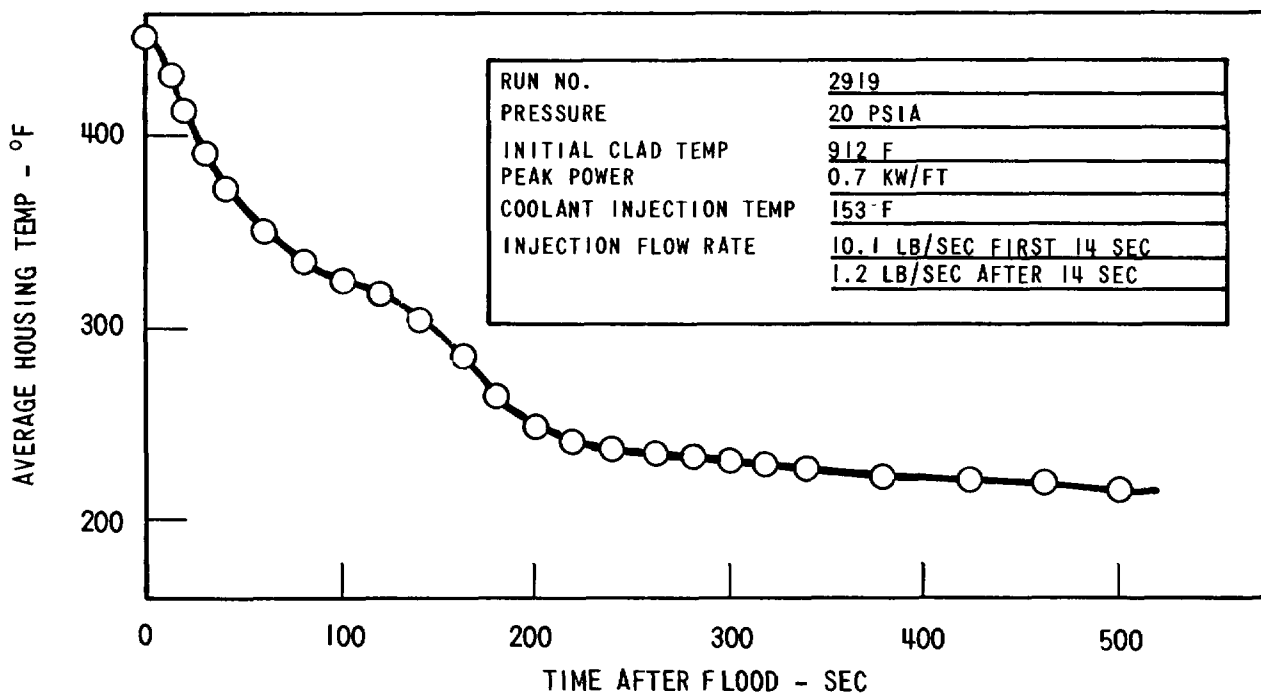
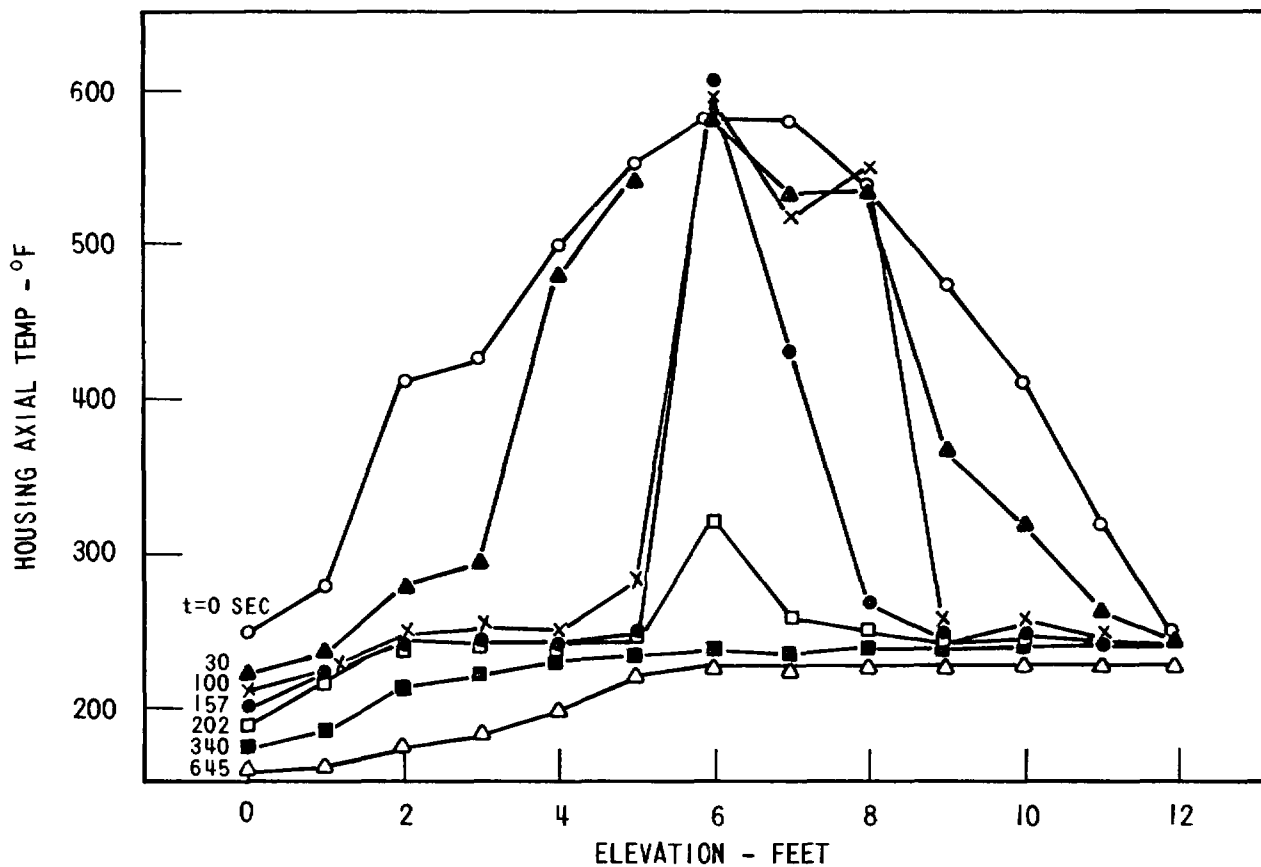


Figure 3-33. Housing Temperature Data - Run 2919

The housing heat release rate prior to 100 seconds was quite high as evidenced by the rapid decrease in the housing average temperature, also shown in Figure 3-33. The initially high heat release rate from the housing can be attributed to the oscillating bundle water level. At the low elevations the heat transfer coefficient at the housing wall surface becomes very high when the water level rises above the surface, resulting in high housing heat release rates. The resulting steam generation entrains large sheets of water droplets, as illustrated in the motion picture, which are carried upward with high velocity. The droplets and steam flowing past the housing midplane do not cause a reduction of the housing midplane temperature until ~ 150 seconds after flood. This can be explained by considering an energy balance on the housing. The housing temperature behavior is determined by the difference between the heat transferred to it by radiation from the heater rods and the heat transferred from it by convection to the steam and droplet flow. Neither the measured exit and inlet flow rates nor the mass accumulated in the bundle changed significantly during the time that the housing midplane quenched. Thus, the heat transferred from the housing by convection did not change significantly. However, there was approximately 35 percent reduction in the radiant heat transfer rates from the heater rods to the housing from the time the heater rod temperature turned around (~ 120 seconds) and the time the housing midplane quenched (~ 175 seconds).

Thus, before the heater rods turned around, the net heat transfer from the housing was approximately zero, but after the heater rods turned around the net heat transfer from the housing became positive and eventually resulted in the quench of the housing. Figure 3-34 shows that the radiation from the rods to the housing was limited primarily to the outer row of rods. The radial temperature profile was very uniform from the third row of rods inward, indicating that the radiation to the housing from the outer row of rods did not affect the temperature behavior of the central rods.

Figure 3-33 also shows that the lower 5 ft of the housing cooled below the saturation temperature, the bottom of the housing being at the coolant inlet condition ($\sim 150^{\circ}\text{F}$) at the end of the test. The lowest housing elevation indicates that the saturation temperature agrees quite well with the zero

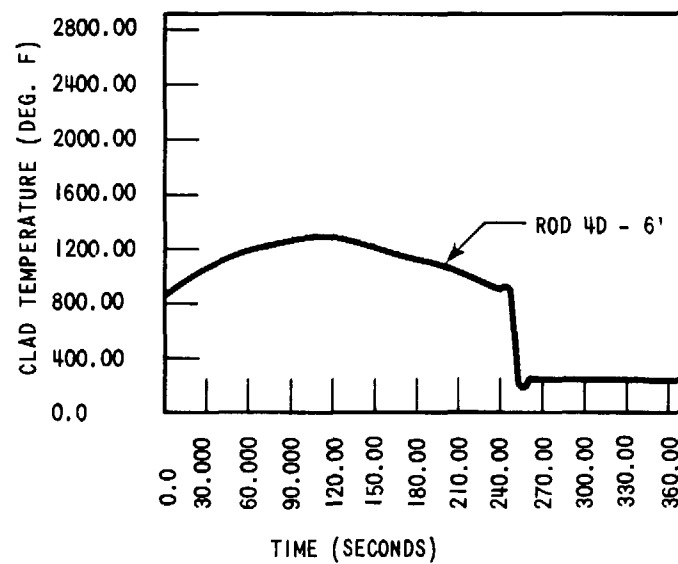
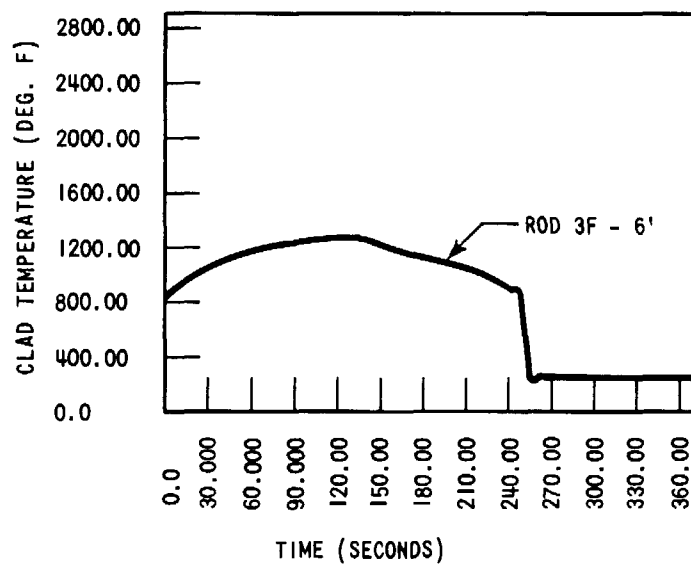
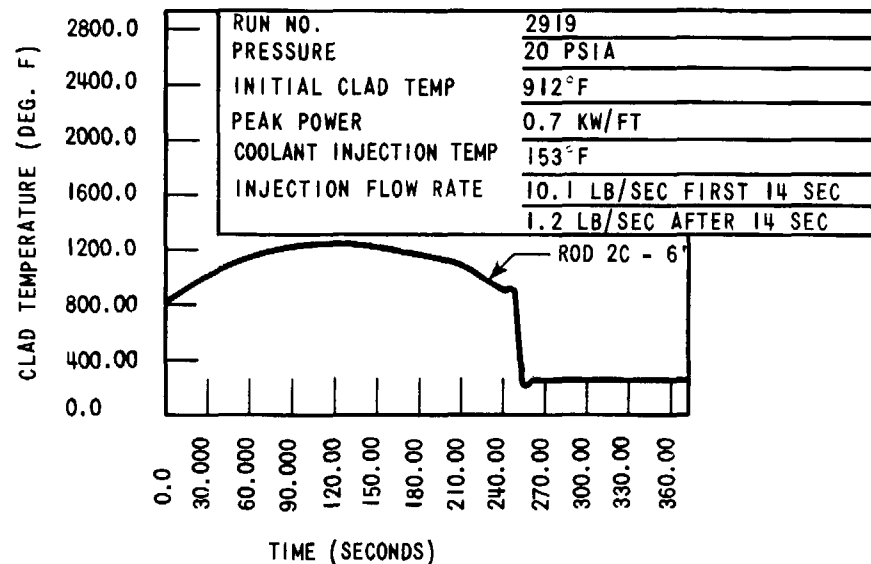
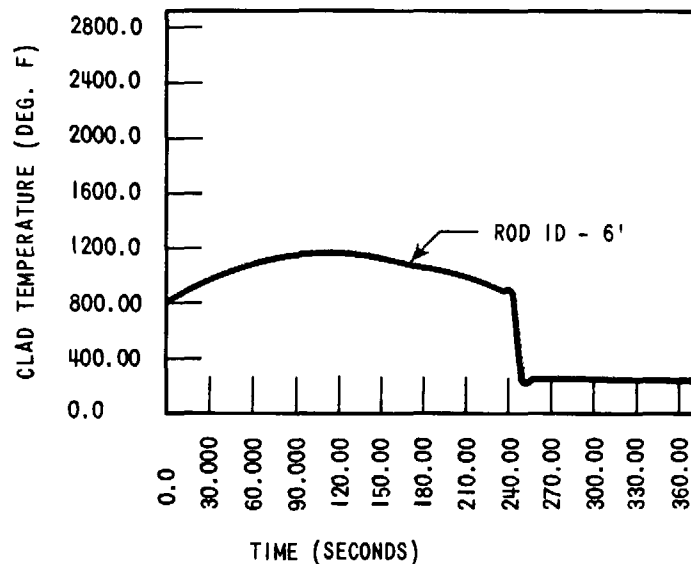


Figure 3-34. Midplane Clad Temperatures at Different Radial Distances from the Test Section Housing Wall - Run 2919

void fraction curve shown in Figure 3-28.

3.3.2.9 Energy Balance

An overall energy balance was performed using the measured mass flow rate and mass storage, the energy inputs from the stored energy in the heater rods and housing walls, and the input electrical energy from the heater rods for the duration of the test (633 seconds). The energy balance was within reasonable limits, being in error by only 9%. The results of the energy balance are summarized as follows:

1. Stored Energy Released by the Heater Rods

$$n \sum_i \rho_i C_i A_i \int_0^{12} (T_i - T_f)_r dz \approx 2.0 \times 10^4 \text{ Btu}$$

where n is the number of heater rods, $\rho_i C_i A_i$ is the product of the density, specific heat, and cross-sectional area of a portion of the heater rod, and $(T_i - T_f)_r$ is the difference between the initial and final rod temperatures.

2. Stored Energy Released by the Housing

$$\rho_h C_h A_h \int_0^{12} (T_i - T_f)_h dz \approx 2.0 \times 10^4 \text{ Btu}$$

where $\rho_h C_h A_h$ is the product of the housing density, specific heat and cross-sectional area, and $(T_i - T_f)_h$ is the difference between the initial and final housing temperatures.

3. Energy Input from Decay Heat

$$P_{\text{initial}} \times I(t) = 16.6 \times 10^4 \text{ Btu}$$

where P_{initial} is the total initial bundle power, and $I(t)$ is the integral of the power decay curve out to 633 seconds after flood.

4. Energy Input from Coolant

$$m_{\text{input}} \times h_{\text{coolant}} = 7.6 \times 10^4 \text{ Btu}$$

where m_{input} is the total mass input to the test section (630 lb),
and h_{coolant} is the enthalpy of the injected coolant.

5. Energy Carried Away by the Steam

$$m_{\text{vapor}} \times h_g \approx 21.5 \times 10^4 \text{ Btu}$$

where m_{vapor} is the total mass of vapor discharged from the
bundle, and h_g is the enthalpy of saturated vapor.

6. Energy Carried Away by the Liquid

$$m_{\text{liquid collected}} \times h_f = 6.8 \times 10^4 \text{ Btu}$$

where $m_{\text{liquid collected}}$ is the mass of liquid collected in the separator
tank at the end of the test, and h_f is the enthalpy of saturated
liquid.

7. Stored Energy Fluid Remaining in the Test Section

$$m_{\text{liquid stored}} \times h_f = 2.4 \times 10^4 \text{ Btu}$$

where $m_{\text{liquid stored}}$ is the water remaining in the test section, upper
plenum, and steam probe tanks at the end of the test, and h_f is
the enthalpy of saturated liquid.

8. Energy Balance

Total energy input	28.2×10^4 Btu
Total energy stored or carried away	30.7×10^4 Btu
Percent error	-9 percent

3.4 HOUSING EFFECTS IN FLECHT-SET TESTS

The rod bundle housing represents a physical boundary not present in a reactor, and thus its effect on the bundle heat transfer and system effects must be analyzed. The hydraulic and stored energy effects of the housing have been thoroughly analyzed in the FLECHT program, and the resulting FLECHT housing criterion has proved to be an acceptable means of controlling the housing heat release so that it releases the same amount of heat as an equivalent row of rods up to the time of the midplane quench.

It was also recognized in the FLECHT program that while the integral of the heat release rate up to the time of the midplane quench was maintained, the local rate of heat release did not match the local heater rod heat release rate at any given point in time between flood and quench.

The rationale behind the criterion used for the initial housing temperature distribution was discussed in Section 2.4. The housing wall was moved away from the heater rod unit cell boundary so that the hydraulic radius of rod flow channels near the wall was the same as the hydraulic radius of an interior flow channel. This resulted in an extra flow area near the housing equivalent to the flow area of 16.8 heater rod flow channels. The housing was heated according to the criterion described in Section 2.4, so that the heat input per unit flow area would be similar to that expected in a PWR during reflood.

The housing effects in the FLECHT-SET tests are further complicated by the dynamic coupling of the flooding rate to the bundle's local heat release rate as discussed previously. To be consistent with the heater rod heat release behavior, the housing must release the proper amount of heat at the correct time or its quenching and steam generation effect will superimpose an abnormal boundary condition in addition to that imposed by the heater rods.

It was decided to investigate three methods of isolating the housing behavior from the bundle heat release rate during a FLECHT-SET transient:

1. Preserve the same power-to-flow area ratio either by heating the housing or increasing the rod power with the housing at the saturation temperature.
2. Vary the housing temperature for the same rod power.
3. Vary the number of heated rods with the housing heated to saturation temperature.

In this fashion, the power to flow area ratio can be varied by either heating the housing, disconnecting rods, or increasing the rod power. These three methods investigate the effect of the power to flow area ratio in the bundle and the effect of whether the energy is input by increasing the rod power or by the release of the housing stored energy.

Table 3-3 lists the test conditions and Figure 3-35 shows the rod hookup for the housing effects tests. All tests were done at 60 psia, 150°F (nominal) injection water temperature, and injection rate (nominal) of 10 lbm/sec for 14 seconds and 1.2 lbm/sec for the remainder of the test.

The effect of the heat input per unit flow area can be based on a local flow area, i.e., the fluid channel near the housing wall or on a total bundle flow area basis. Both seem to correlate the midplane quench time data quite well.

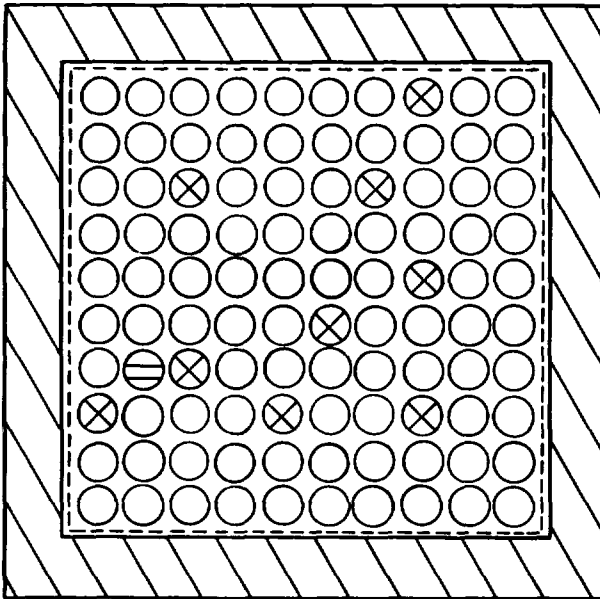
Table 3-4 lists the run conditions and the total heat input to the fluid below the midplane up to the time of the midplane quench. The midplane quench time for all the runs is plotted in Figure 3-36 as a function of the total heat input per unit volume of fluid below the midplane. In Figure 3-36, the midplane quench time varies linearly with the heat input per unit volume.

TABLE 3-3
TEST CONDITIONS FOR HOUSING EFFECTS TESTS

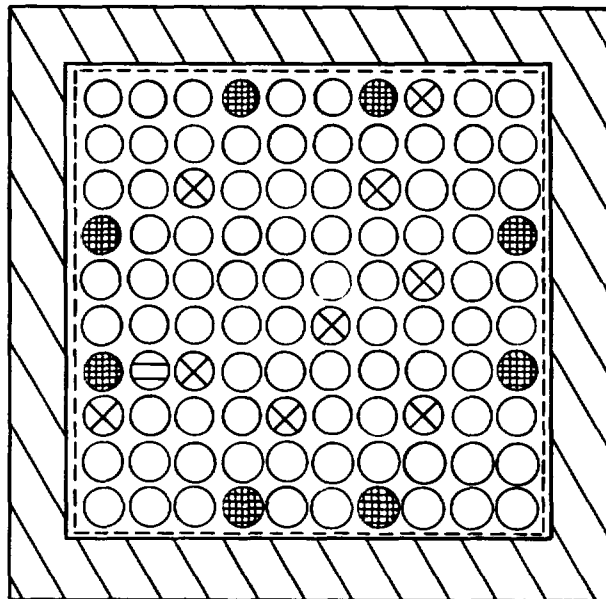
Run No.	No. Heated Rods	Peak Power* (kw/ft)	Avg. Housing Temp (°F)	Coolant Injection Rate (lb/sec)
4311	90	.646	299	9.7 first 14 sec 1.20 onward
4412	82	.646	297	10.9 first 14 sec 1.20 onward
6413	90	.646	614	10.8 first 14 sec 1.25 onward
5214	70	.646	301	10.2 first 14 sec 1.19 onward
5115	90	.759	294	9.0 first 14 sec 1.20 onward
5316	90	.646	424	10.1 first 14 sec 1.18 onward

*All heated rods had the same power. The containment pressure, initial clad temperature, and coolant injection temperature were nearly the same for all runs.

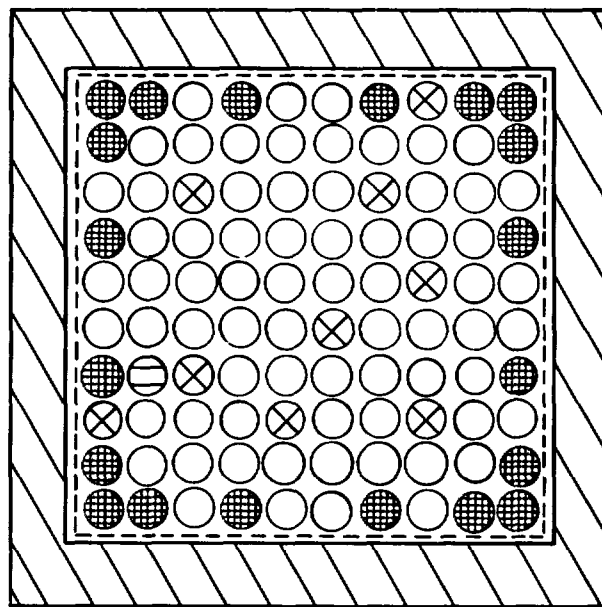
CONFIGURATION FOR RUNS
4311, 5413, 5115 AND 5316



CONFIGURATION FOR RUN 4412



CONFIGURATION FOR RUN 5214



- HEATER ROD
- ⊗ UNHEATED THIMBLE
- ⊖ BURNED OUT ROD
- ⊗ DISCONNECTED HEATER RODS

Figure 3-35. Heater Rod Hookup for Housing Effects Tests

TABLE 3-4

TOTAL HEAT INPUT TO FLUID BELOW MIDPLANE UP TO MIDPLANE QUENCH TIME

Run No.	No. Heated Rods	Peak Power (kw/ft)	Avg. Housing Temp (°F)	Coolant Injection Rate (lb/sec)	Total Energy Released Below Midplane up to 6 ft Quench			
					Housing (Btu)	Rods (Stored) (Btu)	Rods (Generated) (Btu)	Total (Btu)
4311	90	.646	298	9.7 first 14 sec 1.20 onward	$.01 \times 10^4$	1.03×10^4	1.40×10^4	2.44×10^4
4412	82	.646	291	10.9 first 14 sec 1.20 onward	0	$.95 \times 10^4$	1.17×10^4	2.12×10^4
5413	90	.646	603	10.8 first 14 sec 1.25 onward	1.28×10^4	1.32×10^4	1.88×10^4	4.48×10^4
5214	70	.646	302	10.2 first 14 sec 1.19 onward	$.03 \times 10^4$	$.80 \times 10^4$	$.85 \times 10^4$	1.68×10^4
5115	90	.759	294	9.0 first 14 sec 1.20 onward	$.01 \times 10^4$	1.06×10^4	1.76×10^4	2.83×10^4
5316	90	.646	412	10.1 first 14 sec 1.18 onward	$.48 \times 10^4$	1.11×10^4	1.48×10^4	3.07×10^4

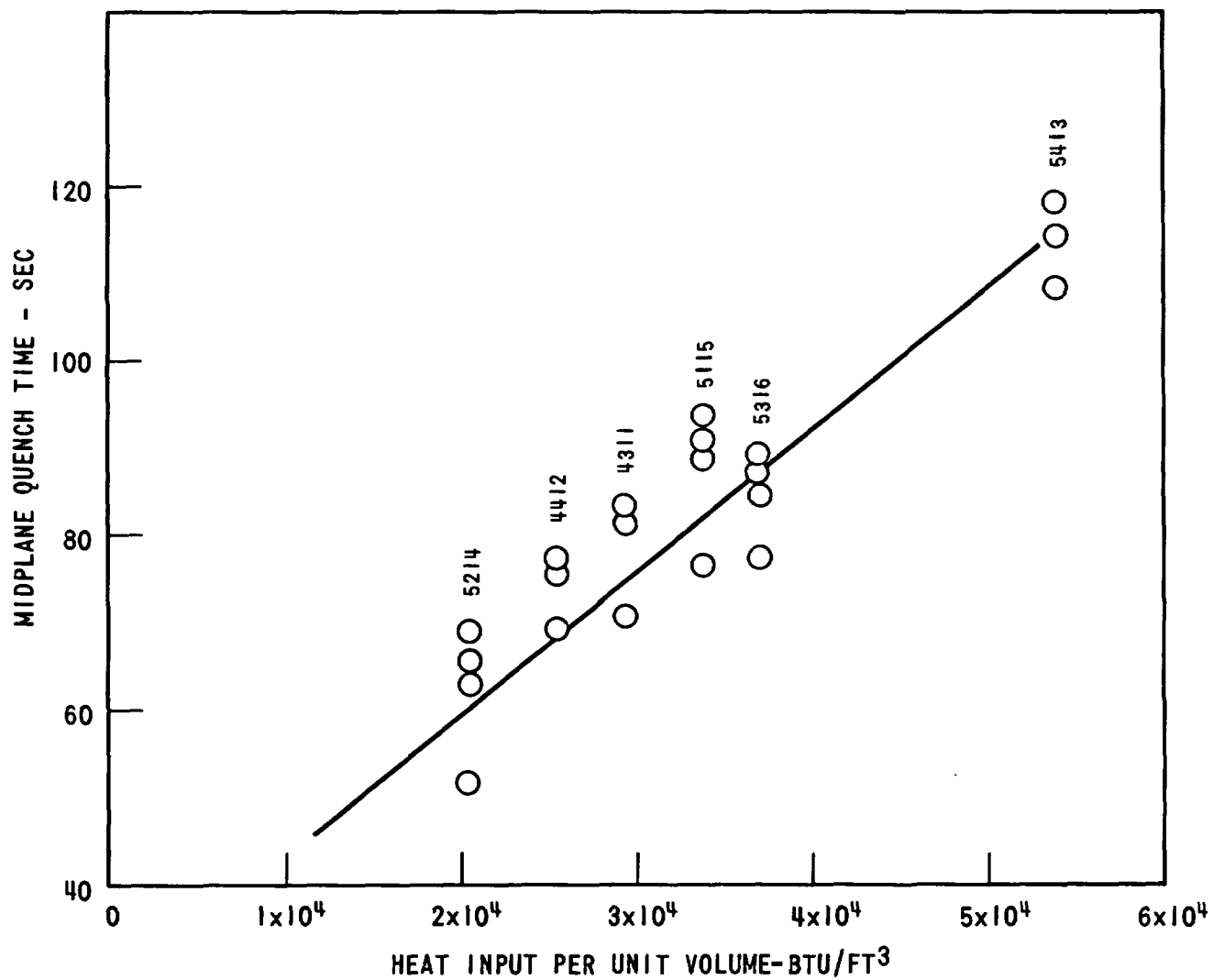


Figure 3-36. Midplane Quench Time vs. Heat Input Below 6' up to 6'
Quench Time per Unit Volume of Fluid Below 6'

Table 3-5 lists the run conditions and the heat input by the housing and the outer row of rods below the midplane up to the time of the midplane quench. All of the runs listed had the same peak power and initial clad temperature so that the central 8 x 8 array of rods had the same initial conditions for all tests. Figure 3-37 shows the midplane quench time plotted as a function of the heat input per unit volume of fluid outside the 8 x 8 array. Again, the variation of quench time with heat input per unit volume was linear.

By comparing Runs 5115 and 5316 the effect of whether the energy is input by the housing or by the rods on the system transient behavior can be observed. Both Runs 5115 and 5316 have approximately the same heat input per unit volume of fluid, as is shown in Table 3-4. However, in Run 5316 the housing is heated above the saturation temperature, while in Run 5115 the additional thermal energy is input by the heater rods, which are at 18 percent higher power, and the housing is heated to the saturation temperature.

The midplane quench time is shown for all runs in Figure 3-36. As can be seen in this figure, the quench times were nearly identical for Runs 5115 and 5316. In fact, the quench front curves for these two runs were nearly identical, as shown in Figure 3-38. As expected, the 10 ft quench times for Runs 5115 and 5316 were different since the criterion used for the housing heat input was based on the 6 ft quench time.

The major differences between the two runs were that the magnitude and duration of the oscillations were much less for the unheated housing run (5115). Figures 3-39 and 3-40 present reduced pen recorder tracings of the downcomer head and loop pressure drop for Runs 5515 and 5316. Of the two runs, only 5316 had an initial housing temperature above the saturation temperature and it had large and long-lasting oscillations. It was also noted that the oscillations ceased as soon as the housing had quenched. The heat release rate from the housing is very high because its surface temperature is low enough for nucleate boiling to take place at the wetted surface. Thus, as the water enters the bundle and reaches the elevation of the unquenched

TABLE 3-5

HEAT INPUT TO PERIPHERY CHANNEL BELOW MIDPLANE UP TO MIDPLANE QUENCH TIME

Run No.	No. Heated Rods in Outer Row	Peak Power (kw/ft)	Avg. Housing Temp (°F)	Coolant Injection Rate (lb/sec)	Energy Released in Periphery Below 6 ft up to 6 ft Quench			
					Housing (Btu)	Rods (Stored) (Btu)	Rods (Generated) (Btu)	Total (Btu)
4311	34	.646	299	9.7 first 14 sec 1.2 onward	$.01 \times 10^4$	$.39 \times 10^4$	$.53 \times 10^4$	$.93 \times 10^4$
4412	26	.646	291	10.9 first 14 sec 1.2 onward	0	$.30 \times 10^4$	$.37 \times 10^4$	$.67 \times 10^4$
5413	34	.646	603	10.8 first 14 sec 1.25 onward	1.28×10^4	$.50 \times 10^4$	$.71 \times 10^4$	2.19×10^4
5214	14	.646	302	10.2 first 14 sec 1.19 onward	$.03 \times 10^4$	$.16 \times 10^4$	$.17 \times 10^4$	$.36 \times 10^4$
5316	34	.646	412	10.1 first 14 sec 1.18 onward	$.48 \times 10^4$	$.42 \times 10^4$	$.56 \times 10^4$	1.46×10^4

3-70

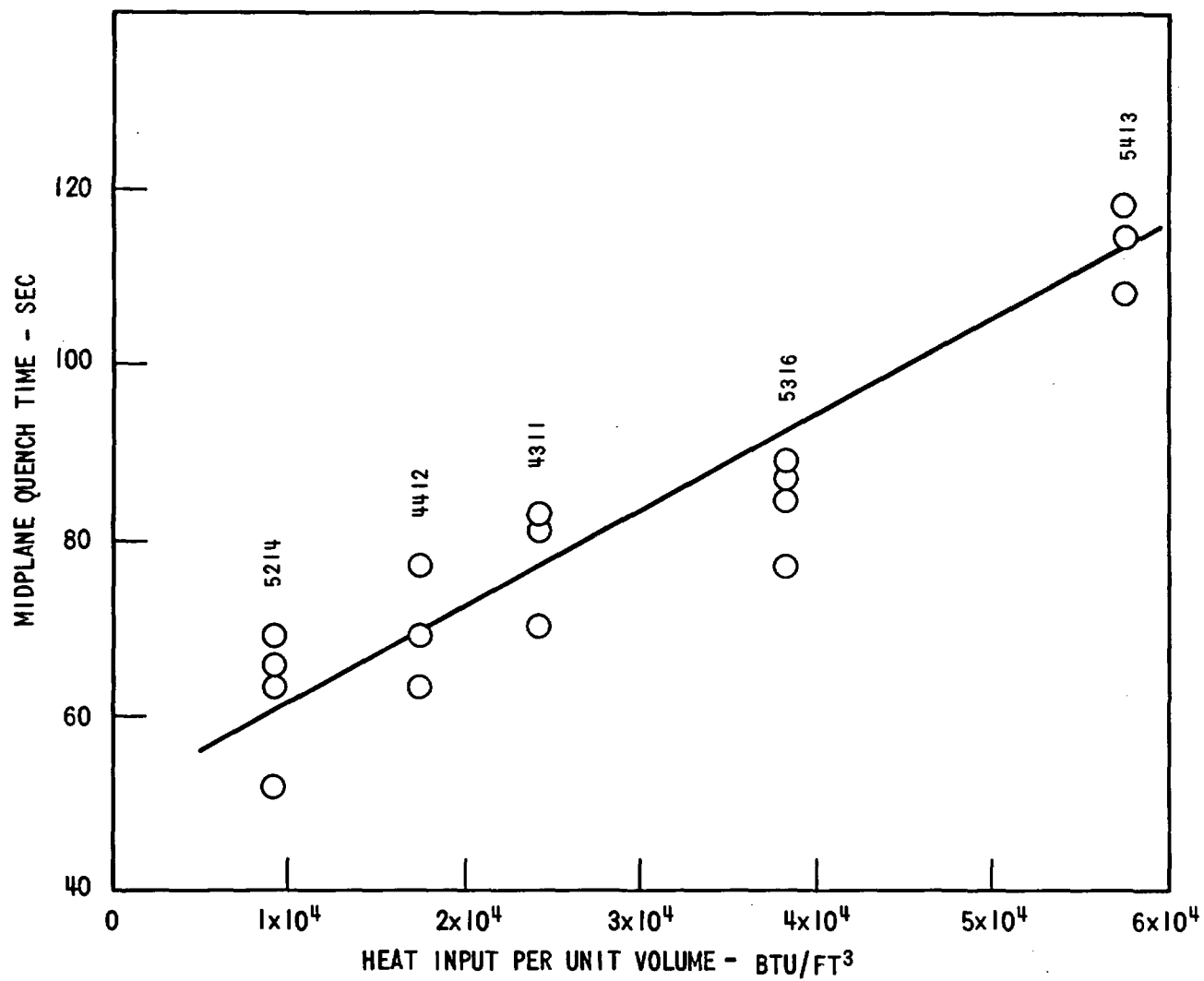


Figure 3-37. Midplane Quench Time vs Heat Input by Housing and Outer Row of Rods Below 6'. Up to 6' Quench Time per Unit Volume of Fluid in Periphery Channel

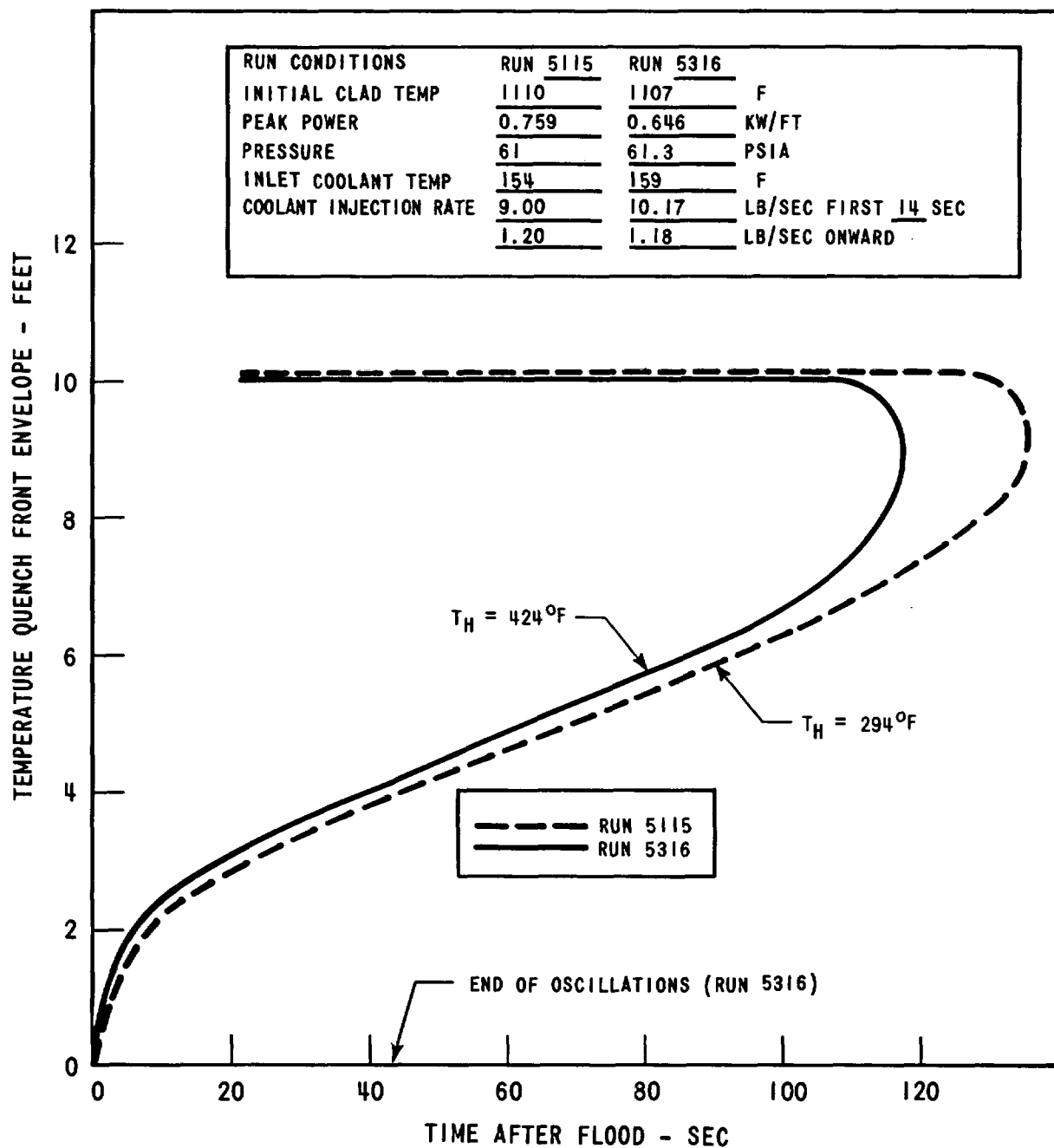


Figure 3-38. Comparison of Quench Front Envelope vs. Time for Runs 5115 and 5316

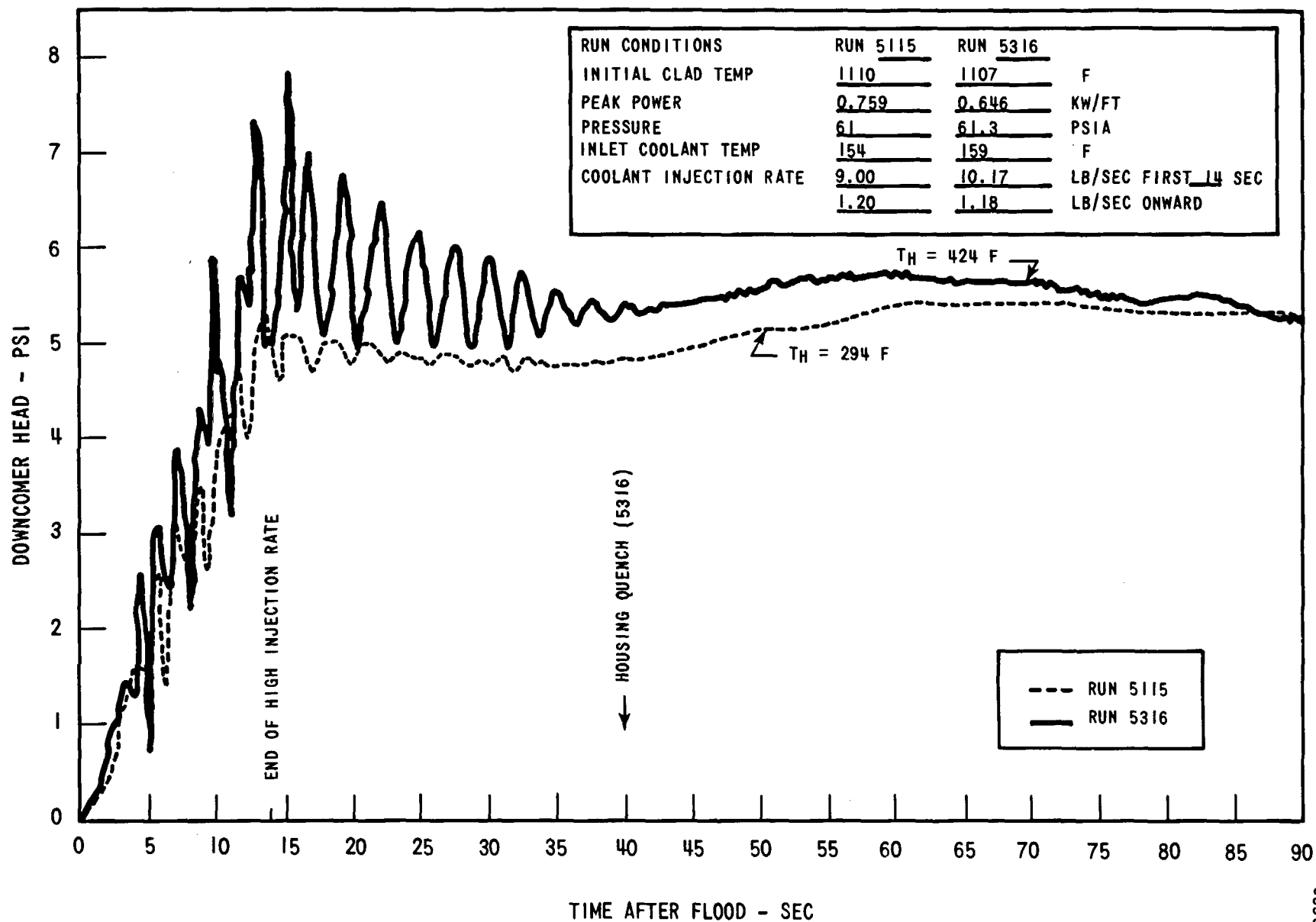


Figure 3-39. Downcomer Head vs. Time for Different Housing Temperatures

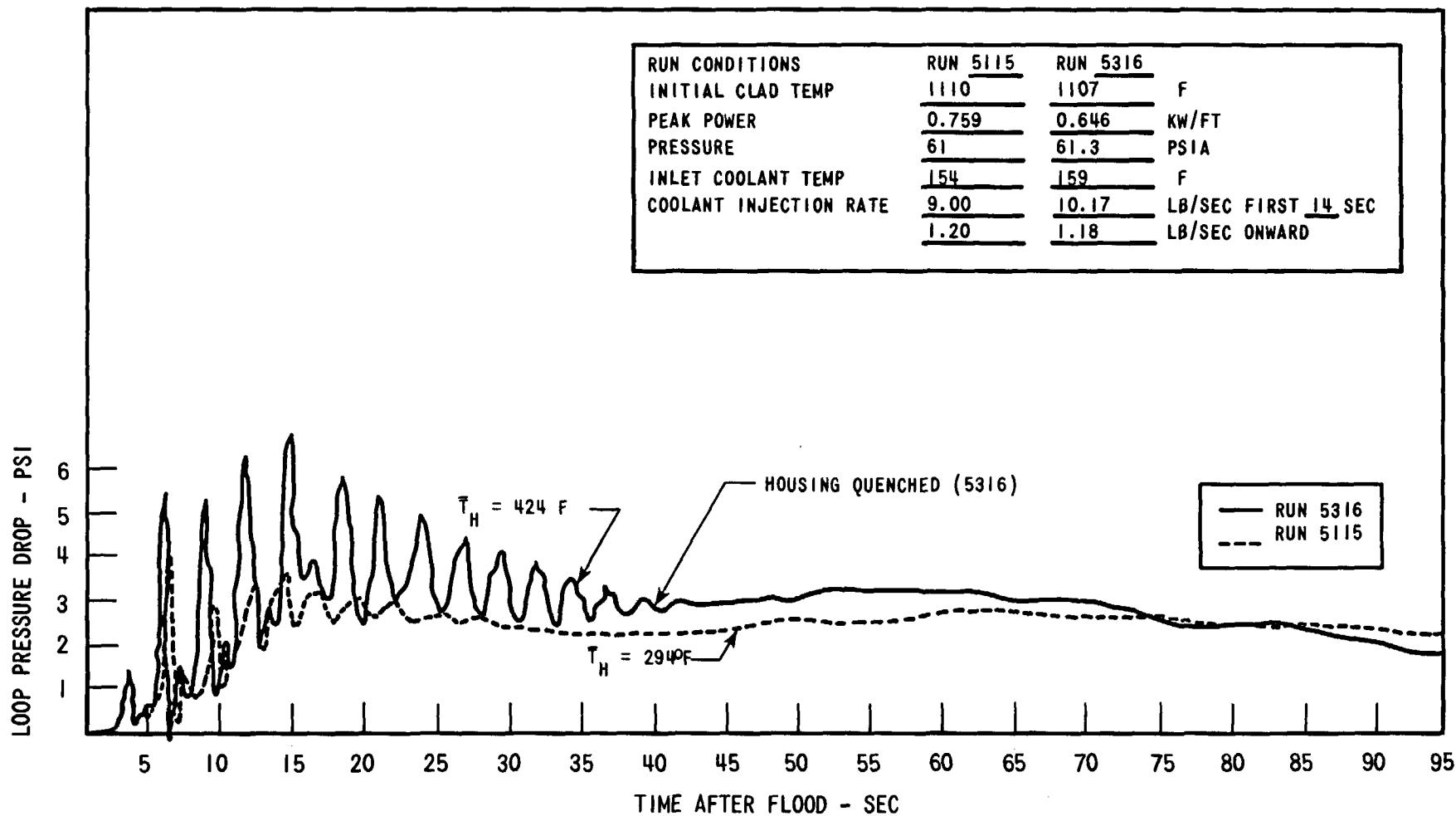


Figure 3-40. Comparison of Loop Pressure Drops for Runs 5115 and 5316

housing, a large volume of steam is produced which must vent through the loop resistance. The resulting pressure increase above the water surface forces the water level down, reducing the steam generation rate because the lower elevations have been quenched. Because of fluid inertia, the bundle water level drops below the equilibrium position. The rising downcomer level creates a large restoring force and the gravitational force eventually cause the downcomer level to fall, forcing water up the bundle until the steam generation rate and the resulting pressure buildup are sufficient to start the process all over again. The heat release rate from the heater rods is apparently not large enough to drive the large oscillations.

A direct comparison of flooding rate in these two runs is not possible since the initial injection rate was higher for Run 5316 than for Run 5115, resulting in about 15 lb more being injected in the first 14 seconds. Even so, the flooding rates were not that different in the first 20 seconds, as shown in Figure 3-41. This was caused by more water storage in the downcomer in Run 5316 than in Run 5115, as shown in Figure 3-39, because of the higher steam flow rate and resulting higher loop pressure drop.

The total amount of mass put into the test section after 25 seconds was higher for the hot housing run (5316), as shown in Figure 3-42. However, if the injection rates had been identical, it is expected that the flooding rate would have been lower for the hot housing run until the housing quench. The steam flow rates are given in Figure 3-43.

Even though more mass entered the test section during the hot housing run (5316) than during Run 5115, less mass remained in the bundle until the housing quenched, as shown in Figure 3-44. Thus, the carryout fraction was significantly higher for the heated housing run as shown in Figure 3-45. The additional vapor carryout is apparent, from Figure 3-43, that the vapor flow rate was higher for the heated housing run (5316) for the first 70 seconds. Although the liquid

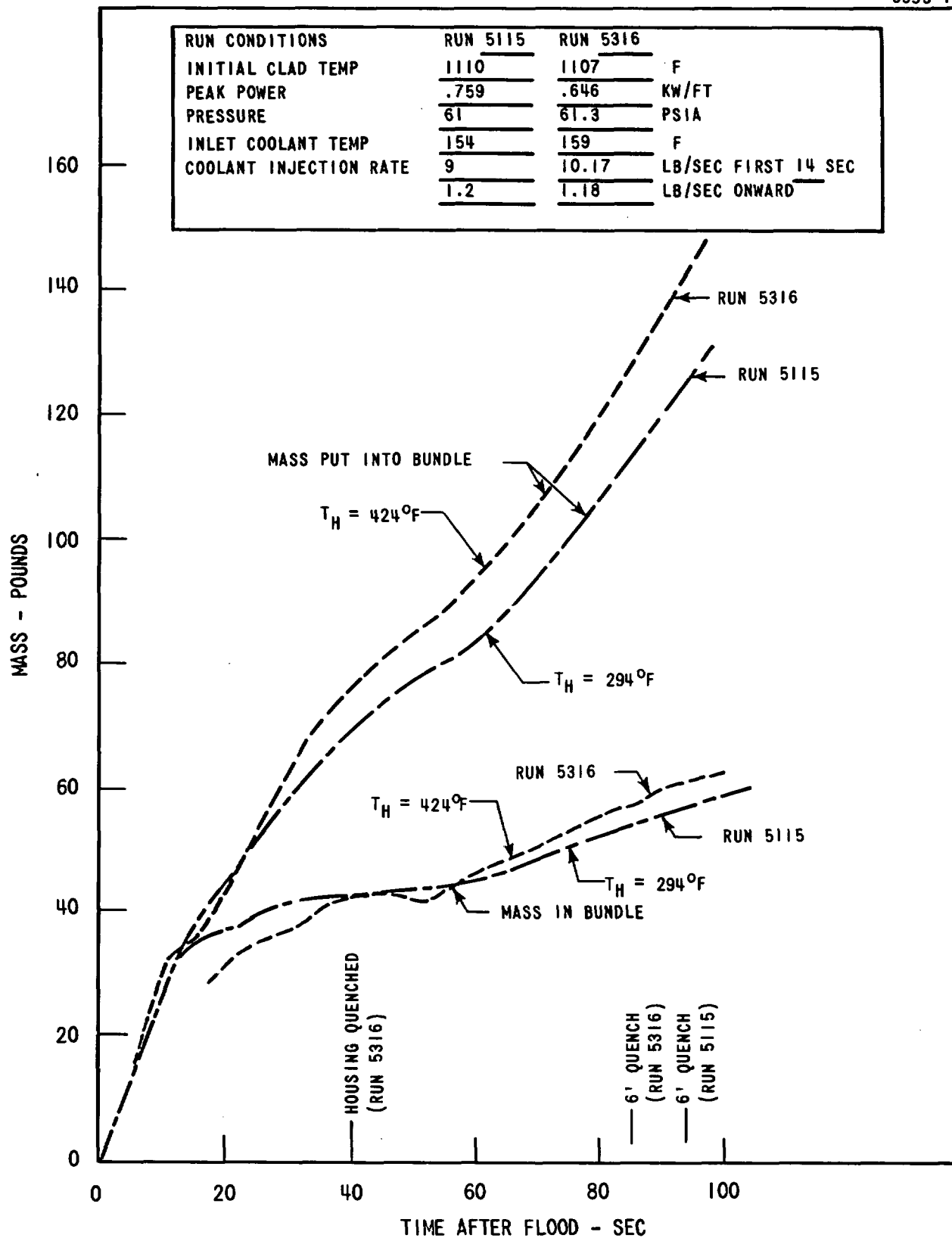


Figure 3-41. Comparison of Mass Put Into Bundle and Mass Remaining in Bundle for Runs 5115 and 5316

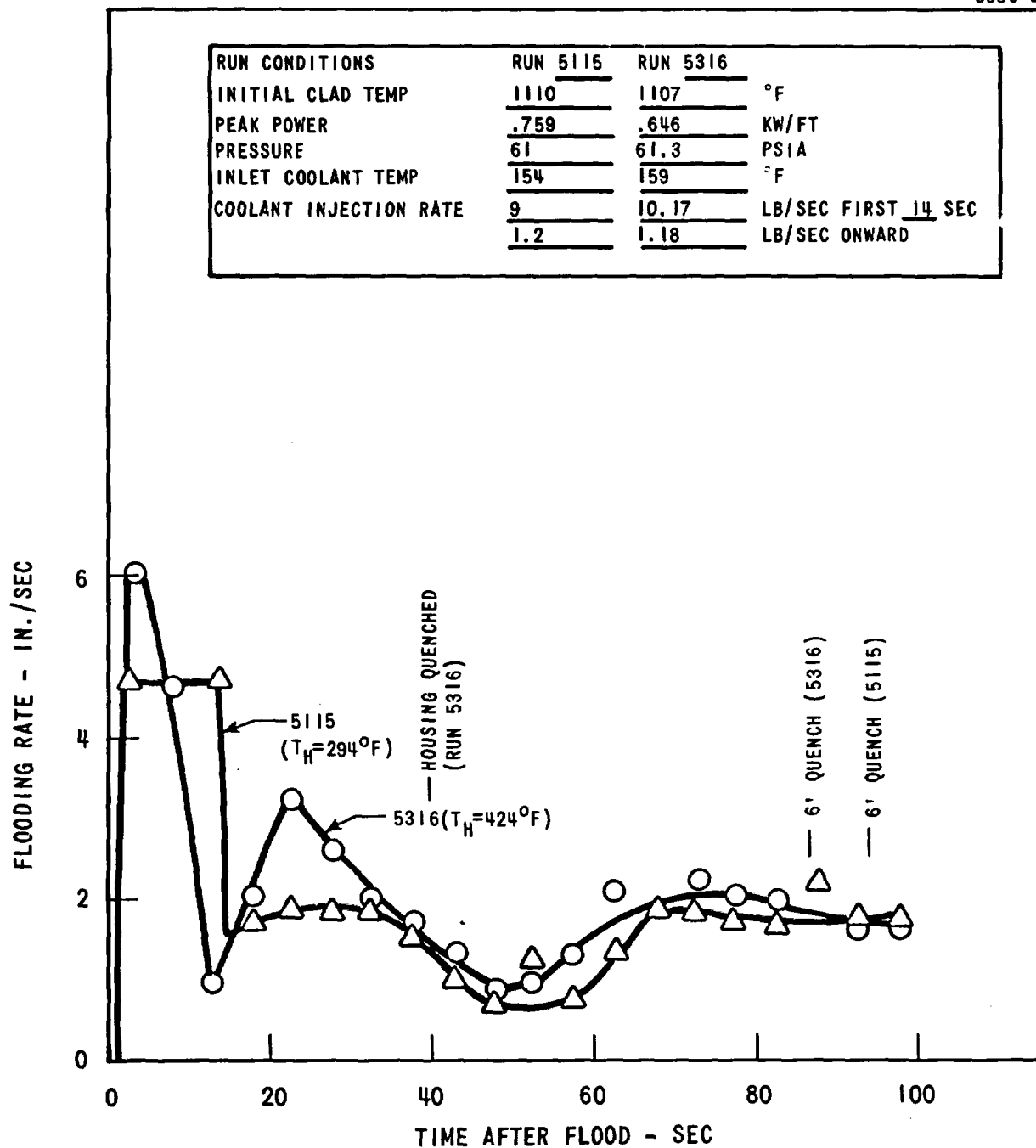


Figure 3-42. Comparison of Flooding Rates for Runs 5316 and 5115

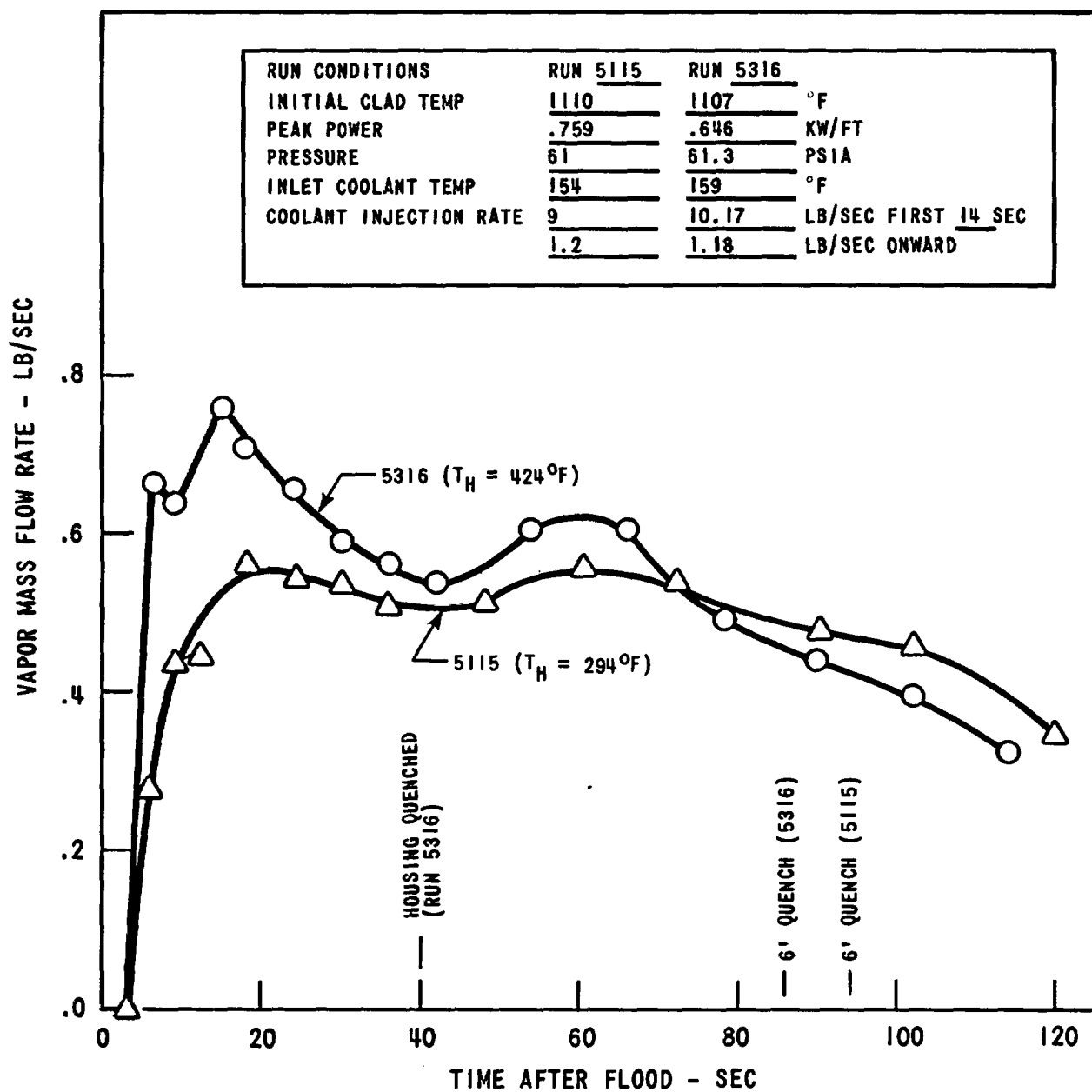


Figure 3-43. Comparison of Vapor Flow Rates for Runs 5316 and 5115

RUN CONDITIONS		RUN 5115	RUN 5316	
INITIAL CLAD TEMP		1110	1107	F
PEAK POWER		.759	.646	KW/FT
PRESSURE		61	61.3	PSIA
INLET COOLANT TEMP		154	159	F
COOLANT INJECTION RATE		9	10.17	LB/SEC FIRST 14 SEC
		1.2	1.18	LB/SEC ONWARD

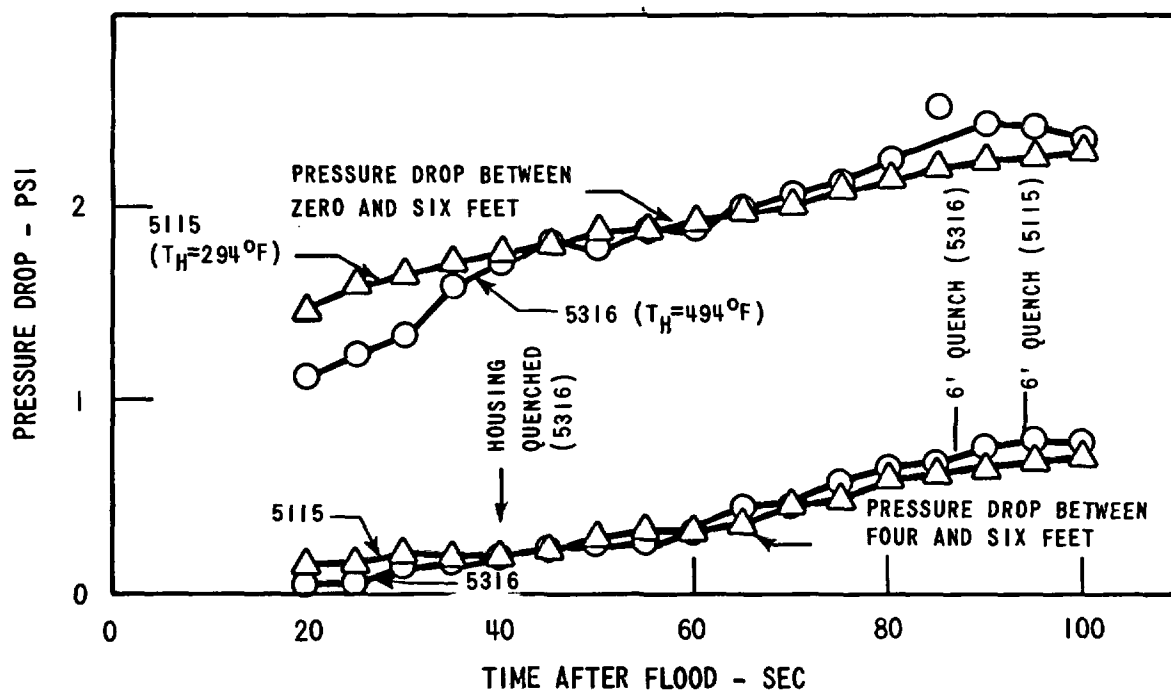


Figure 3-44. Comparison of Bundle Axial Pressure Drops for Runs 5115 and 5316

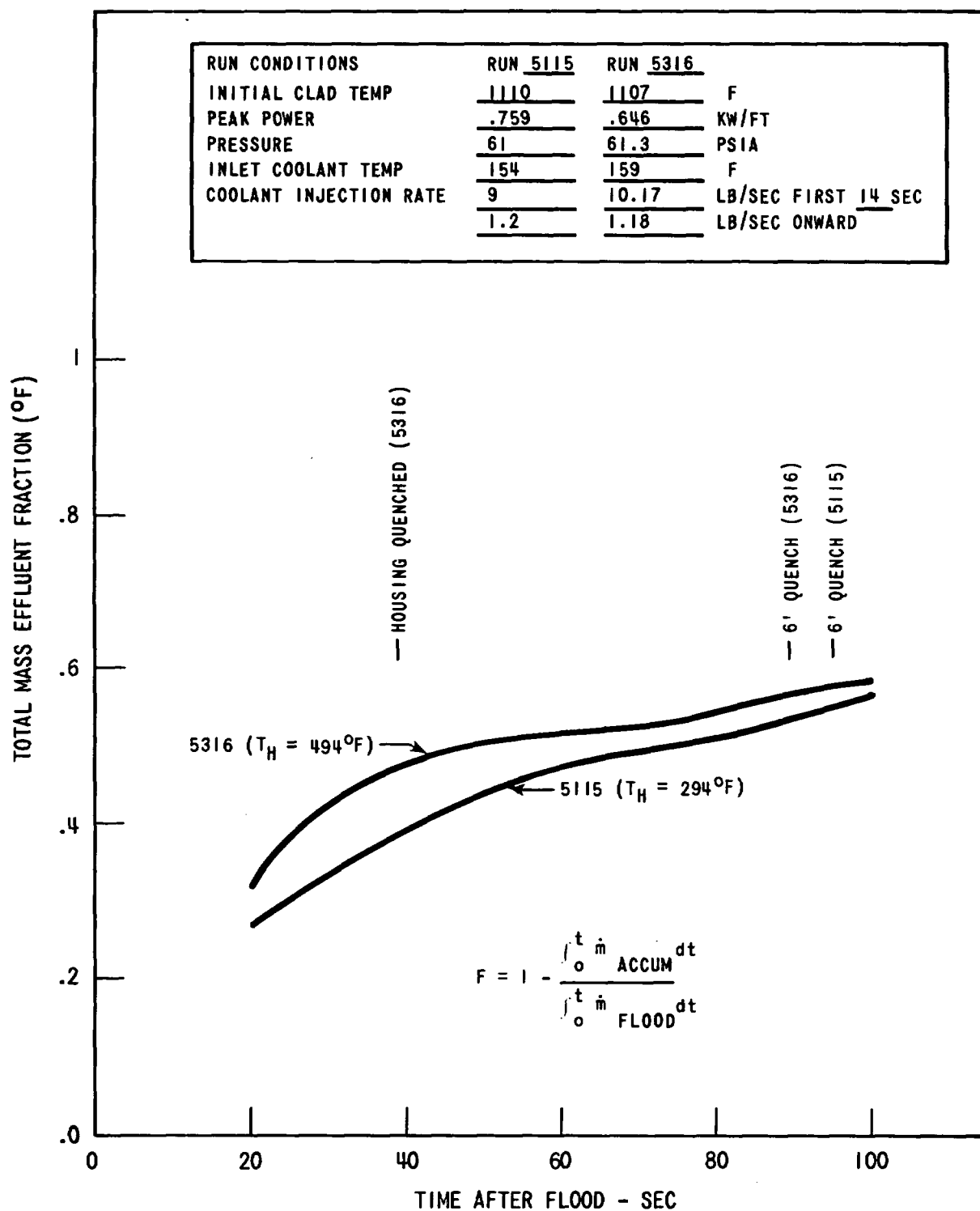


Figure 3-45. Comparison of Total Mass Effluent Fractions
For Runs 5115 and 5316

carryout was not measured directly, Figure 3-46 compares the mass accumulation in the upper plenum extension for the two runs, and the difference between the two runs is very small for the first 80 seconds. Thus, a positive statement cannot be made concerning the difference in liquid carryout for the two runs.

The combination of different injection rates, steam generation rates, etc., yielded the same quench front velocity, as shown in Figure 3-37. However, the midplane heat transfer coefficients are quite different between 10 and 40 seconds after flood as shown in Figure 3-47. The different heat transfer coefficients are reflected in the clad temperature histories shown in the same figure. The midplane clad temperature for heated housing Run 5316 remained near the maximum temperature for a longer time as a result of poorer heat transfer. The heated housing run (5316) had a significantly lower heat transfer coefficient than the unheated housing run (5115) even though the vapor flow rate was higher for heated housing run (5316), as shown in Figure 3-43. The test section axial pressure drop data indicate that there was more water below the 6 ft elevation in Run 5115 than in Run 5316 (hot housing) during the period of time when the heat transfer coefficients were different, as shown in Figure 3-44. Thus, the amount of water remaining in the bundle or the local void fraction apparently had a more dominant effect on the heat transfer coefficient than the vapor flow rate. The effect of heating the housing was to prolong the period during which the 6 ft elevation was cooled by steam and dispersed droplet flow and to delay the transition flow regime.

While a comparison of Runs 5316 and 5115 does indicate the effect of whether the energy is input by increasing the rod power or by the release of the housing stored energy, other effects such as the housing temperature and the number of heated rods influence the bundle heat release rate, local heat transfer coefficient and system response.

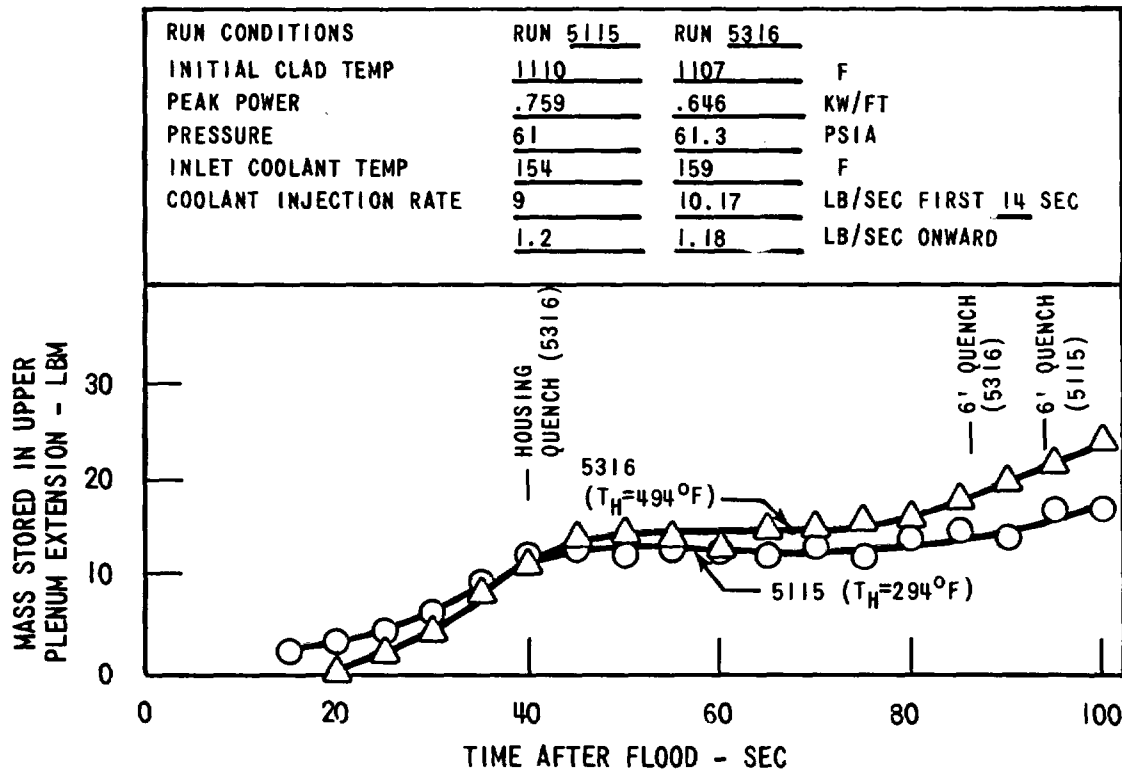


Figure 3-46. Comparison of Mass Stored in Upper Plenum Extension for Runs 5115 and 5316

RUN CONDITIONS	RUN 5115	RUN 5316	
INITIAL CLAD TEMP	1110	1107	F
PEAK POWER	.759	.646	KW/FT
PRESSURE	61	61.3	PSIA
INLET COOLANT TEMP	154	159	F
COOLANT INJECTION RATE	9	10.17	LB/SEC FIRST 14 SEC
	1.2	1.18	LB/SEC ONWARD

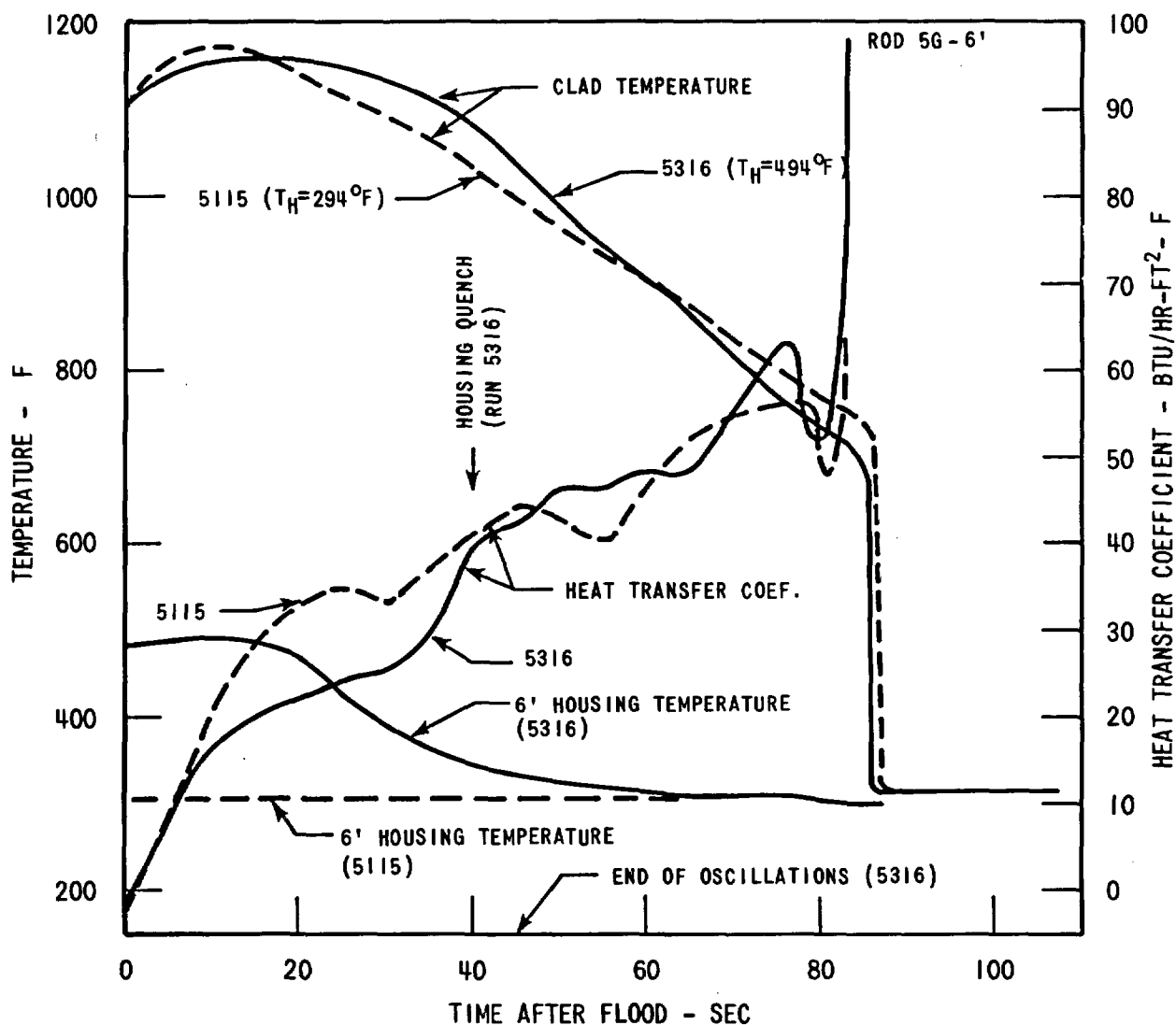


Figure 3-47. Comparison of Midplane Clad Temperature and Heat Transfer Coefficient for Runs 5115 and 5316

Another method of changing the power to flow area ratio for the bundle is to change the number of heated rods. Three such tests were run using 70, 82, and 90 heated rods (rod 2G was already failed and was unheated). The measured rod temperatures and midplane heat transfer are given in Figure 3-48, while the bundle behavior is shown in Figures 3-49, 3-50, and 3-51. The results generally reveal a trend showing that increasing the power-to-flow area ratio increases the vapor flow rate, while the bundle mass storage, flooding rate, and mass input to the bundle generally decrease as the power-to-flow ratio increases. The heat transfer coefficient, mass storage and mass flow rate curves appear to be roughly of the same shape but are shifted in time by approximately the difference in the midplane quench time of the rods.

The effect of changing the power-to-flow area ratio by increasing the rod power for the same housing temperature can be examined in Runs 4311 and 5115. The midplane heat transfer coefficients and peak clad temperatures are shown in Figure 3-52 and indicate that increasing the rod power with the same housing temperature results in a slightly higher heat transfer coefficient and only a small increase in peak clad temperature and quench time. The bundle flooding rates, downcomer behavior, mass storage, and liquid collection rates are nearly identical for these two runs as shown in Figures 3-53, 3-54, and 3-55. These data indicate that if additional energy is added to the fluid by increasing the rod power, the quench front moves up more slowly but the system transient behavior is not significantly changed. This behavior of rod power is different than that of increasing the number of heated rods. In the latter case a larger effect was observed as the power-to-flow area ratio increased.

If energy is added to the fluid by increasing the stored energy in the housing for the same rod power, a more significant effect on the system behavior and local heat transfer coefficient is observed. Runs 4311, 5316, and 5413 all

RUN CONDITIONS	RUN 4311	RUN 4412	RUN 5214	
INITIAL CLAD TEMP	1105	1107	1103	°F
PEAK POWER	.646	.646	.646	KW/FT
PRESSURE	60	61	61	PSIA
INLET COOLANT TEMP	154	159	159	°F
COOLANT INJECTION RATE	9.7	10.9	10.2	LB/SEC FIRST 14 SEC
	1.2	1.2	1.19	LB/SEC ONWARD

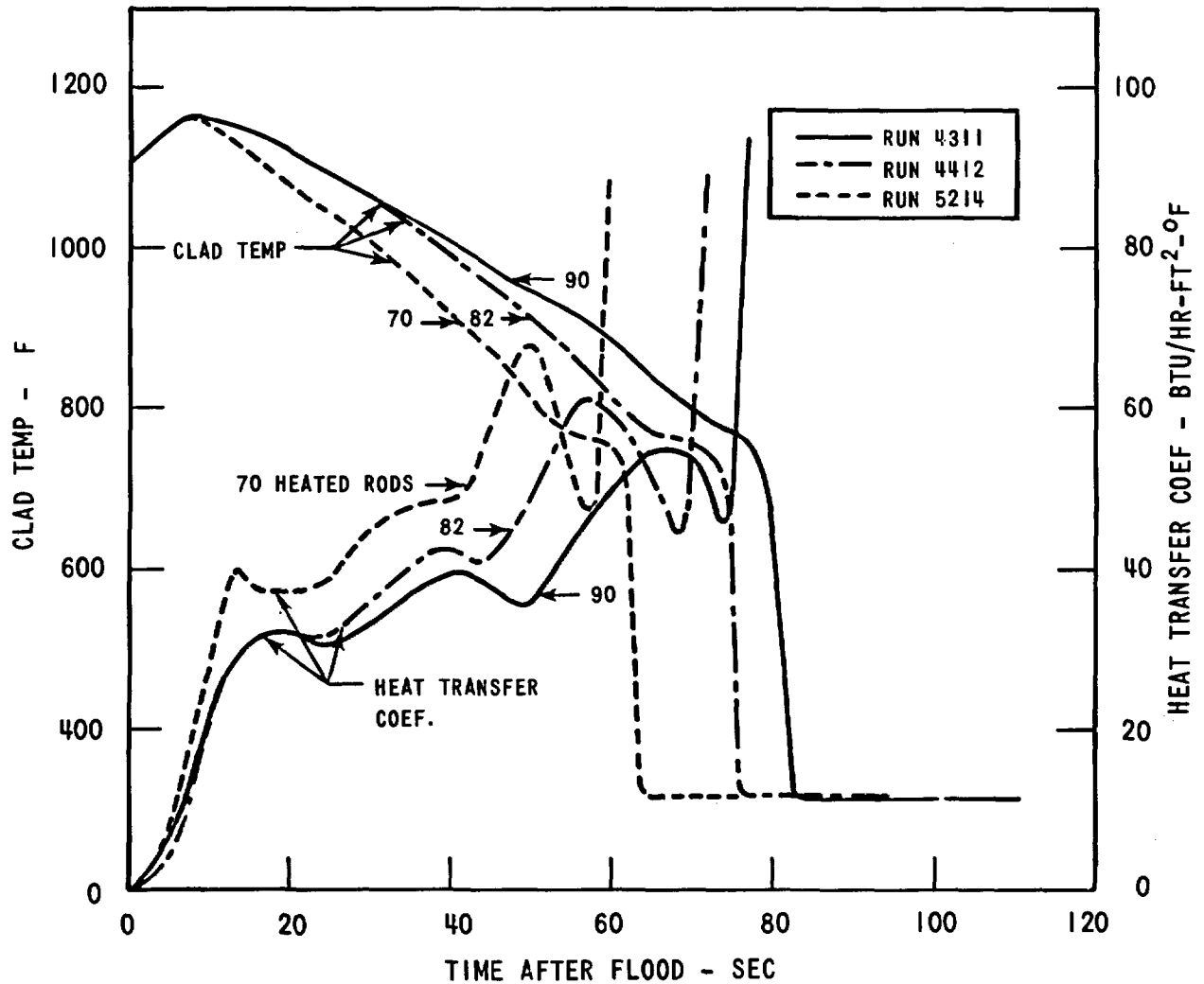


Figure 3-48. Effect of the Number of Heated Rods on Midplane Clad Temperature and Heat Transfer Coefficient

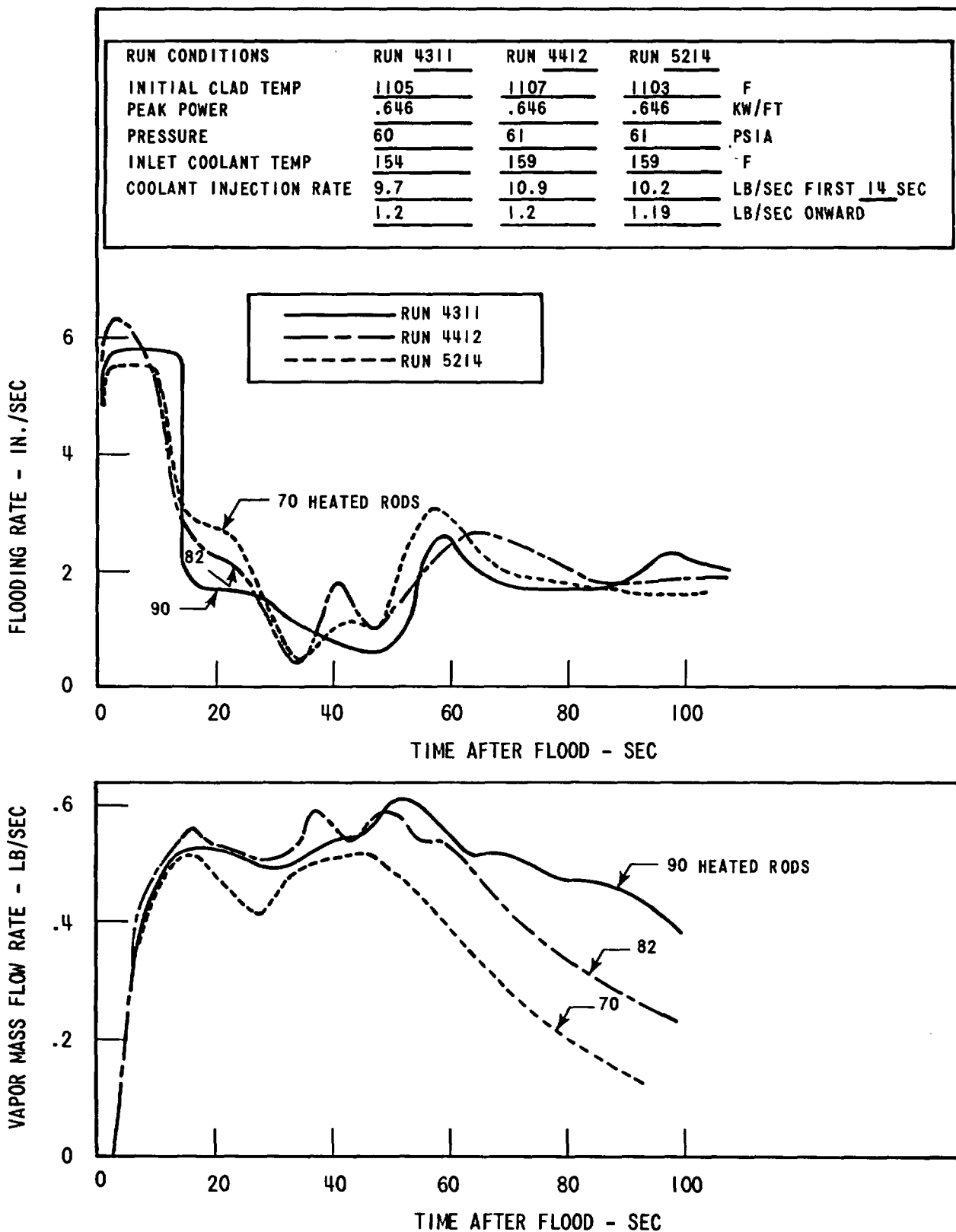


Figure 3-49. Effect of the Number of Heated Rods on the Flooding Rate and Vapor Effluent Mass Flow Rate

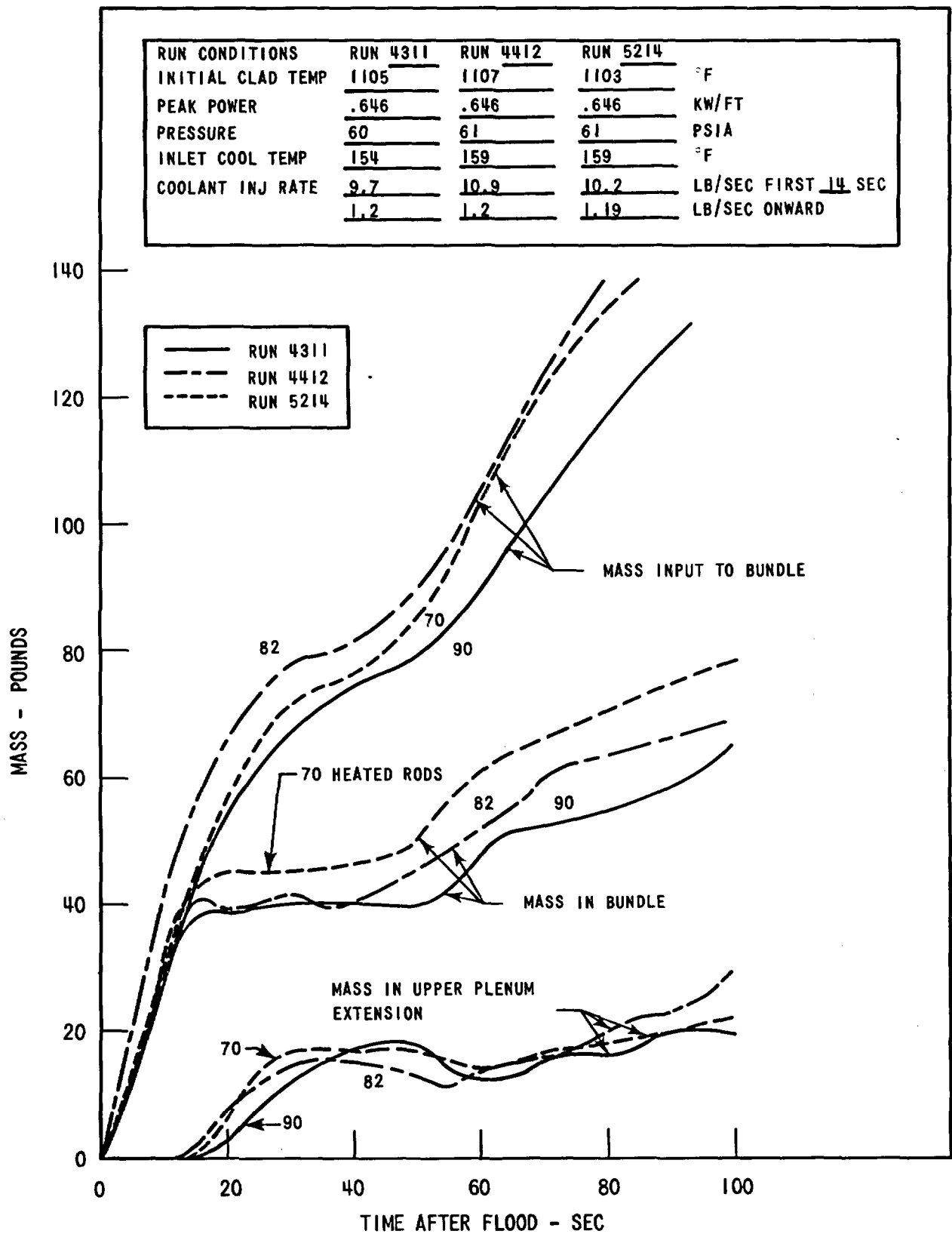


Figure 3-50. Effect of the Number of Heated Rods on the Test Section Mass Input and Storage

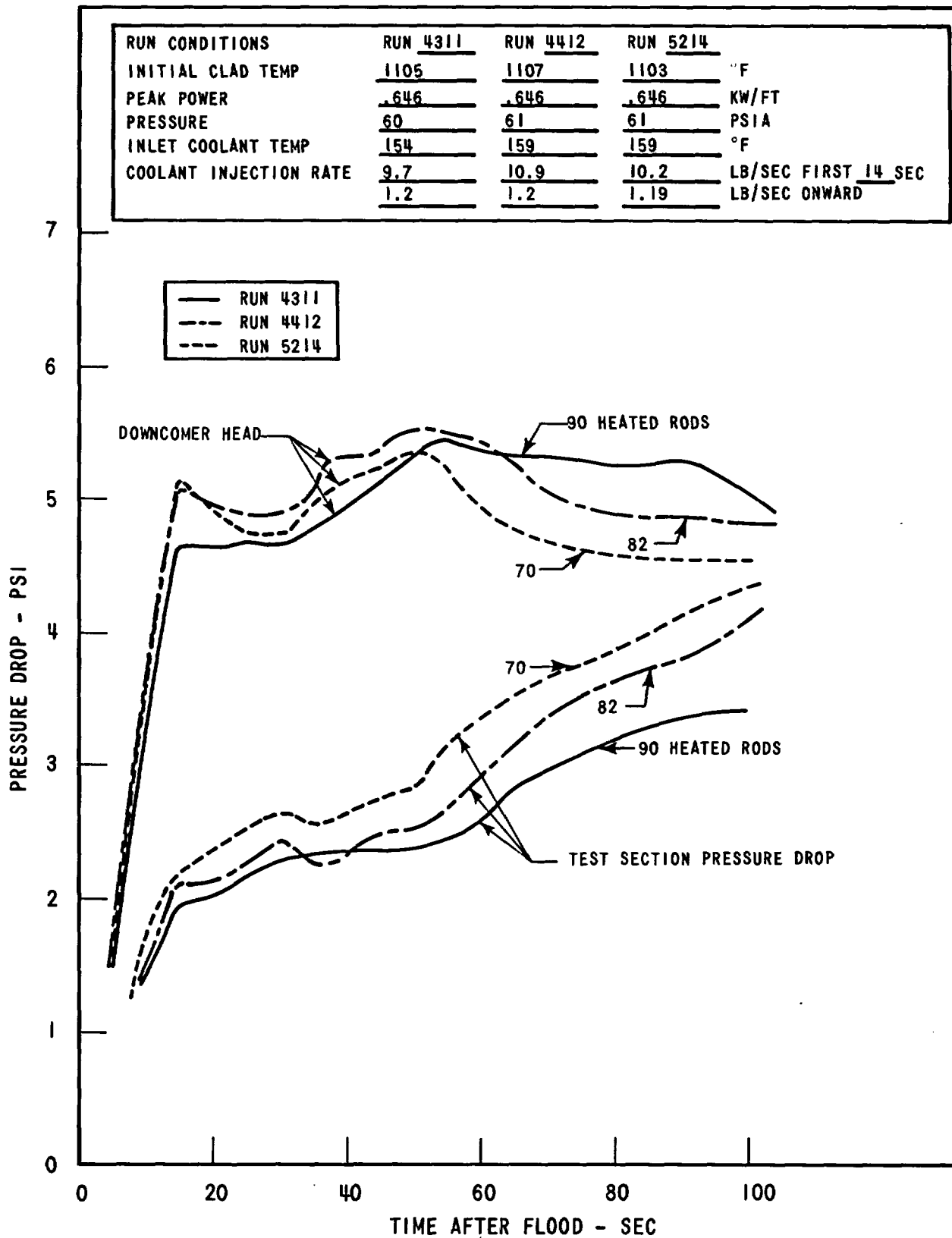


Figure 3-51. Effect of the Number of Heated Rods on Downcomer Head and Test Section Pressure Drop

RUN CONDITIONS	RUN 5115	RUN 4311	
INITIAL CLAD TEMP	1110	1105	°F
PEAK POWER	.759	.646	KW/FT
PRESSURE	61	60	PSIA
INLET COOLANT TEMP	154	154	F
COOLANT INJECTION RATE	9.0	9.7	LB/SEC FIRST 14 SEC
	1.2	1.2	LB/SEC ONWARD

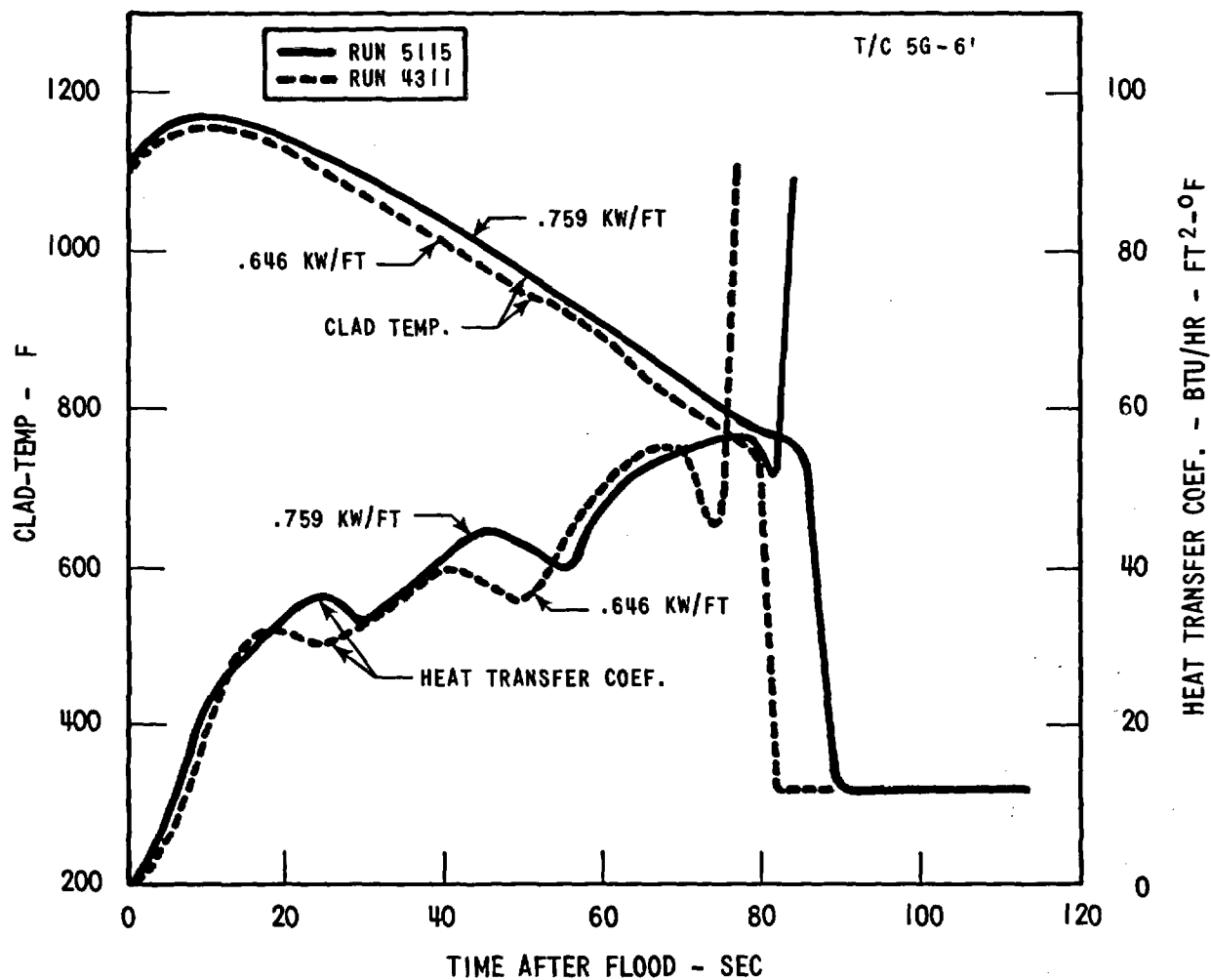


Figure 3-52. Effect of Peak Power on Midplane Clad Temperature and Heat Transfer Coefficient

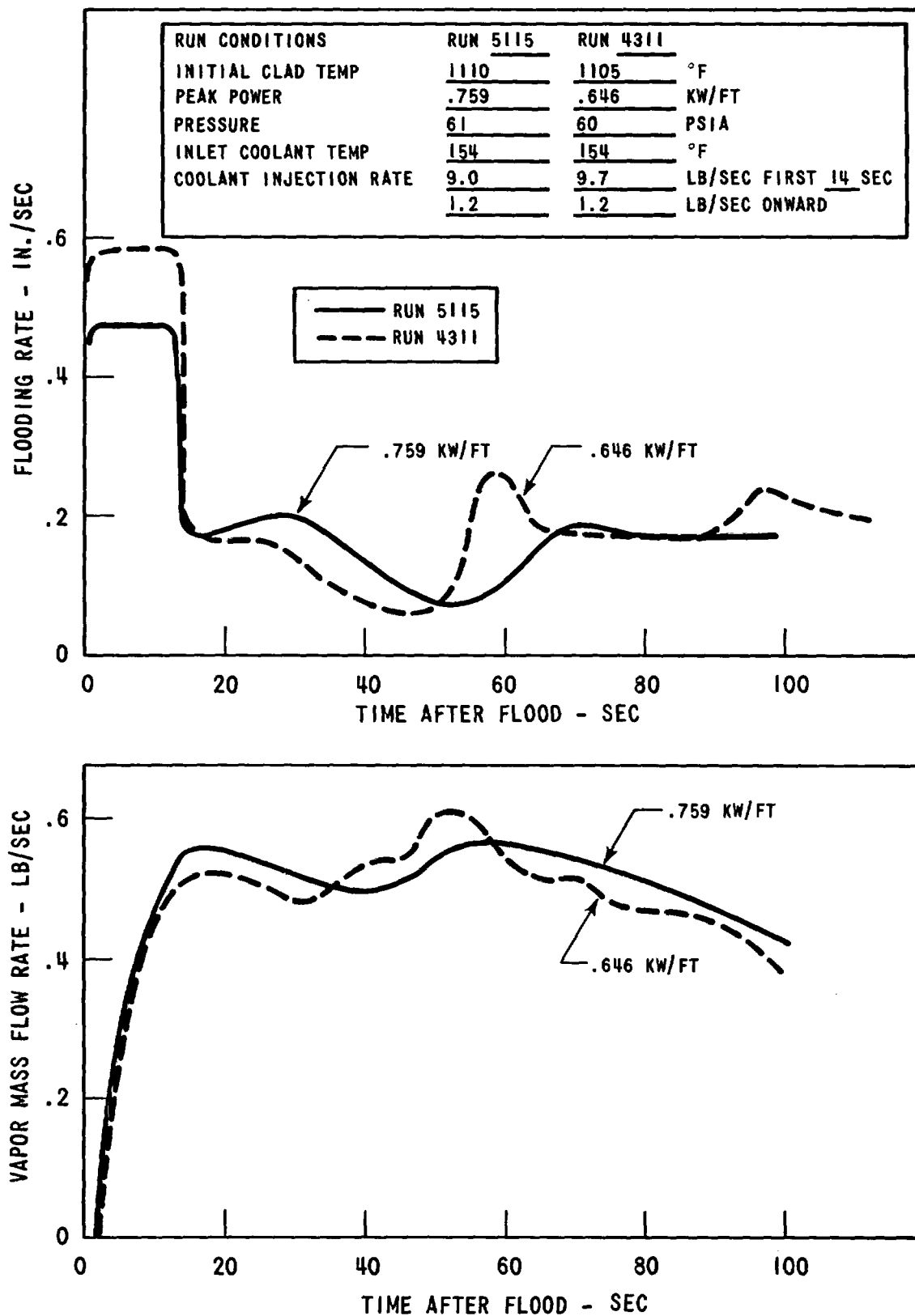


Figure 3-53. Effect of Peak Power on Flooding Rate and Vapor Mass Flow Rate

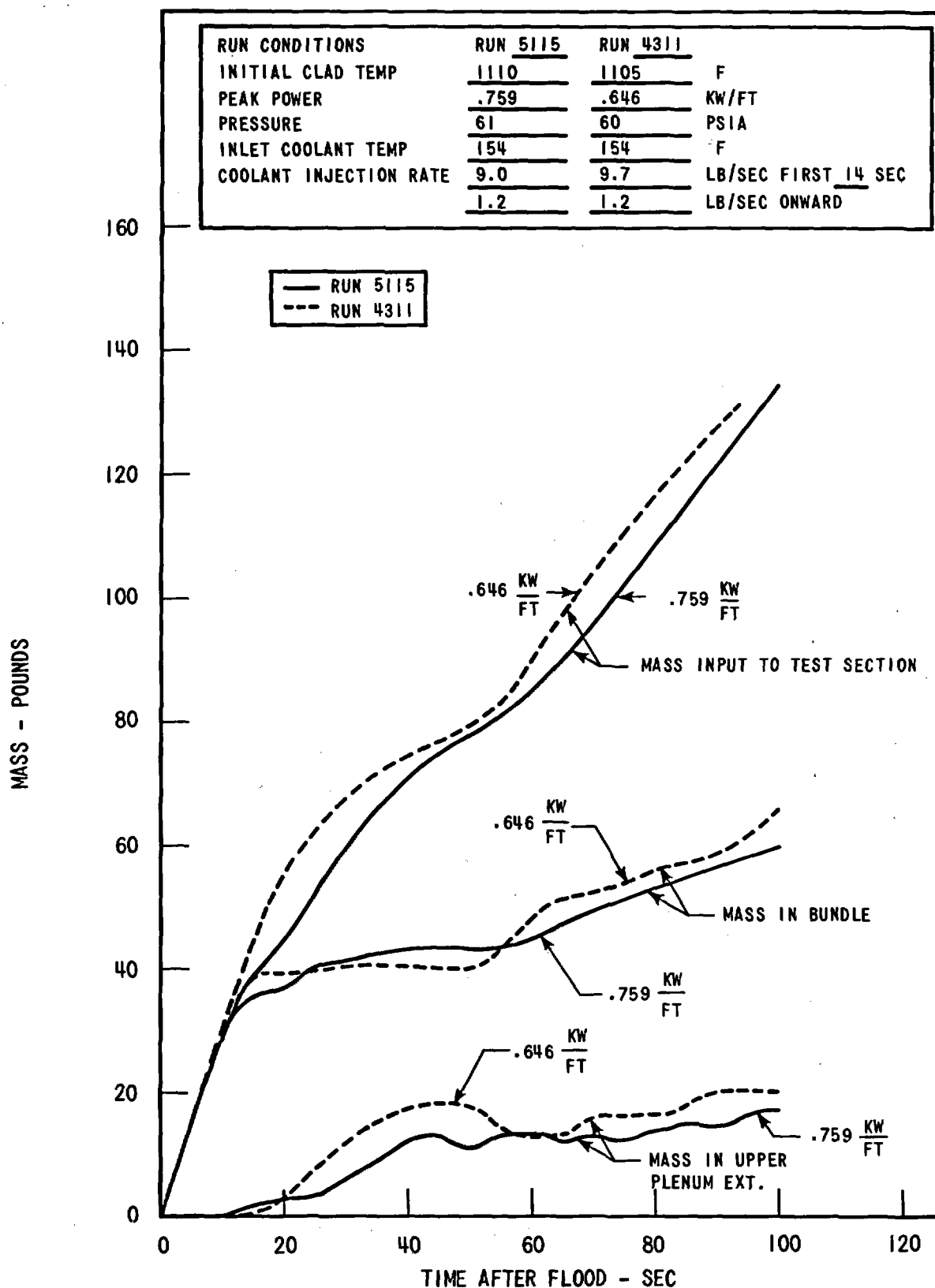


Figure 3-54. Effect of Peak Power on Test Section Mass Input and Storage

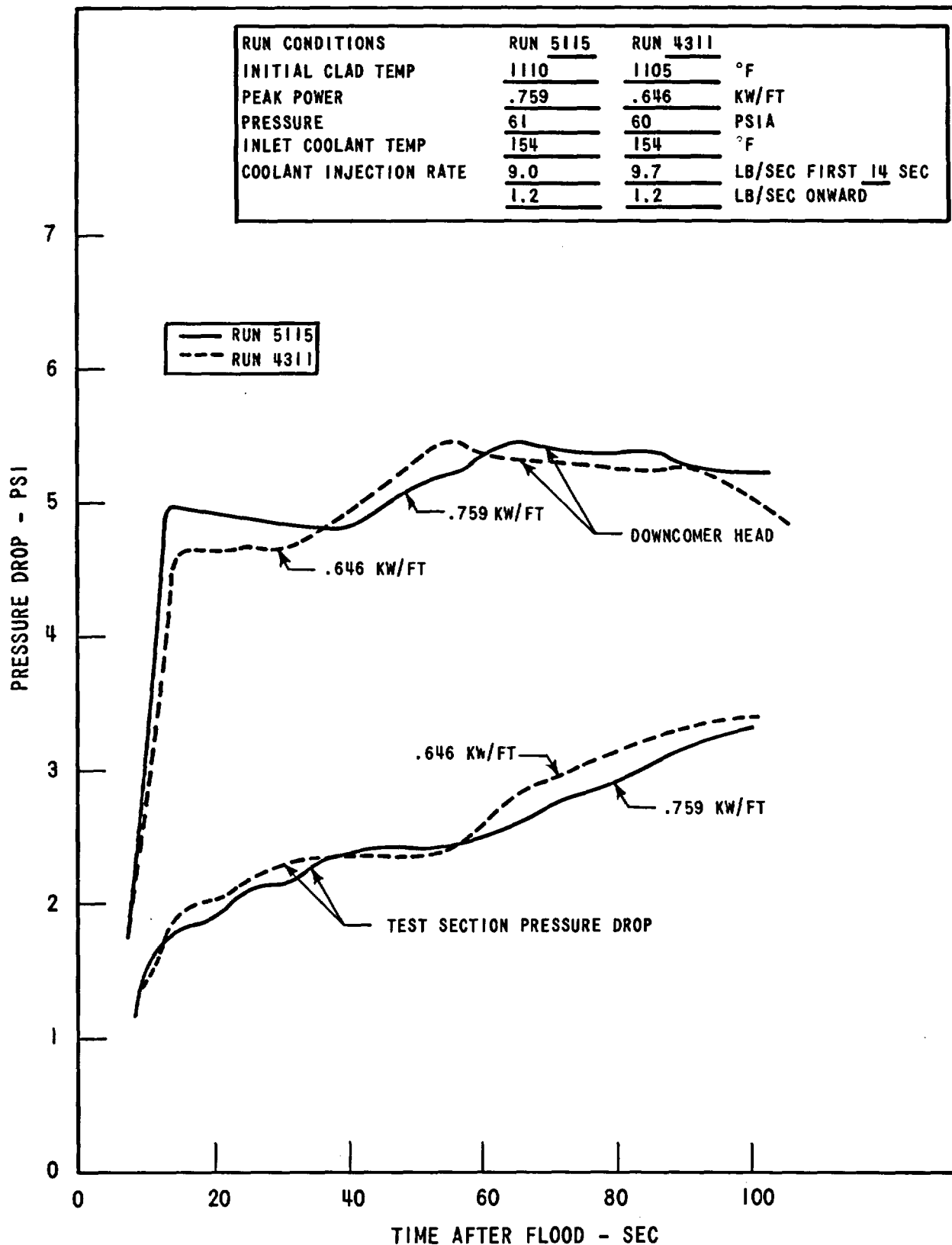


Figure 3-55. Effect of Peak Power on Downcomer Head and Test Section Pressure Drop

were conducted with the same rod power (0.646 kw/ft peak) but with average housing temperatures of 299°F, 424°F, and 614°F respectively. The effect of increasing the housing stored energy on the bundle flooding rate, vapor flow rate, mass storage, and downcomer behavior is shown in Figures 3-56, 3-57, and 3-58. Increasing the housing temperature sharply decreases the heat transfer coefficient as shown in Figure 3-59. The housing releases its heat rapidly at the lower elevations, resulting in a large generation of steam flow as shown in Figure 3-56. The large steam generation rate and resulting loop pressure drop sharply decreases the flooding rate into the bundle and results in a larger mass storage in the downcomer as shown in Figure 3-58. The mass storage in the bundle is decreased as the water is forced back into the downcomer. As the liquid level is forced into the downcomer, the steam generation rate is reduced since the amount of water in the bundle decreases. By the time the steam which has been generated has vented and the steam generation rate has been reduced, the downcomer driving head has substantially increased as shown in Figure 3-58. The larger downcomer driving head then forces the water further into the bundle, quenching more of the rods and housing and the cycle repeats until the housing is quenched. Since the housing is at a lower temperature than the rods, usually below 700°F, the water is able to wet the housing while it cannot wet the higher temperature rods. Thus, the housing causes more steam to be generated than if the housing energy were being accounted for in the higher-temperature heater rods. Therefore, the housing heat release rate and corresponding steam generation rate drive the transient until the housing is quenched. At that time the larger downcomer head rapidly forces water into the bundle, causing a sharp increase in flooding rate.

The data presented indicates that for particular test conditions the steam generation rate is the most important parameter in governing the system performance. When the housing is heated to simulate the heat input of an additional 16.8 heater rods, the large amount of energy stored at low temperatures allows the water to wet the housing, resulting in significantly more steam produced than if the same equivalent number of heater rods had been present. The housing quenching behavior is responsible for driving the large liquid level oscillations during the early stages of reflood. Accounting for

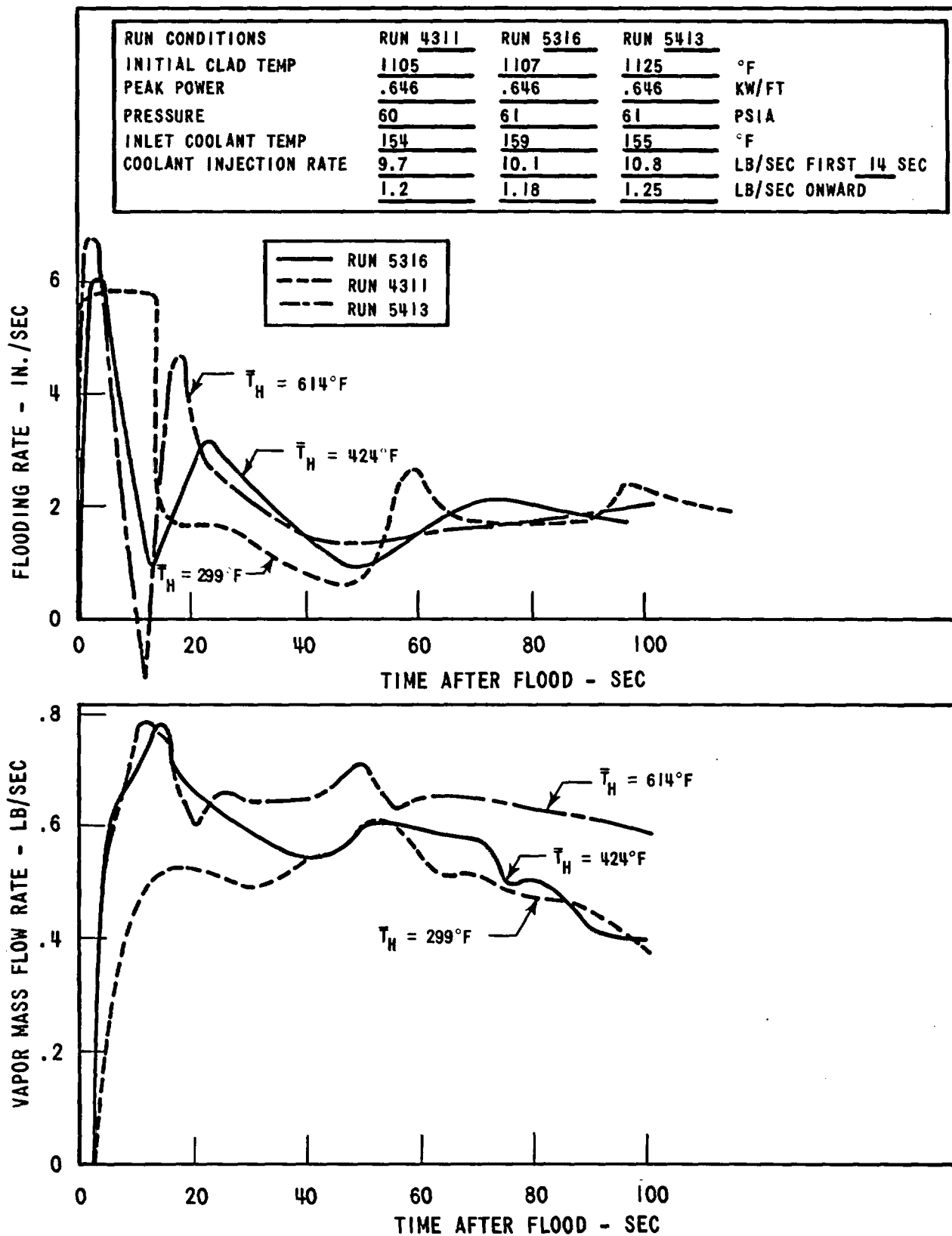


Figure 3-56. Effect of Housing Temperature on Test Section Flooding Rate and Vapor Mass Flow Rate

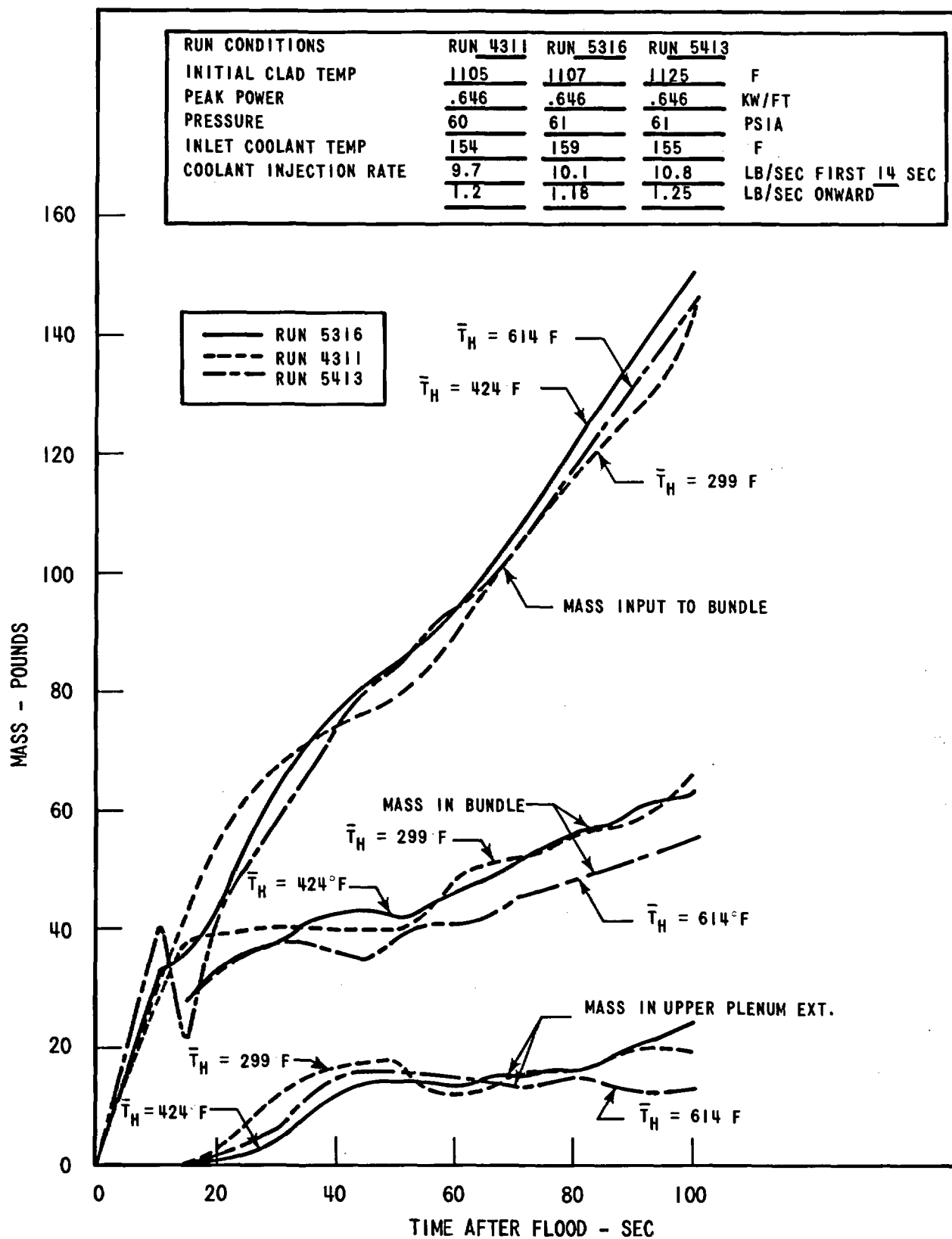


Figure 3-57. Effect of Housing Temperature on Test Section Mass Input and Storage

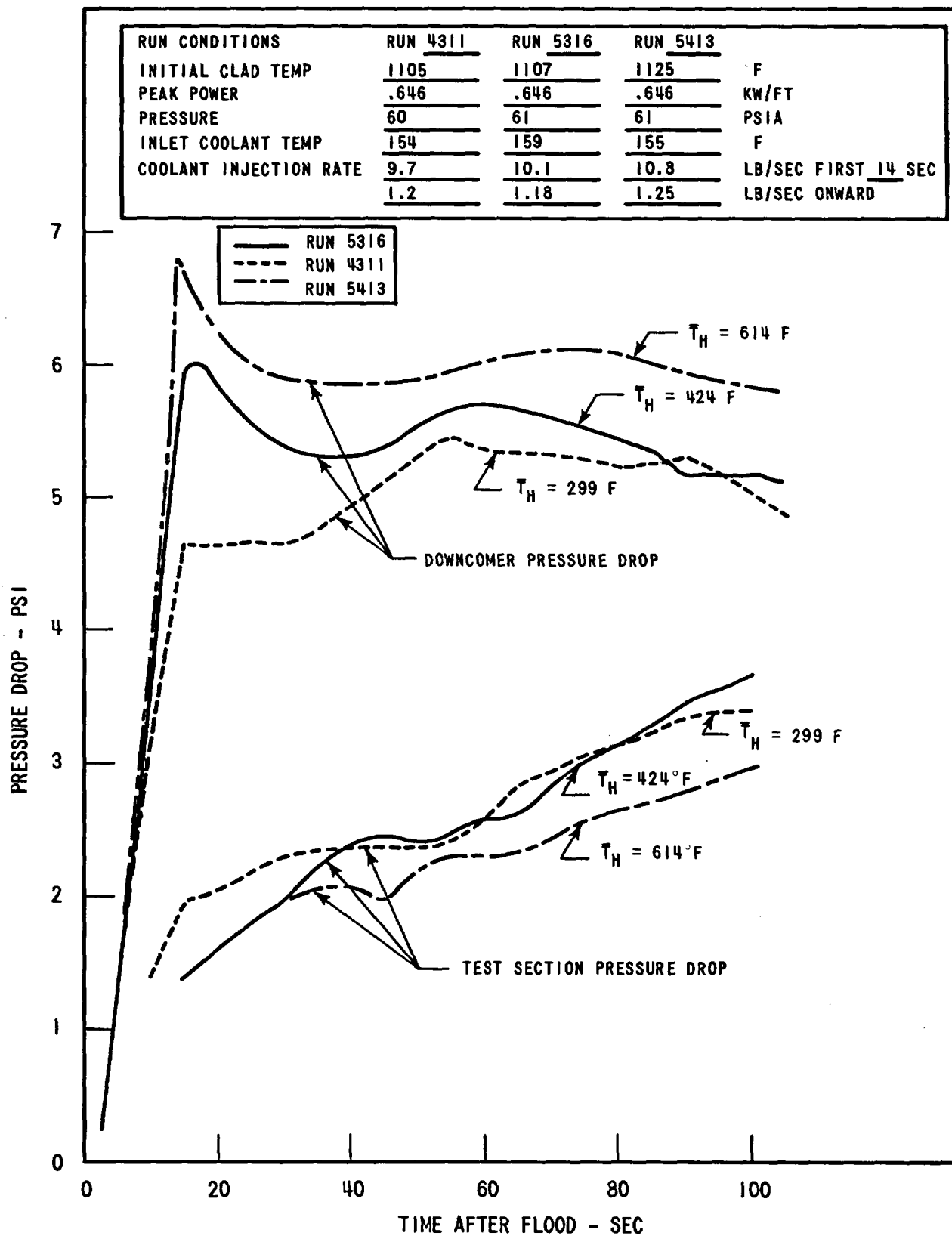


Figure 3-58. Effect of Housing Temperature on Downcomer and Test Section Pressure Drops

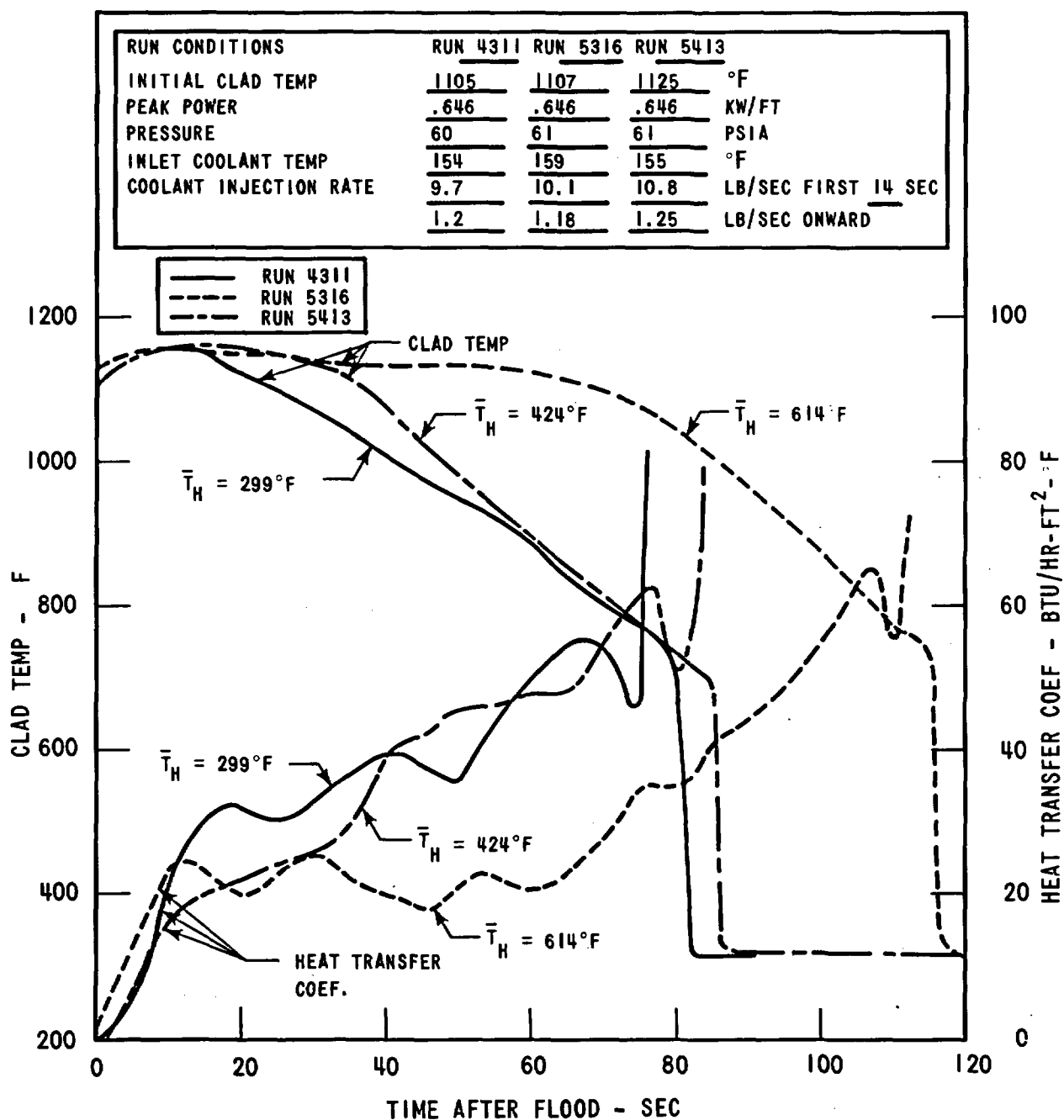


Figure 3-59. Effect of Housing Temperature on Midplane Clad Temperature and Heat Transfer Coefficient

the energy release of 16.8 additional heater rods by increasing the rod power does not result in the same steam generation rate and, therefore, the system transient response as obtained by heating the housing.

The data reported in this section indicates that if the housing is heated to the saturation temperature and the rod peak power is varied, the midplane heat transfer coefficient increases slightly as the power is raised. The opposite trend is noted (Section 3.5) when the housing was heated according to the FLECHT housing criterion. However, the housing temperatures are significantly different for different peak powers when the FLECHT housing criterion is used. The heat transfer coefficients obtained during these runs were nearly the same initially, but the steam generated by the housing resulted in a slower moving quench front and thus a lower heat transfer coefficient later in time.

In the Phase B tests the local heat release and steam generation rate from housing will have to be equal to the equivalent number of rods, or the transient behavior of the system will be forced incorrectly by the housing quenching behavior. Presently, no one easy method exists to accomplish this goal, and tests, already indicated in the Phase B test matrix, will be utilized to investigate some of the following methods proposed to model the housing heat release rate:

1. Decrease the housing temperature but continue to supply heat to the housing so that the total housing energy is released over the correct time period.
2. Increase the power to the outer two rows of heater rods so that the correct power per flow area ratio is maintained and the housing is heated to the saturation temperature. The effect of the location of the hot rods can be examined by using a random pattern of rods with higher power.

3.5 PARAMETER EFFECTS

Bundle and system parameters were varied to determine their effects on the reflooding behavior of the FLECHT-SET system. The bundle parameters were inlet subcooling, initial clad temperature, rod power, containment pressure, and injection rate. These are the same parameters varied in the FLECHT program to determine the reflood heat transfer sensitivity (References 1 and 2).

In the FLECHT program one parameter could be easily varied and the reflooding heat transfer sensitivity determined. In the FLECHT-SET tests the flooding rate was a dependent variable determined by the system response to the bundle parameter changes. Since the system responded to the single parameter change, the effects of this change are difficult to identify and quantify. It should also be noted that some of the earlier runs would have been repeated if both additional time had been available and excessive rod thermocouple failures had not forced termination of the testing. Similar parameter variations will be investigated in the Phase B series.

3.5.1 Inlet Coolant Subcooling

The effect of inlet subcooling on injection water temperature was studied at both 20 and 60 psia containment pressures and was found to be a sensitive parameter. Unfortunately, the coolant subcooling could not be reduced sufficiently at 60 psia to cover the same subcooling range and subcooling effects as at the lower pressure.

As the injection water subcooling decreased:

1. The steam flow increased.
2. The mass stored in the bundle decreased.
3. The resulting flooding rate decreased.
4. The midplane heat transfer coefficient decreased.

The hotter injection water was more easily vaporized in the bundle, resulting in more bundle steam generation. Since the loop resistance was fixed, the increased steam flow increased the loop pressure drop, which retarded the

bundle flooding rate and resulted in less mass inventory stored in the bundle. The calculated flooding rate for the two cases is shown in Figure 3-60, and the bundle mass inventory and the liquid collected are shown in Figure 3-61.

The effect of the decreased injection water subcooling on the quench front and midplane heat transfer coefficient is shown in Figures 3-62 and 3-63, respectively. Decreasing the subcooling results in a decrease in quench front velocity, since both the flooding rate and bundle mass inventory have decreased. The decreased quench front velocity is similar to that observed in FLECHT data (Reference 2).

The midplane heat transfer coefficient was observed to be lower for the hotter injection water case before temperature turnaround. The quench time for Run 3320 was also observed to be longer than for Run 3117. When comparing the subcooling effect in the FLECHT data at 20 psia (Reference 1), the subcooling effect was observed to have a smaller effect on the FLECHT midplane heat transfer coefficient since the flooding rate was constant and was not influenced by the steam generation as in FLECHT-SET. The rod temperature rise was also observed to be higher for the lower subcooling case in Run 3320 due to the reduced flooding rate and midplane heat transfer coefficient.

The decreased subcooling effect on the heat transfer coefficient is more pronounced at later times since both the flooding rate is lower and less mass is stored in the bundle. The decreased subcooling increases the void fraction at the hot spot because of the greater distance from the quench front and results in a decreased heat transfer coefficient. In the FLECHT tests (Reference 2), the decreased injection subcooling had a similar effect although the flooding rate remained constant.

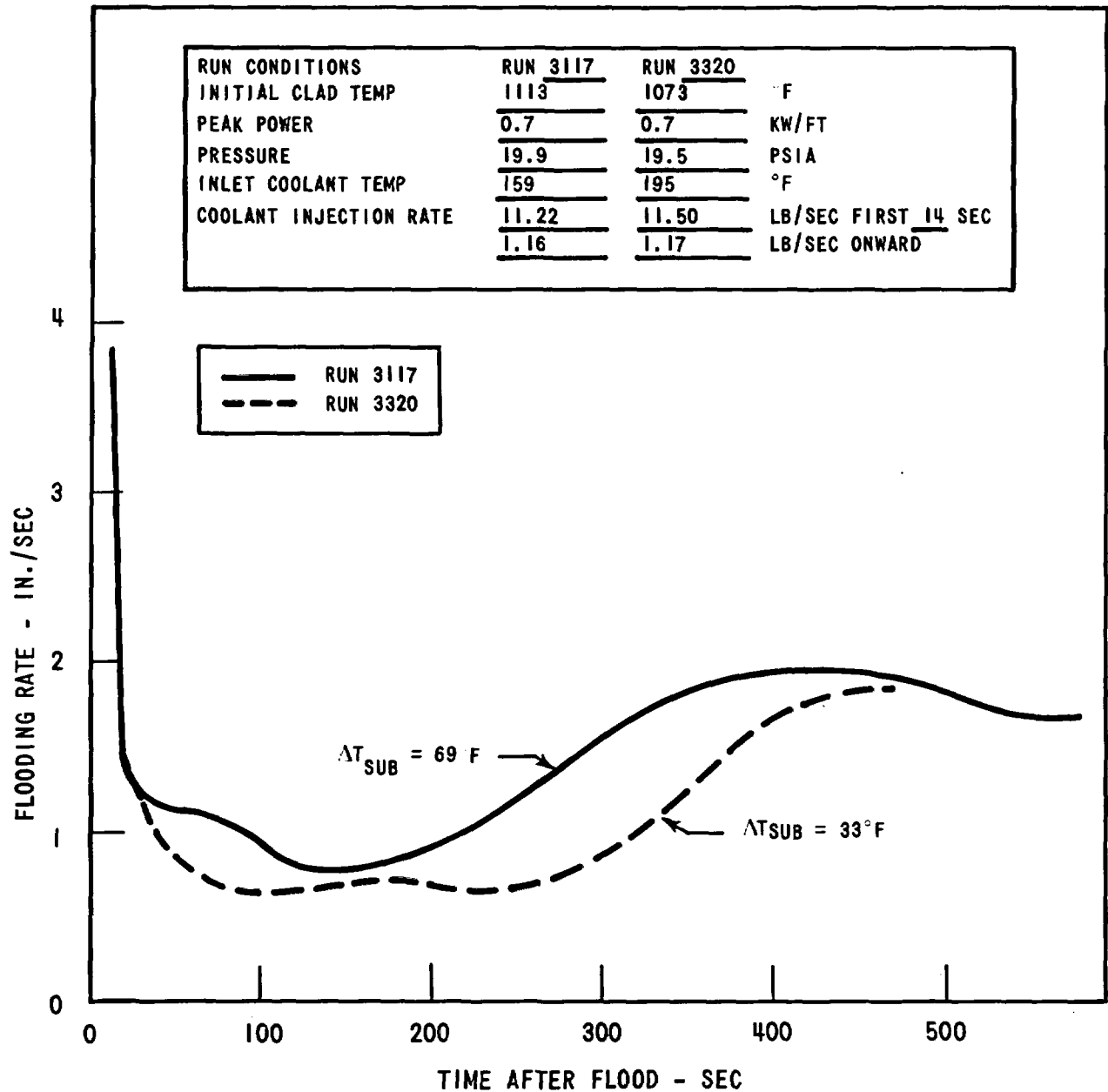


Figure 3-60. Effect of Inlet Subcooling on Flooding Rate at 20 Psia Containment Pressure

RUN CONDITIONS		RUN 3117	RUN 3320	
INITIAL CLAD TEMP		1113	1073	F
PEAK POWER		0.7	0.7	KW/FT
PRESSURE		19.9	19.5	PSIA
INLET COOLANT TEMP		159	195	F
COOLANT INJECTION RATE		11.22	11.50	LB/SEC FIRST 14 SEC
		1.16	1.17	LB/SEC ONWARD

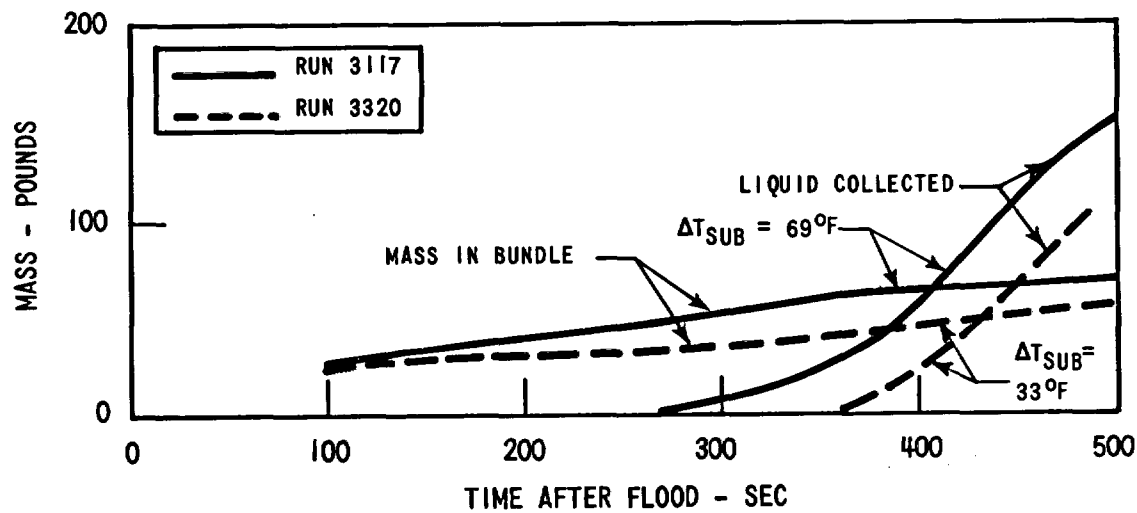


Figure 3-61. Effect of Inlet Subcooling on Mass Stored in the Bundle and Liquid Collected in Separator Tank at 20 Psia Containment Pressure

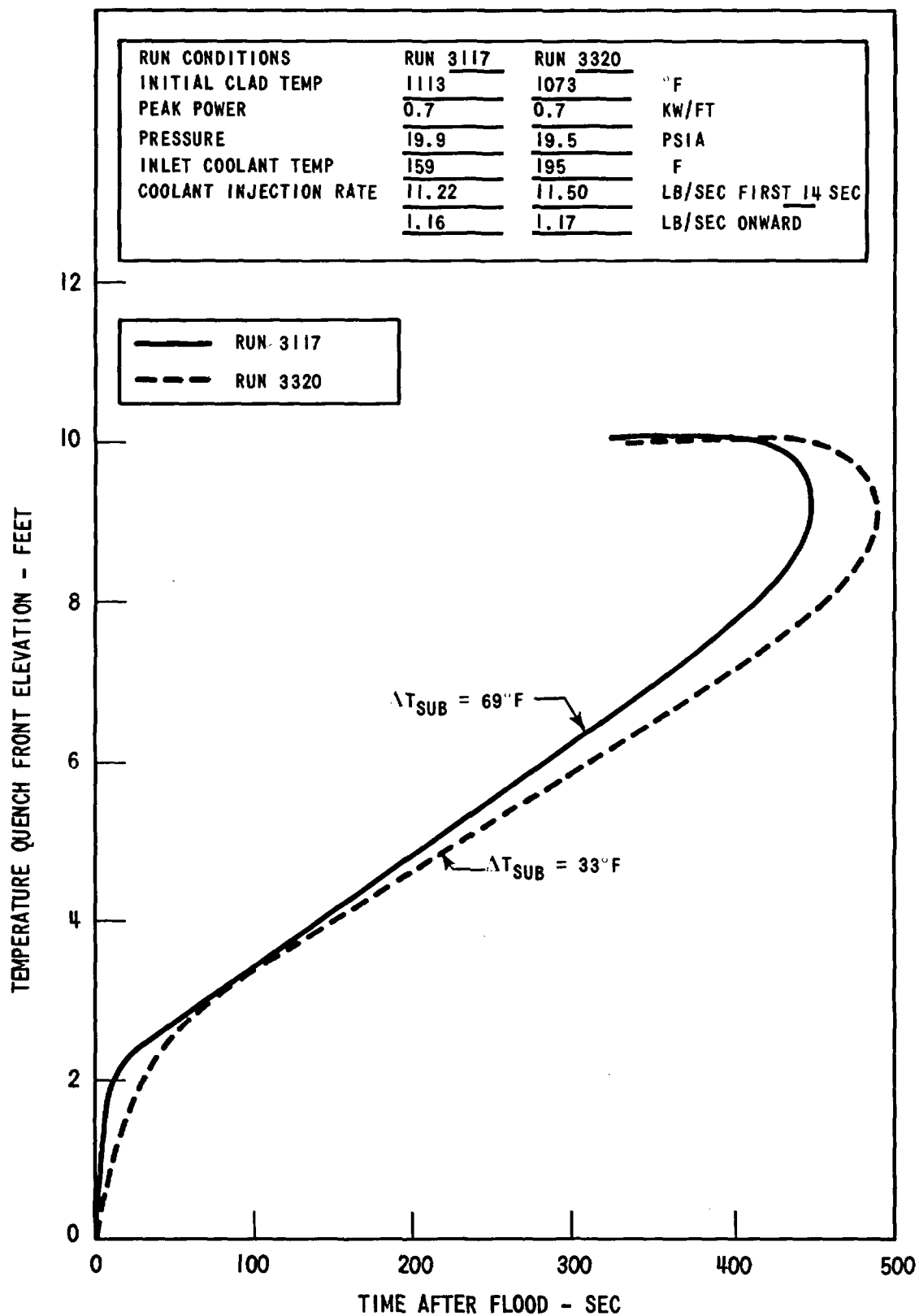


Figure 3-62. Effect of Inlet Subcooling on the Rod Quench Front Envelope at 20 Psia Containment Pressure

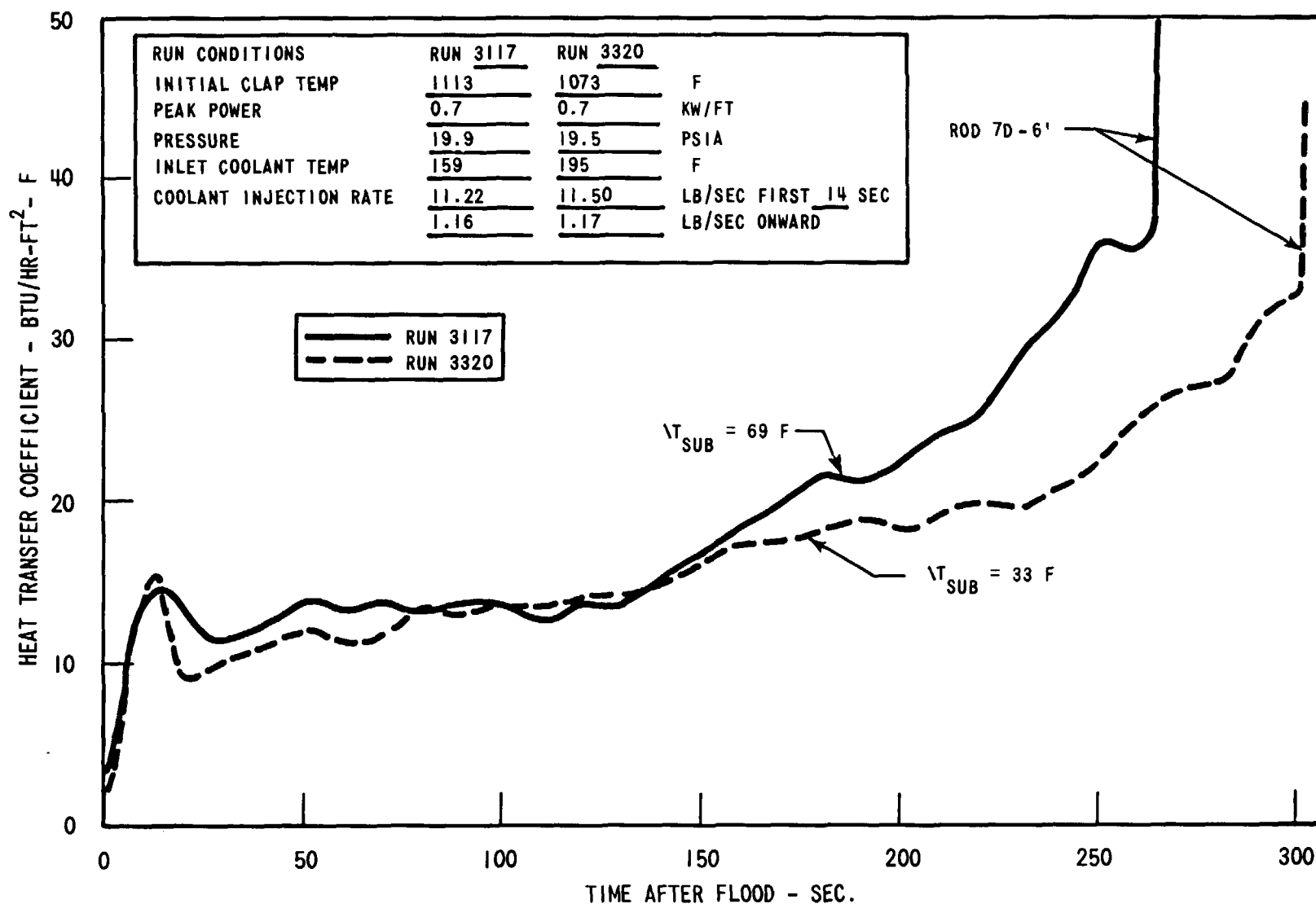


Figure 3-63. Effect of Inlet Subcooling on Midplane Heat Transfer Coefficient at 20 Psia Containment Pressure

Plots of the steam flow, mass storage in the bundle, and the midplane heat transfer coefficient are shown in Figures 3-64 and 3-65 for 60 psia. These plots indicate that the subcooling effect is not nearly as sensitive as for 20 psia.

It is expected that the subcooling effect would not be as sensitive at higher pressures for the same degree of subcooling. Even though the coolant would start boiling at nearly the same elevation in the core for the same flooding rate, the density of saturated steam is 2.8 times higher at 60 psia than at 20 psia. The void fraction in the bundle, the steam velocity, and possibly the liquid entrainment would all be lower at higher pressures. Thus, one would expect that very early in the transient the midplane heat transfer coefficient would be improved at 20 psia over that at 60 psia by decreased subcooling because of the higher steam velocity and liquid entrainment. Later in time, however, the reduction of the midplane heat transfer coefficient should be greater at 20 psia than at 60 psia because of the higher void fraction and greater distance from the quench front at 20 psia.

3.5.2 Initial Clad Temperature

The effect of initial clad temperature was investigated at both 20 psia and 60 psia containment pressures. The results generally showed similar trends at both pressures, namely a faster quench front rise and a higher midplane heat transfer coefficient for lower initial clad temperatures.

The 20 psia runs analyzed were Run 3117 ($T_{\text{initial}} = 1113^{\circ}\text{F}$), Run 2718 ($T_{\text{initial}} = 1400^{\circ}\text{F}$), and Run 2919 ($T_{\text{initial}} = 912^{\circ}\text{F}$). The gross bundle parameters: midplane temperature rise, turnaround time, and quench time, are shown in Figure 3-66. The temperature rise and turnaround time both decreased with increasing initial temperature while the quench time increased (Figure 3-66). Previous FLECHT results (Reference 2) also indicate that temperature rise and turnaround time decrease with increasing initial temperature. However, the FLECHT data indicate that the quench time is not sensitive to the initial temperature, whereas the FLECHT-SET data clearly show that as the initial temperature increases the resulting quench time increases. The increased quench time in FLECHT-SET is due to the feedback effect of the bundle energy

RUN CONDITIONS	RUN 4923	RUN 3928	
INITIAL CLAD TEMP	1111	1102	F
PEAK POWER	0.7	0.7	KW/FT
PRESSURE	61.0	61.9	PSIA
INLET COOLANT TEMP	158	201	F
COOLANT INJECTION RATE	10.52	12.02	LB/SEC FIRST 14 SEC
	1.19	1.37	LB/SEC ONWARD

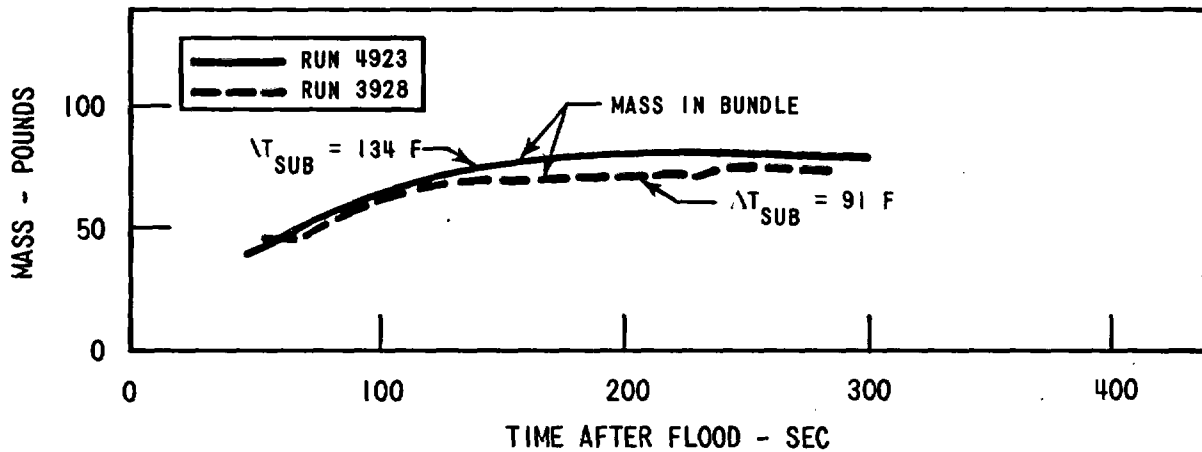
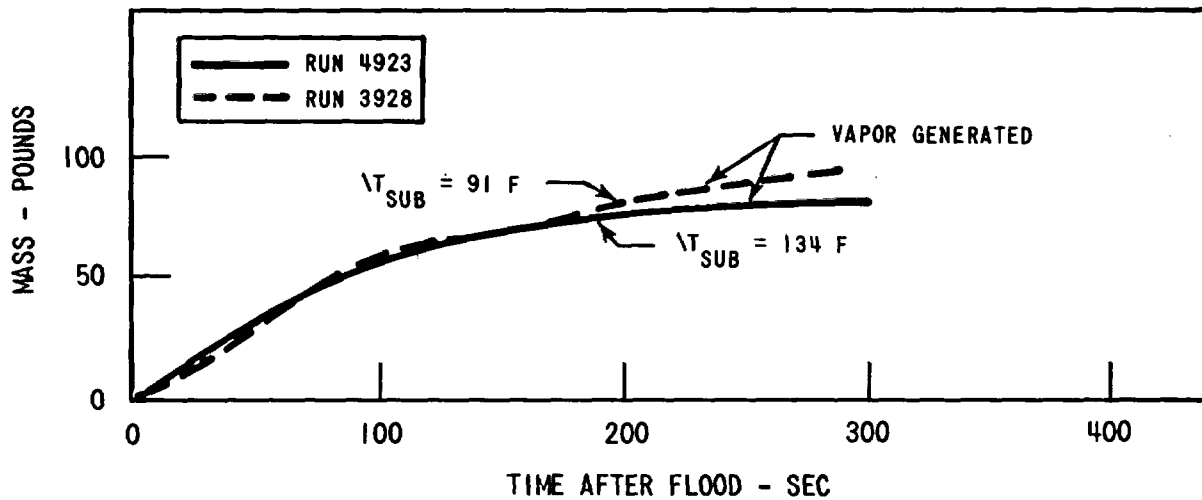


Figure 3-64. Effect of Inlet Subcooling on the Vapor Generated and Mass Stored in the Bundle at 60 Psia Containment Pressure

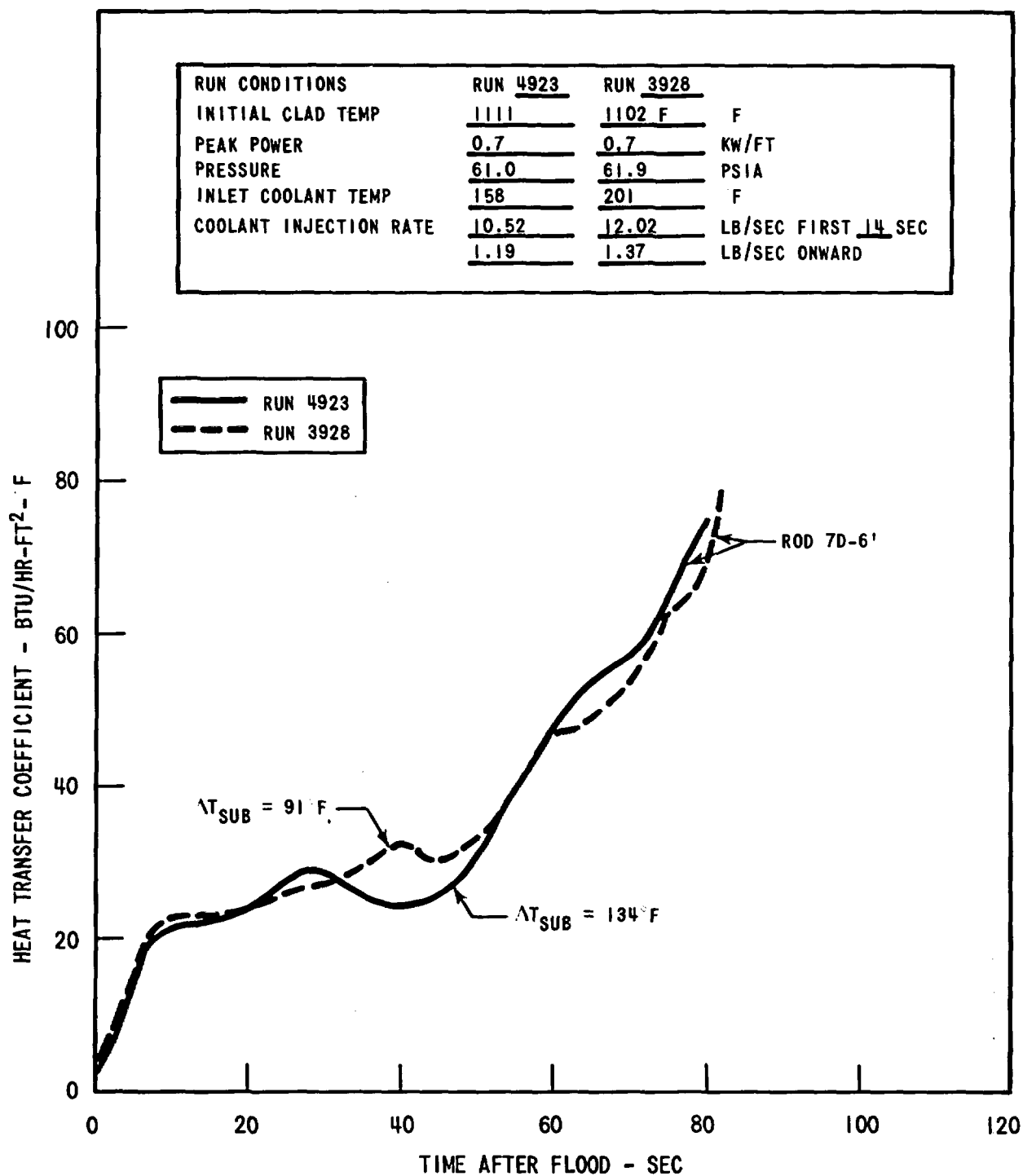


Figure 3-65. Effect of Inlet Subcooling on the Midplane Heat Transfer Coefficient at 60 Psia Containment Pressure

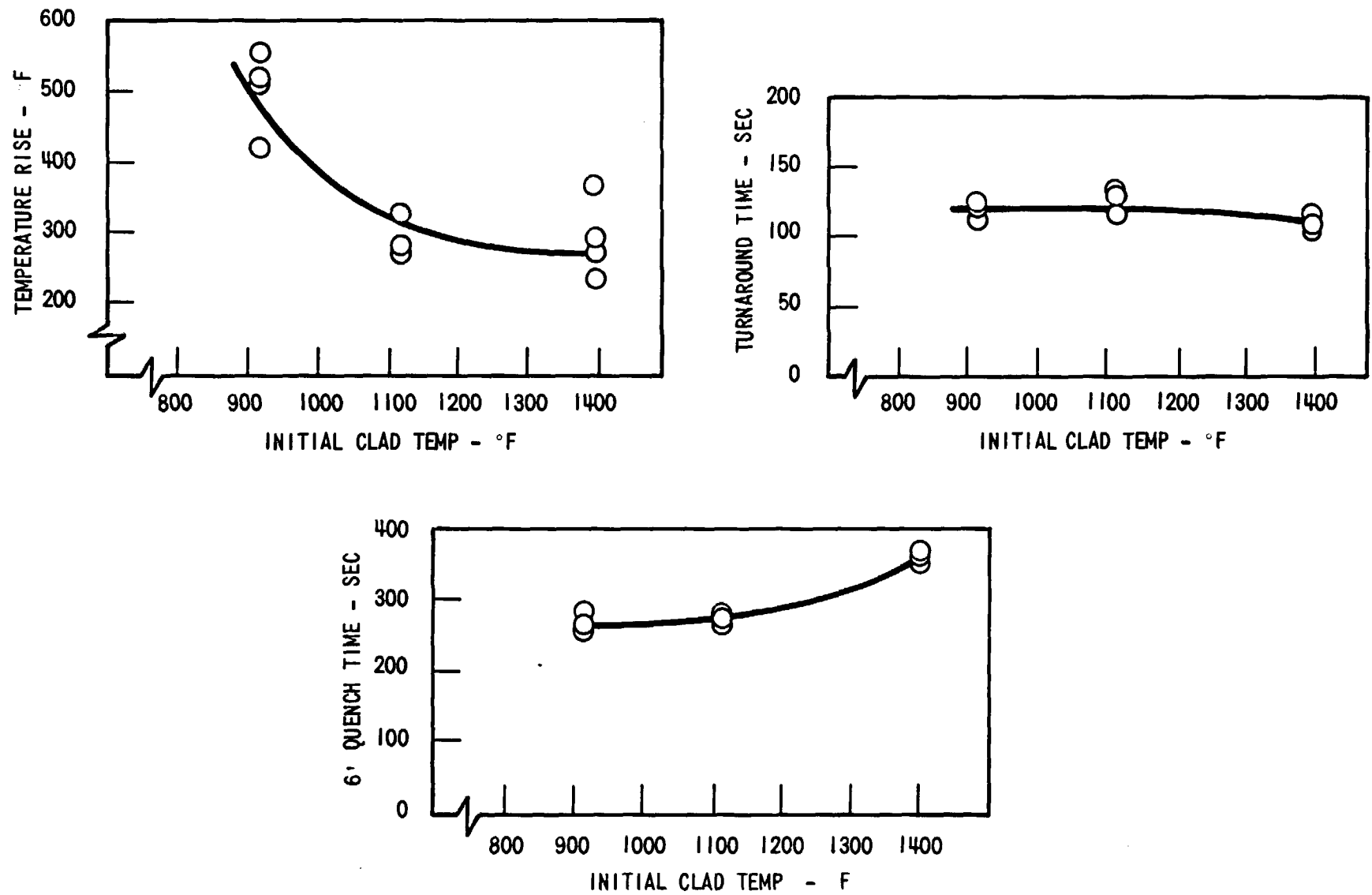


Figure 3-66. Effect of Initial Clad Temperature on 6' Temperature Rise, Turnaround Time, and Quench Time at 20 Psia Containment Pressure

heat releases on the flooding rate. The rod and the housing initial temperatures are increased for Run 2718 such that the total stored energy in the bundle is increased. Since more energy must be removed for a given loop pressure drop, and therefore steam flow rate, it takes longer to quench the bundle.

A closer examination of the data indicates that increasing the initial clad temperature decreases the mass storage in the bundle and the average flooding rate, and delays the time at which liquid collection begins as shown in Figure 3-67. The calculated flooding rates are shown in Figure 3-68 and the quench front profile in Figure 3-69 for these cases. The measured midplane heat transfer coefficient is shown in Figure 3-70 and indicates that the heat transfer coefficient is nearly the same for all three runs in the very early portion of the transient ($t < 20$ seconds), after which the heat transfer coefficient for the higher initial temperature runs increased more slowly.

The observed heat transfer behavior can be related to the mass storage in the bundle at different times. For both Runs 3117 and 2919, the mass storage is greater than for Run 2718, resulting in an increase in the midplane heat transfer coefficient. The flooding rate also has an effect on the heat transfer behavior but it appears to be less sensitive than the bundle mass storage effect.

Similar trends in temperature rise, turnaround time, and quench time were observed in the 60 psia runs as shown in Figure 3-71. The runs analyzed in detail were: Run 4825 ($T_{\text{initial}} = 712^{\circ}\text{F}$), Run 4923 ($T_{\text{initial}} = 1111^{\circ}\text{F}$), and run 4024 ($T_{\text{initial}} = 1402^{\circ}\text{F}$). The details of the runs were, however, different than those observed at 20 psia.

The vapor flow and, therefore, the loop pressure drop were observed to increase with increasing initial temperature. This resulted in decreased mass storage in the bundle as the initial temperature increased as shown in Figure 3-72. The increased mass storage in the bundle for the lower

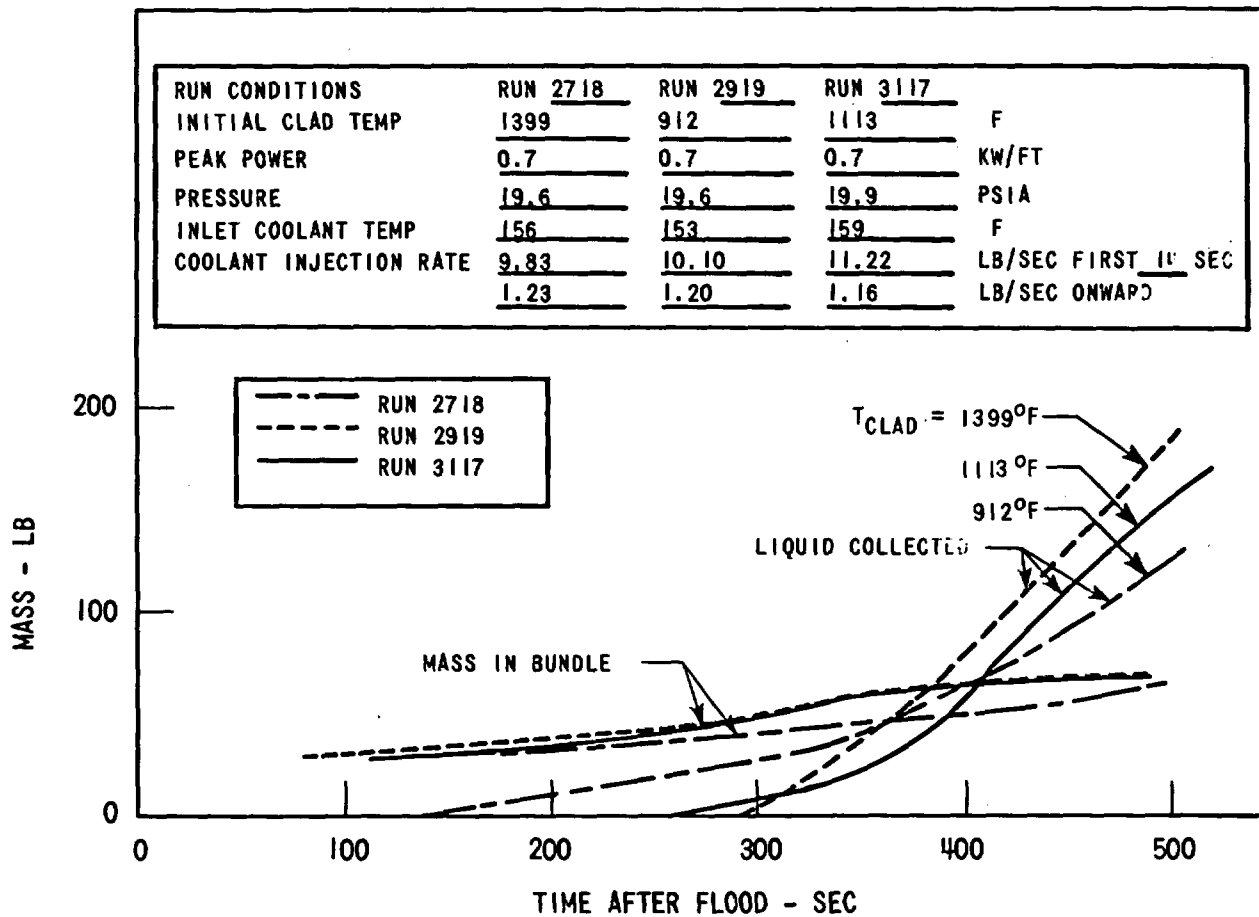


Figure 3-67. Effect of Initial Clad Temperature on the Mass Remaining in the Bundle and the Mass of Liquid Collected in the Separator Tank at 20 Psia Containment Pressure

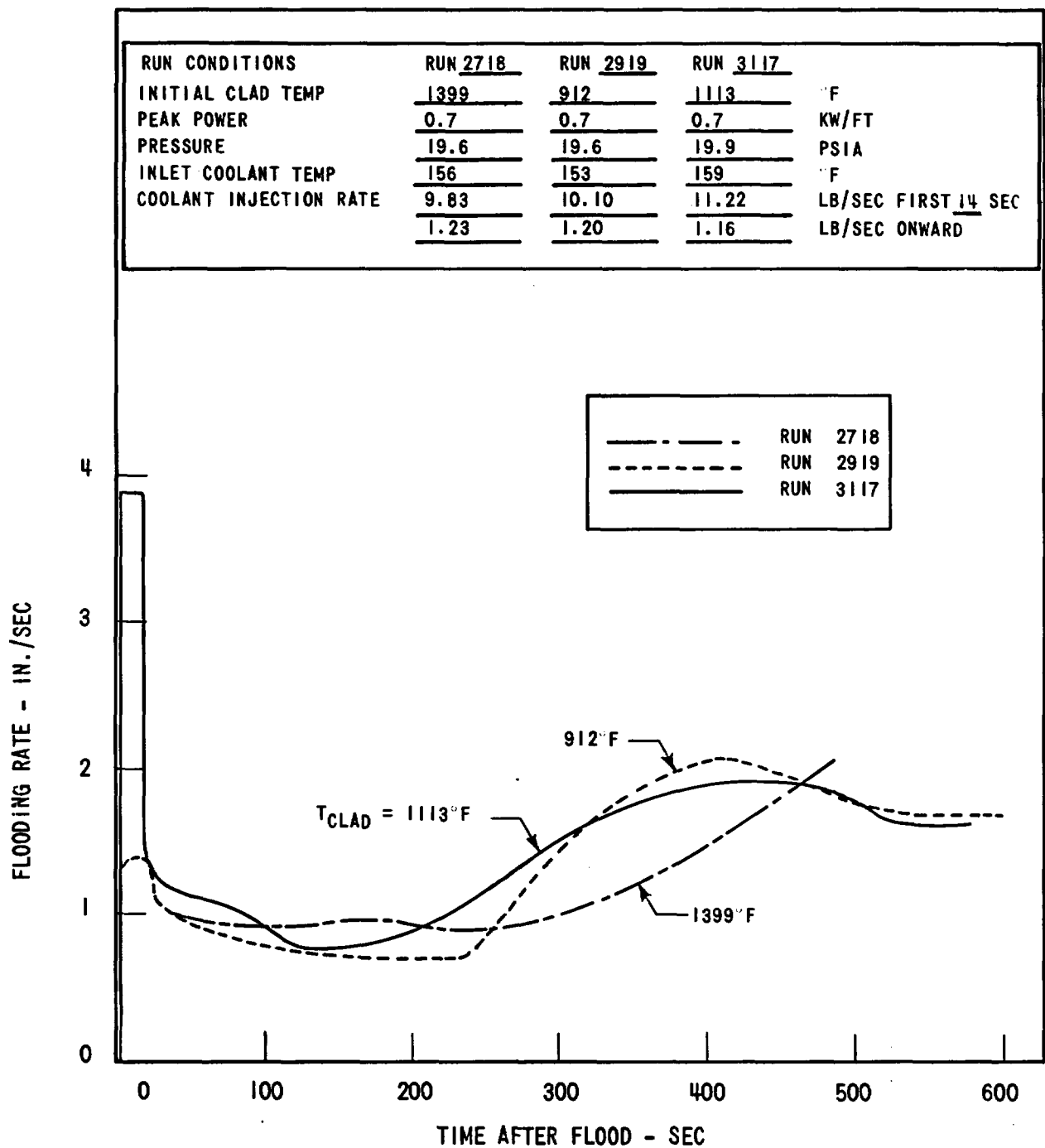


Figure 3-68. Effect of Initial Clad Temperature on Flooding Rate at 20 Psia Containment Pressure

RUN CONDITIONS		RUN 2718	RUN 2919	RUN 3117	
INITIAL CLAD TEMP		1399	912	1113	°F
PEAK POWER		0.7	0.7	0.7	KW/FT
PRESSURE		19.6	19.6	19.9	PSIA
INLET COOLANT TEMP		156	153	159	°F
COOLANT INJECTION RATE		9.83	10.10	11.22	LB/SEC FIRST 14 SEC
		1.23	1.20	1.16	LB/SEC ONWARD

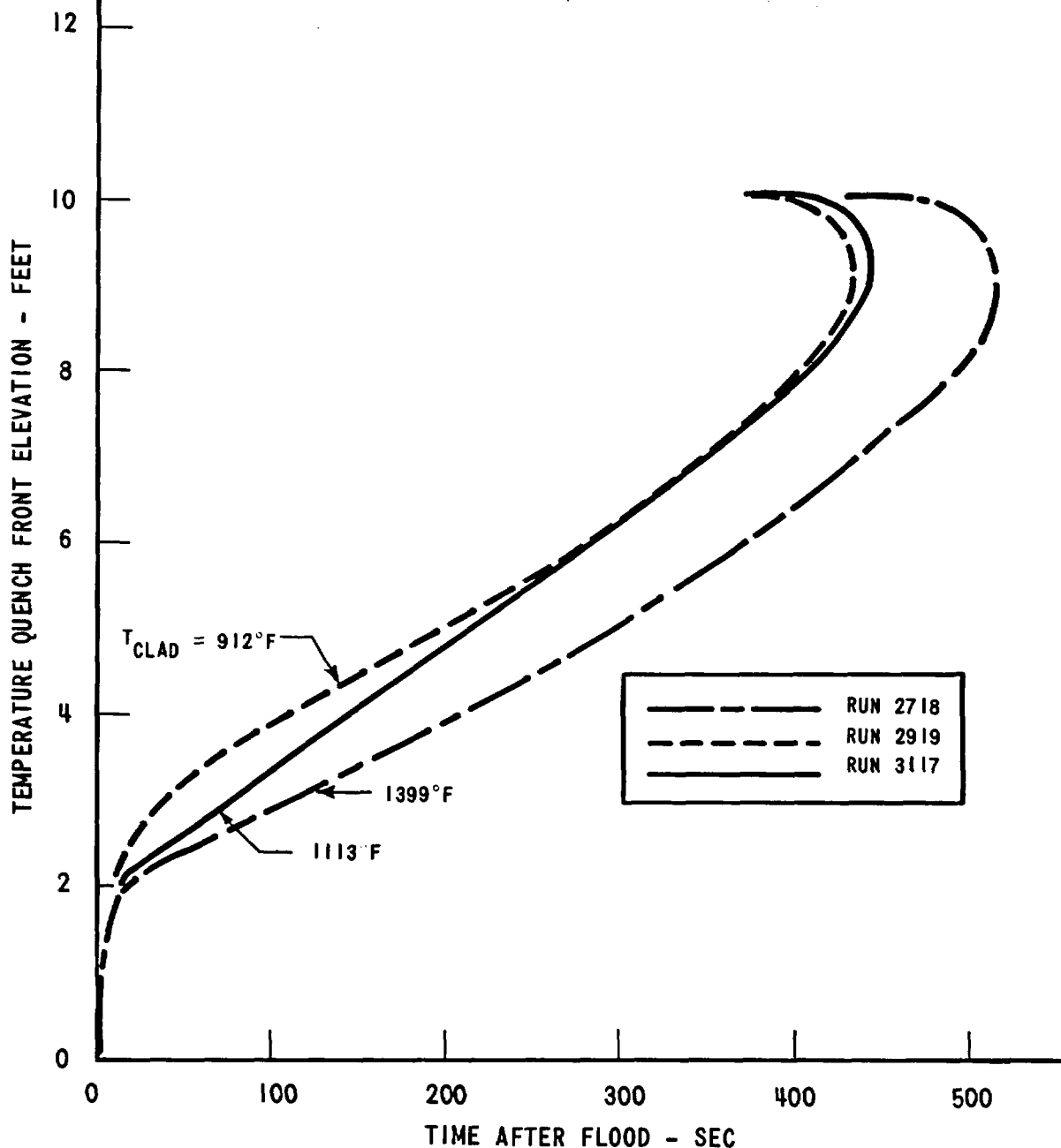


Figure 3-69. Effect of Initial Clad Temperature on Rod Quench Front Behavior at 20 Psia Containment Pressure

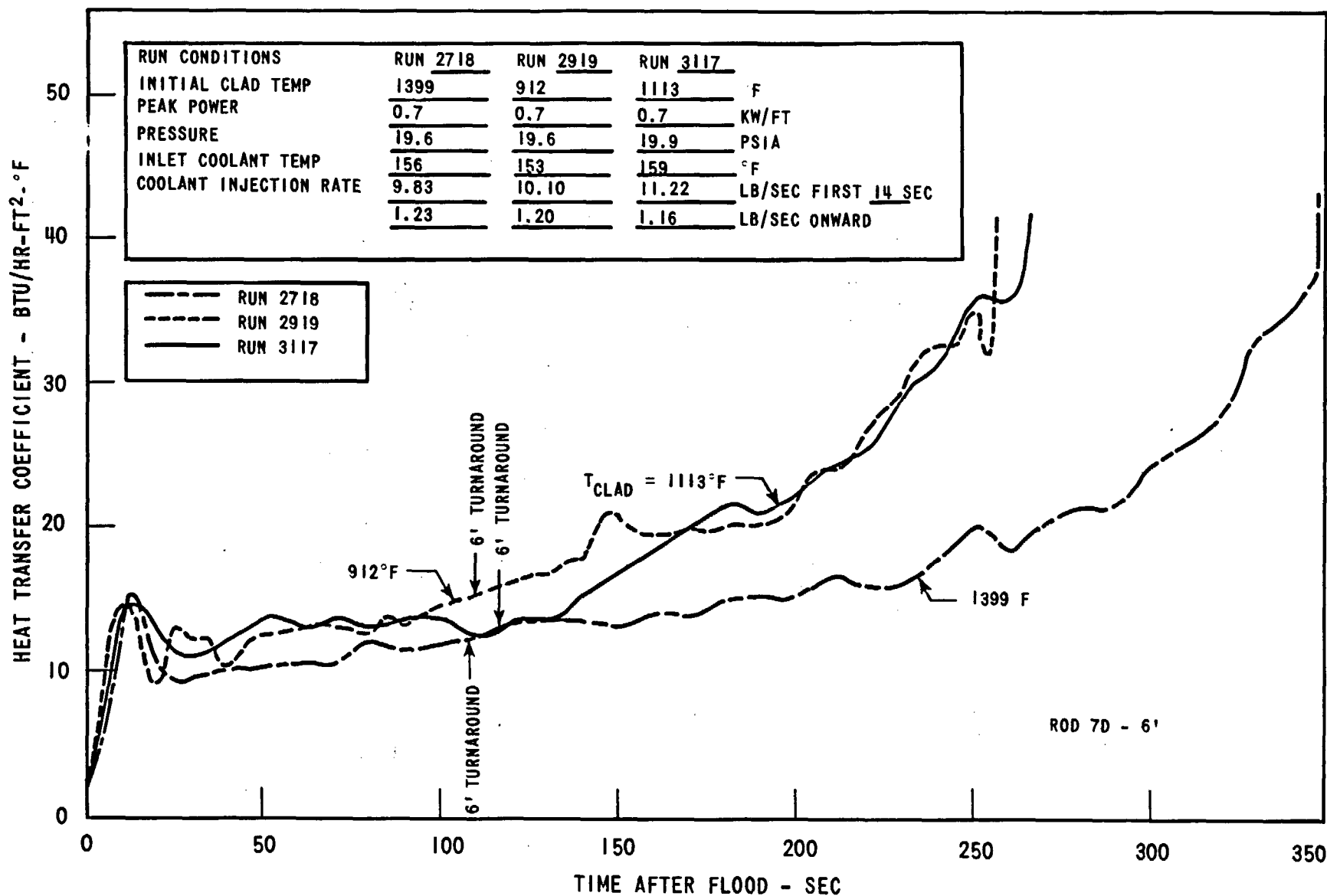


Figure 3-70. Effect of Initial Clad Temperature on Midplane Heat Transfer Coefficient at 20 Psia Containment Pressure

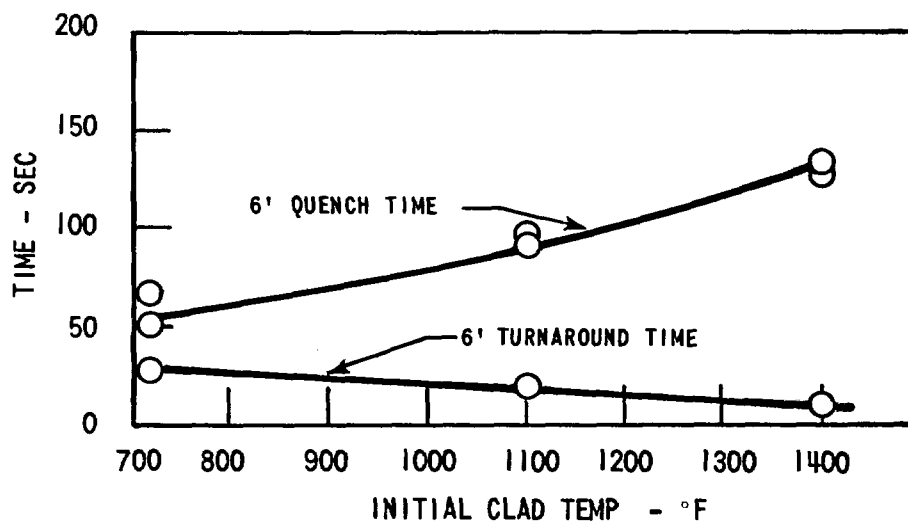
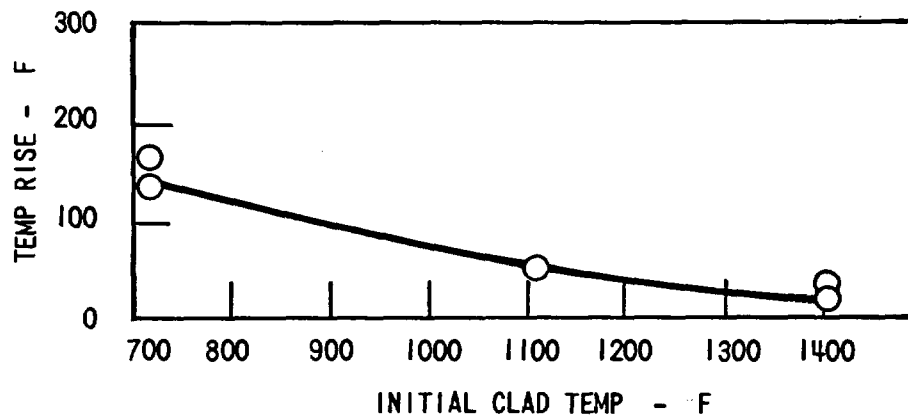


Figure 3-71. Effect of Initial Clad Temperature on Midplane Temperature Rise, Turnaround Time, and Quench Time at 60 Psia Containment Pressure

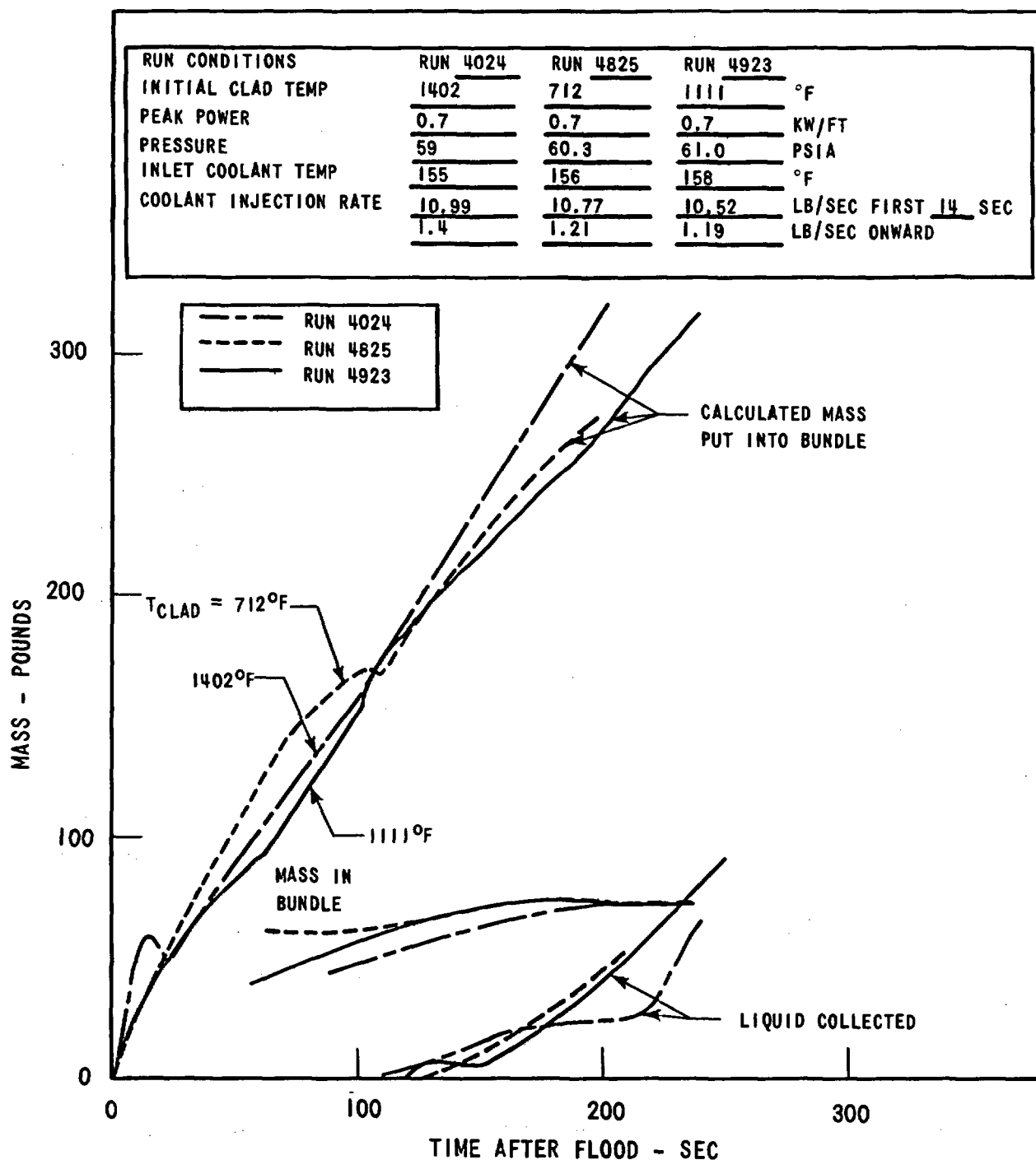


Figure 3-72. Effect of Initial Clad Temperature on the Mass put into the Bundle, Mass Remaining in the Bundle, and Liquid Collected in the Separator Tank at 60 Psia Containment Pressure

the bundle to quench faster, resulting in improved flooding rate and heat transfer as shown in Figures 3-73, 3-74, and 3-75. There was no indication of a significant increase in the onset of liquid collection with increasing initial temperature as shown in Figure 3-72. The rate of liquid collection was somewhat lower for the higher initial temperature, indicating more vaporization occurring in the bundle above the quench front.

3.5.3 Peak Power Generation

The effect of peak power generation was investigated at both 20 psia and 60 psia. The three 20 psia runs analyzed were: Run 2822 (0.4 kw/ft peak), Run 3117 (0.7 kw/ft peak), and Run 3421 (1.0 kw/ft peak). The injection flow rates and pressure conditions were nearly the same for these runs as well as the downstream loop resistance. As the rod peak power increased, the housing initial temperature was increased according to the FLECHT housing criterion as given in Section 2.4. This series of tests then became a two-parameter series of tests (Section 3.4): rod peak power and housing initial stored energy. The effect of rod peak power with the housing heated to the saturation temperature was discussed in Section 3.4 and it was observed that increasing the rod power increased the rod quench time but did not significantly change the midplane heat transfer coefficient.

By heating the housing to match the heat input of an equivalent row of rods, a housing effect was superimposed on Runs 2822, 3117, and 3421. The midplane temperature rise, turnaround time, and quench time all increased with increasing peak rod power and housing temperature as shown in Figure 3-76. The mass balance for each run indicates that, as the rod power and housing temperature increase, the mass stored in the bundle decreases, steam flow in the loops increases, and the rate of water collection in the collection tanks decreases. These trends indicate that as the rod power and housing temperature increase, more of the water is vaporized before leaving the bundle. The mass storage in the bundle and the liquid collected are shown in Figure 3-77, and the flooding rate is shown in Figure 3-78.

RUN CONDITIONS	RUN 4024	RUN 4825	RUN 4923	
INITIAL CLAD TEMP	1402	712	1111	F
PEAK POWER	0.7	0.7	0.7	KW/FT
PRESSURE	59.0	60.3	61.0	PSIA
INLET COOLANT TEMP	155	156	158	F
COOLANT INJECTION RATE	10.99	10.77	10.52	LB/SEC FIRST 14 SEC
	1.4	1.21	1.19	LB/SEC ONWARD

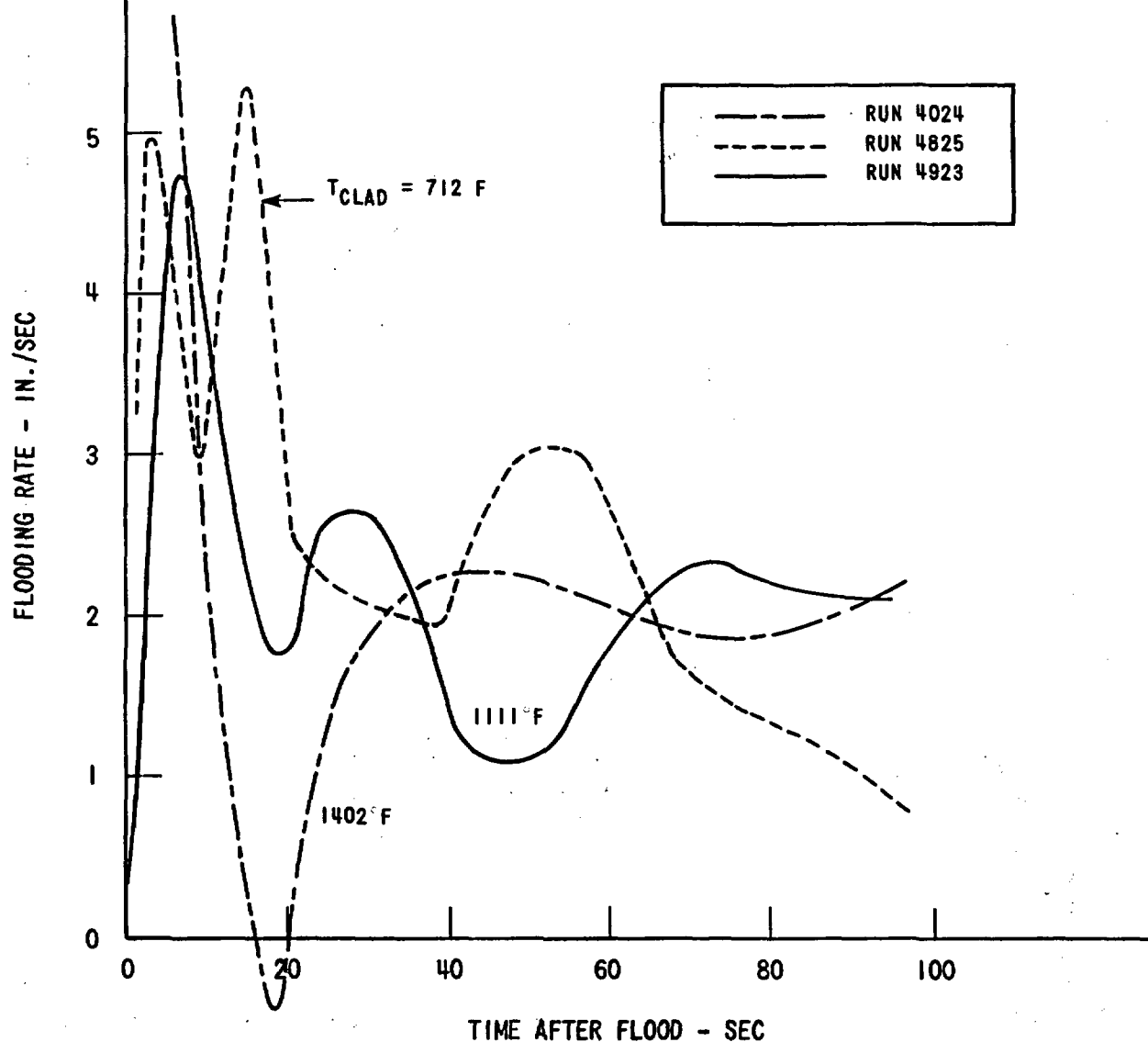


Figure 3-73. Effect of Initial Clad Temperature on Flooding Rate at 60 Psia Containment Pressure

RUN CONDITIONS	RUN 4024	RUN 4825	RUN 4923	
INITIAL CLAD TEMP	1402	712	1111	F
PEAK POWER	0.7	0.7	0.7	KW/FT
PRESSURE	59.0	60.3	61.0	PSIA
INLET COOLANT TEMP	155	156	158	F
COOLANT INJECTION RATE	10.99	10.77	10.52	LB/SEC FIRST 14 SEC
	1.4	1.21	1.19	LB/SEC ONWARD

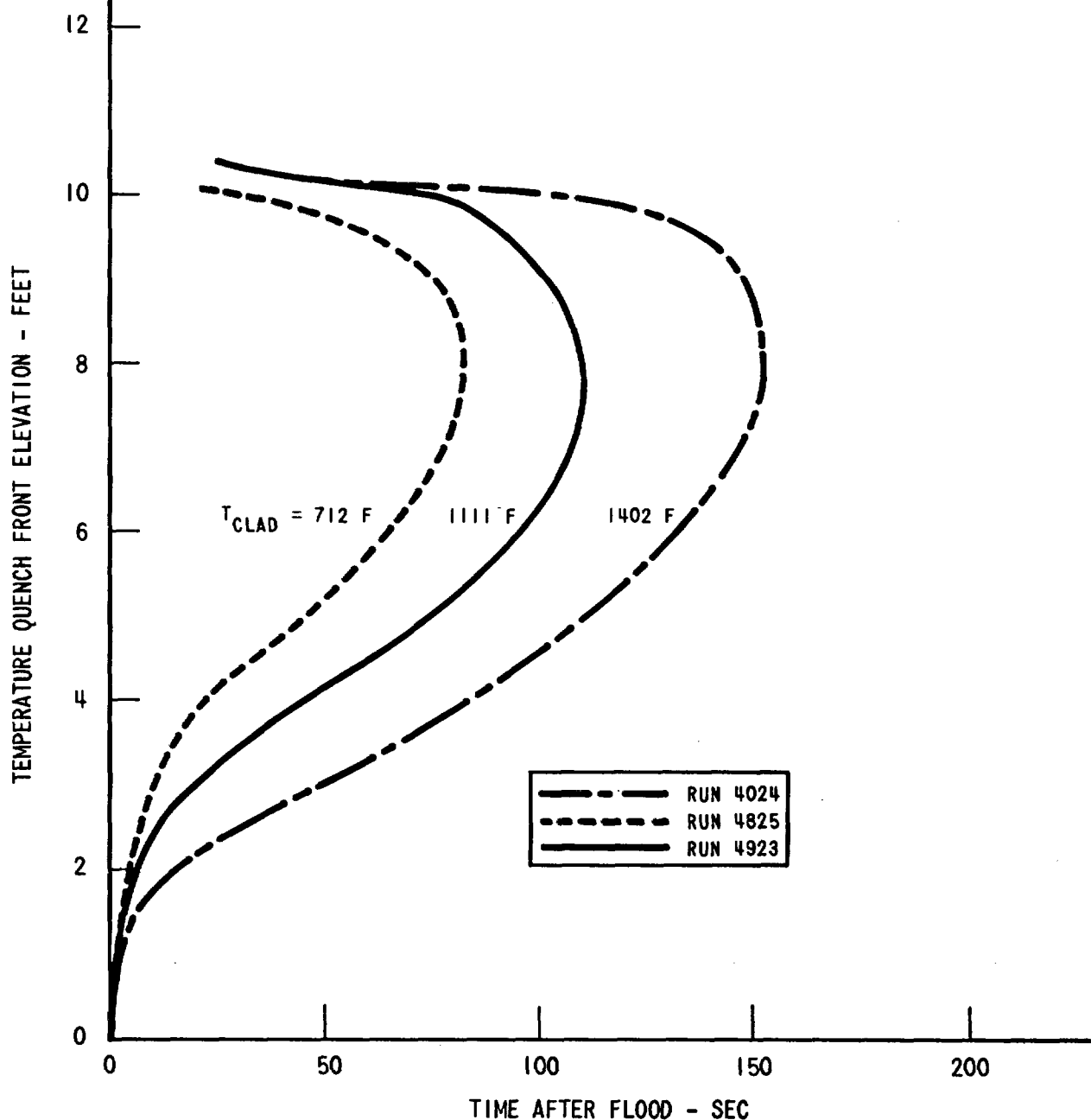


Figure 3-74. Effect of Initial Clad Temperature on Rod Quench Front Behavior at 60 Psia Containment Pressure

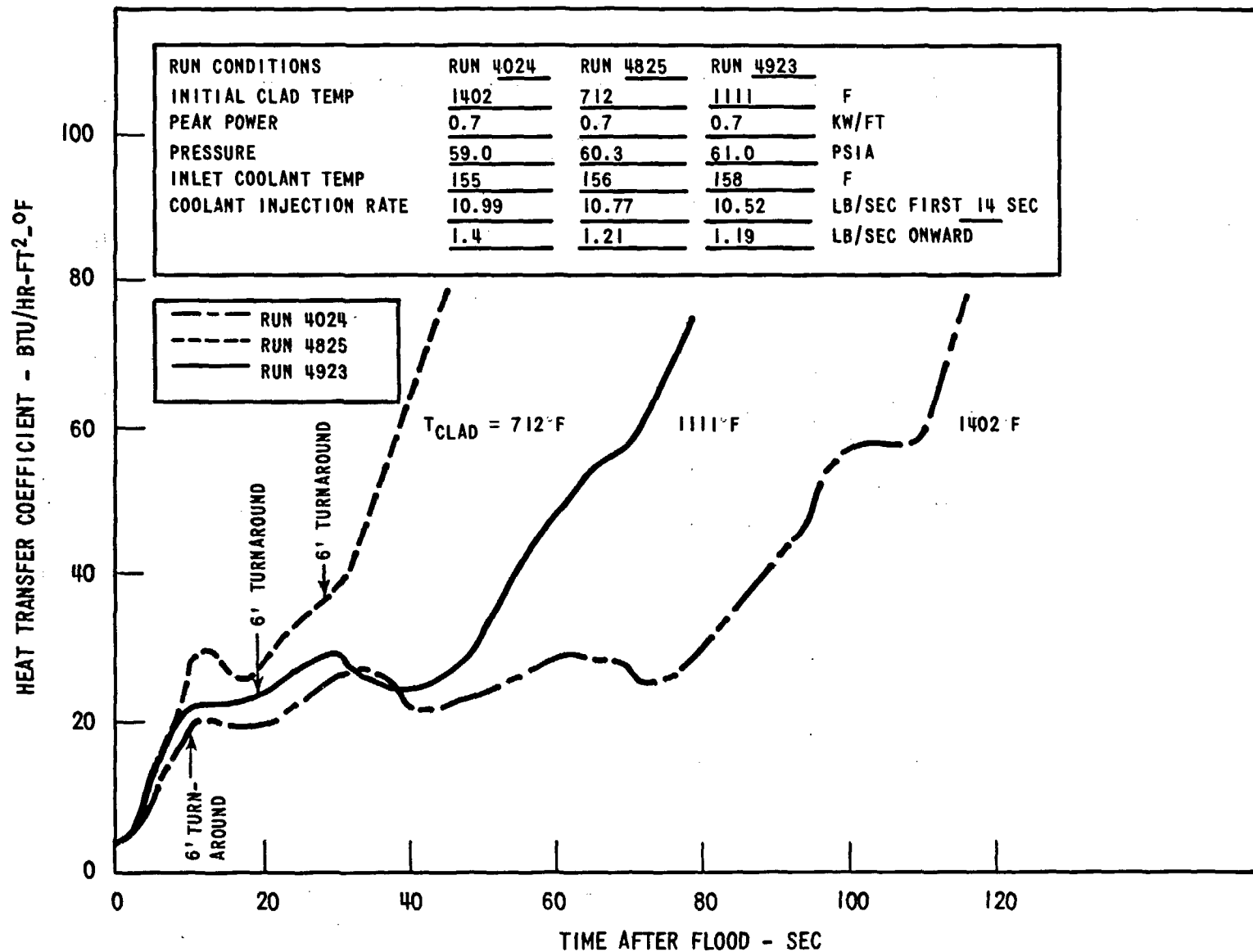


Figure 3-75. Effect of Initial Clad Temperature on Midplane Heat Transfer Coefficient at 60 Psia Containment Pressure

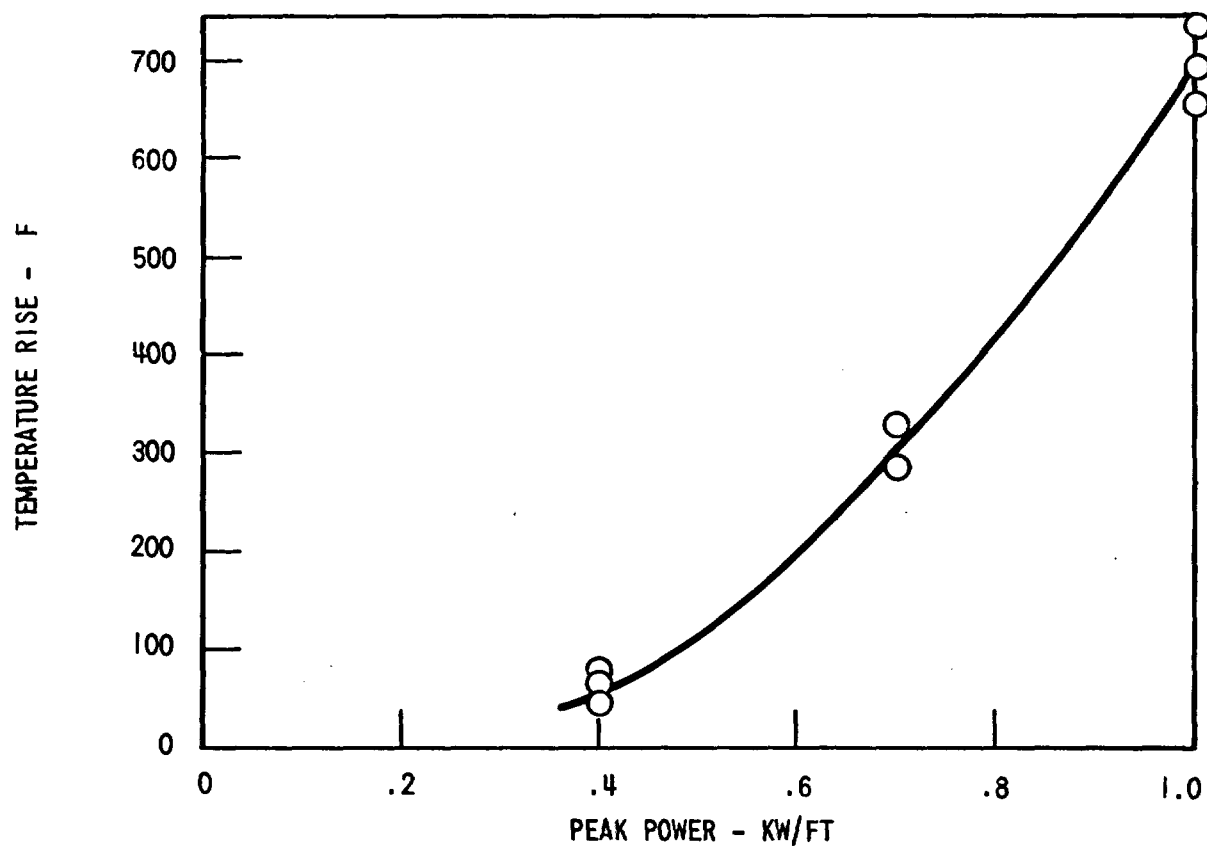
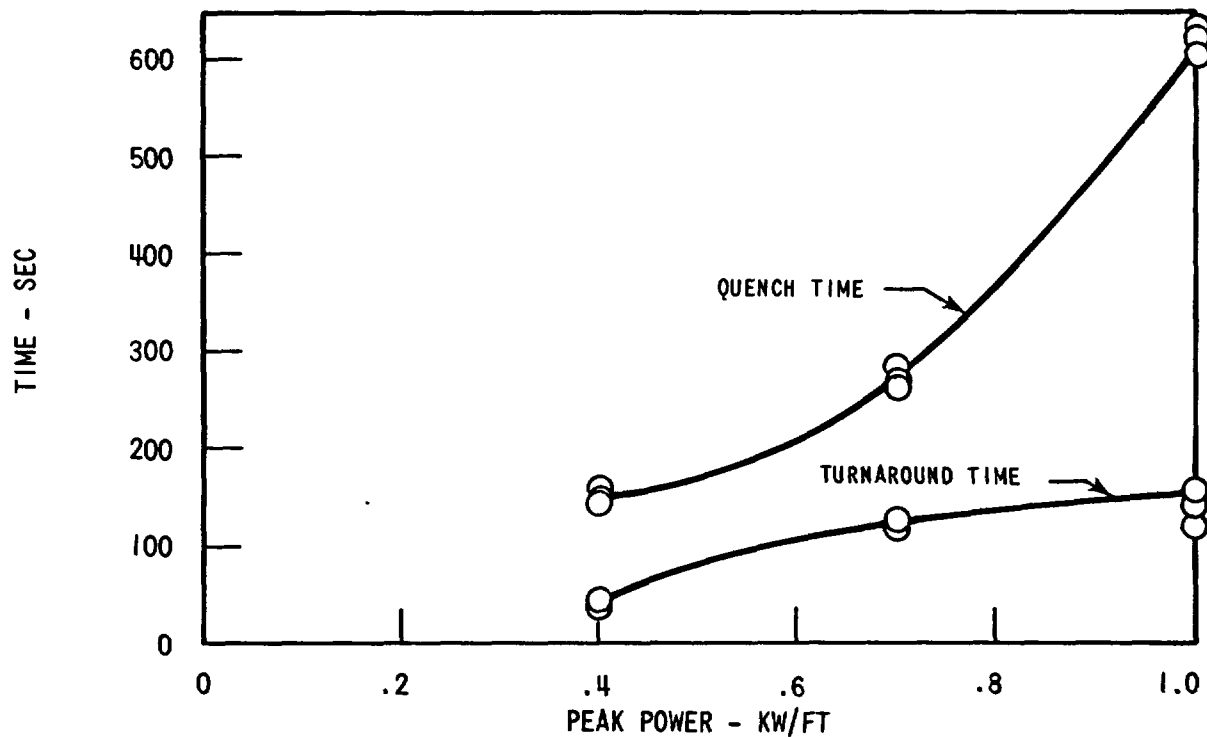


Figure 3-76. Effect of Peak Power on 6' Quench Time, Turnaround Time and Temperature Rise at 20 Psia Containment Pressure

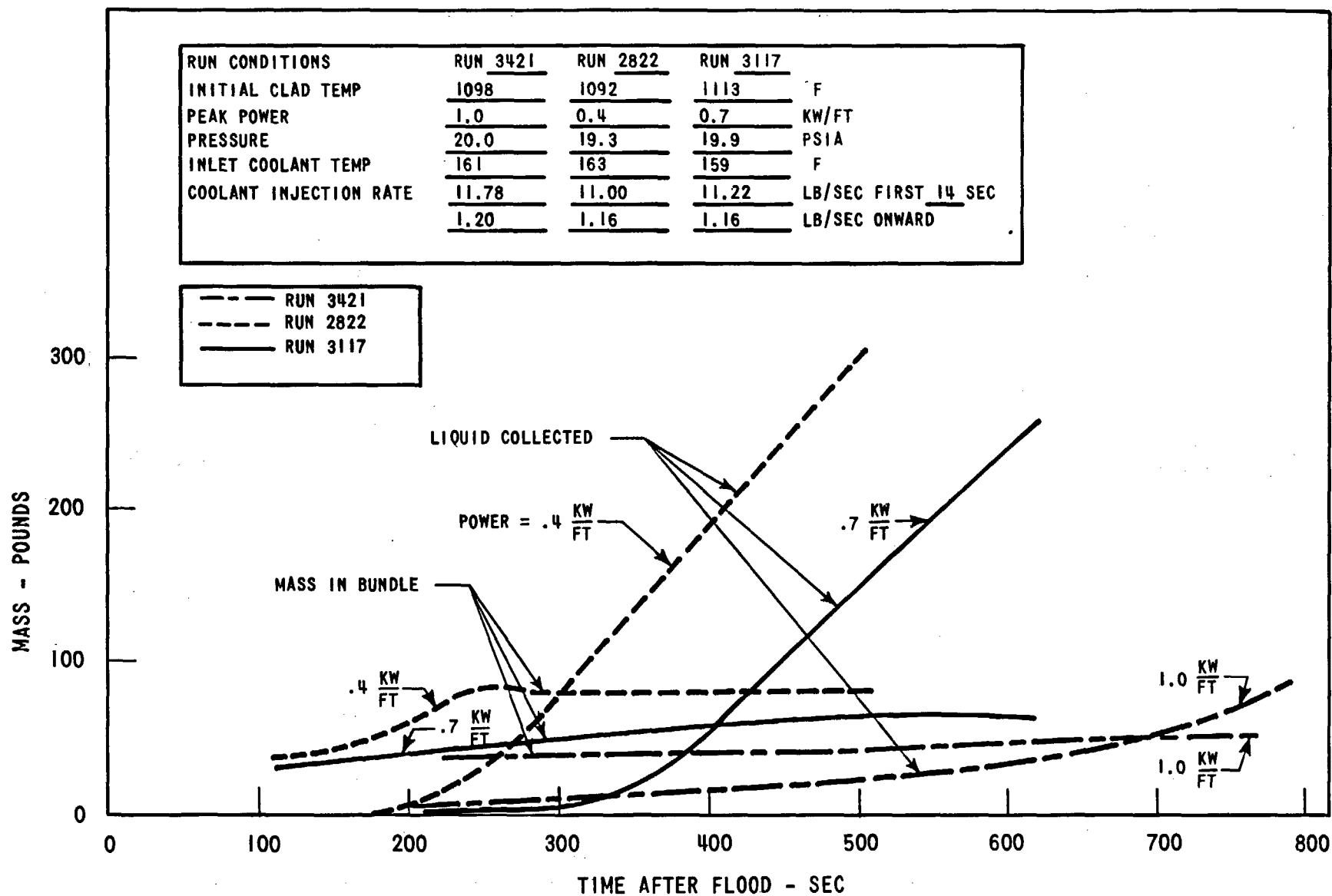


Figure 3-77. Effect of Peak Power on the Mass Remaining in the Bundle and the Liquid Collected in the Separator Tank at 20 Psia Containment Pressure

RUN CONDITIONS	RUN 3421	RUN 2822	RUN 3117
INITIAL CLAD TEMP	1098	1092	1113 °F
PEAK POWER	1.0	0.4	0.7 KW/FT
PRESSURE	20.0	19.3	19.9 PSIA
INLET COOLANT TEMP	161	163	159 °F
COOLANT INJECTION RATE	11.78	11.00	11.22 LB/SEC FIRST 14 SEC
	1.20	1.16	1.16 LB/SEC ONWARD

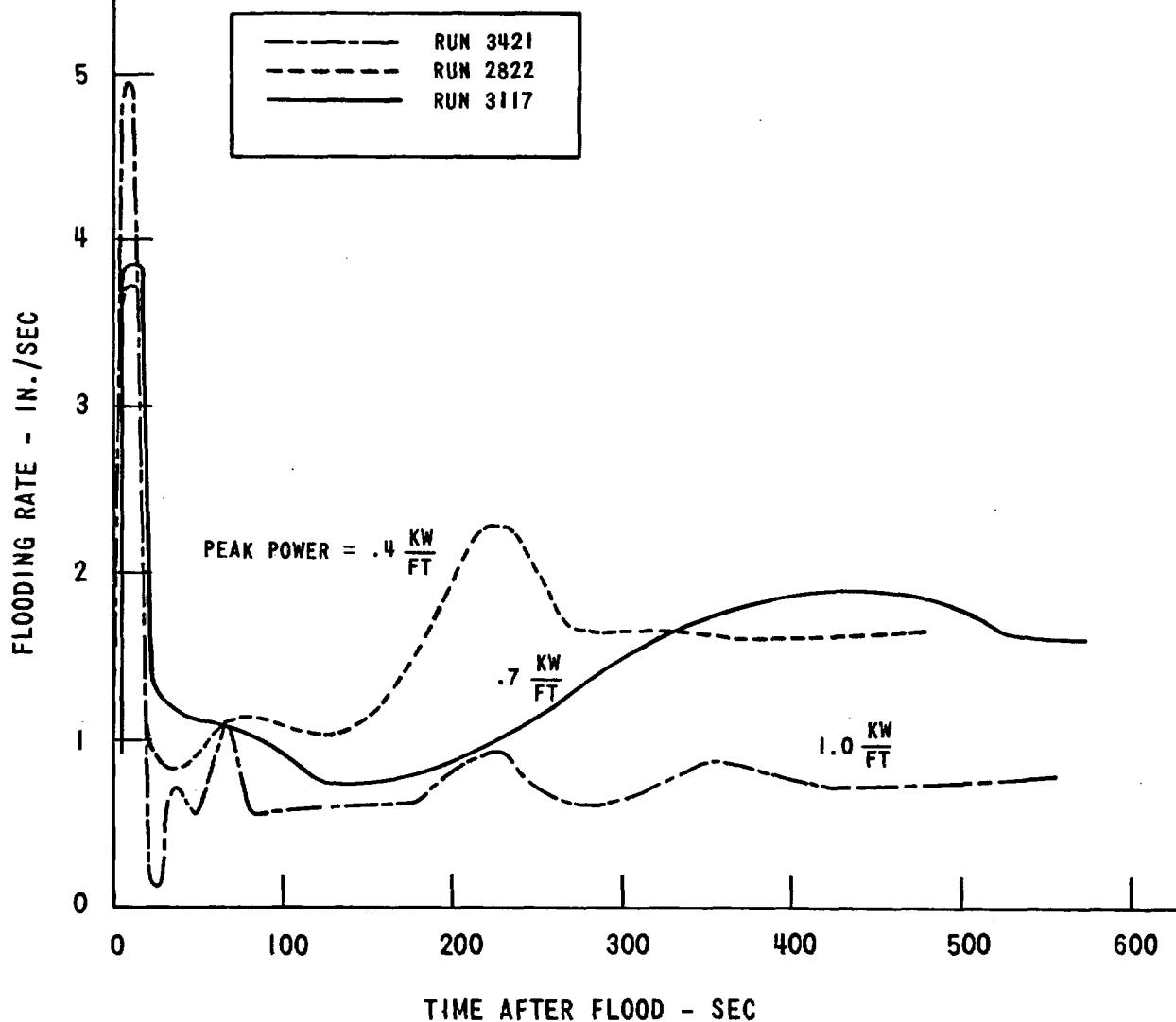


Figure 3-78. Effect of Peak Power on the Flooding Rate at 20 Psia Containment Pressure

The effect of increasing the steam flow rate with increasing rod power and housing temperature results in a larger loop pressure drop which, in turn, decreases the bundle flooding rate, shown in Figure 3-78. The result of decreasing the flooding rate and the mass storage in the bundle is reflected in the slower quench front velocity (Figure 3-79) and lower midplane heat transfer coefficient (Figure 3-80).

The effect of peak power variation was also investigated at 60 psia; however, these tests were some of the earliest Phase A tests conducted and used coolant injection at the top of the downcomer. The condensation problem observed using this mode of injection has already been discussed and these tests were to be rerun. However, the heater rod thermocouple complement was less than 50 percent of the original number forcing the termination of testing before these runs were repeated. These test conditions will be examined in Phase B of FLECHT-SET.

3.5.4 Containment Pressure

The effect of containment pressure was analyzed in Run 3117 (20 psia), Run 4530 (40 psia), and Run 4923 (60 psia). All other conditions were approximately the same except that the high injection flow rate was somewhat lower for the 20 psia test. Since the inlet temperature was maintained the same, the subcooling was different for each test, making this comparison a double parameter effect instead of just a single parameter test.

Another problem which hinders data interpretation is the condensation effect observed in the overflow tanks for the 20 psia run. As mentioned in Section 3.3.2, when overflow occurred the steam in the overflow tank condensed, causing a local pressure difference between the downcomer and the containment tank which resulted in flow from the containment to the downcomer. This additional pressure drop, resulting from the steam flow through a small diameter vent line, was estimated to be between 1 and 2 psia while overflow occurred and caused a reduction in the effective downcomer head. Decreasing the downcomer driving head reduced the mass storage in the bundle, the flooding rate, and resulted in increased temperature rise, turnaround times, and quench times for the 20 psia tests. The Phase B design had addressed this

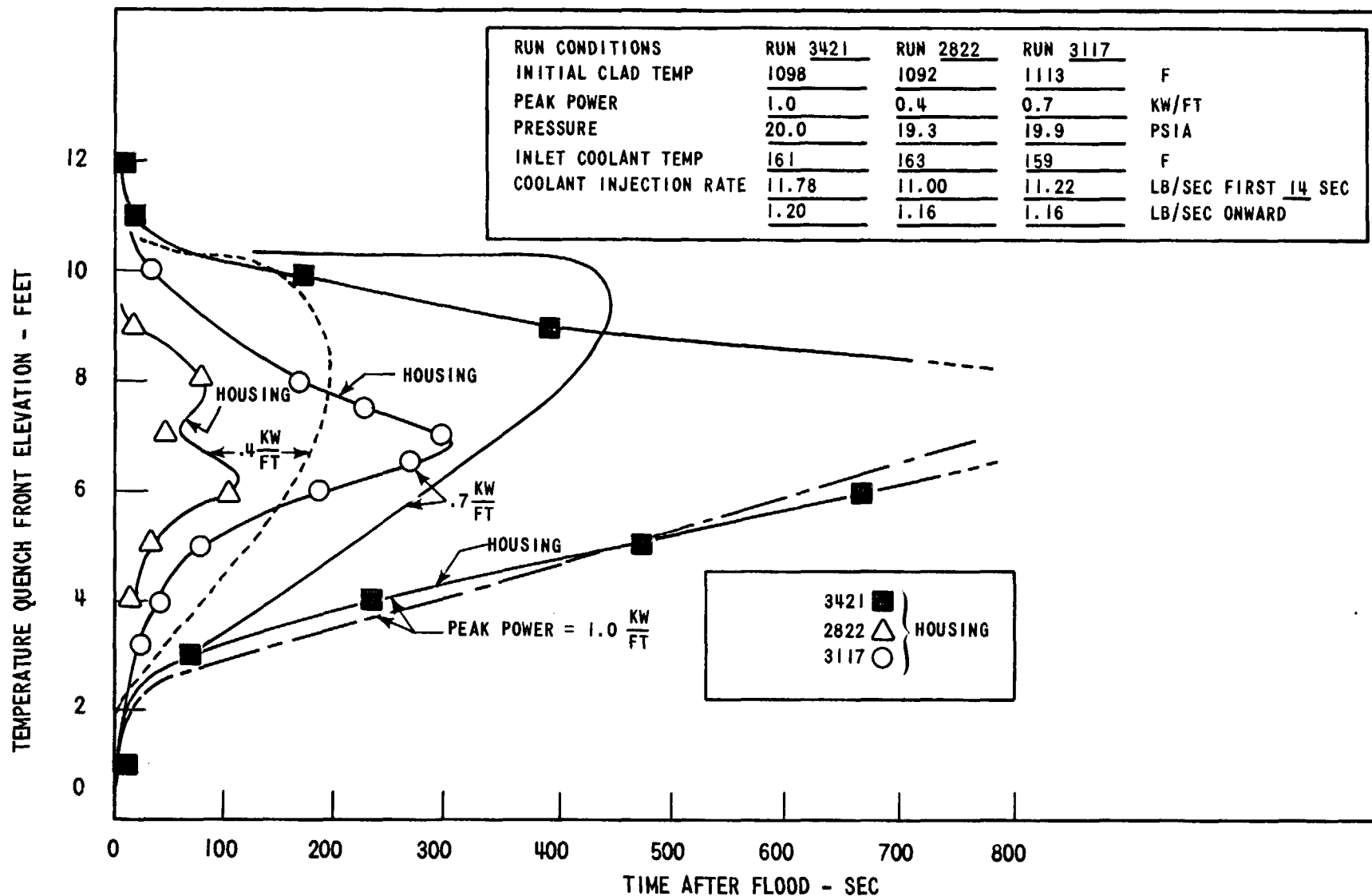


Figure 3-79. Effect of Peak Power on Rod and Housing Quench Front Behavior at 20 Psia Containment Pressure

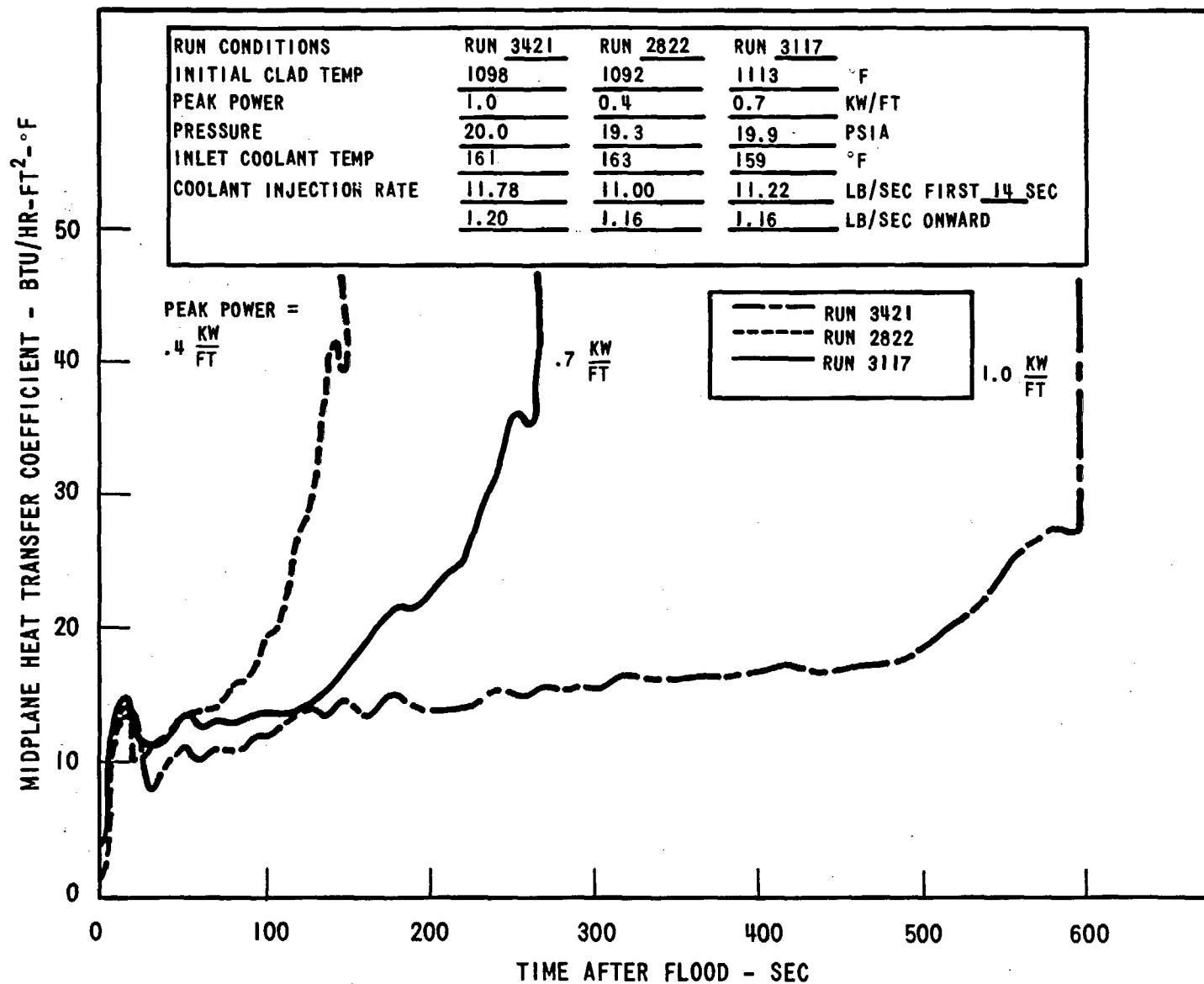


Figure 3-80. Effect of Peak Power on Midplane Heat Transfer Coefficient at 20 Psia Containment Pressure

problem, and a larger vent path from the downcomer to the containment has been provided. It is believed that by allowing ample flow from the containment, the pressure at the top of the downcomer should not decrease. While the housing effect was not analyzed at 20 psia, it is felt that the large initial steam generation rates caused by the housing heat release had a significant effect on the 20 psia data. The larger volume of steam generated at 20 psia would have reduced the flooding rate the bundle mass storage and the midplane heat transfer coefficient even more than was observed at 60 psia.

The combined effects of subcooling and pressure on the bundle midplane temperature rise, turnaround time, and quench time are shown in Figure 3-81. All three quantities are shown to decrease as containment pressure increases. Similar trends have been observed in the FLECHT program over a wider range of pressures with constant subcooling effects (Reference 2).

The loop resistance was the same for these tests and it was observed that the experimentally measured loop pressure drop was also very nearly the same. Since the steam mass flow through the loop is proportional to the square root of the product of the vapor density and loop pressure drop, increasing the system pressure increases the fluid density and results in an increased vapor mass flow for the same loop pressure drop. Thus a 19 percent higher mass flow can be achieved at 60 psia than at 40 psia which is consistent with the measurements. A comparison of the measured vapor flow rates is given in Figure 3-82. Since more steam can pass through the loop for a given loop pressure drop, more heat can be removed from the bundle (enthalpy of vaporization differences are small) and the quench front will advance more rapidly into the bundle for higher pressures as shown in Figure 3-83. Figure 3-84 shows that the bundle mass storage increases with increasing pressure, and that the majority of the entrained water does not reach the collection tank until after the bundle has quenched for the 60 psia and 40 psia runs. In this case, the large collection rate in the collection tanks is due to overflow, since the bundle steam generation has sharply decreased as shown in Figure 3-82.

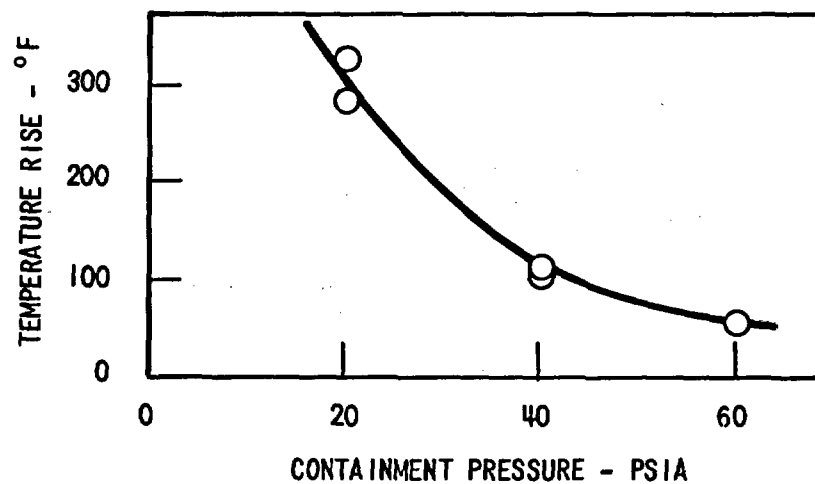
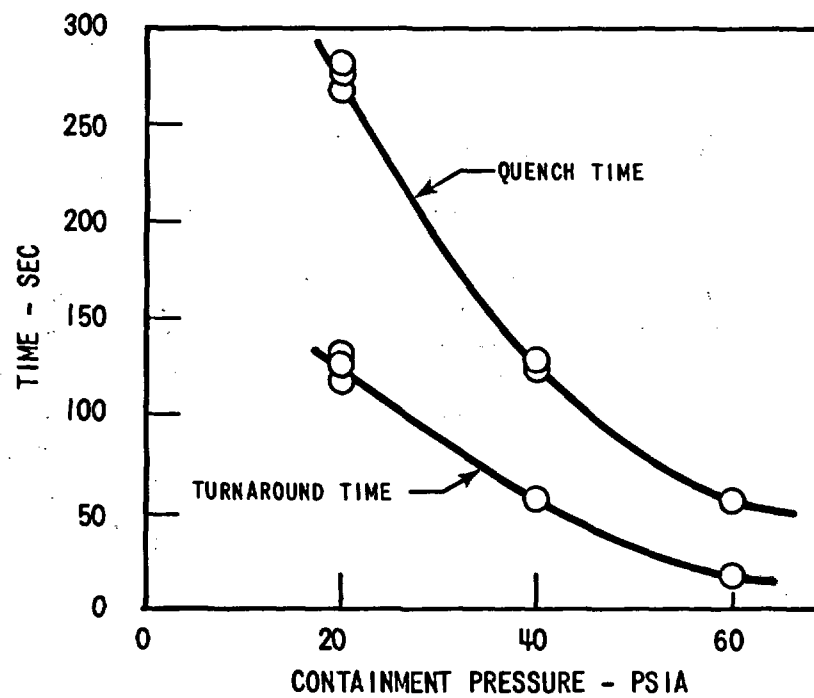


Figure 3-81. Effect of Containment Pressure on Midplane Quench Time, Turnaround Time, and Temperature Rise

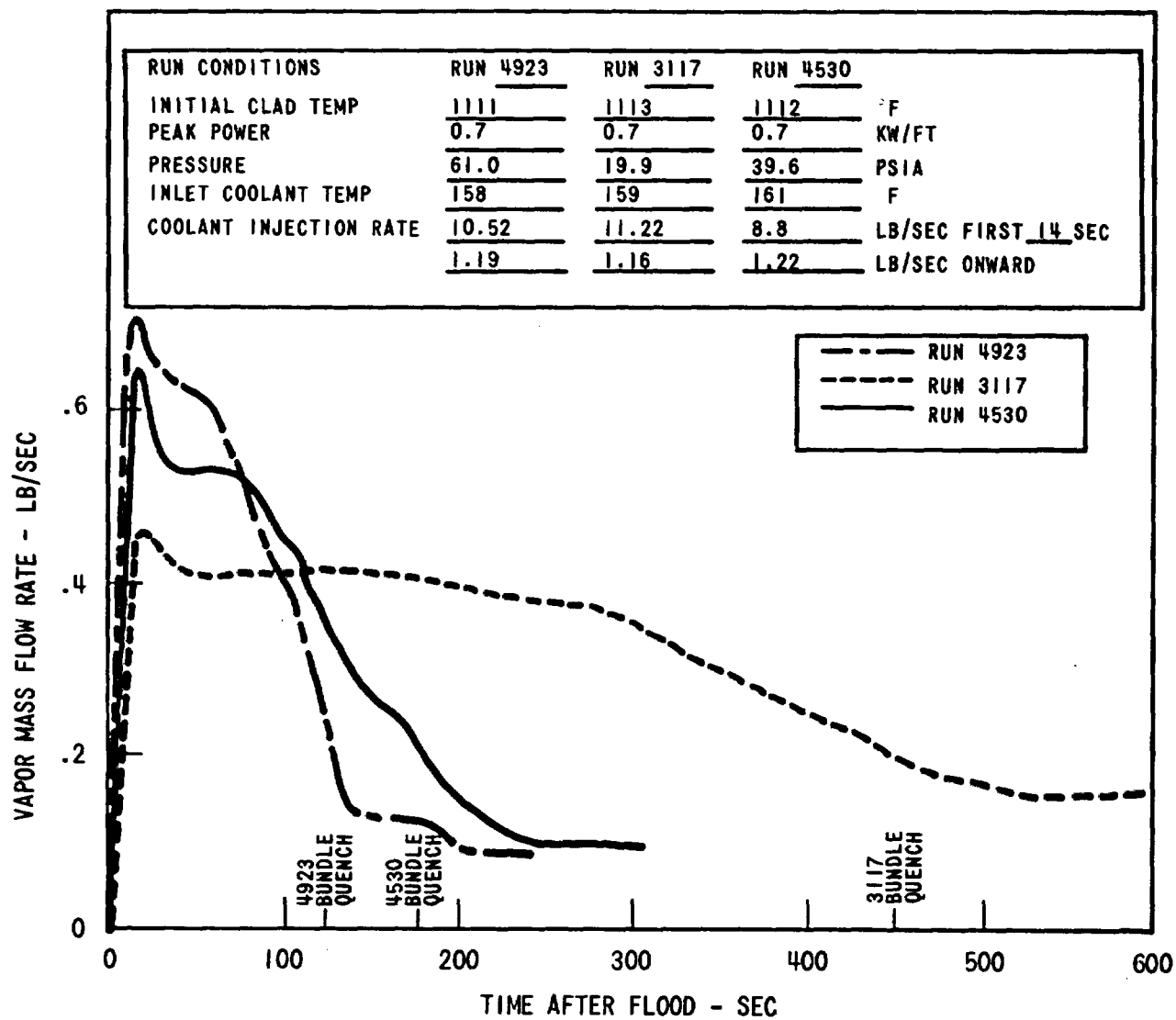


Figure 3-82. Effect of Containment Pressure on the Vapor Mass Flow Rate

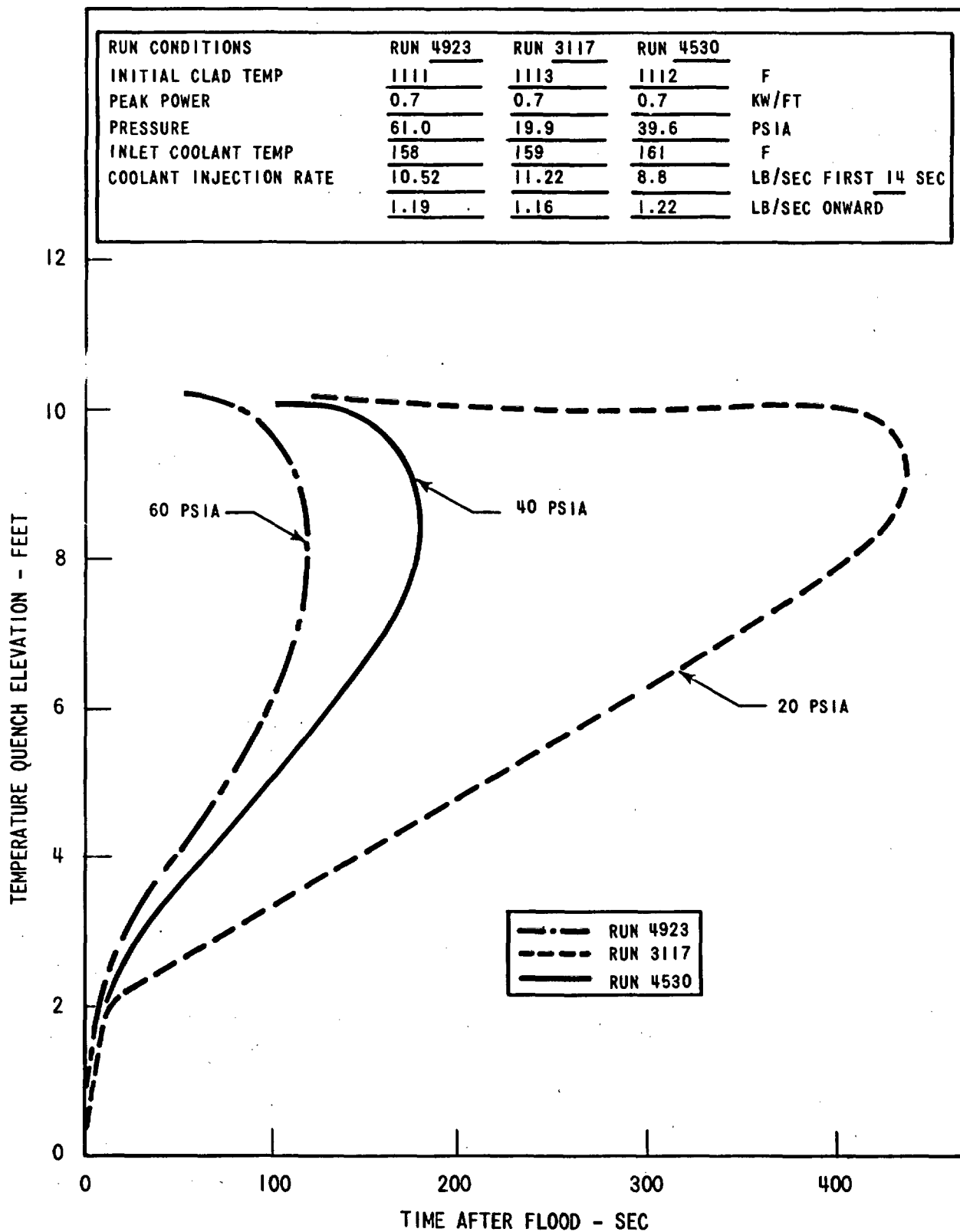


Figure 3-83. Effect of Containment Pressure on the Rod Quench Front Envelope

RUN CONDITIONS	RUN 4923	RUN 3117	RUN 4530	
INITIAL CLAD TEMP	1111	1113	1112	°F
PEAK POWER	0.7	0.7	0.7	KW/FT
PRESSURE	61.0	19.9	39.6	PSIA
INLET COOLANT TEMP	158	159	161	°F
COOLANT INJECTION RATE	10.52	11.22	8.8	LB/SEC FIRST 14 SEC
	1.19	1.16	1.22	LB/SEC ONWARD

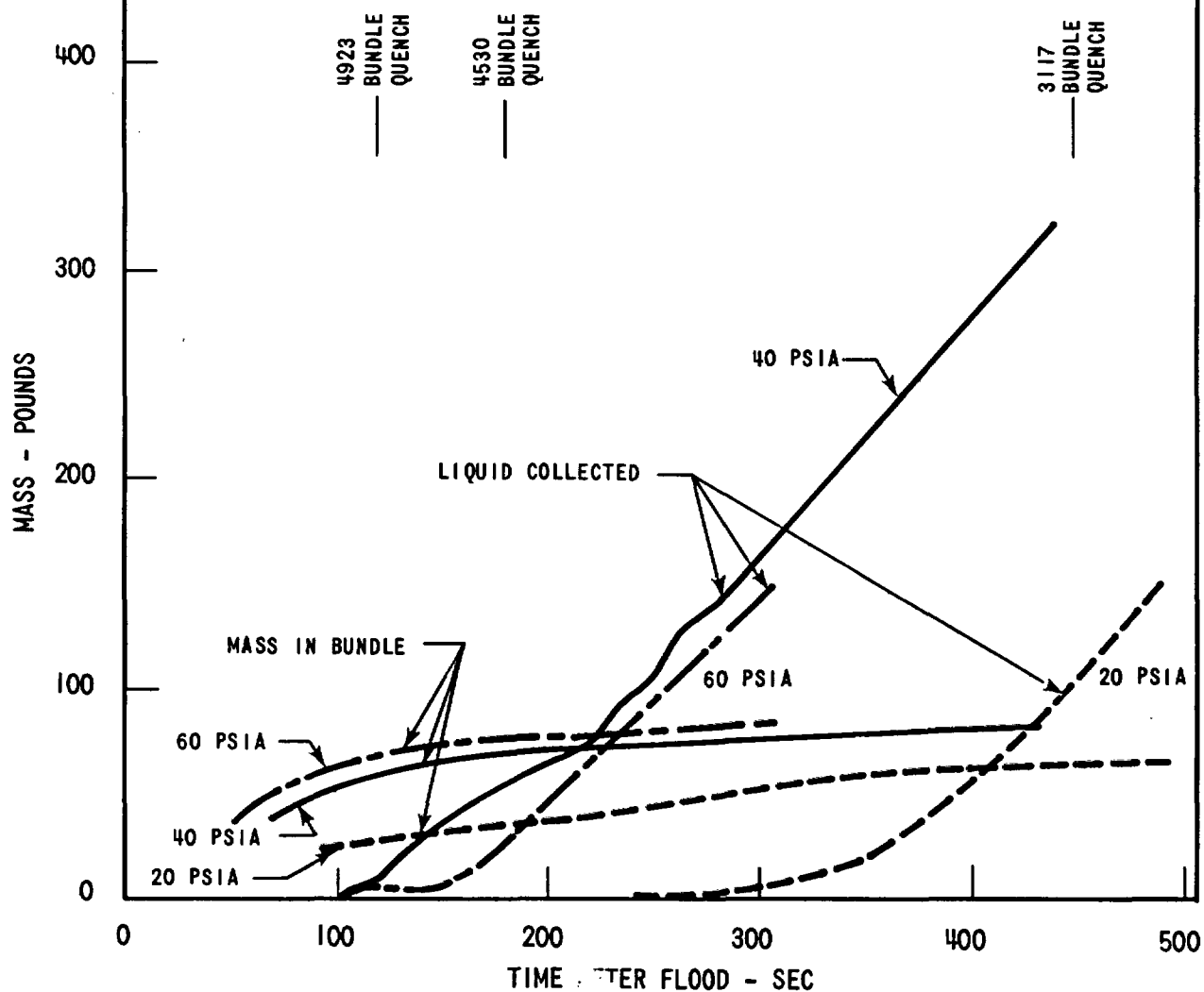
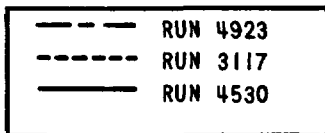


Figure 3-84. Effect of Containment Pressure on Mass Remaining in Bundle and Liquid Collected in Separator Tank

A comparison of the flooding rates is shown in Figure 3-85 for the three different tests. While the 60 psia and 40 psia tests had the same amount of mass injected into the bundle for the first 200 seconds, more mass remained in the bundle for the 60 psia test, which thereby increased the heat transfer coefficient as seen in Figure 3-86. The 20 psia run had a considerably lower flooding rate, less mass storage, and poorer heat transfer coefficient than either of the other higher pressure tests. Again, it should be emphasized that the housing effect would be more severely felt at the lower pressure than at higher pressures. Also, the condensation observed in the downcomer also decreases the driving head at 20 psia as compared with the other pressures. These two additional effects help make the 20 psia heat transfer data lower than the higher pressure data.

The flooding rate variations seen in Figure 3-85 are due to the transient interaction of the steam generation, loop pressure drop, and mass accumulation in the bundle. A detailed description of the flooding rate history and these interactions has been given in Section 3.3.1.

3.5.5 Injection Rate

The effect of coolant injection rate into the downcomer was examined at both 60 and 20 psia. The 20 psia runs examined were Run 3006 (1.17 lbm/sec constant injection), Run 2605 (5.7 lb/sec for 28 seconds and 1.23 lb/sec onward), and Run 3117 (11.22 lbm/sec for 14 seconds and 1.16 lbm/sec onward). The injection rates for all three cases are shown in Figure 3-87, while the calculated bundle flooding rates are shown in Figure 3-88. As can be seen in Figure 3-88, the tests with the larger initial injection rate have an early surge of coolant into the bundle. This is caused by the larger downcomer driving head for the higher initial injection rates, which forces the coolant further into the bundle and results in a rapid rise of the vapor for rate which retard the inflow of water.

The mean downcomer head for each run is shown in Figure 3-89, indicating that the higher injection rate quickly fills the downcomer and results in a larger driving head earlier in time. The initial surge of water into the

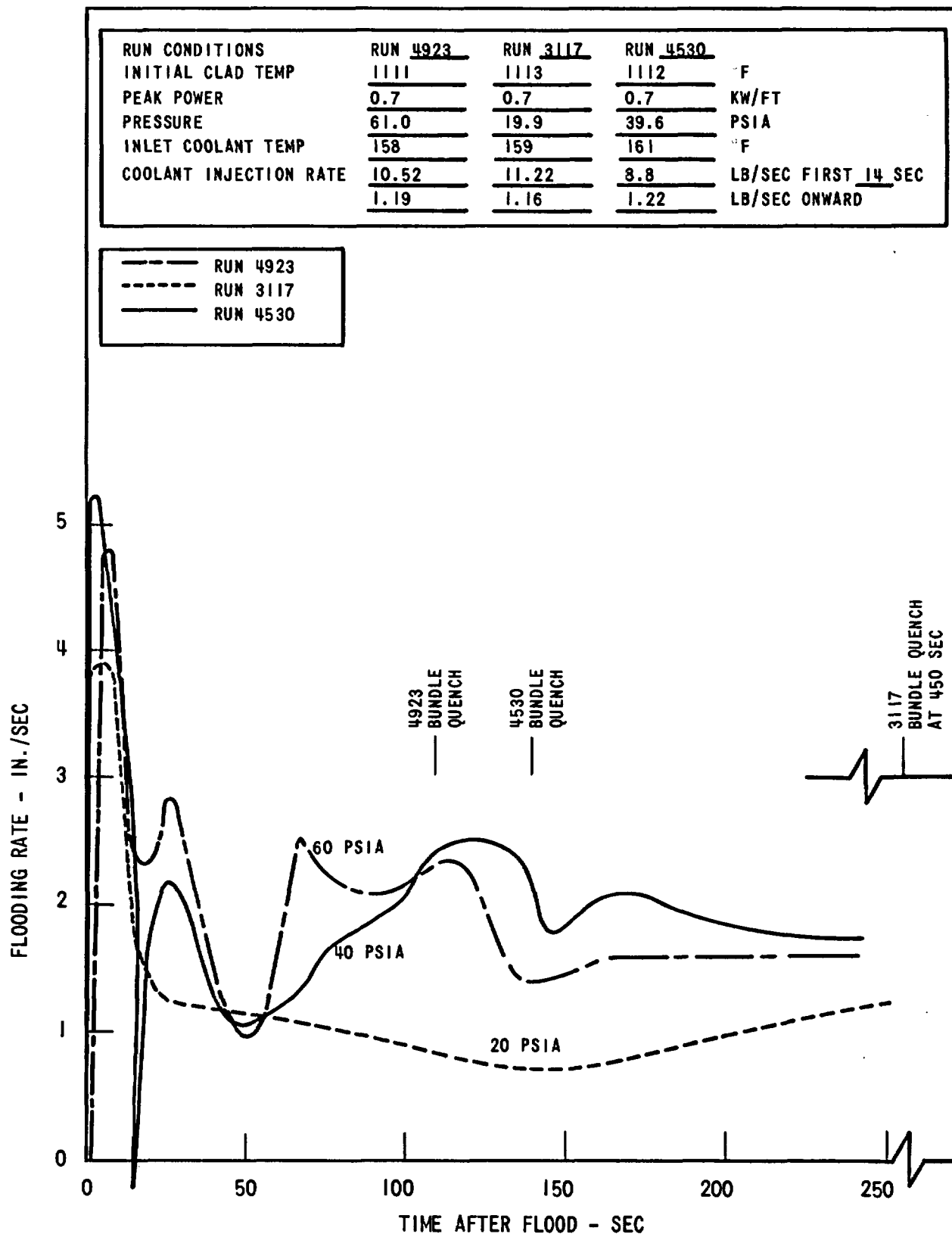


Figure 3-85. Effect of Containment Pressure on Flooding Rate

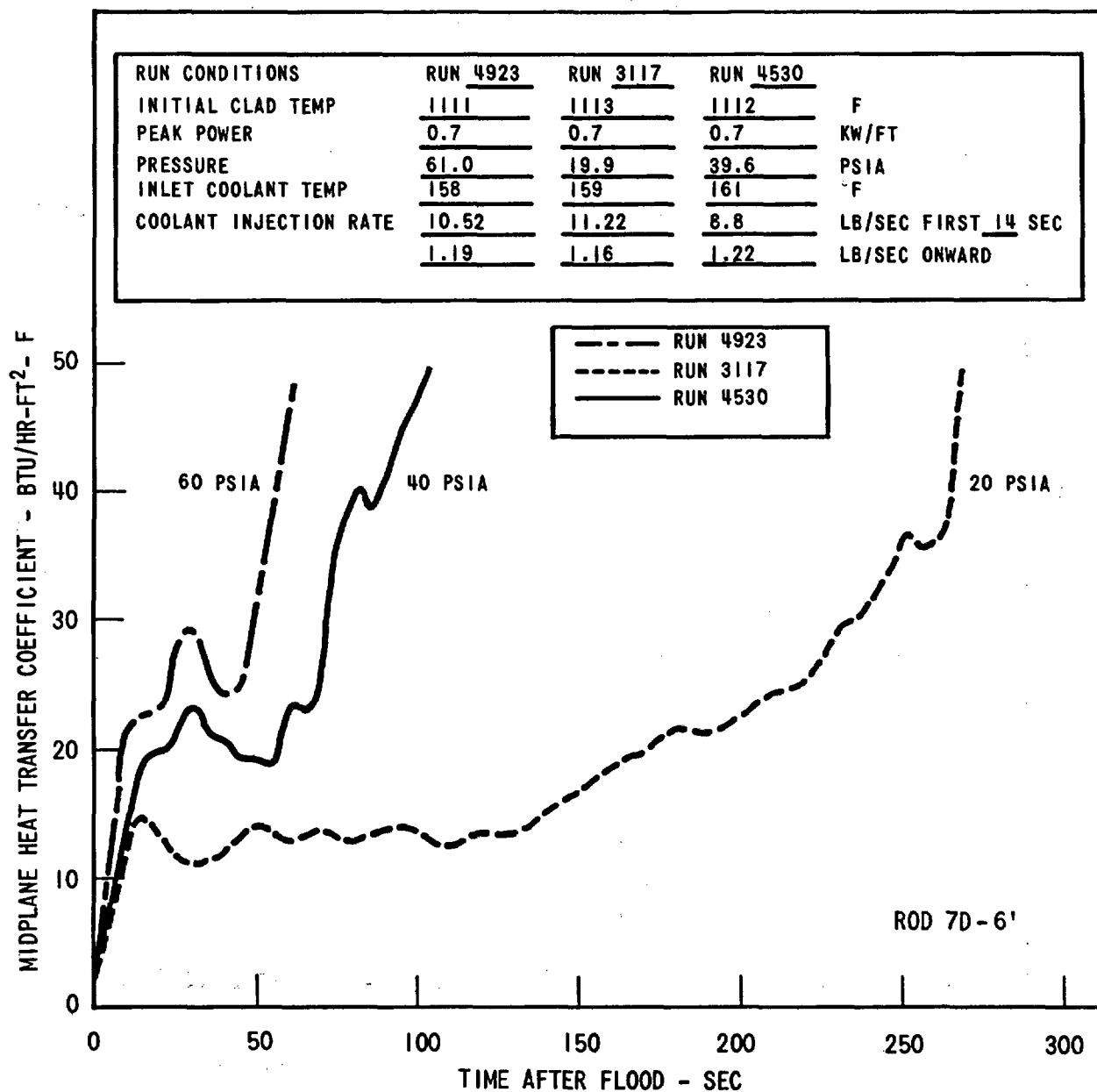


Figure 3-86. Effect of Containment Pressure on Midplane Heat Transfer Coefficient

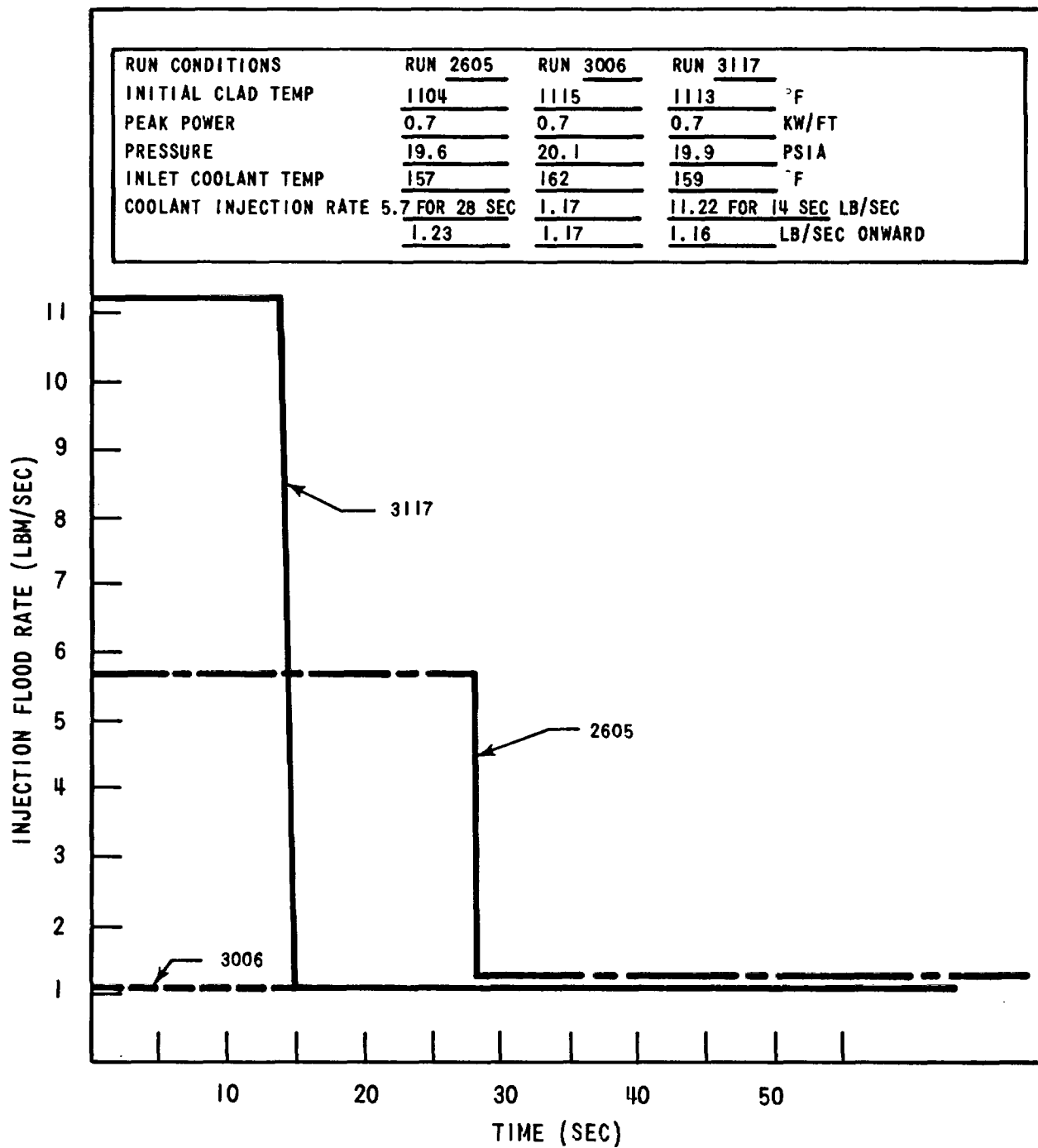


Figure 3-87. Injection Flood Rates at 20 Psia

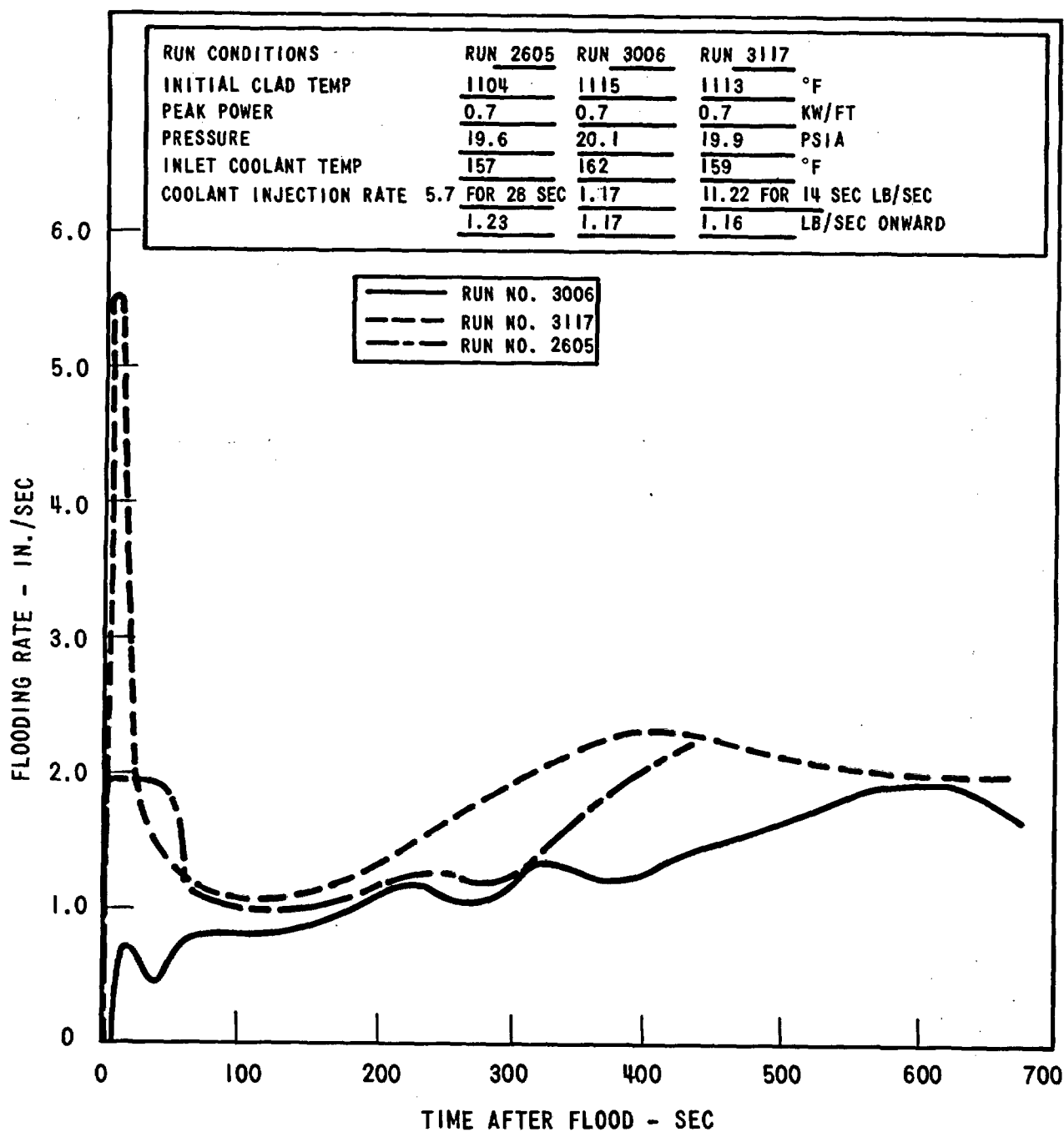


Figure 3-88. Flooding Rates for Runs 3117, 3006, and 2605

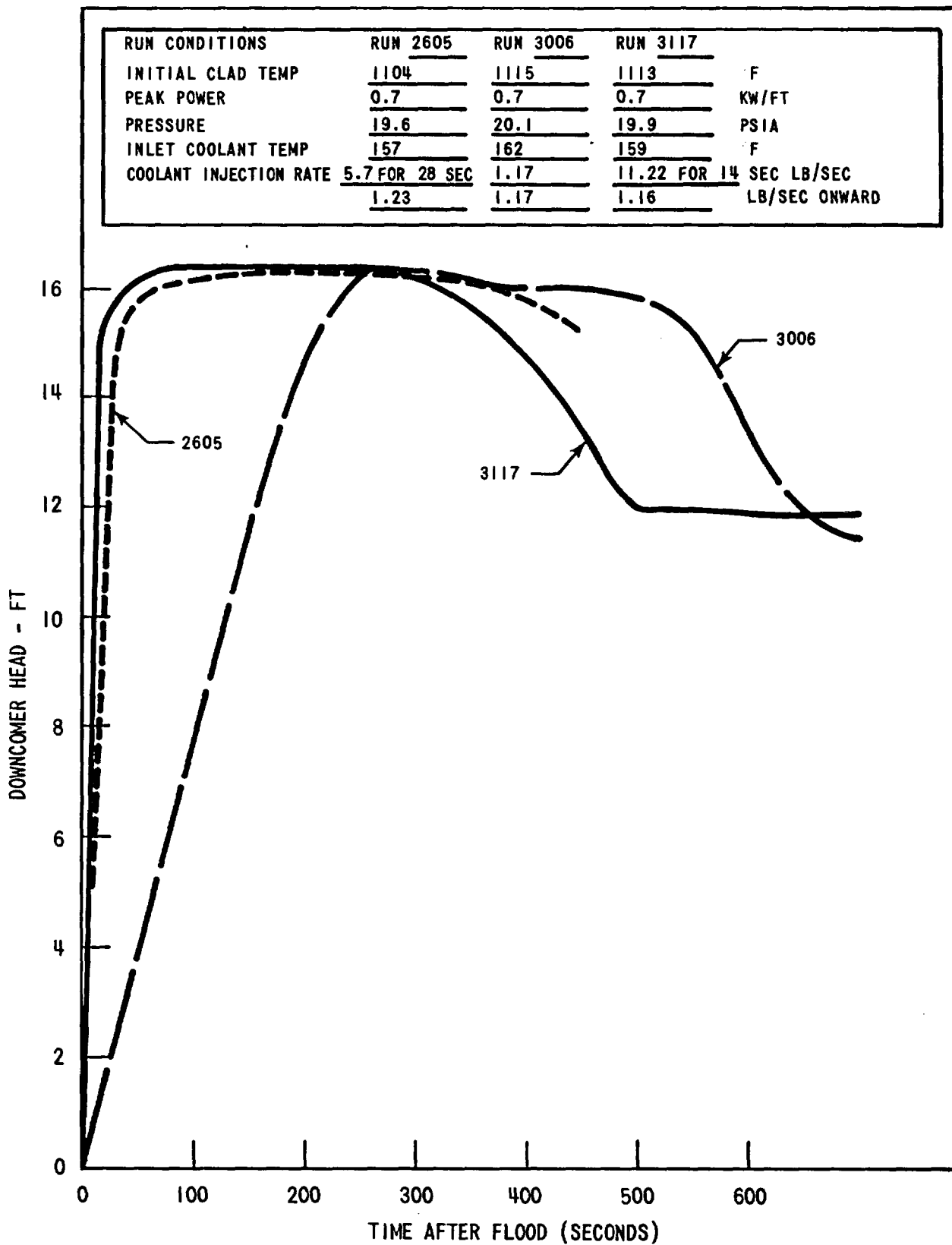


Figure 3-89. Downcomer Elevation for Runs 2605, 3006, and 3117

bundle is reflected in the larger heat transfer coefficients during the early portion of the transient, as shown in Figure 3-90 and the faster moving quench front, as shown in Figure 3-91. Both Runs 3117 and 2605 had higher midplane heat transfer coefficients initially and for the remainder of the transient than did Run 3006, which had a lower constant injection rate.

The rate at which the water is injected into the downcomer also influences the heat transfer coefficient, particularly at early times. Comparing Runs 3117 and 2605, the high injection rates were such that in Run 2605 the mass injection rate was reduced to nearly one-half that of Run 3117, but it was extended for twice the time so that nearly the same total mass was injected into the downcomer. The effect of different initial mass injection rates at early times can be seen in Figure 3-90, which indicates that the larger the initial injection rate, the greater the rod heat transfer coefficient in the initial period of the transient. It is believed that the heat transfer coefficient increase is caused by the larger downcomer head which forces more coolant into the bundle resulting in a lower void fraction at the hot spot and more steam generation (energy removed). At later times, the heat transfer coefficients are nearly the same because, at later times, the downcomer head, bundle mass storage and vapor flow rate are nearly the same for the two runs.

The effect of injection rate on the midplane heat transfer was also investigated at 60 psia by examining Runs 2023 (10.04 lbm/sec for 14 seconds and 1.38 lbm/sec onward), and Run 1709 (1.316 lbm/sec constant). The same trends were observed in the 60 psia data as in the 20 psia data, except that the difference in the heat transfer coefficient was more pronounced. The heat transfer coefficients for these two tests are shown in Figure 3-92, which clearly indicates that the higher injection rate at early time improves the heat transfer coefficient considerably. The corresponding flooding rates and downcomer elevations for these two tests are shown in Figure 3-93 and indicate that the higher injection rate quickly built up a large downcomer driving head which forced water into the bundle. Because of the large difference in the density of saturated steam and degree of subcooling between the 60 psia and 20 psia tests, the same downcomer head will result in more mass storage in the bundle and less loop pressure drop. Therefore, the

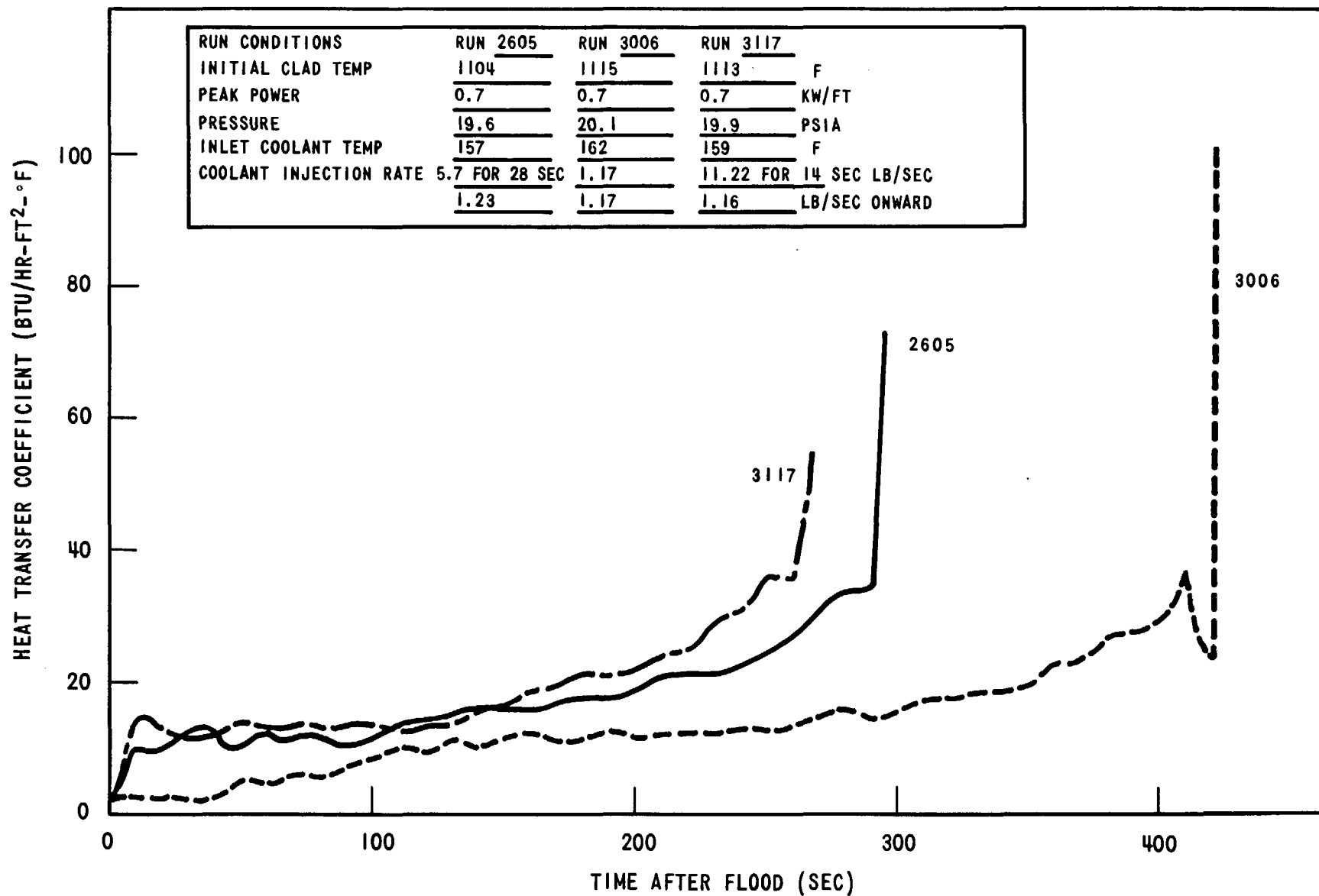


Figure 3-90. Midplane Heat Transient Coefficient for Runs 2605, 3006, and 3117

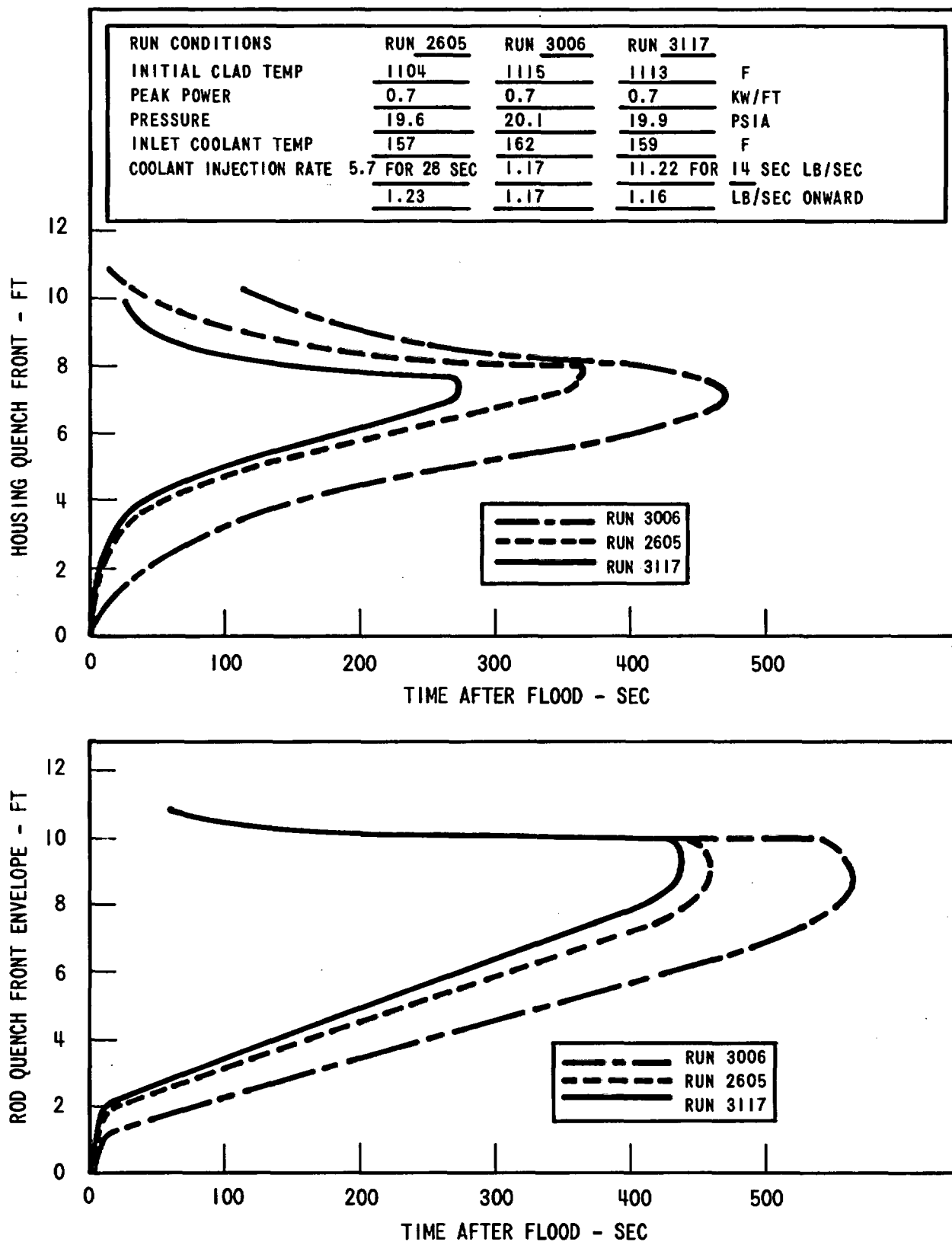


Figure 3-91. Rod Quench Envelope and Housing Quench Front for Runs 3117, 2605, and 3006

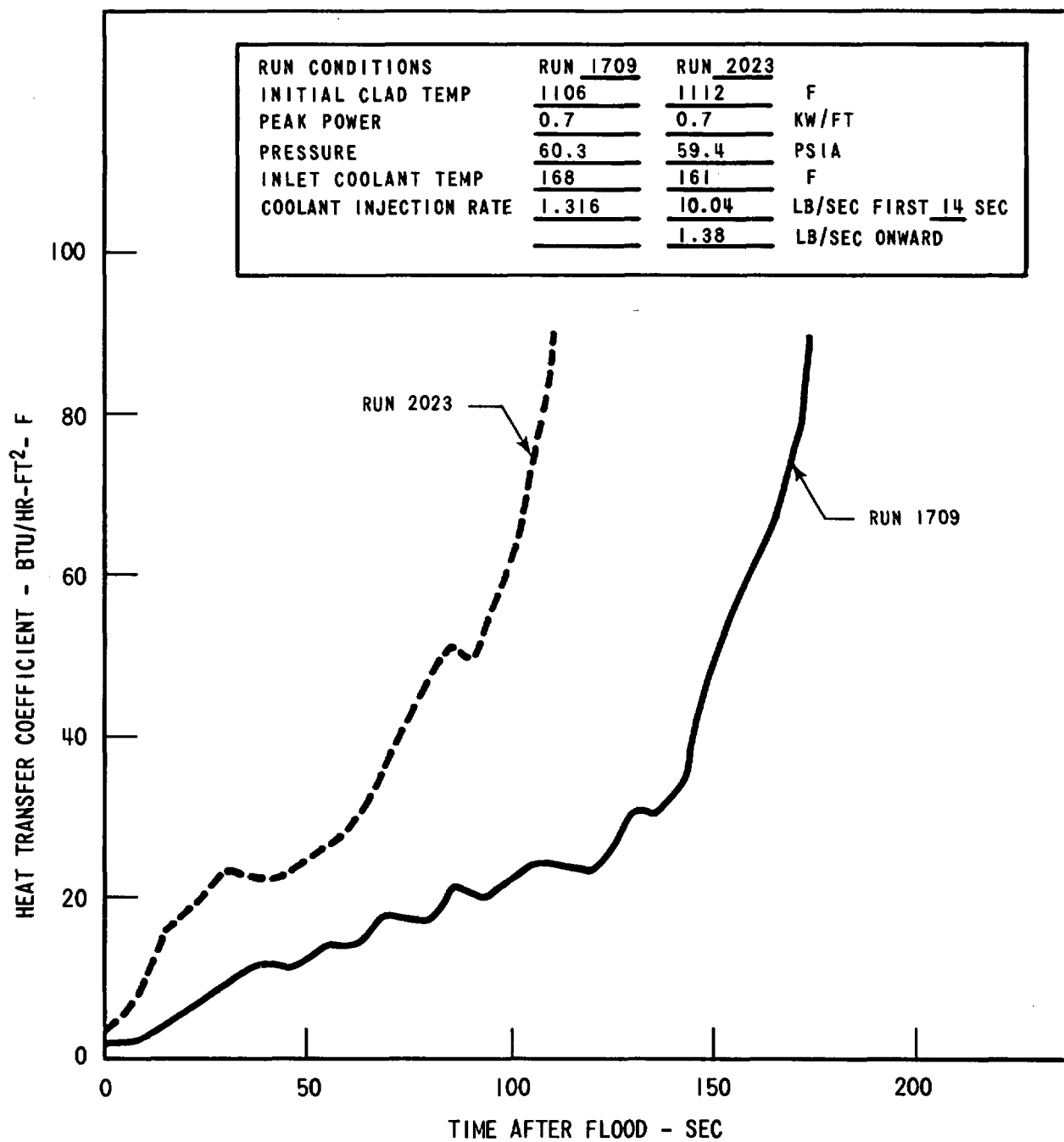


Figure 3-92. Midplane Heat Transfer Coefficient for Runs 1709 and 2023, Rod 7D

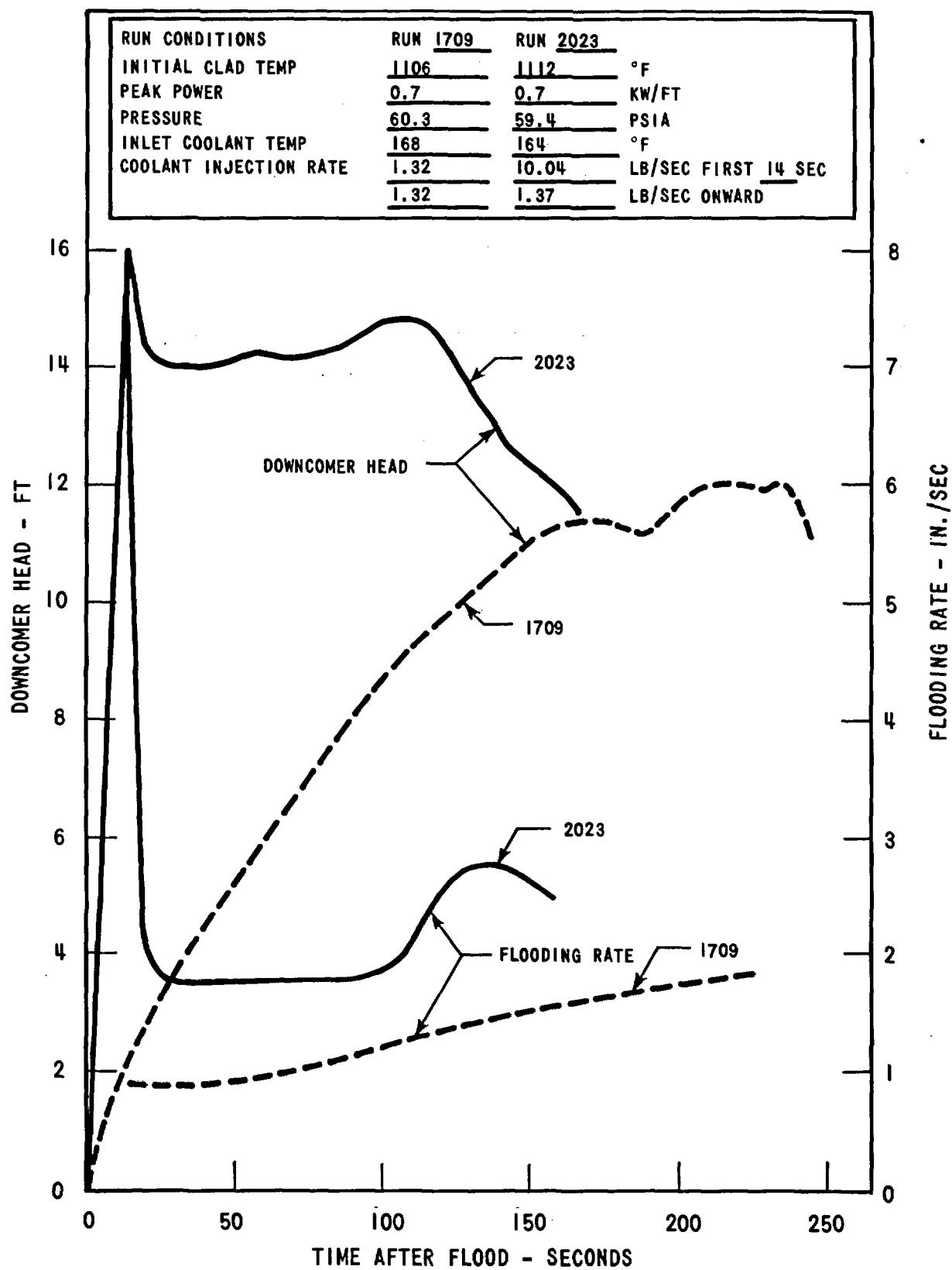


Figure 3-93. Downcomer Elevations and Flooding Rate, Runs 1709 and 2023

initially high flooding rate quenches the bundle and housing at the lower elevations very quickly and thereby allows a higher flooding rate, more mass storage in the bundle, and a larger midplane heat transfer coefficient. Both of these 60 psia tests were conducted with injection at the top of the downcomer and were affected by the condensation in the downcomer as discussed in Section 3.3.2.

Therefore, both 20 and 60 psia reflood heat transfer coefficients improve as the initial injection flow rate into the downcomer is increased.

SECTION 4

SUMMARY AND CONCLUSIONS

4.1 FLECHT-SET PHASE A CONCLUSIONS

1. The flooding rate transient generally began with large oscillations in the liquid levels in the downcomer and test section. The period of the oscillations was ~ 3 seconds, which is the period of liquid level oscillations of a U-tube with the same dimensions. The oscillations are driven by the very high heat release rate present early in the transient. It was found that the quenching of the test section housing was largely responsible for the initially high heat release rate. It is expected that similar oscillations, although of smaller amplitude, would occur during the reflood of a PWR.
2. The measured midplane heat transfer coefficients generally show considerable margin over those obtained from the FLECHT heat transfer correlations presented in Reference 1, using the measured flooding rate and a simple time shift to account for the flooding rate history. The margin in measured over predicted heat transfer coefficients existed for tests exhibiting large and small oscillations of the core liquid level (i.e., Runs 4923 and 4311). It was also noted that when there were liquid level oscillations but the mean flooding rate was nearly constant, as in Runs 1709 and 3006, the margin between measured and predicted heat transfer coefficients was considerably reduced. Thus, the largest margin exists when there are large variations in the mean flooding rate. Therefore, the method used to predict the heat transfer coefficient is very conservative when the mean flooding rate varies with time. An improved method is required to better predict the heat transfer coefficients when the flooding rate varies with time to remove some of the conservatism which exists in the present method.

3. There was a significant delay (100 to 200 seconds) before water from the test section collected in the separator at the end of the hot leg. The delay was caused by the storage of water in the upper plenum and upper plenum extension of the test section. The effect the test section geometry had on the accumulation of water in the upper plenum and upper plenum extension is not known at this time. Additional tests are planned in Phase B to determine the importance of the upper plenum geometry. However, this separation effect is present in a PWR upper plenum and it is expected that a PWR upper plenum would also accumulate a significant amount of water. The separation effect of the upper plenum is important since it affects the two-phase quality of the mixture flowing into the steam generators and the energy release rate to the containment.
4. The average flooding rates determined for the tests were observed to fluctuate considerably even after the large 3-second-period oscillations had decayed. The fluctuations in flooding rate are caused by the same phenomenon observed in many two-phase flow systems and have been described as density wave oscillations. A perturbation which results in an increase in flooding rate initially causes a decrease in steam flow rate as the void generation is decreased. The resulting decreased loop pressure drop results in a further increase in flooding rate. Eventually the steam generation rate increases because the quench front moves up faster, releasing more stored heat; also the difference between test section pressure drop and downcomer head results in less driving head and the flooding rate decreases. These fluctuations have been observed to have a period of ~50 seconds. Similar fluctuations are expected to occur in a PWR.
5. As expected from the constant flooding rate FLECHT tests, the containment pressure had the most significant effect on the transient. The quench time, turnaround times and temperature rise generally decreased and heat transfer coefficients increased as the containment pressure increased.

6. Similar to the constant flooding rate FLECHT tests, the inlet subcooling had a significant effect. The steam flow rate increased while the mass stored in the bundle, flooding rate, and midplane heat transfer coefficient decreased as the subcooling decreased. This is to be expected since the core elevation where void generation begins decreases as the subcooling decreases for a given flooding rate.
7. Increasing the initial clad temperature resulted in decreased midplane temperature rise and turnaround time and increased quench times. With 20 psia containment pressures an increased initial clad temperature resulted in water being collected in the separator tank earlier in time, indicating that more entrained liquid was carried out of the test section. With 60 psia containment pressures, an increased initial clad temperature also increased the vapor flow rate and decreased the mass stored in the bundle. There was no indication of a significant increase in the time of liquid collection with increasing initial clad temperatures at 60 psia.
8. Increasing the peak power resulted in increased midplane temperature rise, turnaround time, and quench times and decreased the midplane heat transfer coefficient. In addition, raising the peak power resulted in higher steam flow rates, lower flooding rates, and less mass remaining in the bundle. It should be emphasized that if the FLECHT housing criterion is used, increasing the peak power also means that the housing initial temperature is increased. When the peak power was increased with the housing temperature unchanged, the midplane heat transfer coefficient was slightly improved.
9. The effect of the housing when heated according to the FLECHT housing criterion has been shown to be conservative. However, it has also been shown to have a significant effect on the test results. Since the housing initial stored energy depends of the initial stored energy of the heater rods and on the power input up to the expected midplane quench time, any parameter variation such as rod power, initial clad temperature, containment pressure, etc., also changes the housing temperature. The housing heat release rate and steam generation rate are much higher than for an equivalent row of rods early in the transient. First, the housing heat

release rate is sufficient to drive oscillations in the core and downcomer liquid levels which are much larger and longer lasting than those which exist when the housing is passive. Second, the test results, such as the midplane rod heat transfer coefficient, are more affected early in the transient by the change in housing temperature than by the parameter variation being investigated. For example, it was found that if the housing temperature was unchanged and the rod peak power was raised, the resulting midplane heat transfer coefficient was slightly higher. However, when the FLECHT housing criterion was applied and the housing temperature increased, the resulting midplane heat transfer coefficient was reduced in the critical early part of the transient when the rod temperature was being turned around.

Although the housing effect was not investigated at 20 psia, it is believed that it would have been even more significant at the lower pressure. Since the midplane quench times were longer at 20 psia than at 60 psia, the FLECHT criterion increased the difference between the housing temperature and the saturation temperature. This, combined with the fact that the volume of steam produced per Btu is approximately 2.8 times higher at 20 psia than at 60 psia, indicates that the housing effect is more dominant at the lower pressure. Tests are planned in Phase B to investigate the effect of the housing temperature at 20 psia.

4.2 LOW CLAD TEMPERATURE FLECHT TESTS

These tests extend the range of the FLECHT conditions as close as possible to the saturation temperature over the initial temperature range from 250°F to 750°F. The following conclusions may be drawn:

1. Both the amount of liquid entrained and the average mass effluent fraction are significantly lower than in the high temperature FLECHT tests.
2. With initial clad temperatures very close to saturation temperature, the bundle quenches at nearly the cold fill rate with little or no liquid entrainment.

3. As the initial clad temperature increases, the temperature quench front diverges progressively further from the cold fill rate. This effect is greater at 20 psia than at 60 psia, but in both cases the 4 ft elevation is reached before significant mass effluent fractions are measured.
4. The mass of liquid collected and the average mass effluent fraction up to the time of the midplane quench increase as:
 - a. Flooding rate decreases
 - b. Initial clad temperature increases
 - c. Pressure decreases
 - d. Peak power increases

Coolant subcooling showed no significant effect.

4.3 TOP INJECTION TESTS

The top injection tests performed in FLECHT-SET Phase A indicate that core cooling can be obtained by this mode of ECC injection. It is also evident that the individual rod temperatures will remain at elevated temperatures for longer periods of time than a comparable bottom flooding FLECHT test with the same injection flow rate. The top injection flow distribution is a sensitive parameter in these tests and can result in only marginal cooling for rods which are removed from the coolant injection location.

The most significant parameters on the temperature history and rod heat transfer were the amount of injection water subcooling, injection flow rate, and whether the water was allowed to accumulate in the lower plenum of the test section. The hot injection water resulted in more steam generation which helped to maximize any flow redistribution effects within the bundle so that better cooling was promoted. Cold injection water resulted in cold water channeling which created bundle hot spots.

If sufficient injection water is used, the flow maldistribution effects are also minimized and all rods receive some cooling. It should be noted that the injection flow rate was increased by a factor of 2.3 at approximately 82°F and the resulting peak temperatures were higher than the case with lower injection flow which was heated to 180°F. Therefore, the primary mechanism for mixing and promoting improved cooling appears to be the amount of steam generation in the bundle.

If the top injection water is allowed to accumulate in the bundle, the cooling performance of the bundle is significantly improved so that rod quenches typical of FLECHT occur. The maximum temperatures observed in this system configuration were lower than those observed in tests with similar system parameters but, in which no water was allowed to accumulate in the bundle.

SECTION 5

REFERENCES

1. F. F. Cadek, D. P. Dominicis, H. C. Yeh, R. H. Leyse, "PWR FLECHT Final Report Supplement," WCAP-7931, October 1972.
2. F. F. Cadek, D. P. Dominicis, R. H. Leyse, "PWR FLECHT: (Full Length Emergency Cooling Heat Transfer) Final Report," WCAP-7665, April 1971.
3. J. O. Cermak, A. S. Kitzes, F. F. Cadek, R. H. Leyse, D. P. Dominicis, "PWR Full Length Emergency Cooling Heat Transfer (FLECHT) Group I Test Report," WCAP-7435, January 1970.

APPENDIX A
FLECHT-SET DATA SHEETS

)

)

)

—

FLECHT-SET RUN SUMMARY SHEET

RUN NO. 1510

DATE 8/18/72

A. RUN CONDITIONS

Containment Pressure	55.2	psia
Initial Clad Temperature	1112	°F
Peak Power	0.7	kw/ft
Coolant Supply Temperature	164	°F
Injection Rate	10.44 lb/sec first 14 sec, 1.37 lb/sec after 14 sec	
Loop Resistance Coefficient ($\Delta p_{loop} / 1/2 \rho v_{hotleg}^2$)	30.0	

B. INITIAL HOUSING TEMPERATURES

Elevation (ft)	Initial Temperature (°F)
0	294
2	405
4	508
6	548
8	507
10	420
12	350

FLECHT-SET RUN SUMMARY SHEET (Cont)

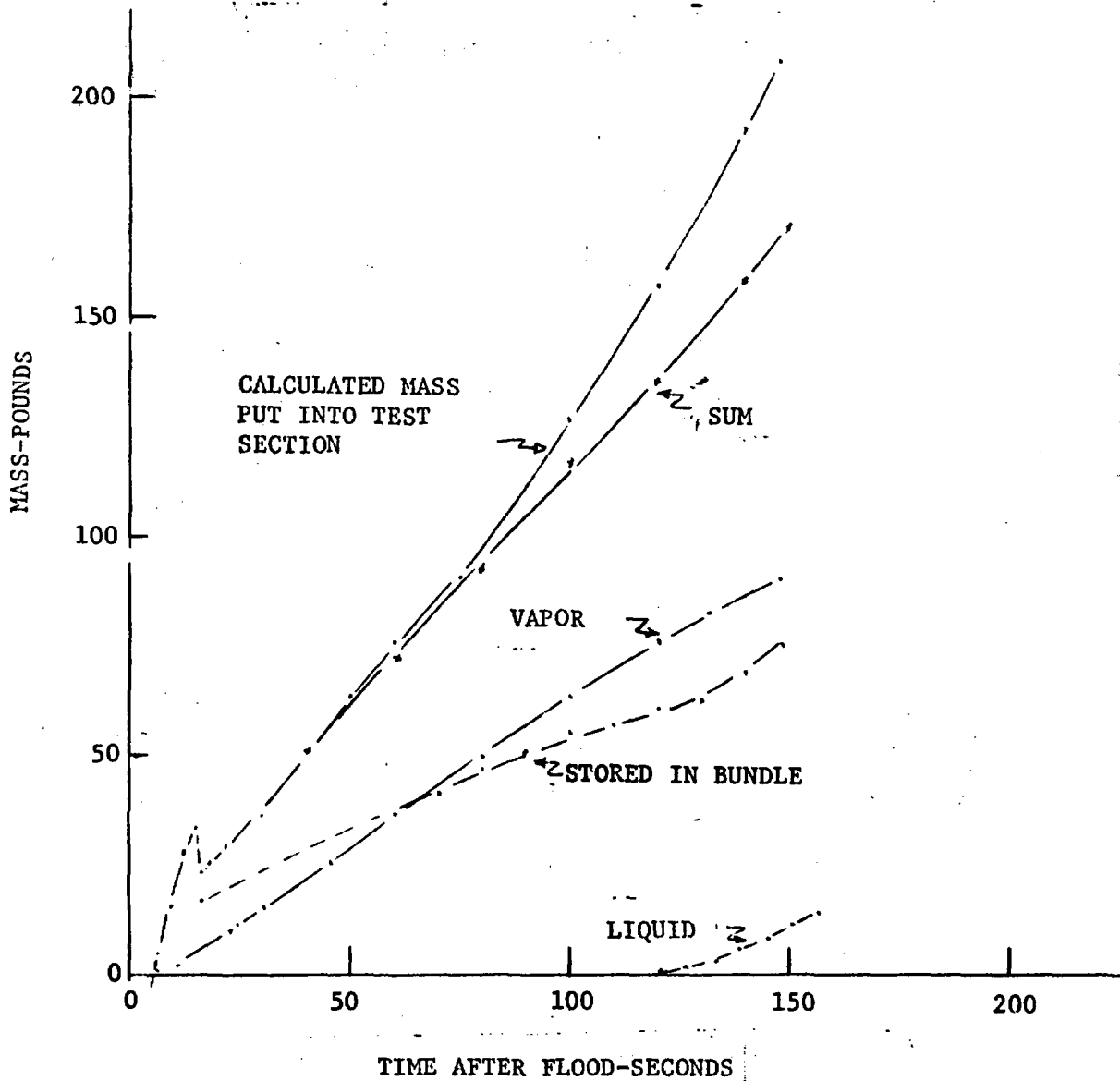
RUN NO. 1510

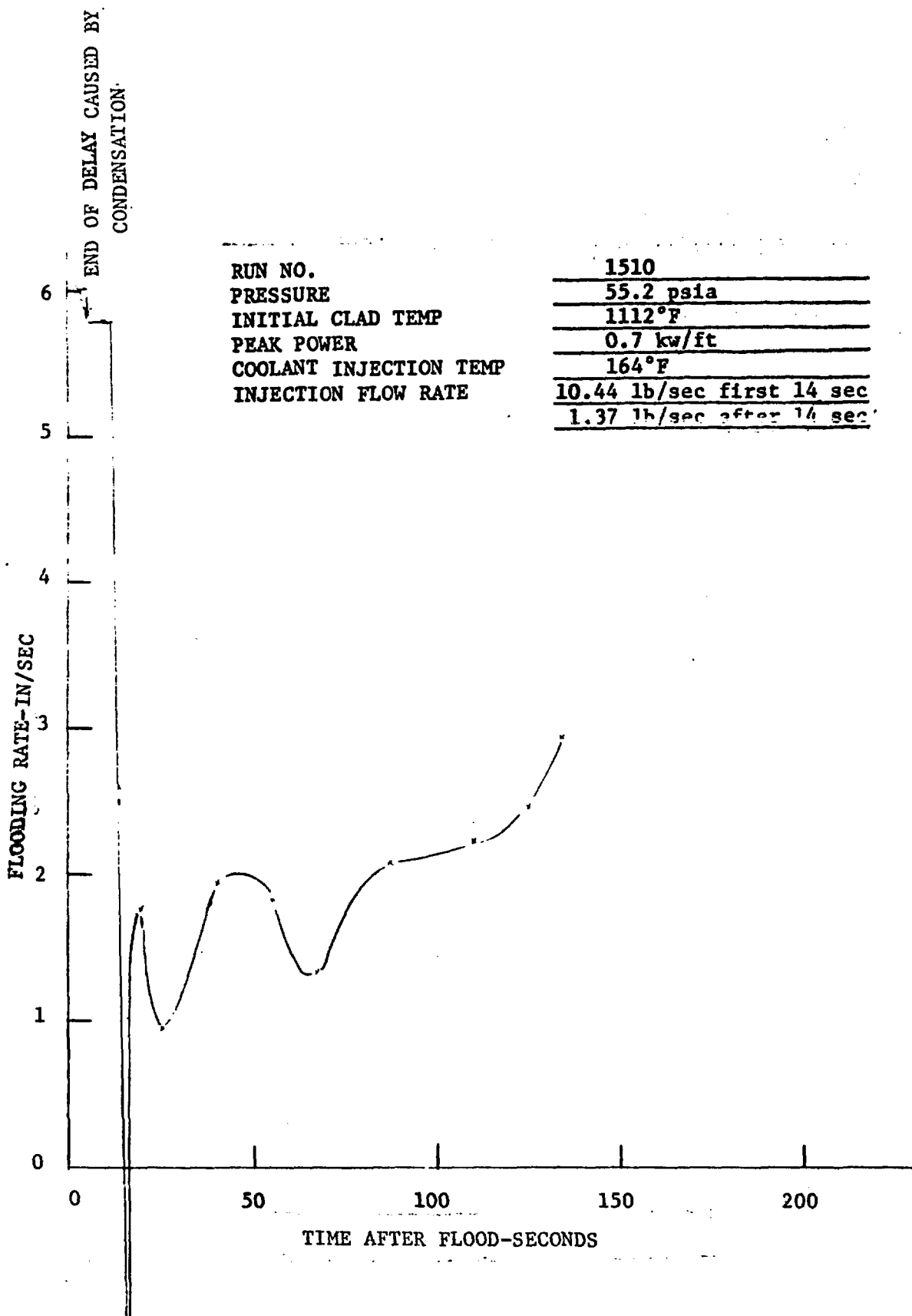
DATE 8/18/72

C. HEATER THERMOCOUPLE DATA

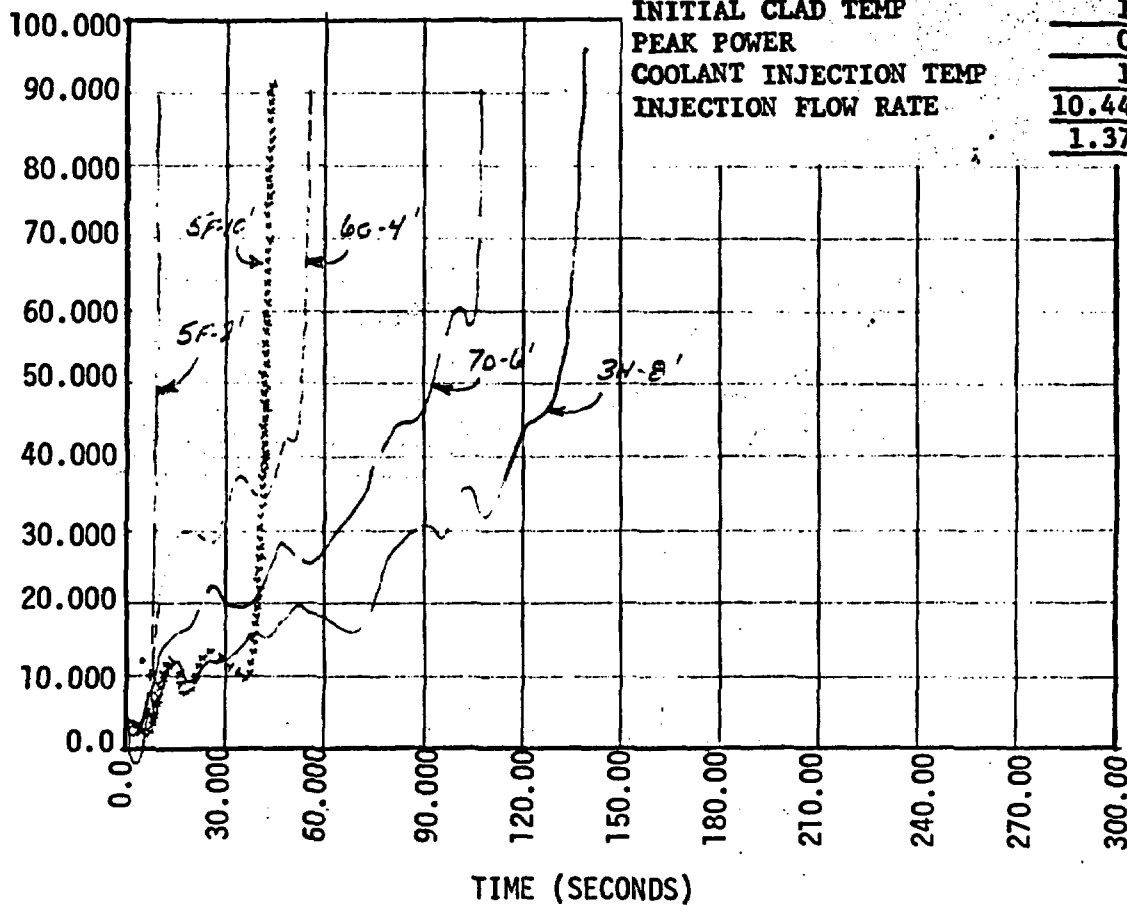
Rod/Elev.	Initial Temp. (°F)	Max. Temp. (°F)	Turnaround Time (Sec)	Quench Time (Sec)
5F/2'	675	713	8	15
5F/4'				
5F/6'				
5F/8'				
5F/10'	712	808	40	51
5G/2'	664	707	9	16
5G/4'				
5G/6'	1112	1263	41	121
5G/8'	978	1109	41	146
5G/10'	706	799	41	91
6G/2'	674	714	9	16
6G/4'	946	1008	10	63
6G/6'				
6G/8'				
6G/10'	698	775	37	64
3H/2'				
3H/4'	943	1008	34	71
3H/6'	1077	1243	35	117
3H/8'	906	1101	72	146
3H/10'	657	773	77	136
4G/4'	1041	1108	10	65
4G/6'	1108	1279	41	115
4G/10'	687	784	43	62
4H/4'	945	1118	15	72
4H/6'				
4H/10'	688	792	49	113
7D/4'	939	1003	10	68
7D/6'	1047	1175	40	115
7D/10'				

RUN NO.	1510
PRESSURE	55.2 psia
INITIAL CLAD TEMP	1112°F
PEAK POWER	0.7 kw/ft
COOLANT INJECTION TEMP	164°F
INJECTION FLOW RATE	10.44 lb/sec first 14 sec
	1.37 lb/sec after 14 sec





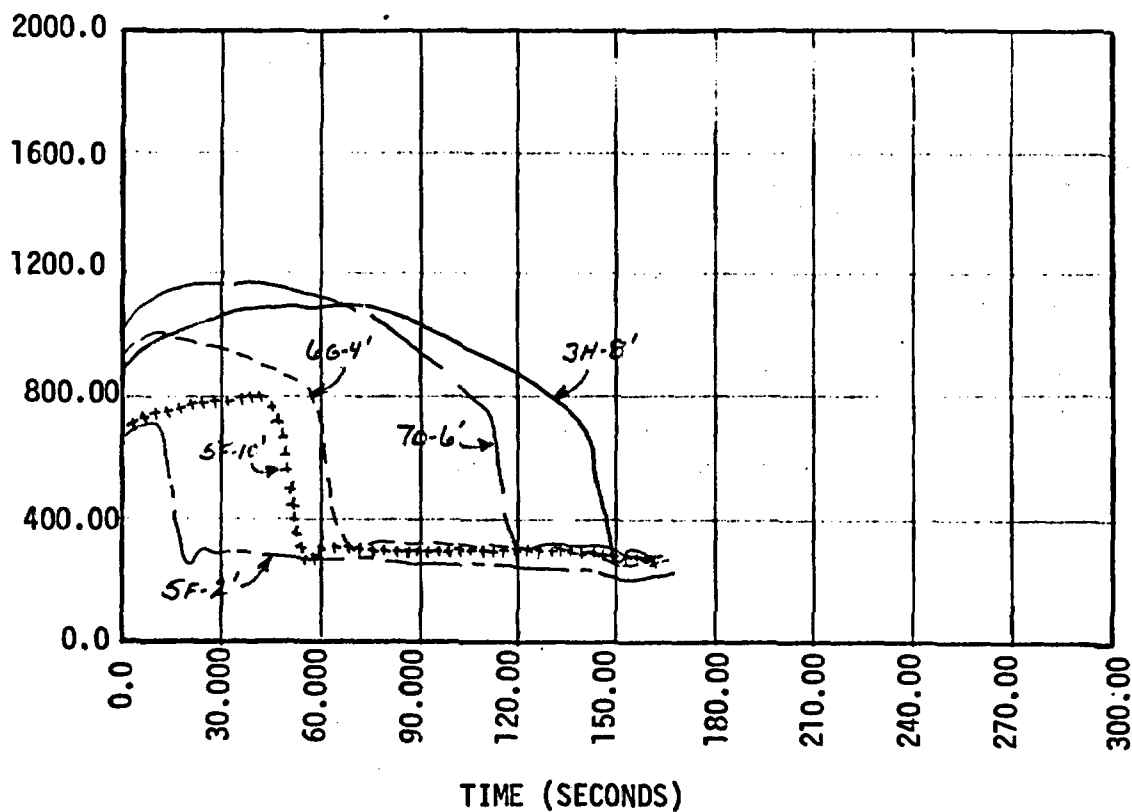
HEAT TRANSFER COEFFICIENT (BTU/HR/FT**2) (G F)



RUN NO.
PRESSURE
INITIAL CLAD TEMP
PEAK POWER
COOLANT INJECTION TEMP
INJECTION FLOW RATE

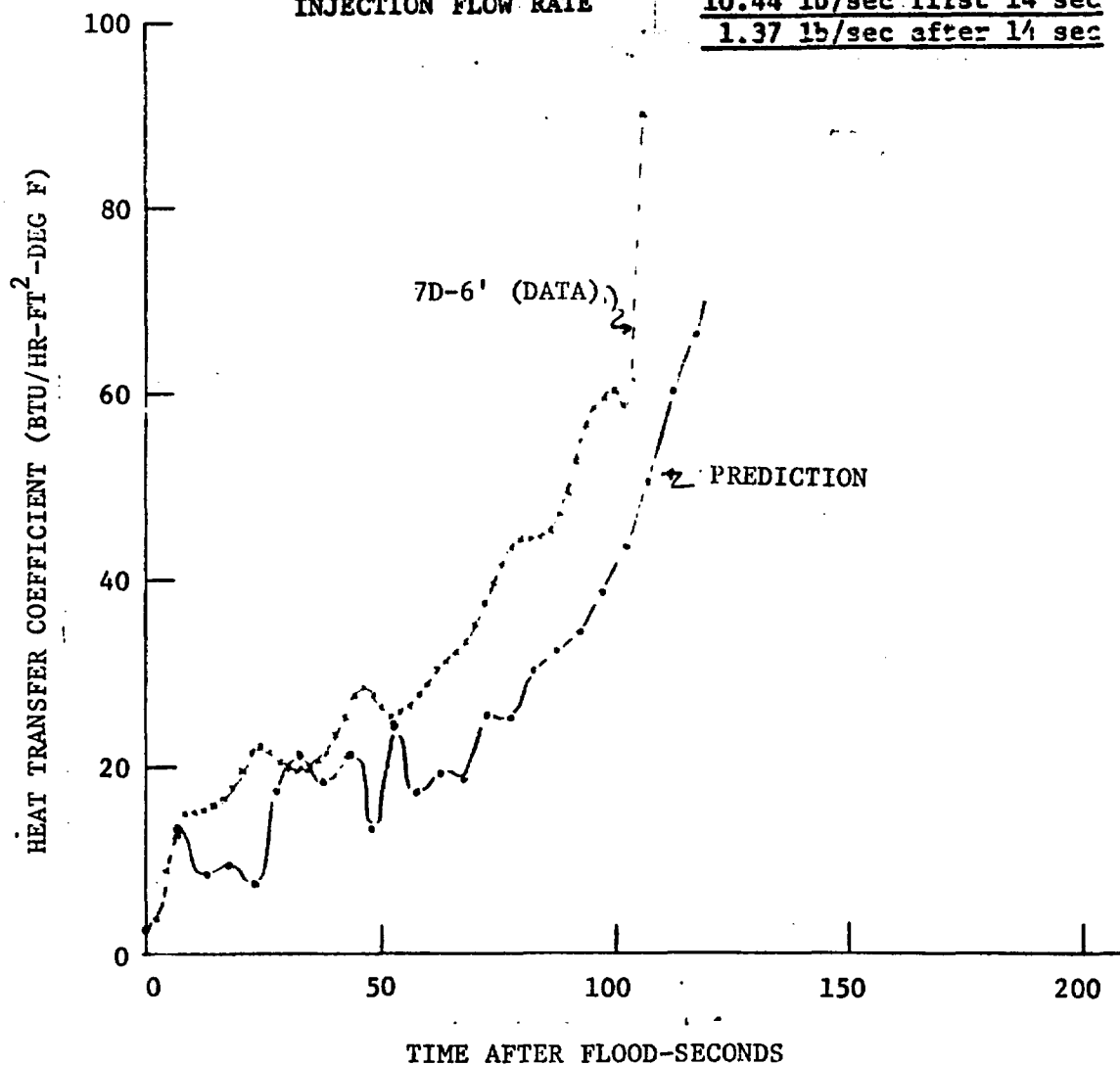
1510
55.2 psia
1112°F
0.7 kw/ft
164°F
10.44 lb/sec first 14 sec
1.37 lb/sec after 14 sec

CLAD TEMPERATURE (DEG. F)



RUN NO.
 PRESSURE
 INITIAL CLAD TEMP
 PEAK POWER
 COOLANT INJECTION TEMP
 INJECTION FLOW RATE

1510
55.2 psia
1112°F
0.7 kw/ft
164°F
10.44 lb/sec first 14 sec
1.37 lb/sec after 14 sec



FLECHT-SET RUN SUMMARY SHEET

RUN NO. 1709

DATE 8/23/72

A. RUN CONDITIONS

Containment Pressure	60.3	psia
Initial Clad Temperature	1106	°F
Peak Power	0.7	kw/ft
Coolant Supply Temperature	168	°F
Injection Rate	1.32 lb/sec first	sec, 1b/sec after sec
Loop Resistance Coefficient	$(\Delta p_{loop} / 1/2 \rho V_{hotleg}^2)$	29.1

B. INITIAL HOUSING TEMPERATURES

Elevation (ft)	Initial Temperature (°F)
0	285
2	406
4	482
6	540
8	510
10	408
12	292

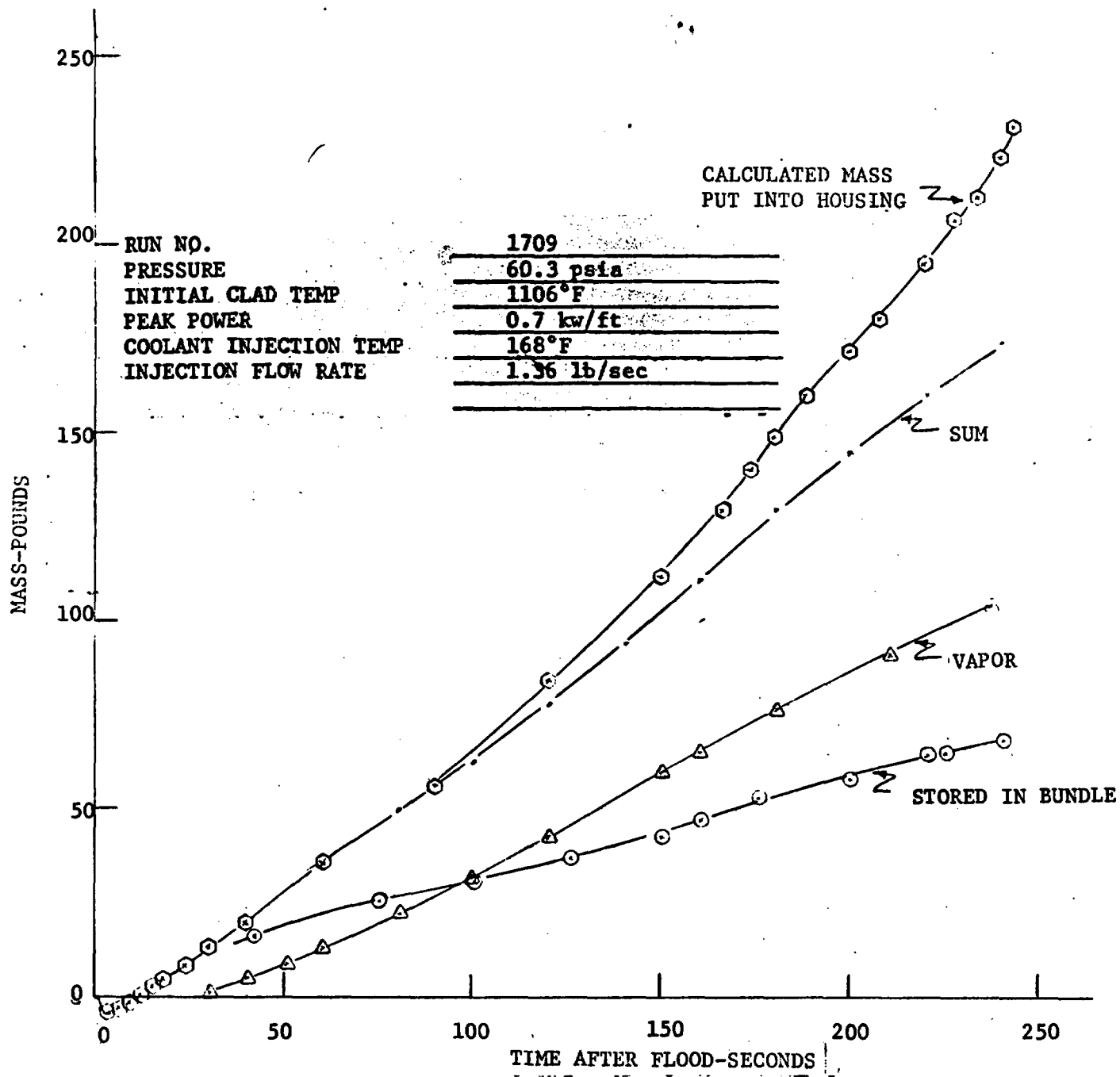
FLECHT-SET RUN SUMMARY SHEET (Cont)

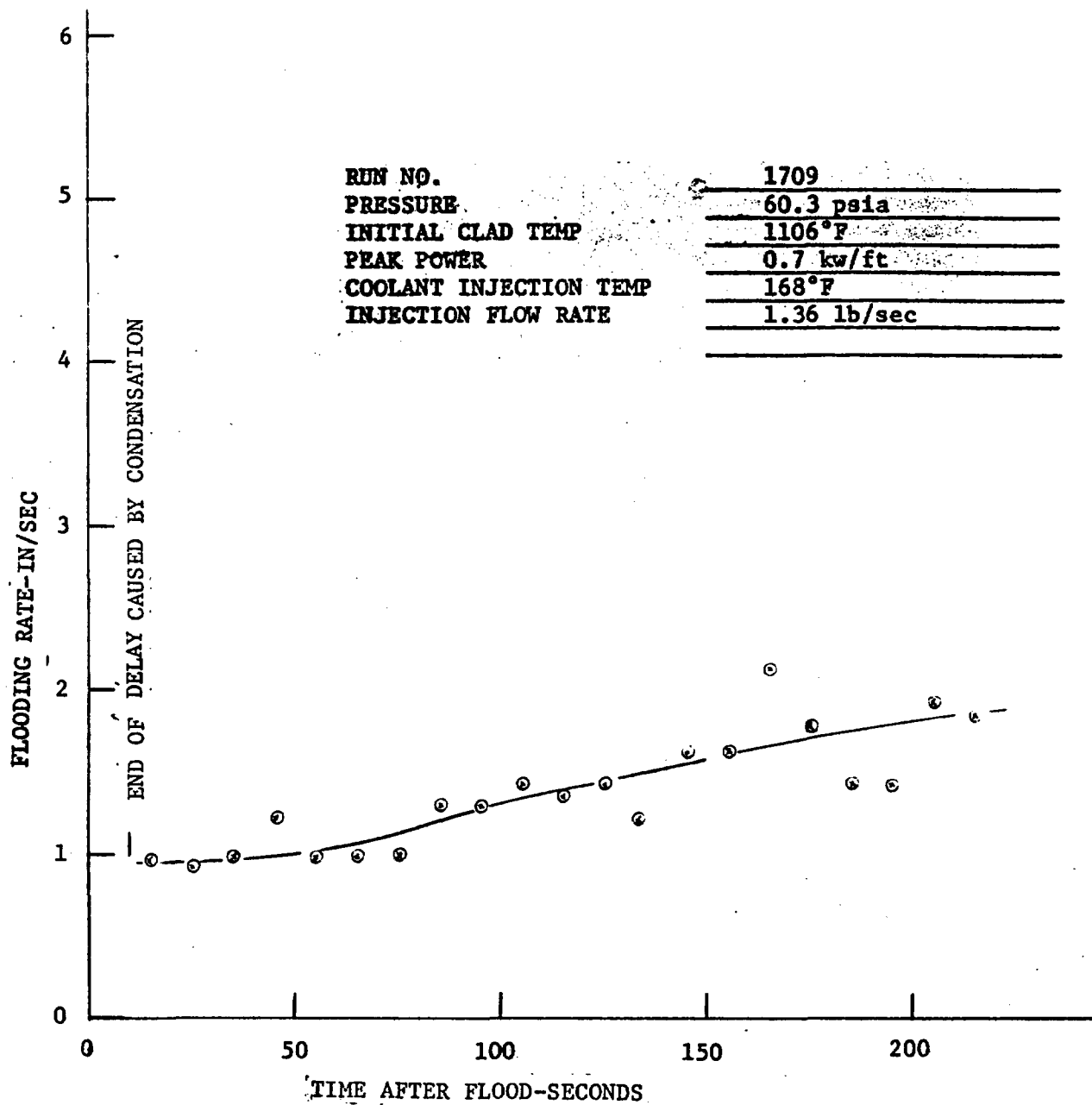
RUN NO. 1709

DATE 8/23/72

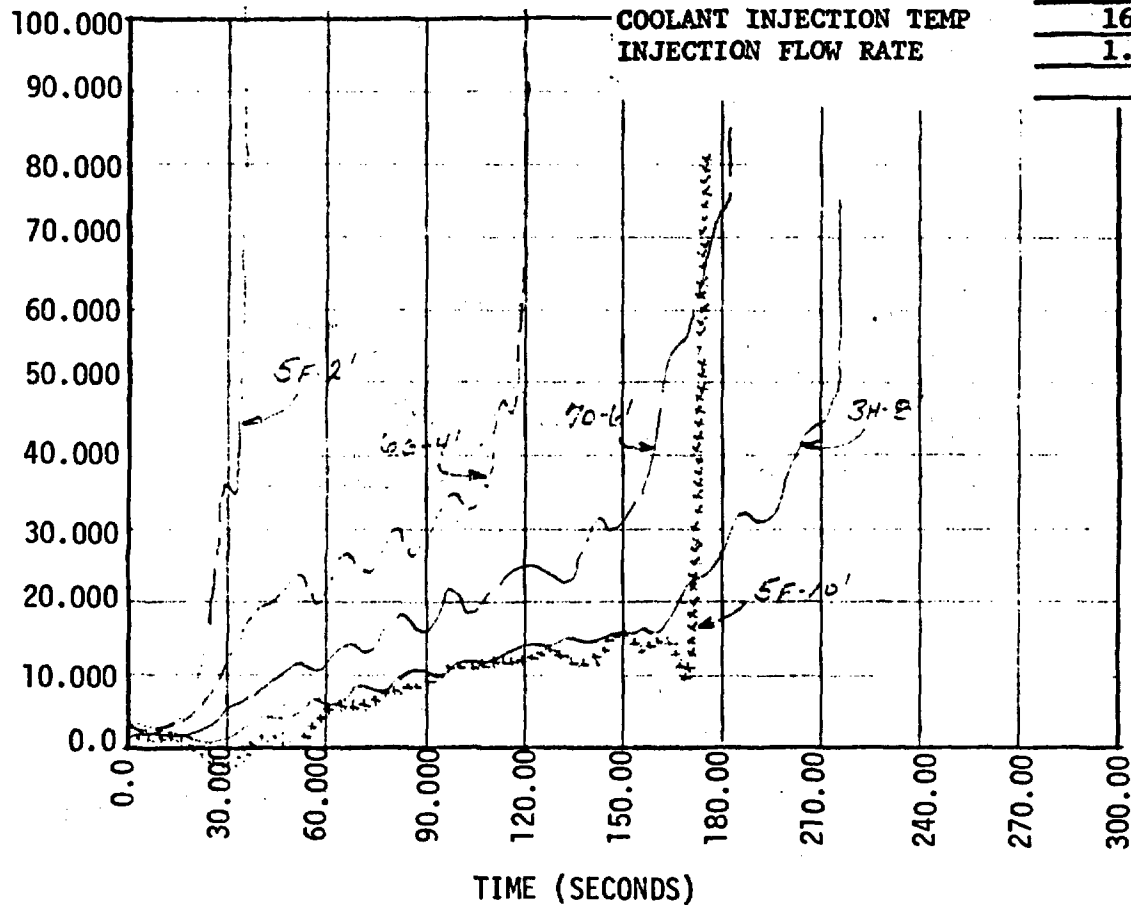
C. HEATER THERMOCOUPLE DATA

Rod/Elev.	Initial Temp. (°F)	Max. Temp. (°F)	Turnaround Time (Sec)	Quench Time (Sec)
5F/2'	651	752	25	41
5F/4'				
5F/6'				
5F/8'				
5F/10'	726	1039	93	181
5G/2'	641	741	24	42
5G/4'				
5G/6'	1106	1551	77	192
5G/8'	990	1453	98	238
5G/10'	712	1021	89	194
6G/2'	651	752	24	42
6G/4'	923	1140	36	126
6G/6'				
6G/8'				
6G/10'	699	974	90	184
3H/2'				
3H/4'	902	1146	38	126
3H/6'	1055	1489	75	187
3H/8'	907	1378	99	223
3H/10'	652	978	94	234
4G/4'	1016	1268	40	130
4G/6'	1104	1581	83	188
4G/10'	696	1007	92	199
4H/4'	917	1165	54	132
4H/6'				
4H/10'	691	1004	92	213
7D/4'	921	1153	35	127
7D/6'	1055	1460	76	191
7D/10'				





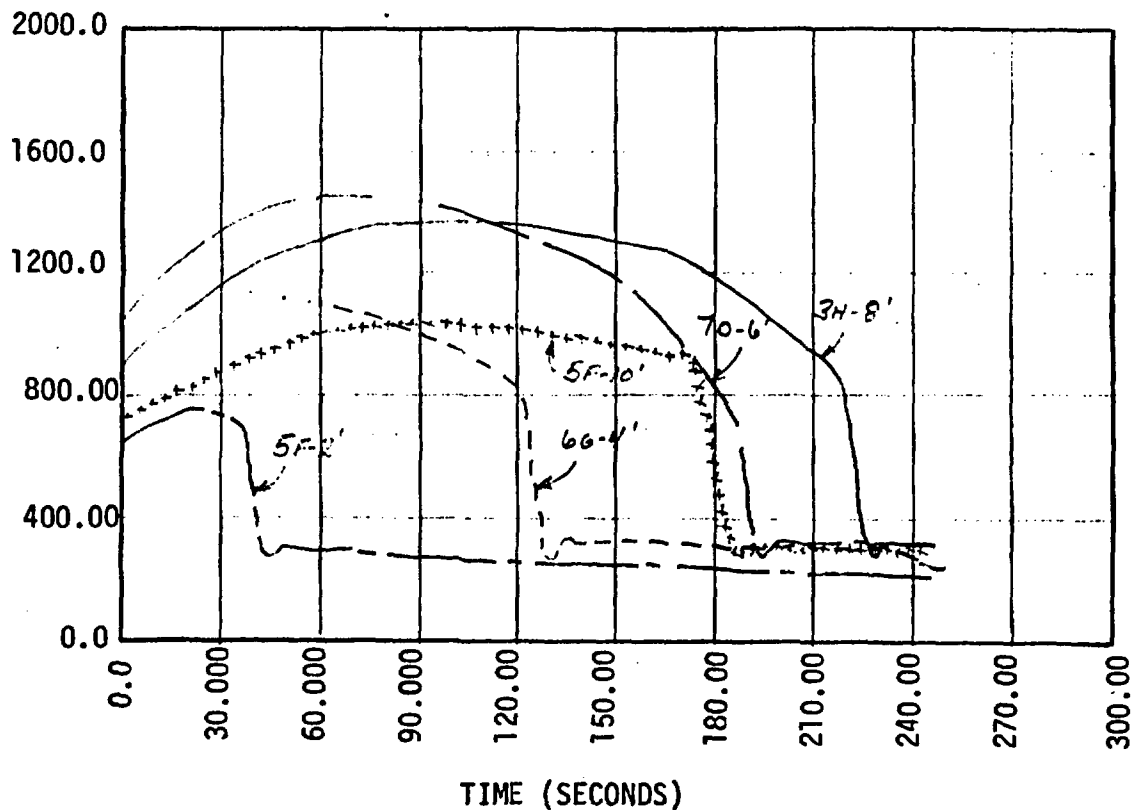
HEAT TRANSFER COEFFICIENT (BTU/HR/FT**2/DEG F)

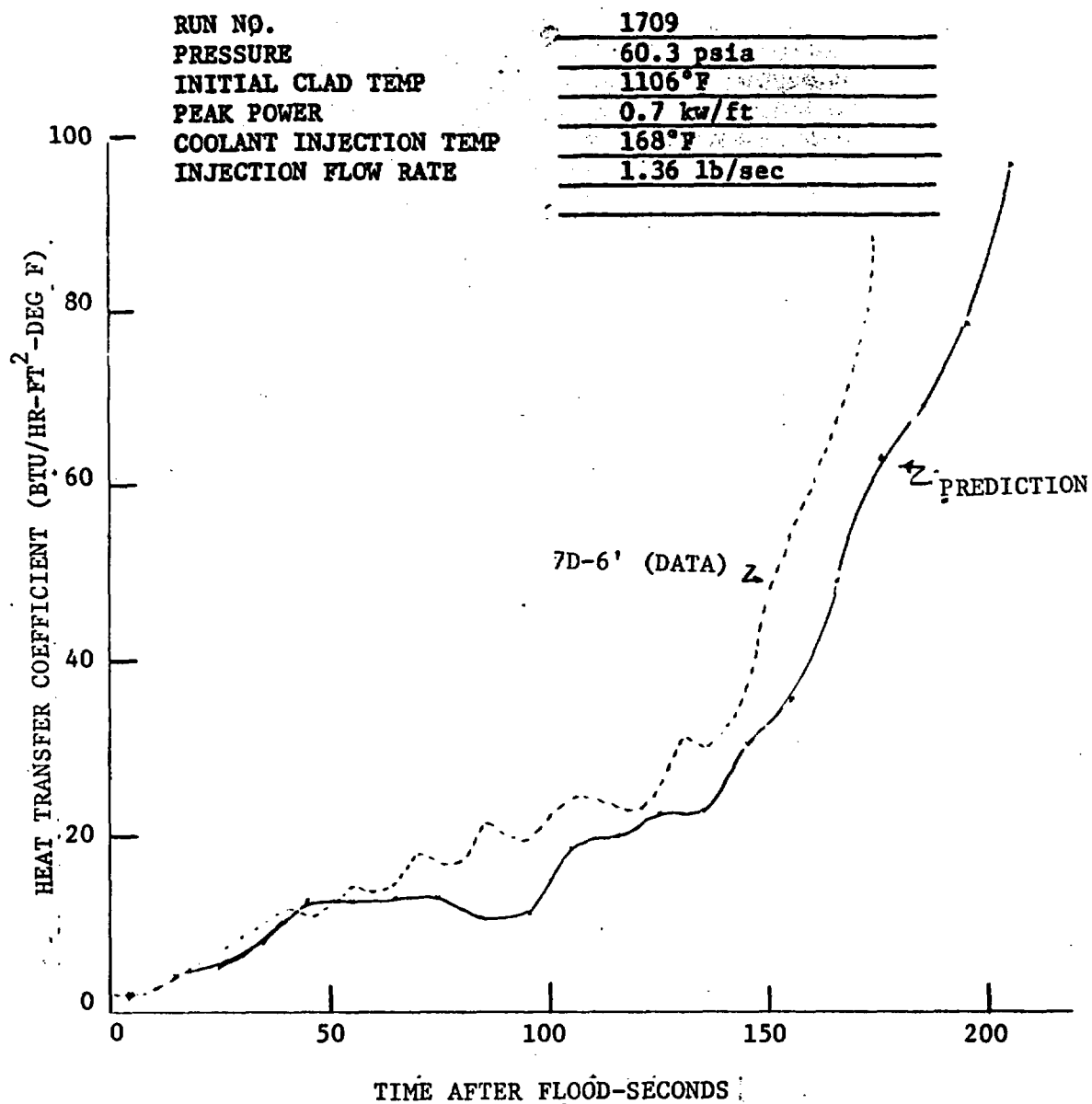


PRESSURE
INITIAL CLAD TEMP
PEAK POWER
COOLANT INJECTION TEMP
INJECTION FLOW RATE

60.3 psia
1106°F
0.7 kw/ft
168°F
1.36 lb/sec

CLAD TEMPERATURE (DEG. F)





FLECHT-SET RUN SUMMARY SHEET

RUN NO. 1827

DATE 8/28/72

A. RUN CONDITIONS

Containment Pressure	59.5	psia
Initial Clad Temperature	1112	°F
Peak Power	0.4	kw/ft
Coolant Supply Temperature	161	°F
Injection Rate	9.63 lb/sec first 14 sec, 1.36 lb/sec after 14 sec	
Loop Resistance Coefficient	$(\Delta p_{\text{loop}} / 1/2 \rho V_{\text{hotleg}}^2)$ 28.0	

B. INITIAL HOUSING TEMPERATURES

Elevation (ft)	Initial Temperature (°F)
0	290
2	375
4	437
6	472
8	440
10	365
12	290

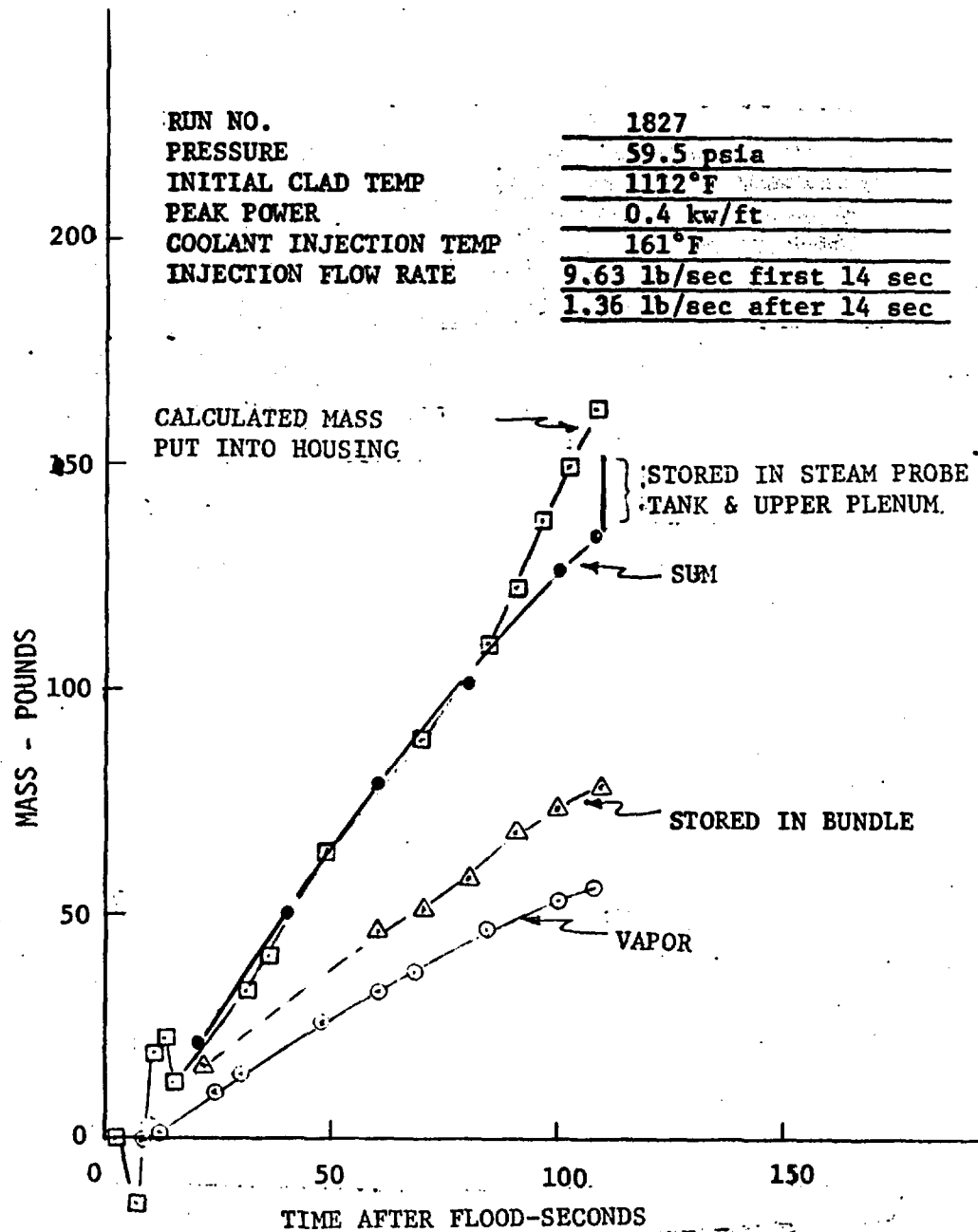
FLECHT-SET RUN SUMMARY SHEET (Cont)

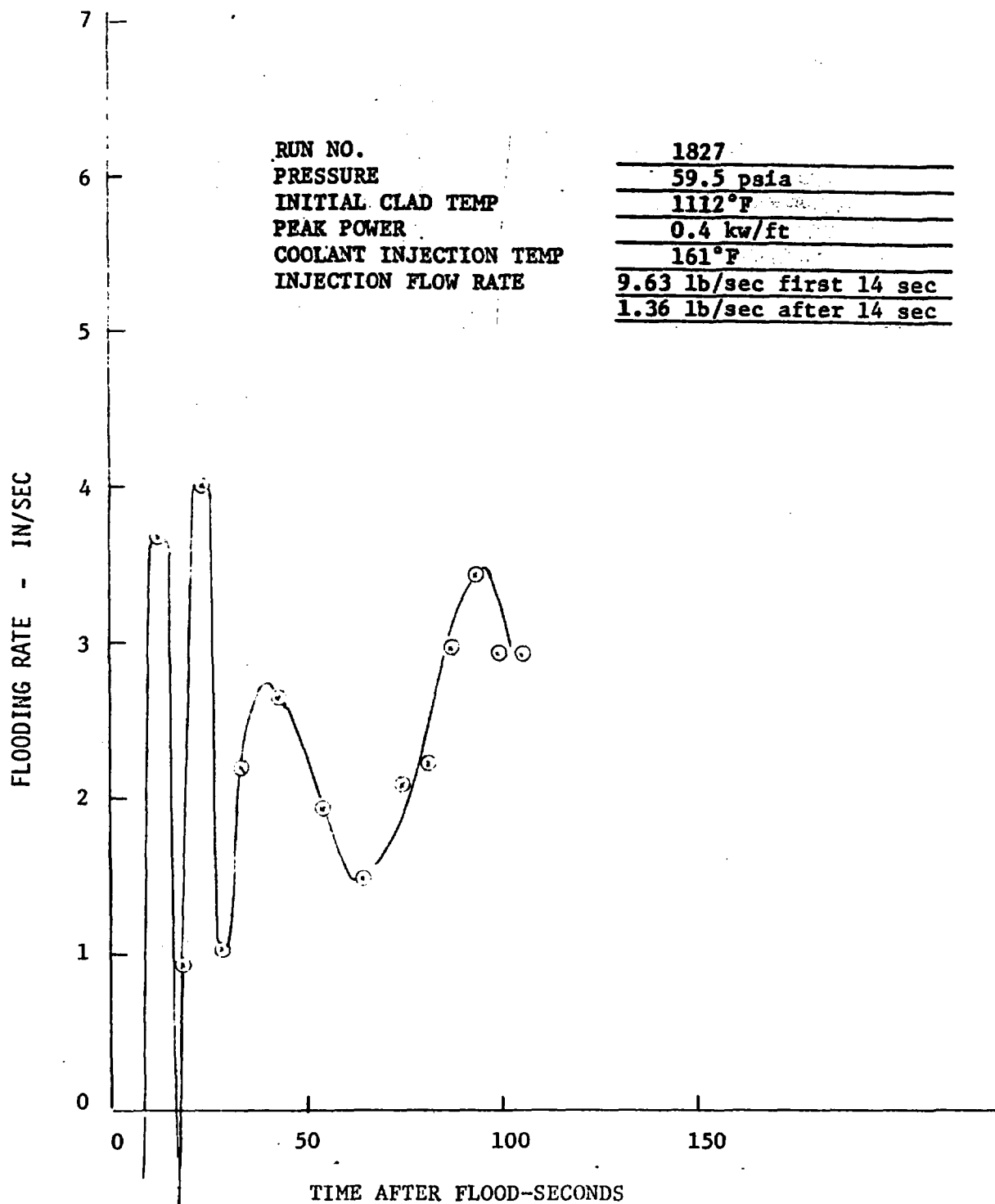
RUN NO. 1827

DATE 8/28/72

C. HEATER THERMOCOUPLE DATA

Rod/Elev.	Initial Temp. (°F)	Max. Temp. (°F)	Turnaround Time (Sec)	Quench Time (Sec)
5F/2'	709	736	8	26
5F/4'				
5F/6'				
5F/8'	909	956	23	78
5F/10'	694	729	29	36
5G/2'	701	726	7	22
5G/4'				
5G/6'	1112	1150	12	93
5G/8'	963	999	20	90
5G/10'	678	711	29	35
6G/2'	707	731	8	22
6G/4'	952	978	9	56
6G/6'				
6G/8'				
6G/10'	669	689	18	36
3H/2'				
3H/4'	938	970	11	60
3H/6'	1052	1091	23	83
3H/8'	875	911	16	91
3H/10'	589	634	28	48
4G/4'	1036	1063	11	50
4G/6'	1100	1138	14	83
4G/10'	653	678	19	29
4H/4'	941	975	12	60
4H/6'				
4H/10'	743	761	15	36
7D/4'	949	979	9	61
7D/6'	1067	1103	12	87
7D/10'	669	716	25	46

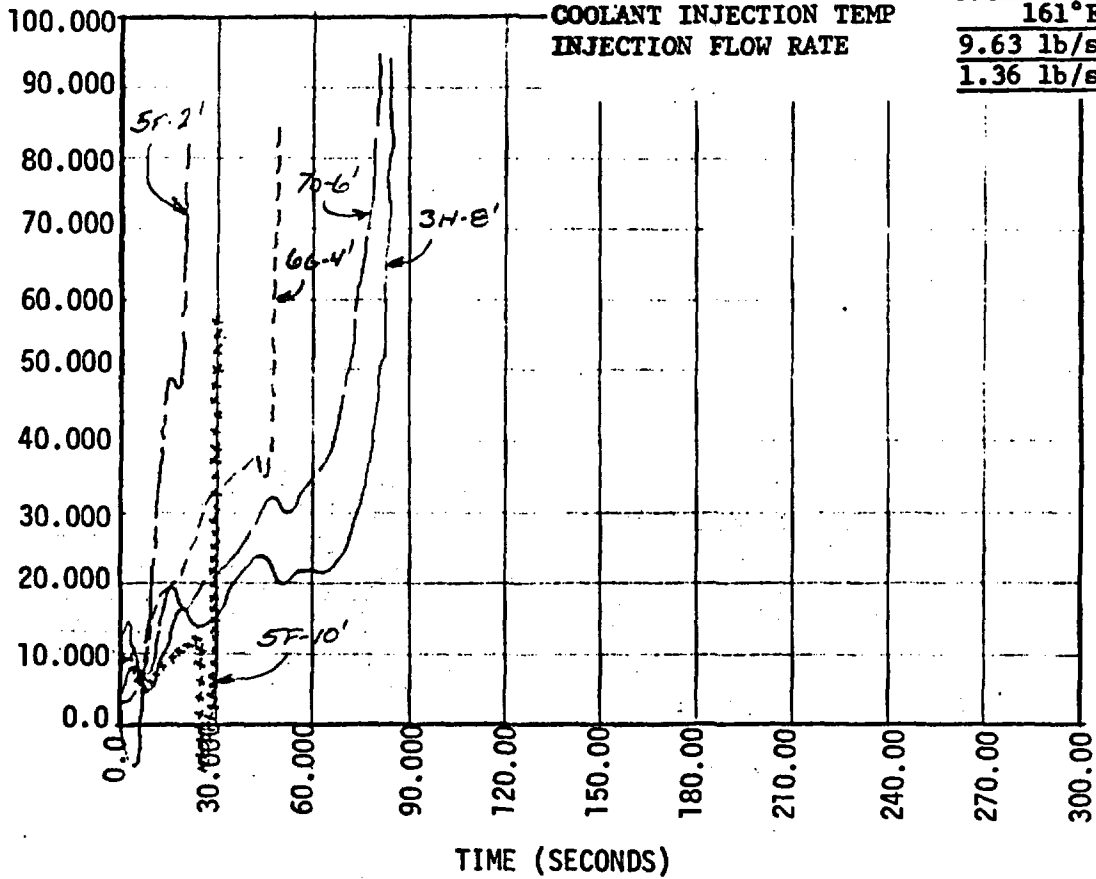




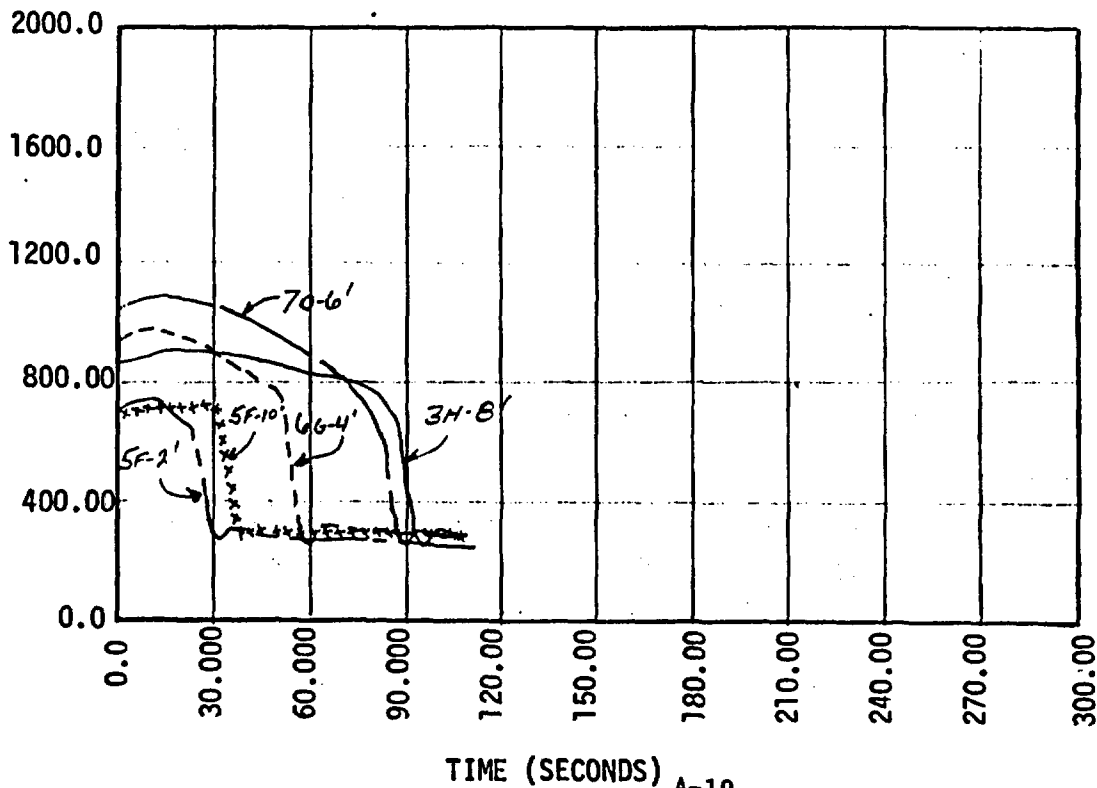
RUN NO.
 PRESSURE
 INITIAL CLAD TEMP
 PEAK POWER
 COOLANT INJECTION TEMP
 INJECTION FLOW RATE

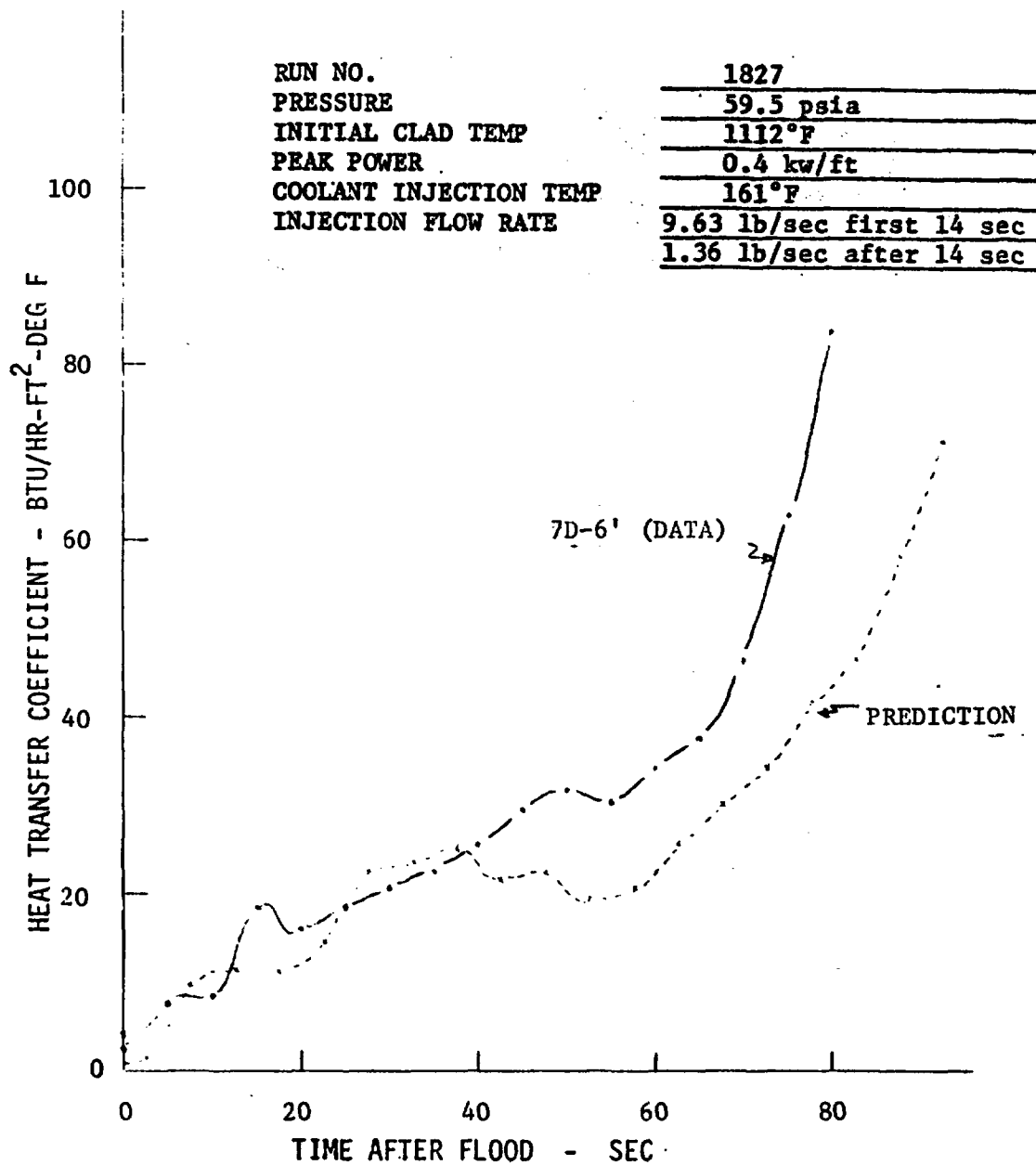
1827
59.5 psia
1112°F
0.4 kw/ft
161°F
9.63 lb/sec first 14 sec
1.36 lb/sec after 14 sec

HEAT TRANSFER COEFFICIENT (BTU/HR/FT**2/DEG F)



CLAD TEMPERATURE (DEG. F)





FLECHT-SET RUN SUMMARY SHEET

RUN NO. 1926

DATE 8/29/72

A. RUN CONDITIONS

Containment Pressure	59.2	psia
Initial Clad Temperature	1120	°F
Peak Power	1.0	kw/ft
Coolant Supply Temperature	163	°F
Injection Rate	12.91 lb/sec first 14 sec,	1.65 lb/sec after 14 sec
Loop Resistance Coefficient	$(\Delta p_{loop}/1/2 \rho V_{hotleg}^2)$	27.0

B. INITIAL HOUSING TEMPERATURES

Elevation (ft)	Initial Temperature (°F)
0	332
2	506
4	596
6	716
8	664
10	520
12	393

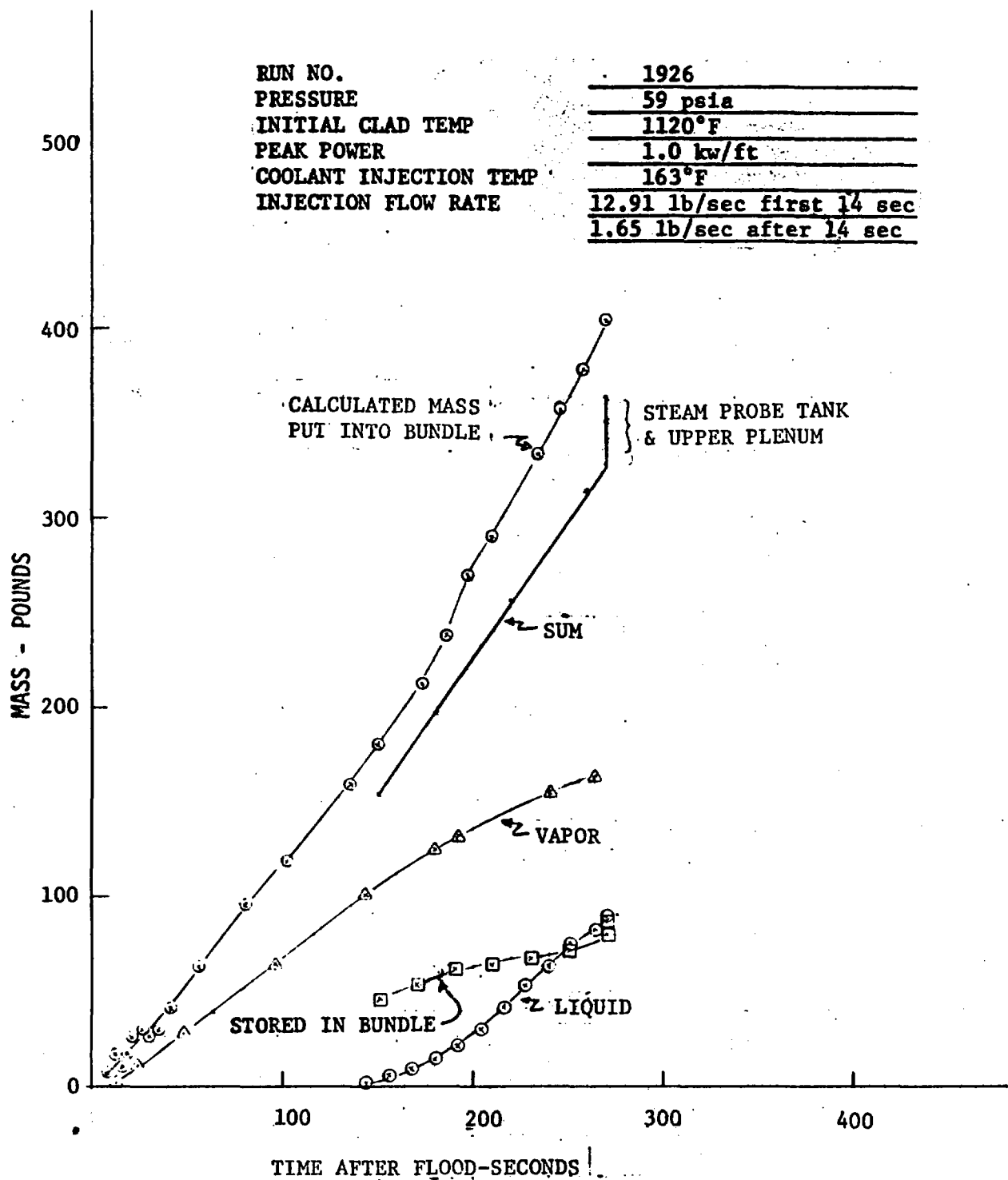
FLECHT-SET RUN SUMMARY SHEET (Cont)

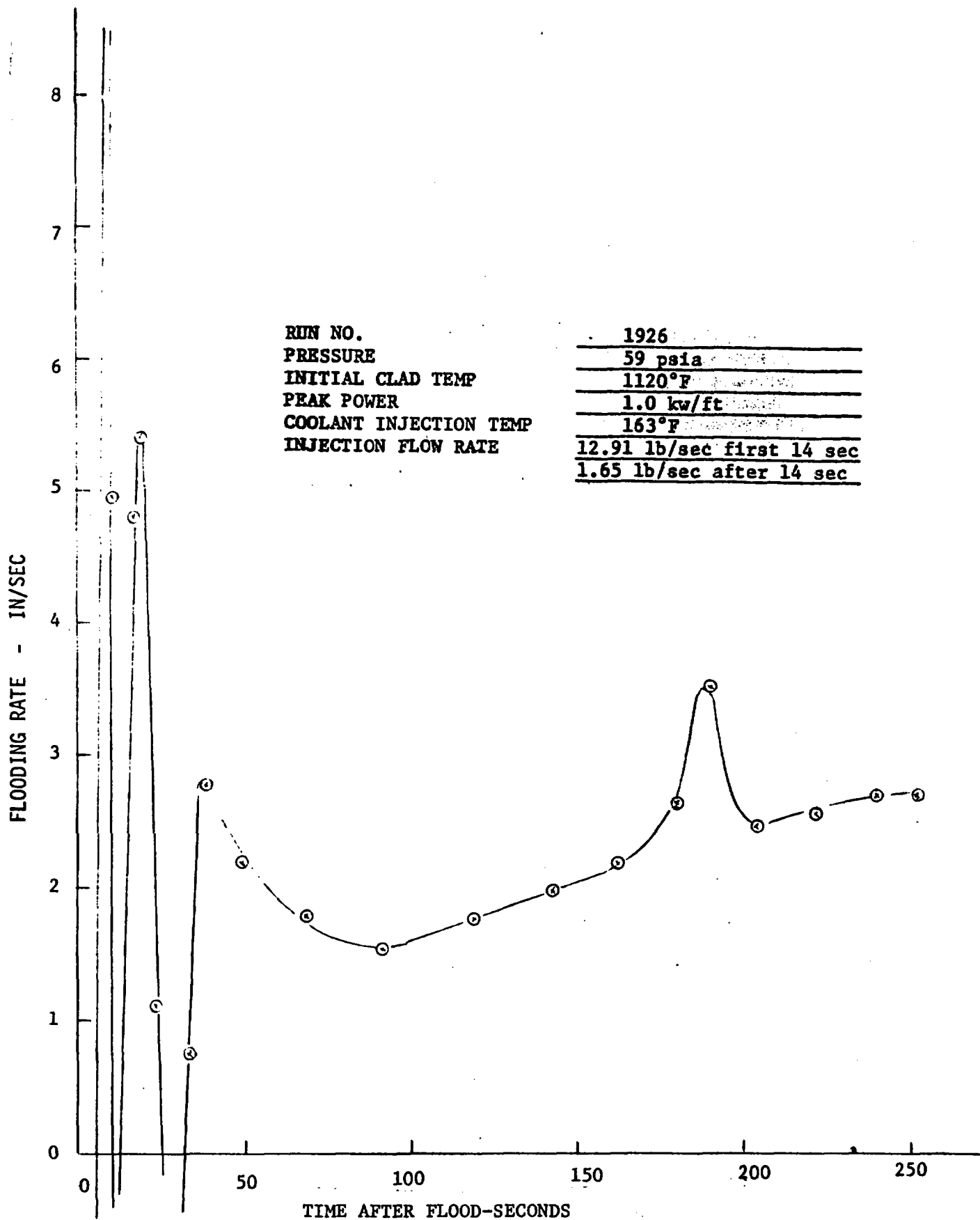
RUN NO. 1926

DATE 8/29/72

C. HEATER THERMOCOUPLE DATA

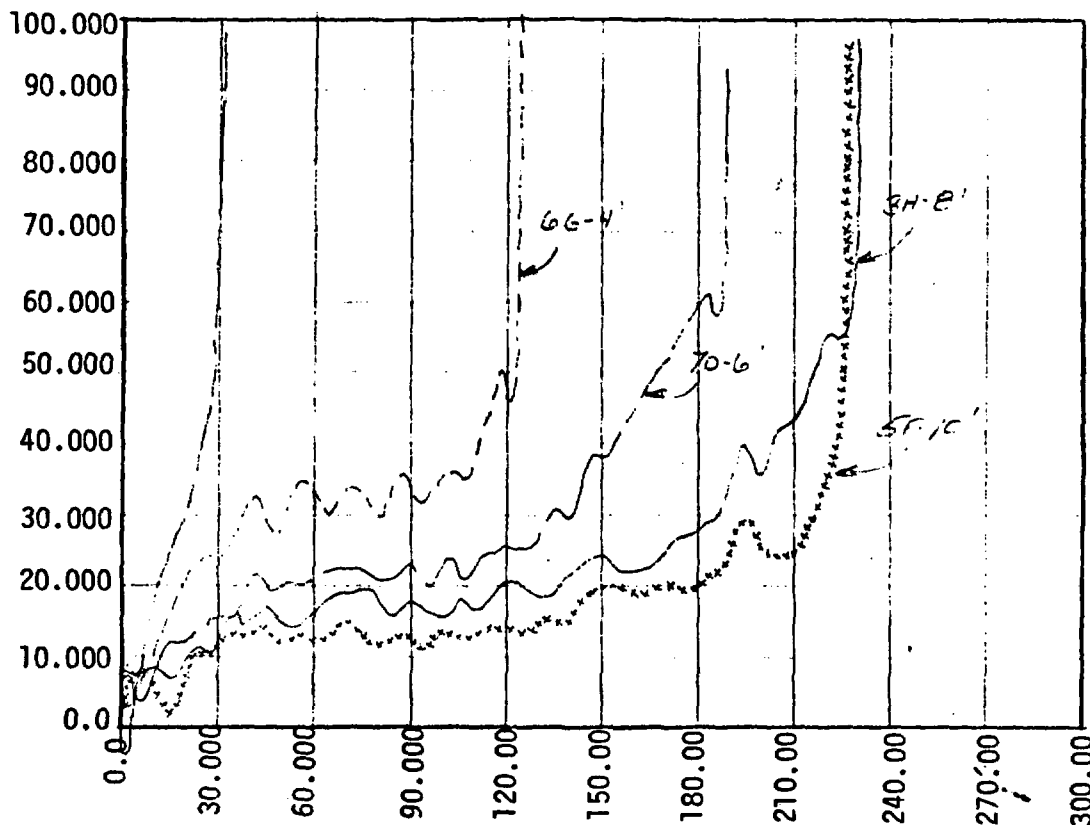
Rod/Elev.	Initial Temp. (°F)	Max. Temp. (°F)	Turnaround Time (Sec)	Quench Time (Sec)
5F/2'	731	787	13	39
5F/4'				
5F/6'				
5F/8'	936	1226	44	231
5F/10'	734	1003	128	231
5G/2'	720	781	16	37
5G/4'				
5G/6'	1116	1529	96	202
5G/8'	986	1360	105	256
5G/10'	725	994	102	204
6G/2'	726	791	15	36
6G/4'	969	1138	32	130
6G/6'				
6G/8'				
6G/10'	713	946	113	165
3H/2'				
3H/4'	964	1143	36	129
3H/6'	1099	1487	93	197
3H/8'	907	1322	113	238
3H/10'	660	960	128	259
4G/4'	1057	1288	36	135
4G/6'	1120	1580	104	202
4G/10'	698	974	122	199
4H/4'	971	1173	37	136
4H/6'				
4H/10'	696	990	115	243
7D/4'	970	1150	33	131
7D/6'	1074	1418	85	196
7D/10'				





RUN NO.	1926
PRESSURE	59 psia
INITIAL CLAD TEMP	1120°F
PEAK POWER	1.0 kw/ft
COOLANT INJECTION TEMP	163°F
INJECTION FLOW RATE	12.91 lb/sec first 14 sec
	1.65 lb/sec after 14 sec

HEAT TRANSFER COEFFICIENT (BTU/HR/FT**2/DEG F)

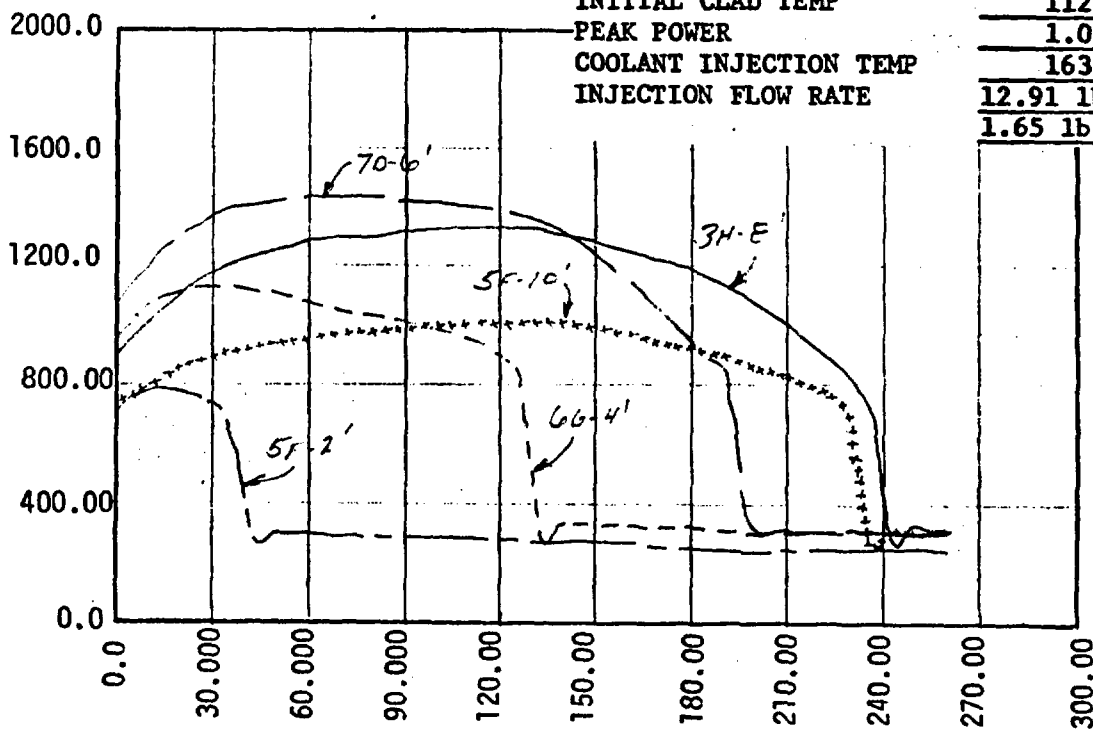


TIME (SECONDS)

RUN NO.
PRESSURE
INITIAL CLAD TEMP
PEAK POWER
COOLANT INJECTION TEMP
INJECTION FLOW RATE

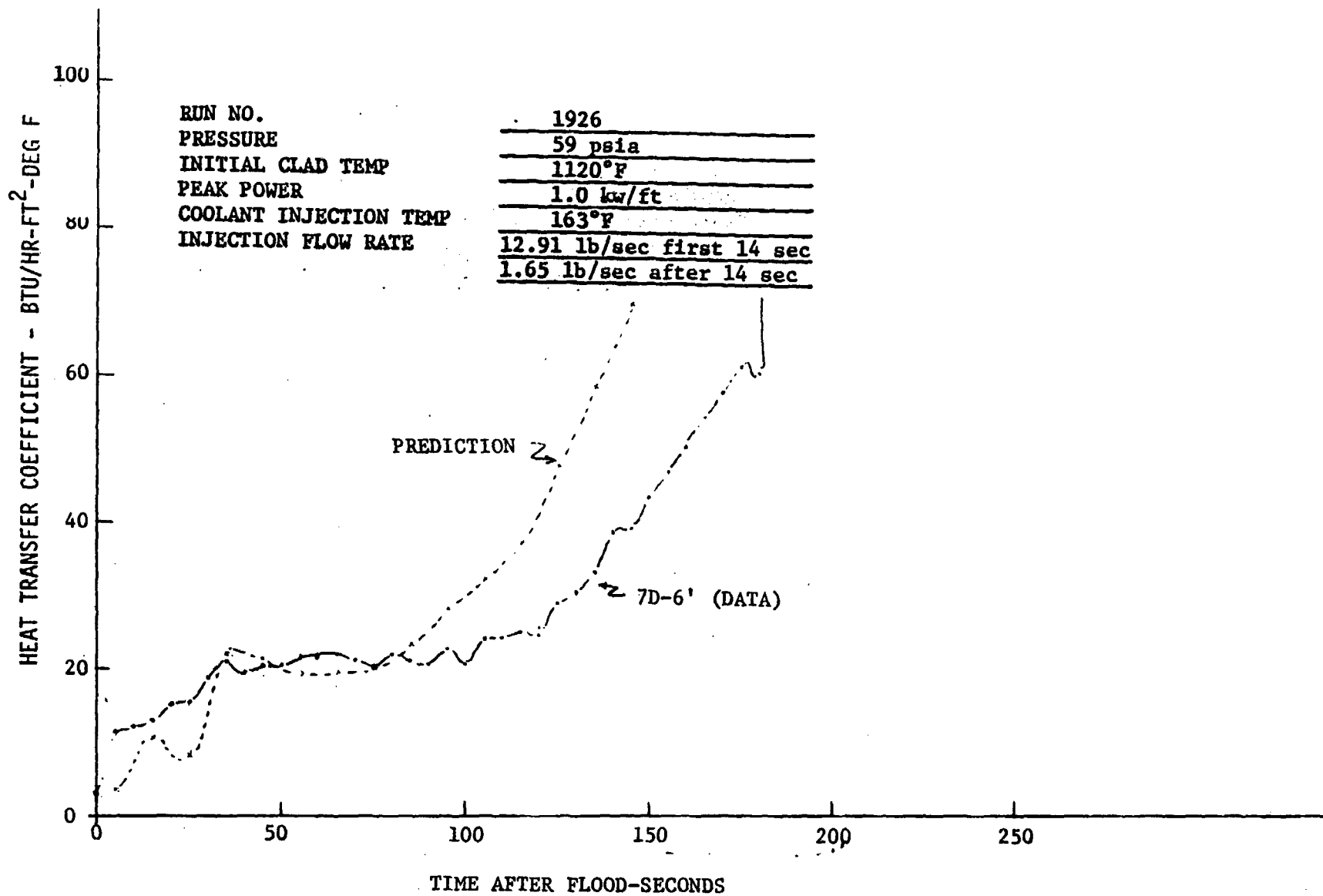
1926
59 psia
1120°F
1.0 kw/ft
163°F
12.91 lb/sec first 14 sec
1.65 lb/sec after 14 sec

CLAD TEMPERATURE (DEG. F)



TIME (SECONDS)

A-26



FLECHT-SET RUN SUMMARY SHEET

RUN NO. 2023

DATE 9/1/72

A. RUN CONDITIONS

Containment Pressure	59.4	psia
Initial Clad Temperature	1112	°F
Peak Power	0.7	kw/ft
Coolant Supply Temperature	161	°F
Injection Rate	10.04 lb/sec first 14 sec, 1.38 lb/sec after 14 sec	
Loop Resistance Coefficient ($\Delta p_{loop}/1/2 \rho V^2_{hotleg}$)	29.9	

B. INITIAL HOUSING TEMPERATURES

Elevation (ft)	Initial Temperature (°F)
0	287
2	435
4	471
6	525
8	485
10	402
12	293

FLECHT-SET RUN SUMMARY SHEET (Cont)

RUN NO. 2023

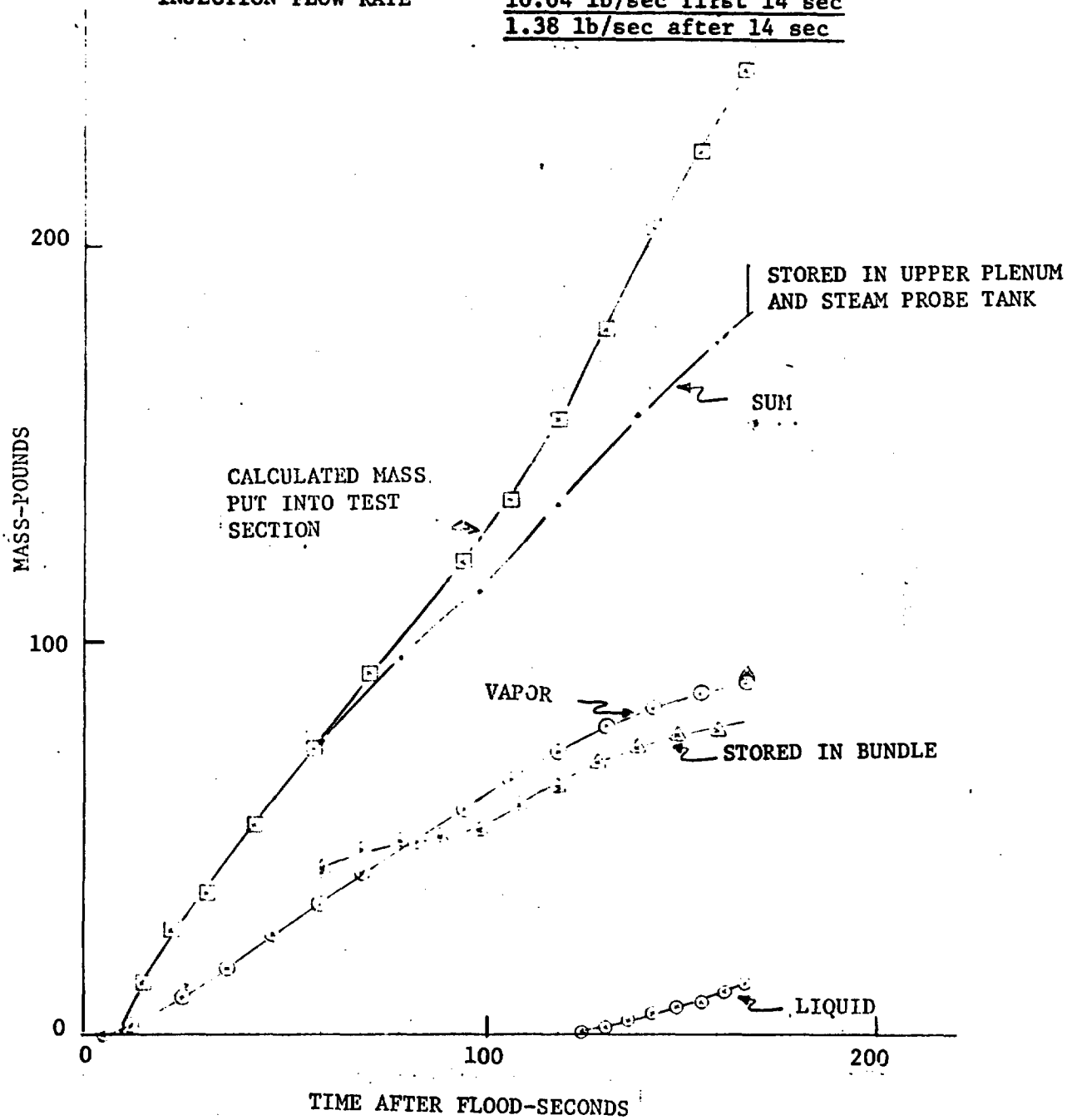
DATE 9/1/72

C. HEATER THERMOCOUPLE DATA

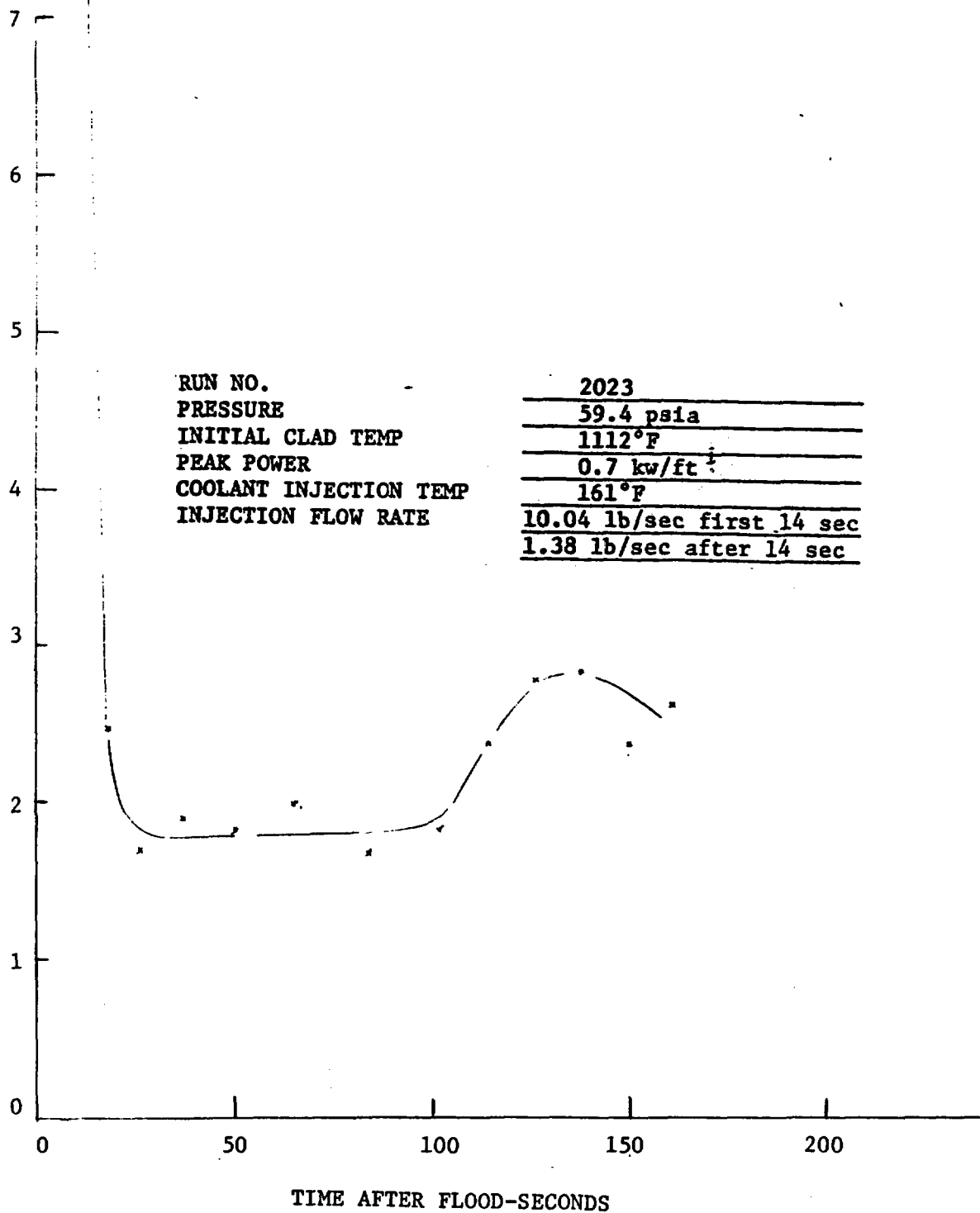
Rod/Elev.	Initial Temp. (°F)	Max. Temp. (°F)	Turnaround Time (Sec)	Quench Time (Sec)
5F/2'	702	739	7	11
5F/4'				
5F/6'				
5F/8'	891	1004	20	119
5F/10'	678	776	48	119
5G/2'	691	734	7	26
5G/4'				
5G/6'	1112	1250	25	121
5G/8'	956	1092	49	150
5G/10'	666	761	47	117
6G/2'	698	739	7	12
6G/4'	949	1010	11	68
6G/6'				
6G/8'				
6G/10'				
3H/2'				
3H/4'	947	1022	16	75
3H/6'	1047	1220	33	116
3H/8'	875	1038	59	130
3H/10'	607	731	46	57
4G/4'	1054	1135	17	66
4G/6'	1110	1278	41	111
4G/10'	641	754	34	50
4H/4'	946	1033	19	77
4H/6'				
4H/10'	642	747	36	57
7D/4'	948	1010	11	72
7D/6'	1052	1176	27	119
7D/10'	623	738	25	106

RUN NO.
 PRESSURE
 INITIAL CLAD TEMP
 PEAK POWER
 COOLANT INJECTION TEMP
 INJECTION FLOW RATE

2023
59.4 psia
1112°F
0.7 kw/ft
161°F
10.04 lb/sec first 14 sec
1.38 lb/sec after 14 sec



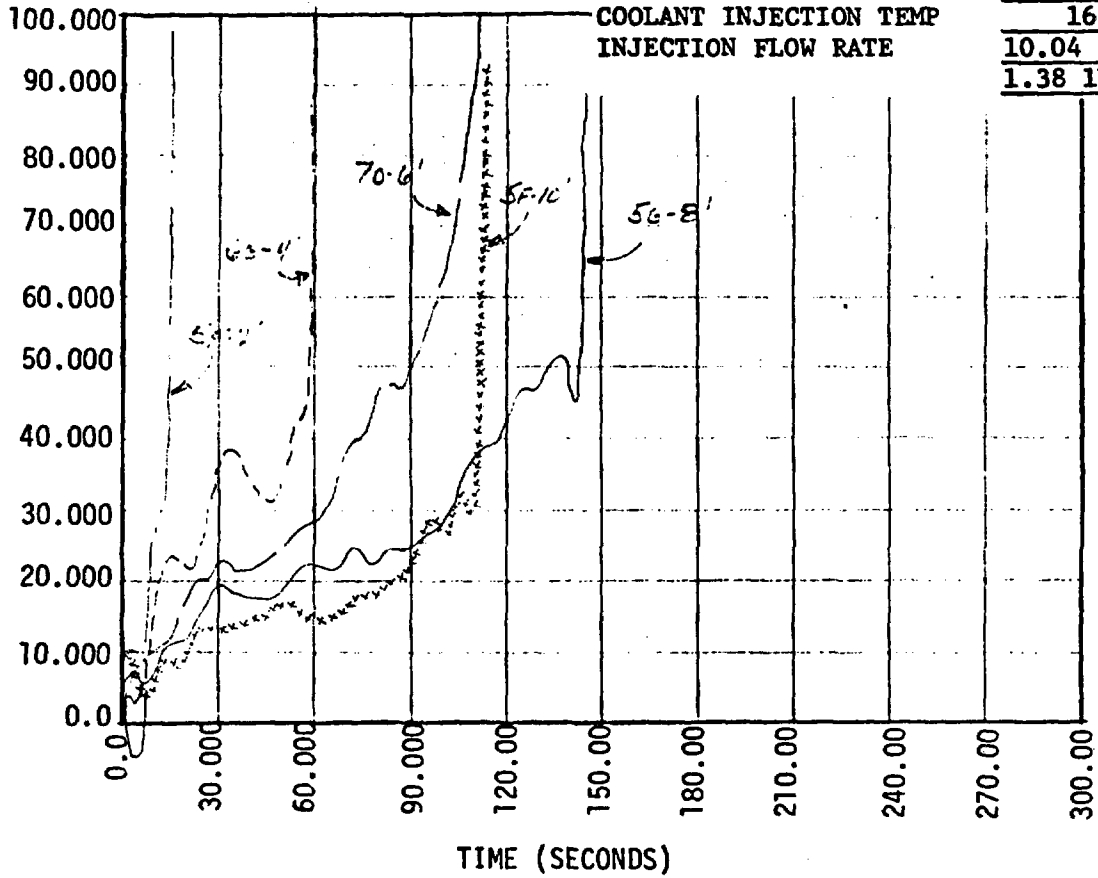
FLOODING RATE-IN/SEC



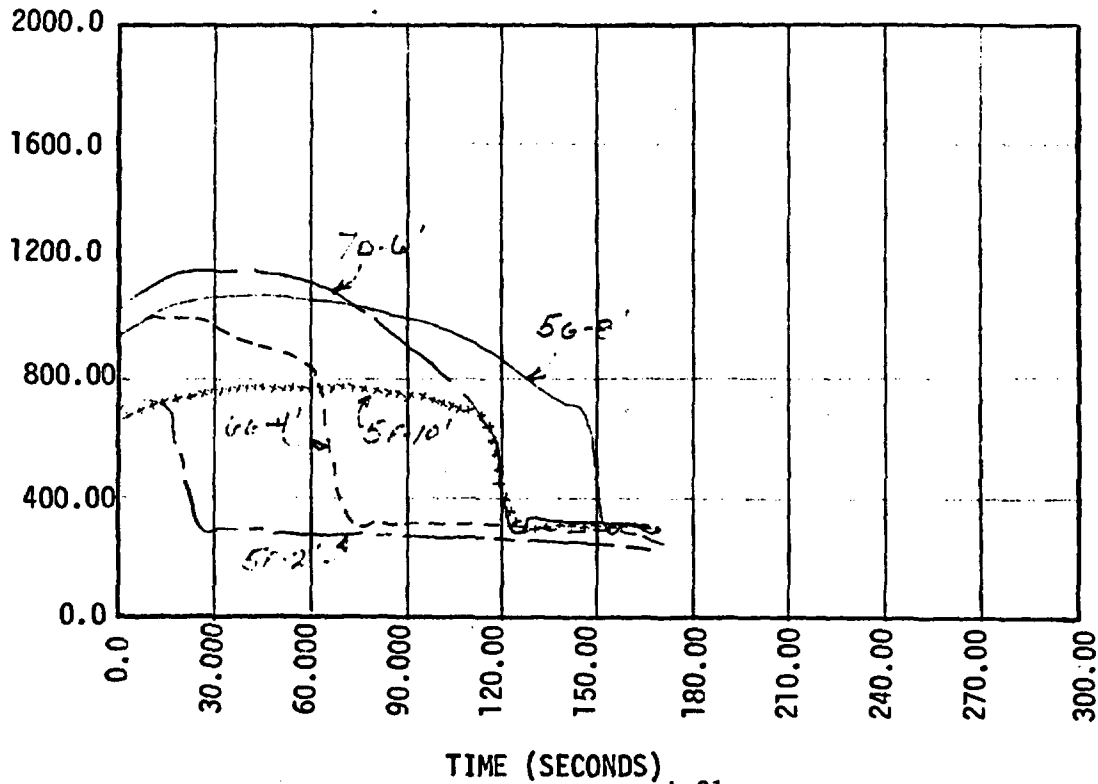
RUN NO.
 PRESSURE
 INITIAL CLAD TEMP
 PEAK POWER
 COOLANT INJECTION TEMP
 INJECTION FLOW RATE

2023
 59.4 psia
 1112°F
 0.7 kw/ft
 161°F
 10.04 lb/sec first 14 sec
 1.38 lb/sec after 14 sec

HEAT TRANSFER COEFFICIENT (BTU/HR/FT**2/DEG F)

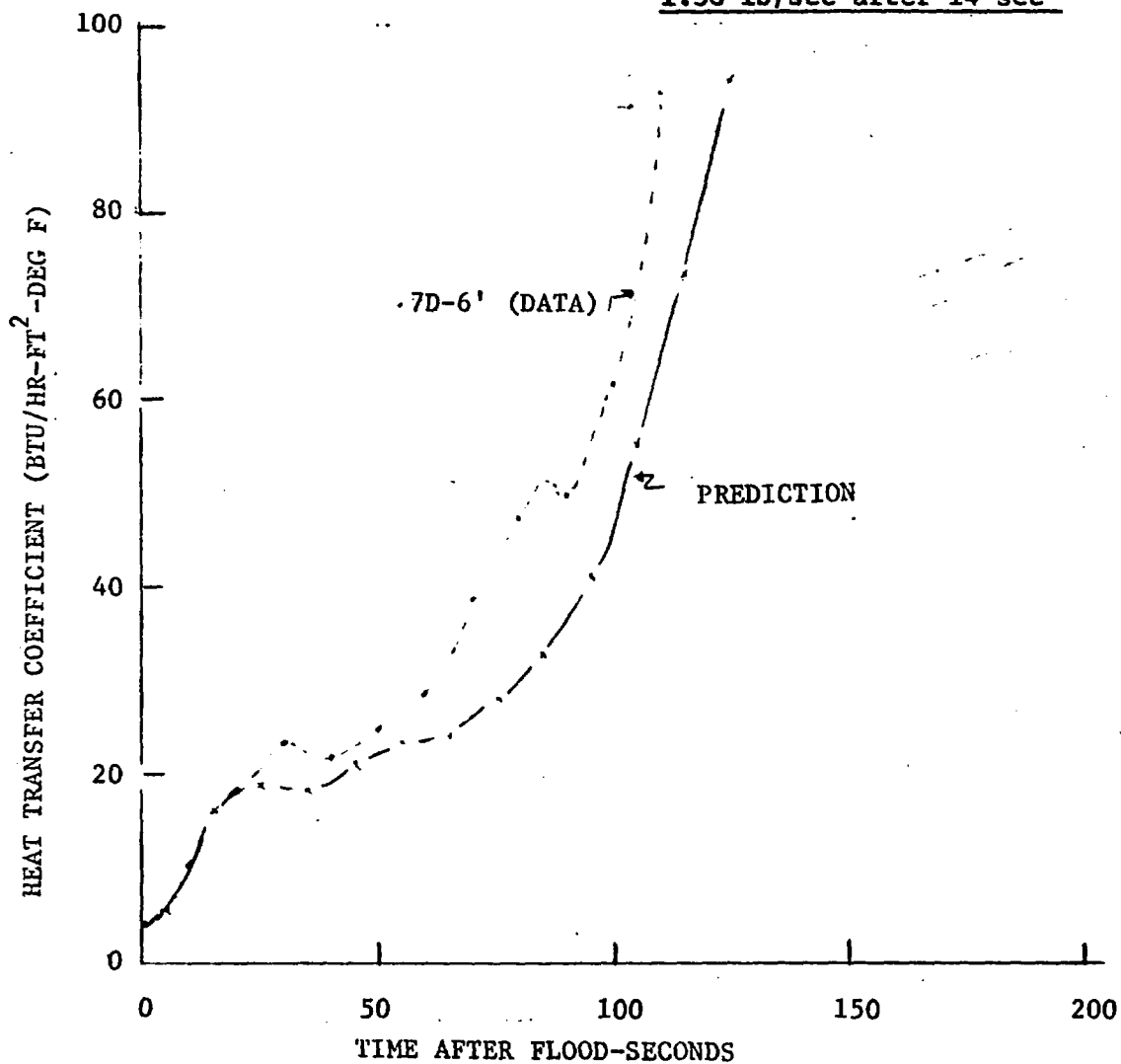


CLAD TEMPERATURE (DEG. F)



RUN NO.
 PRESSURE
 INITIAL CLAD TEMP
 PEAK POWER
 COOLANT INJECTION TEMP
 INJECTION FLOW RATE

2023
59.4 psia
1112°F
0.7 kw/ft ²
161°F
10.04 lb/sec first 14 sec
1.38 lb/sec after 14 sec



FLECHT-SET RUN SUMMARY SHEET

RUN NO. 2207

DATE 10/5/72

A. RUN CONDITIONS

Containment Pressure	22* psia
Initial Clad Temperature	1100 °F
Peak Power	0.7 kw/ft
Coolant Supply Temperature	160 °F
Injection Rate	12.12 lb/sec first 14 sec., 1.19 lb/sec after 14 sec.
Loop Resistance Coefficient ($\Delta p_{loop}/1/2\rho V^2$ hotleg)	31

B. INITIAL HOUSING TEMPERATURES

Elevation (ft)	Initial Temperature (°F)
0	231
2	428
4	488
6	599
8	568
10	428
12	295

*Pressure control was not good, 20.3 psia to 23.5 psia

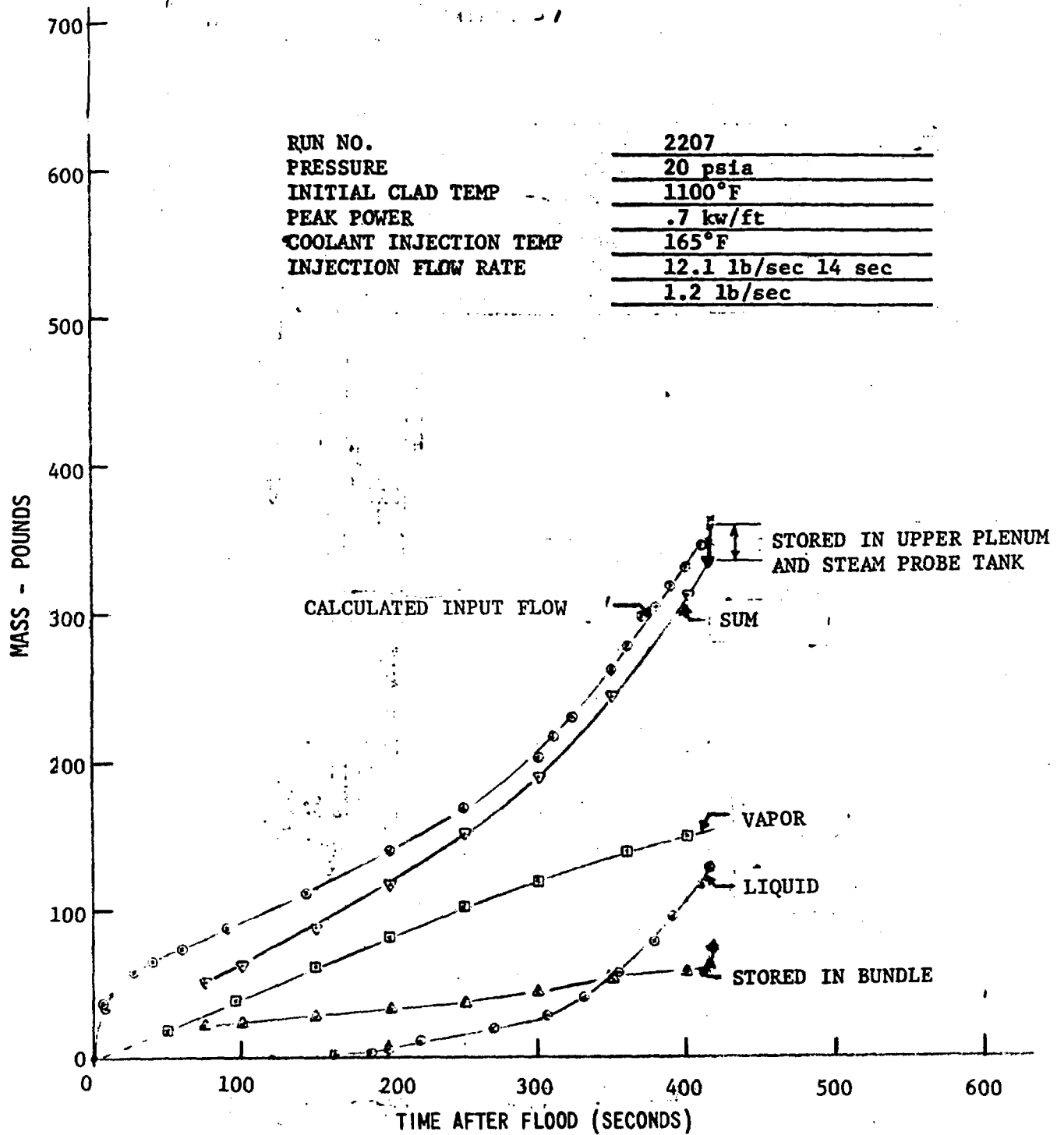
FLECHT-SET RUN SUMMARY SHEET (Cont)

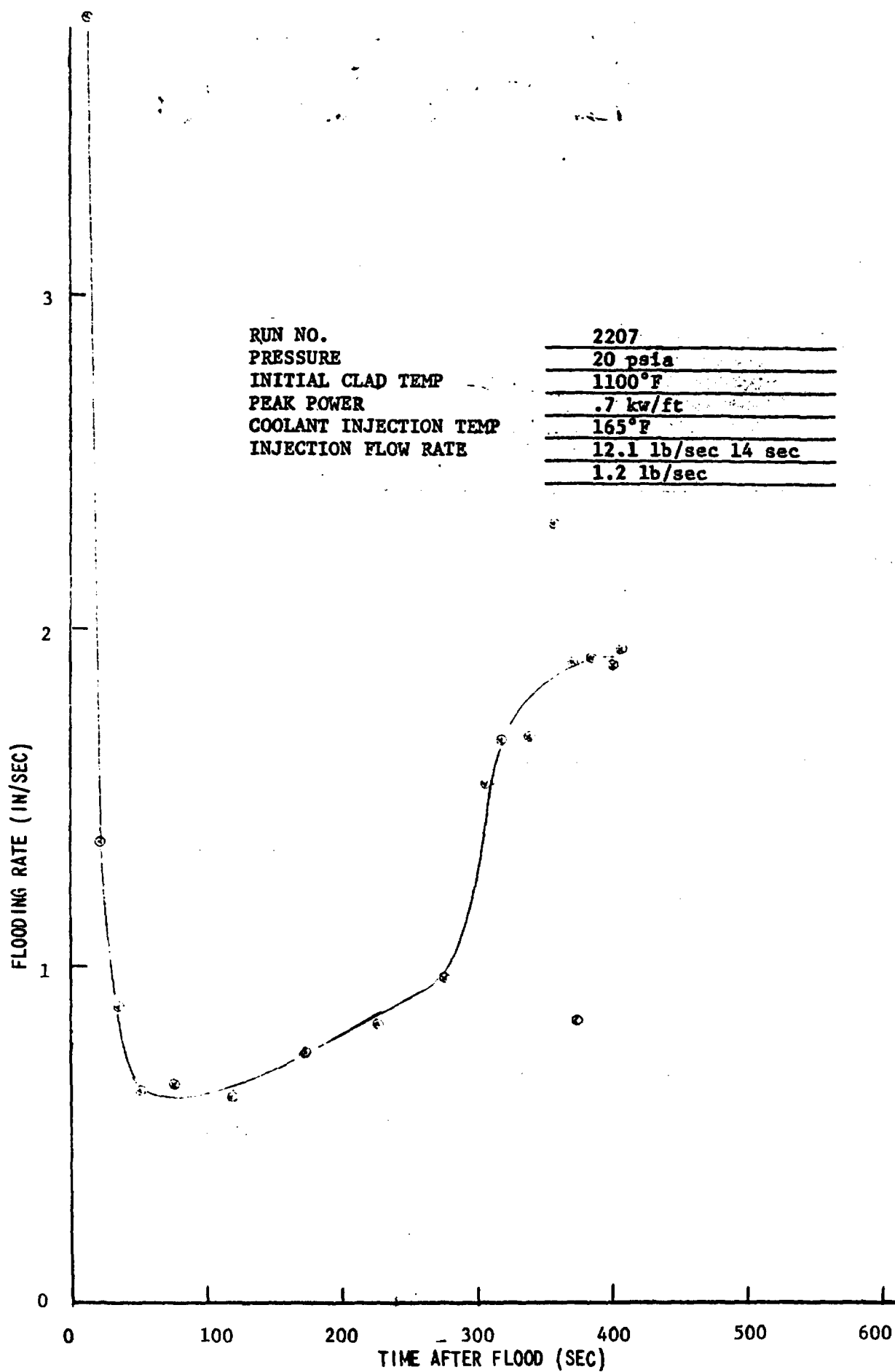
RUN NO. 2207

DATE 10/5/72

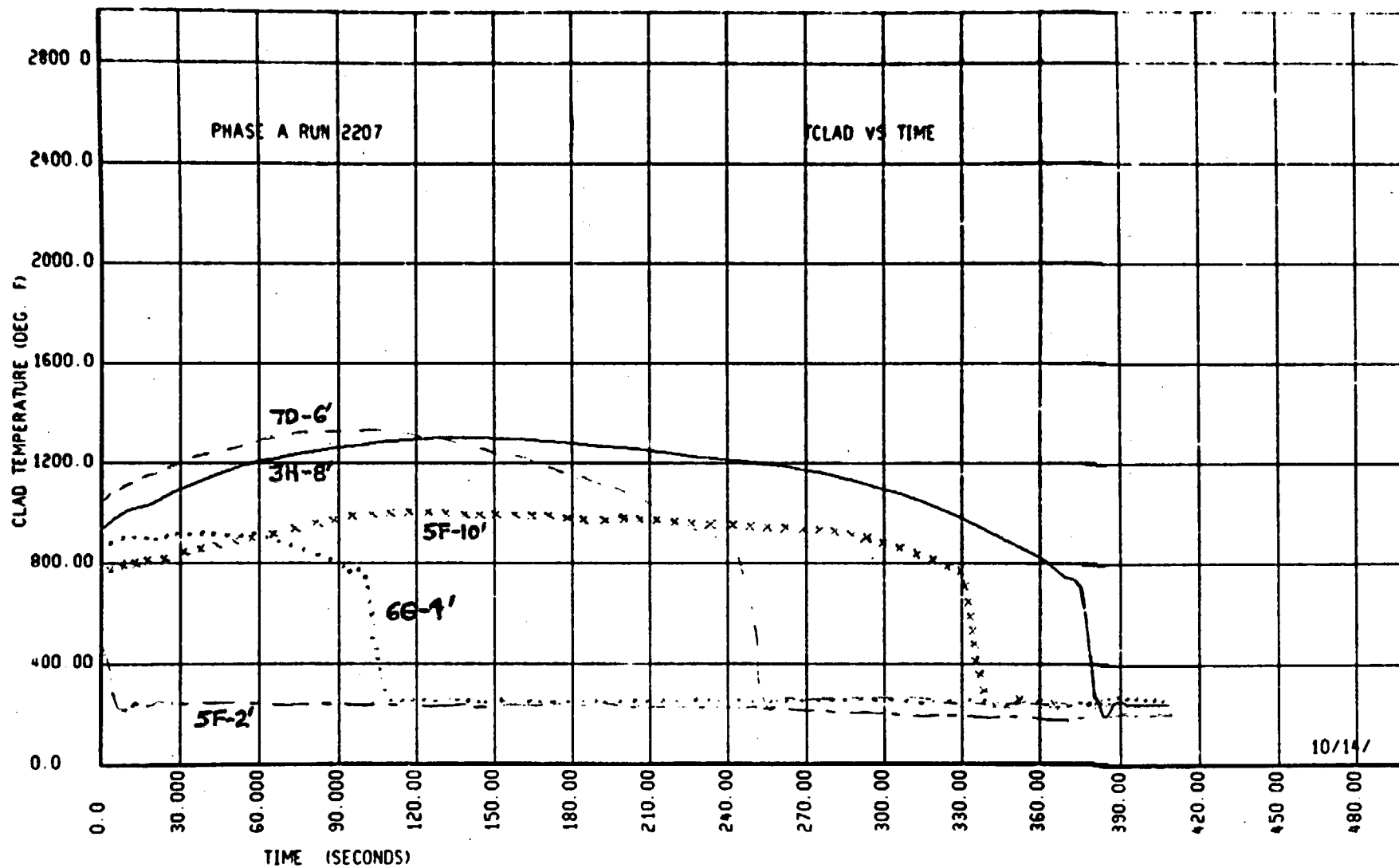
C. HEATER THERMOCOUPLE DATA

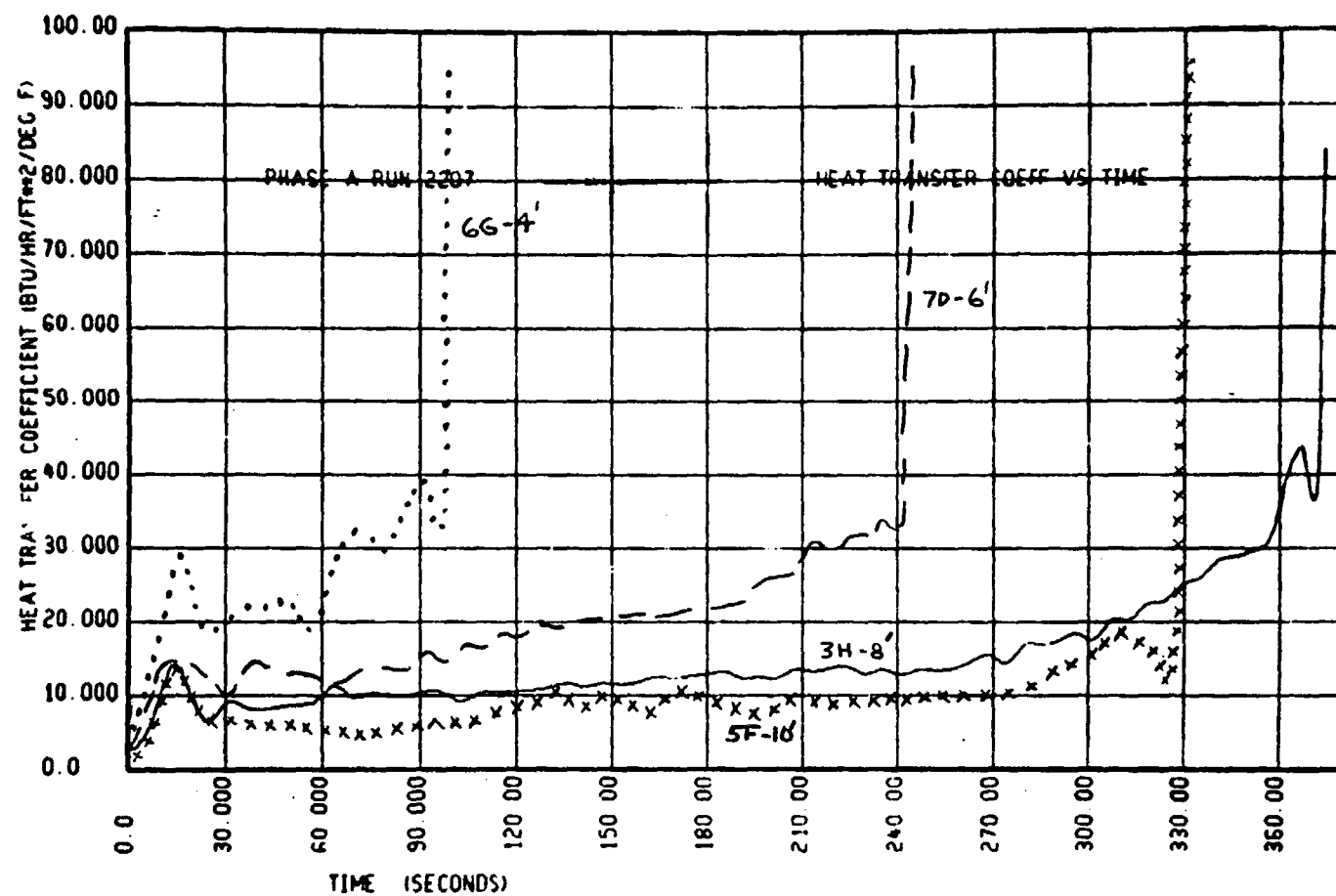
Rod/Elev.	Initial Temp. (°F)	Max. Temp. (°F)	Turnaround Time (Sec)	Quench Time (Sec)
5F/2'	---			
5F/4'	---			
5F/6'	---			
5F/8'	948	1261	162	361
5F/10'	750	991	123	328
5G/2'	538	538	0	5
5G/4'	---			
5G/6'	1087	1457	101	258
5G/8'	1010	1338	130	338
5G/10'	737	983	119	308
6G/2'	550	550	0	5
6G/4'	856	918	54	98
6G/6'	---			
6G/8'	---			
6G/10'	723	945	135	297
3H/2'	---			
3H/4'	---			
3H/6'	1061	1400	106	253
3H/8'	943	1304	132	372
3H/10'	690	941	137	>407
4G/4'	961	1019	56	113
4G/6'	1100	1489	107	270
4G/10'	722	921	159	206
4H/4'	873	990	56	109
4H/6'	---			
4H/10'	722	967	130	367
7D/4'	862	922	41	93
7D/6'	1031	1322	99	242
7D/10'	---			



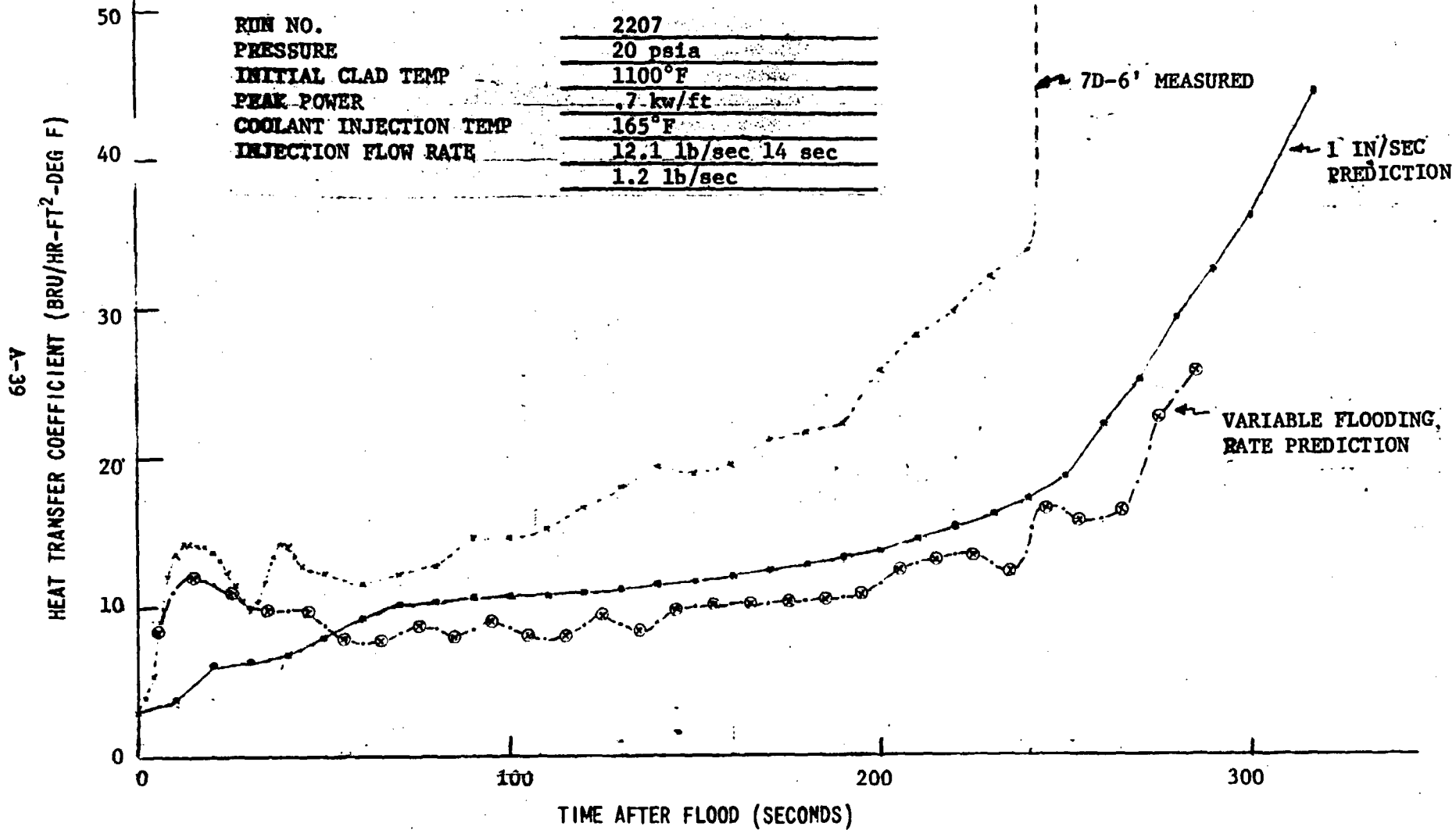


A-37





MIDPLANE HEAT TRANSFER COEFFICIENT RUN 2207



1

2

3

4

FLECHT-SET RUN SUMMARY SHEET

RUN NO. 2605

DATE 10/18/72

A. RUN CONDITIONS

Containment Pressure	19.6 psia
Initial Clad Temperature	1104 °F
Peak Power	0.7 kw/ft
Coolant Supply Temperature	157 °F
Injection Rate	5.7 lb/sec first 28 sec., 1.23 lb/sec. after 28
Loop Resistance Coefficient ($\Delta p_{loop}/1/2\rho V^2_{hotleg}$)	30

B. INITIAL HOUSING TEMPERATURES

Elevation (ft)	Initial Temperature (°F)
0	254
2	420
4	521
6	636
8	600
10	428
12	241

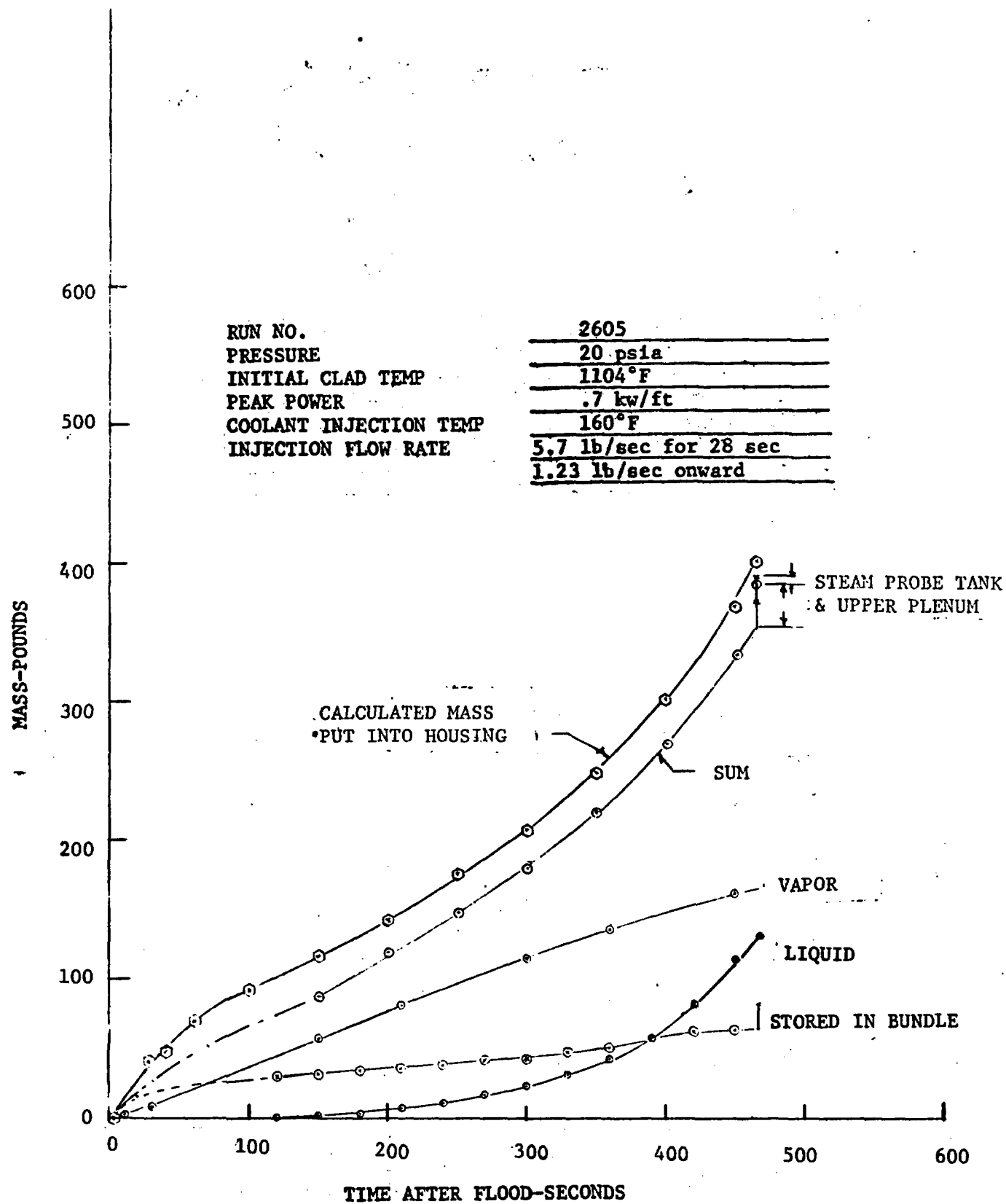
FLECHT-SET RUN SUMMARY SHEET (Cont)

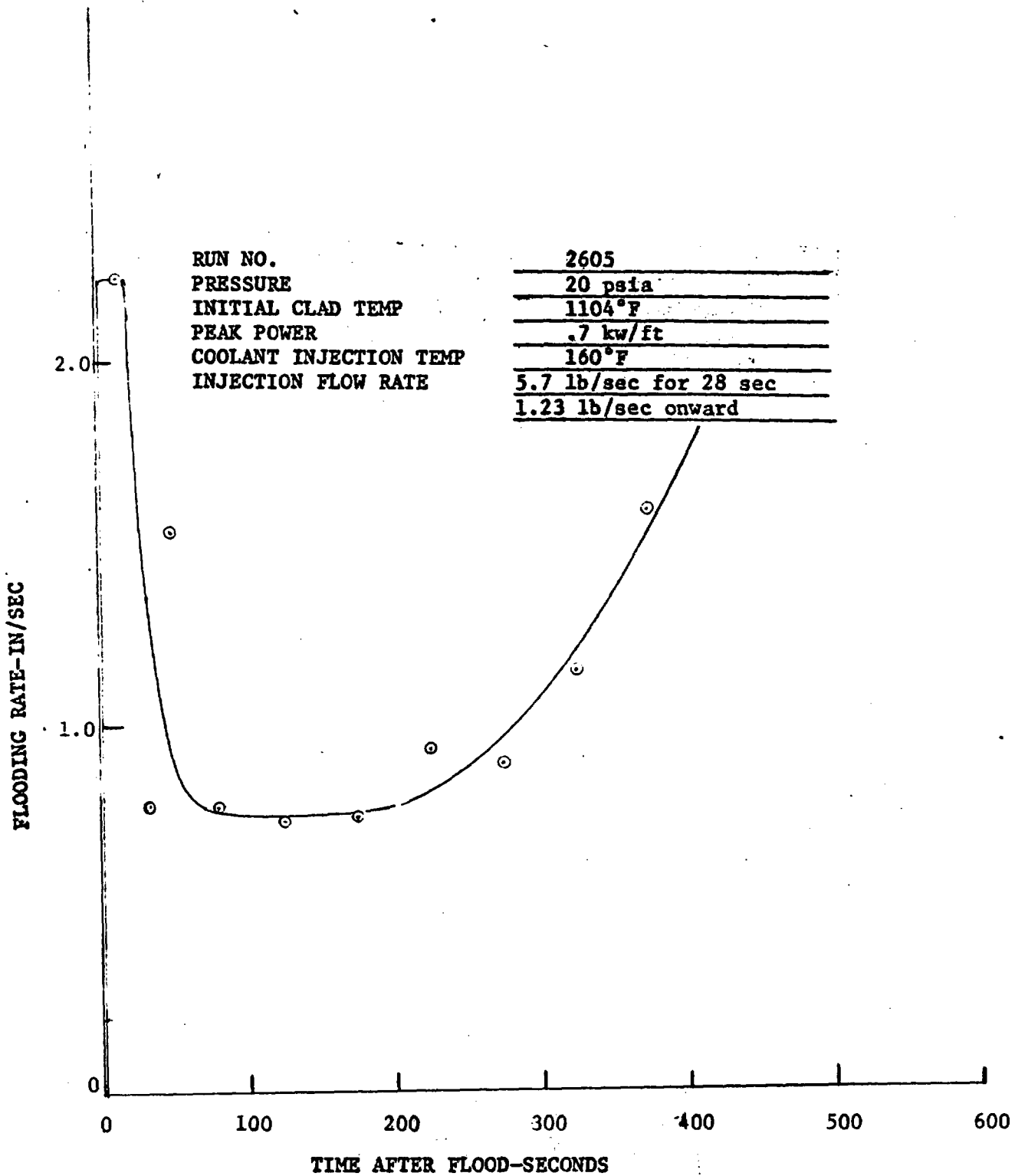
RUN NO. 2605

DATE 10/18/72

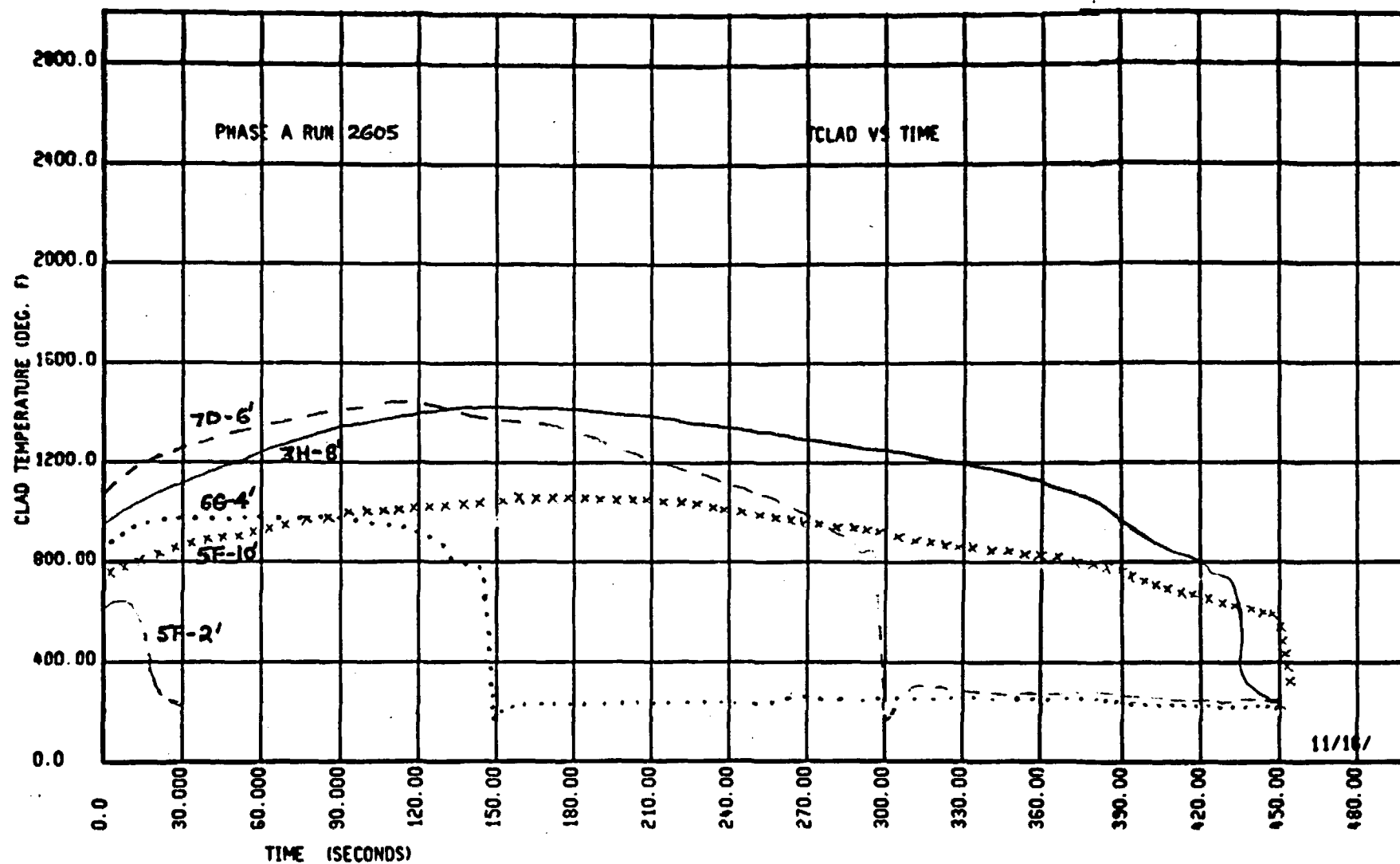
C. HEATER THERMOCOUPLE DATA

Rod/Elev.	Initial Temp. (°F)	Max. Temp. (°F)	Turnaround Time (Sec.)	Quench Time (Sec.)
5F/2'	596	630	13	16
5F/4'	---			
5F/6'	---			
5F/8'	962	1265	151	426
5F/10'	733	1038	183	448
5G/2'	586	615	10	17
5G/4'	---			
5G/6'	1097	1511	132	311
5G/8'	1001	1356	152	448
5G/10'	718	1017	180	299
6G/2'	594	628	11	16
6G/4'	884	883	81	140
6G/6'	---			
6G/8'	---			
6G/10'	708	982	168	382
3H/2'	---			
3H/4'	878	1013	88	145
3H/6'	1069	1473	123	300
3H/8'	935	1398	156	431
3H/10'	660	969	168	436
4G/4'	983	1150	77	157
4G/6'	1104	1551	136	322
4G/10'	700	977	159	327
4H/4'	893	1082	88	151
4H/6'	---			
4H/10'	698	992	170	410
4D/4'	883	1012	34	131
7D/6'	1048	1406	113	294
7D/10'	---			

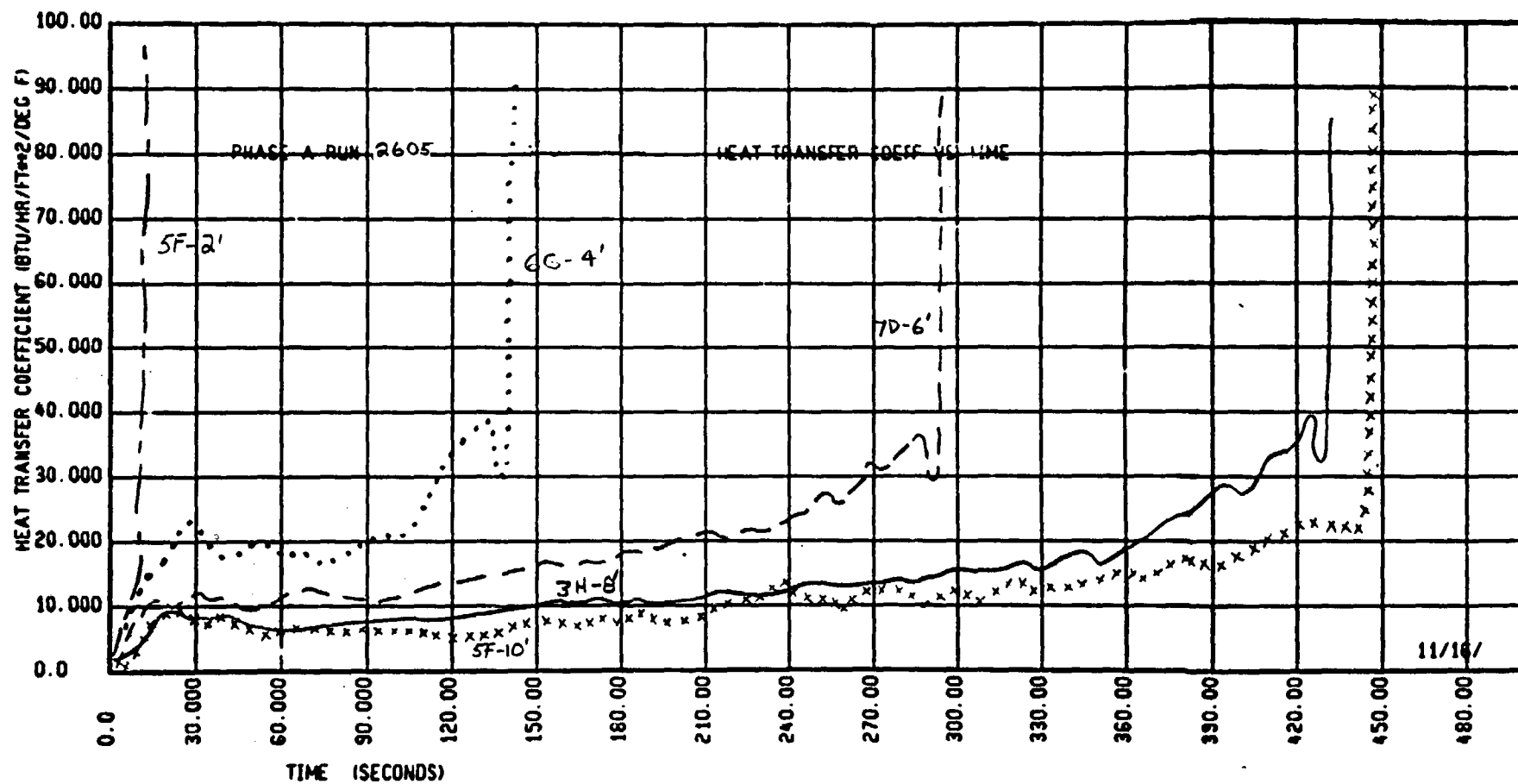




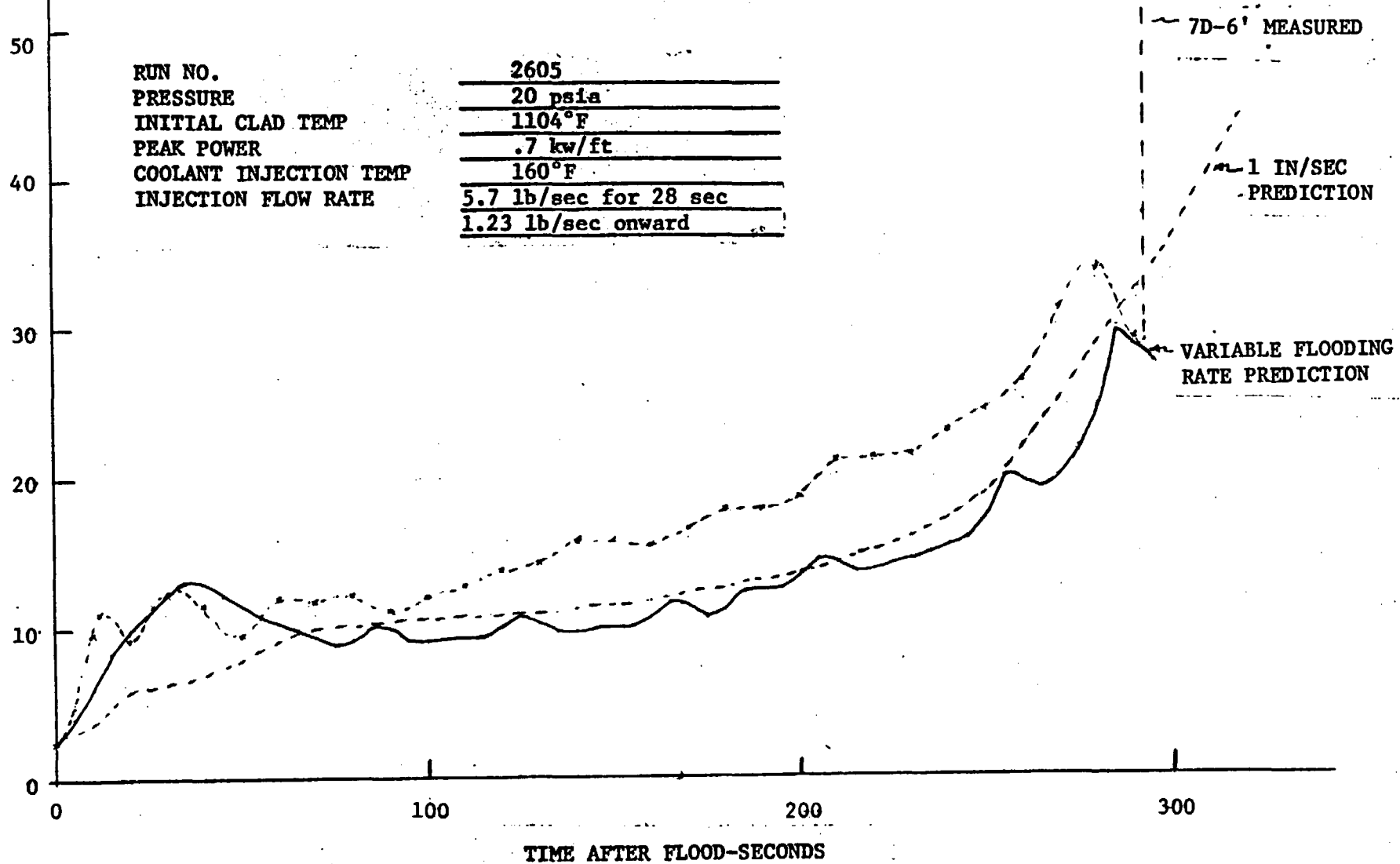
A-45



A-46



A-47

HEAT TRANSFER COEFFICIENT - BTU/HR-FT²-DEG F

1

2

3

4

5

FLECHT-SET RUN SUMMARY SHEET

RUN NO. 2718

DATE 10/19/72

A. RUN CONDITIONS

Containment Pressure	19.6 psia
Initial Clad Temperature	1399 °F
Peak Power	0.7 kw/ft
Coolant Supply Temperature	156 °F
Injection Rate	9.83 lb/sec. first 14 sec., 1.23 lb/sec. after 14 sec.
Loop Resistance Coefficient	$(\Delta p_{\text{loop}} / 1/2 \rho V_{\text{hotleg}}^2)$ 31

B. INITIAL HOUSING TEMPERATURES

Elevation (ft)	Initial Temperature (°F)
0	247
2	429
4	547
6	654
8	603
10	453
12	292

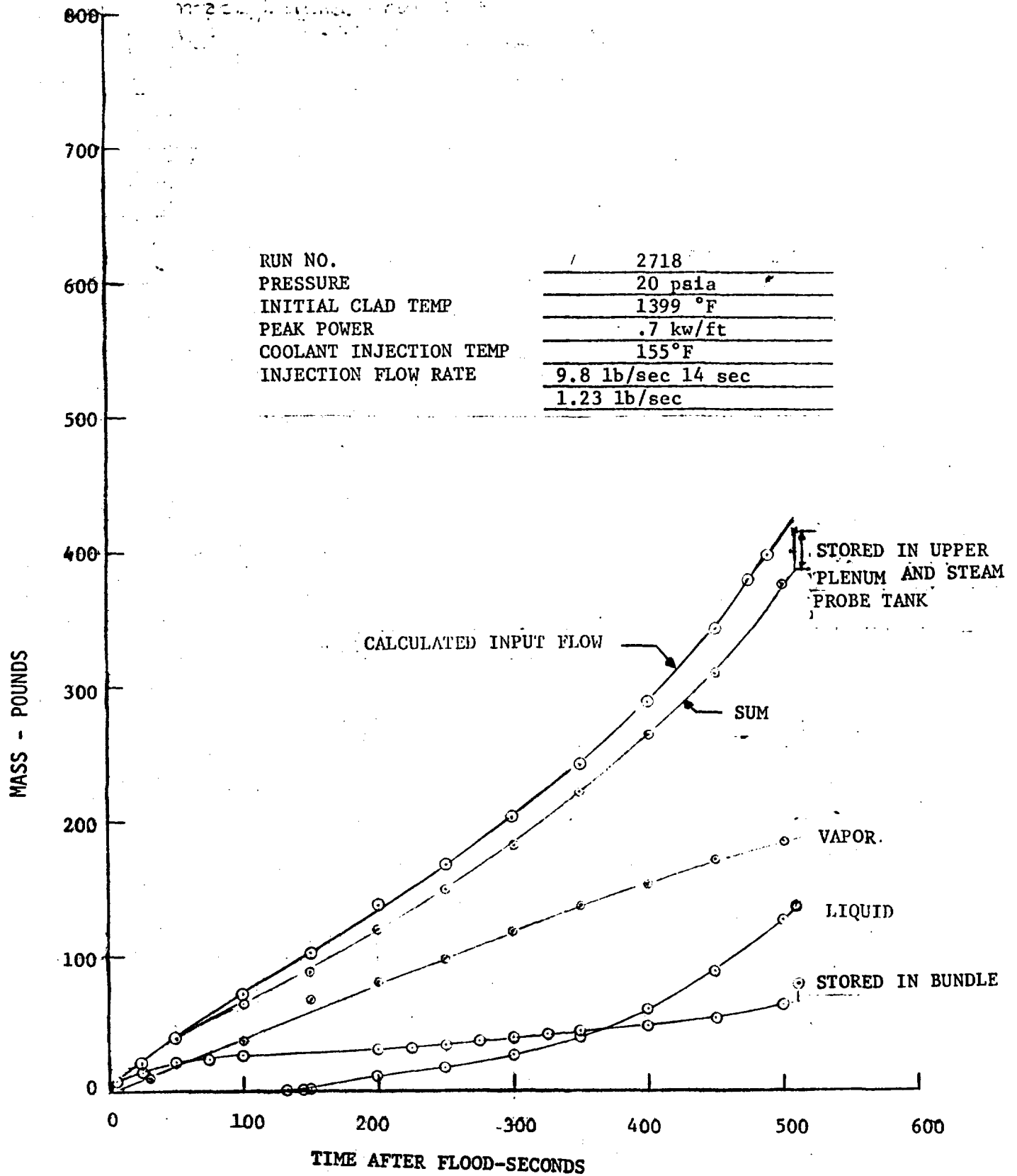
FLECHT-SET RUN SUMMARY SHEET (Cont)

RUN NO. 2718

DATE 10/19/72

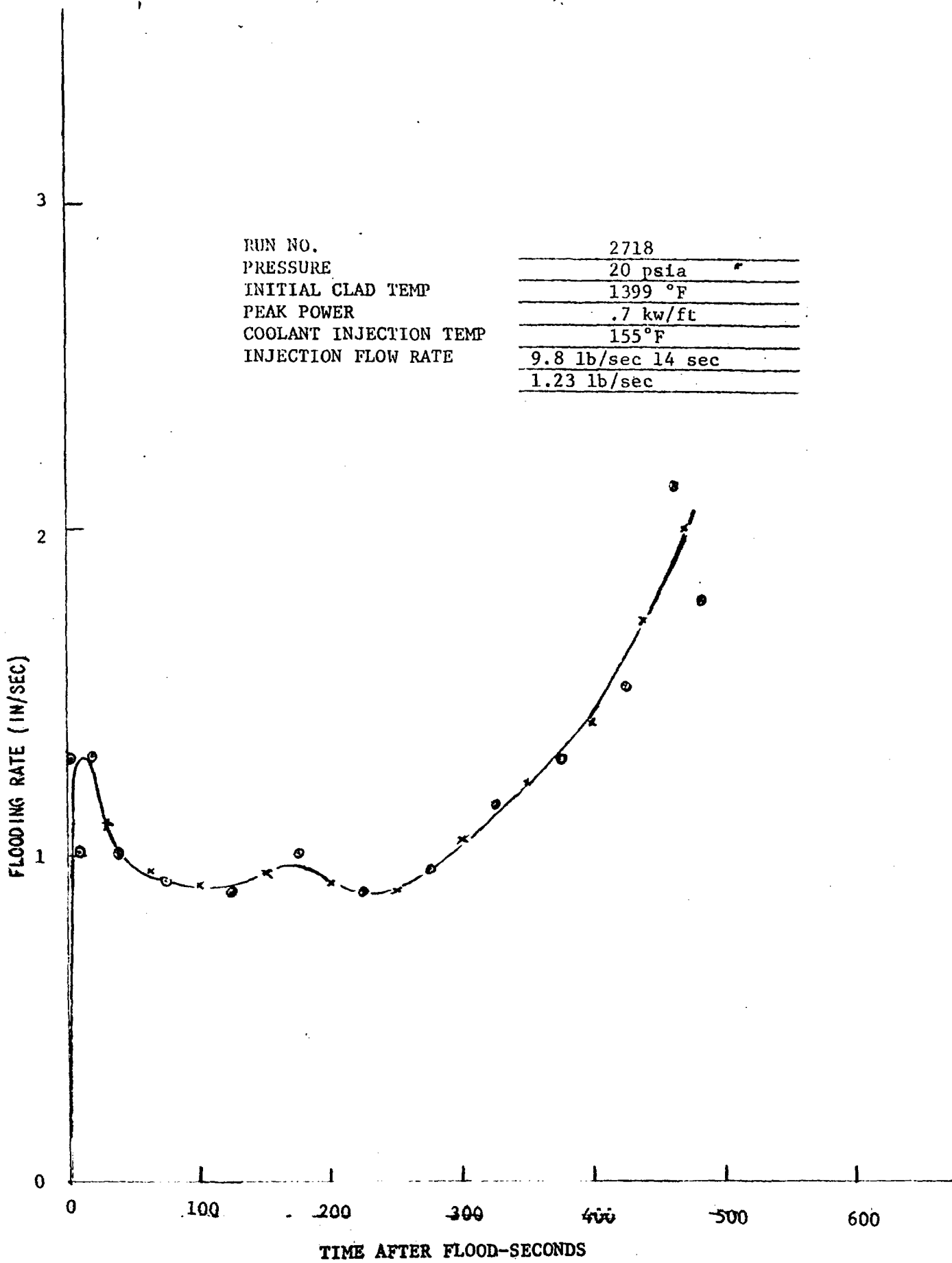
C. HEATER THERMOCOUPLE DATA

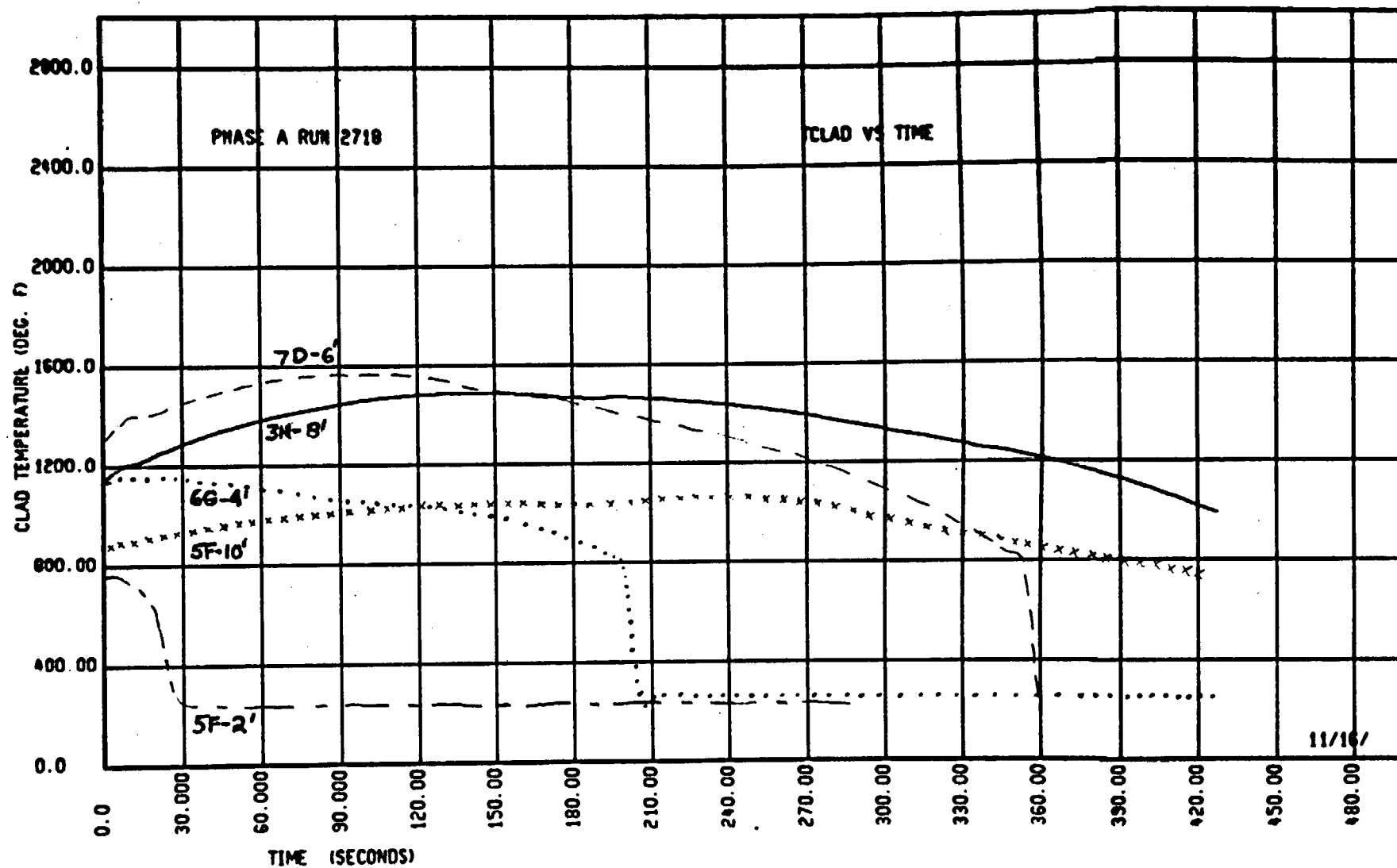
Rod/Elev.	Initial Temp. (°F)	Max. Temp. (°F)	Turnaround Time (Sec.)	Quench Time (Sec.)
5F/2'	752	764	5	22
5F/4'	---			
5F/6'	---			
5F/8'	1172	1417	80	488
5F/10'	859	1055	234	449
5G/2'	739	753	5	13
5G/4'	---			
5G/6'	1397	1686	102	361
5G/8'	1236	1425	51	484
5G/10'	845	1021	144	315
6G/2'	751	764	4	12
6G/4'	1125	1157	8	196
6G/6'	---			
6G/8'	---			
6G/10'	833	977	145	405
3H/2'	---			
3H/4'	1126	1173	10	200
3H/6'	1358	1630	115	356
3H/8'	1151	1489	143	486
3H/10'	791	965	148	348
4G/4'	1261	1302	9	211
4G/6'	1399	1769	120	373
4G/10'	825	993	130	316
4H/4'	1141	1199	26	206
4H/6'	---			
4H/10'	830	995	147	409
4D/4'	1131	1172	9	197
7D/6'	1331	1565	108	350
7D/10'	---			



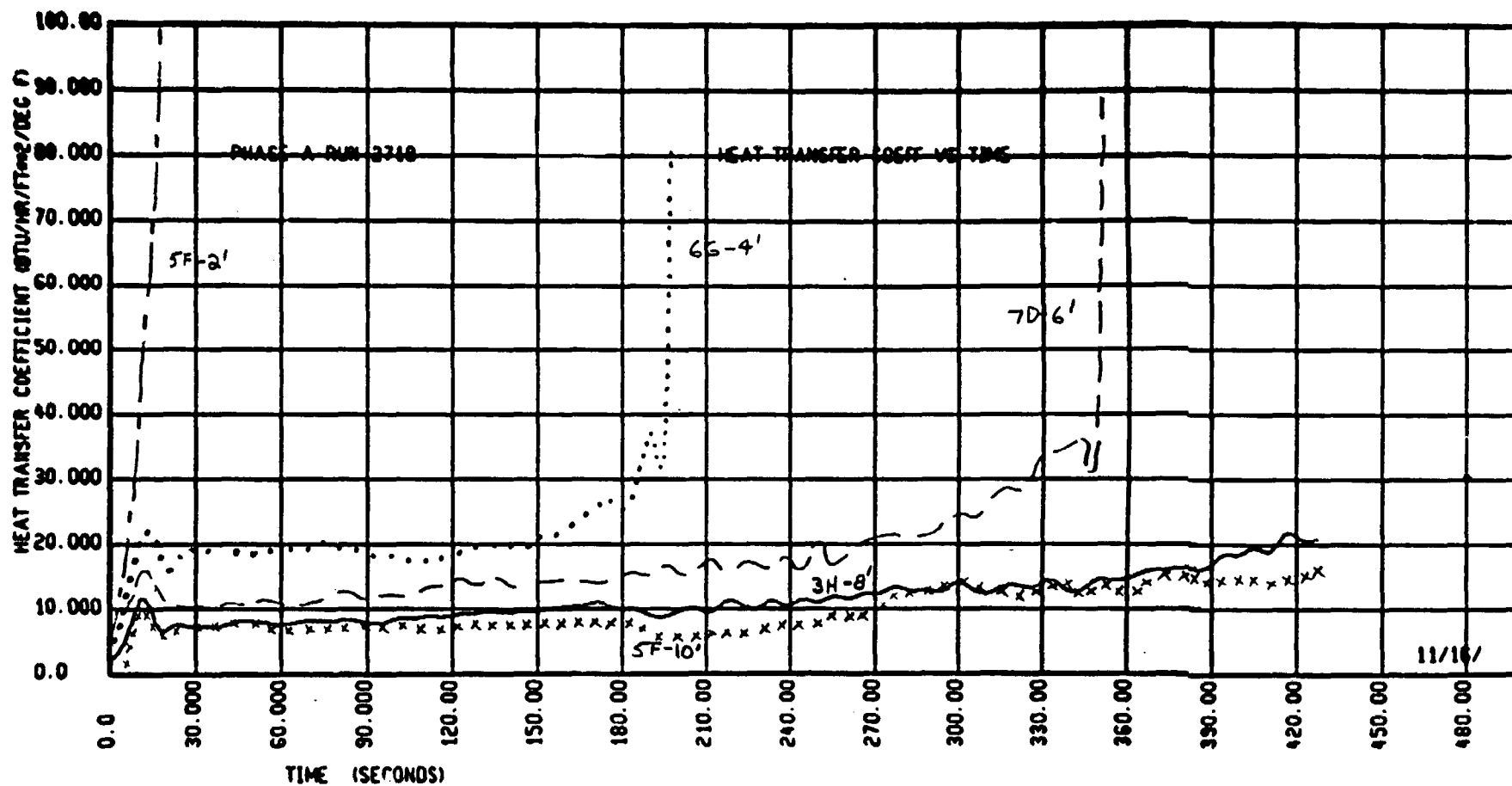
RUN NO.
 PRESSURE
 INITIAL CLAD TEMP
 PEAK POWER
 COOLANT INJECTION TEMP
 INJECTION FLOW RATE

2718
20 psia
1399 °F
.7 kw/ft
155°F
9.8 lb/sec 14 sec
1.23 lb/sec

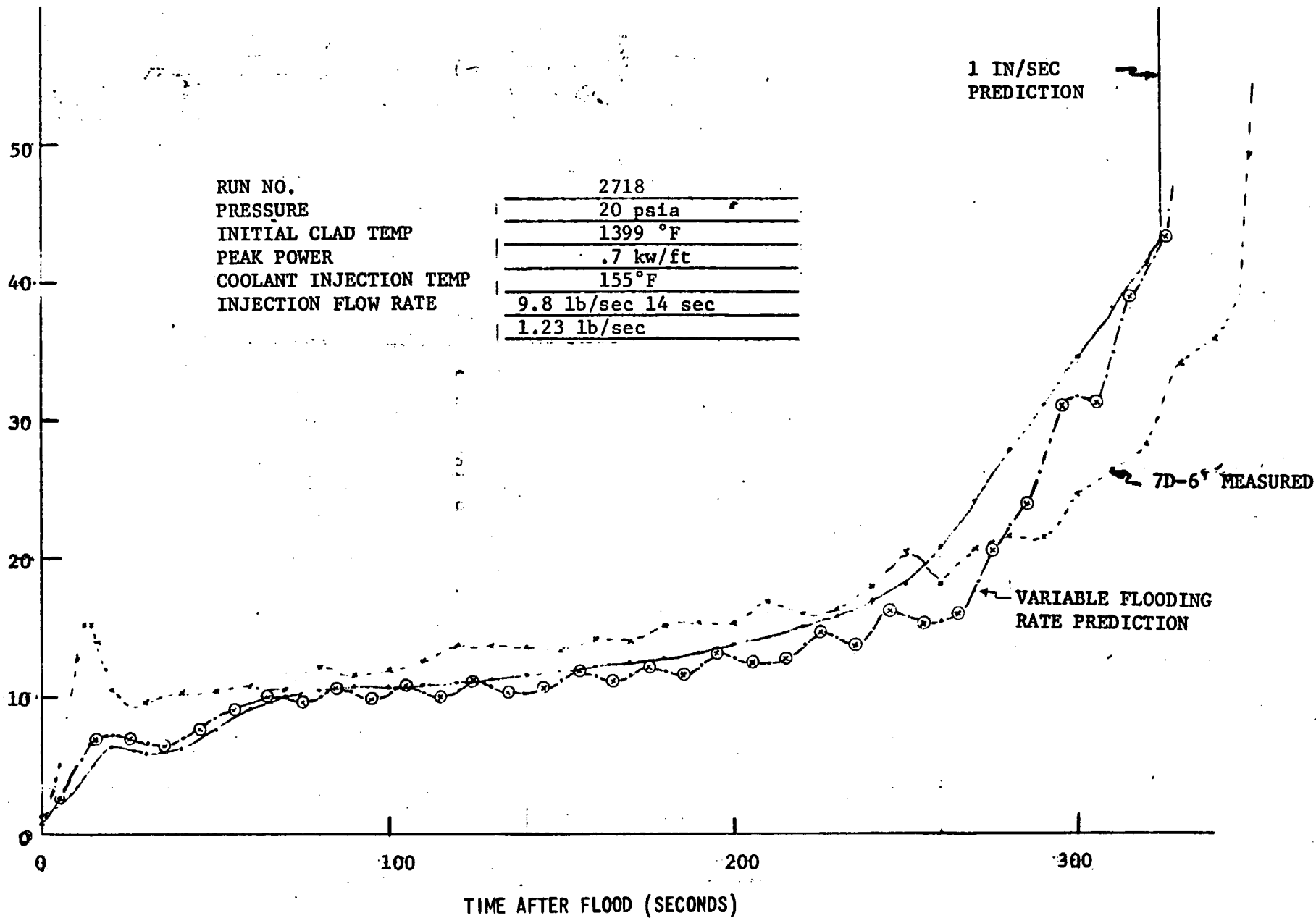




A-54



SS-V

HEAT TRANSFER COEFFICIENT (BTU/HR-FT² DEG F)

1

2

3

4

FLECHT-SET RUN SUMMARY SHEET

RUN NO. 2822

DATE 10/20/72

A. RUN CONDITIONS

Containment Pressure	19.3 psia
Initial Clad Temperature	1092 °F
Peak Power	0.4 kw/ft
Coolant Supply Temperature	163 °F
Injection Rate	11.0 lb/sec. first 14 sec., 1.16 lb/sec. after 14 sec.
Loop Resistance Coefficient	$(\Delta p_{loop}/1/2\rho V^2_{hotleg})$ 33

B. INITIAL HOUSING TEMPERATURES

Elevation (ft)	Initial Temperature (°F)
0	219
2	358
4	425
6	502
8	474
10	350
12	270

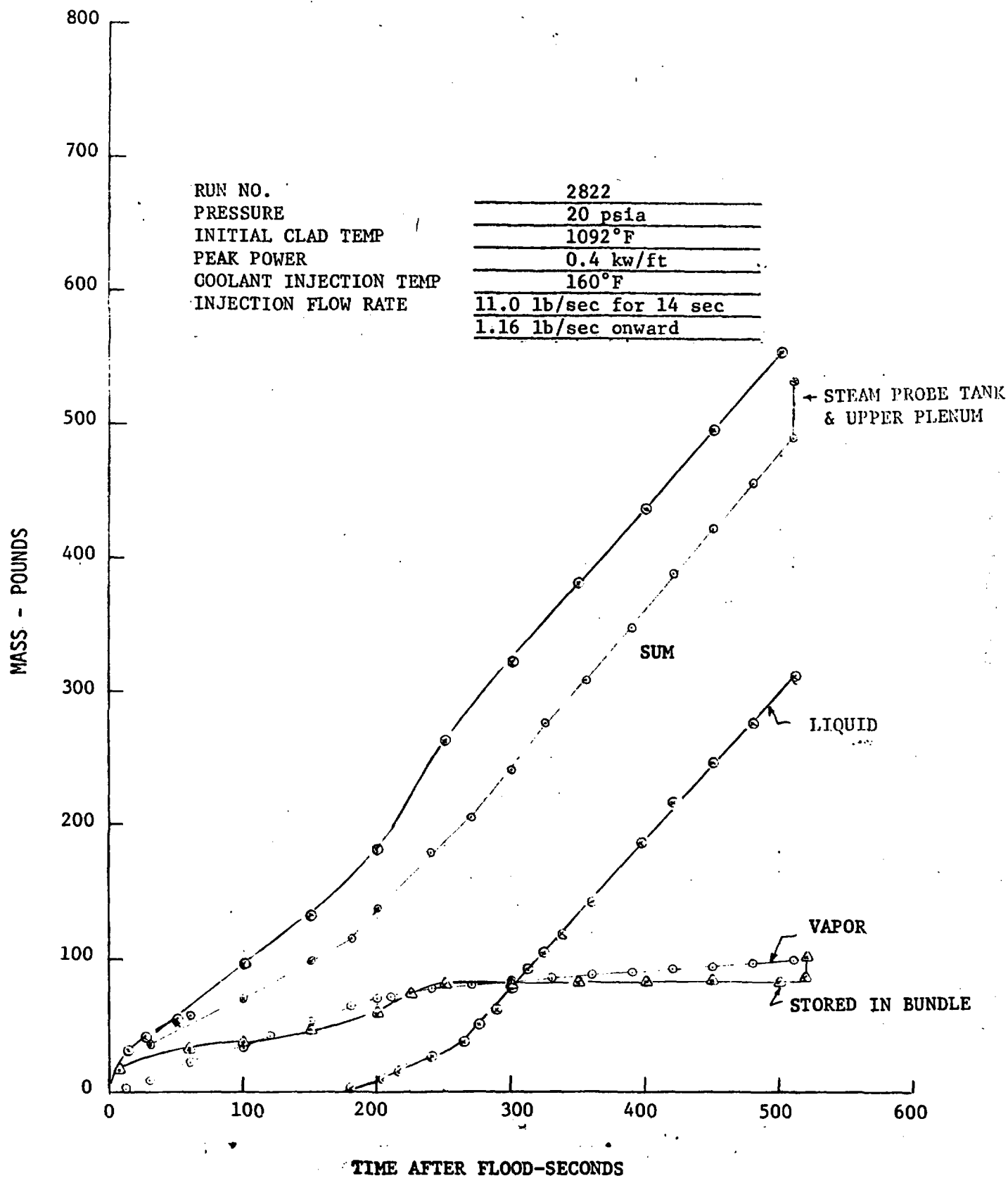
FLECHT-SET RUN SUMMARY SHEET (Cont)

RUN NO. 2822

DATE 10/20/72

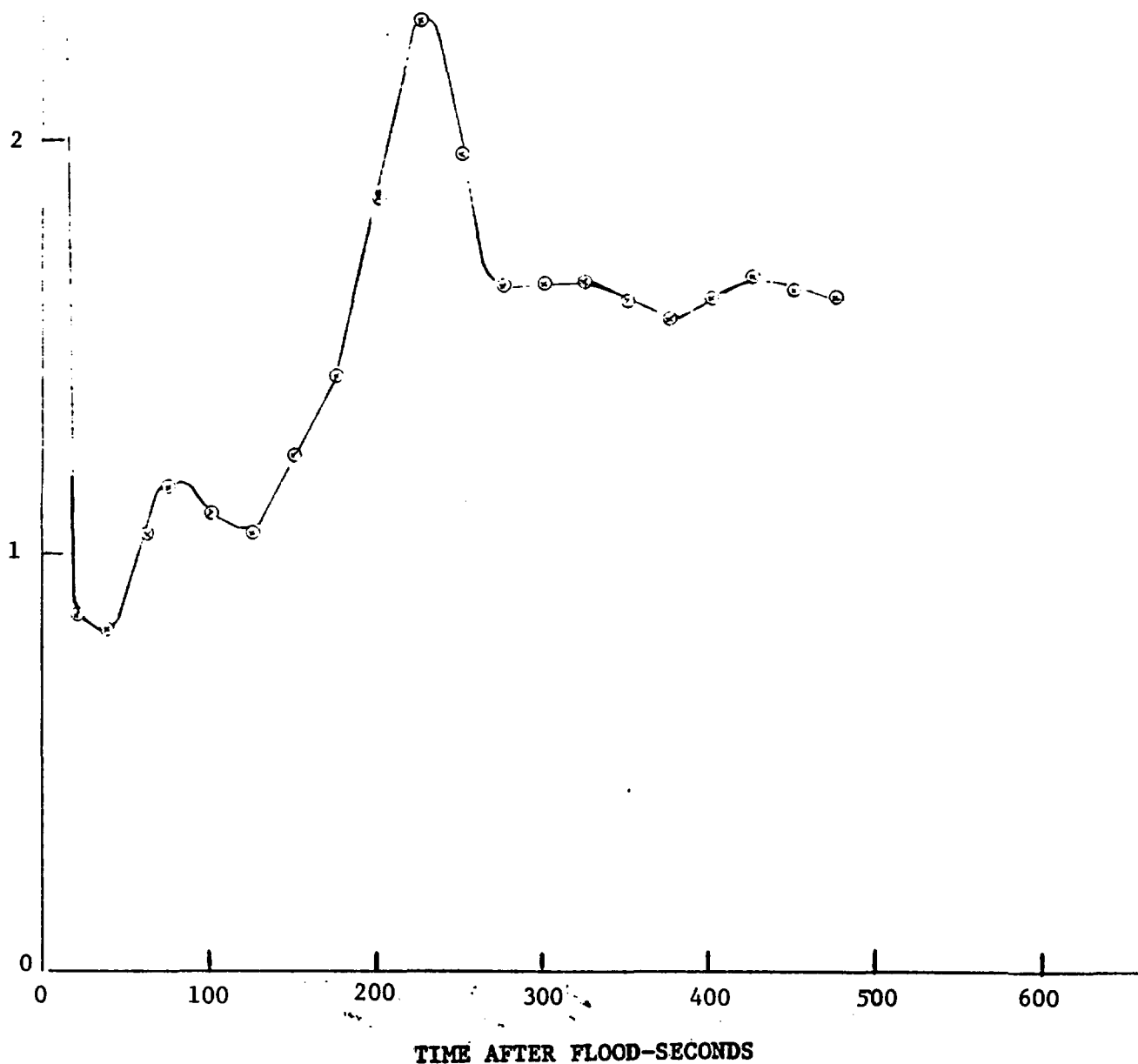
C. HEATER THERMOCOUPLE DATA

Rod/Elev.	Initial Temp. (°F)	Max. Temp. (°F)	Turnaround Time (Sec.)	Quench Time (Sec.)
5F/2'	604	612	3	9
5F/4'	---			
5F/6'	---			
5F/8'	927	984	26	180
5F/10'	696	712	11	38
5G/2'	594	600	4	7
5G/4'	---			
5G/6'	1089	1163	45	159
5G/8'	968	1016	31	180
5G/10'	684	718	50	52
6G/2'	602	611	5	6
6G/4'	887	901	6	58
6G/6'	---			
6G/8'	---			
6G/10'	671	700	47	119
3H/2'	---			
3H/4'	886	904	7	77
3H/6'	1055	1118	41	149
3H/8'	907	999	51	191
3H/10'	634	679	39	69
4G/4'	987	1002	8	78
4G/6'	1092	1170	40	155
4G/10'	670	713	30	32
4H/4'	904	921	12	83
4H/6'	---			
4H/10'	665	682	28	43
7D/4'	889	903	6	79
7D/6'	1038	1085	43	150
7D/10'	---			

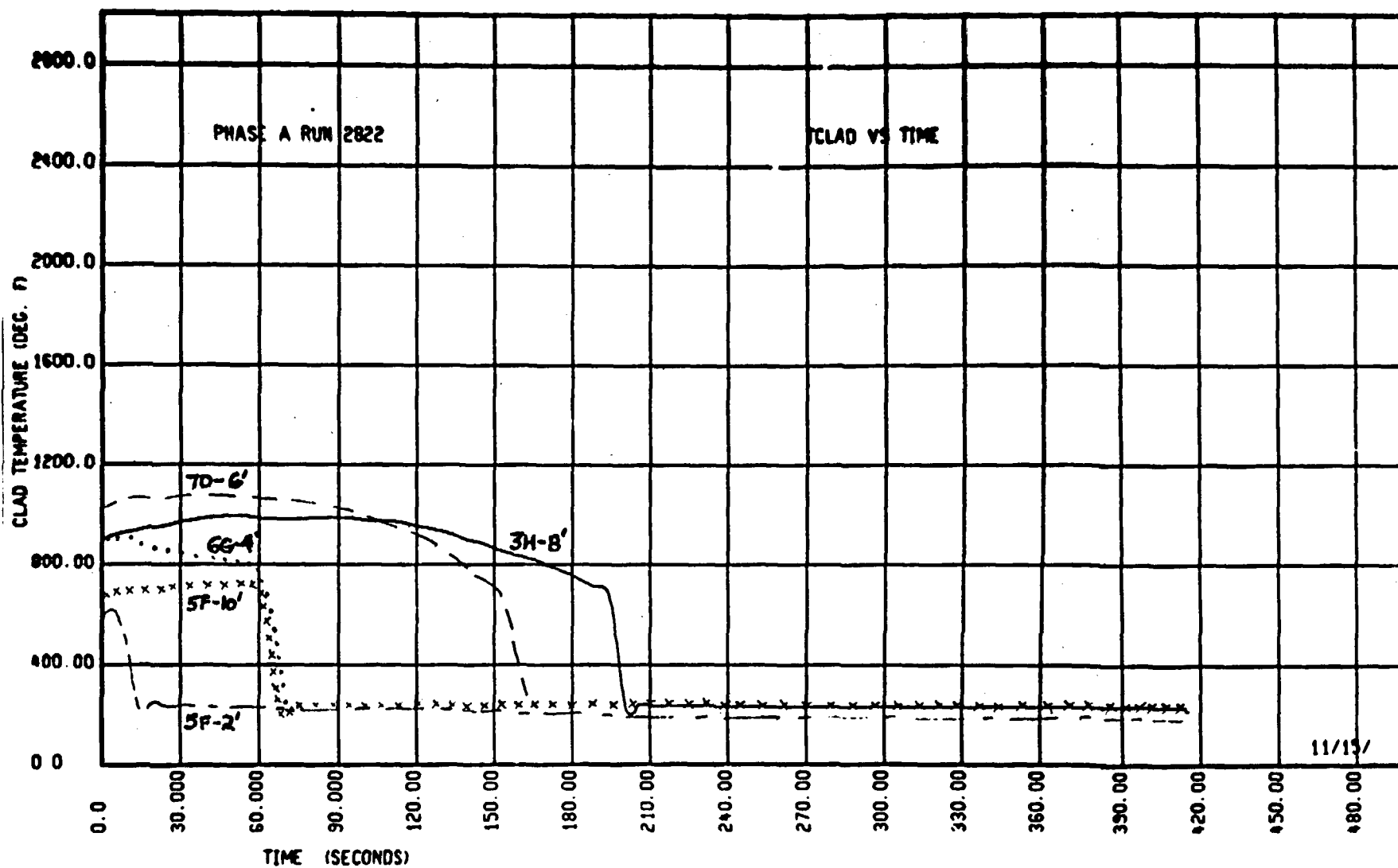


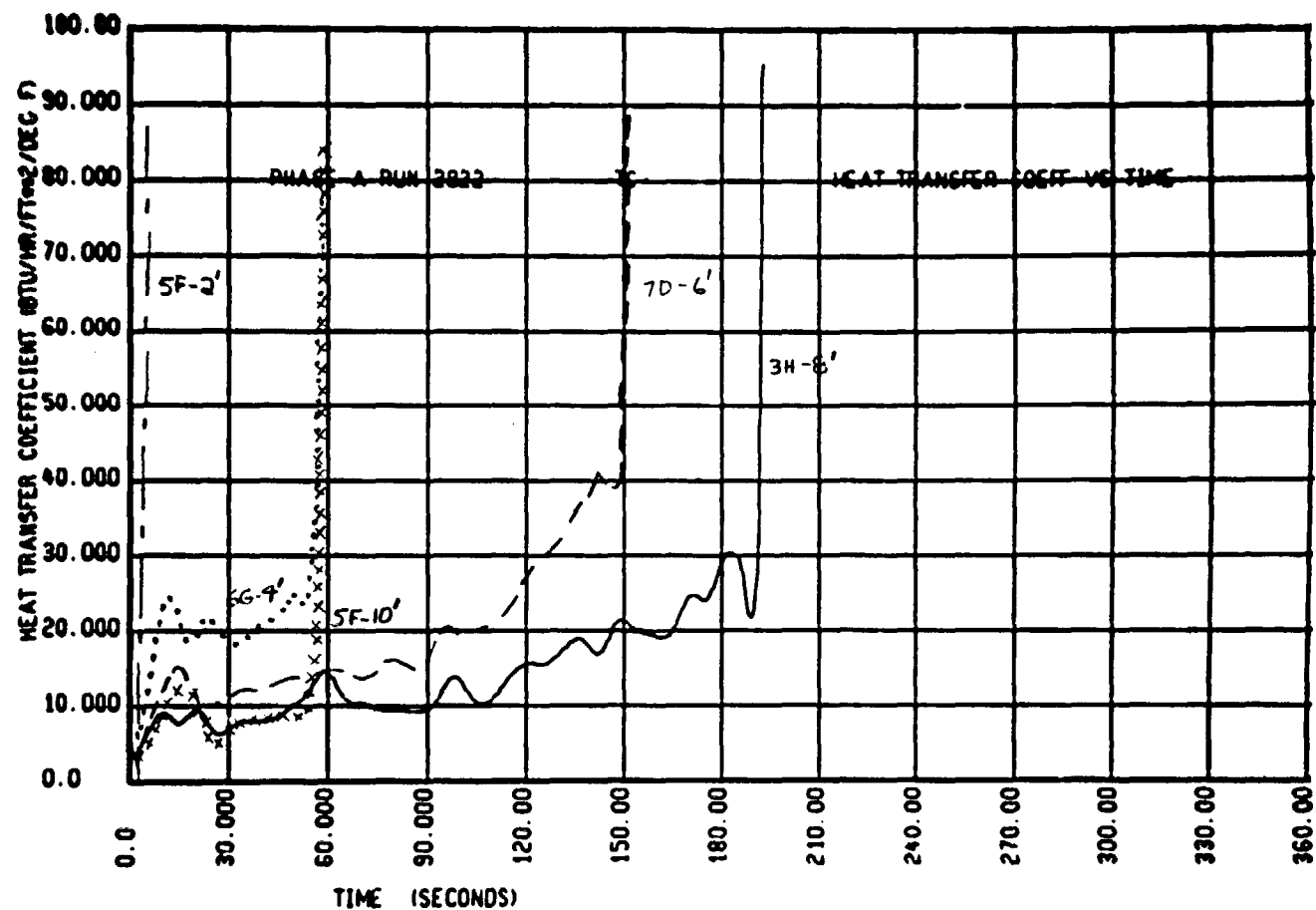
RUN NO.	2822
PRESSURE	20 psia
INITIAL CLAD TEMP	1092°F
PEAK POWER	0.4 kw/ft
COOLANT INJECTION TEMP	160°F
INJECTION FLOW RATE	11.0 lb/sec for 14 sec
	1.16 lb/sec onward

FLOODING RATE-IN/SEC

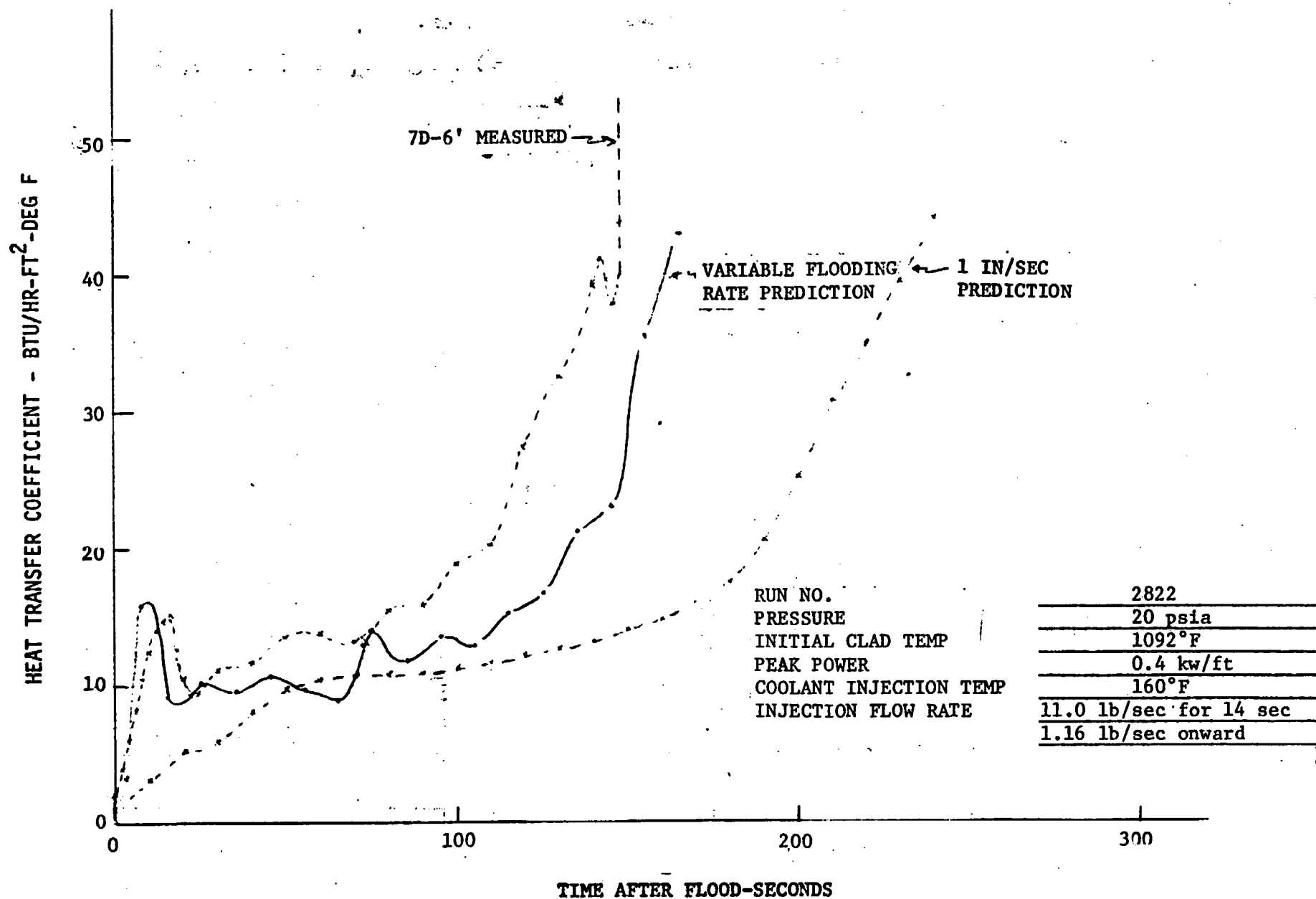


A-61





A-63



1

2

3

4

FLECHT-SET RUN SUMMARY SHEET

RUN NO. 2919

DATE 10/21/72

A. RUN CONDITIONS

Containment Pressure	20.1	psia
Initial Clad Temperature	912	°F
Peak Power	0.7	kw/ft
Coolant Supply Temperature	153	°F
Injection Rate	10.1 lb/sec first 14 sec,	1.2 lb/sec after 14 sec
Loop Resistance Coefficient	$(\Delta p_{loop}/1/2 \rho V_{hotleg}^2)$	33.1

B. INITIAL HOUSING TEMPERATURES

Elevation (ft)	Initial Temperature (°F)
0	248
2	411
4	500
6	584
8	536
10	410
12	239

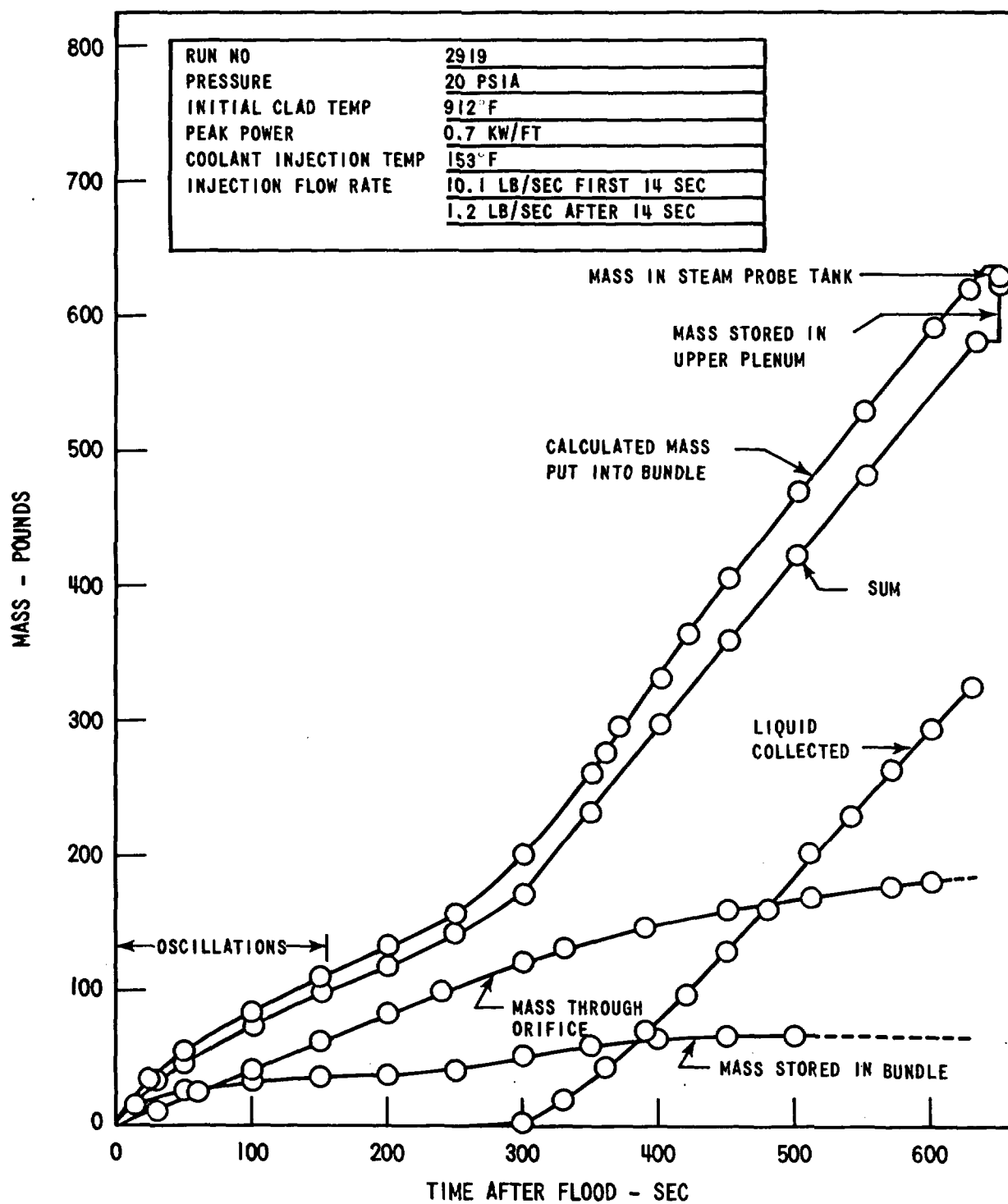
FLECHT-SET RUN SUMMARY SHEET (Cont)

RUN NO. 2919

DATE 10/21/72

C. HEATER THERMOCOUPLE DATA

Rod/Elev.	Initial Temp. (°F)	Max. Temp. (°F)	Turnaround Time (Sec)	Quench Time (Sec)
5F/2'	555	581	6	11
5F/4'	---			
5F/6'				
5F/8'	818	1173	112	376
5F/10'	640	945	145	295
5G/2'	545	566	5	7
5G/4'	---			
5G/6'	911	1430	125	268
5G/8'	839	1322	141	403
5G/10'	626	946	156	277
6G/2'	552	574	4	5
6G/4'	775	912	53	103
6G/6'	---			
6G/8'	---			
6G/10'	614	958	215	328
3H/2'	---			
3H/4'	756	935	58	102
3H/6'	880	1386	114	265
3H/8'	773	1299	201	377
3H/10'	571	898	218	352
4G/4'	837	1048	65	118
4G/6'	912	1476	122	285
4G/10'	610	755	39	40
4H/4'	775	994	61	114
4H/6'	---			
4H/10'	603	760	57	226
7D/4'	772	923	52	103
7D/6'	879	1308	110	256
7D/10'	---			



89-A

FLOODING RATE - IN./SEC

5

4

3

2

1

0

0

100

200

300

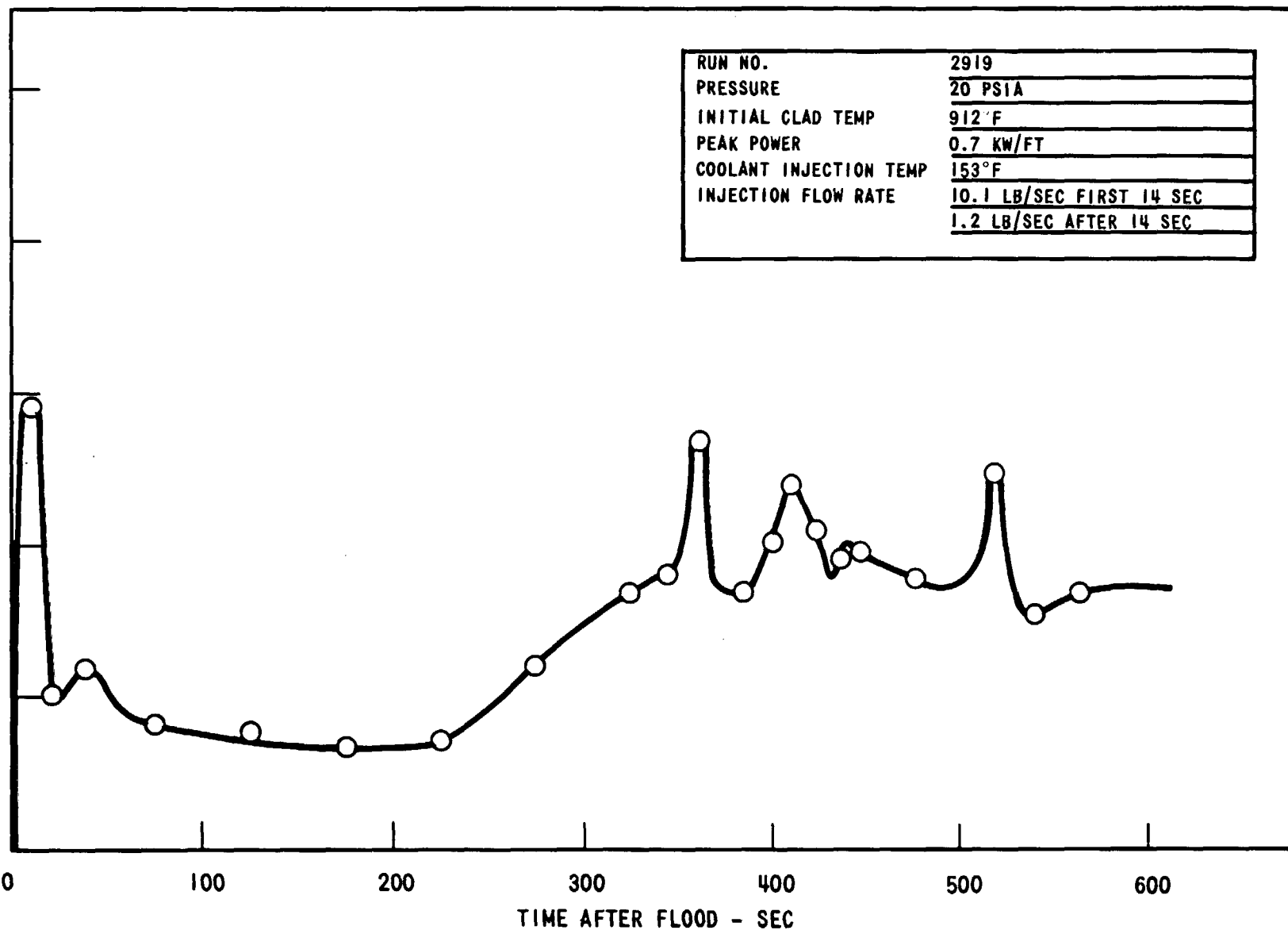
400

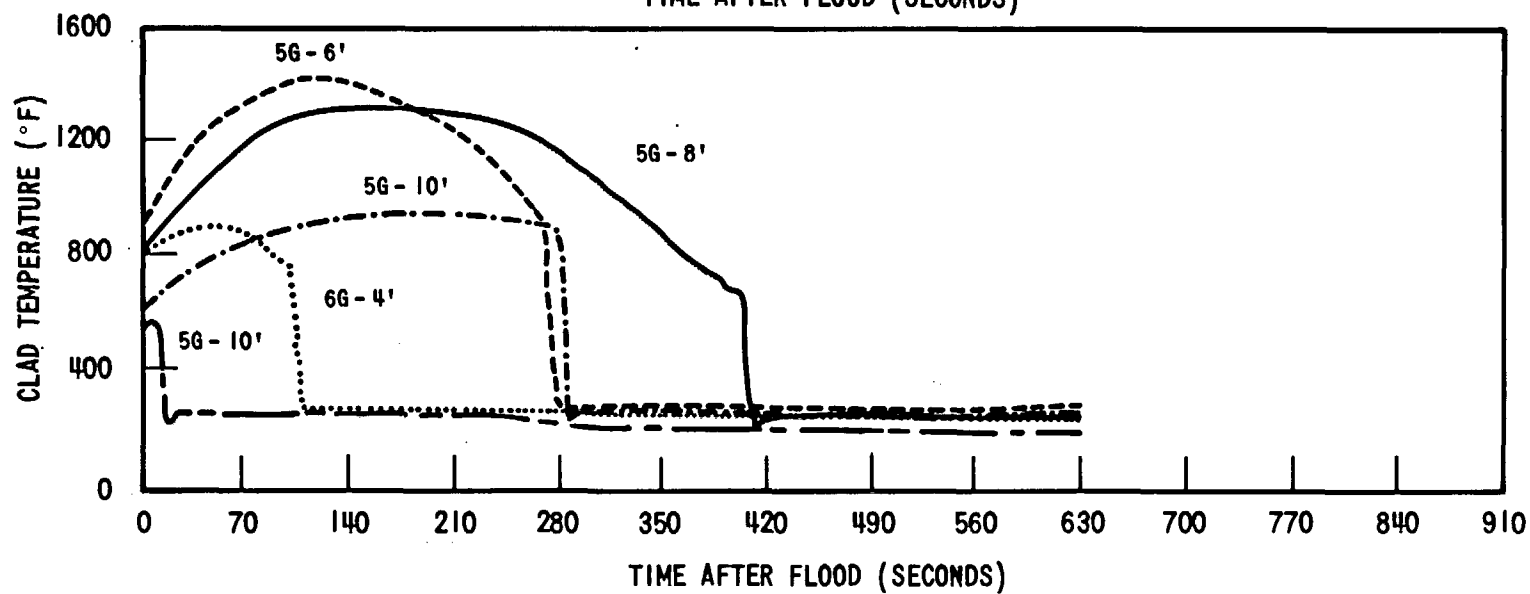
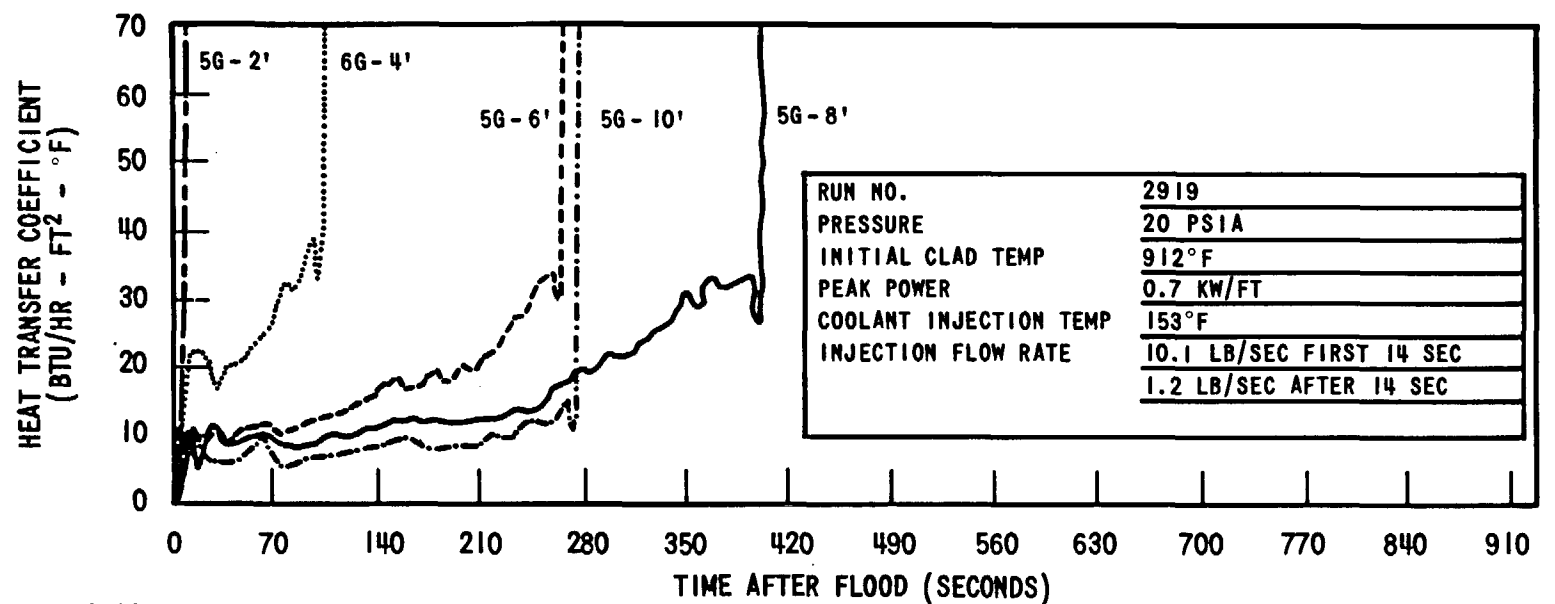
500

600

TIME AFTER FLOOD - SEC

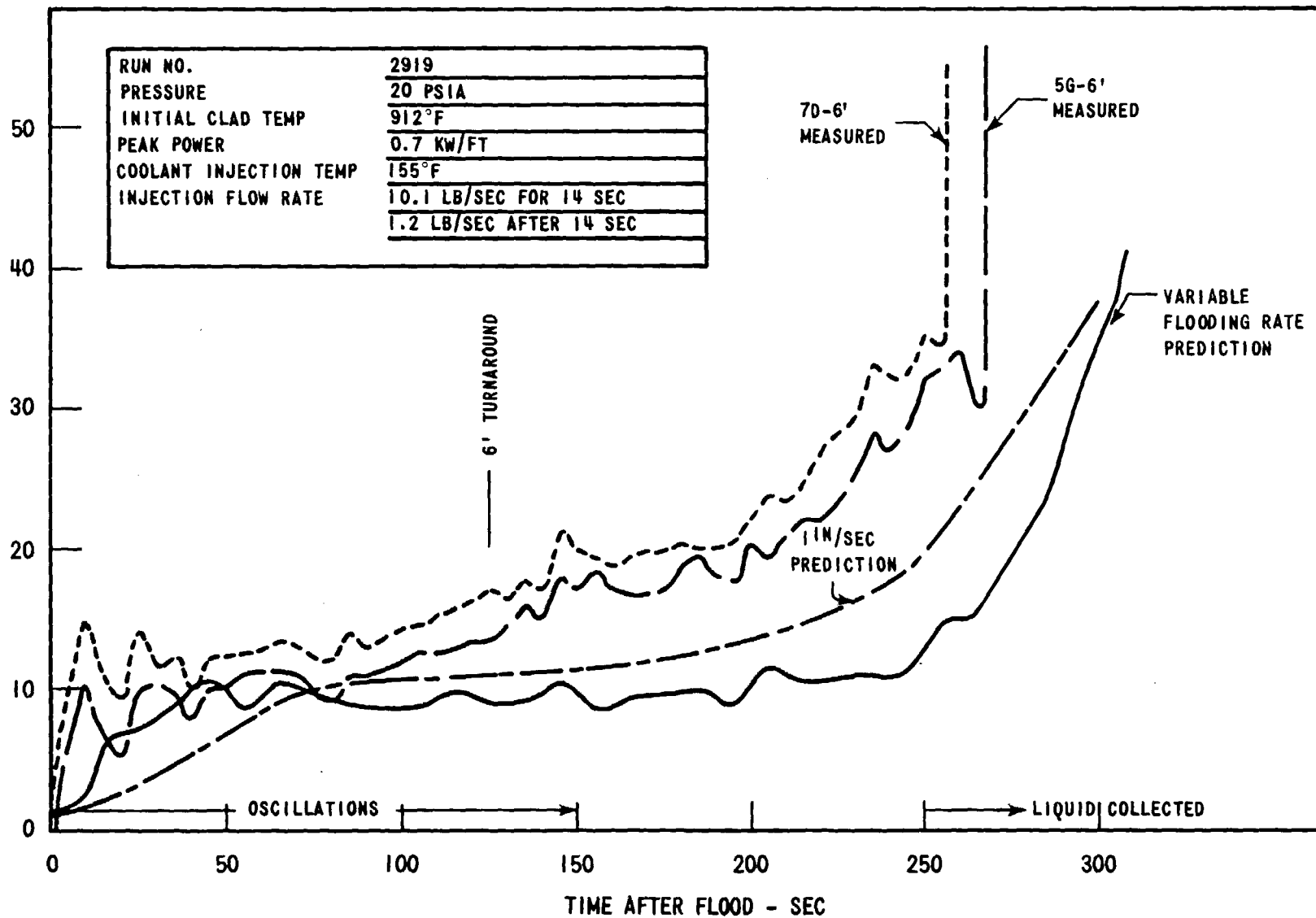
RUN NO.	2919
PRESSURE	20 PSIA
INITIAL CLAD TEMP	912°F
PEAK POWER	0.7 KW/FT
COOLANT INJECTION TEMP	153°F
INJECTION FLOW RATE	10.1 LB/SEC FIRST 14 SEC
	1.2 LB/SEC AFTER 14 SEC





A-70

HEAT TRANSFER COEFFICIENT - BTU/HR-FT²-°F



FLECHT-SET RUN SUMMARY SHEET

RUN NO. 3006

DATE 10/24/72

A. RUN CONDITIONS

Containment Pressure	20.1	psia	
Initial Clad Temperature	1115	°F	
Peak Power	0.7	kw/ft	
Coolant Supply Temperature	162	°F	
Injection Rate	1.17 lb/sec first	sec,	1b/sec after sec
Loop Resistance Coefficient	$(\Delta p_{loop}/1/2 \rho V_{hotleg}^2)$	32	

B. INITIAL HOUSING TEMPERATURES

Elevation (ft)	Initial Temperature (°F)
0	259
2	4236
4	546
6	652.3
8	613.5
10	420
12	249

FLECHT-SET RUN SUMMARY SHEET (Cont)

RUN NO. 3006

DATE 10/24/72

C. HEATER THERMOCOUPLE DATA

Rod/Elev.	Initial Temp. (°F)	Max. Temp. (°F)	Turnaround Time (Sec)	Quench Time (Sec)
5F/2'	644	762	37	80
5F/4'	---			
5F/6'	---			
5F/8'	996	1697	185	554
5F/10'	774	1211	144	347
5G/2'	630	752	36	79
5G/4'	---			
5G/6'	1110	1785	137	432
5G/8'	1026	1690	149	542
5G/10'	758	1158	120	364
6G/2'	640	764	36	78
6G/4'	934	1260	75	280
6G/6'	---			
6G/8'	---			
6G/10'	745	1150	131	520
3H/2'	---			
3H/4'	909	1226	76	287
3H/6'	1073	1677	134	428
3H/8'	942	1559	175	555
3H/10'	678	1083	137	364
4G/4'	1017	1427	91	304
4G/6'	1115	1819	139	439
4G/10'	736	1166	139	354
4H/4'	935	1329	102	304
4H/6'	---			
4H/10'	724	1172	129	409
7D/4'	929	1292	73	283
7D/6'	1067	1722	122	421
7D/10'	---			

RUN NO.	3006
PRESSURE	20 psia
INITIAL CLAD TEMP	1115°F
PEAK POWER	0.7 kw/ft
COOLANT INJECTION TEMP	170°F
INJECTION FLOW RATE	1.17 lb/sec

MASS - POUNDS

800
700
600
500
400
300
200
100
0

0 100 200 300 400 500 600

TIME AFTER FLOOD-SECONDS

A-73

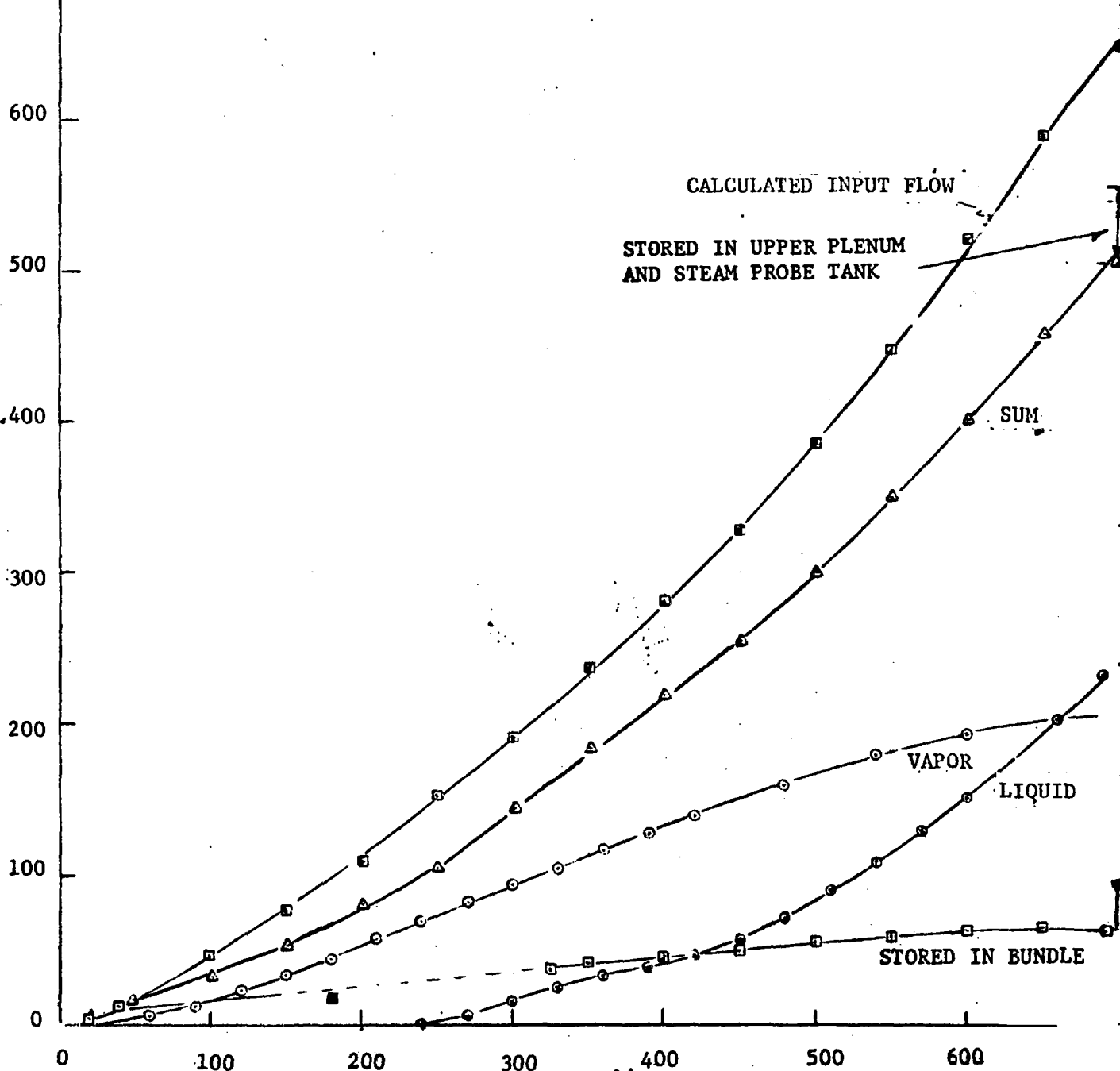
CALCULATED INPUT FLOW
STORED IN UPPER PLENUM
AND STEAM PROBE TANK

SUM

VAPOR

LIQUID

STORED IN BUNDLE



FLOODING RATE-IN/SEC

3.0

2.0

1.0

0

RUN NO.
PRESSURE
INITIAL CLAD TEMP
PEAK POWER
COOLANT INJECTION TEMP
INJECTION FLOW RATE

3006

20 psia

1115°F

0.7 kw/ft

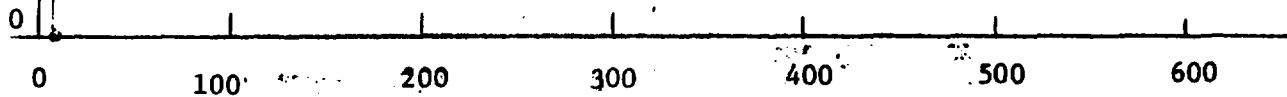
170°F

1.17 lb/sec

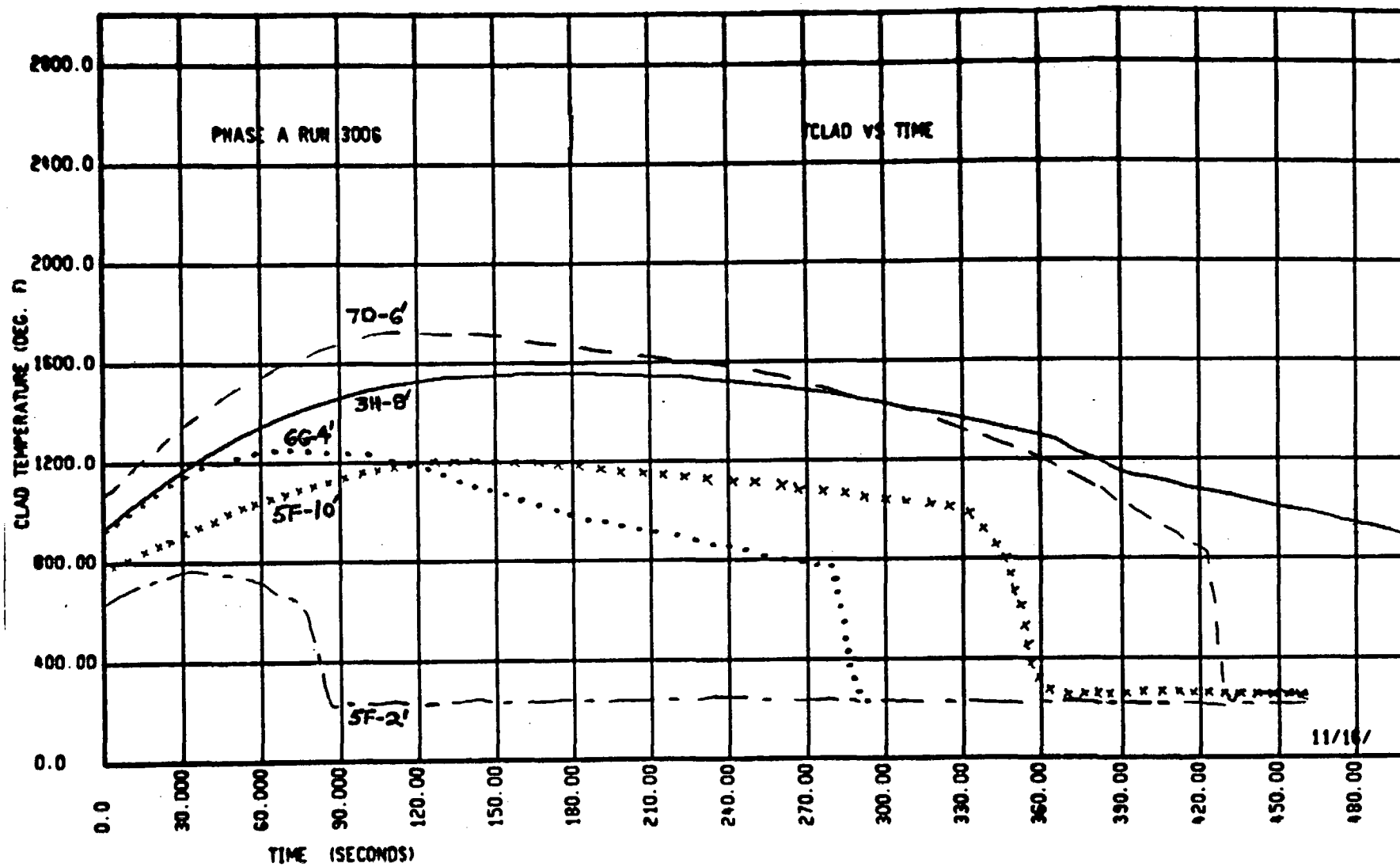
0 100 200 300 400 500 600

TIME AFTER FLOOD-SECONDS

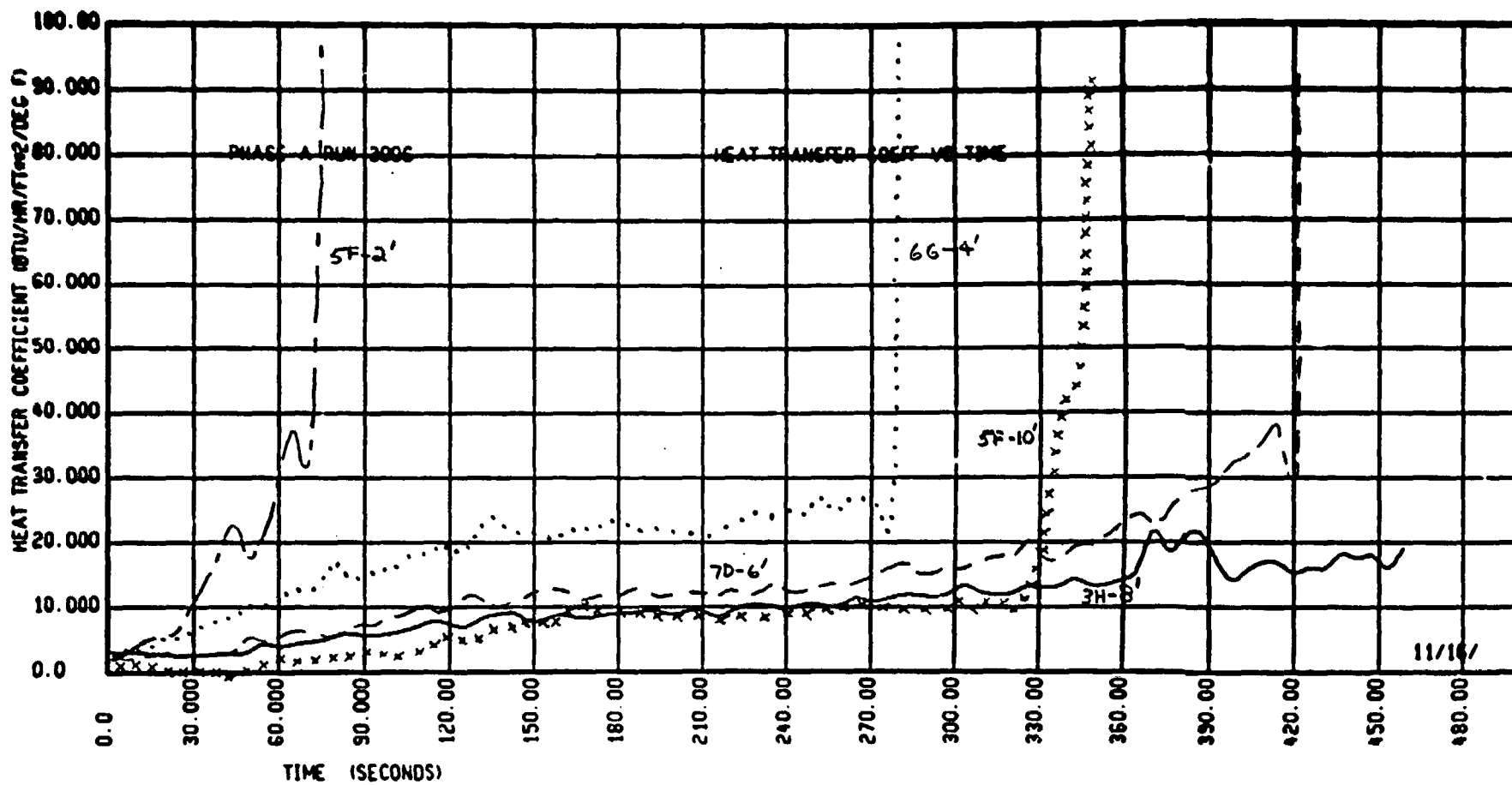
A-74



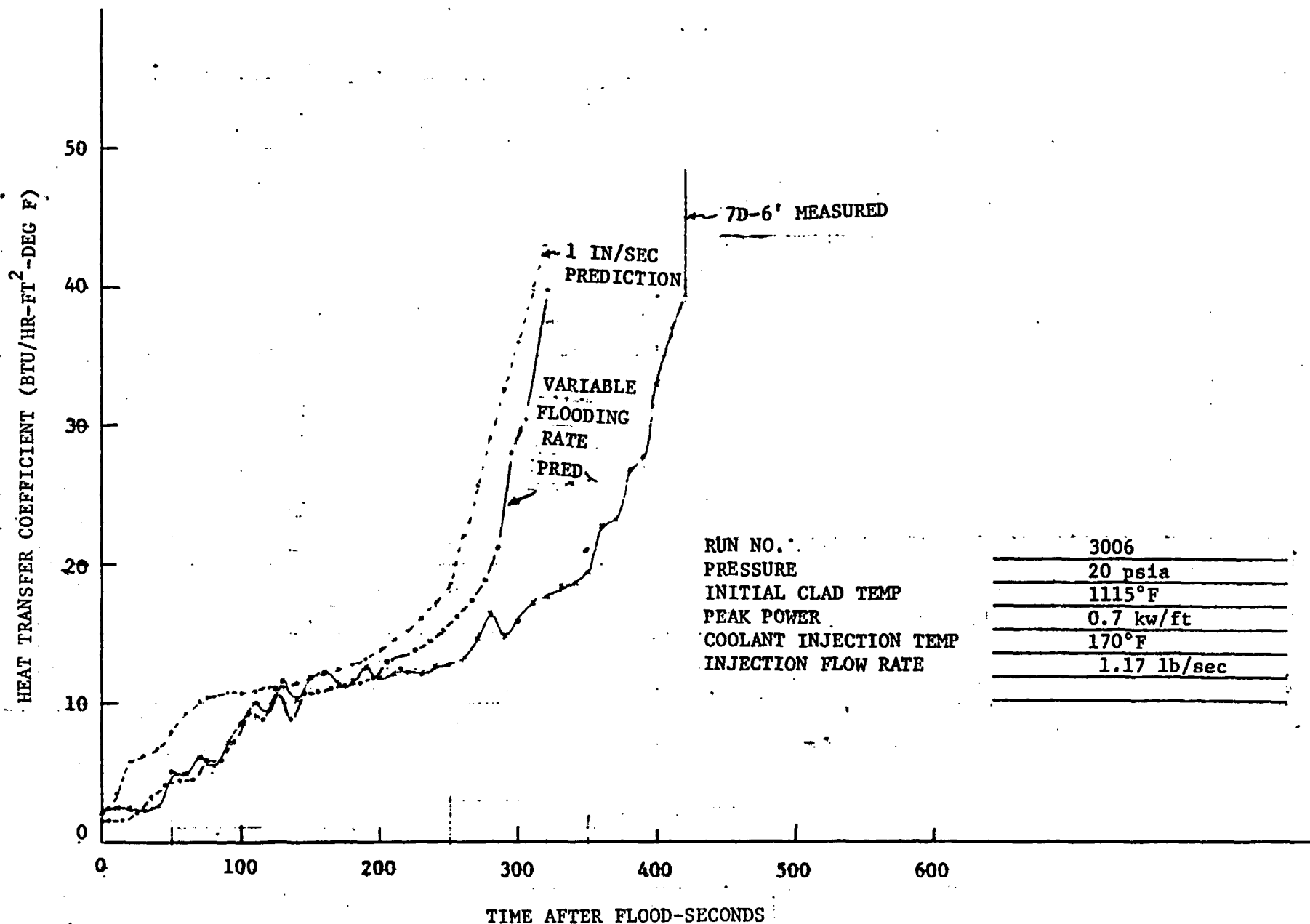
A-75



A-76



A-77



—

—

—

FLECHT-SET RUN SUMMARY SHEET

RUN NO. 3117

DATE 10/25/72

A. RUN CONDITIONS

Containment Pressure	19.9	psia
Initial Clad Temperature	1113	°F
Peak Power	0.7	kw/ft
Coolant Supply Temperature	159	°F
Injection Rate	11.22 lb/sec first 14 sec, 1.16 lb/sec after 14 sec	
Loop Resistance Coefficient ($\Delta p_{loop}/1/2 \rho V_{hotleg}^2$)	27.9	

B. INITIAL HOUSING TEMPERATURES

Elevation (ft)	Initial Temperature (°F)
0	2255
2	441
4	508.5
6	607.0
8	584.5
10	420
12	242

FLECHT-SET RUN SUMMARY SHEET (Cont)

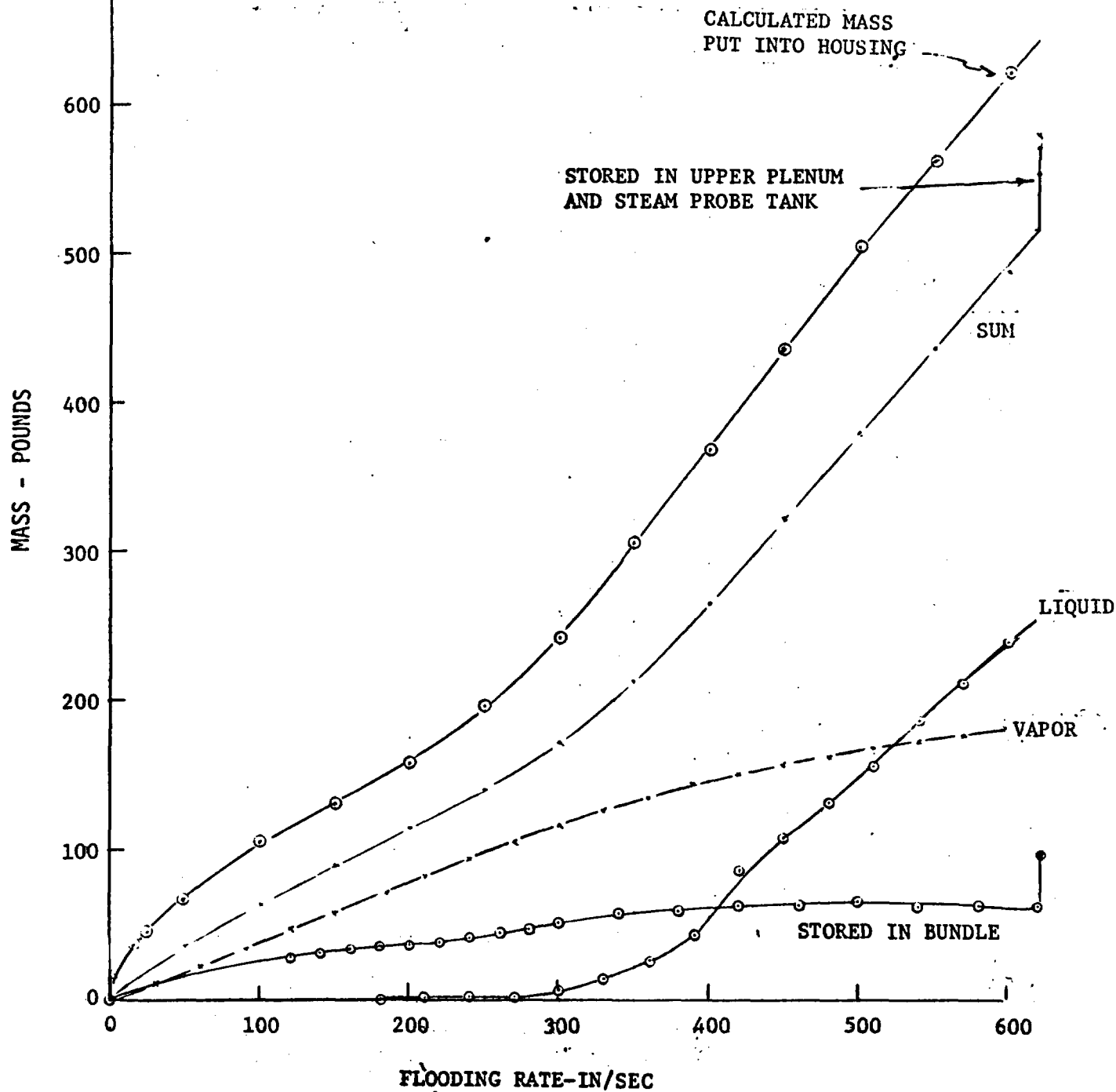
RUN NO. 3117

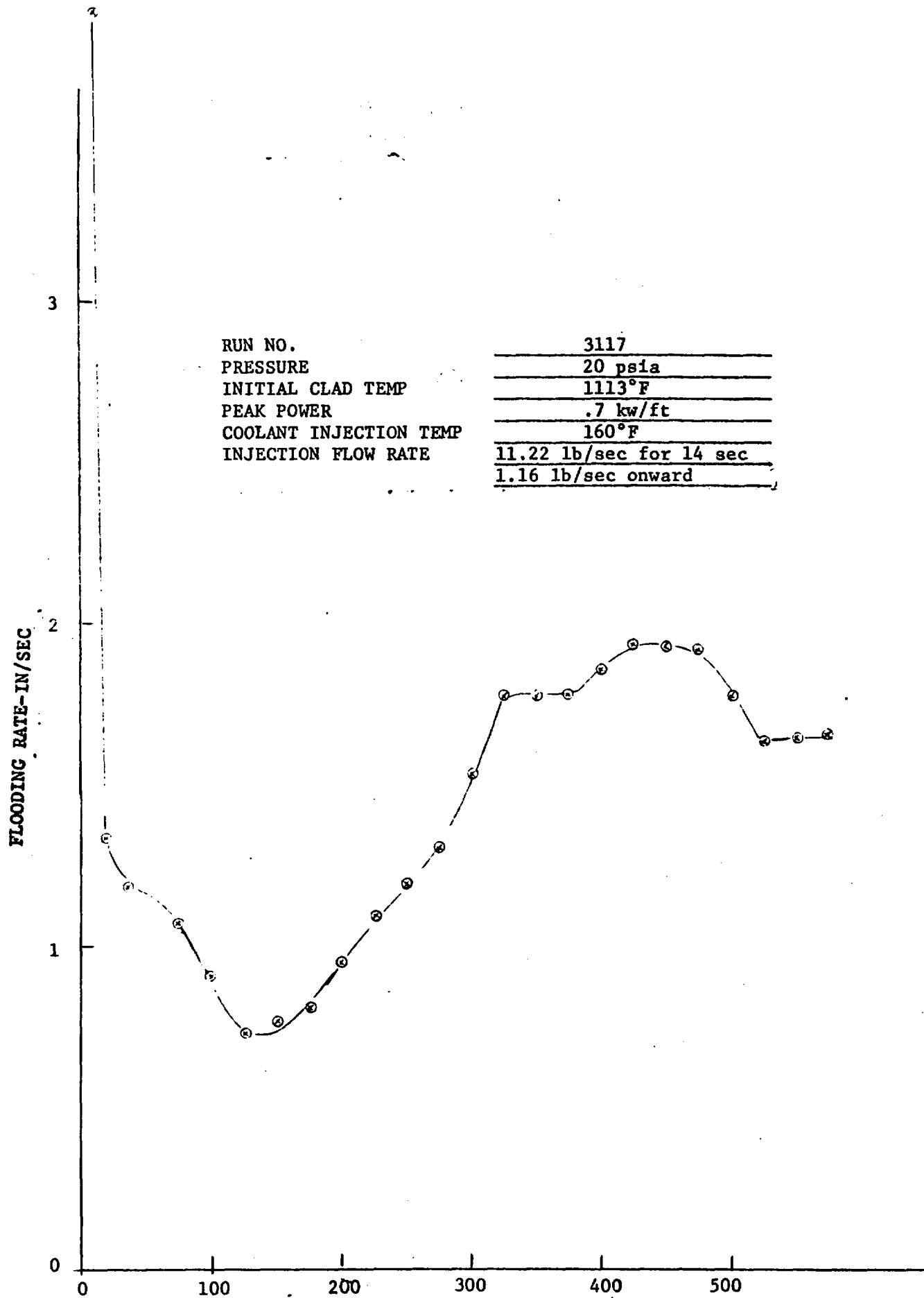
DATE 10/25/72

C. HEATER THERMOCOUPLE DATA

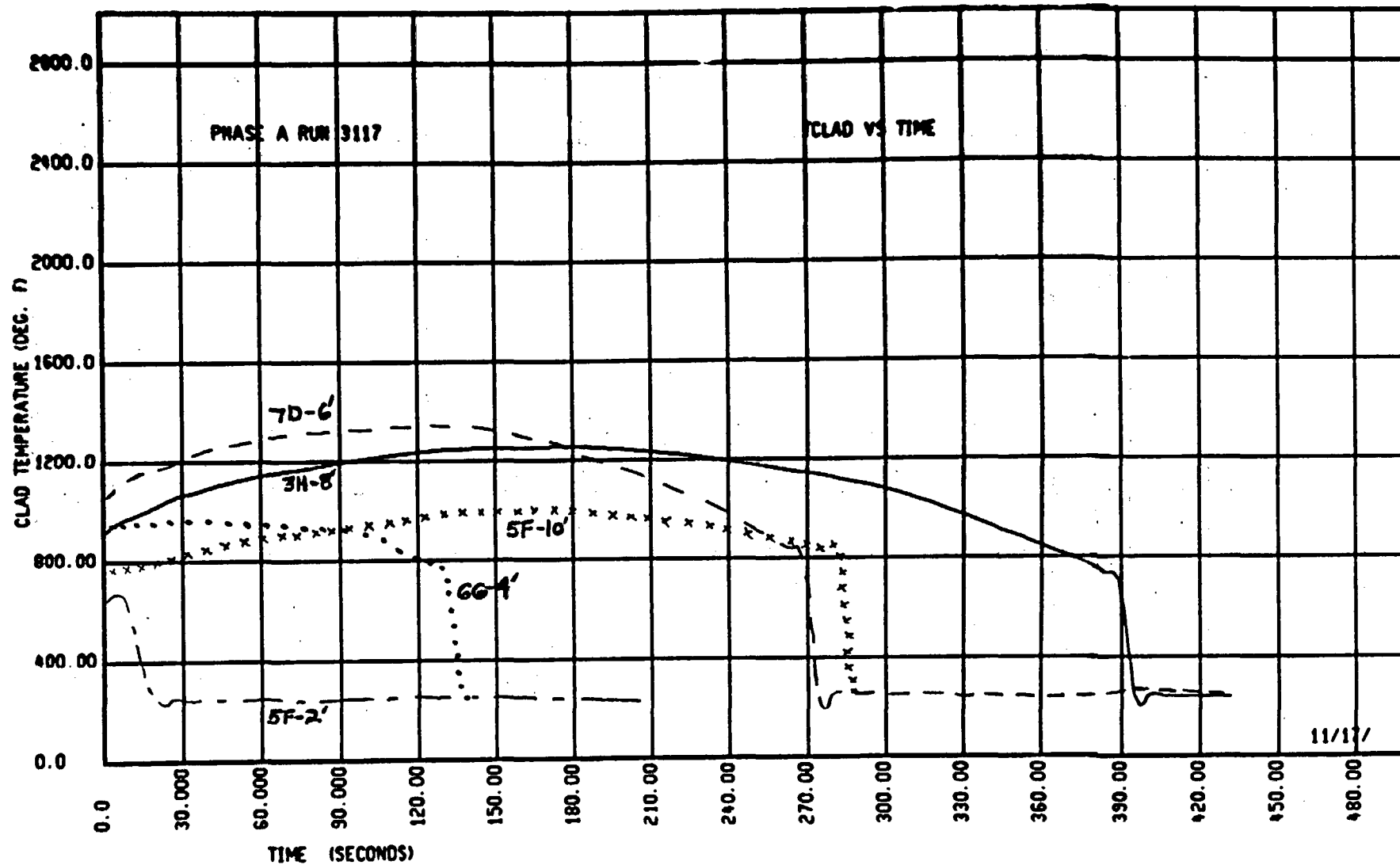
Rod/Elev.	Initial Temp. (°F)	Max. Temp. (°F)	Turnaround Time (Sec)	Quench Time (Sec)
5F/2'	655	673	4	11
5F/4'	---			
5F/6'	---			
5F/8'	972	1259	150	386
5F/10'	---			
5G/2'	642	653	4	10
5G/4'	---			
5G/6'	1113	1437	133	281
5G/8'	1007	1308	149	408
5G/10'	718	1000	171	294
6G/2'	653	672	5	7
6G/4'	923	962	31	129
6G/6'	---			
6G/8'	---			
6G/10'	701	957	170	304
3H/2'	---			
3H/4'	906	973	58	133
3H/6'	1077	1405	127	272
3H/8'	923	1256	175	387
3H/10'	633	897	163	420
4G/4'	1020	1103	63	143
4G/6'	---			
4G/10'	698	950	222	265
4H/4'	926	1046	68	139
4H/6'	---			
4H/10'	682	962	155	375
7D/4'	921	978	34	129
7D/6'	1070	1350	117	266
7D/10'	693	976	187	419

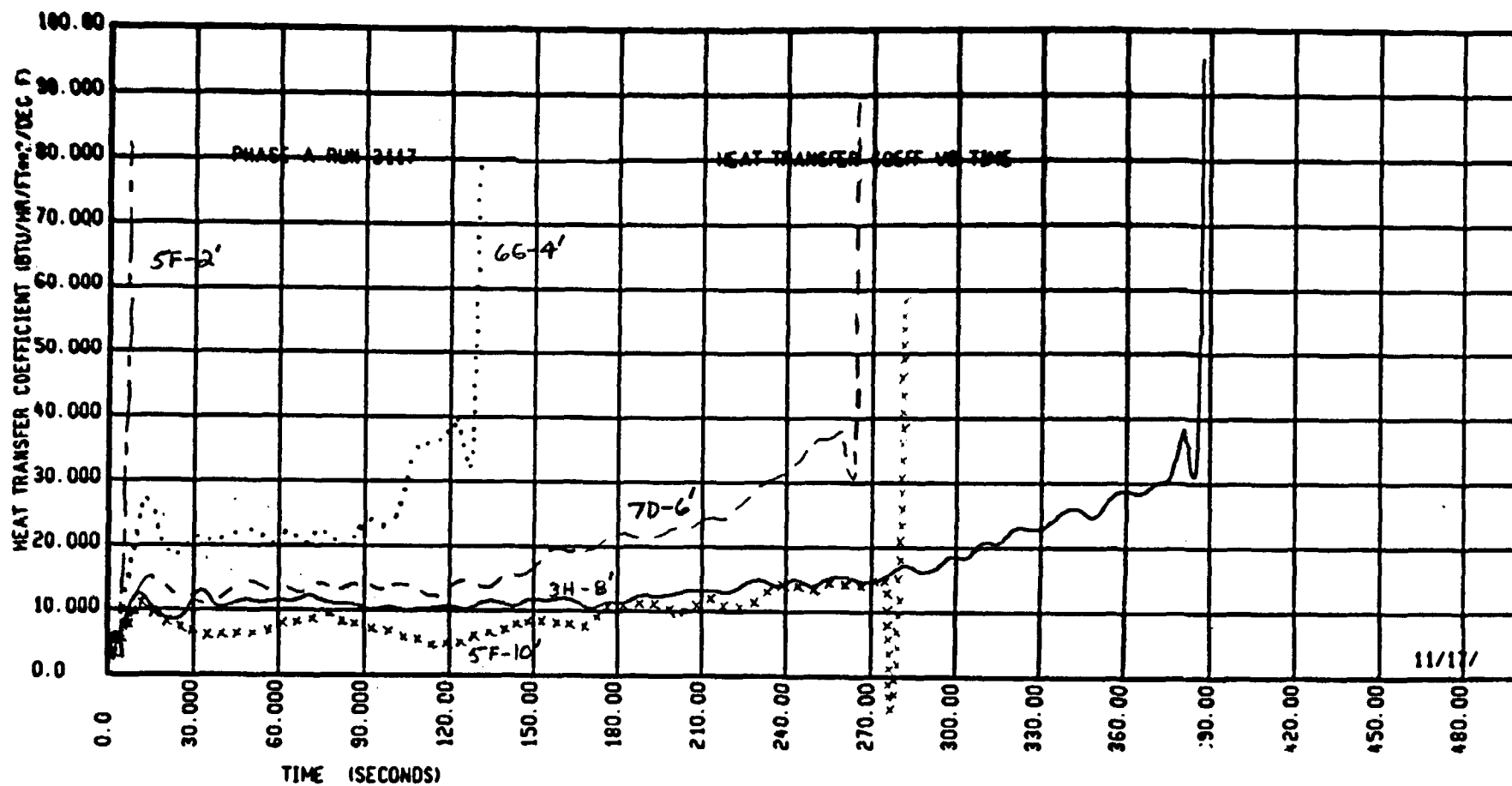
RUN NO.	3117
PRESSURE	20 psia
INITIAL CLAD TEMP	1113°F
PEAK POWER	.7 kw/ft
COOLANT INJECTION TEMP	160°F
INJECTION FLOW RATE	11.22 lb/sec for 14 sec
	1.16 lb/sec onward





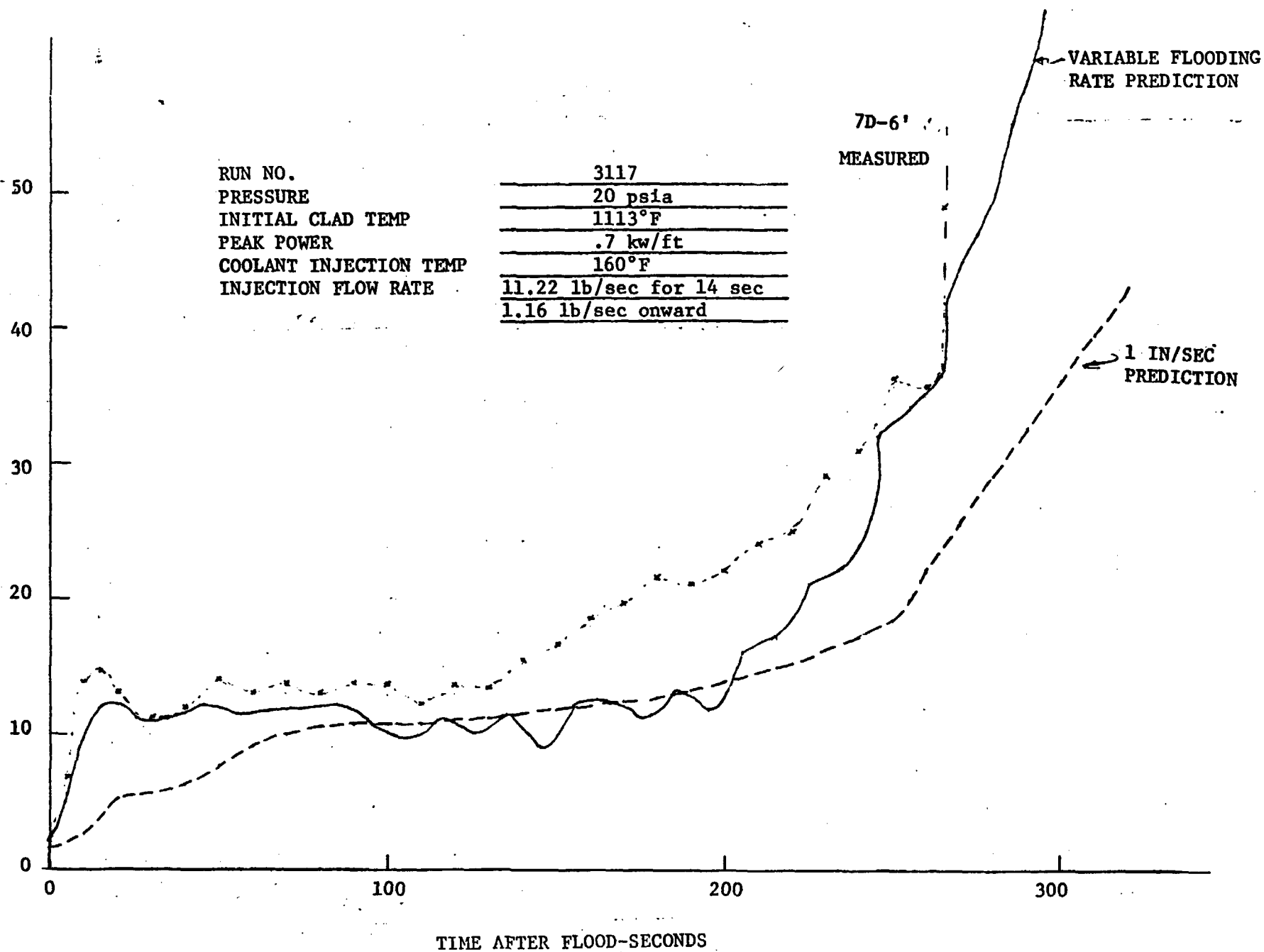
RUN NO.	3117
PRESSURE	20 psia
INITIAL CLAD TEMP	1113°F
PEAK POWER	.7 kw/ft
COOLANT INJECTION TEMP	160°F
INJECTION FLOW RATE	11.22 lb/sec for 14 sec
	1.16 lb/sec onward





A-85

HEAT TRANSFER COEFFICIENT - BTU/HR-FT²-DEG F



1

2

3

4

FLECHT-SET RUN SUMMARY SHEET

RUN NO. 3320

DATE 10/27/72

A. RUN CONDITIONS

Containment Pressure	19.5	psia
Initial Clad Temperature	1073	°F
Peak Power	0.7	kw/ft
Coolant Supply Temperature	195	°F
Injection Rate	11.5 lb/sec first 14 sec,	1.17 lb/sec after 14 sec
Loop Resistance Coefficient ($\Delta p_{loop} / 1/2 \rho V_{hotleg}^2$)	31	

B. INITIAL HOUSING TEMPERATURES

Elevation (ft)	Initial Temperature (°F)
0	228
2	389
4	494
6	574
8	531
10	371
12	215

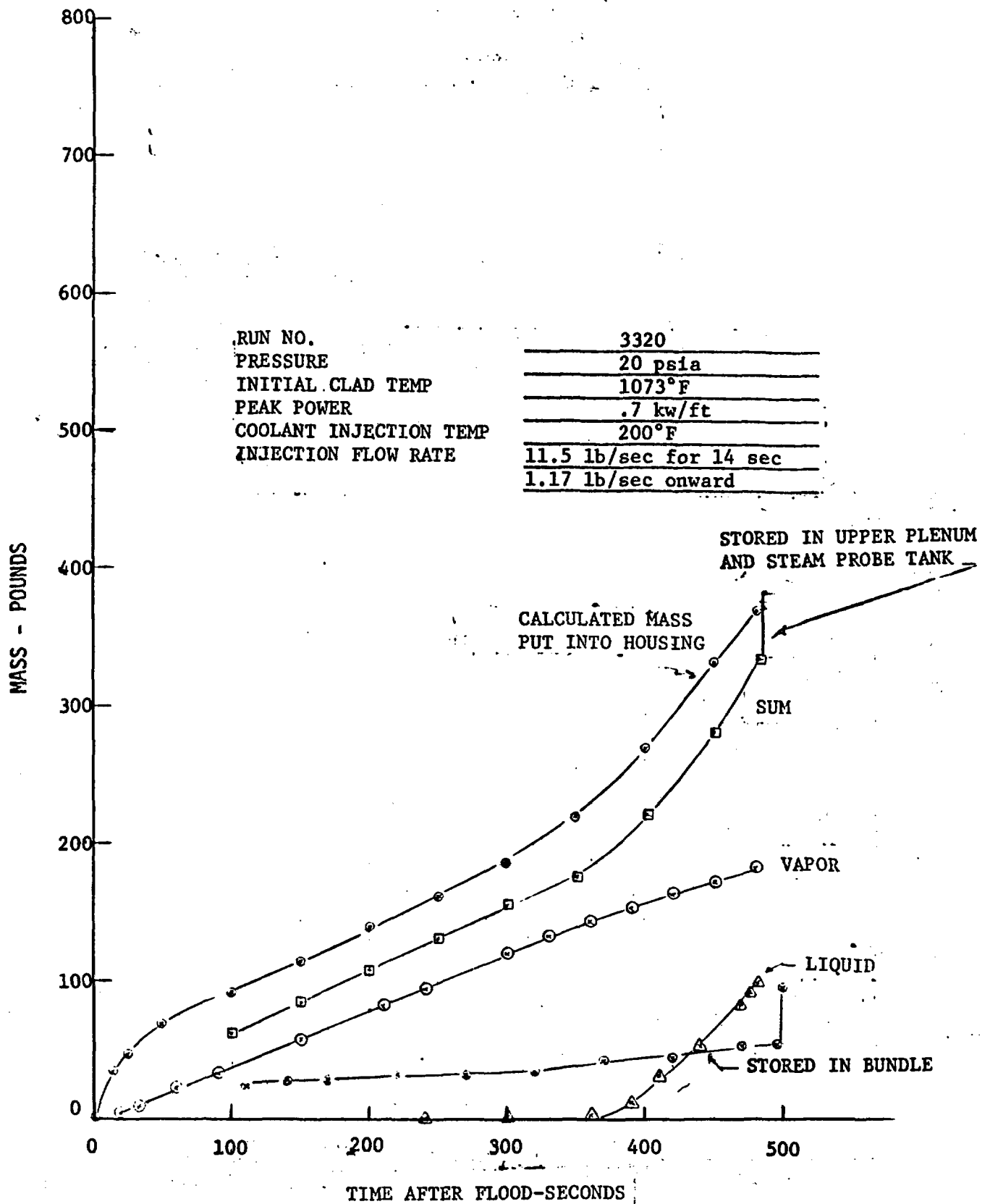
FLECHT-SET RUN SUMMARY SHEET (Cont)

RUN NO. 3320

DATE 10/27/72

C. HEATER THERMOCOUPLE DATA

Rod/Elev.	Initial Temp. (°F)	Max. Temp. (°F)	Turnaround Time (Sec)	Quench Time (Sec)
5F/2'	659	677	5	29
5F/4'	---			
5F/6'	---			
5F/8'	957	1319	159	438
5F/10'	709	1026	160	370
5G/2'	645	658	6	20
5G/4'	---			
5G/6'	1009	1451	118	309
5G/8'	995	1336	146	>451
5G/10'	695	1025	168	432
6G/2'	654	668	5	31
6G/4'	933	993	42	131
6G/6'	---			
6G/8'	---			
6G/10'	683	997	192	401
3H/2'	---			
3H/4'	917	1000	55	131
3H/6'	1073	1426	116	308
3H/8'	912	1267	149	>451
3H/10'	627	951	159	445
4G/4'	1031	1147	71	147
4G/6'	---			
4G/10'	676	980	249	400
4H/4'	936	1077	57	141
4H/6'	---			
4H/10'	669	968	158	317
7D/4'	931	1005	43	137
7D/6'	1060	1369	117	301
7D/10'	677	990	193	>451



FLOODING RATE-IN/SEC

3

2

1

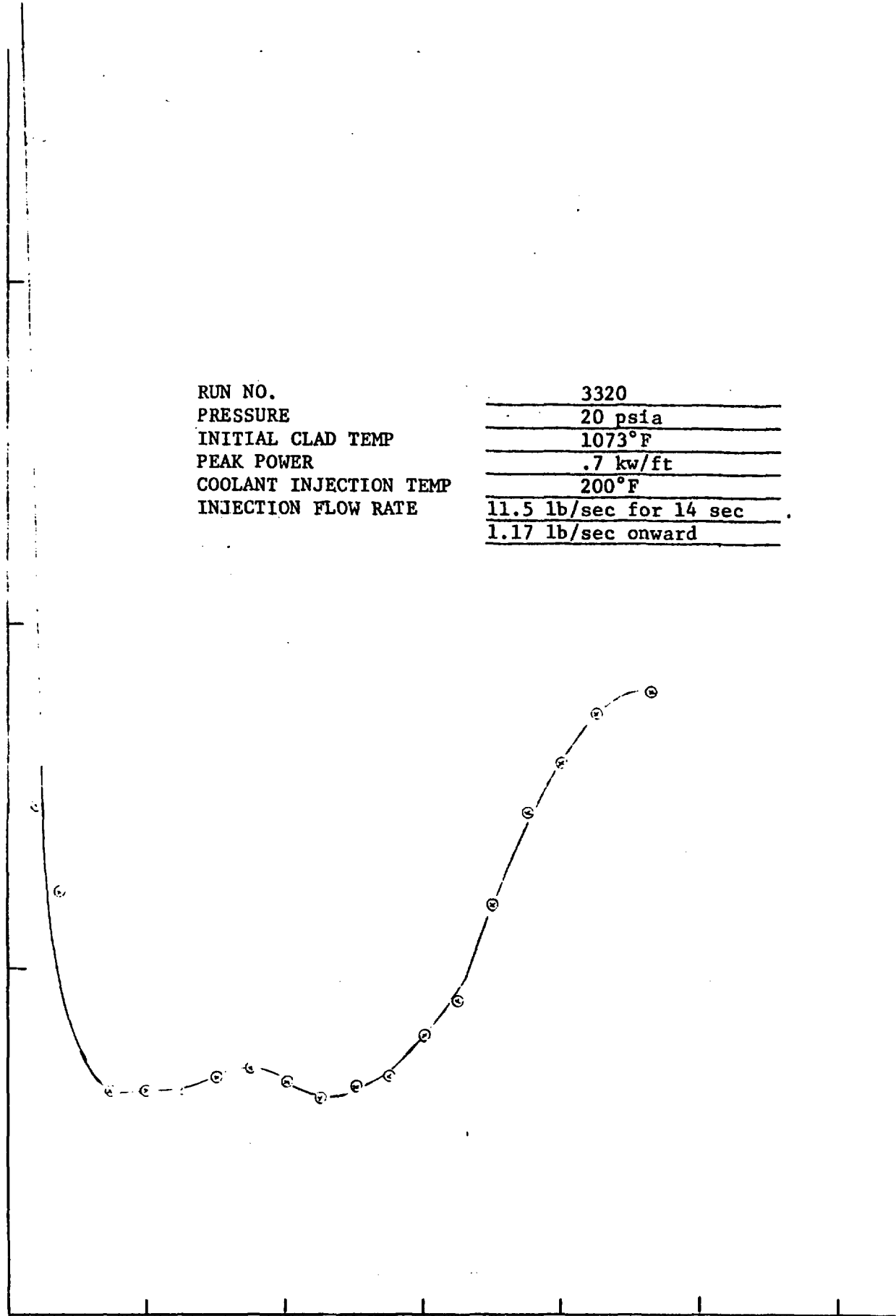
0

RUN NO.
PRESSURE
INITIAL CLAD TEMP
PEAK POWER
COOLANT INJECTION TEMP
INJECTION FLOW RATE

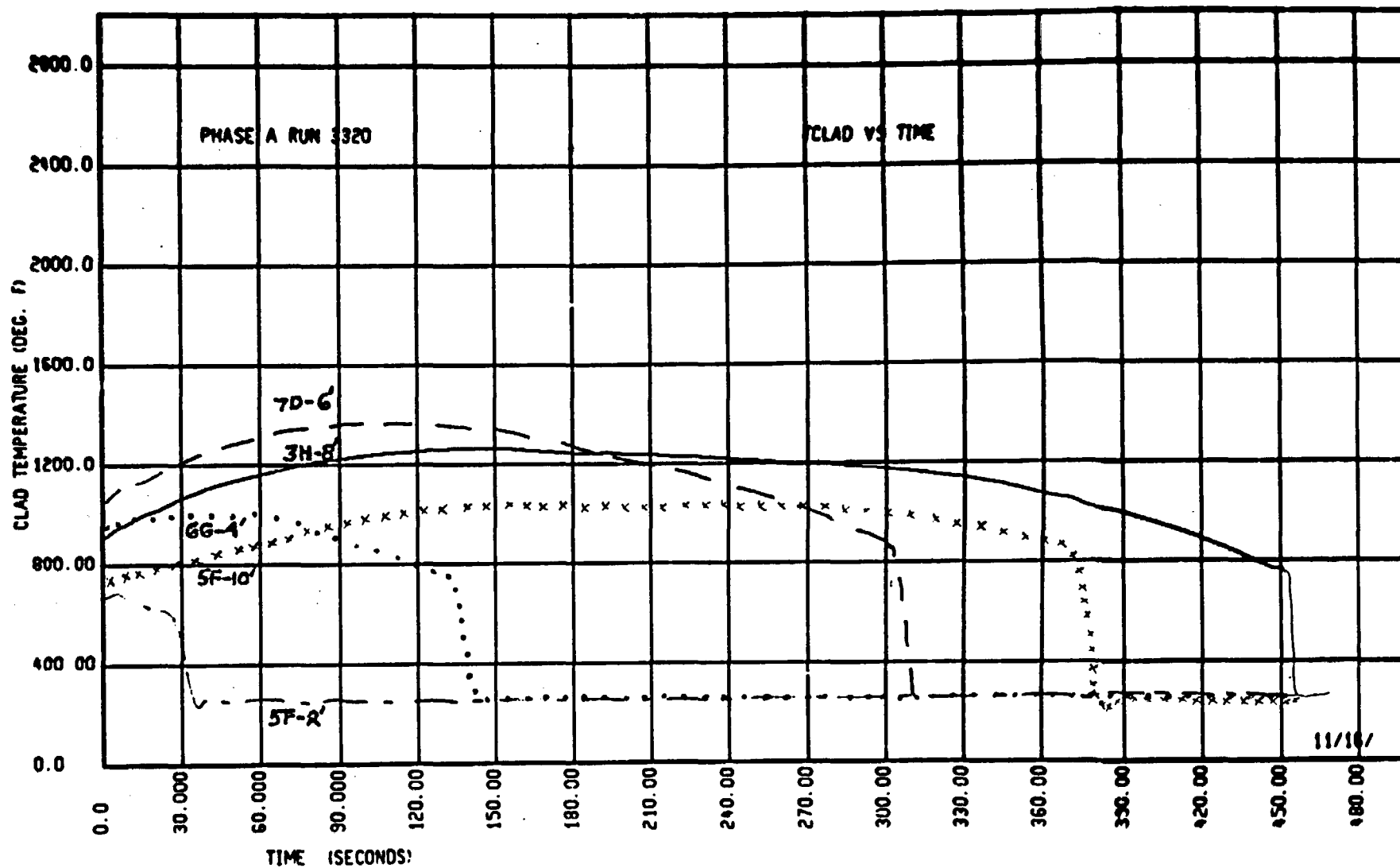
3320
20 psia
1073°F
.7 kw/ft
200°F
11.5 lb/sec for 14 sec
1.17 lb/sec onward

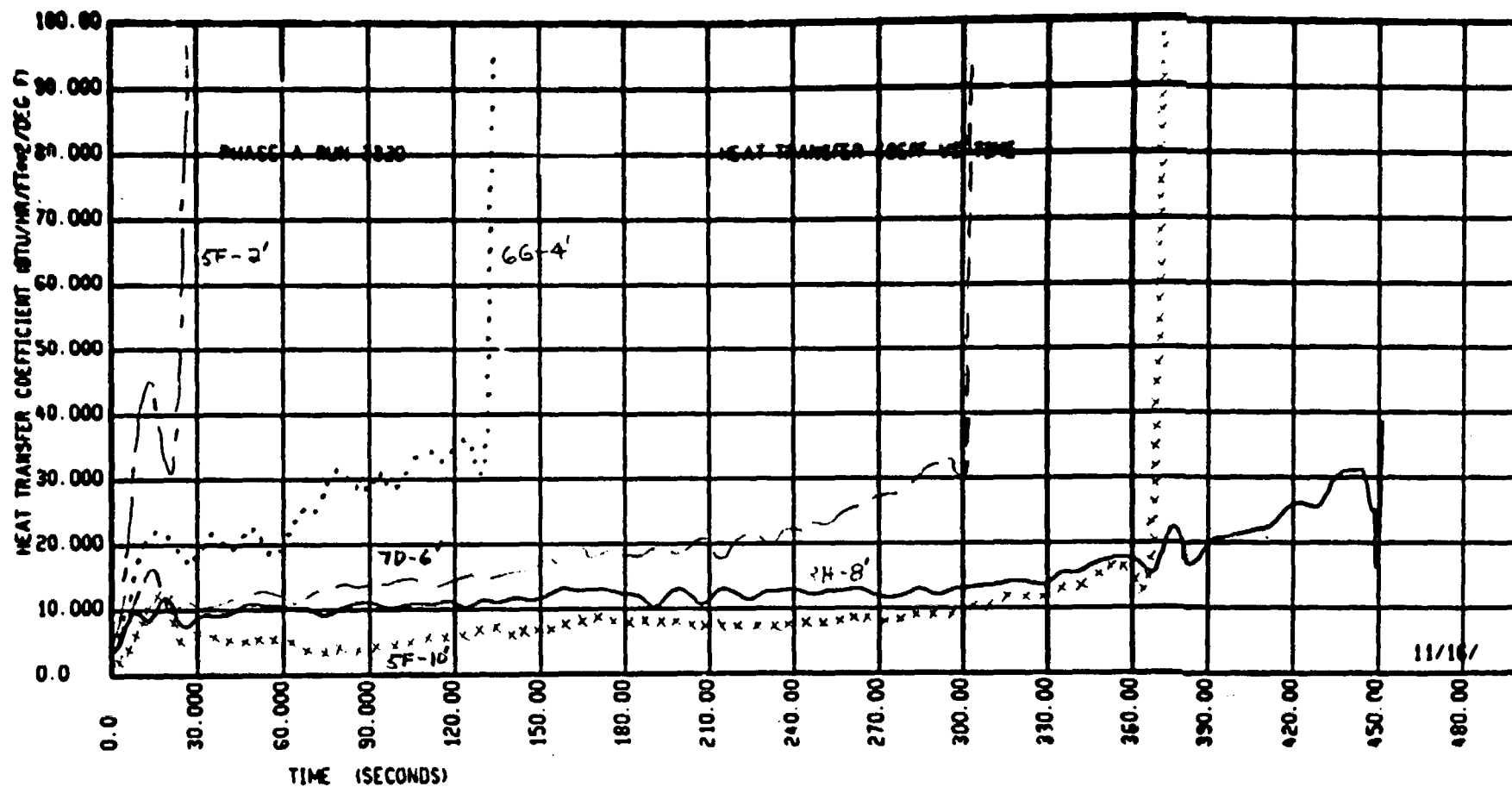
0 100 200 300 400 500 600

TIME AFTER FLOOD-SECONDS A-90

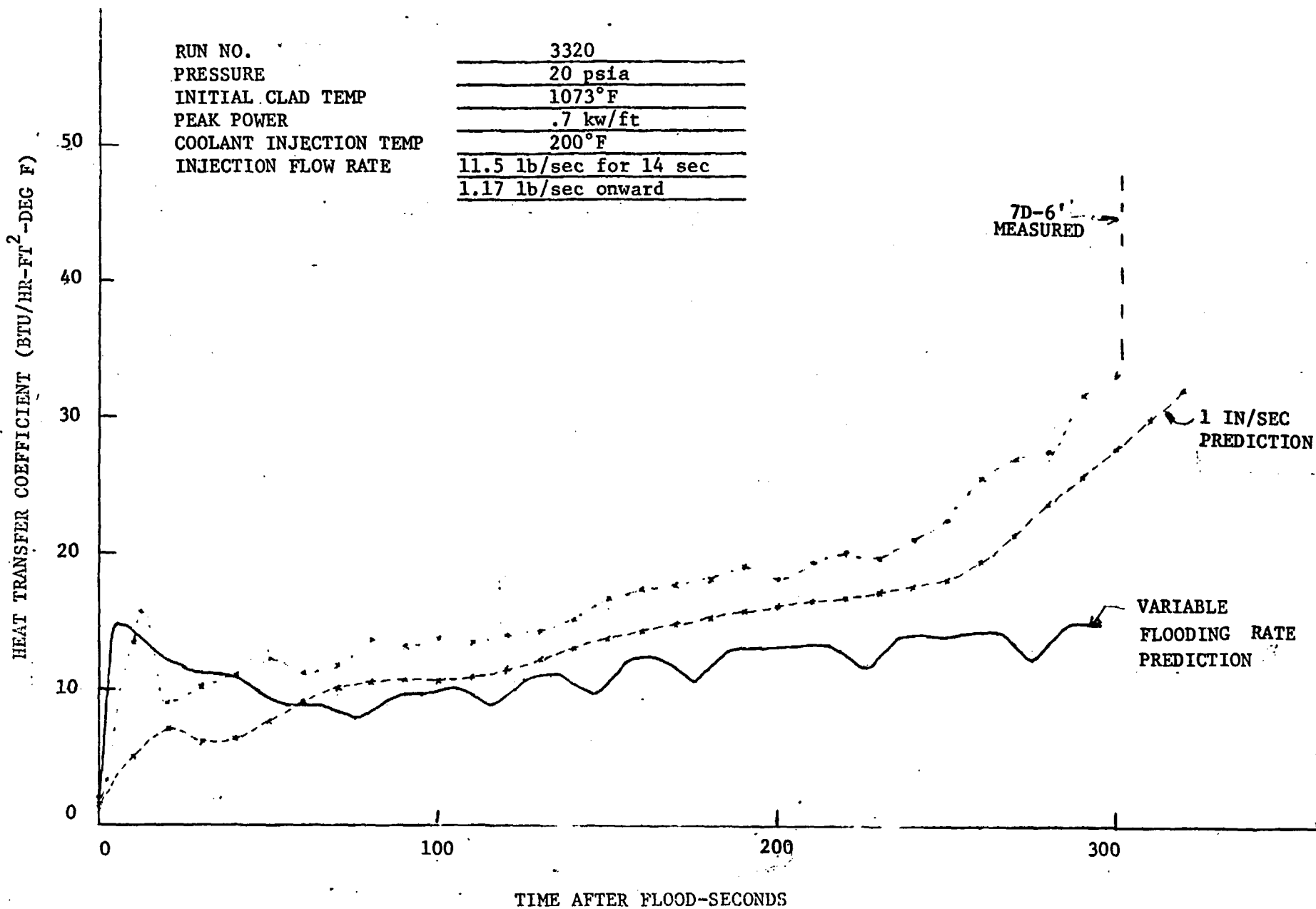


T6-V





86-A



1

2

3

4

FLECHT-SET RUN SUMMARY SHEET

RUN NO. 3421

DATE 10/31/72

A. RUN CONDITIONS

Containment Pressure	19.6	psia
Initial Clad Temperature	1098	°F
Peak Power	1.0	kw/ft
Coolant Supply Temperature	161	°F
Injection Rate	11.78 lb/sec first 14 sec, 1.2 lb/sec after 14 sec	
Loop Resistance Coefficient	$(\Delta p_{loop}/1/2 \rho V_{hotleg}^2)$ 27.3	

B. INITIAL HOUSING TEMPERATURES

Elevation (ft)	Initial Temperature (°F)
0	232
2	551
4	704
6	848
8	799
10	556
12	319

FLECHT-SET RUN SUMMARY SHEET (Cont)

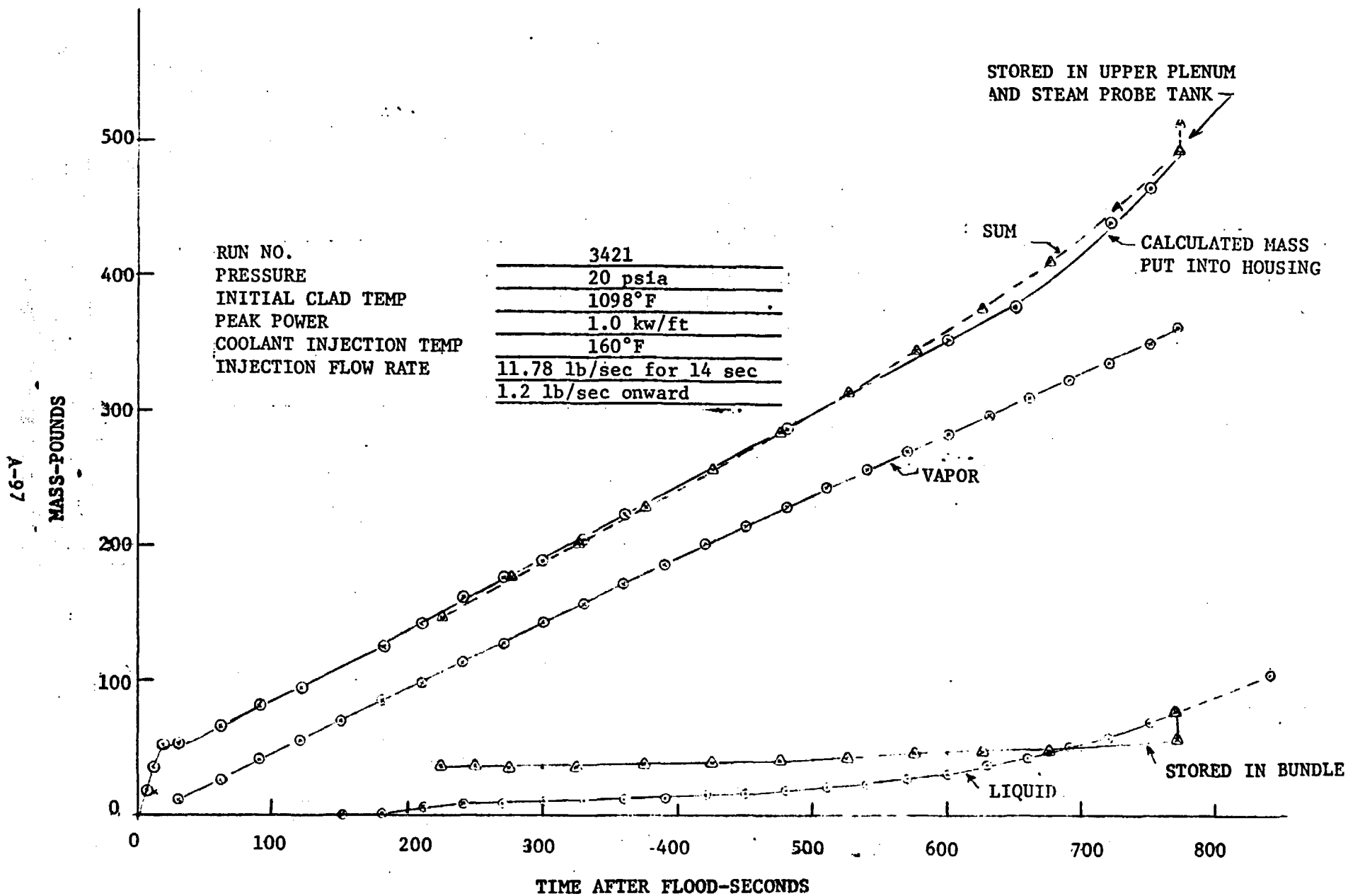
RUN NO. 3421

DATE 10/31/72

C. HEATER THERMOCOUPLE DATA

Rod/Elev.	Initial Temp. (°F)	Max. Temp. (°F)	Turnaround Time (Sec)	Quench Time (Sec)
5F/2'	656	677	5	16
5F/4'	---			
5F/6'	---			
5F/8'	1025	1913	339	*
5F/10'	800	1624	390	*
5G/2'	643	666	6	12
5G/4'	---			
5G/6'	1115	1807	123	631
5G/8'	1051	1857	330	*
5G/10'	758	1581	402	*
6G/2'	653	680	6	12
6G/4'	932	1217	101	284
6G/6'	---			
6G/8'	---			
6G/10'	767	1562	408	*
3H/2'	---			
3H/4'	914	1263	138	283
3H/6'	1098	1834	149	627
3H/8'	984	1739	309	*
3H/10'	716	1397	360	*
4G/4'	997	1467	142	311
4G/6'	---			
4G/10'	763	1538	383	*
4H/4'	944	1386	138	300
4H/6'	---			
4H/10'	754	1481	390	*
7D/4'	933	1276	121	280
7D/6'	1092	1747	163	603
7D/10'				

*Water supply depleted before quench (775 sec.)



FLOODING RATE-IN/SEC

3.0

2.0

1.0

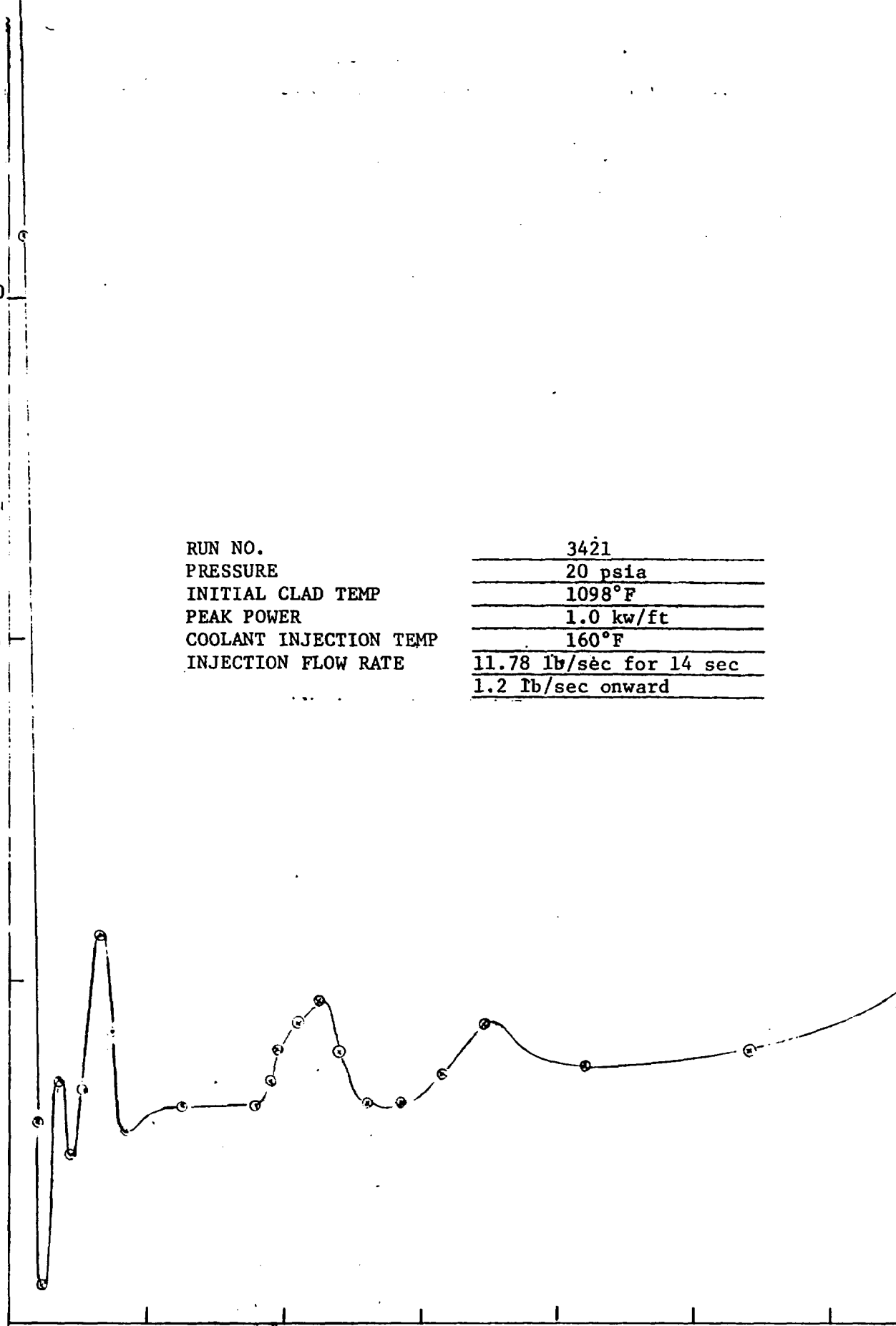
0

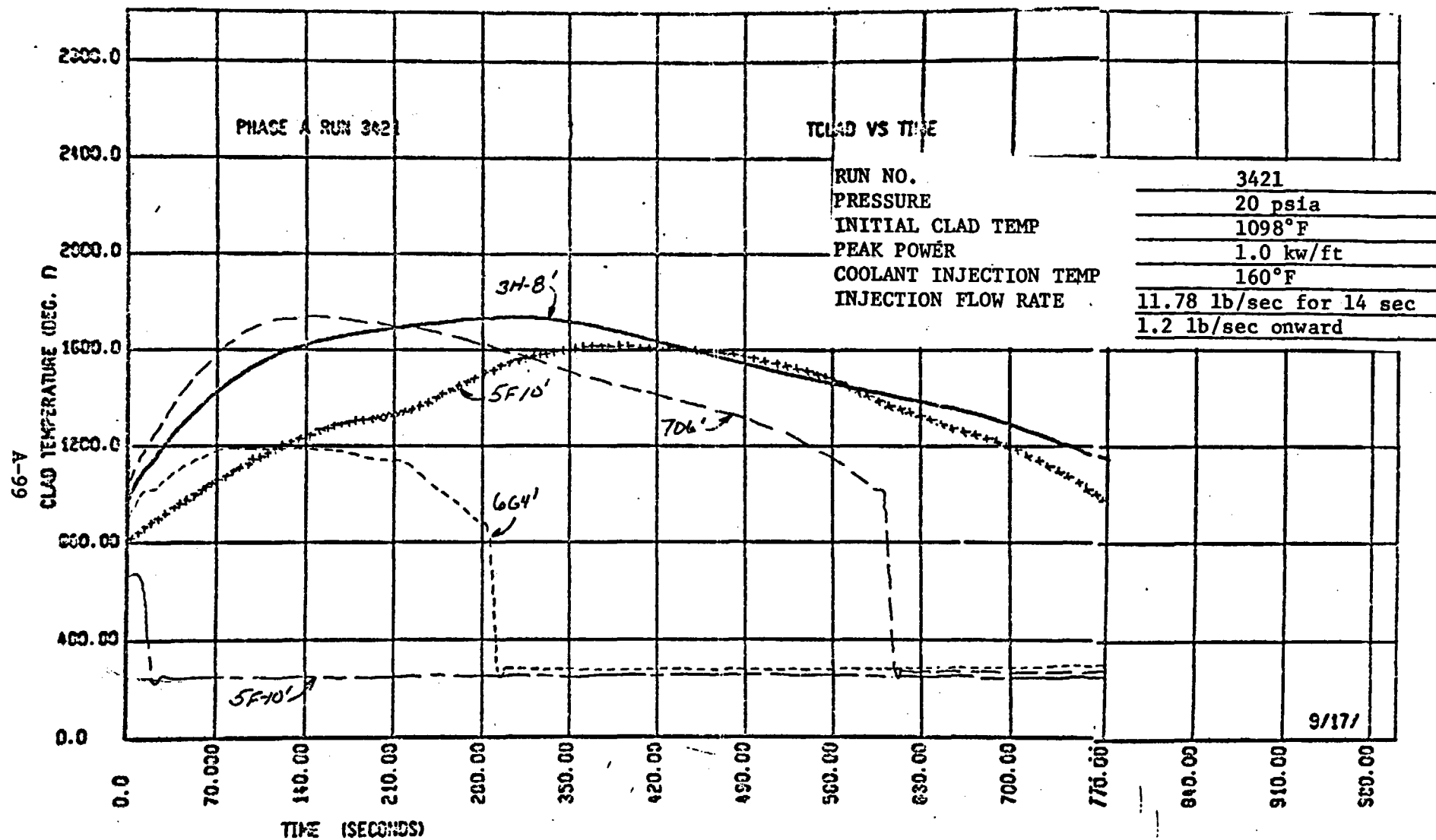
RUN NO.	3421
PRESSURE	20 psia
INITIAL CLAD TEMP	1098°F
PEAK POWER	1.0 kw/ft
COOLANT INJECTION TEMP	160°F
INJECTION FLOW RATE	11.78 lb/sec for 14 sec
	1.2 lb/sec onward

0 100 200 300 400 500 600

TIME AFTER FLOOD-SECONDS

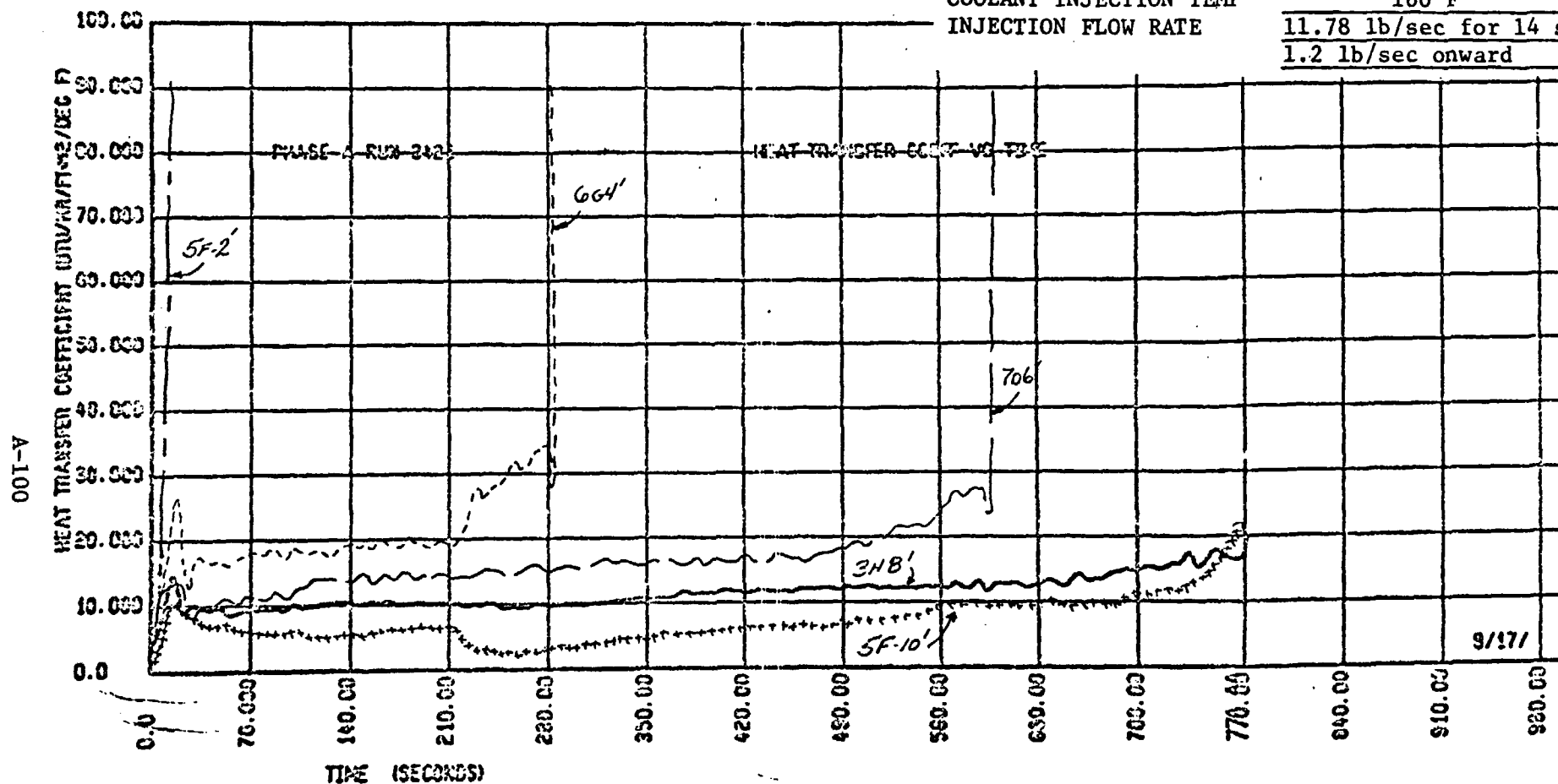
A-98



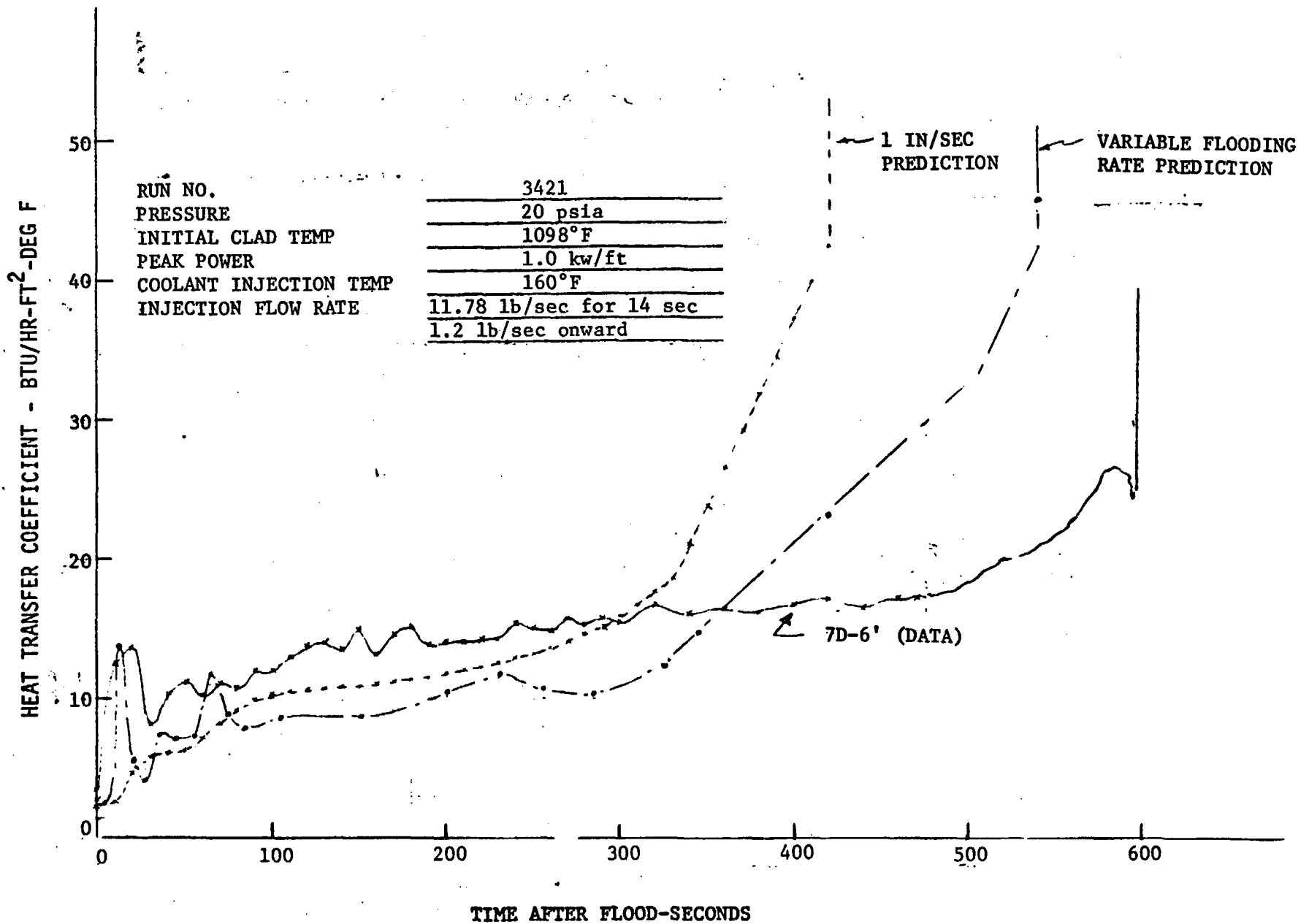


RUN NO.
 PRESSURE
 INITIAL CLAD TEMP
 PEAK POWER
 COOLANT INJECTION TEMP
 INJECTION FLOW RATE

3421
 20 psia
 1098°F
 1.0 kw/ft
 160°F
 11.78 lb/sec for 14 sec
 1.2 lb/sec onward



A-101



1

2

3

4

FLECHT-SET RUN SUMMARY SHEET

RUN NO. 3928

DATE 2/1/73

A. RUN CONDITIONS

Containment Pressure	61.9	psia
Initial Clad Temperature	1102	°F
Peak Power	0.7	kw/ft
Coolant Supply Temperature	201	°F
Injection Rate	12.02 lb/sec first 14 sec, 1.37 lb/sec after 14 sec	
Loop Resistance Coefficient ($\Delta p_{loop}/1/2 \rho V^2_{hotleg}$)	32.0	

B. INITIAL HOUSING TEMPERATURES

Elevation (ft)	Initial Temperature (°F)
0	291
2	392
4	496
6	528
8	470
10	391
12	296

FLECHT-SET RUN SUMMARY SHEET (Cont)

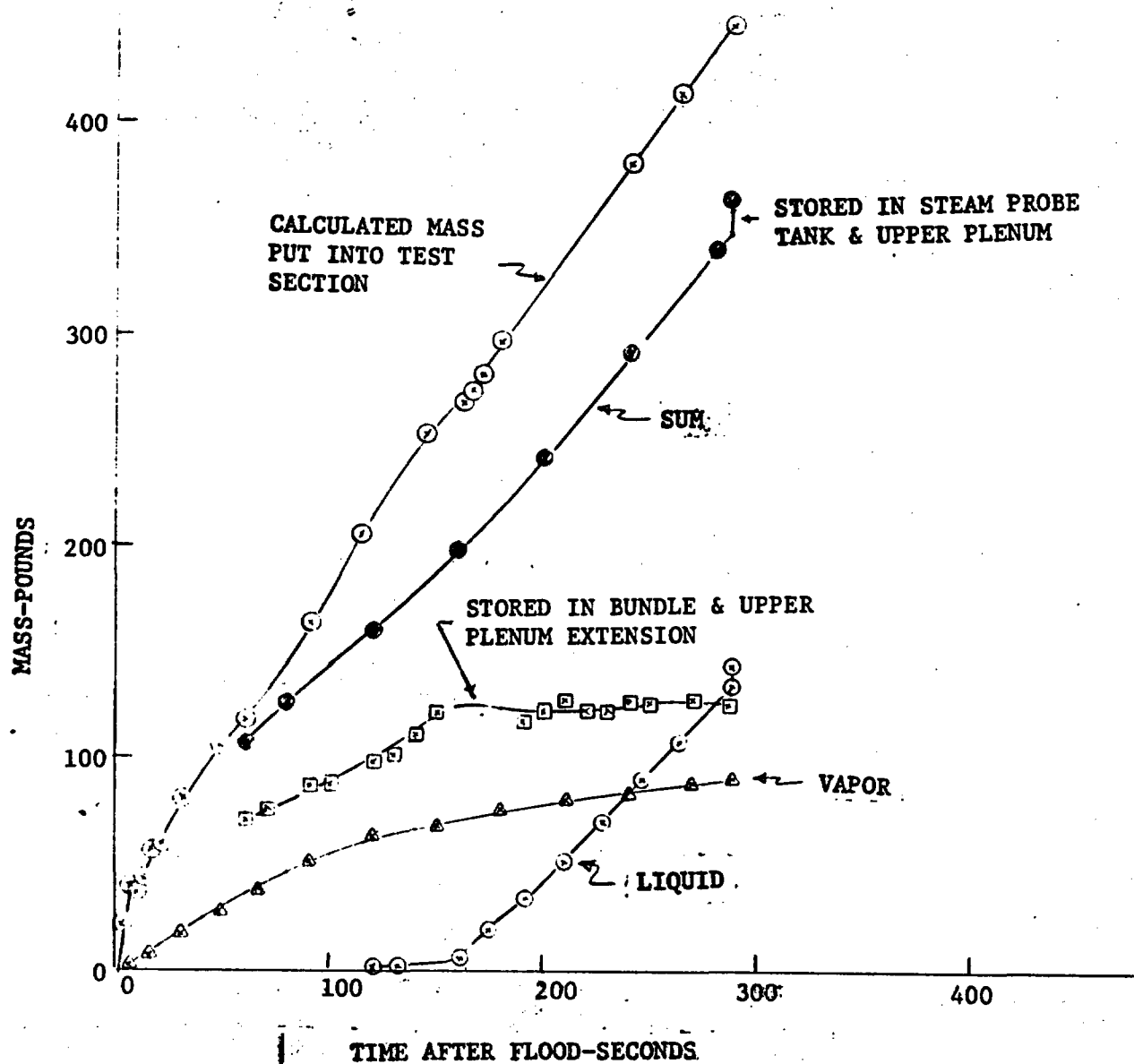
RUN NO. 3928

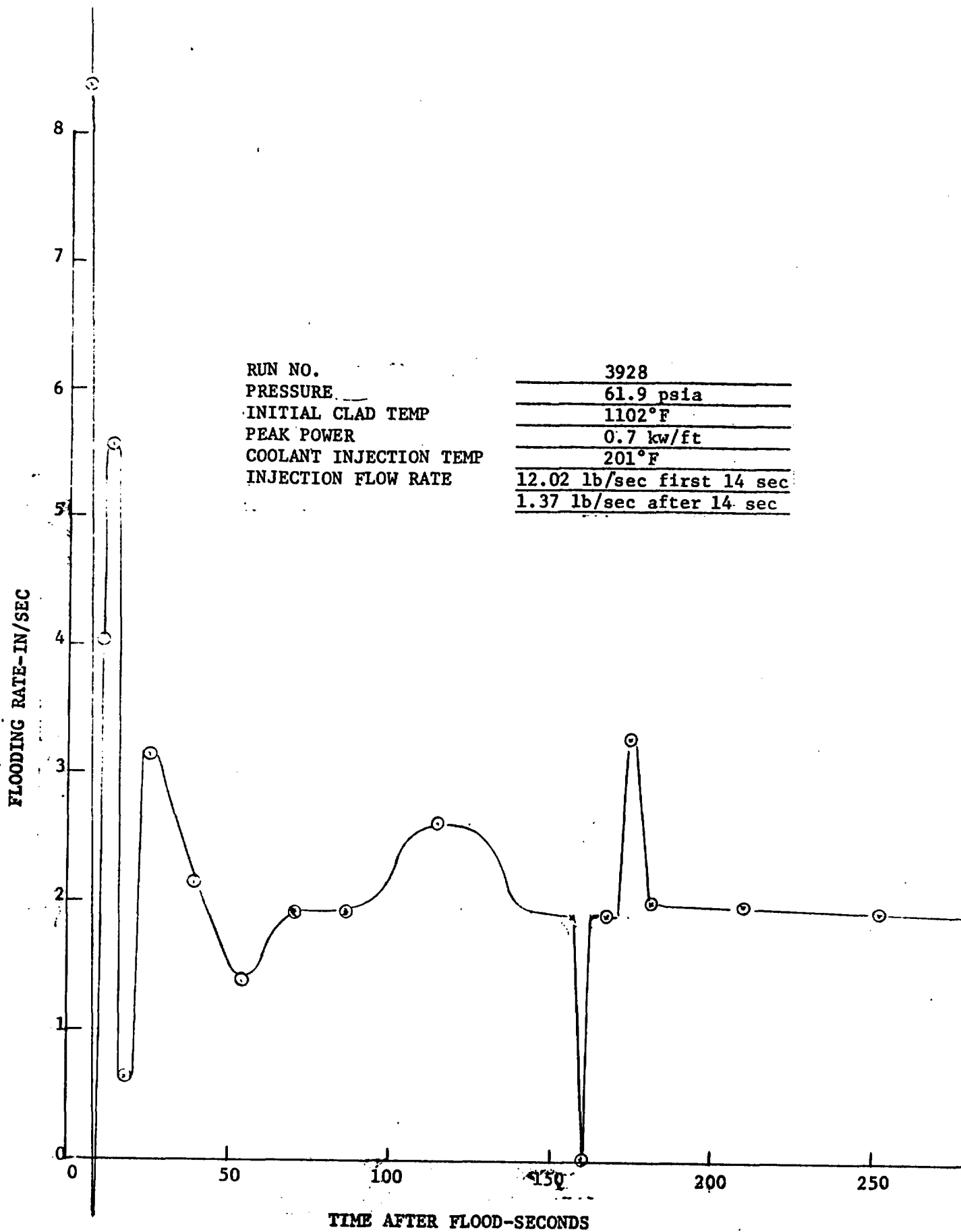
DATE 2/1/73

C. HEATER THERMOCOUPLE DATA

Rod/Elev.	Initial Temp. (°F)	Max. Temp. (°F)	Turnaround Time (Sec)	Quench Time (Sec)
5F/2'	656	664	2	7
5F/4'				
5F/6'				
5F/8'				
5F/10'	635	697	25	43
5G/2'	643	658	3	8
5G/4'				
5G/6'	1102	1167	20	96
5G/8'	936	1020	24	115
5G/10'	627	681	23	70
6G/2'	650	668	3	8
6G/4'	939	969	6	37
6G/6'				
6G/8'				
6G/10'	683	740	16	23
3H/2'				
3H/4'				
3H/6'				
3H/8'	918	1025	57	106
3H/10'	594	672	28	56
4G/4'	1061	1087	4	41
4G/6'				
4G/10'	616	682	25	32
4H/4'	955	994	8	41
4H/6'				
4H/10'	680	740	11	29
7D/4'	943	977	6	46
7D/6'	1024	1099	20	90
7D/10'				

RUN NO.	3928
PRESSURE	61.9 psia
INITIAL CLAD TEMP	1102°F
PEAK POWER	0.7 kw/ft
COOLANT INJECTION TEMP	201°F
INJECTION FLOW RATE	12.02 lb/sec first 14 sec
	1.37 lb/sec after 14 sec

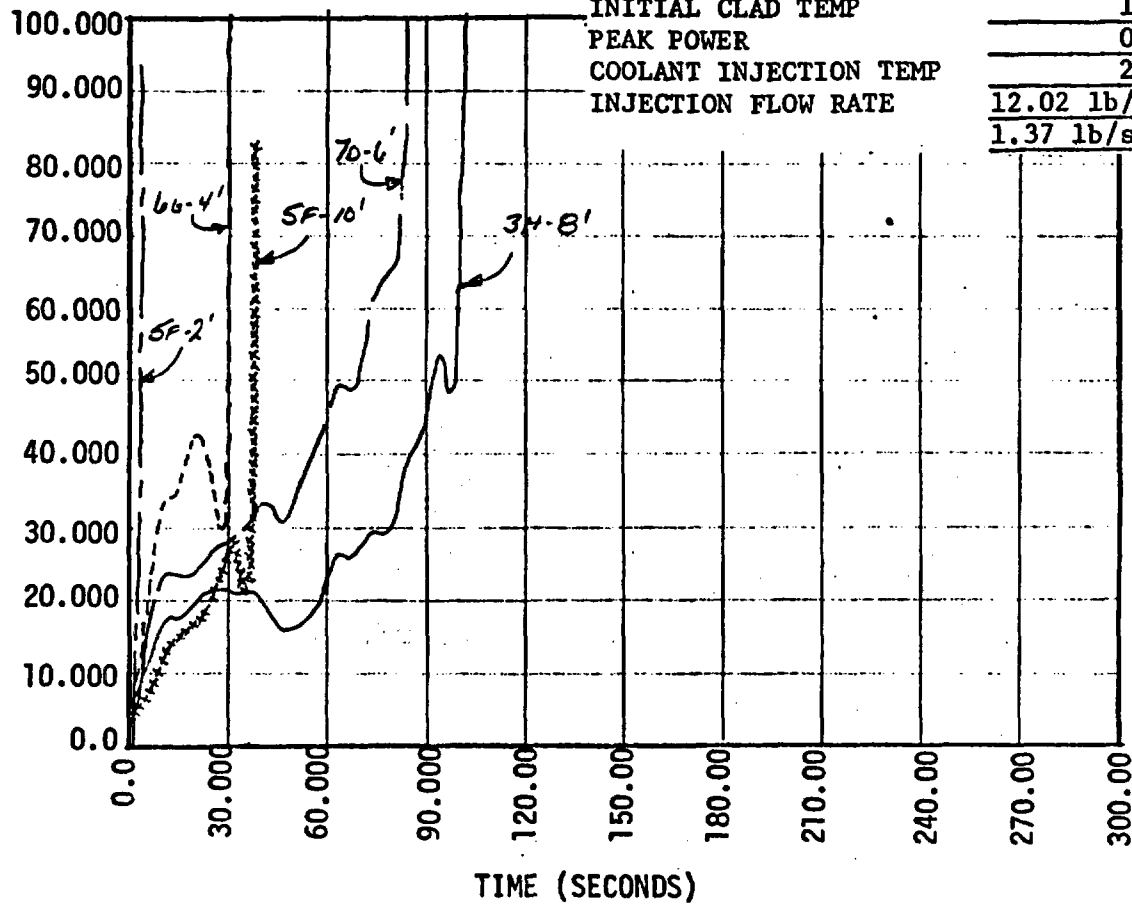




RUN NO.
PRESSURE
INITIAL CLAD TEMP
PEAK POWER
COOLANT INJECTION TEMP
INJECTION FLOW RATE

3928
61.9 psia
1102°F
0.7 kw/ft
201°F
12.02 lb/sec first 14 sec
1.37 lb/sec after 14 sec

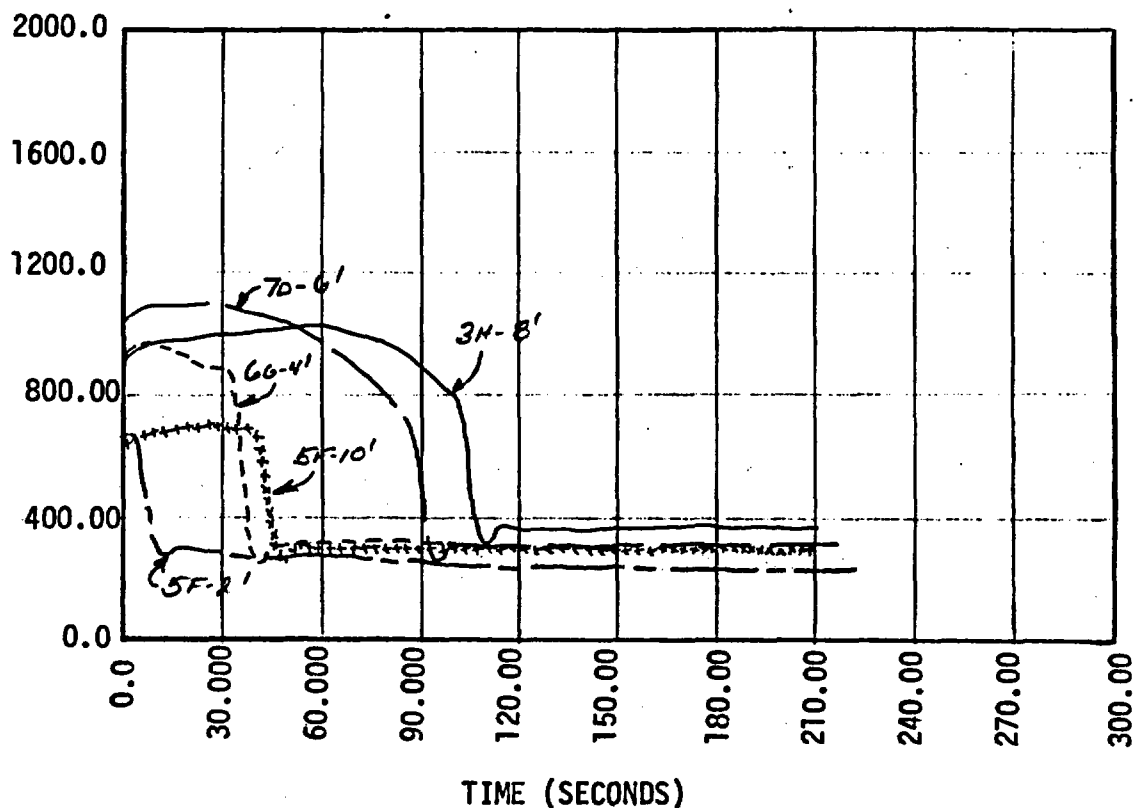
HEAT TRANSFER COEFFICIENT (BTU/HR/FT**2/DEG F)

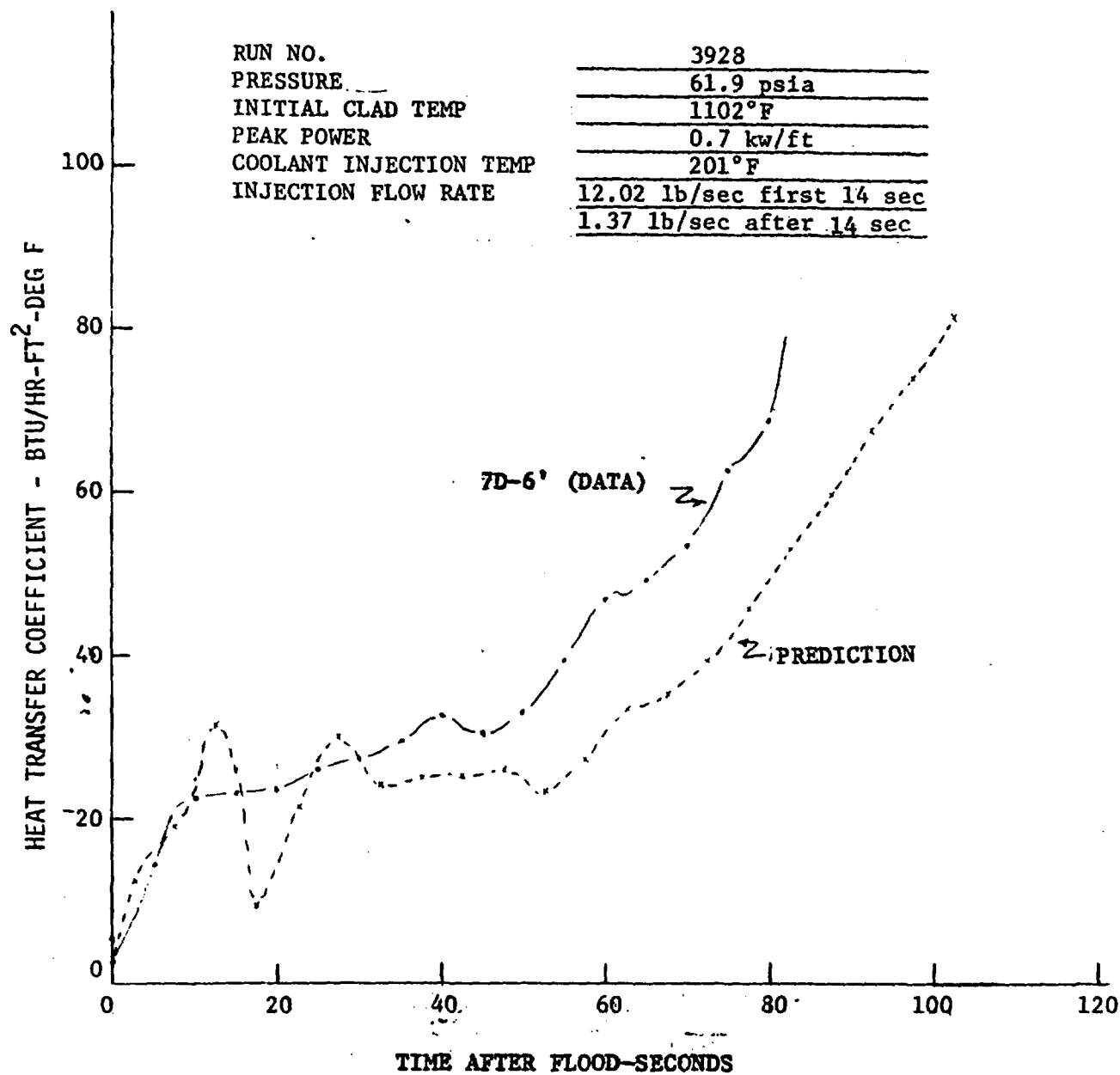


RUN NO. 3928
 PRESSURE 61.9 psia
 INITIAL CLAD TEMP 1102°F
 PEAK POWER 0.7 kw/ft
 COOLANT INJECTION TEMP 201°F
 INJECTION FLOW RATE 12.02 lb/sec first 14 sec.
 1.37 lb/sec after 14 sec

3928
 61.9 psia
 1102°F
 0.7 kw/ft
 201°F
 12.02 lb/sec first 14 sec.
 1.37 lb/sec after 14 sec

CLAD TEMPERATURE (DEG. F)





FLECHT-SET RUN SUMMARY SHEET

RUN NO. 4024

DATE 2/4/73

A. RUN CONDITIONS

Containment Pressure	59	psia
Initial Clad Temperature	1402	°F
Peak Power	0.7	kw/ft
Coolant Supply Temperature	155	°F
Injection Rate	10.99 lb/sec first 14 sec, 1.4 lb/sec after 14 sec	
Loop Resistance Coefficient	$(\Delta\rho_{loop}/1/2 \rho V_{hotleg}^2)$	28.8

B. INITIAL HOUSING TEMPERATURES

Elevation (ft)	Initial Temperature (°F)
0	291
2	491
4	582
6	600
8	581
10	462
12	324

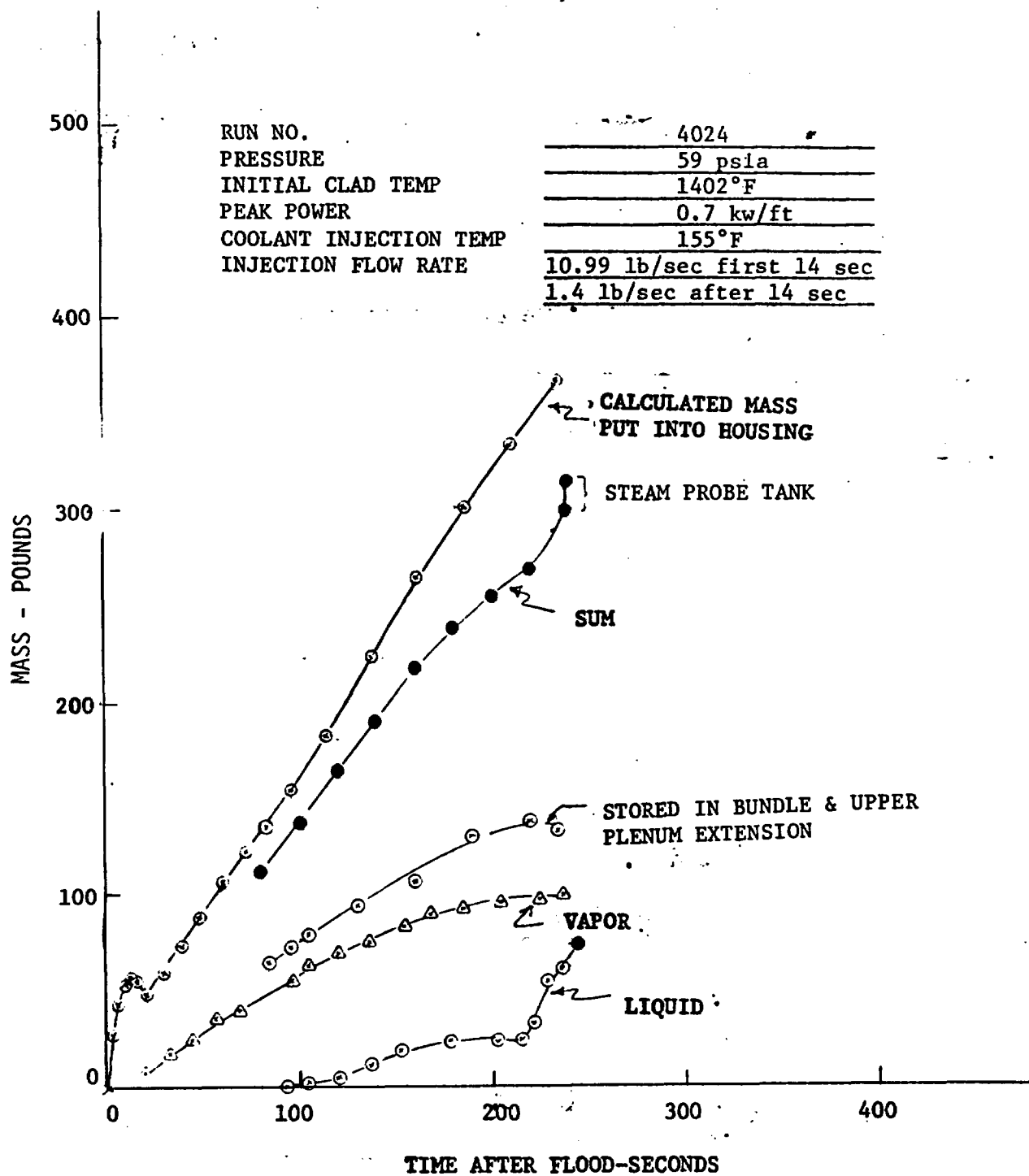
FLECHT-SET RUN SUMMARY SHEET (Cont)

RUN NO. 4024

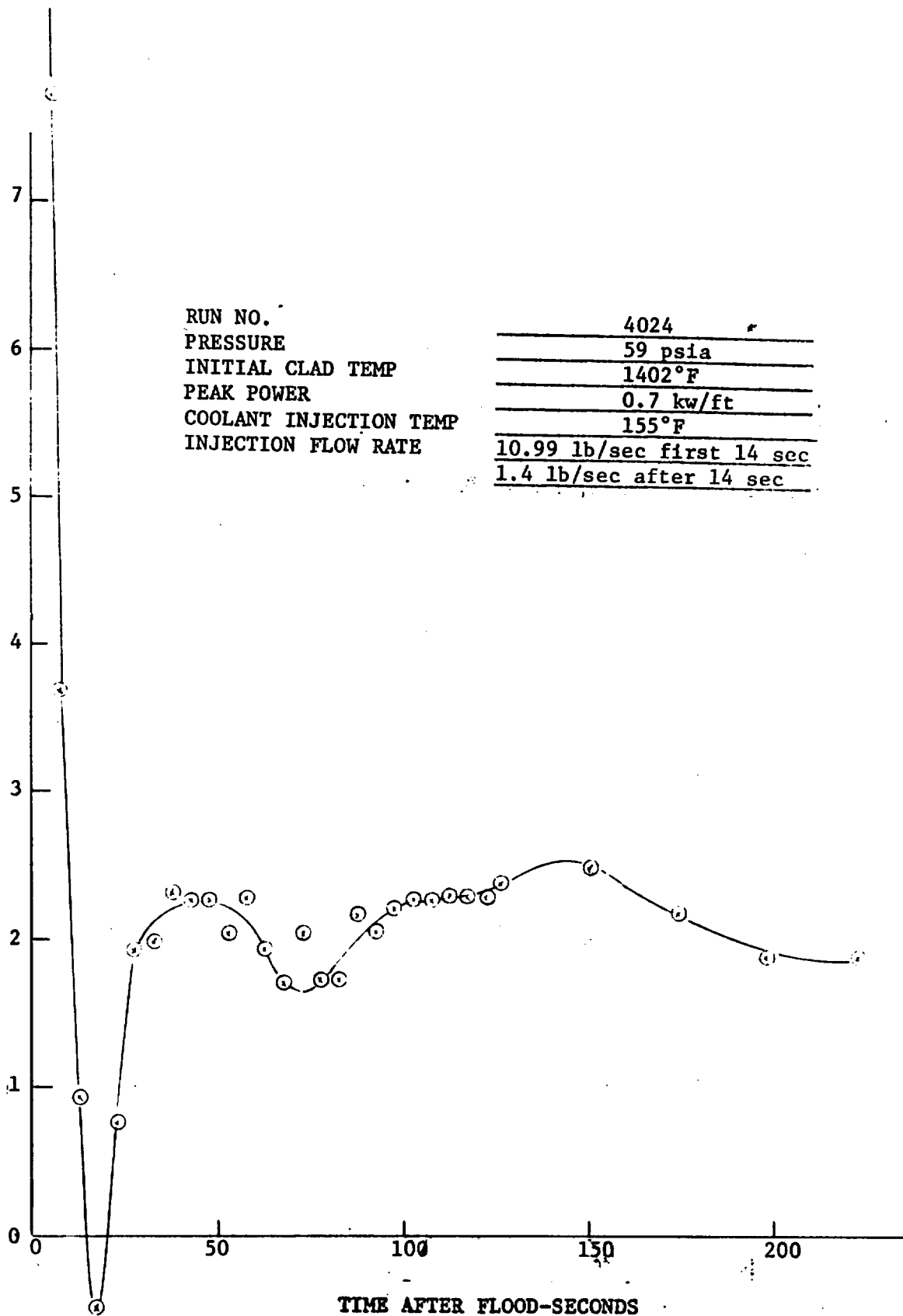
DATE 2/4/73

C. HEATER THERMOCOUPLE DATA

Rod/Elev.	Initial Temp. (°F)	Max. Temp. (°F)	Turnaround Time (Sec)	Quench Time (Sec)
5F/2'	876	882	3	12
5F/4'				
5F/6'				
5F/8'				
5F/10'	734	803	40	48
5G/2'	865	870	3	17
5G/4'				
5G/6'	1420	1433	7	133
5G/8'	1148	1180	27	153
5G/10'	725	785	50	71
6G/2'	878	883	3	13
6G/4'	1268	1288	5	74
6G/6'				
6G/8'				
6G/10'	784	834	46	65
3H/2'				
3H/4'	1250	1266	4	84
3H/6'				
3H/8'	1088	1155	43	148
3H/10'	683	777	56	94
4G/4'	1383	1401	4	79
4G/6'				
4G/10'	716	783	53	63
4H/4'	1275	1301	5	82
4H/6'				
4H/10'	785	838	47	73
7D/4'	1277	1301	5	85
7D/6'	1335	1371	8	125
7D/10'				

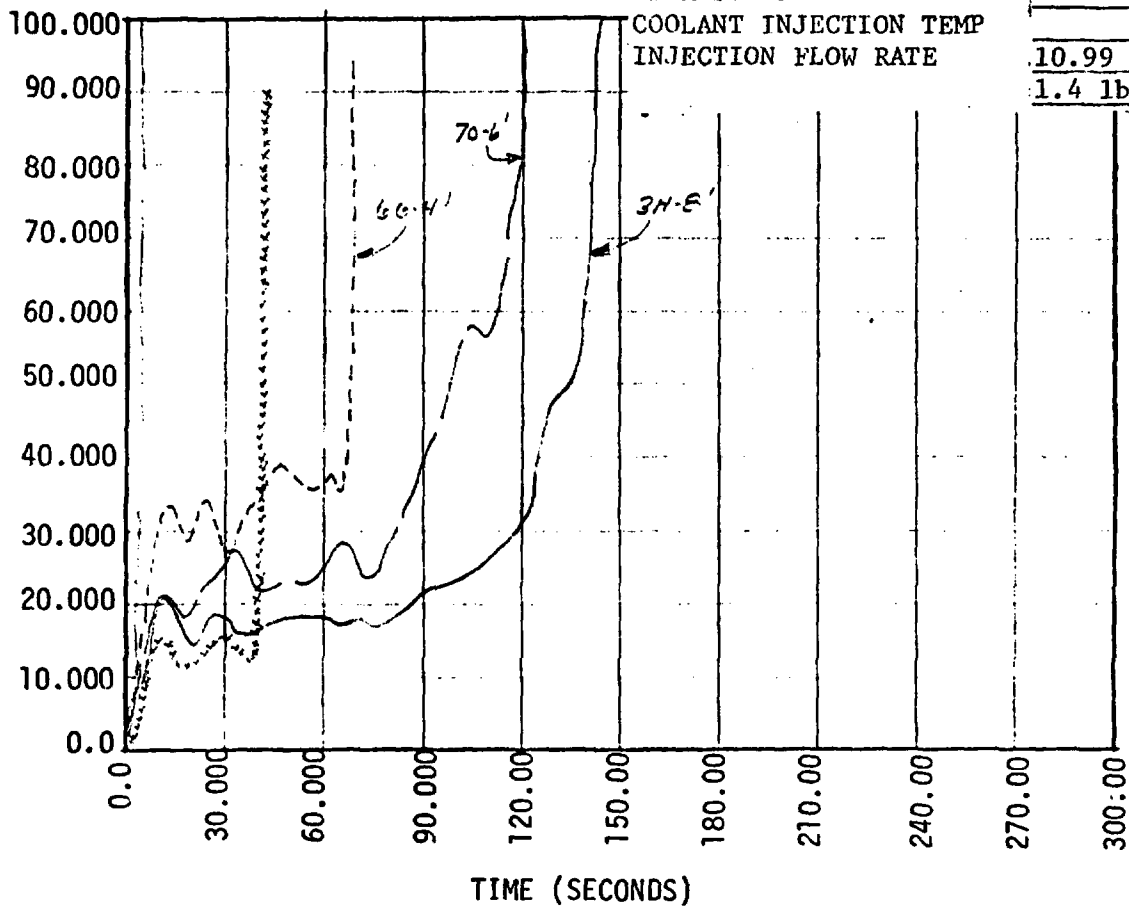


FLOODING RATE-IN/SEC



RUN NO.	4024
PRESSURE	59 psia
INITIAL CLAD TEMP	1402°F
PEAK POWER	0.7 kw/ft
COOLANT INJECTION TEMP	155°F
INJECTION FLOW RATE	10.99 lb/sec first 14 sec
	1.4 lb/sec after 14 sec

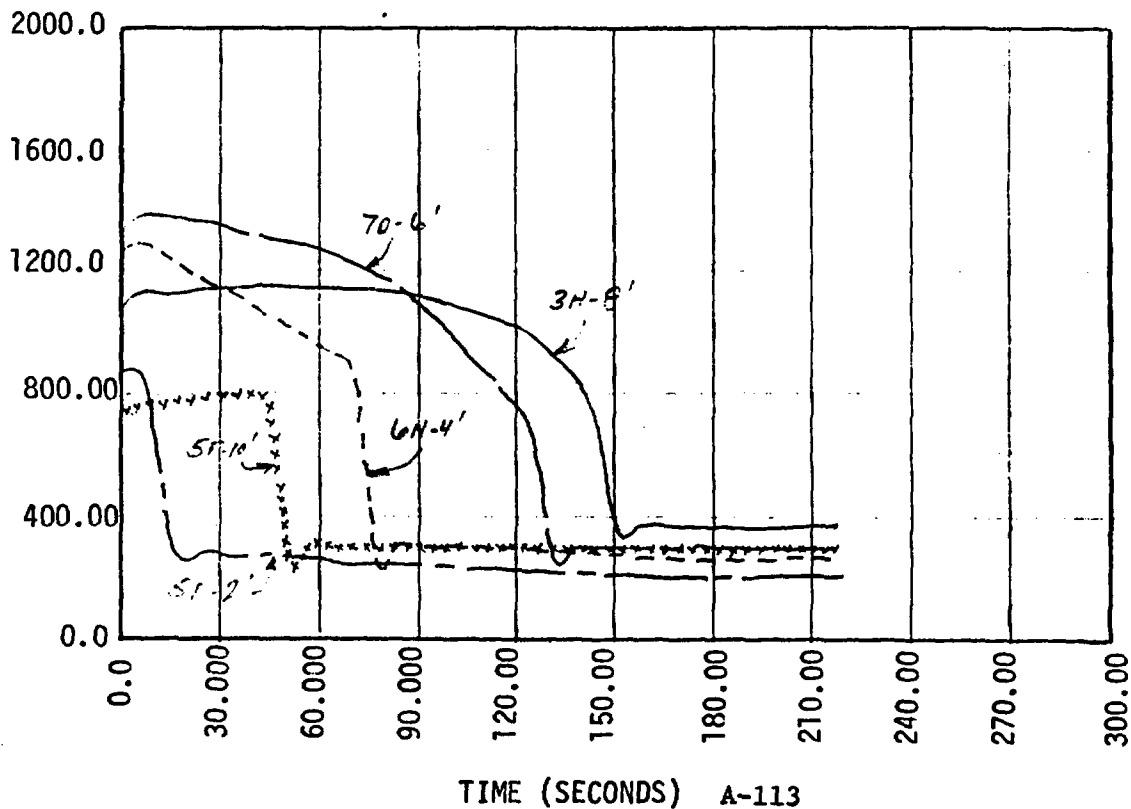
HEAT TRANSFER COEFFICIENT (BTU/HR/FT**2/DEG F)



RUN NO.
PRESSURE
INITIAL CLAD TEMP
PEAK POWER
COOLANT INJECTION TEMP
INJECTION FLOW RATE

4024
59 psia
1402°F
0.7 kw/ft
155°F
10.99 lb/sec first 14 sec
1.4 lb/sec after 14 sec

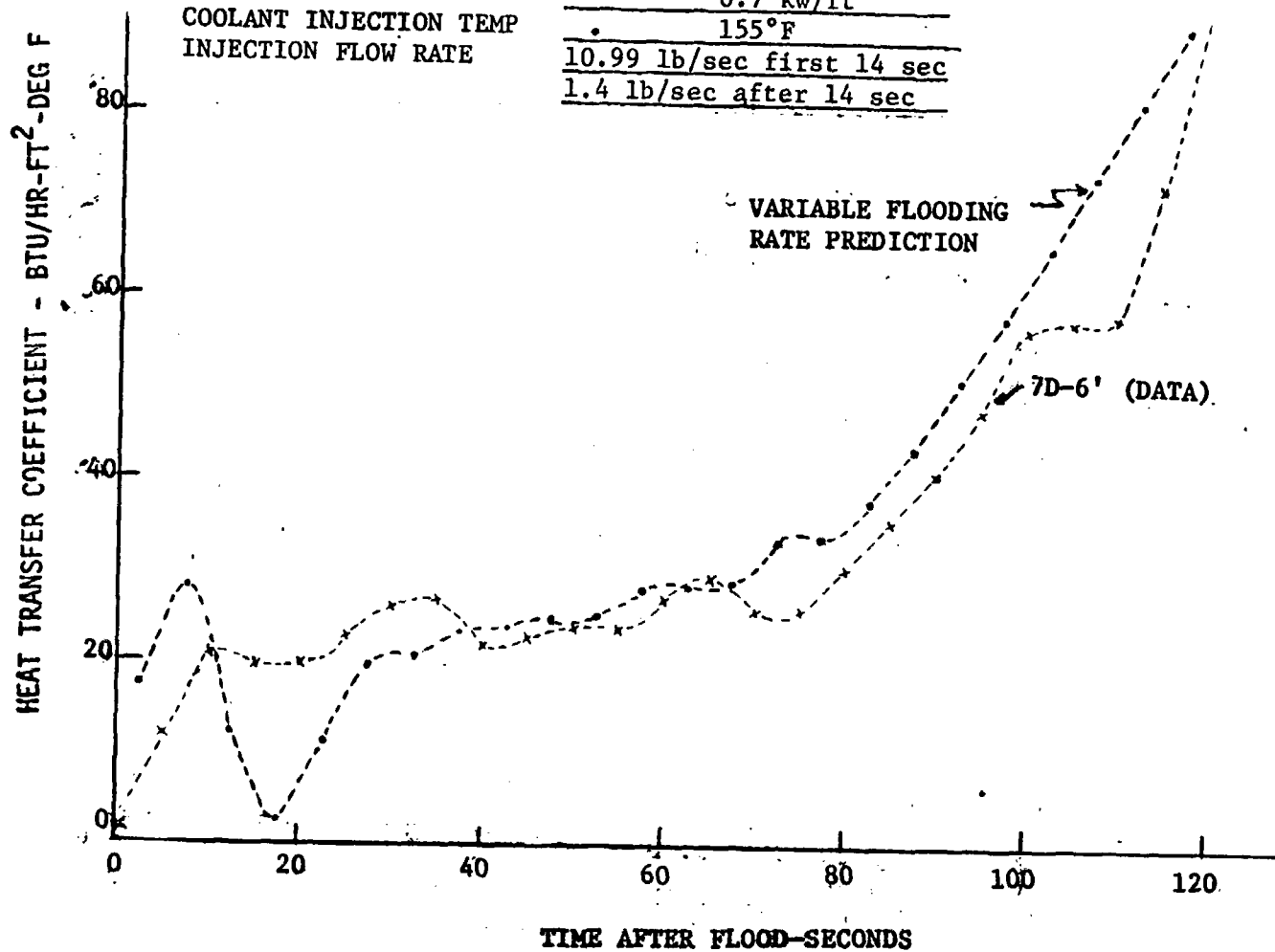
CLAD TEMPERATURE (DEG. F)



A-114

RUN NO.
PRESSURE
INITIAL CLAD TEMP
PEAK POWER
COOLANT INJECTION TEMP
INJECTION FLOW RATE

4024
59 psia
1402°F
0.7 kw/ft
155°F
10.99 lb/sec first 14 sec
1.4 lb/sec after 14 sec



FLECHT-SET RUN SUMMARY SHEET

RUN NO. 4311

DATE 2/19/73

A. RUN CONDITIONS

Containment Pressure	59.5	psia
Initial Clad Temperature	1105	°F
Peak Power	.646*	kw/ft
Coolant Supply Temperature	154	°F
Injection Rate	9.70 lb/sec first 14 sec, 1.20 lb/sec after 14 sec	
Loop Resistance Coefficient ($\Delta p_{loop}/1/2 \rho V_{hotleg}^2$)	32.1	

B. INITIAL HOUSING TEMPERATURES

Elevation (ft)	Initial Temperature (°F)
0	238
2	304
4	317
6	307
8	296
10	302
12	259

*All 90 heater rods had the same power.

FLECHT-SET RUN SUMMARY SHEET (Cont)

RUN NO. 4311

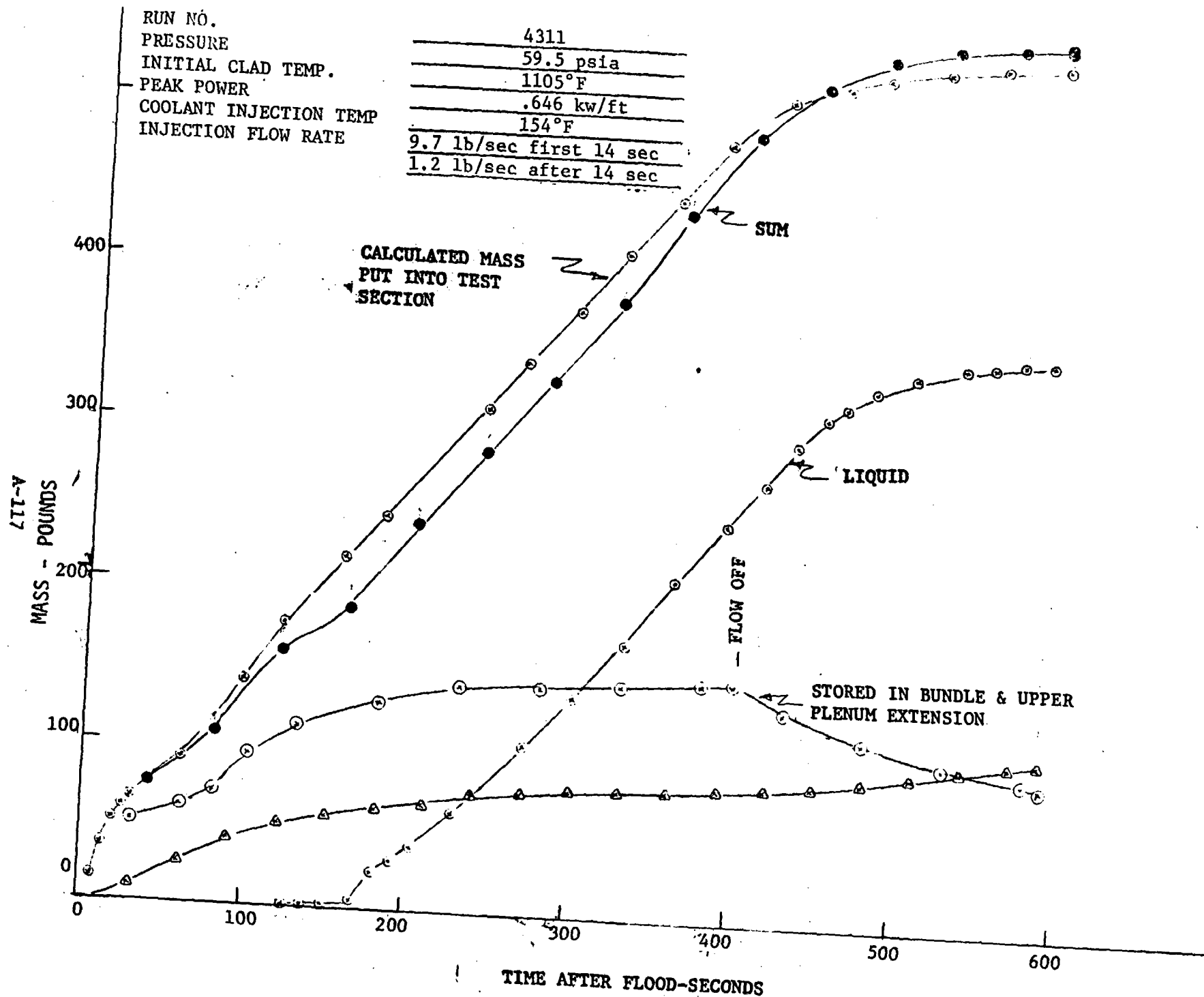
DATE 2/19/73

C. HEATER THERMOCOUPLE DATA

Rod/Elev.	Initial Temp. (°F)	Max. Temp. (°F)	Turnaround Time (Sec)	Quench Time (Sec)
5F/2'	635	636	1	6
5F/4'				
5F/6'				
5F/8'				
5F/10'	636	680	12	31
5G/2'	623	627	1	6
5G/4'				
5G/6'	1105	1163	9	83
5G/8'	960	1018	5	107
5G/10'	623	648	54	73
6G/2'	632	637	1	6
6G/4'	902	927	5	34
6G/6'				
6G/8'				
6G/10'	690	733	13	20
3H/2'				
3H/4'	910	944	7	33
3H/6'				
3H/8'	930	1032	55	104
3H/10'	600	662	35	42
4G/4'	1036	1065	6	28
4G/6'				
4G/10'	617	661	18	24
4H/4'	920	952	7	40
4H/6'				
4H/10'	683	727	12	42
7D/4'	905	934	6	40
7D/6'	1033	1090	8	70
7D/10'				

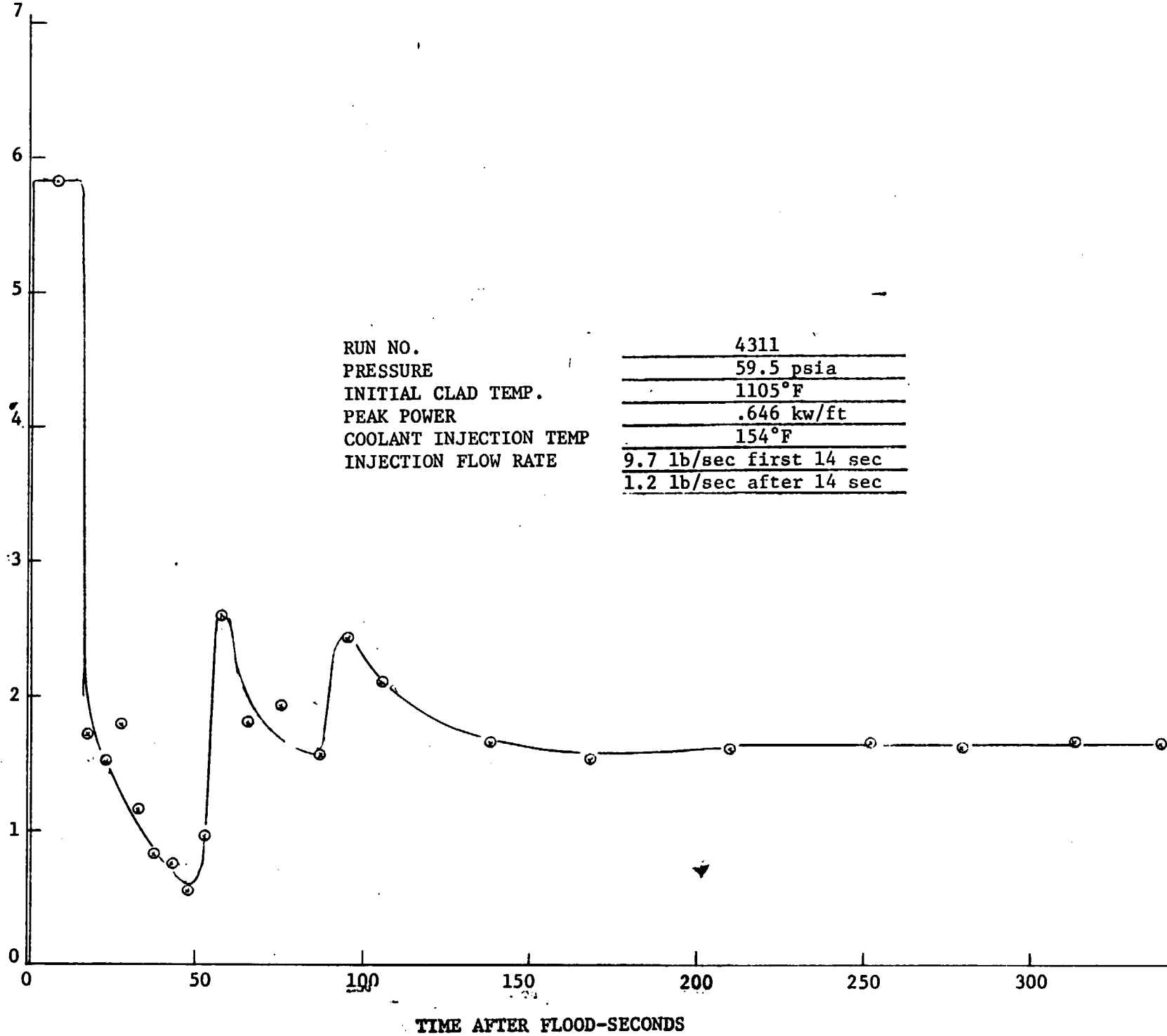
RUN NO.
 PRESSURE
 INITIAL CLAD TEMP.
 PEAK POWER
 COOLANT INJECTION TEMP
 INJECTION FLOW RATE

4311
59.5 psia
1105°F
.646 kw/ft
154°F
9.7 lb/sec first 14 sec
1.2 lb/sec after 14 sec

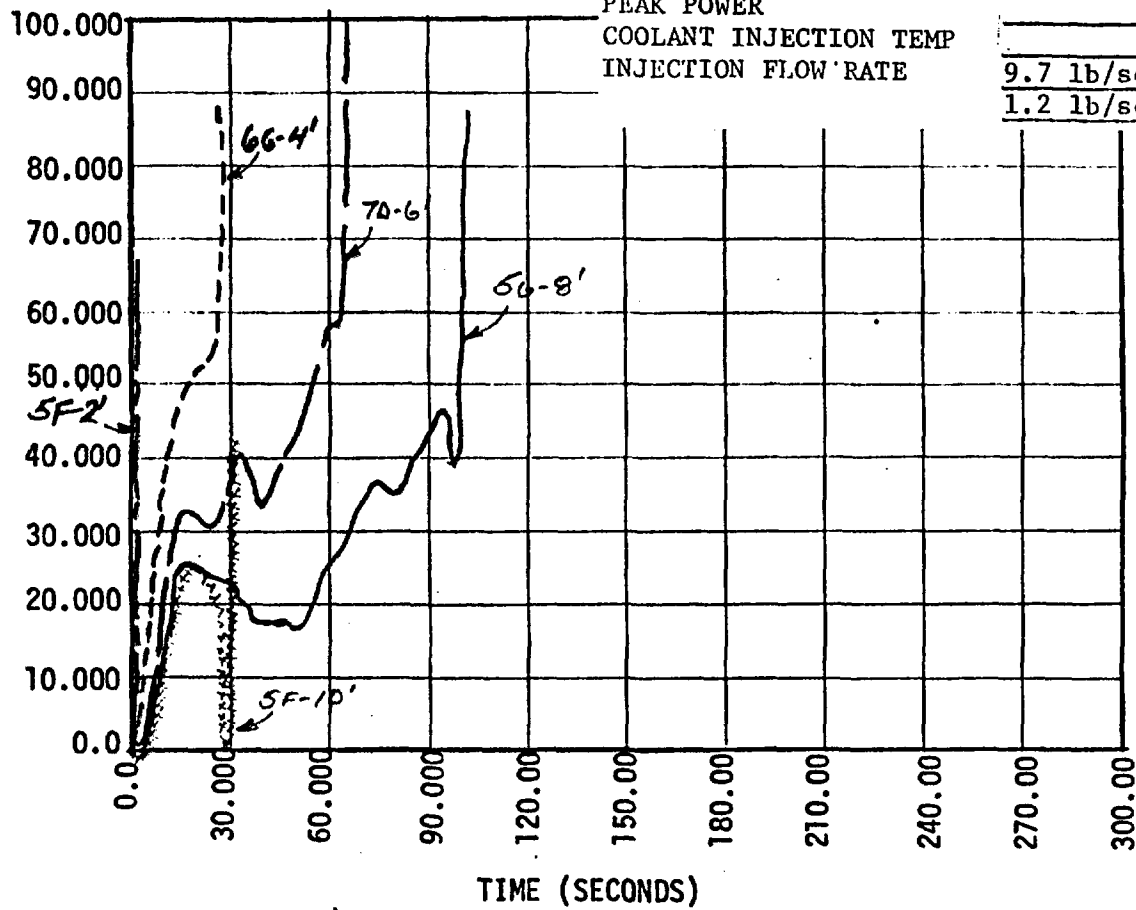


811-V

FLOODING RATE-IN/SEC



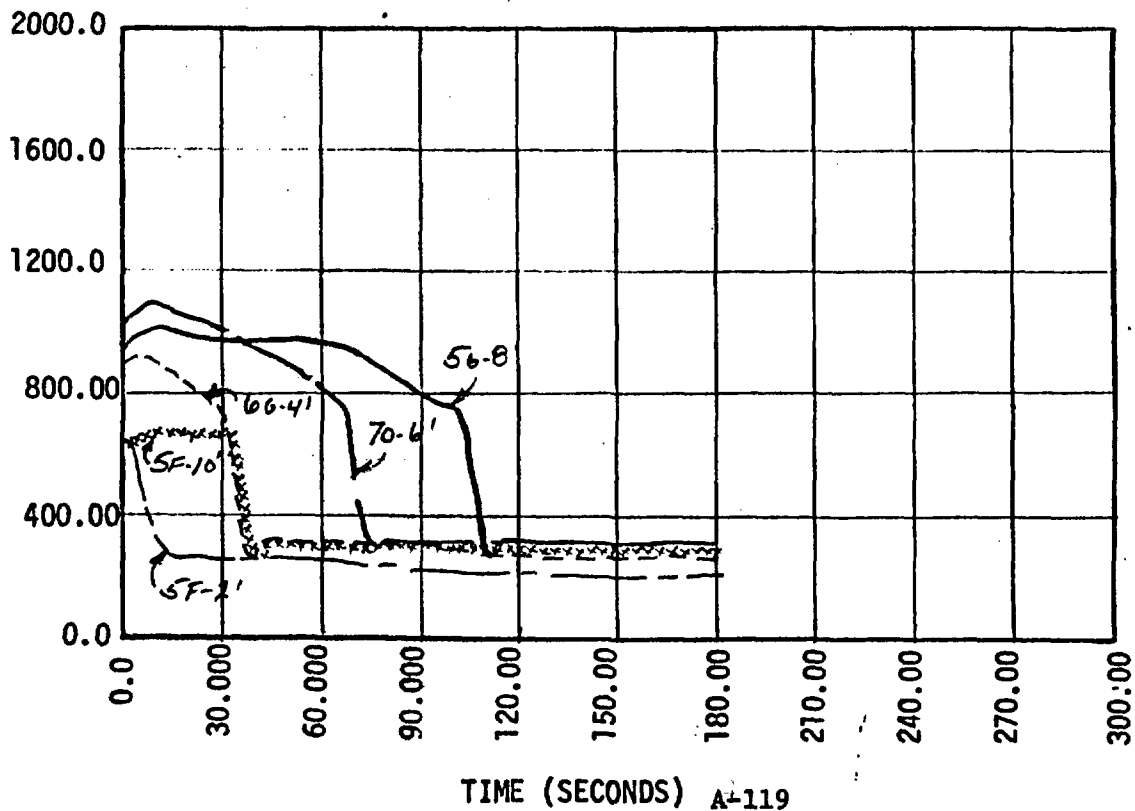
HEAT TRANSFER COEFFICIENT (BTU/HR/FT**2/DEG F)



RUN NO.
PRESSURE
INITIAL CLAD TEMP.
PEAK POWER
COOLANT INJECTION TEMP
INJECTION FLOW RATE

4311
59.5 psia
1105°F
.646 kw/ft
154°F
9.7 lb/sec first 14 sec
1.2 lb/sec after 14 sec

CLAD TEMPERATURE (DEG. F)



5

6

7

8

9

FLECHT-SET RUN SUMMARY SHEET

RUN NO. 4412

DATE 2/20/73

A. RUN CONDITIONS

Containment Pressure	61.4	psia
Initial Clad Temperature	1107	°F
Peak Power	0.646*	kw/ft
Coolant Supply Temperature	159	°F
Injection Rate	10.93 lb/sec first 14 sec, 1.22 lb/sec after 14 sec	
Loop Resistance Coefficient	$(\Delta p_{loop}/1/2 \rho V^2_{hotleg})$	29.5

B. INITIAL HOUSING TEMPERATURES

Elevation (ft)	Initial Temperature (°F)
0	239
2	296
4	305
6	303
8	298
10	307
12	271

*All 82 heater rods had the same power. Rods 4A, 7A, 1D, 1G, 4K, 7K, 10D and 10G were disconnected from the power supply.

FLECHT-SET RUN SUMMARY SHEET (Cont)

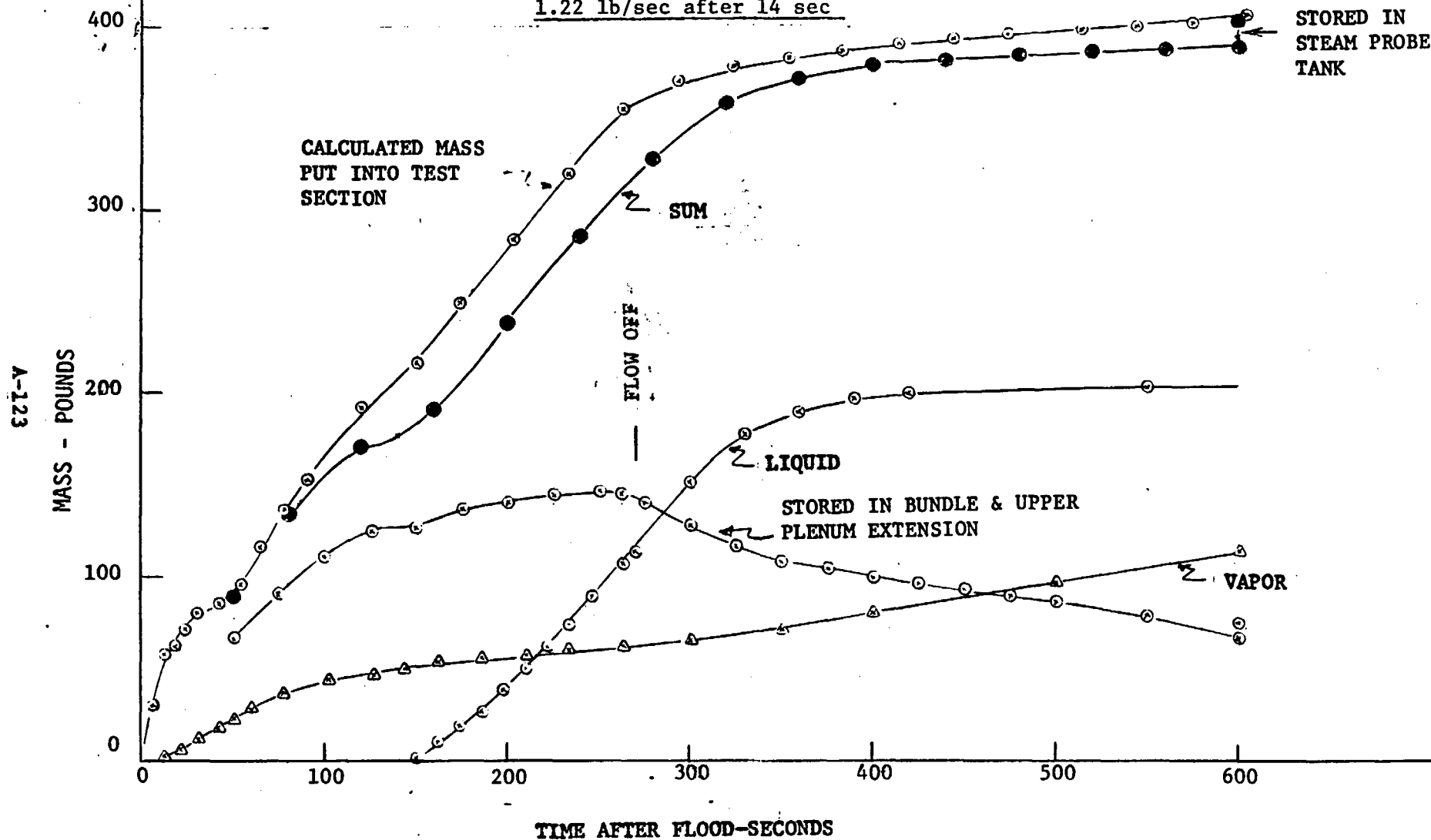
RUN NO. 4412

DATE 2/20/73

C. HEATER THERMOCOUPLE DATA

Rod/Elev.	Initial Temp. (°F)	Max. Temp. (°F)	Turnaround Time (Sec)	Quench Time (Sec)
5F/2'	647	648	1	7
5F/4'				
5F/6'				
5F/8'				
5F/10'	659	700	11	25
5G/2'	637	640	2	7
5G/4'				
5G/6'	1107	1164	9	75
5G/8'	971	1034	11	95
5G/10'	646	689	11	46
6G/2'	648	652	2	7
6G/4'	914	934	5	25
6G/6'				
6G/8'				
6G/10'	702	754	13	21
3H/2'				
3H/4'				
3H/6'				
3H/8'				
3H/10'	615	664	12	46
4G/4'	1030	1052	5	27
4G/6'				
4G/10'	642	688	12	30
4H/4'	918	943	7	34
4H/6'				
4H/10'	695	752	14	21
7D/4'	909	934	6	30
7D/6'	1033	1089	9	63
7D/10'				

RUN NO.	4412
PRESSURE	61.4 psia
INITIAL CLAD TEMP	1107°F
PEAK POWER	0.646 kw/ft
COOLANT INJECTION TEMP	159°F
INJECTION FLOW RATE	10.93 lb/sec first 14 sec
	1.22 lb/sec after 14 sec

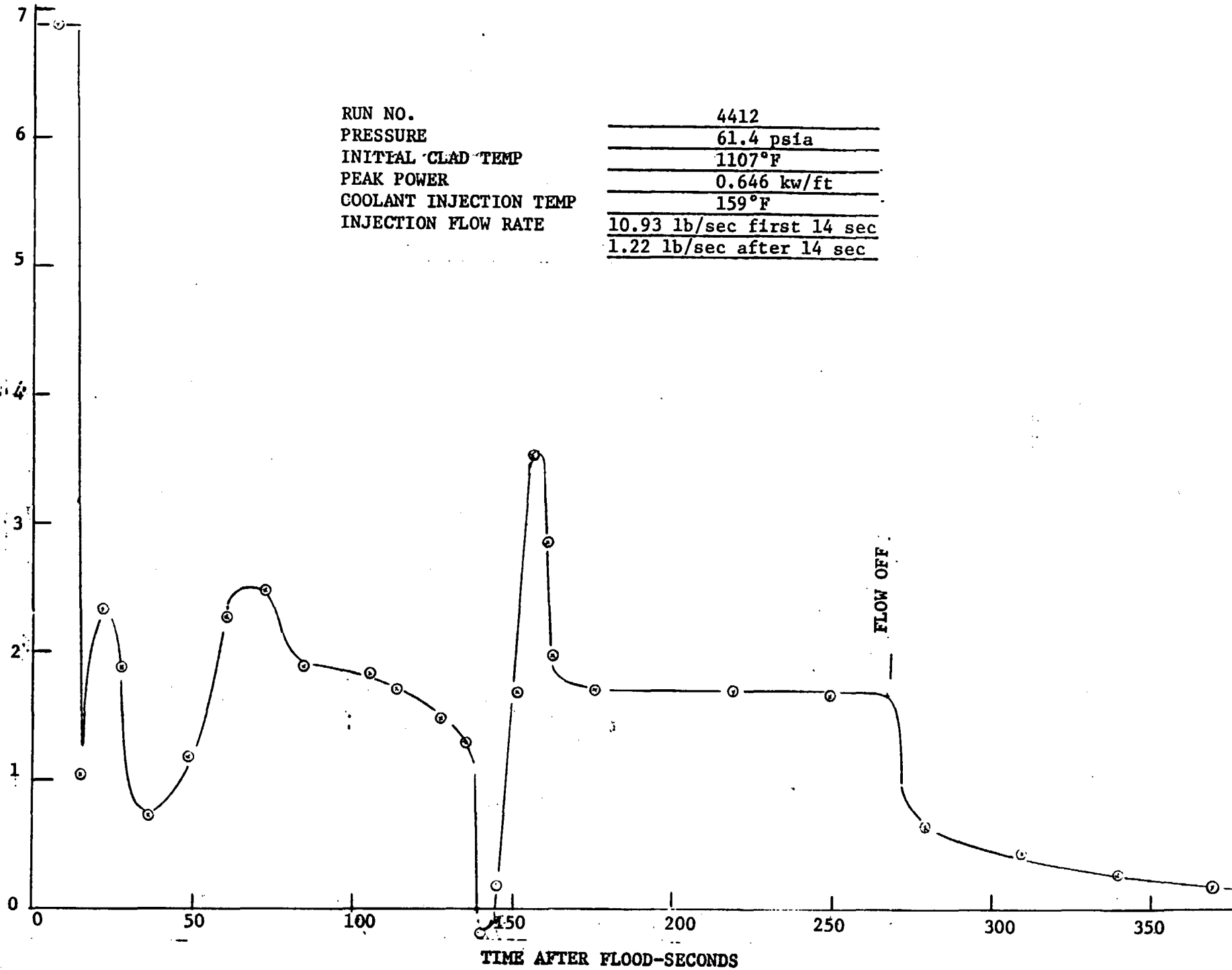


RUN NO.
PRESSURE
INITIAL CLAD TEMP
PEAK POWER
COOLANT INJECTION TEMP
INJECTION FLOW RATE

4412
61.4 psia
1107°F
0.646 kw/ft
159°F
10.93 lb/sec first 14 sec
1.22 lb/sec after 14 sec

A-124

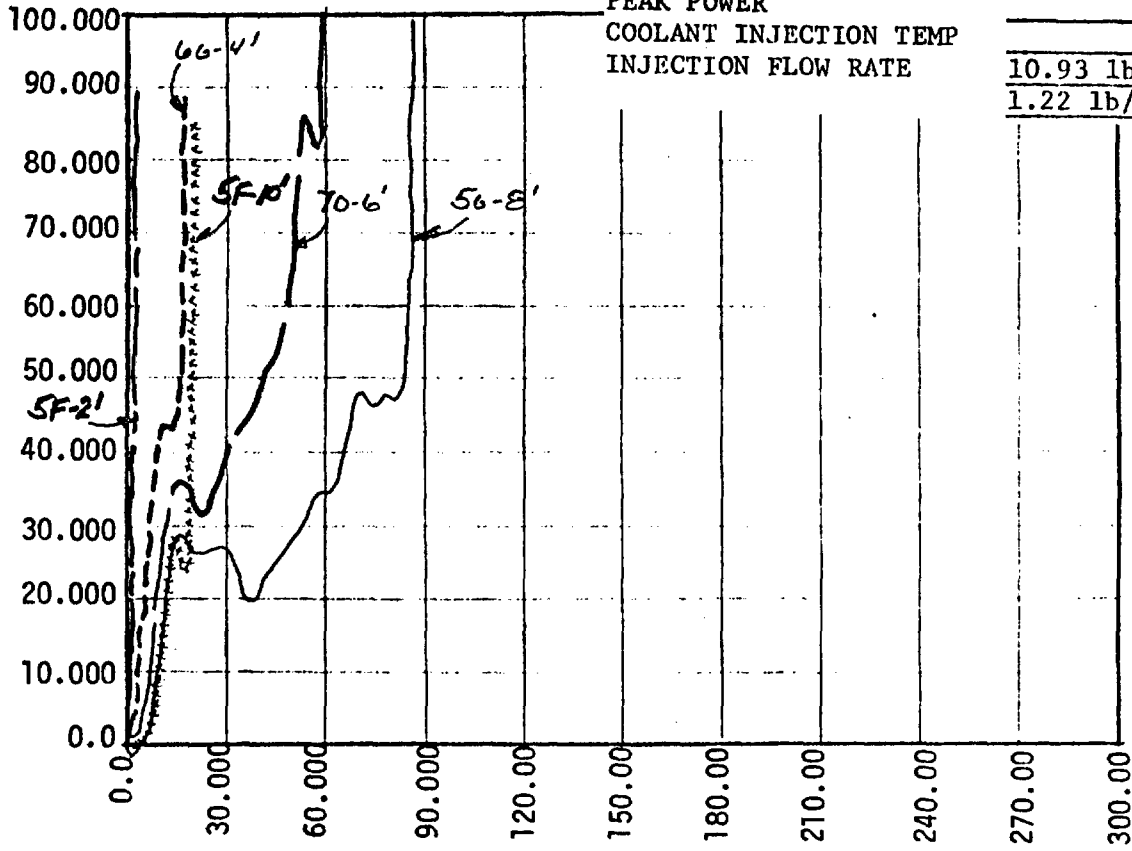
FLOODING RATE-IN/SEC



RUN NO.
 PRESSURE
 INITIAL CLAD TEMP
 PEAK POWER
 COOLANT INJECTION TEMP
 INJECTION FLOW RATE

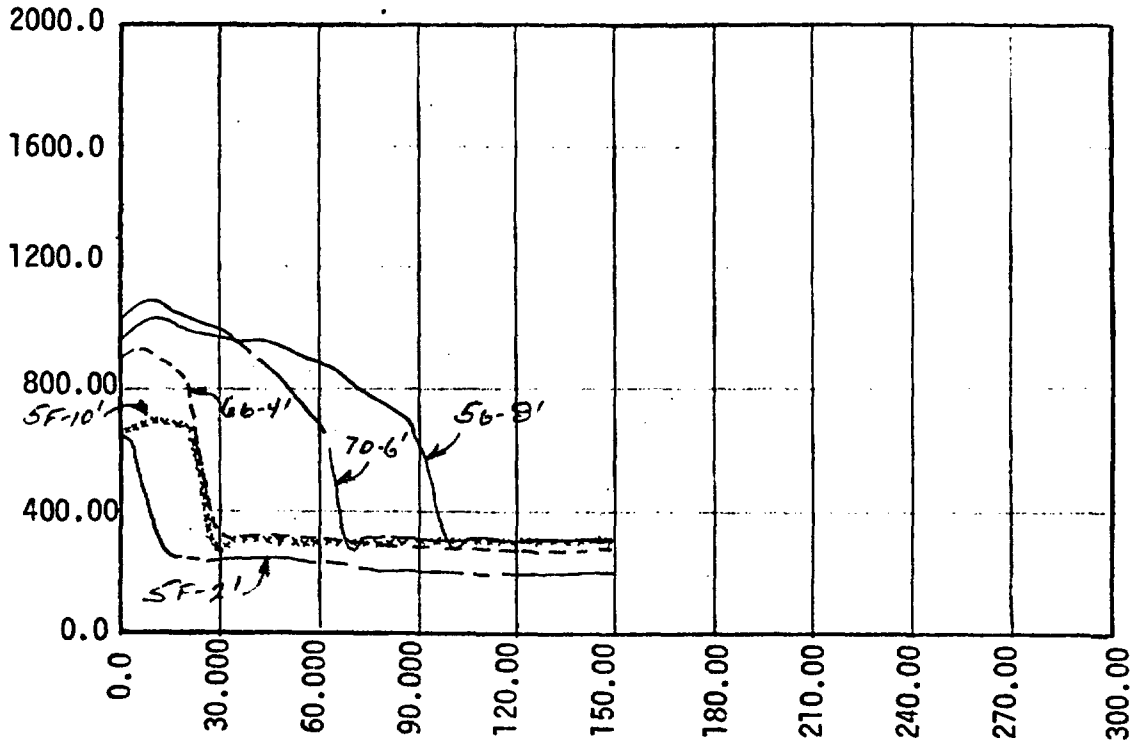
4412
 61.4 psia
 1107°F
 0.646 kw/ft
 159°F
 10.93 lb/sec first 14 sec
 1.22 lb/sec after 14 sec

HEAT TRANSFER COEFFICIENT (BTU/HR/FT**2/DEG F)



TIME (SECONDS)

CLAD TEMPERATURE (DEG. F)



TIME (SECONDS)

A-125

1

2

3

4

5

FLECHT-SET RUN SUMMARY SHEET

RUN NO. 4530

DATE 2/21/73

A. RUN CONDITIONS

Containment Pressure	39.6	psia
Initial Clad Temperature	1112	°F
Peak Power	0.7	kw/ft
Coolant Supply Temperature	161	°F
Injection Rate	8.8 lb/sec first 14 sec, 1.22 lb/sec after 14 sec	
Loop Resistance Coefficient ($\Delta\rho_{loop}/1/2 \rho V_{hotleg}^2$)	30.9	

B. INITIAL HOUSING TEMPERATURES

Elevation (ft)	Initial Temperature (°F)
0	265
2	387
4	506
6	533
8	531
10	385
12	292

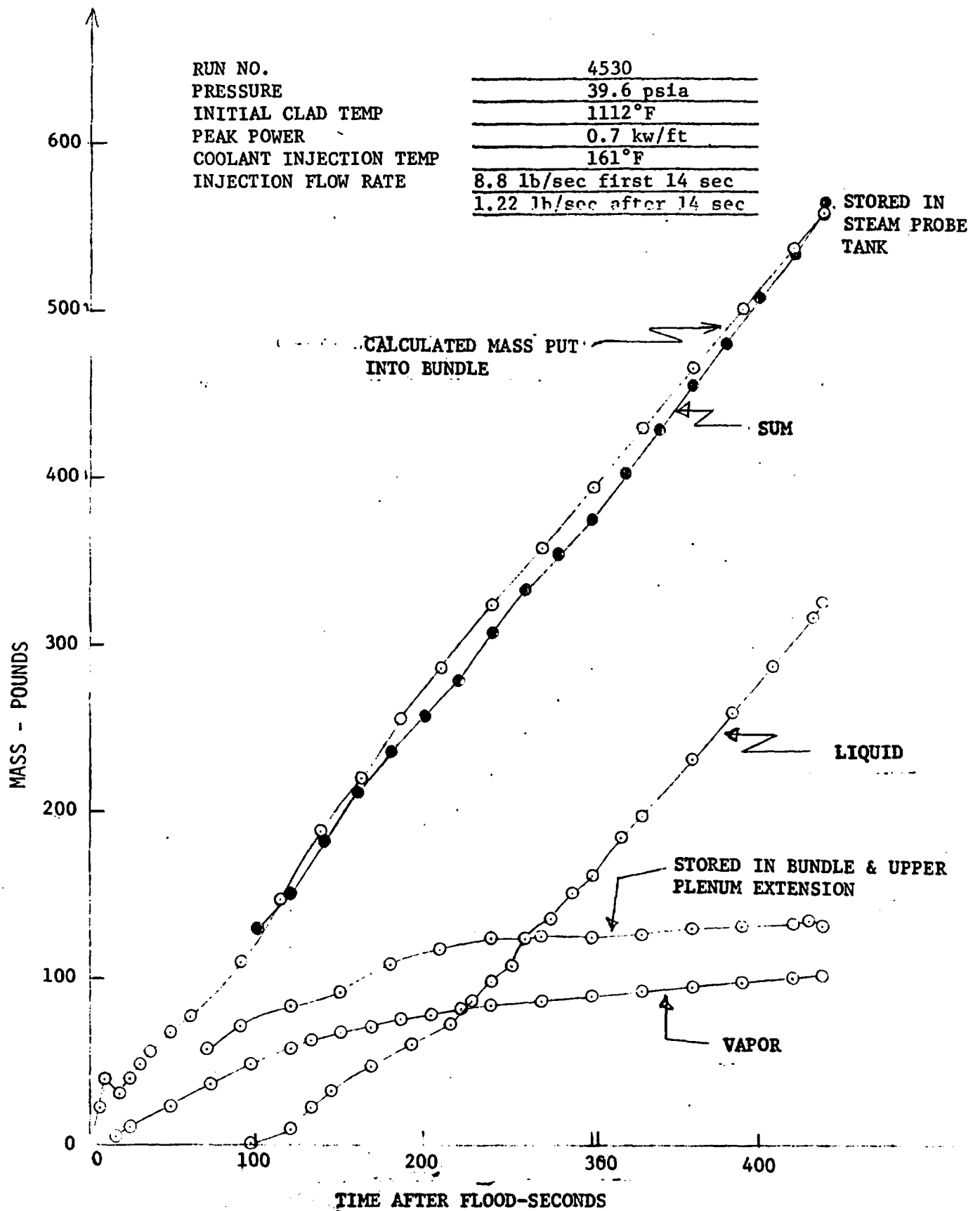
FLECHT-SET RUN SUMMARY SHEET (Cont)

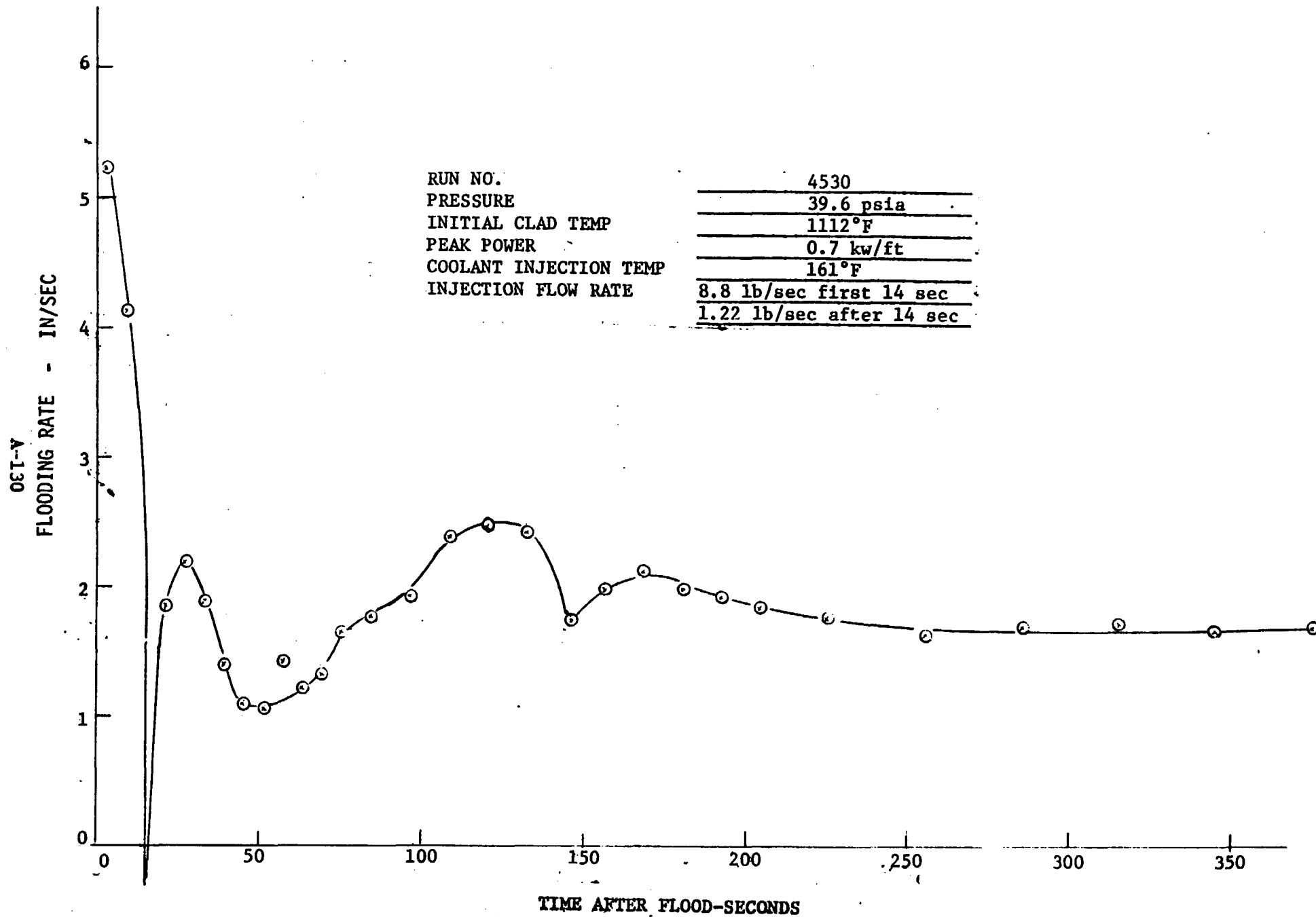
RUN NO. 4530

DATE 2/21/73

C. HEATER THERMOCOUPLE DATA

Rod/Elev.	Initial Temp. (°F)	Max. Temp. (°F)	Turnaround Time (Sec)	Quench Time (Sec)
5F/2'	642	646	2	7
5F/4'				
5F/6'				
5F/8'				
5F/10'	721	824	59	65
5G/2'	630	636	2	7
5G/4'				
5G/6'	1112	1224	56	129
5G/8'	996	1237	42	176
5G/10'	704	789	60	119
6G/2'	641	650	2	7
6G/4'	937	968	7	45
6G/6'				
6G/8'				
6G/10'	754	835	72	99
3H/2'				
3H/4'				
3H/6'				
3H/8'	981	1117	72	154
3H/10'	646	751	64	92
4G/4'	1039	1082	10	62
4G/6'				
4G/10'	692	773	56	81
4H/4'	950	986	8	62
4H/6'				
4H/10'	747	811	47	71
7D/4'	938	976	8	63
7D/6'	1054	1155	57	126
7D/10'				

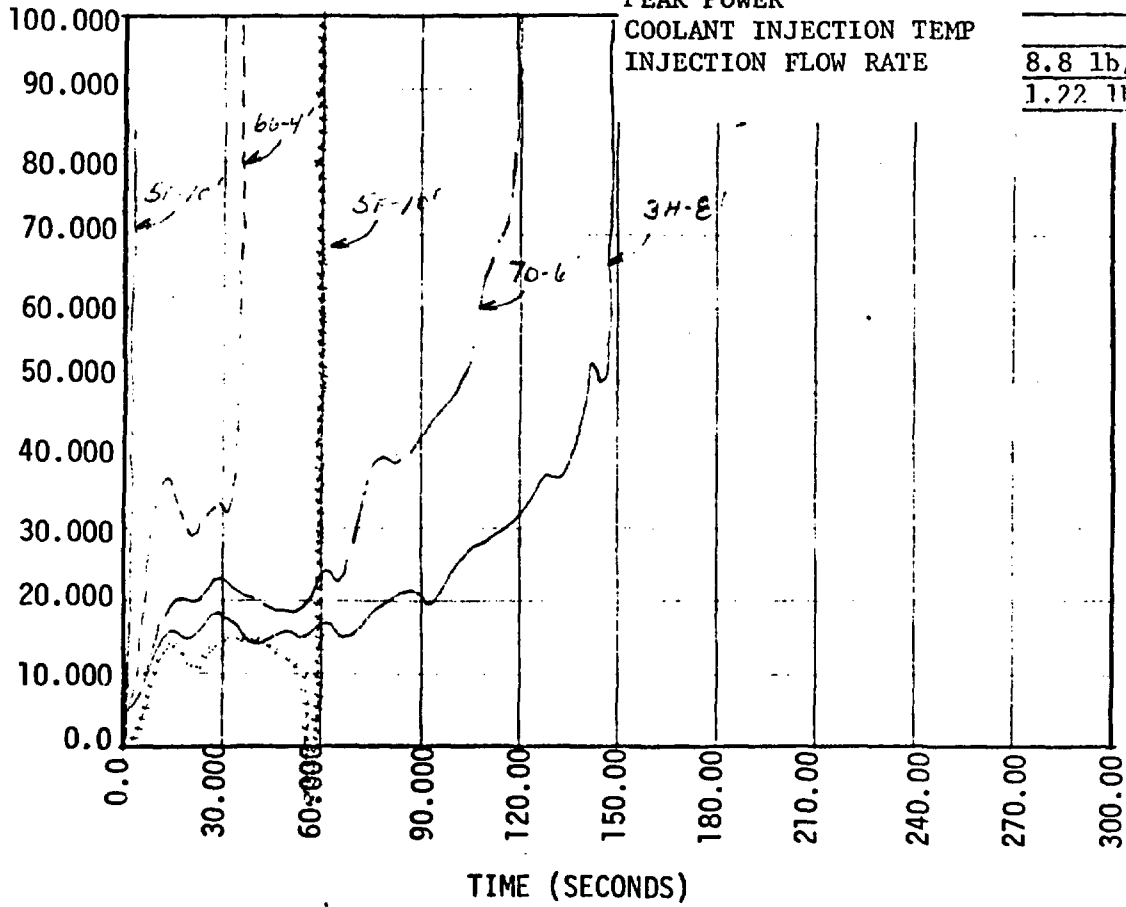




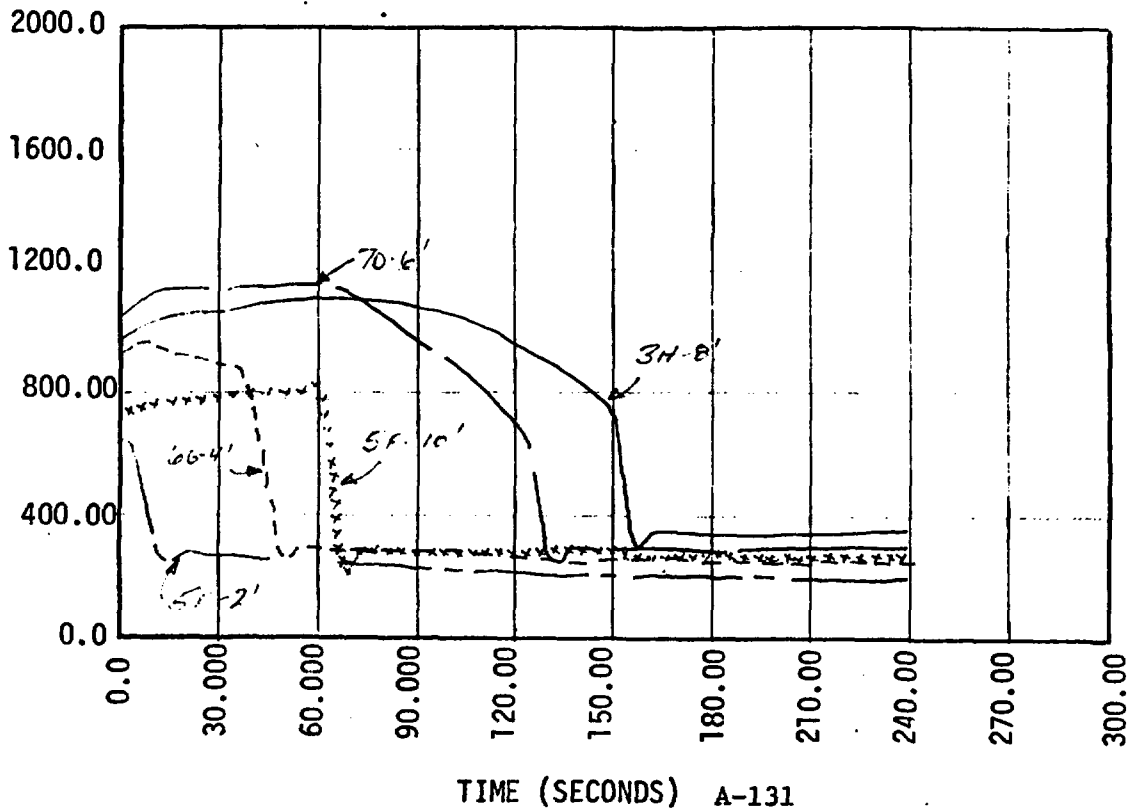
RUN NO.
 PRESSURE
 INITIAL CLAD TEMP
 PEAK POWER
 COOLANT INJECTION TEMP
 INJECTION FLOW RATE

4530
39.6 psia
1112°F
0.7 kw/ft
161°F
8.8 lb/sec first 14 sec
1.22 lb/sec after 14 sec

HEAT TRANSFER COEFFICIENT (BTU/HR/FT**2/DEG F)



CLAD TEMPERATURE (DEG. F)



(

(

(

|

FLECHT-SET RUN SUMMARY SHEET

RUN NO. 4825

DATE 2/27/73

A. RUN CONDITIONS

Containment Pressure	60.3	psia
Initial Clad Temperature	712	°F
Peak Power	0.7	kw/ft
Coolant Supply Temperature	156	°F
Injection Rate	10.77 lb/sec first 14 sec, 1.21 lb/sec after 14 sec	
Loop Resistance Coefficient	$(\Delta\rho_{\text{loop}}/1/2 \rho V^2_{\text{hotleg}})$	30.6

B. INITIAL HOUSING TEMPERATURES

Elevation (ft)	Initial Temperature (°F)
0	247
2	375
4	423
6	462
8	447
10	374
12	283

FLECHT-SET RUN SUMMARY SHEET (Cont)

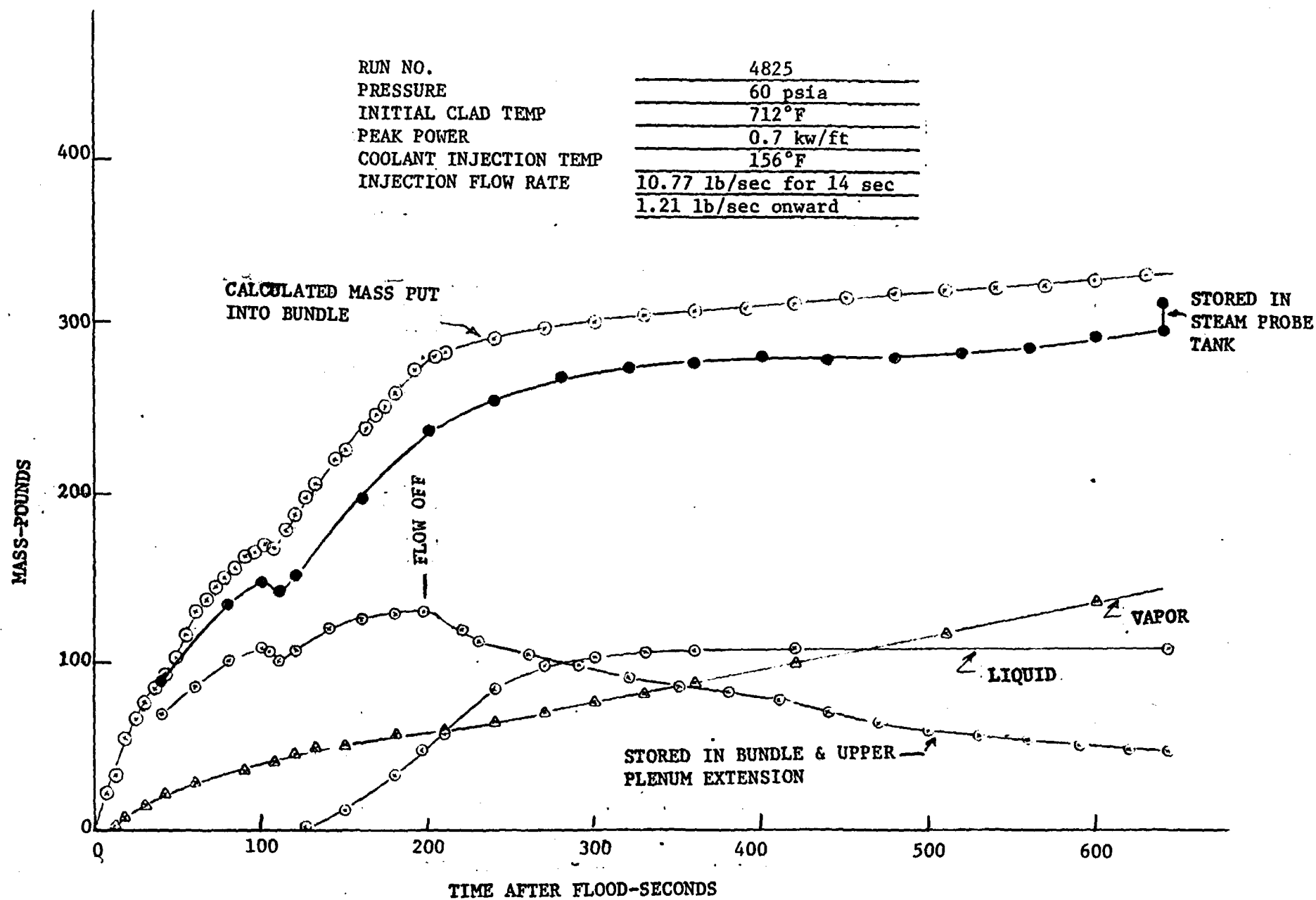
RUN NO. 4825

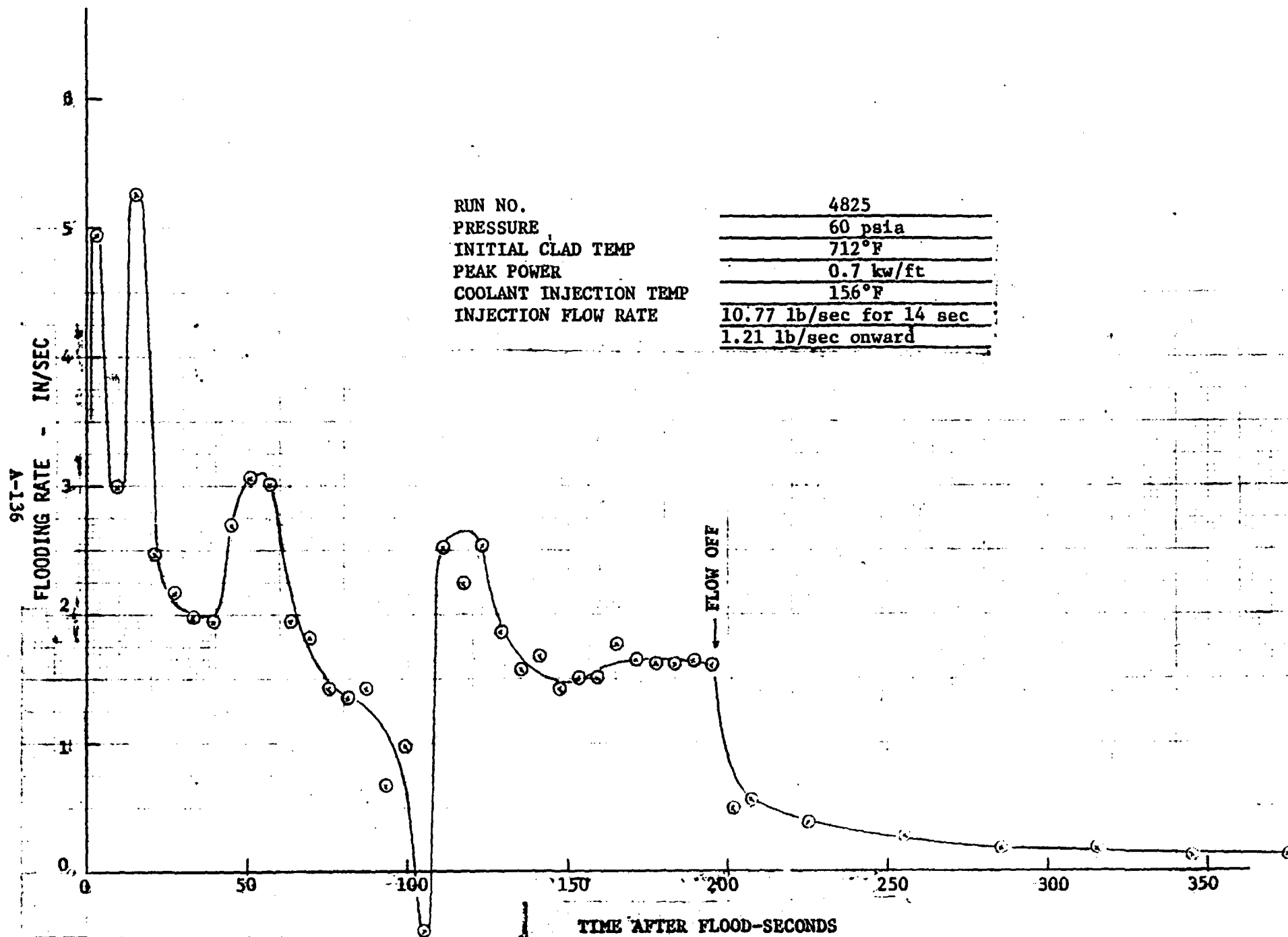
DATE 2/27/73

C. HEATER THERMOCOUPLE DATA

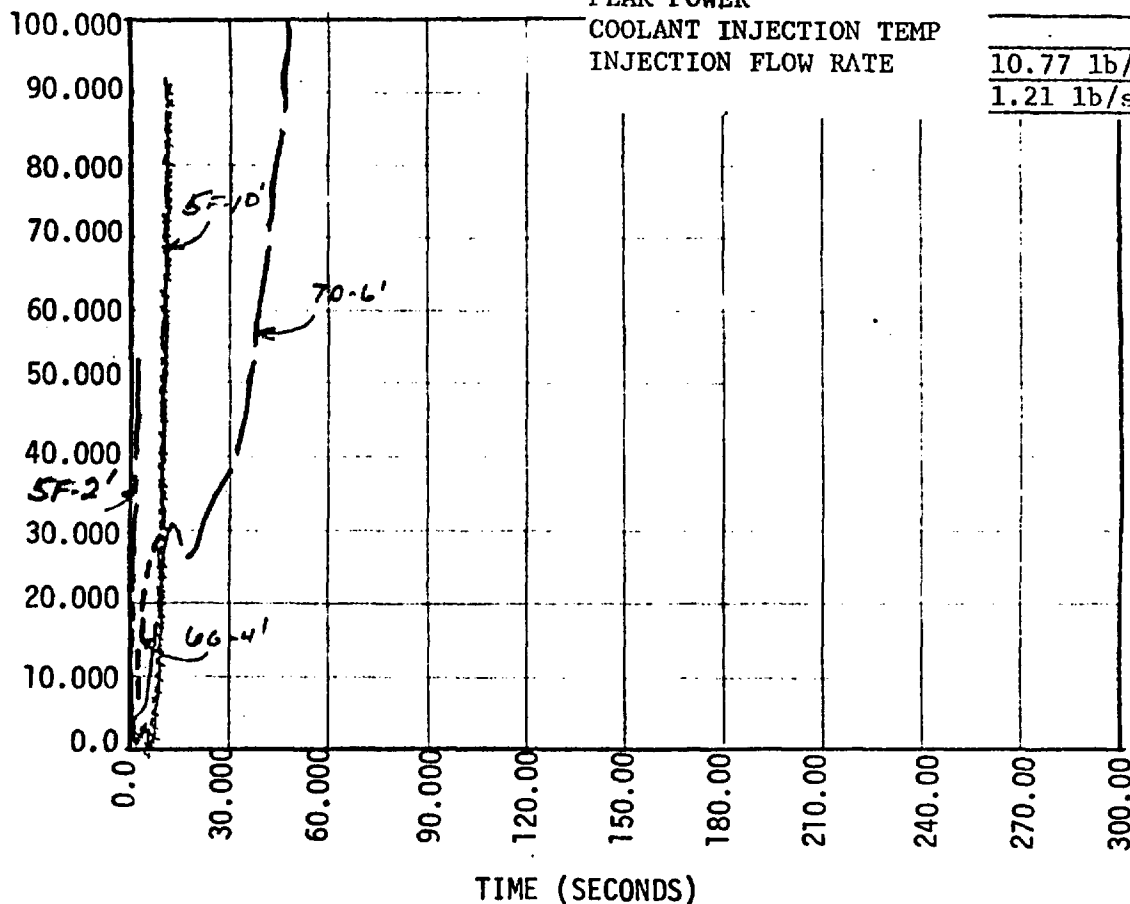
Rod/Elev.	Initial Temp. (°F)	Max. Temp. (°F)	Turnaround Time (Sec)	Quench Time (Sec)
5F/2'	517	519	1	3
5F/4'				
5F/6'				
5F/8'				
5F/10'	477	526	9	13
5G/2'	509	513	2	4
5G/4'				
5G/6'	712	877	27	66
5G/8'				
5G/10'	465	526	19	22
6G/2'	513	521	2	4
6G/4'	645	705	12	18
6G/6'				
6G/8'				
6G/10'	527	586	10	14
3H/2'				
3H/4'				
3H/6'				
3H/8'	539	806	36	46
3H/10'	434	489	11	25
4G/4'	695	762	8	17
4G/6'				
4G/10'	458	513	9	12
4H/4'	650	718	14	22
4H/6'				
4H/10'	521	580	10	15
7D/4'	642	699	7	15
7D/6'	689	820	28	54
7D/10'				

A-135





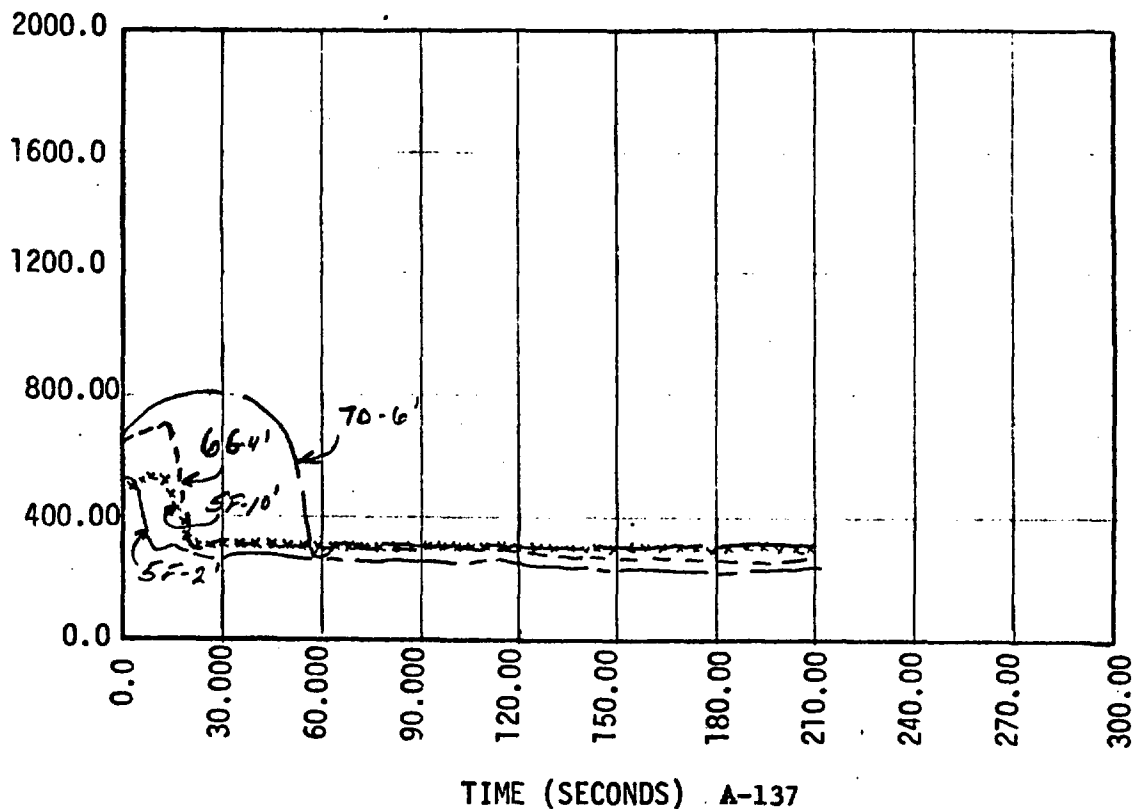
HEAT TRANSFER COEFFICIENT (BTU/HR/FT**2/DEG F)



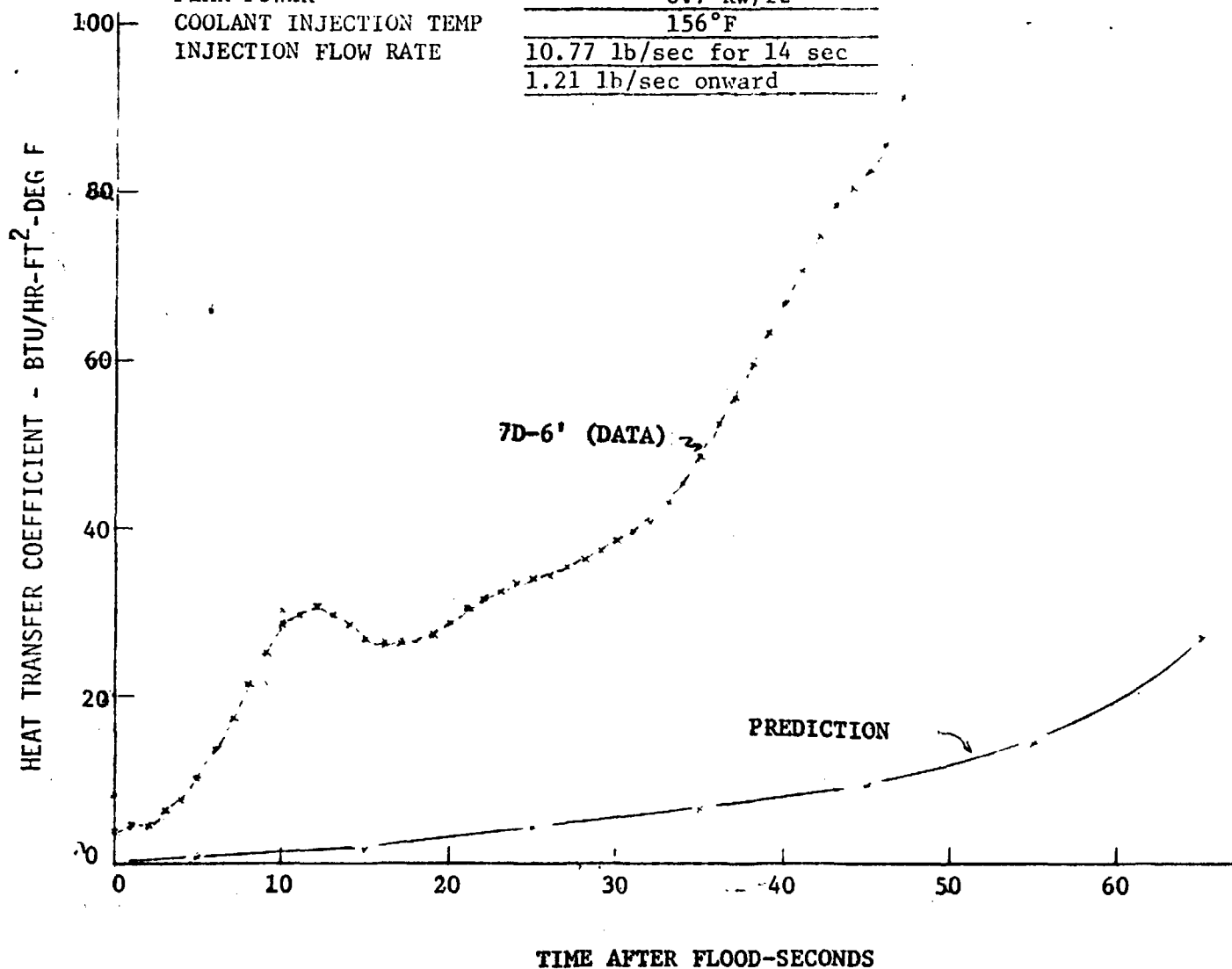
RUN NO.
PRESSURE
INITIAL CLAD TEMP
PEAK POWER
COOLANT INJECTION TEMP
INJECTION FLOW RATE

4825
60 psia
712°F
0.7 kw/ft
156°F
10.77 lb/sec for 14 sec
1.21 lb/sec onward

CLAD TEMPERATURE (DEG. F)



RUN NO.	4825
PRESSURE	60 psia
INITIAL CLAD TEMP	712°F
PEAK POWER	0.7 kw/ft
COOLANT INJECTION TEMP	156°F
INJECTION FLOW RATE	10.77 lb/sec for 14 sec
	1.21 lb/sec onward



FLECHT-SET RUN SUMMARY SHEET

RUN NO. 4923

DATE 2/28/73

A. RUN CONDITIONS

Containment Pressure	61	psia
Initial Clad Temperature	1111	°F
Peak Power	0.7	kw/ft
Coolant Supply Temperature	158	°F
Injection Rate	10.52 lb/sec first 14 sec, 1.19 lb/sec after 14 sec	
Loop Resistance Coefficient ($\Delta\rho_{loop}/1/2 \rho V_{hotleg}^2$)	31.1	

B. INITIAL HOUSING TEMPERATURES

Elevation (ft)	Initial Temperature (°F)
0	268
2	409
4	501
6	545
8	531
10	406
12	305

FLECHT-SET RUN SUMMARY SHEET (Cont)

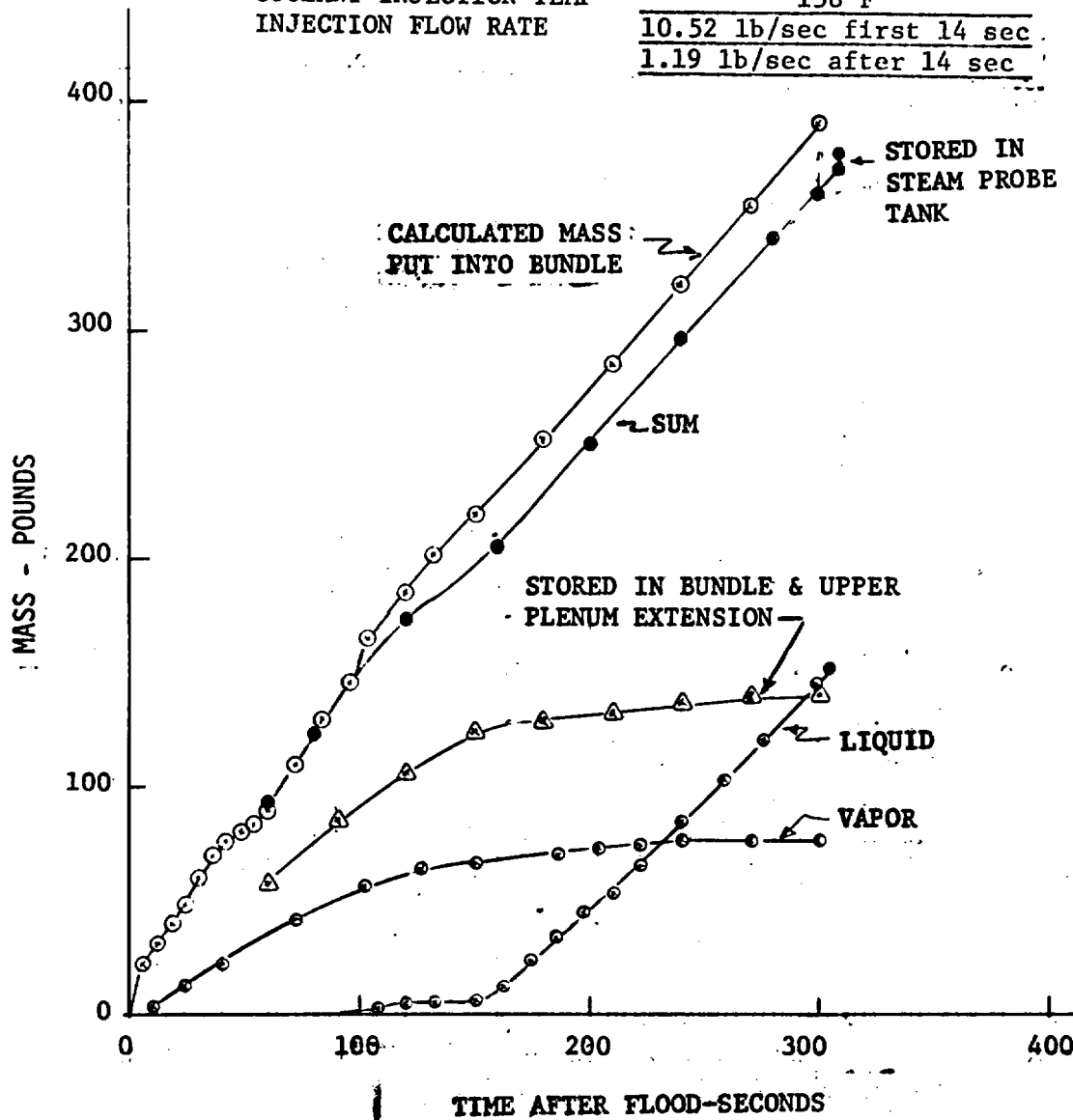
RUN NO. 4923

DATE 2/28/73

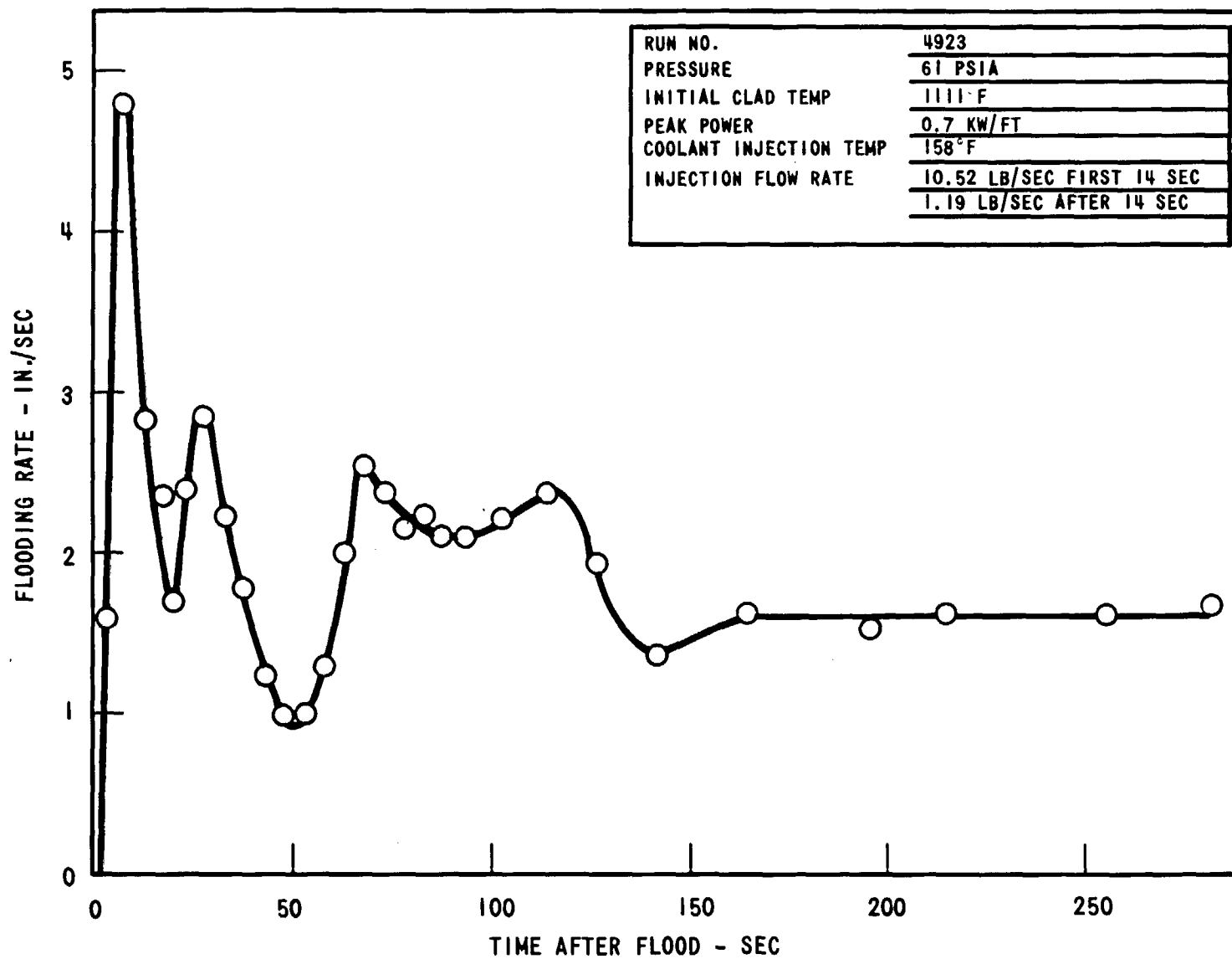
C. HEATER THERMOCOUPLE DATA

Rod/Elev.	Initial Temp. (°F)	Max. Temp. (°F)	Turnaround Time (Sec)	Quench Time (Sec)
5F/2'	699	700	1	7
5F/4'				
5F/6'				
5F/8'				
5F/10'	675	724	23	46
5G/2'	690	696	2	7
5G/4'				
5G/6'	1111	1167	19	97
5G/8'	943	1055	26	115
5G/10'	638	714	14	80
6G/2'	697	706	2	8
6G/4'	960	985	3	37
6G/6'				
6G/8'				
6G/10'	714	770	21	28
3H/2'				
3H/4'				
3H/6'				
3H/8'	929	1042	53	105
3H/10'	613	681	48	63
4G/4'	1065	1085	4	44
4G/6'				
4G/10'	652	701	24	52
4H/4'	970	994	7	46
4H/6'				
4H/10'	714	759	26	61
7D/4'	959	990	7	43
7D/6'	1057	1108	19	89
7D/10'				

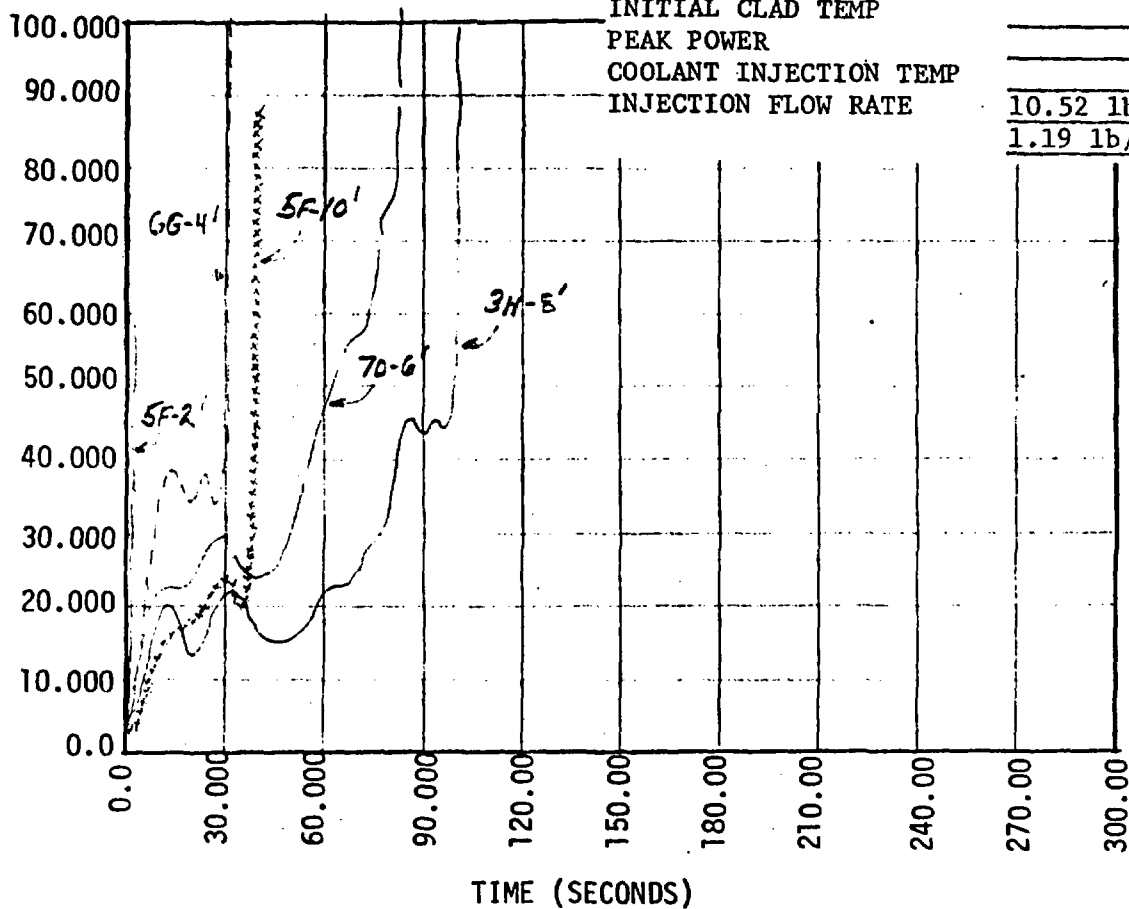
RUN NO.	4923
PRESSURE	61 psia
INITIAL CLAD TEMP	1111°F
PEAK POWER	0.7 kw/ft
COOLANT INJECTION TEMP	158°F
INJECTION FLOW RATE	10.52 lb/sec first 14 sec
	1.19 lb/sec after 14 sec



A-142



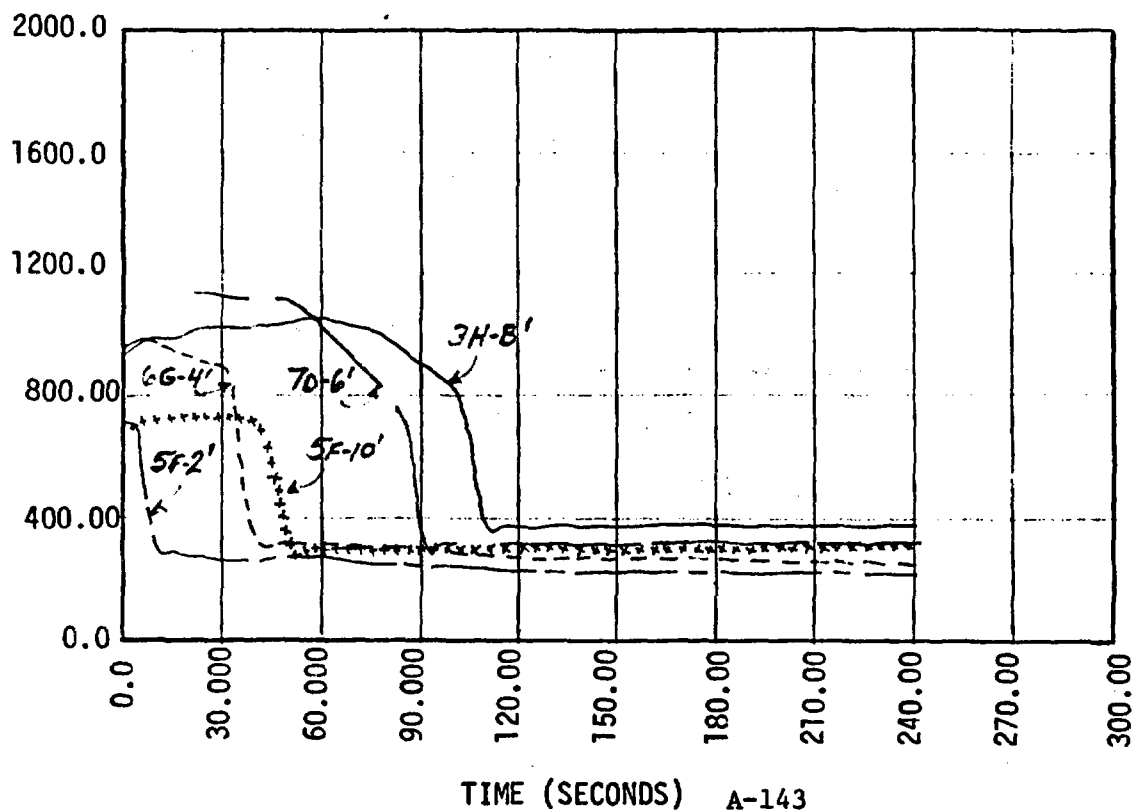
HEAT TRANSFER COEFFICIENT (BTU/HR/FT**2/DEG F)



RUN NO.
PRESSURE
INITIAL CLAD TEMP
PEAK POWER
COOLANT INJECTION TEMP
INJECTION FLOW RATE

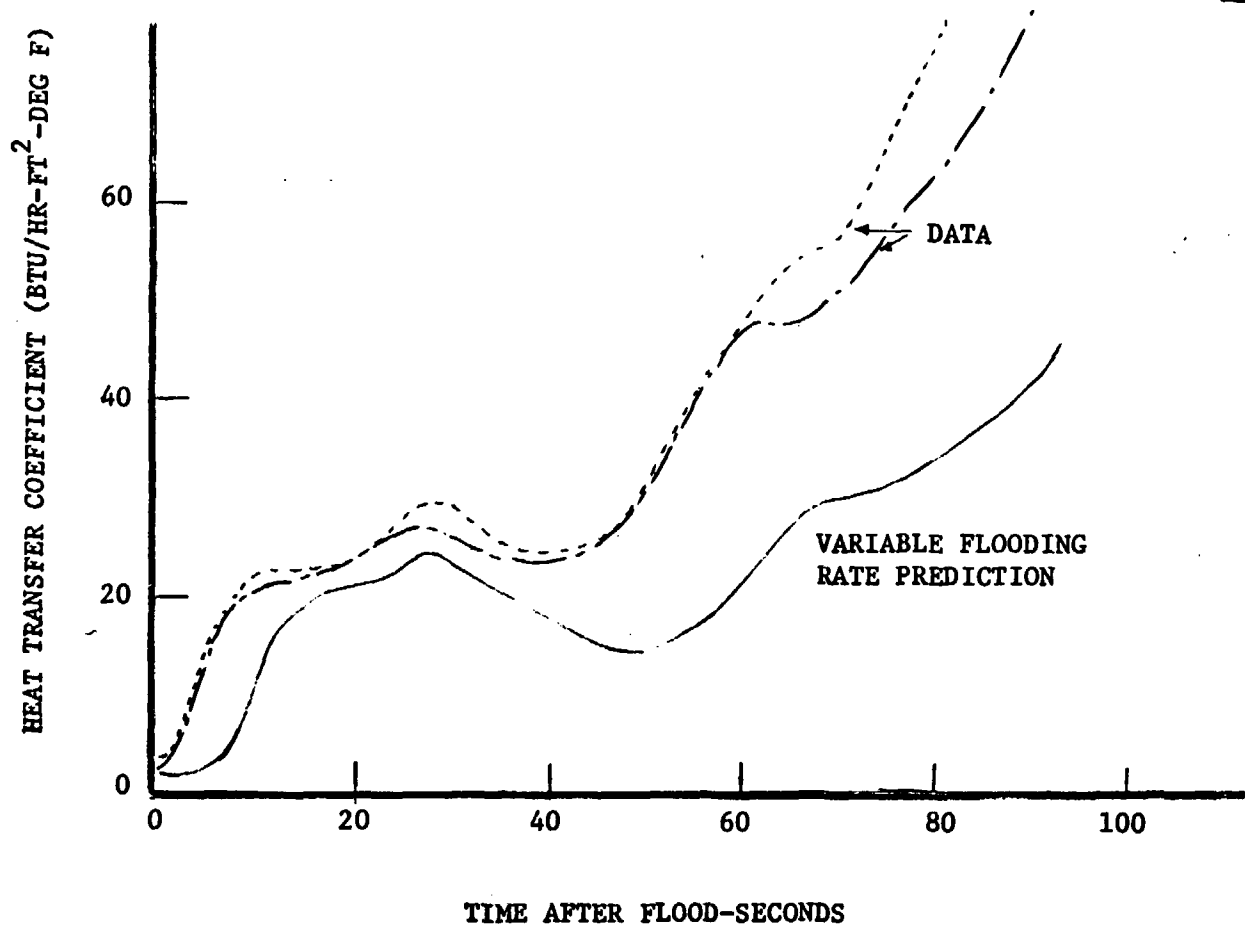
4923
61 psia
1111°F
0.7 kw/ft
158°F
10.52 lb/sec first 14 sec
1.19 lb/sec after 14 sec

CLAD TEMPERATURE (DEG. F)



RUN NO.
PRESSURE
INITIAL CLAD TEMP
PEAK POWER
COOLANT INJECTION TEMP
INJECTION FLOW RATE

4923
61 psia
1111°F
0.7 kw/ft
158°F
10.52 lb/sec first 14 sec
1.19 lb/sec after 14 sec



FLECHT-SET RUN SUMMARY SHEET

RUN NO. 5115

DATE 3/2/73

A. RUN CONDITIONS

Containment Pressure	61.0	psia
Initial Clad Temperature	1110	°F
Peak Power	0.759*	kw/ft
Coolant Supply Temperature	154	°F
Injection Rate	9.0 lb/sec first 14 sec, 1.2 lb/sec after 14 sec	
Loop Resistance Coefficient	$(\Delta\rho_{loop}/1/2 \rho V_{hotleg}^2)$	30.8

B. INITIAL HOUSING TEMPERATURES

Elevation (ft)	Initial Temperature (°F)
0	265
2	301
4	307
6	300
8	298
10	290
12	258

*All 90 heater rod had same initial power.

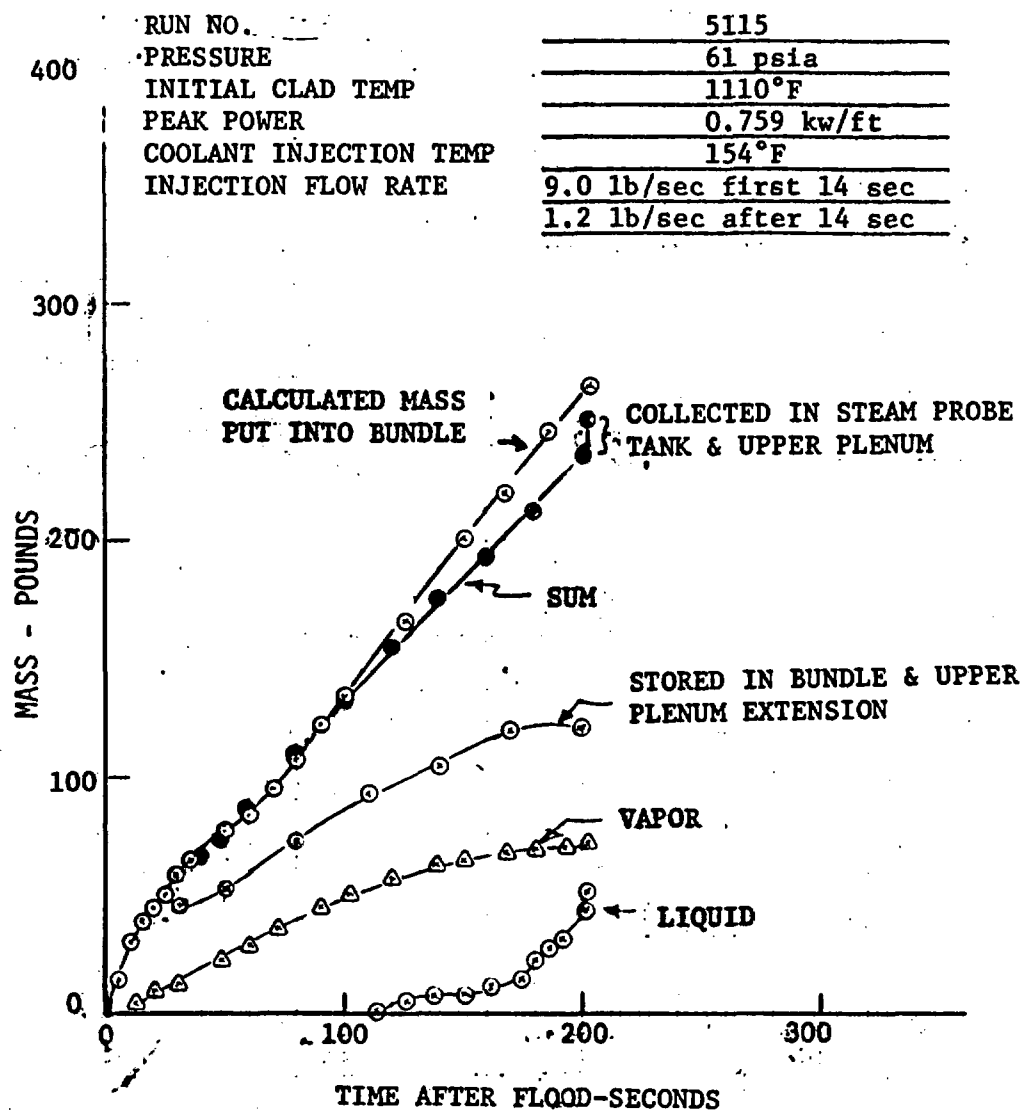
FLECHT-SET RUN SUMMARY SHEET (Cont)

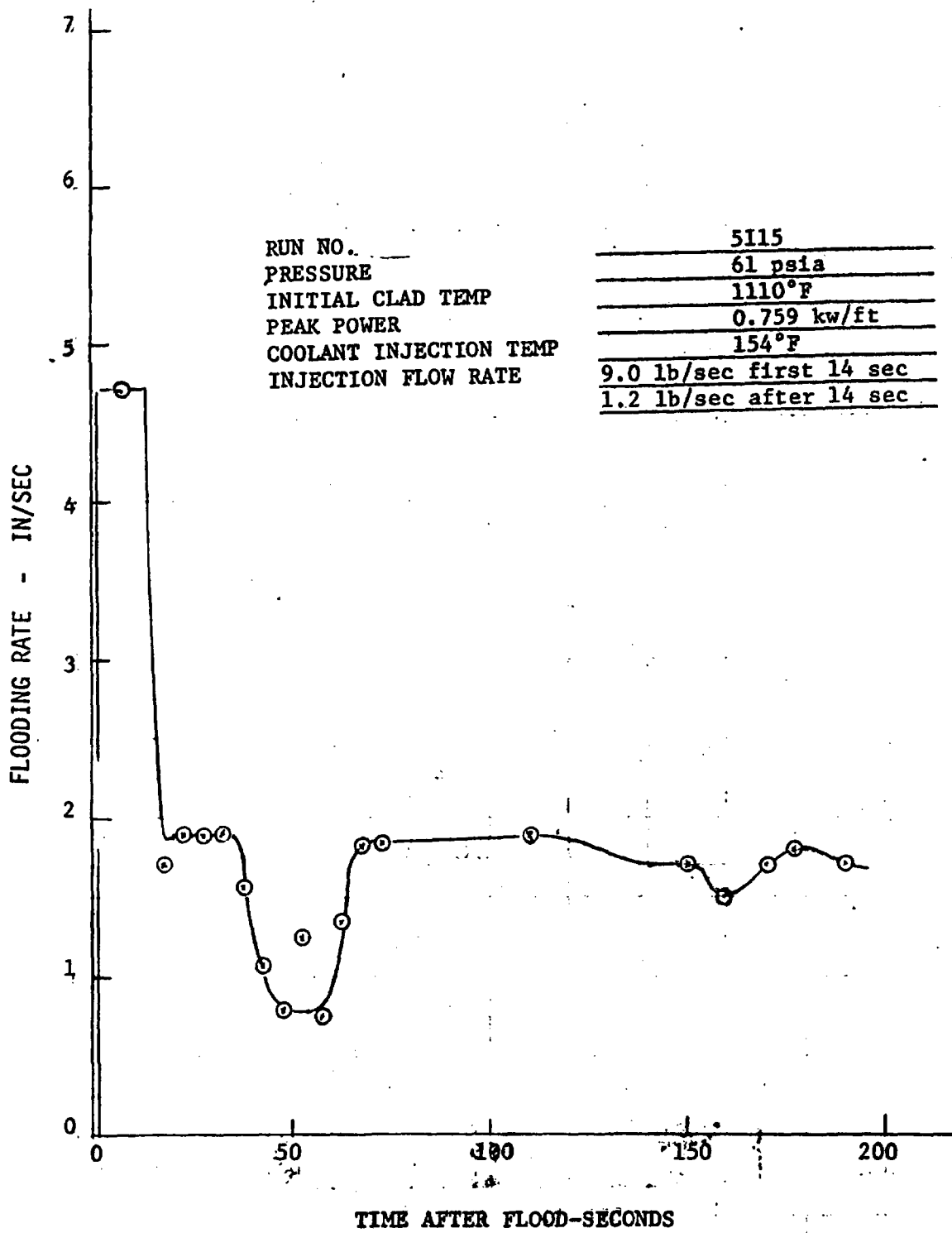
RUN NO. 5115

DATE 3/2/73

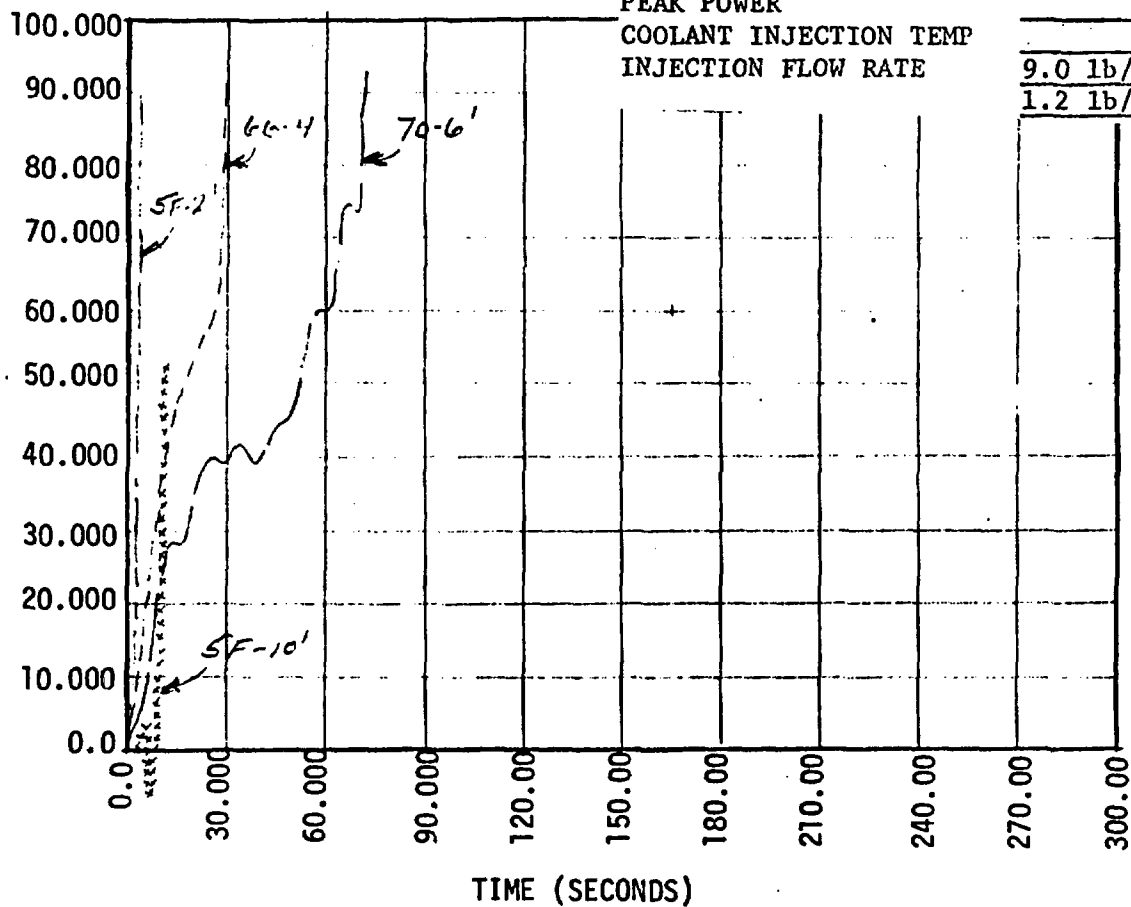
C. HEATER THERMOCOUPLE DATA

Rod/Elev.	Initial Temp. (°F)	Max. Temp. (°F)	Turnaround Time (Sec)	Quench Time (Sec)
5F/2'	646	652	2	8
5F/4'				
5F/6'				
5F/8'				
5F/10'	626	675	10	16
5G/2'	633	643	2	8
5G/4'				
5G/6'	1110	1172	10	90
5G/8'				
5G/10'	606	680	12	76
6G/2'	641	652	3	9
6G/4'	910	948	7	36
6G/6'				
6G/8'				
6G/10'	695	747	14	22
3H/2'				
3H/4'				
3H/6'				
3H/8'				
3H/10'	611	675	26	98
4G/4'	1052	1091	7	30
4G/6'				
4G/10'	622	669	12	26
4H/4'	933	975	9	46
4H/6'				
4H/10'	694	751	14	22
7D/4'	915	950	7	42
7D/6'	1038	1105	10	76
7D/10'				





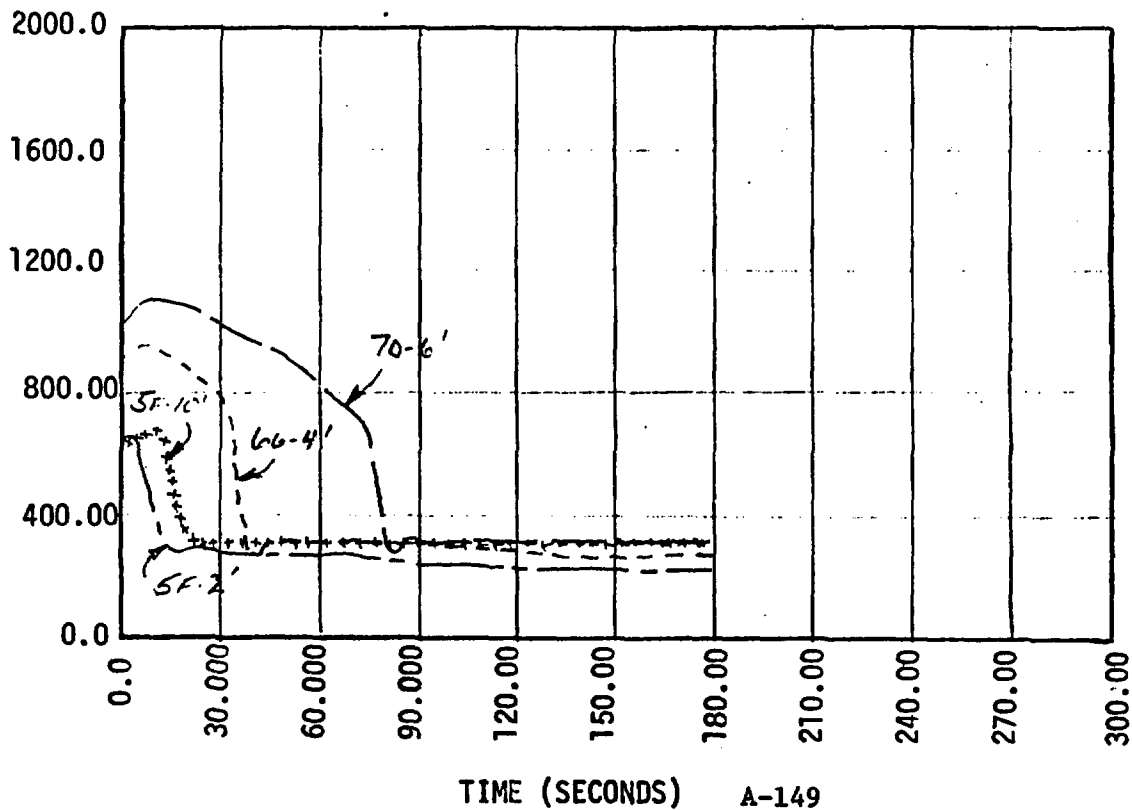
HEAT TRANSFER COEFFICIENT (BTU/HR/FT**2/DEG F)



RUN NO. _____
 PRESSURE _____
 INITIAL CLAD TEMP _____
 PEAK POWER _____
 COOLANT INJECTION TEMP _____
 INJECTION FLOW RATE _____

5115
61 psia
1110°F
0.759 kw/ft
154°F
9.0 lb/sec first 14 sec
1.2 lb/sec after 14 sec

CLAD TEMPERATURE (DEG. F)



C

C

C

|

FLECHT-SET RUN SUMMARY SHEET

RUN NO. 5214

DATE 3/3/73

A. RUN CONDITIONS

Containment Pressure	61	psia
Initial Clad Temperature	1103	°F
Peak Power	0.646*	kw/ft
Coolant Supply Temperature	159	°F
Injection Rate	10.2 lb/sec first 14 sec, 1.19 lb/sec after 14 sec	
Loop Resistance Coefficient	$(\Delta\rho_{loop}/1/2 \rho V_{hotleg}^2)$	29.1

B. INITIAL HOUSING TEMPERATURES

Elevation (ft)	Initial Temperature (°F)
0	274
2	303
4	308
6	314
8	299
10	299
12	268

*All 70 heater rods had same power. Rods 1A, 2A, 4A, 7A, 9A, 10A, 1B, 10B, 1D, 10D, 1G, 10G, 1J, 10J, 1K, 2K, 4K, 7K, 9K, and 10K were disconnected from power supply.

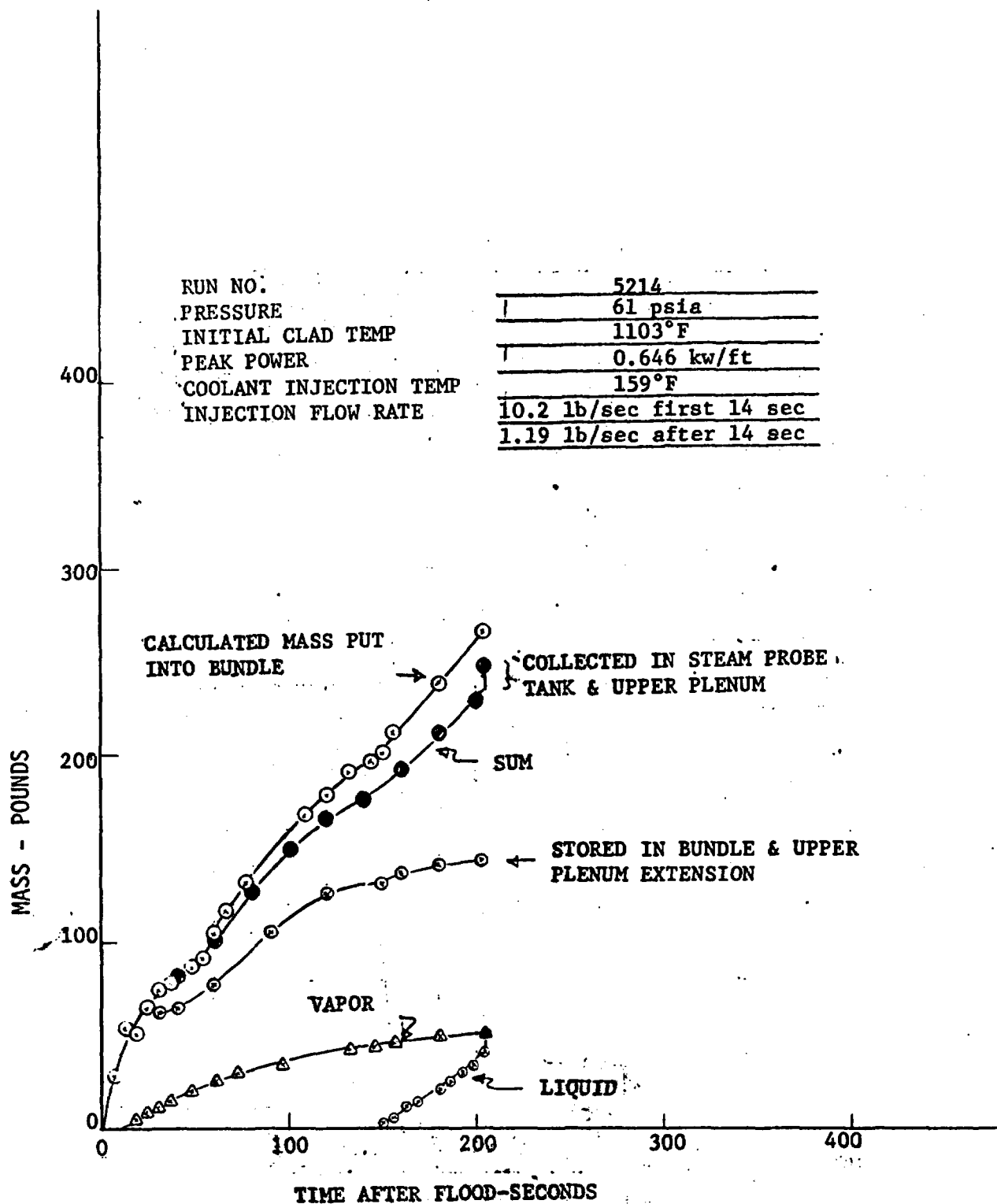
FLECHT-SET RUN SUMMARY SHEET (Cont)

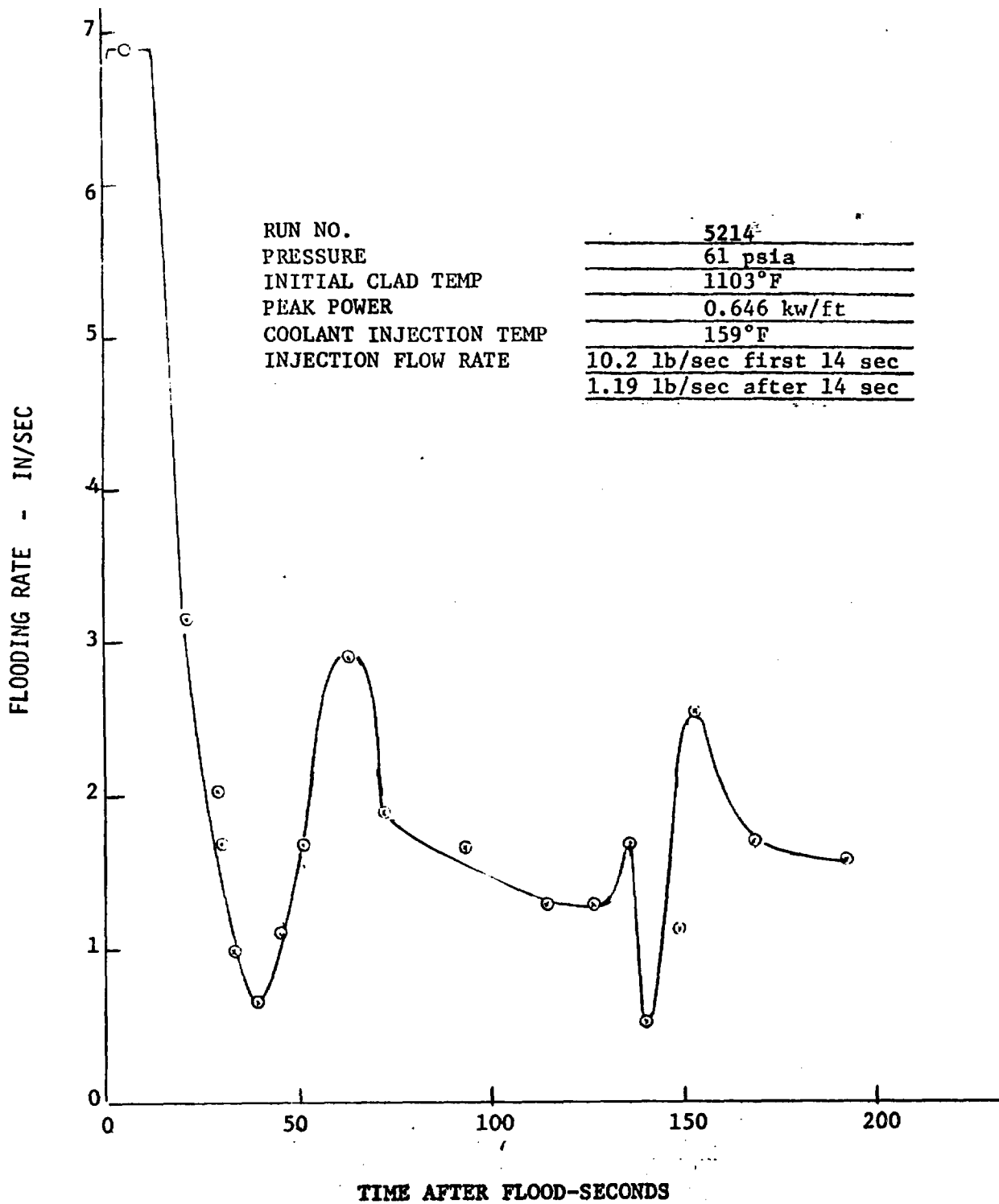
RUN NO. 5214

DATE 3/3/73

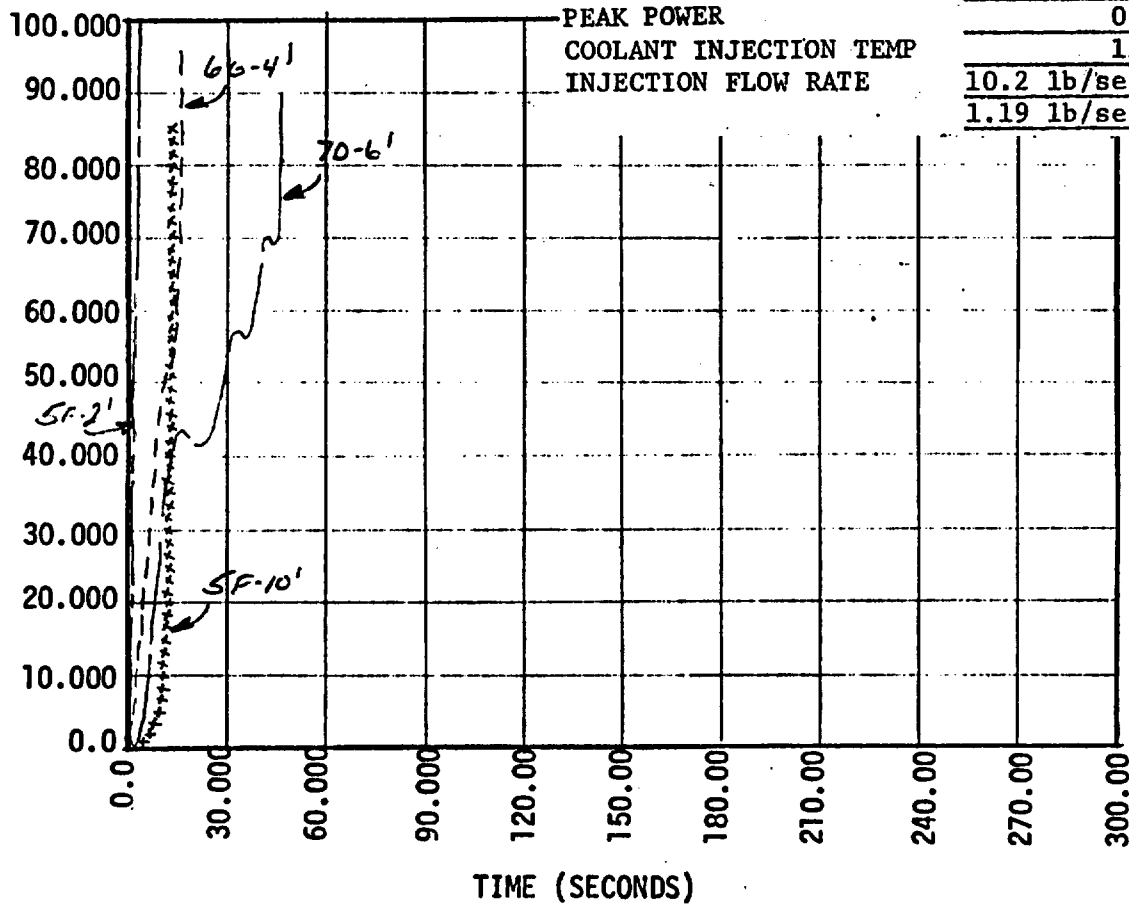
C. HEATER THERMOCOUPLE DATA

Rod/Elev.	Initial Temp. (°F)	Max. Temp. (°F)	Turnaround Time (Sec)	Quench Time (Sec)
5F/2'	633	634	1	7
5F/4'				
5F/6'				
5F/8'				
5F/10'	633	679	12	19
5G/2'	633	634	1	6
5G/4'				
5G/6'	1103	1156	8	64
5G/8'				
5G/10'	673	673	0	24
6G/2'	643	644	1	6
6G/4'	905	922	5	23
6G/6'				
6G/8'				
6G/10'	697	743	12	20
3H/2'				
3H/4'				
3H/6'				
3H/8'				
3H/10'	617	661	11	40
4G/4'	1032	1068	6	22
4G/6'				
4G/10'	628	670	11	24
4H/4'	924	954	7	28
4H/6'				
4H/10'	697	748	13	20
7D/4'	905	927	6	28
7D/6'	1030	1082	8	52
7D/10'				





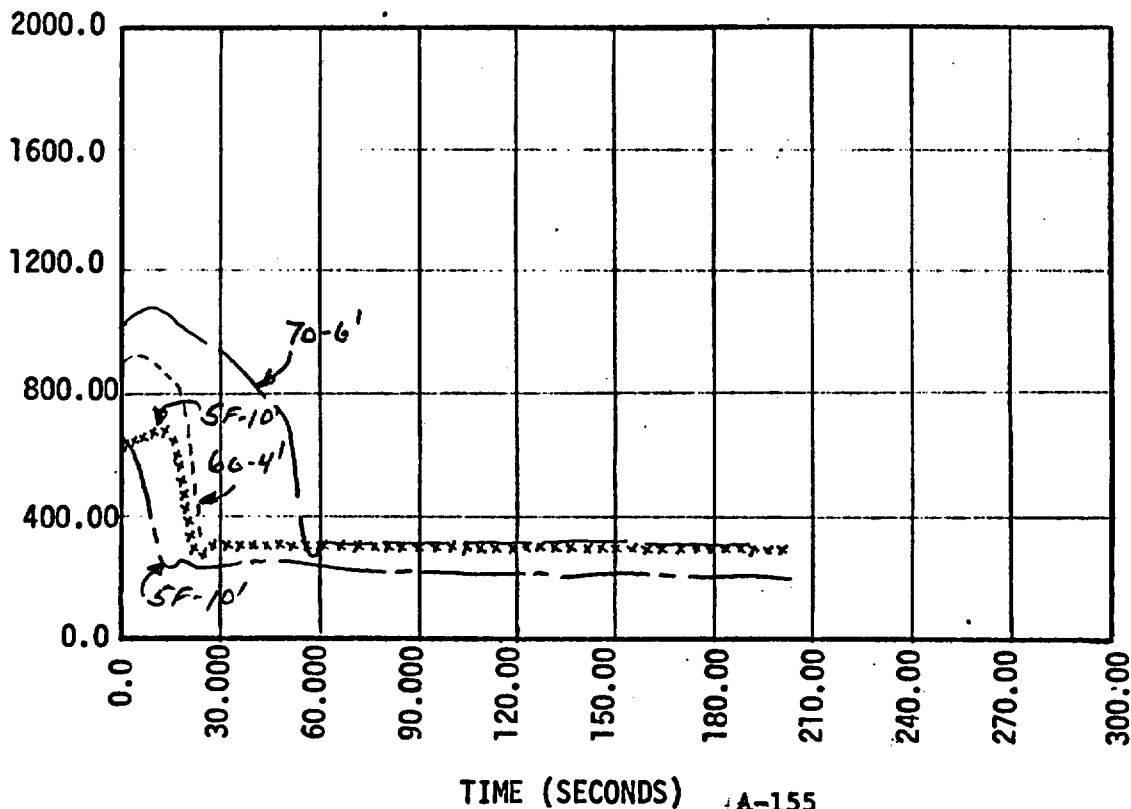
HEAT TRANSFER COEFFICIENT (BTU/HR/FT**2/DEG F)



PRESSURE
INITIAL CLAD TEMP
PEAK POWER
COOLANT INJECTION TEMP
INJECTION FLOW RATE

61 psia
1103°F
0.646 kw/ft
159°F
10.2 lb/sec first 14 sec
1.19 lb/sec after 14 sec

CLAD TEMPERATURE (DEG. F)



FLECHT-SET RUN SUMMARY SHEET

RUN NO. 5316

DATE 3/9/73

A. RUN CONDITIONS

Containment Pressure	61.3	psia
Initial Clad Temperature	1107	°F
Peak Power	.646*	kw/ft
Coolant Supply Temperature	159	°F
Injection Rate	10.17 lb/sec first 14 sec, 1.18 lb/sec after 14 sec	
Loop Resistance Coefficient ($\Delta\rho_{loop}/1/2 \rho V^2_{hotleg}$)	32.0	

B. INITIAL HOUSING TEMPERATURES

Elevation (ft)	Initial Temperature (°F)
0	287
2	393
4	454
6	488
8	456
10	423
12	310

*All 90 heater rods had same power.

FLECHT-SET RUN SUMMARY SHEET (Cont)

RUN NO. 5316

DATE 3/9/73

C. HEATER THERMOCOUPLE DATA

Rod/Elev.	Initial Temp. (°F)	Max. Temp. (°F)	Turnaround Time (Sec)	Quench Time (Sec)
5F/2'	671	675	1	7
5F/4'				
5F/6'				
5F/8'				
5F/10'	654	690	31	37
5G/2'	662	668	2	7
5G/4'				
5G/6'	1107	1160	12	89
5G/8'				
5G/10'	644	702	22	59
6G/2'	671	681	2	7
6G/4'	946	969	6	30
6G/6'				
6G/8'				
6G/10'	712	758	15	22
3H/2'				
3H/4'				
3H/6'				
3H/8'				
3H/10'	612	676	25	47
4G/4'	1059	1081	5	38
4G/6'				
4G/10'	639	686	24	32
4H/4'	958	985	6	34
4H/6'				
4H/10'	712	761	20	31
7D/4'	944	971	6	39
7D/6'	1055	1106	11	77
7D/10'				

RUN NO.

5316

PRESSURE

61.3 psia

INITIAL CLAD TEMP

1107°F

PEAK POWER

.646 kw/ft

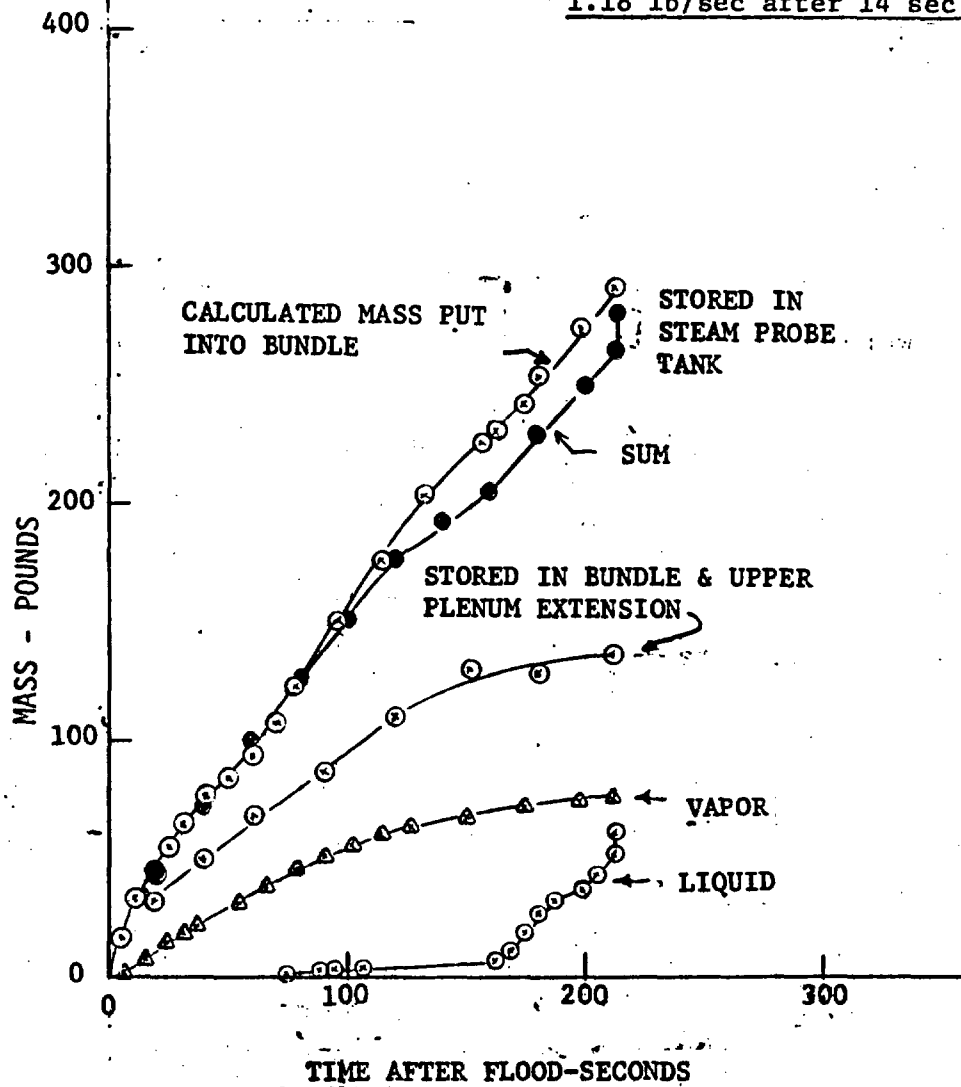
COOLANT INJECTION TEMP

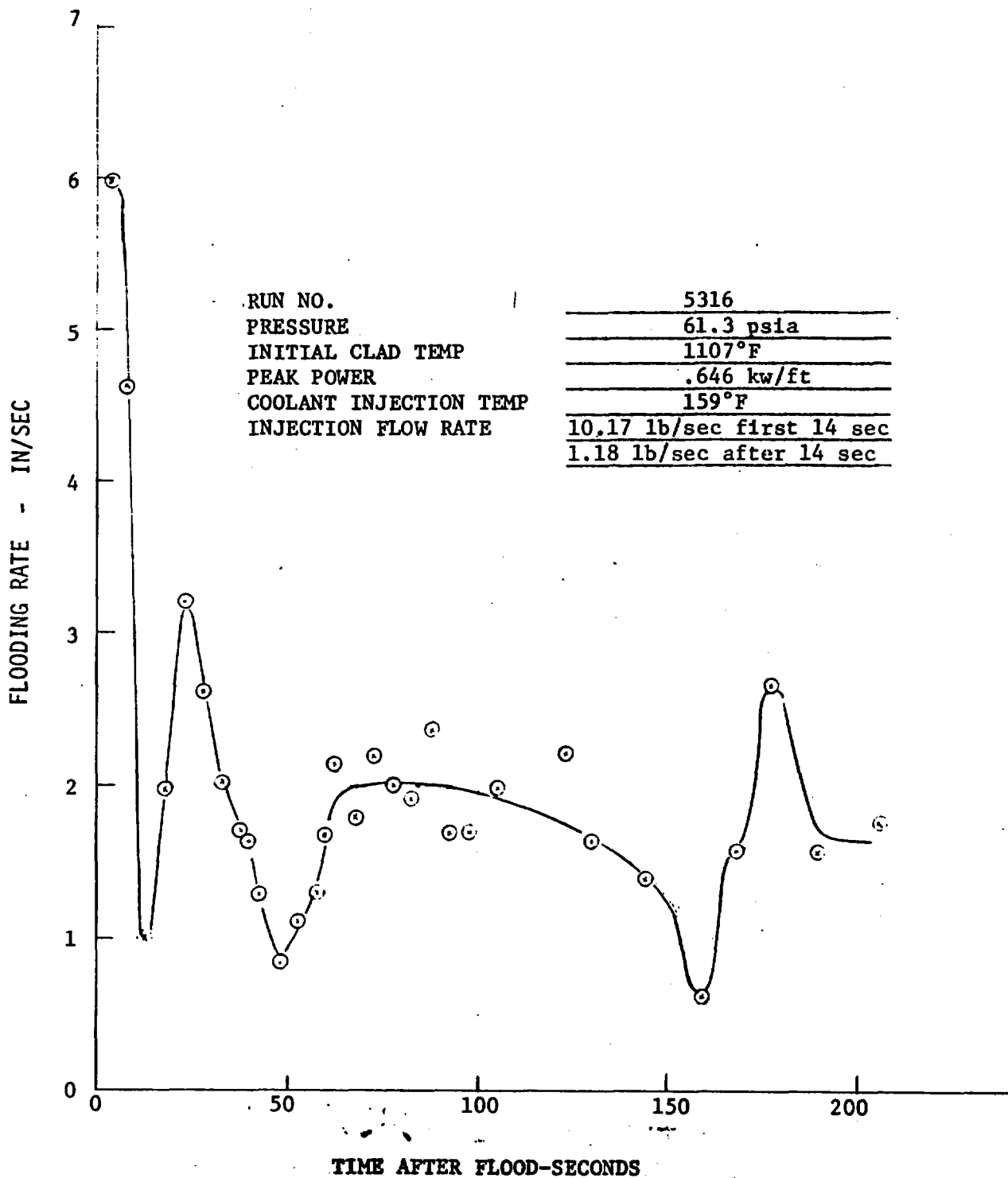
159°F

INJECTION FLOW RATE

10.17 lb/sec first 14 sec

1.18 lb/sec after 14 sec

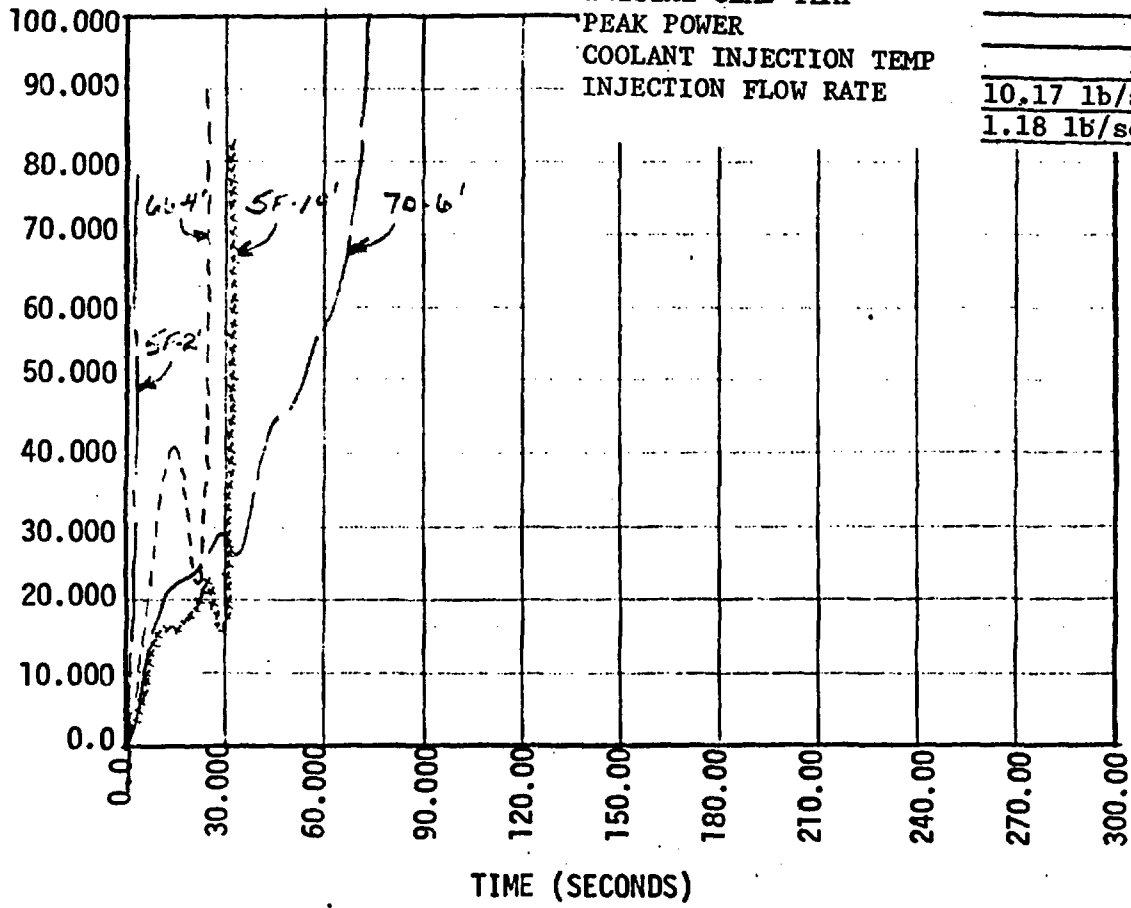




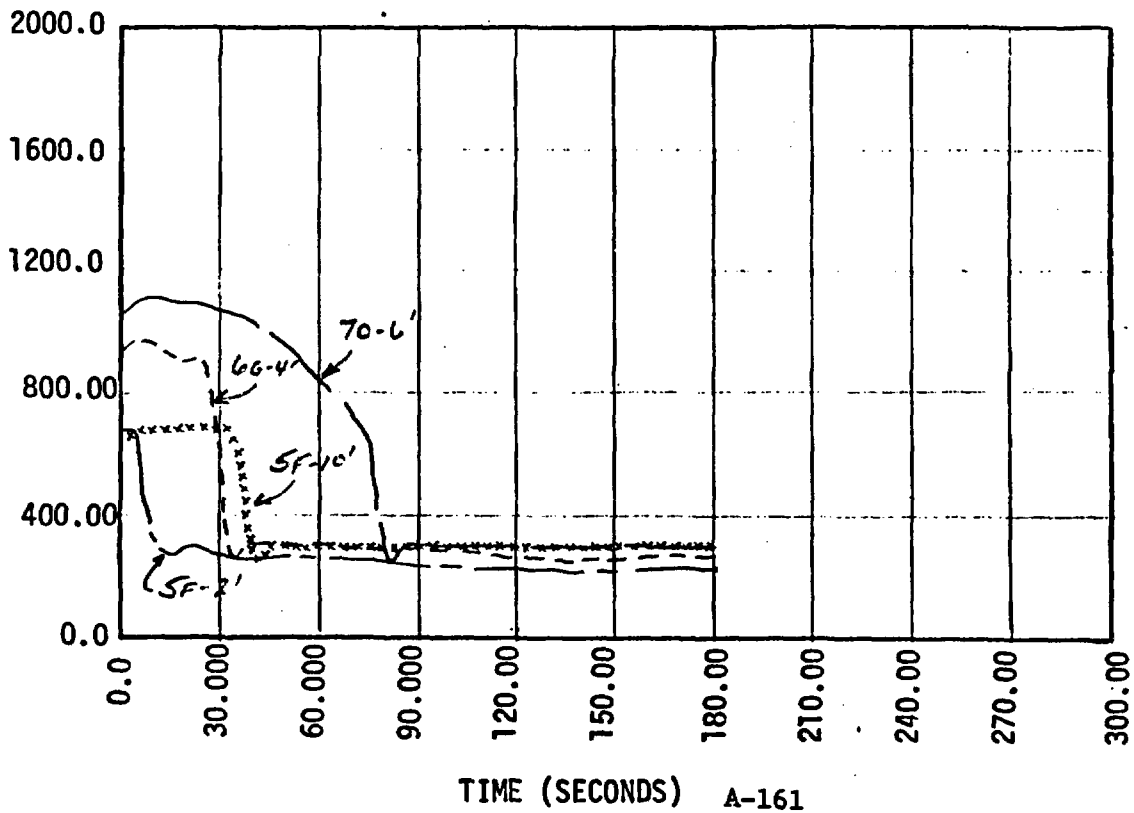
RUN NO.
PRESSURE
INITIAL CLAD TEMP
PEAK POWER
COOLANT INJECTION TEMP
INJECTION FLOW RATE

5316
61.3 psia
1107°F
.646 kw/ft
159°F
10.17 lb/sec first 14 sec
1.18 lb/sec after 14 sec

HEAT TRANSFER COEFFICIENT (BTU/HR/FT**2/DEG F)



CLAD TEMPERATURE (DEG. F)



1

.

2

3

4

5

FLECHT-SET RUN SUMMARY SHEET

RUN NO. 5413

DATE 3/10/73

A. RUN CONDITIONS

Containment Pressure	60.9	psia
Initial Clad Temperature	1125	°F
Peak Power	0.646*	kw/ft
Coolant Supply Temperature	155	°F
Injection Rate	10.8 lb/sec first 14 sec,	1.25 lb/sec after 14 sec
Loop Resistance Coefficient	$(\Delta p_{loop}/1/2 \rho V^2_{hotleg})$	30.5

B. INITIAL HOUSING TEMPERATURES

Elevation (ft)	Initial Temperature (°F)
0	304
2	545
4	712
6	797
8	715
10	545
12	344

*All 90 heater rods had same power.

FLECHT-SET RUN SUMMARY SHEET (Cont)

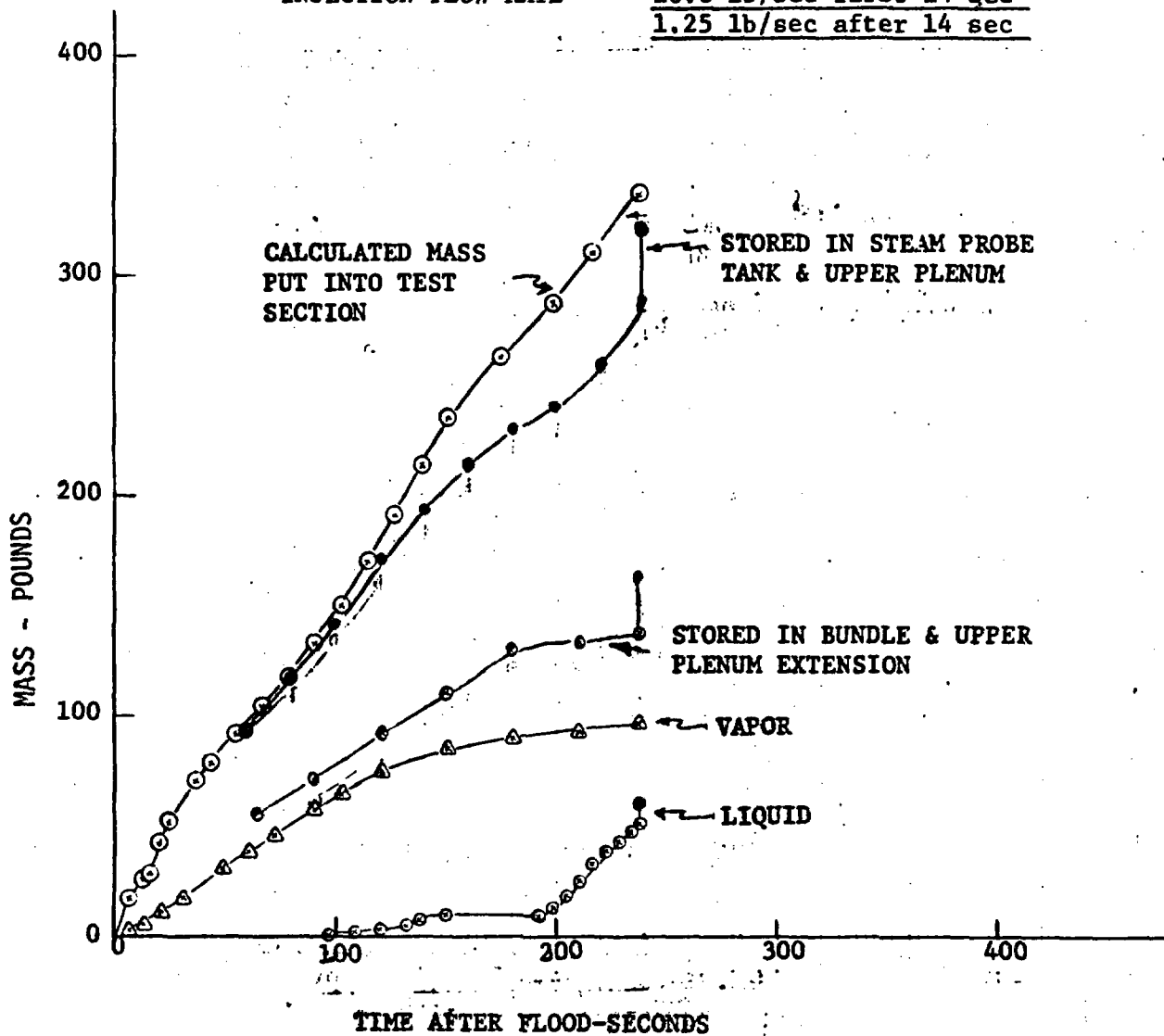
RUN NO. 5413

DATE 3/10/73

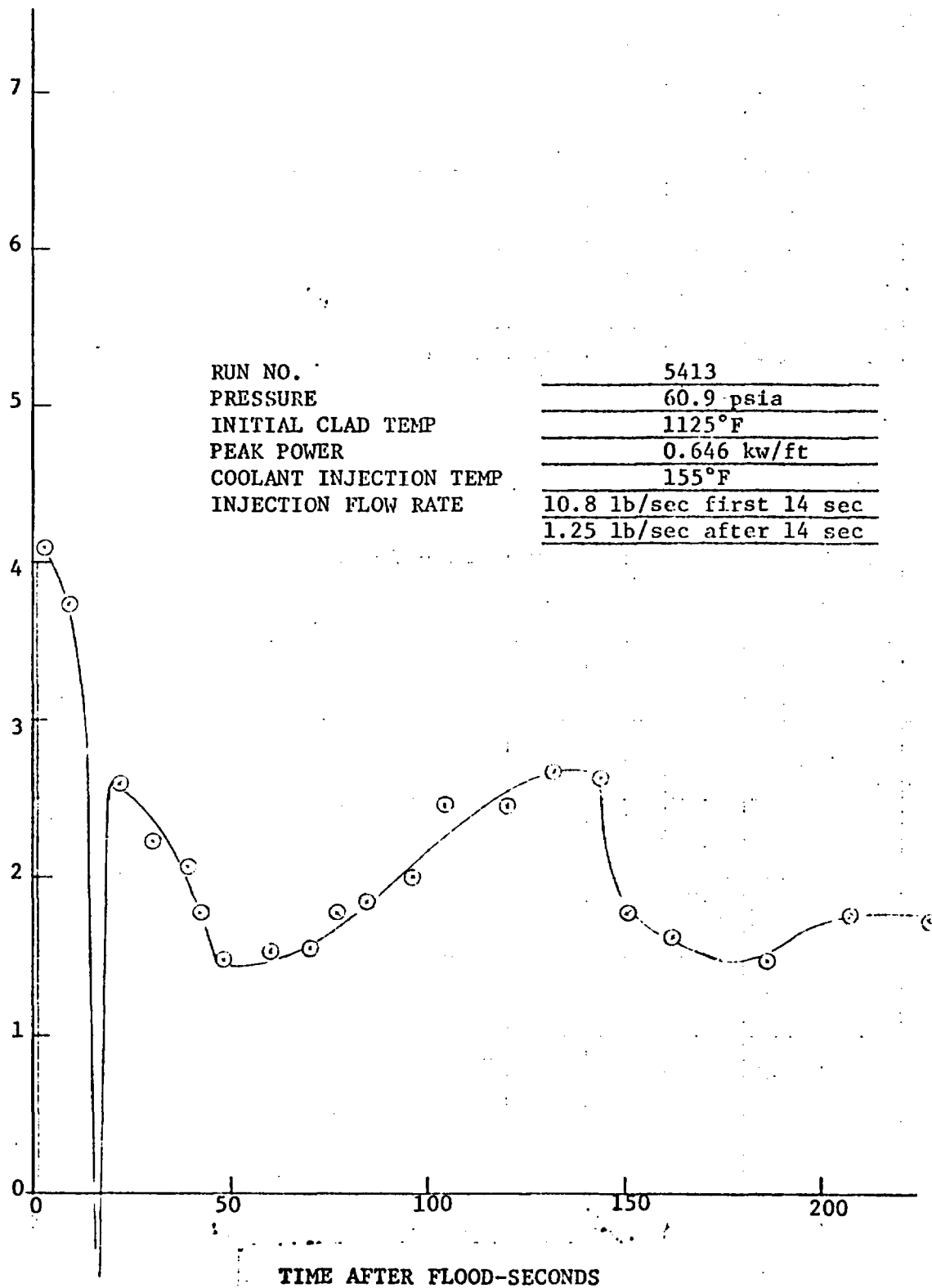
C. HEATER THERMOCOUPLE DATA

Rod/Elev.	Initial Temp. (°F)	Max. Temp. (°F)	Turnaround Time (Sec)	Quench Time (Sec)
5F/2'	762	762	0	7
5F/4'				
5F/6'				
5F/8'				
5F/10'	626	671	22	38
5G/2'	760	760	0	8
5G/4'				
5G/6'	1125	1159	7	118
5G/8'				
5G/10'				
6G/2'	765	768	1	9
6G/4'	1067	1071	2	48
6G/6'				
6G/8'				
6G/10'	680	724	16	23
3H/2'				
3H/4'				
3H/6'				
3H/8'				
3H/10'	580	629	24	44
4G/4'	1151	1161	2	57
4G/6'				
4G/10'	607	649	21	28
4H/4'	1079	1087	3	59
4H/6'				
4H/10'				
7D/4'	1060	1066	2	53
7D/6'	1072	1110	7	108
7D/10'				

RUN NO.	5413
PRESSURE	60.9 psia
INITIAL CLAD TEMP	1125°F
PEAK POWER	0.646 kw/ft
COOLANT INJECTION TEMP	155°F
INJECTION FLOW RATE	10.8 lb/sec first 14 sec
	1.25 lb/sec after 14 sec



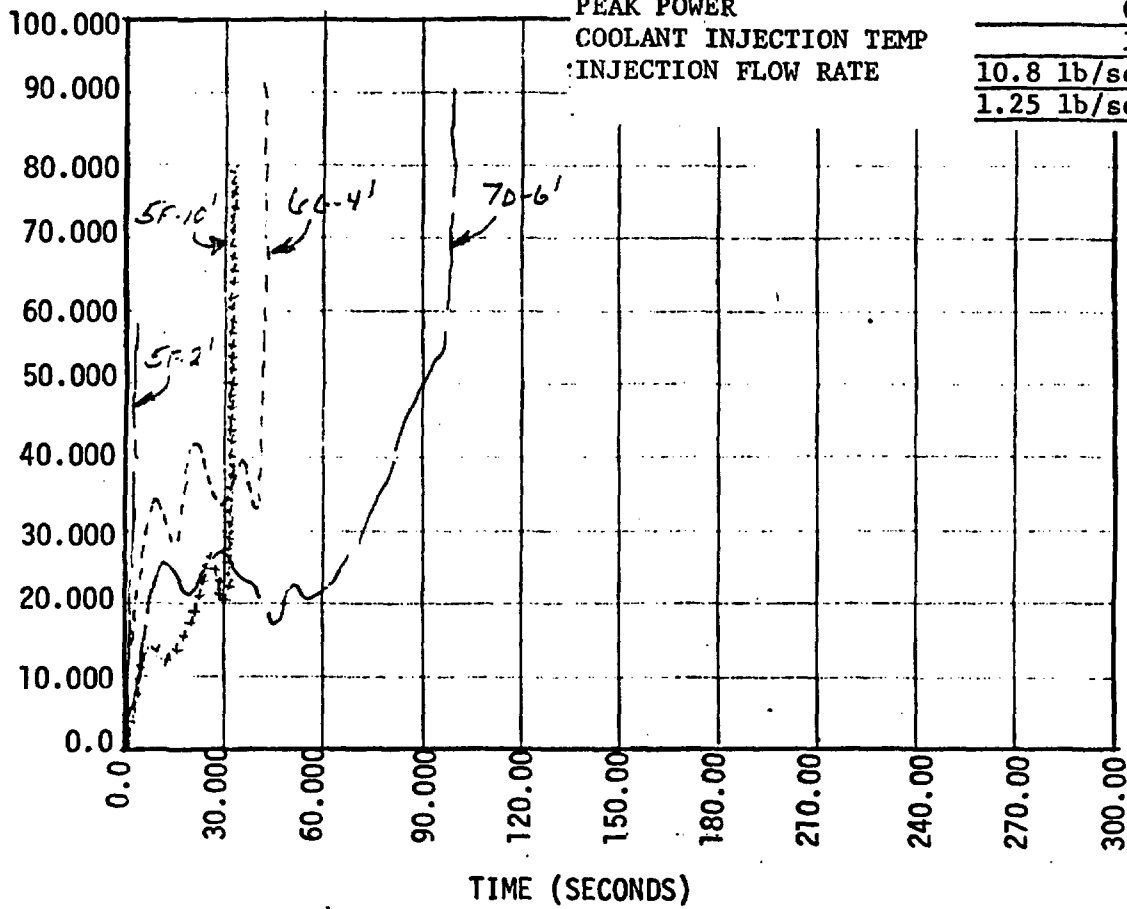
FLOODING RATE - IN/SEC



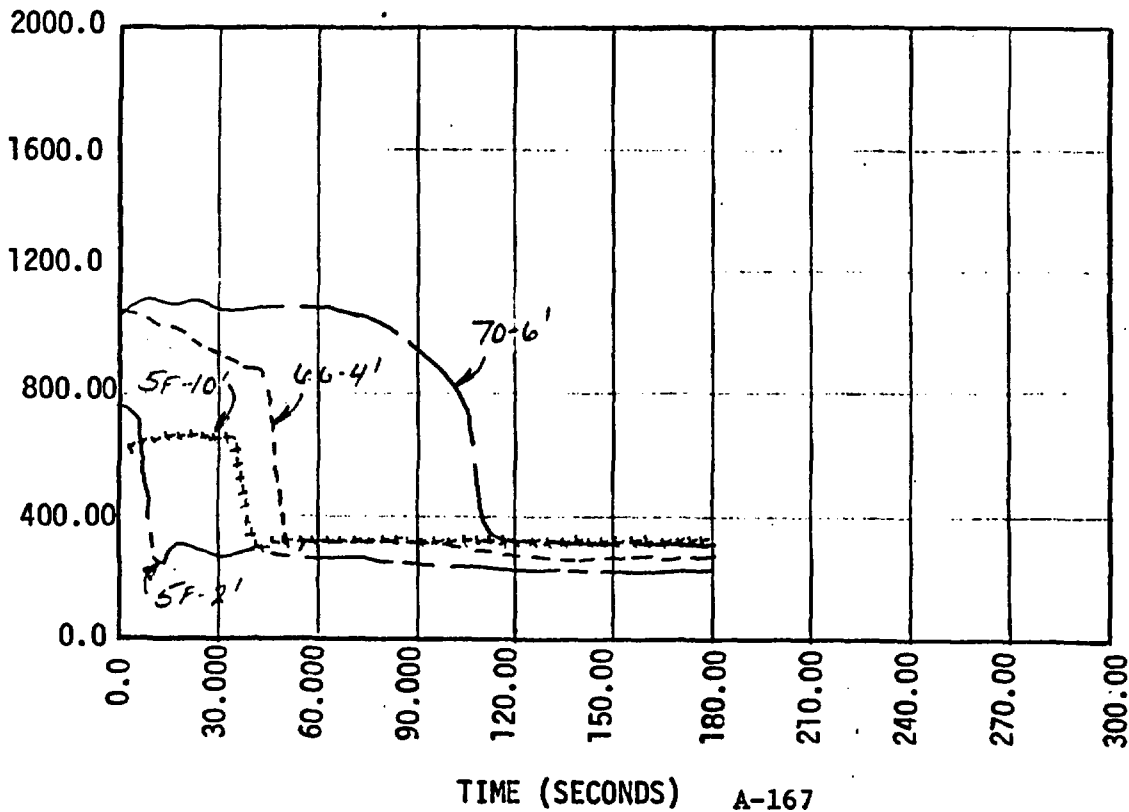
RUN NO.
 PRESSURE
 INITIAL CLAD TEMP
 PEAK POWER
 COOLANT INJECTION TEMP
 INJECTION FLOW RATE

5413
 60.9 psia
 1125°F
 0.646 kw/ft
 155°F
 10.8 lb/sec first 14 sec
 1.25 lb/sec after 14 sec

HEAT TRANSFER COEFFICIENT (BTU/HR/FT**2/DEG F)



CLAD TEMPERATURE (DEG. F)





APPENDIX B

LOW CLAD TEMPERATURE FLECHT TESTS

B.1 INTRODUCTION

B.1.1 Rationale for Tests

After the blowdown phase of a LOCA in a PWR the radial temperature distribution of the fuel pins will vary over a wide range and will be a function of the steady-state radial power profile. To determine the peak clad temperature encountered, the conditions of the hottest and average fuel assemblies are used for testing and analysis. Accordingly, correlations for total mass effluent have been developed for these conditions. The colder assemblies, however, will generate less steam and therefore entrain less liquid, resulting in less mass effluent. Consideration of this effect would result in the prediction of higher flooding rates into the core after a LOCA, thereby improving heat transfer and reducing calculated peak clad temperatures.

The original series of FLECHT tests covered a range of initial peak clad temperatures at the time of bottom of core recovery of 800°F to 2200°F. This additional series of tests extended the range of initial temperatures down to nearly saturation temperature.

B.1.2 Objective

The objective of the tests was to determine the amount of entrained liquid collected as well as the total mass effluent for a series of low initial peak clad temperature FLECHT tests. A run schedule was developed which varied the peak clad temperature, the peak linear power, the pressure, the flooding rate, and the amount of coolant subcooling.

B.2 TEST DESCRIPTION

B.2.1 Facility Layout

The tests were similar to the FLECHT series (Reference 1) and did not use the FLECHT-SET simulated loop piping and system components. A forced injection directly into the lower plenum of the test section was employed, and the bundle was vented through a pressure control valve located in a short exhaust line. A baffle was also located in the upper plenum directly in front of the exhaust line to separate entrained liquid from the exhaust flow as shown in Figure B-1. The upper plenum did not contain the aluminum filler plates used for Phase A FLECHT-SET and was continuously drained into a vertical collection tank.

B.2.2 Instrumentation and Data Acquisition

The test section flow housing and rod bundle instrumentation were the same as that used in FLECHT-SET Phase A (see Section 2.2). These low clad temperature tests were performed before the additional housing axial differential pressure transducers were added at the higher elevations. The injection flow was measured using the same Brooks rotameters as for Phase A tests and the output recorded on a pen recorder. For some of the tests with constant injection rate a different 0-35 gpm nonrecording rotameter was used. The upper plenum pressure, rather than containment pressure as in Phase A, was maintained constant and was recorded on a pen recorder.

The addition of the liquid collection tank necessitated supplementary instrumentation in addition to that of Phase A. This consisted of two wall thermocouples and a differential pressure transducer to indicate temperature and water level in the liquid collection tank. The data acquisition systems used were the same as in the Phase A testing.

B.2.3 Test Procedure

The flow housing was initially heated to the proper temperature profile as specified by the FLECHT criteria (see Section 2.4) except as noted below. Because many of the tests were run at very low temperatures, the specified housing temperature was often very close to the desired initial peak clad

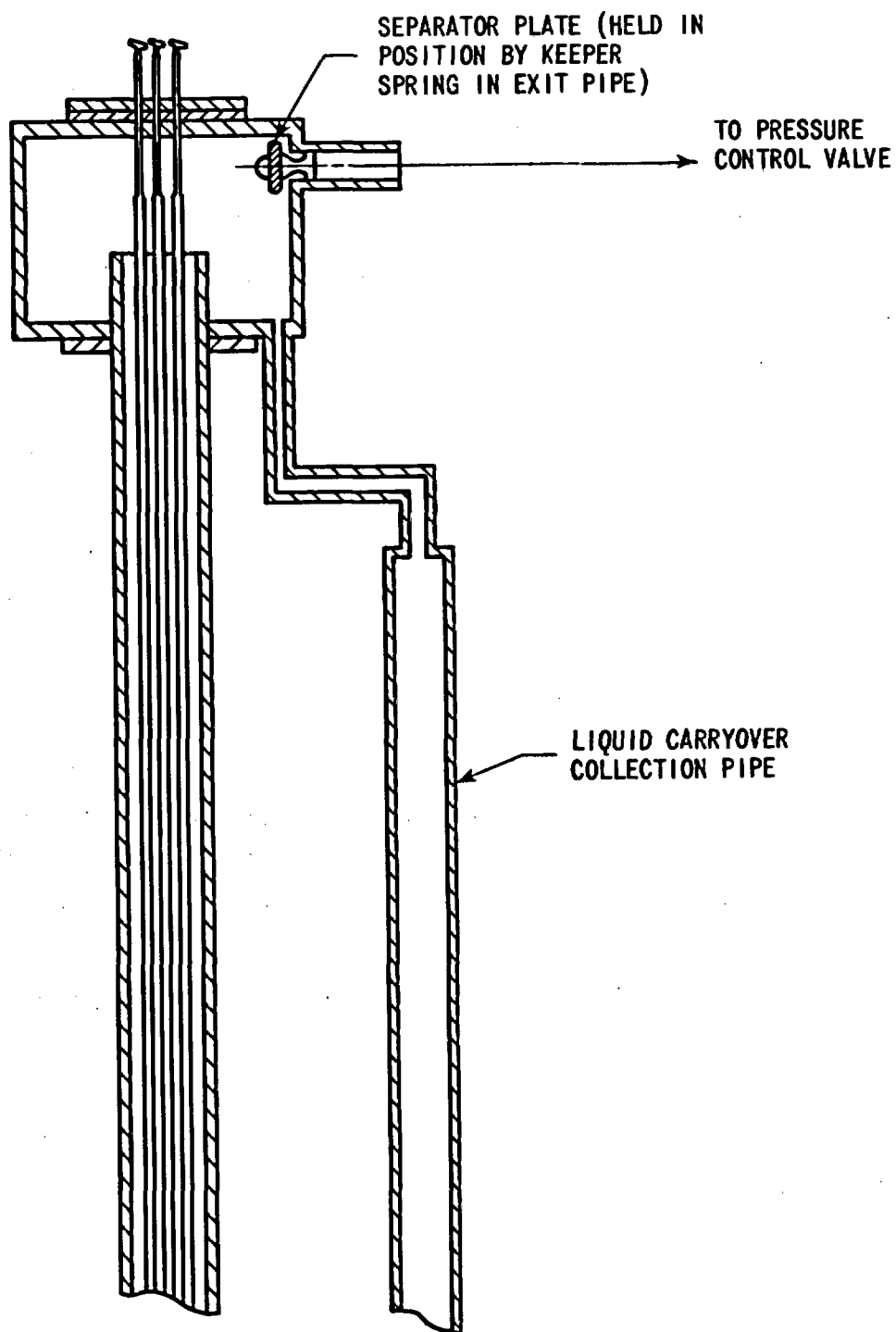


Figure B-1. Low Initial Temperature Series Test Section Configuration

temperature. Thus, it was not possible to heat the housing, as in Phase A tests by radiation from periodically energized heater rods, without heating the rods above the desired initial temperature. Additional strip heaters were consequently added to the test section housing along with several temperature controllers such that the desired temperature distribution could be obtained.

For some of the runs with very low initial clad temperatures, the FLECHT criteria specified housing temperatures that were higher than the desired initial clad temperature. In these cases, the housing was heated to the same temperature profile as the rods. In a few of the runs, with the specified initial rod temperatures very close to the saturation temperature, the housing was heated uniformly to saturation temperature.

The liquid collection tank and upper plenum were heated to 20°F above saturation temperature to avoid condensation. The lower plenum was heated to the temperature of the injection coolant. After the desired wall temperatures were attained, the test section was pressurized and full power applied to the rods. Flooding was automatically initiated when the desired temperature was reached by the designated heater rod. The test continued until a sufficient quantity of liquid was collected, which was often after the bundle had completely quenched. After the run was terminated by ceasing injection flow and bundle power, the test section was depressurized. At this time the water in the liquid collection tank was drained and weighed. During the run the thermocouple and differential and absolute pressure data were recorded by the data acquisition system previously described in Section B.2.2.

The stepped flooding rates specified for many of the runs were produced by operating various combinations of electrically actuated valves controlled by timing devices. This technique was satisfactory and produced repeatable flow rates.

B.3 CALCULATIONS AND DATA REDUCTION

The purpose of these tests was to measure the total mass effluent and the amount of liquid collected as a function of the various test parameters. As a result, the data reduction and analysis concentrated on these two quantities.

The rod thermocouple data were recorded and converted to engineering units. The data for selected thermocouples were then examined to determine initial clad temperature, maximum clad temperature, quench temperature, turnaround time, and quench time. This information is presented in the summary sheets in Appendix B-1.

The housing axial differential pressure data, the absolute pressure data, the liquid collection tank differential pressure data, and the wall thermocouple data were converted to engineering units. The housing axial pressure data were used to calculate the mass stored in the test section. It was assumed that the friction and acceleration pressure drop terms were negligible and that the pressure drop indicated elevation head only. This assumption is justified in Section 3.2. The mass storage data are presented along with the mass of liquid collected and the mass injected data in the summary sheets for each run.

For the parametric studies, two quantities were considered:

1. The mass of liquid collected by the time of the midplane quench.
2. The average mass effluent fraction calculated up to the time of the midplane quench.

The first variable is obtained directly from the data. The second quantity is derived from the following definition:

$$\text{Average mass effluent fraction} = \frac{\text{Mass out of test section}}{\text{Mass injected into test section}} \quad (1)$$

The mass out of the test section was not measured, but since

$$\text{Mass out of test section} = \text{Mass injected into test section} - \text{Mass stored in test section} \quad (2)$$

Equation (1) may be written as:

$$\text{Average mass effluent fraction} = 1 - \frac{\text{Mass stored in test section}}{\text{Mass injected into test section}}$$

This equation was evaluated at the time of the quench of the midplane heater rod thermocouples, assuming that the mass stored in the test section was indicated by the housing axial pressure data.

B.4 DISCUSSION OF TEST RESULTS

B.4.1 Run Summary

Table B-1 presents a run schedule with initial conditions and a summary of results. Detailed data sheets for each run are contained in Appendix B-1.

It should be noted with regard to the determination of quench times and temperatures, turnaround times and temperatures, and initial temperature that the VIDAR recorded data every 5.5 seconds and in some test runs the rods were completely quenched in about 40 seconds. The 2 ft level thermocouple usually quenched in less than 10 seconds. The error for the turnaround times and quench times is approximately ± 3 seconds.

Figure B-2 shows the different nominal flooding rates that were used and which are referenced in Table B-1. The data sheets for each run present the actual measured flooding rate with the exception of those runs for which the flow was not recorded. For those runs, the flooding rates were assumed to be the nominal specified values.

TABLE B-1

LOW INITIAL CLAD TEMPERATURE FLECHT TESTS - RUN CONDITIONS AND RESULTS

Run No.	Run Schedule			Pen Recorder Results					
	Pressure (psia)	Peak Power (kw/ft)	Initial Temp (°F)	Flooding Rate (in./sec)	Coolant Temp (°F)	T _{max} 6' (°F)	t _{turn} 6' (sec)	t _{6'} quench (sec)	t _{1.c} ** (sec)
0104	57	0.7	459	3.0	143	747	27	30	42
0203	60	0.7	360	3.0	144	664	27	28	41
0306	59	0.7	559	3.0	156	800	26	36	42
0405	59	0.7	449	4.0	144	627	14	15	34
0507	59	0.7	654	3.0	154	847	21	40	36
0608	60	0.7	754	3.0	149	928	20	48	33
0701	23	0.7	375	3.0	140	690	47	49	41
0802	20	0.7	453	3.0	142	729	54	78	33
1109	20	0.7	311	3.0	149	668	50	52	35
1212	19	0.7	253	A*	139	825	74	125	70
1516	22	1.0	320	B*	145	998	90	149	42
1617	24	1.2	272	B*	149	1114	96	153	33
1715	20	0.7	401	B*	147	790	86	88	45
1812	59	0.7	502	B*	151	780	42	49	75
1913	58	1.0	310	B*	156	597	15	15	60
2014	60	1.2	320	B*	150	760	25	26	36
2122	59	0.7	498	D*	149	845	38	60	138
2324	60	1.2	653	B*	145	1136	67	123	29
2420	60	0.7	508	1.5	146	963	47	78	80
2519	61	0.7	603	1.5	145	1039	48	90	60
2618	59	0.7	401	1.5	146	897	46	70	81
2823	58	0.7	670	B*	147	887	28	60	100
2921	59	0.7	660	B*	171	852	26	64	115

TABLE B-1 (Cont)

NOTES:

*The nominal flooding rates, shown in Figure B-2, are as follows:

- A. 6 in./sec for 0 3 sec
1 in./sec for 3 end
- B. 6 in./sec for 0 3 sec
3 in./sec for 3 15 sec
1 in./sec for 15 end
- C. 1.5 in./sec for 0 end
- D. 6 in./sec for 0 3 sec
3 in./sec for 3 9 sec
1 in./sec for 9 end

The actual measured flooding rates are shown on the data summary sheets for each run.

**Time when liquid collection from the upper plenum drain begins.

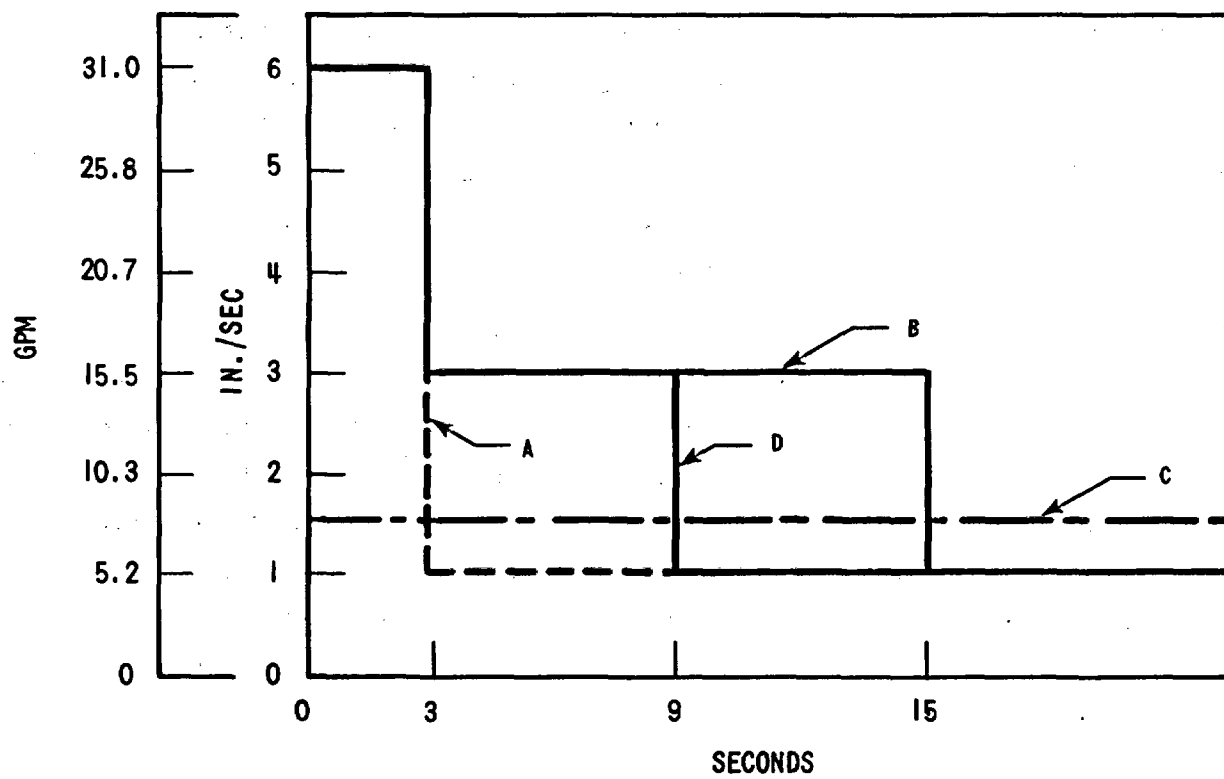


Figure B-2. Flooding Rate Profiles

B.4.2 Typical Test Results

Figures B-3 through B-6 present results for a typical test run. The first figure shows the temperature quench envelope as well as the range of quench times for each elevation. Also shown is the cold fill line. As seen, the quench envelope curve closely follows the cold fill line until the 4 ft elevation is reached. At this point it begins to diverge significantly. This indicates that there is very little steam generation until the 4 ft elevation is reached. This was true for all of the test runs performed (initial midplane clad temperature less than 750°F). The same effect is also shown by the housing axial differential pressure data, Figure B-4. The measurements plotted are the pressure difference between the particular elevation and a pressure tap in the upper plenum of the test section. The accuracy of these measurements is approximately $\pm 1\%$ of full scale or 0.1 psi.

The calculated mass balance of the test section is shown in Figure B-5. The mass injected, mass of liquid collected, and mass stored in the housing are obtained directly from the data, where the housing axial differential pressure data were assumed to indicate the mass of water stored (i.e., friction and acceleration pressure drop terms are assumed negligible). By subtracting the mass stored from the mass injected, the mass out curve is obtained. This curve shows that until about 40 seconds very little mass left the test section. Since the 4 ft elevation quenched at 36 seconds, this confirms the conclusion derived from the quench data that there is little steam generation until the 4 ft elevation is reached.

The difference between the mass out curve and the mass of liquid collected curve is the amount of steam that left the test section and possibly entrained water that left due to imperfect separation by the upper plenum exit baffle. There was no direct measurement of this quantity. Energy balance calculations indicate that the exit flow did contain some entrained water.

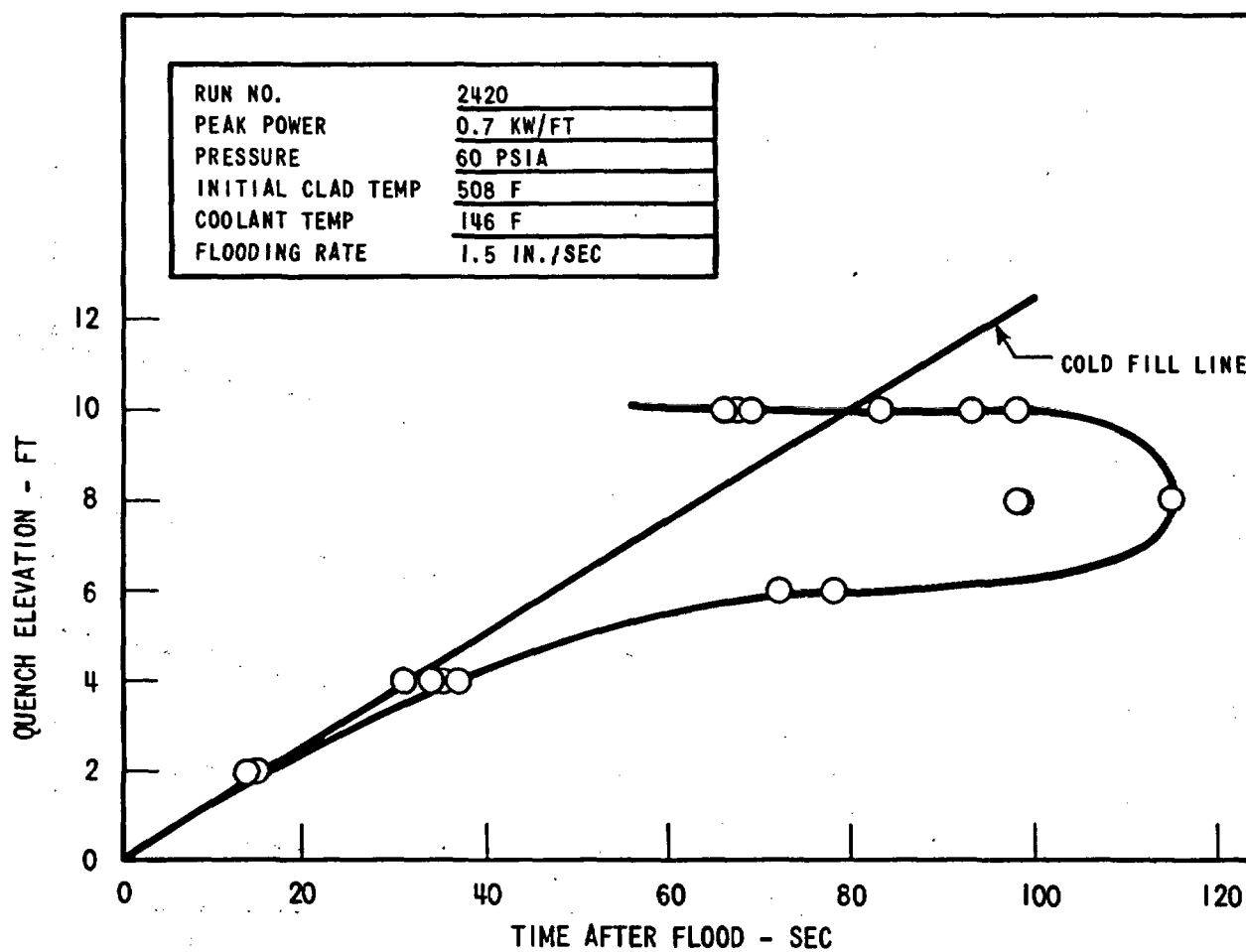


Figure B-3. Envelope of Temperature Quench Front - Run 2420

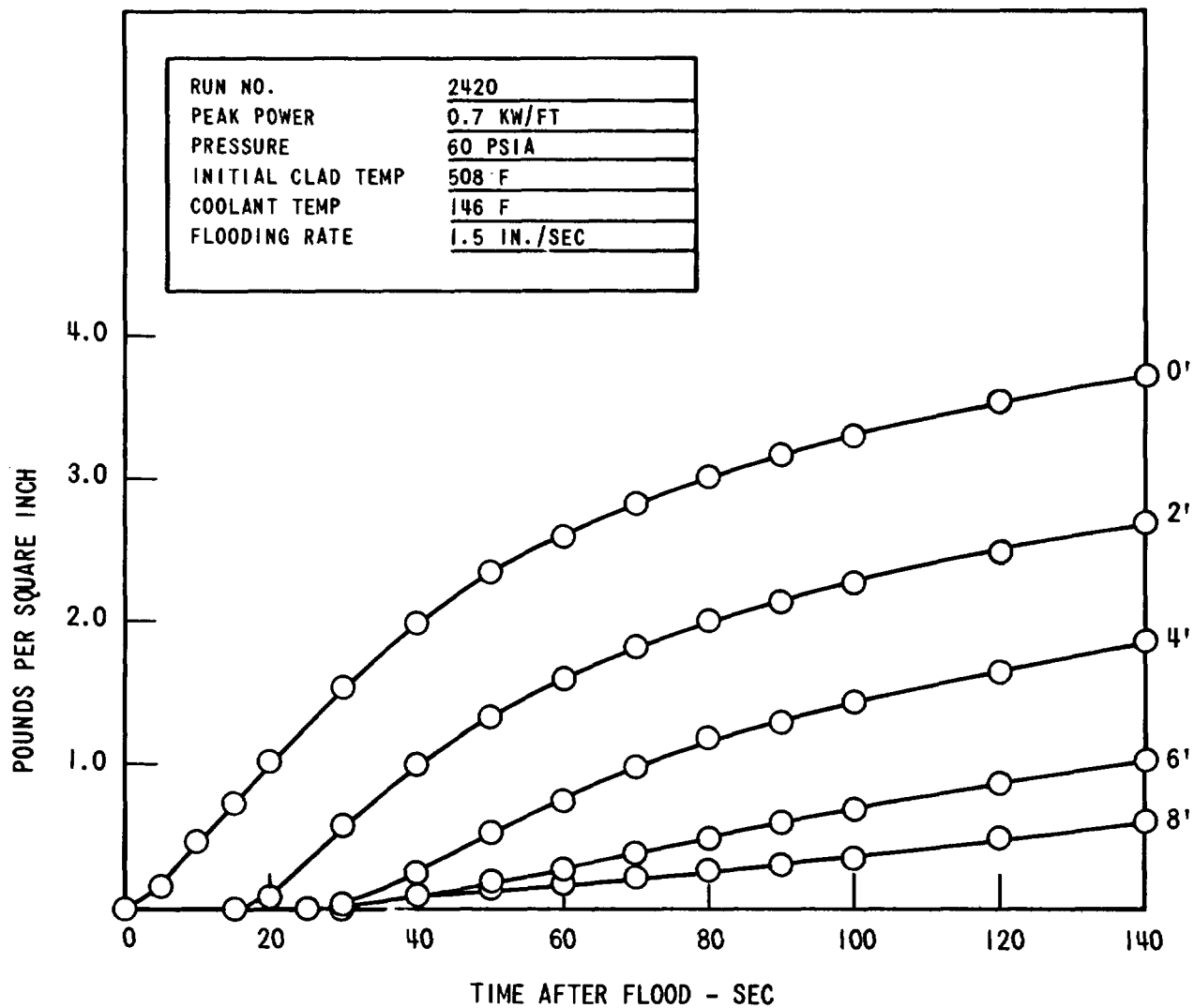


Figure B-4. Housing Axial Pressure Data - Run 2420

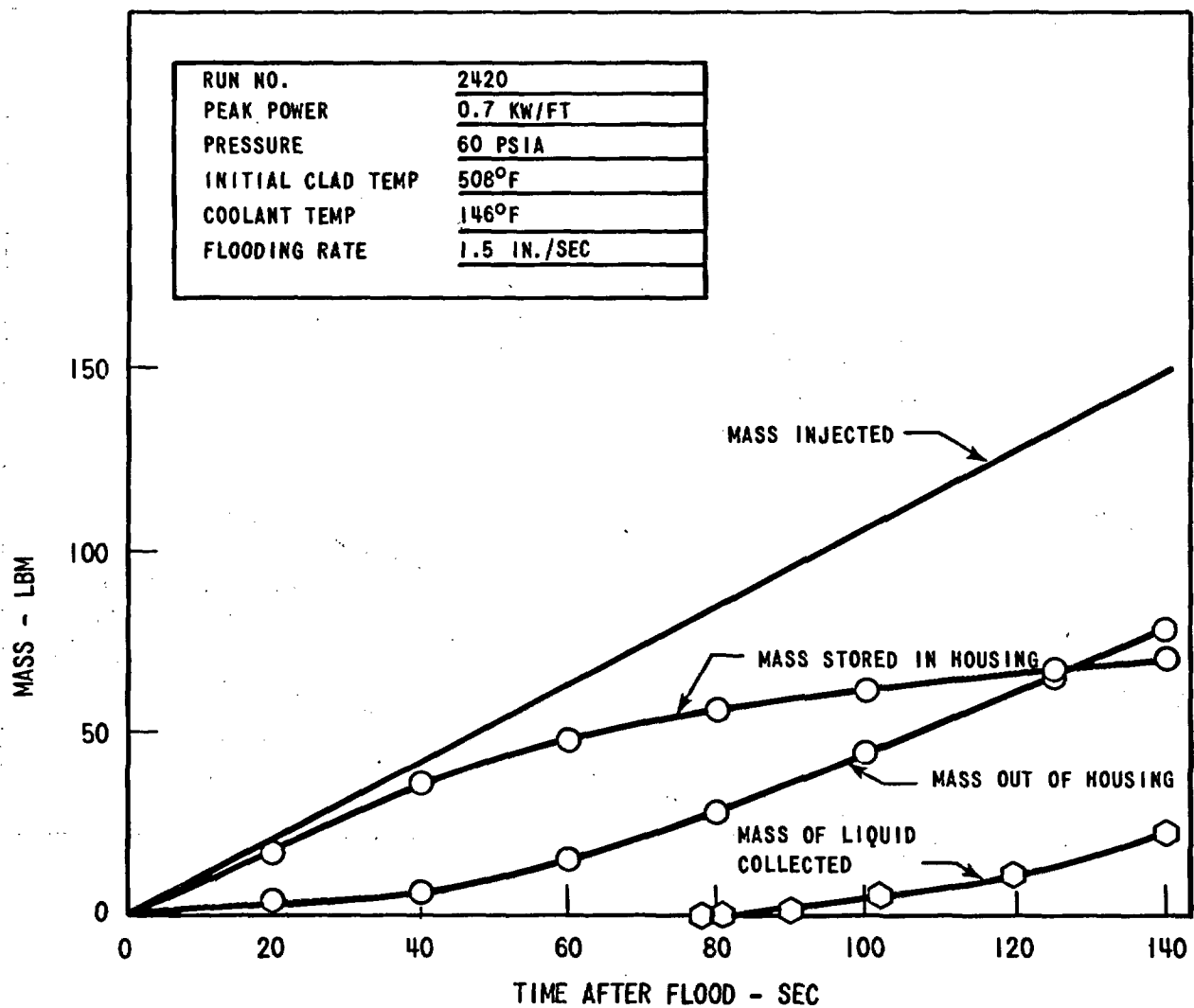


Figure B-5. Mass Calculation - Run 2420

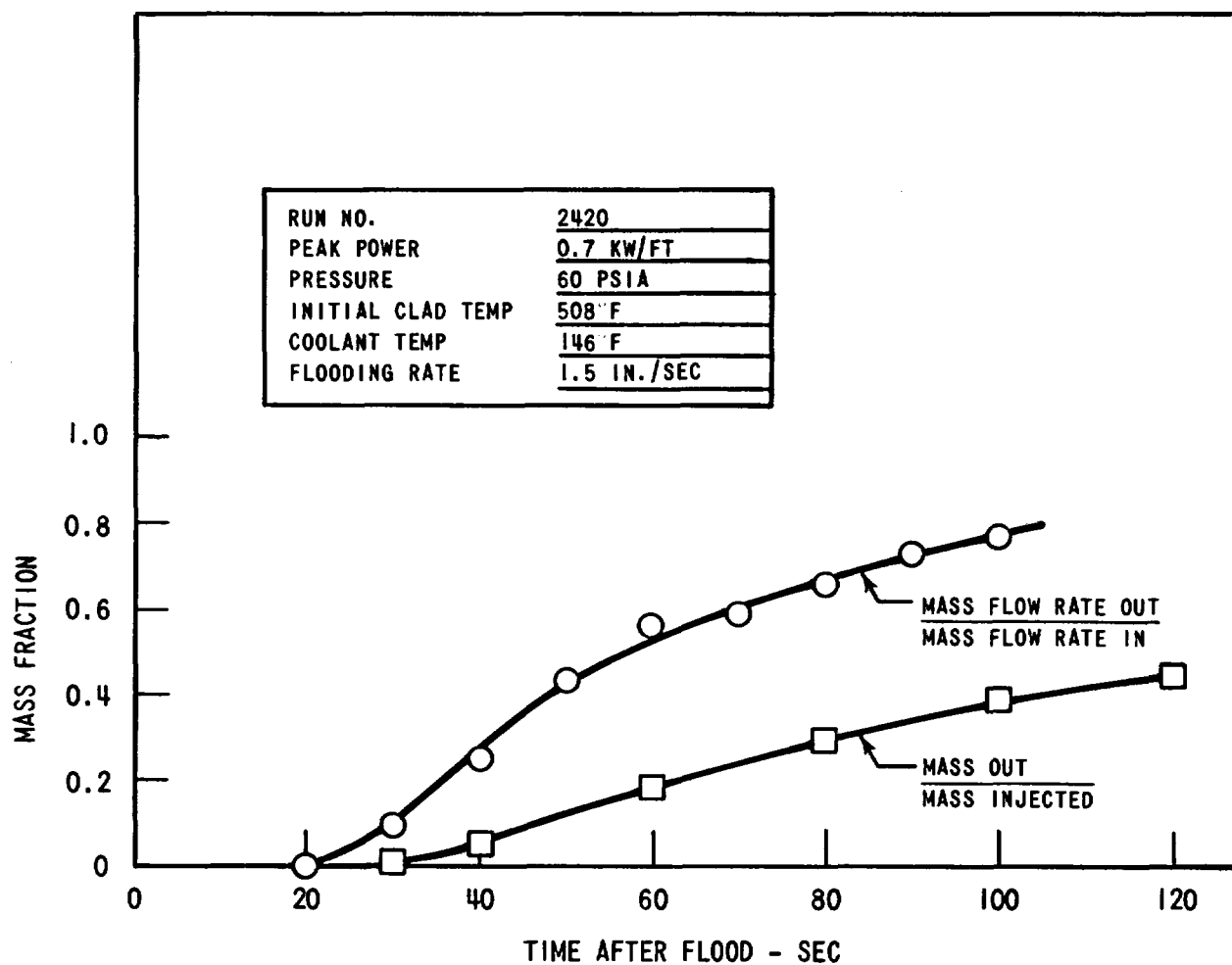


Figure B-6. Mass Effluent Fraction - Run 2420

The graph in Figure B-6 contains the ratio of mass out to mass injected shown as a function of time as is the ratio of mass flow rate out to mass flow rate injected. These values are significantly lower than those obtained from higher temperature FLECHT data (mass flow rate out/mass flow rate in ≈ 0.8).

The amount of energy initially stored in the heater rods and flow housing is lower in these tests than for high temperature FLECHT runs with the same peak linear heating rate. This is due to the lower initial temperatures, as shown in Figure B-7 for the test run considered above. The lower heat release results in less steam generation and therefore less entrainment of liquid.

B.4.3 Housing Axial Pressure Data

The housing axial pressure data are compared to the rod temperature quench envelope for several test runs in Figures B-8 through B-14. The pressure data have been converted to feet of water, assuming a density equal to that of saturated water at the test pressure. Actually, the mass indicated by the pressure data is distributed within the test section with a varying density. The comparison shows, however, the difference between the mass storage calculated using temperature quench data and that calculated from the pressure data. The temperature quench times plotted are for the longest quench time at each elevation, thus representing an envelope of all the quenches.

The level calculated from the differential pressure data is higher than that derived from the temperature quench front data for the greater portion of most of the test runs. This indicates that there is storage of mass in the bundle above the quench front. Hence, the use of the pressure drop data to calculate mass effluent fraction will yield values which are lower than those calculated by using the quench front data. The pressure drop data indicate the total mass in the test section; thus the calculated mass effluent fraction is for the mass leaving the test section, not the quench front. By the time of the 8 ft elevation quench, however, the total or average mass effluent fractions calculated by the two methods are only slightly different. The levels indicated by the pressure and quench data show better agreement for the test runs with higher flooding rate, lower initial clad temperature, and higher system pressure.

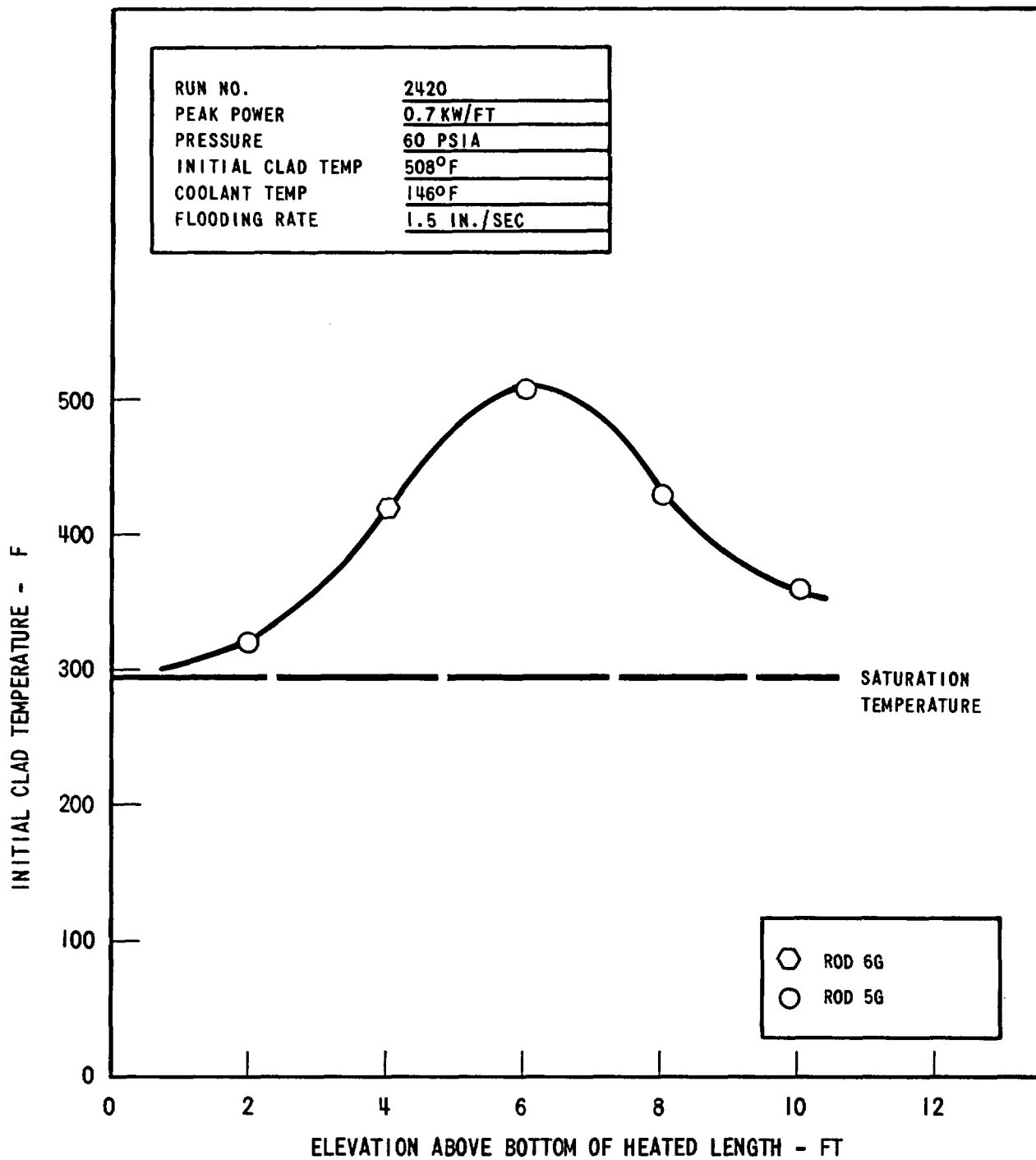


Figure B-7. Initial Clad Temperature vs. Elevation

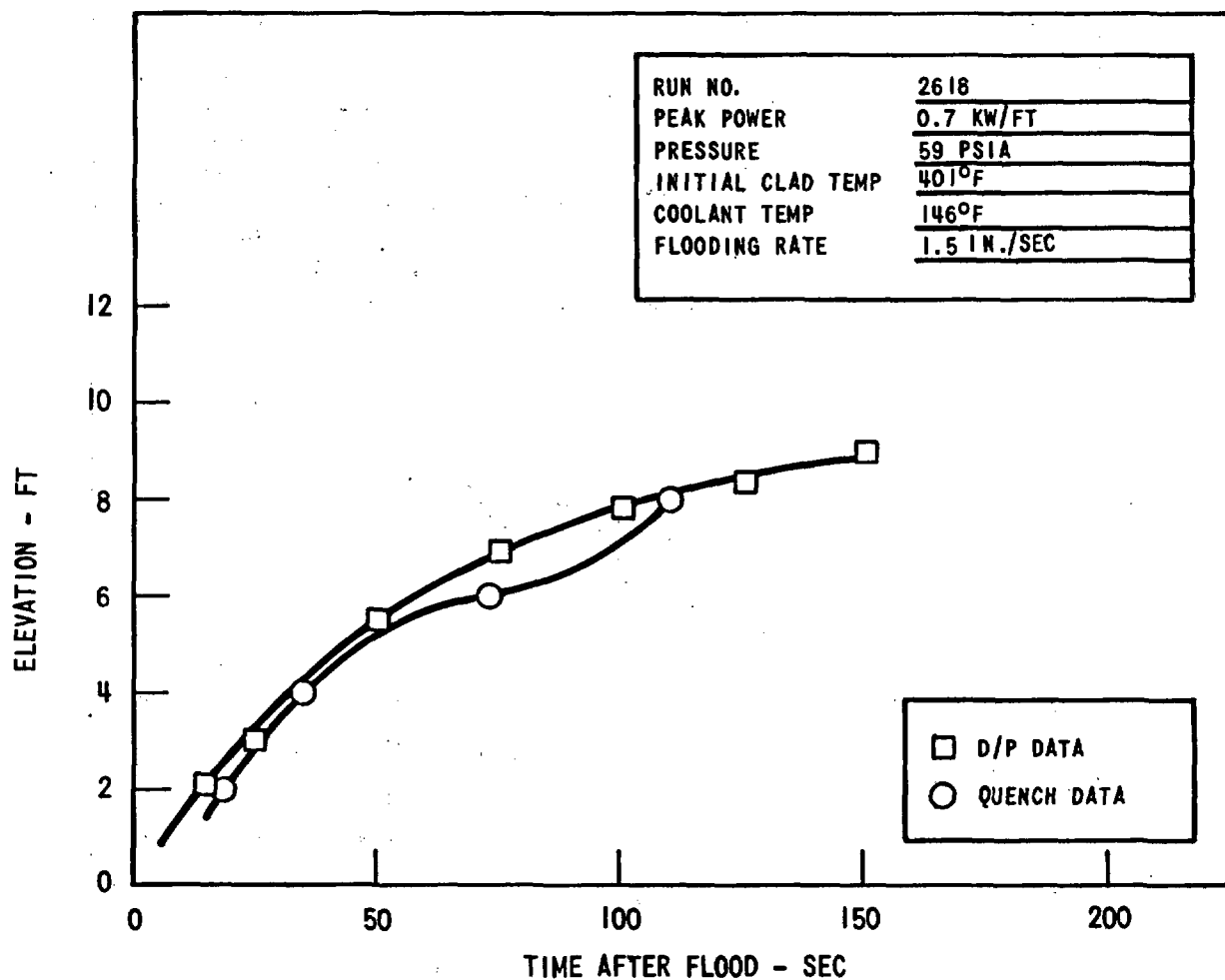


Figure B-8. Comparison of Quench Front and Differential Pressure Data

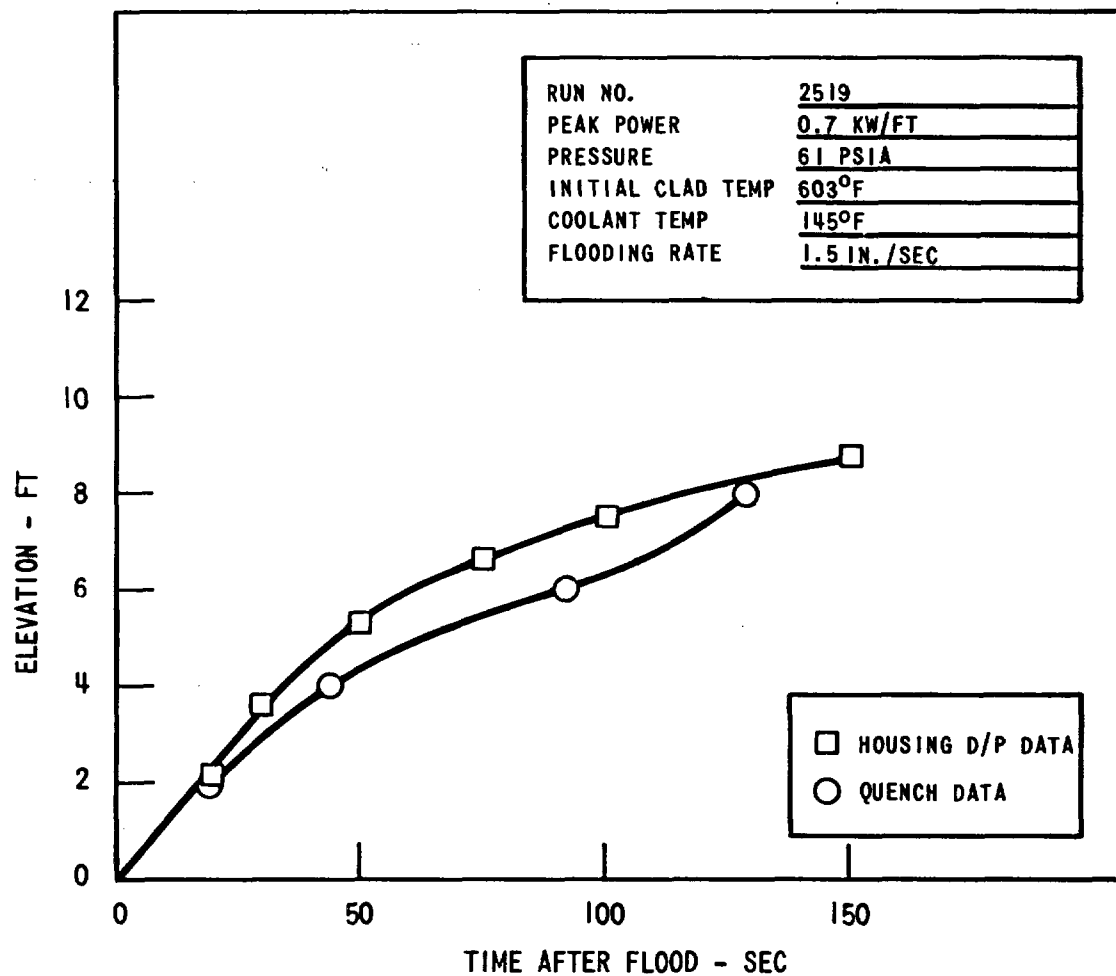


Figure B-9. Comparison of Quench Front and Differential Pressure Data

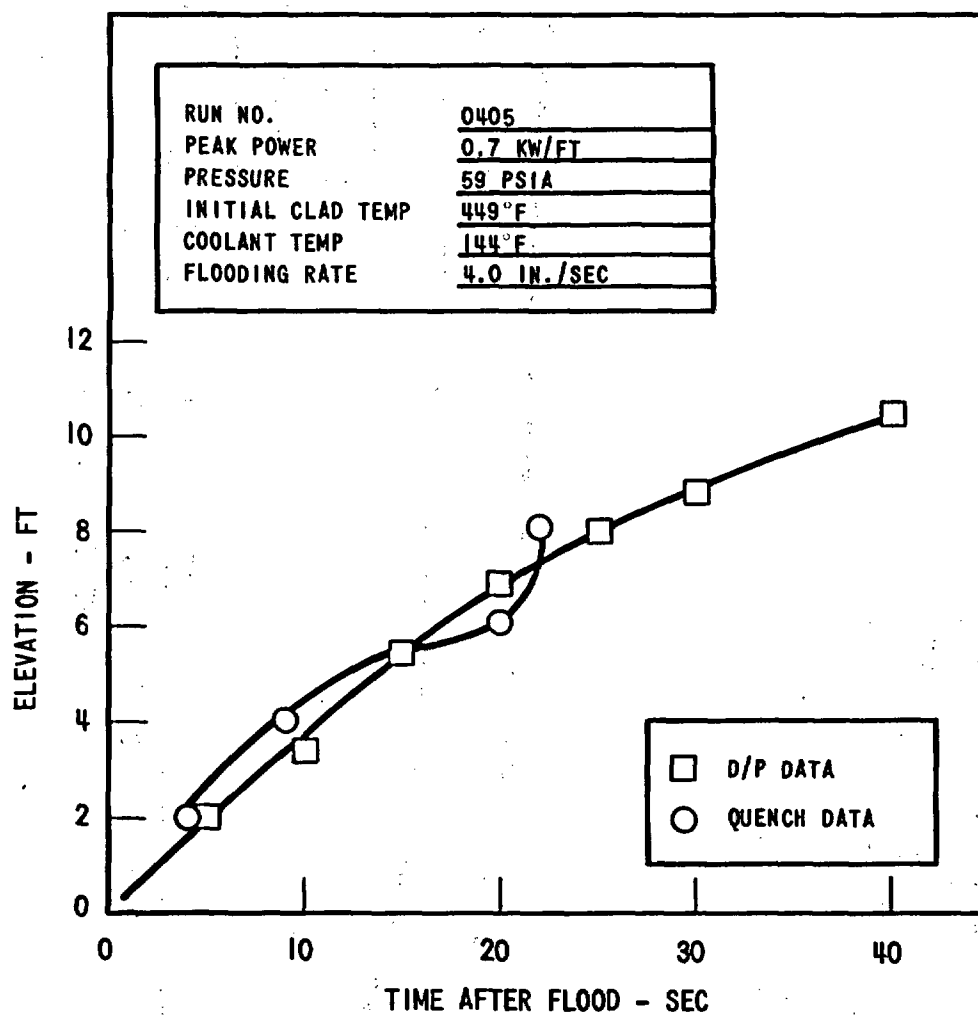


Figure B-10. Comparison of Quench Front and Differential Pressure Data

B-20

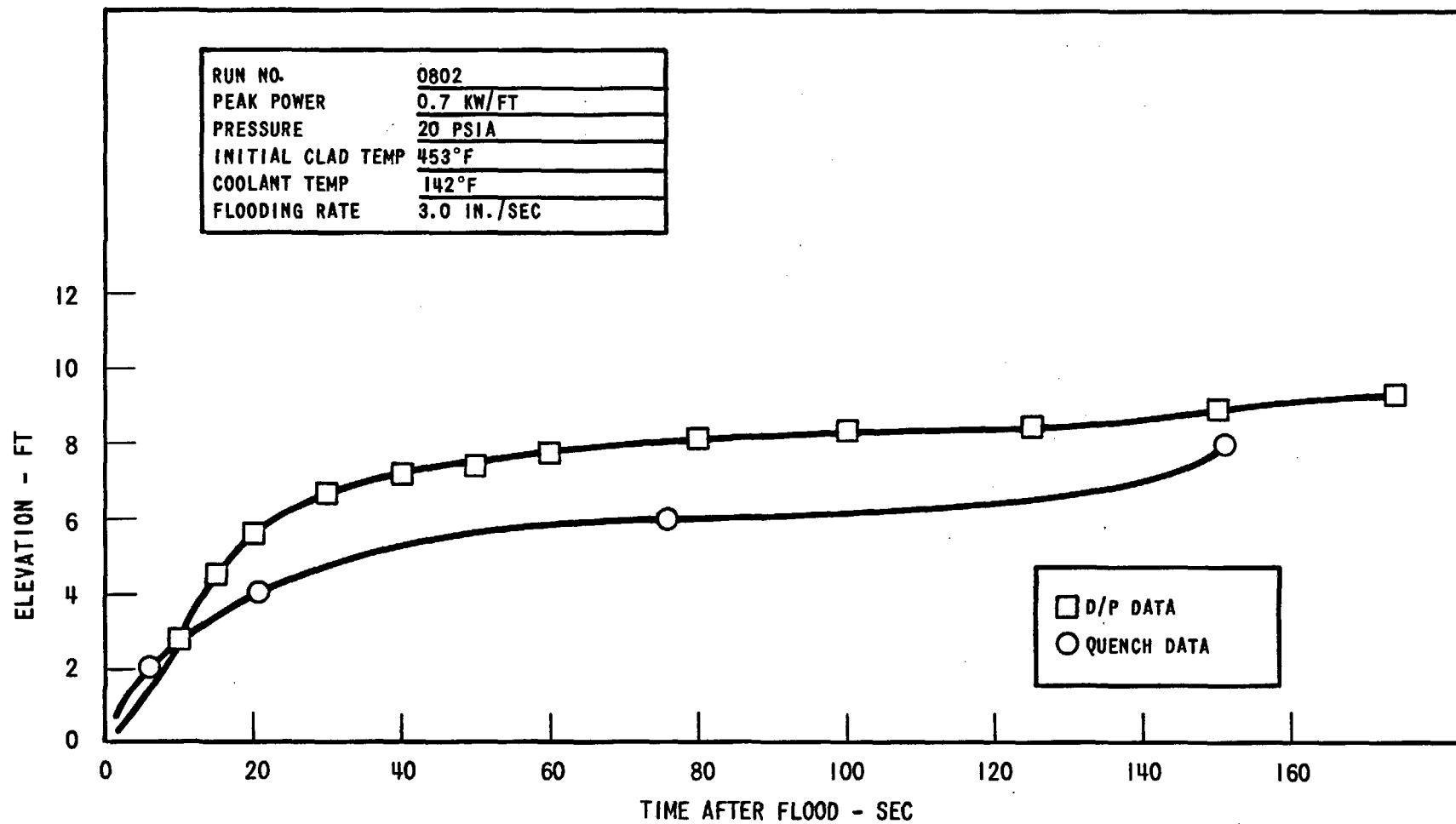


Figure B-11 . Comparison of Quench Front and Differential Pressure Data

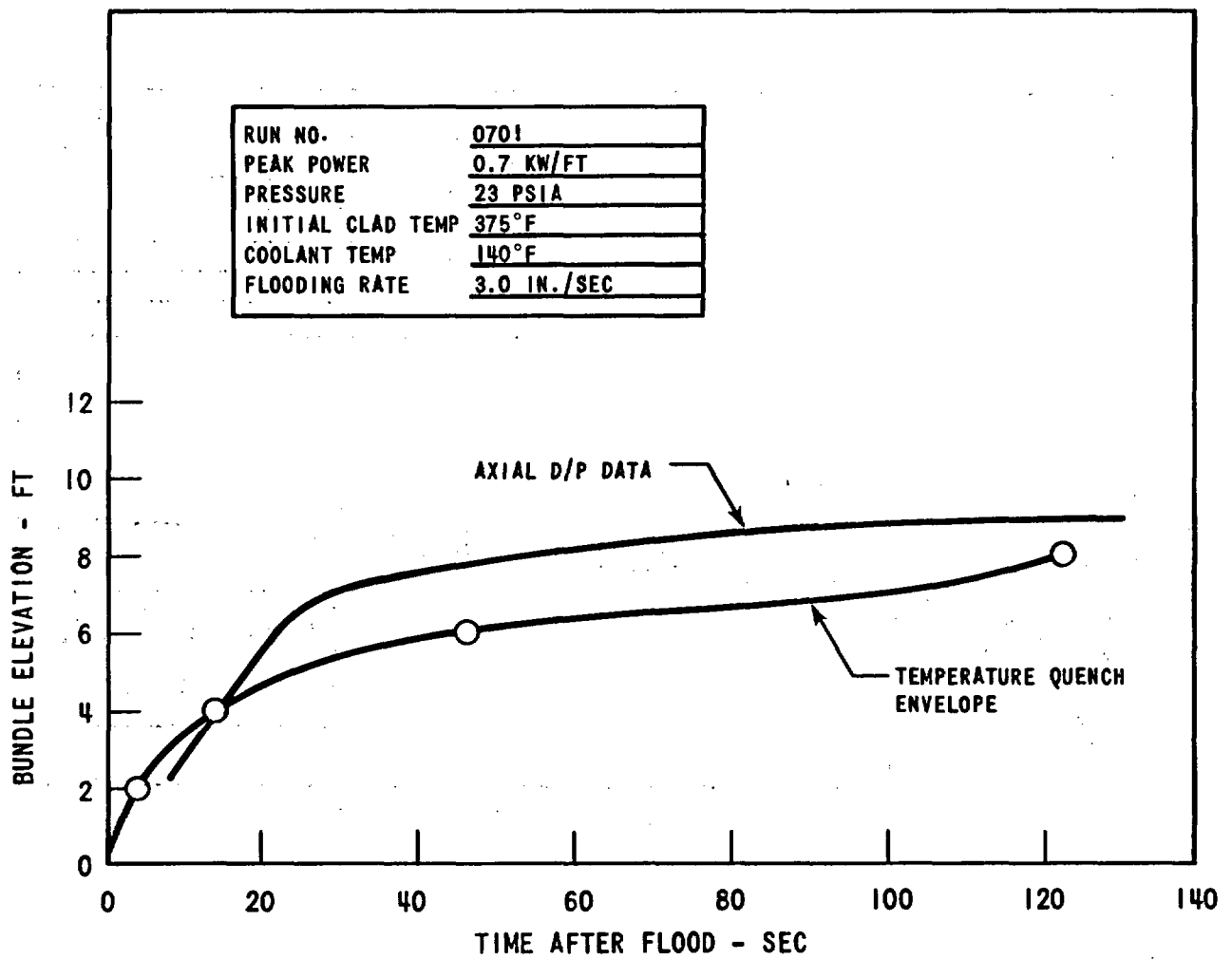


Figure B-12. Comparison of Quench Front and Differential Pressure Data

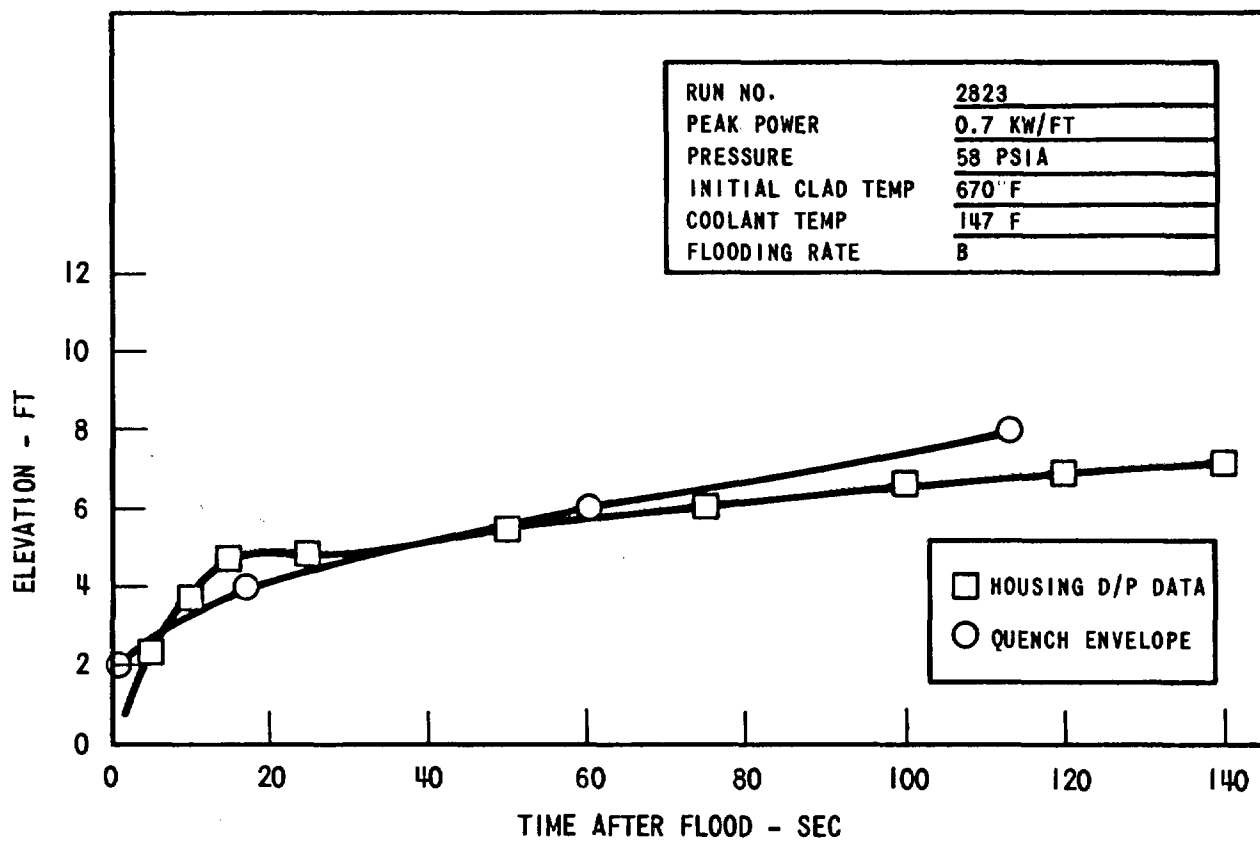


Figure B-13. Comparison of Quench Front with Differential Pressure Data

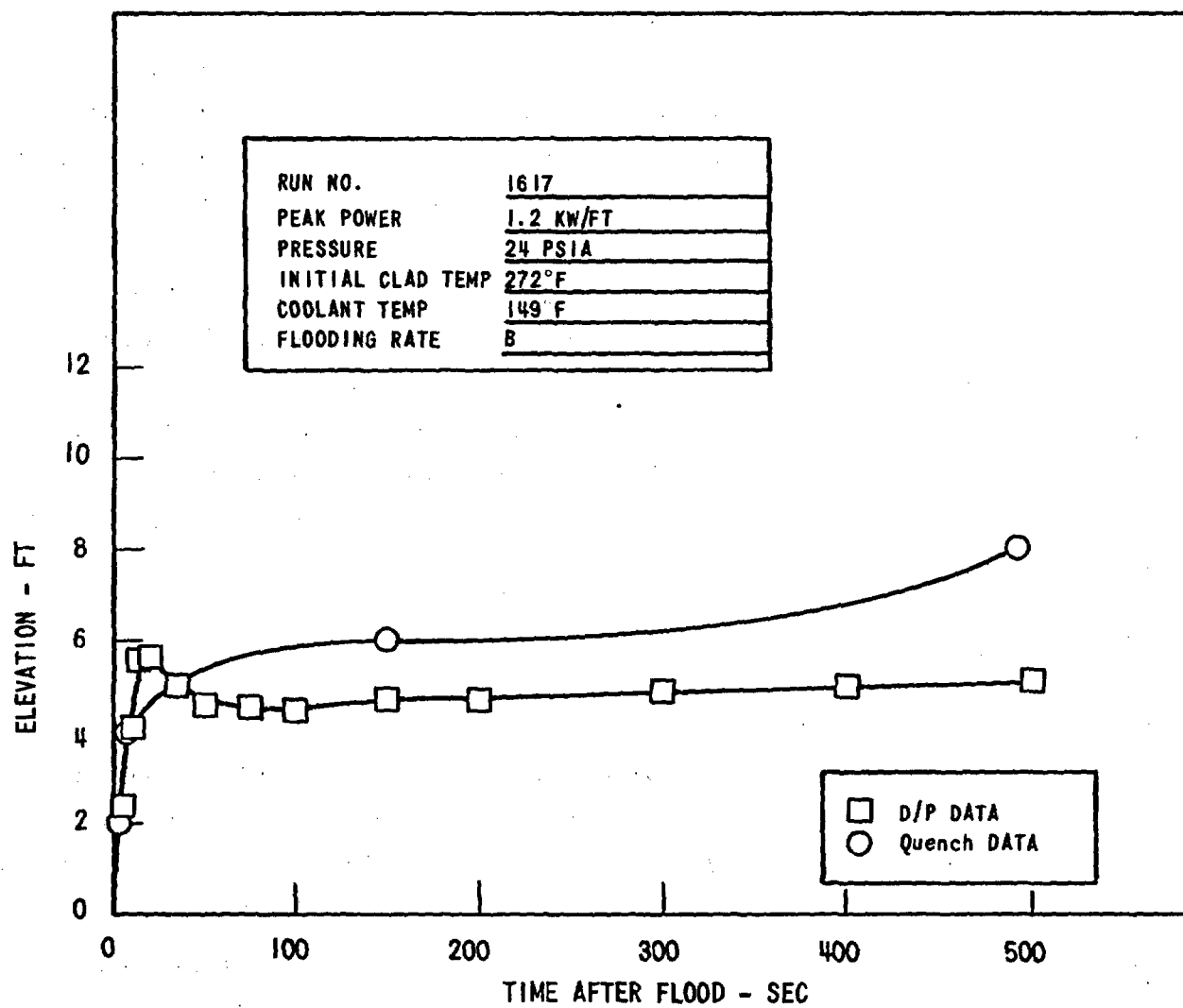


Figure B-14. Comparison of Quench Front and Differential Pressure Data

These conditions result in lower steam volumetric flux and thus less entrainment of liquid and less storage of mass above the quench front.

In test Run 1617, shown in Figure B-14, the temperature quench data indicate, for most of the run, a higher level in the bundle than the differential pressure data. After cessation of the high flooding rate (15 seconds after initiation of flood), the high power in this test (1.2 kw/ft) results in a large void fraction in the bundle. The injection rate at this time was 1 in./sec, which equals 0.7 lbm/sec. The housing differential pressure data indicate that the saturation point was below the 2 ft level for the entire run, i.e., the void fraction was greater than zero from at least the 2 ft level upward, indicating that a large void fraction below the quench front existed. In addition, the high power results in increased vaporization of entrained liquid, which is confirmed by the liquid collection measurements, as shown in Appendix B-1 for these tests. Both of these effects contribute to the low differential pressure reading. These results are consistent with those obtained in higher temperature FLECHT tests at low pressure, high power, and low flooding rate given in Reference 1.

B.5 PARAMETER EFFECTS

B.5.1 Initial Clad Temperature

A comparison between a low clad temperature FLECHT run and high temperature FLECHT runs is shown in Figure B-15. The low temperature run refloods at nearly the cold fill rate, while the high temperature runs require 4 to 5 times the cold fill time for the quench front to reach the bundle midplane.

The temperature quench envelopes of three low temperature runs are compared in Figure B-16. As expected, the higher the initial clad temperature, the longer the quench time. Figure B-17 shows the maximum clad temperatures measured in those runs at the 6 and 8 foot elevations. The values are plotted as a function of initial peak clad temperature. The difference between the

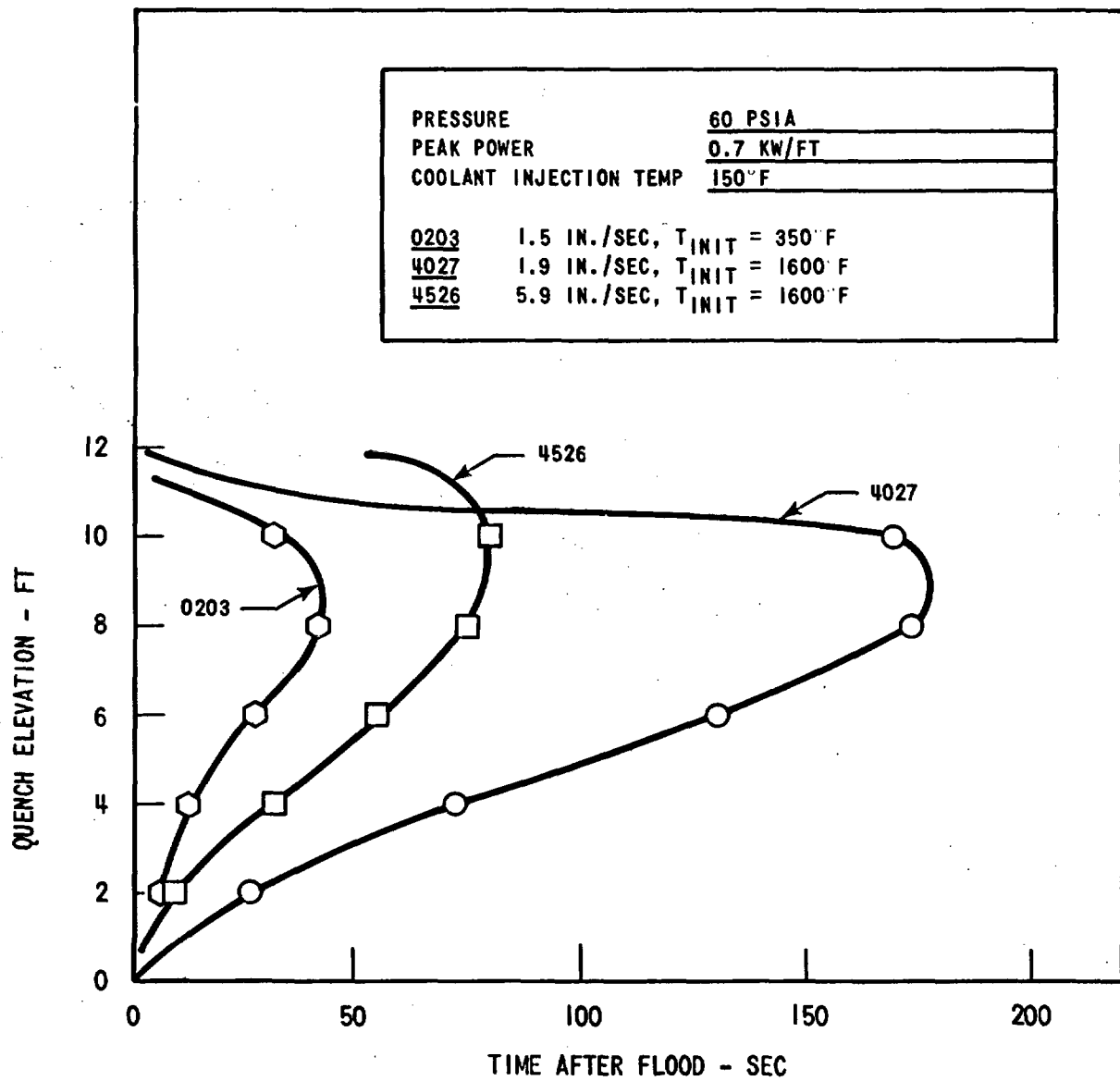


Figure B-15. Comparison of FLECHT Temperature Quench Fronts with Low Clad Temperature FLECHT

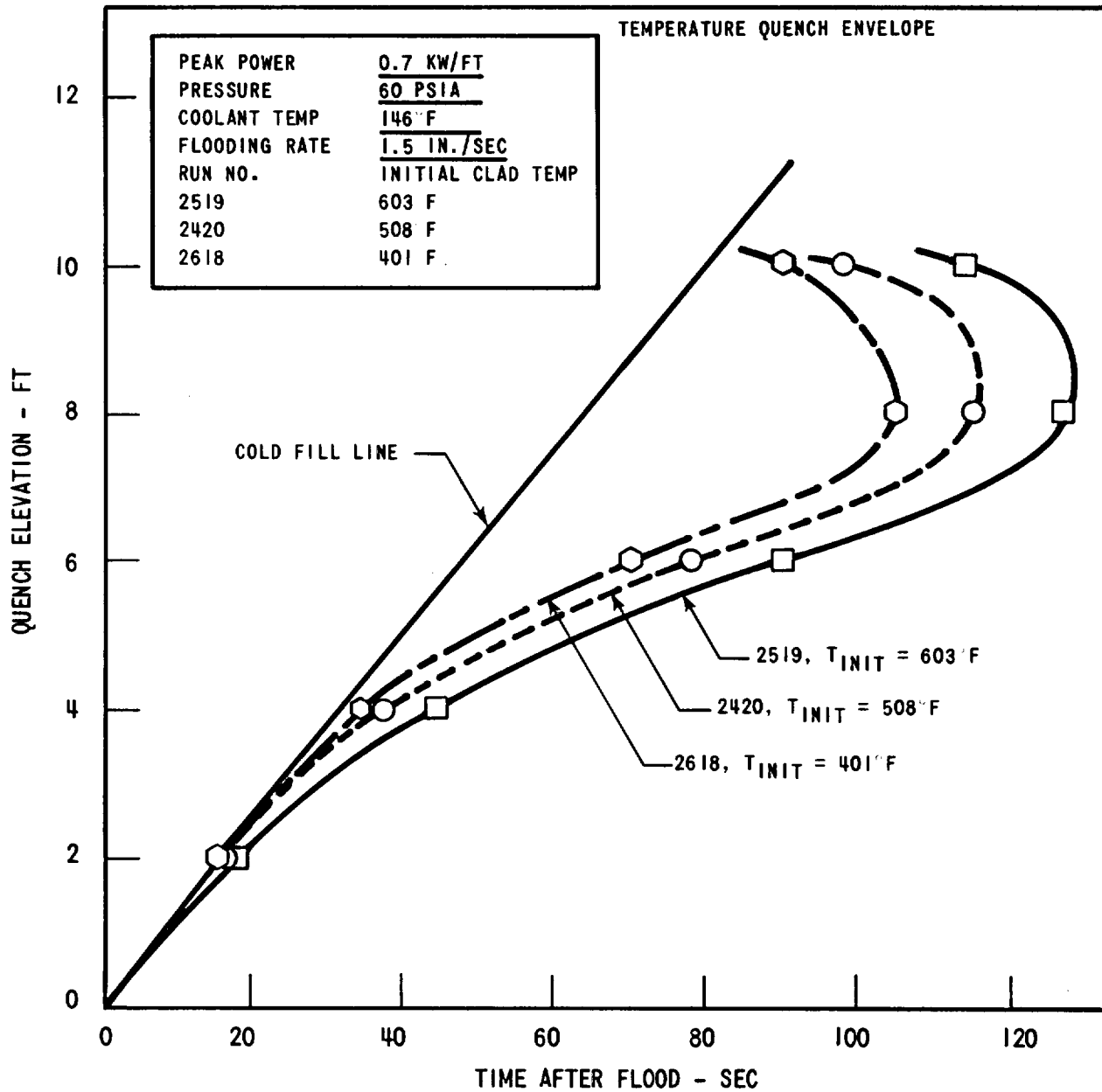


Figure B-16. Effect of Initial Temperature on Quench Front

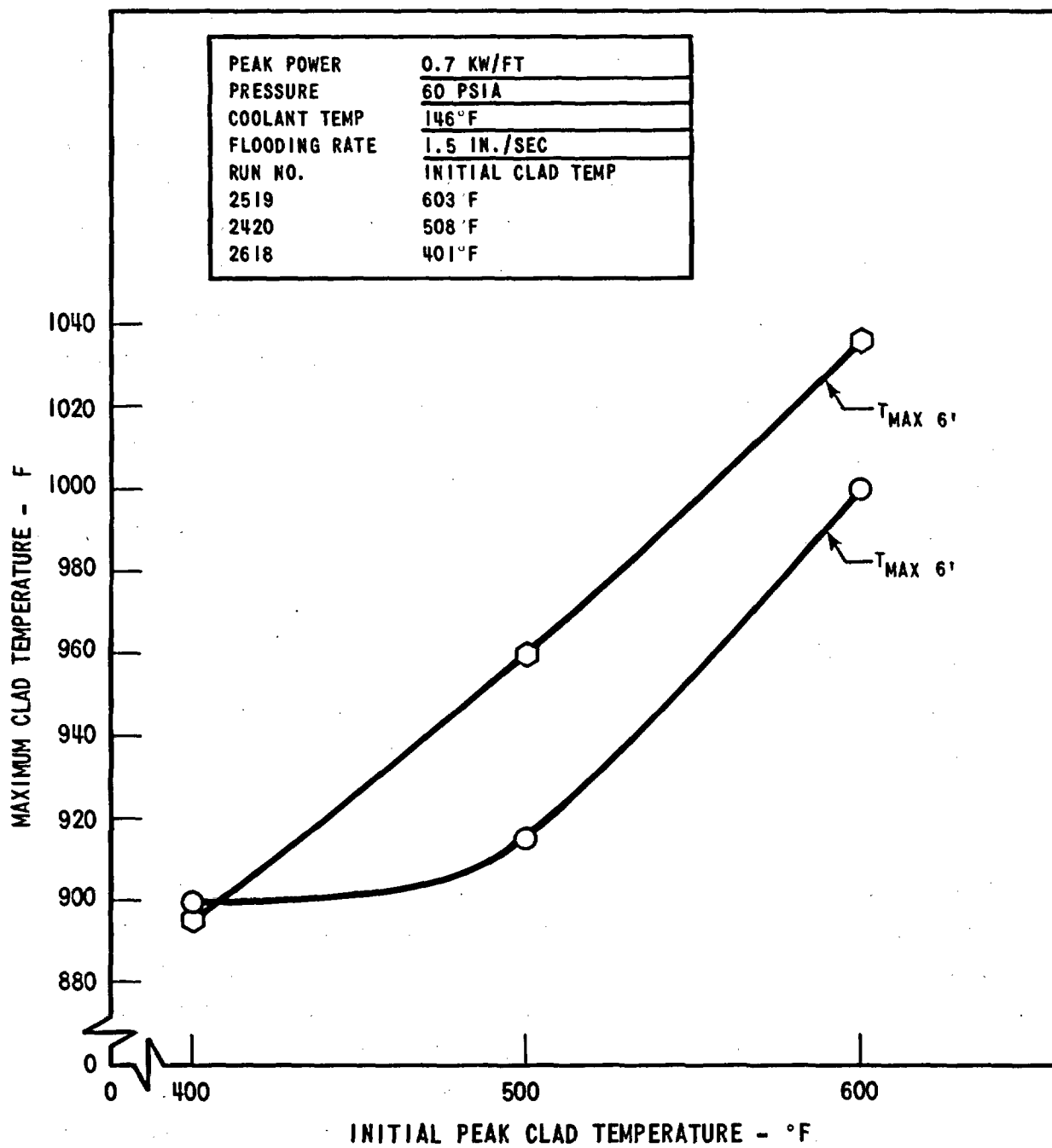


Figure B-17. Effect of Initial Clad Temperature on Maximum Clad Temperature

6 and 8 ft maximum temperatures is seen to decrease as the initial temperature is lowered. This effect is due to the smaller amounts of steam generated as the temperature decreases. Less steam generation results in less cooling at the upper elevations by convection and radiation to the steam. Consequently, the rise in the temperatures of the 8-ft-elevation thermocouples tends to be larger than the rise of the 6-ft-elevation thermocouple temperatures. The effect sometimes causes the 8-ft-elevation thermocouples to reach higher maximum temperatures than the 6-ft-elevation thermocouples.

The mass of liquid collected for each of these runs is plotted in Figure B-18 as a function of $t/t_{8, \text{quench}}$. This nondimensional time scale reveals the effect of clad temperature only on the amount of liquid collected. It is clear that less water is entrained at lower initial clad temperature as a result of the lower rate of steam generation.

Figures B-19, B-20, and B-21 present similar results for runs with a lower flooding rate.

B.5.2 Coolant Subcooling

Figure B-22 shows the effect of different amounts of coolant subcooling. There is no significant effect for these conditions.

B.5.3 Pressure

Figure B-23 presents plots of mass of liquid collected and average mass effluent fraction up to the time of the 6 ft quench as a function of the initial clad temperature for pressures of 20 and 60 psia. The graphs indicate that there is more entrained liquid and a larger mass effluent fraction at lower pressure. While the data for 60 psia show a definite threshold temperature for liquid entrainment, the 20 psia data indicate that for these conditions liquid will be entrained at all temperatures above $\sim 300^\circ\text{F}$.

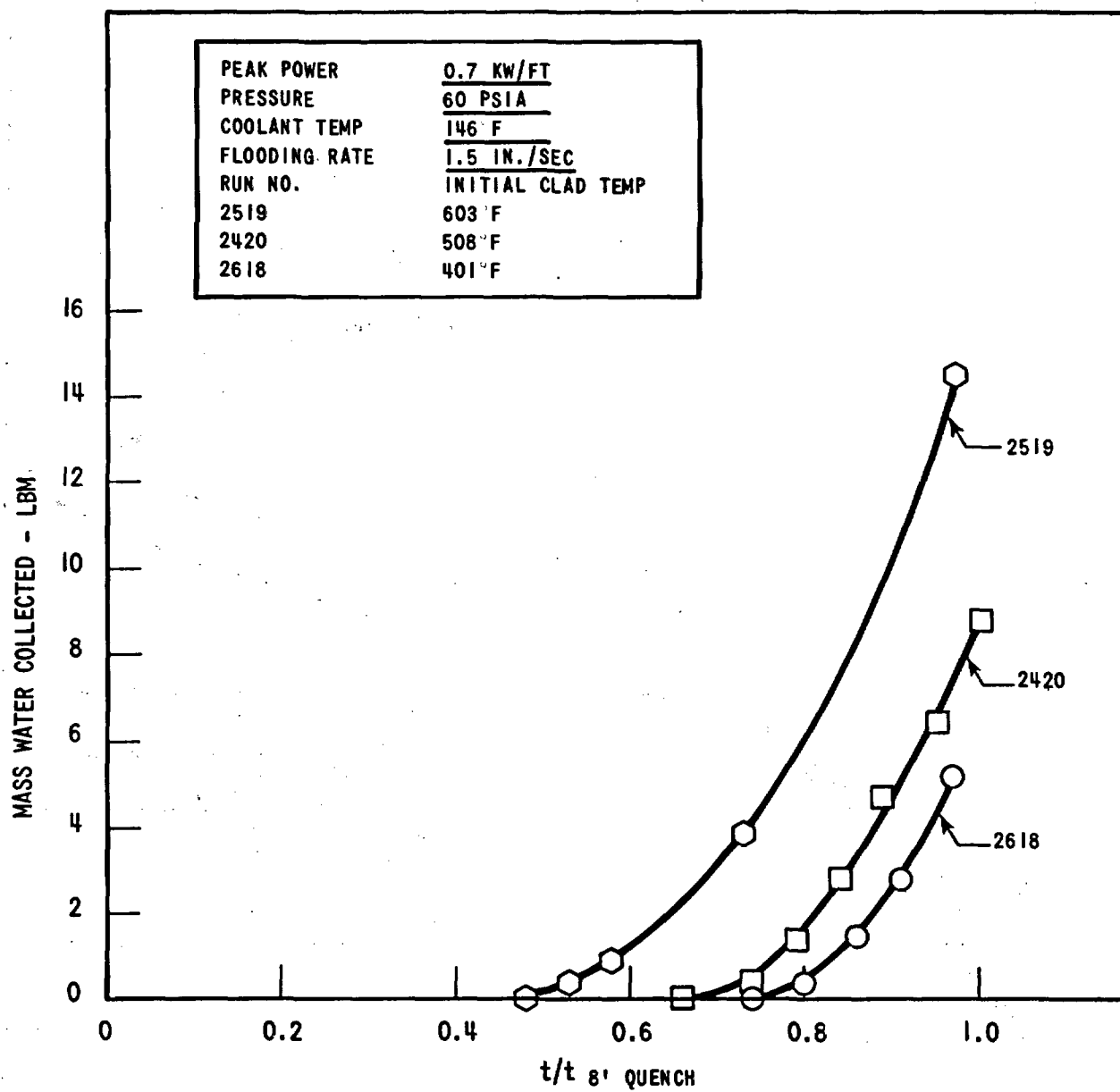


Figure B-18. Effect of Initial Clad Temperature on Entrainment

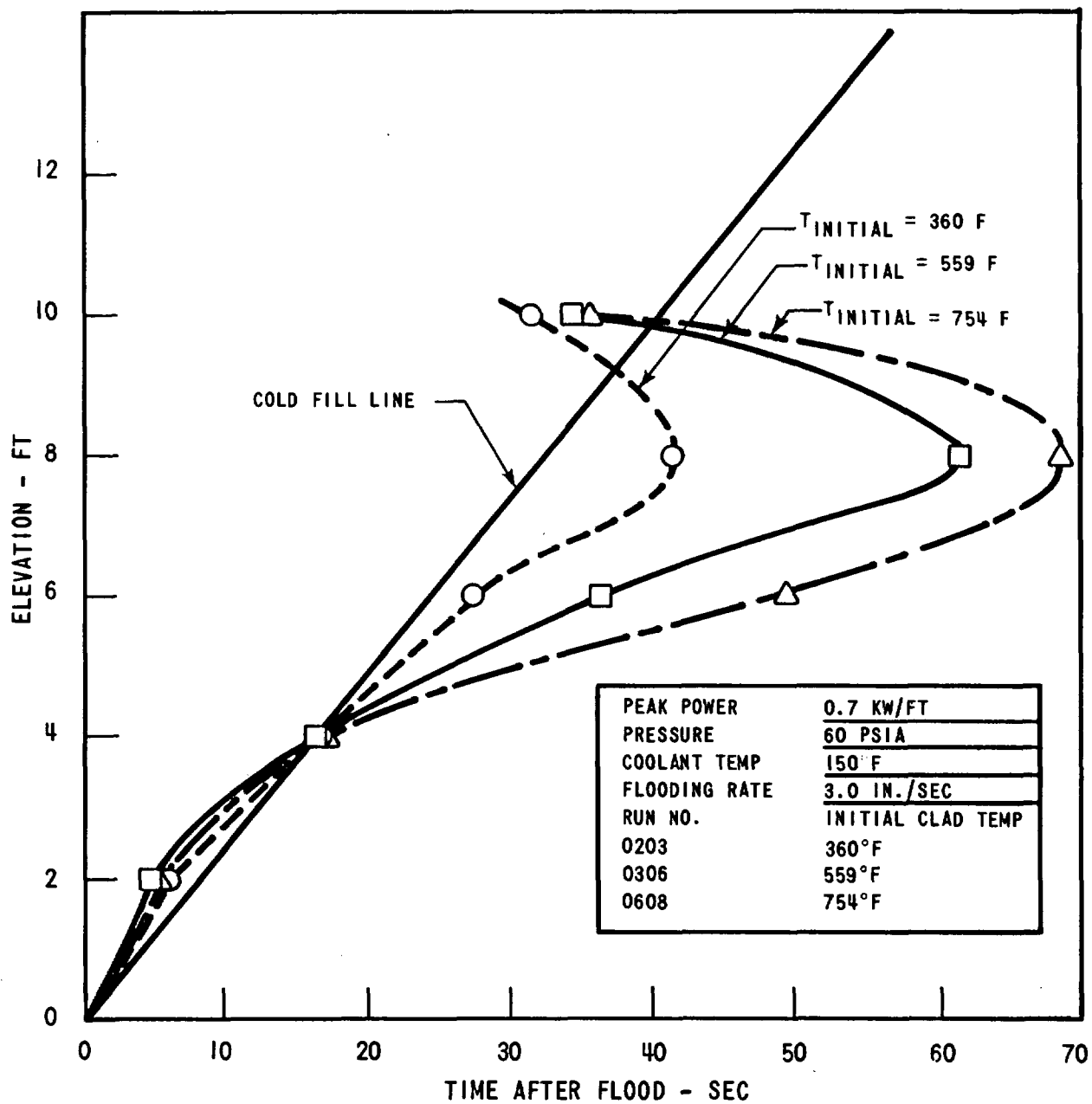


Figure B-19. Effect of Initial Clad Temperature on Quench Front

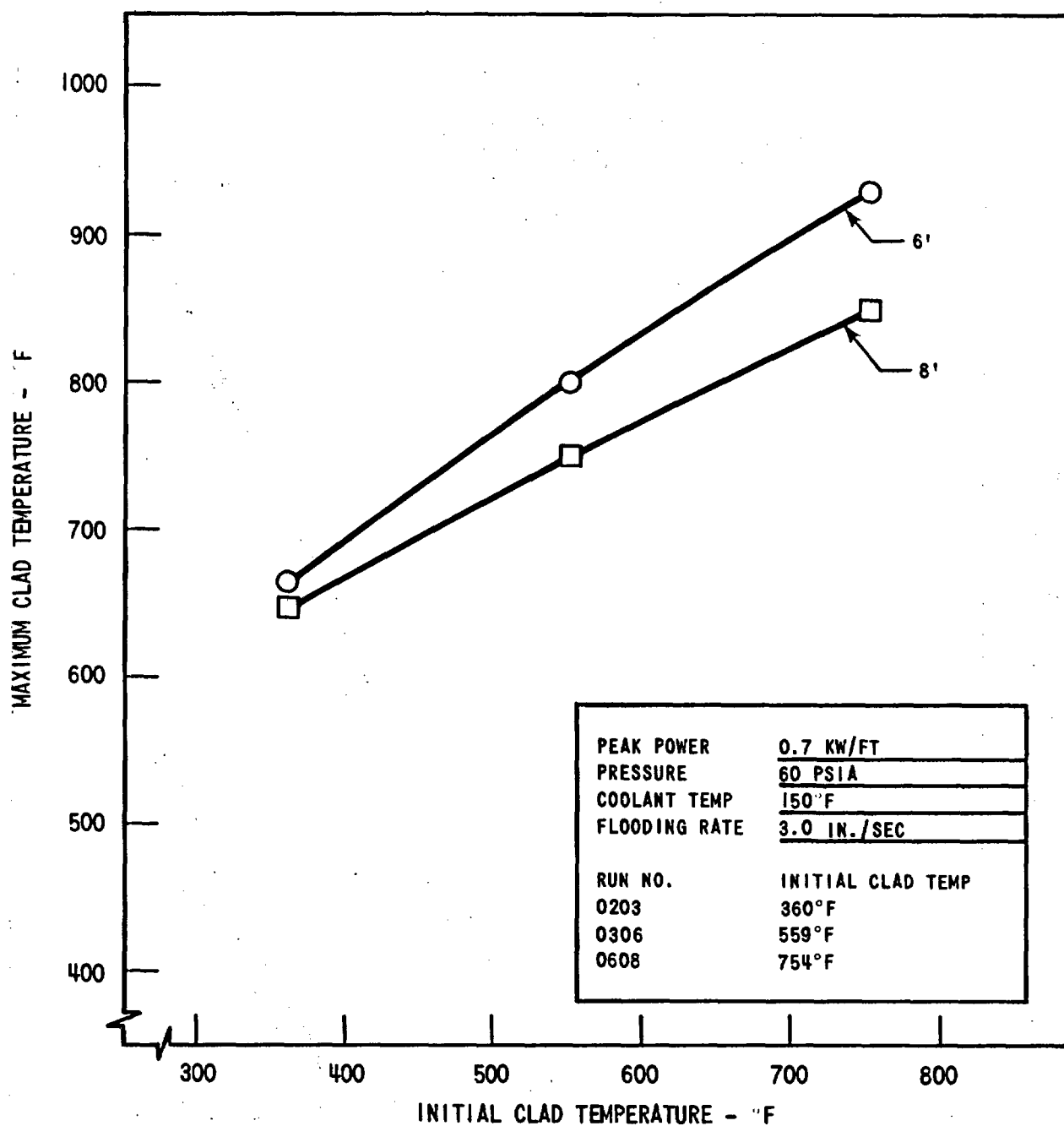


Figure B-20. Effect of Initial Clad Temperature on Maximum Clad Temperature

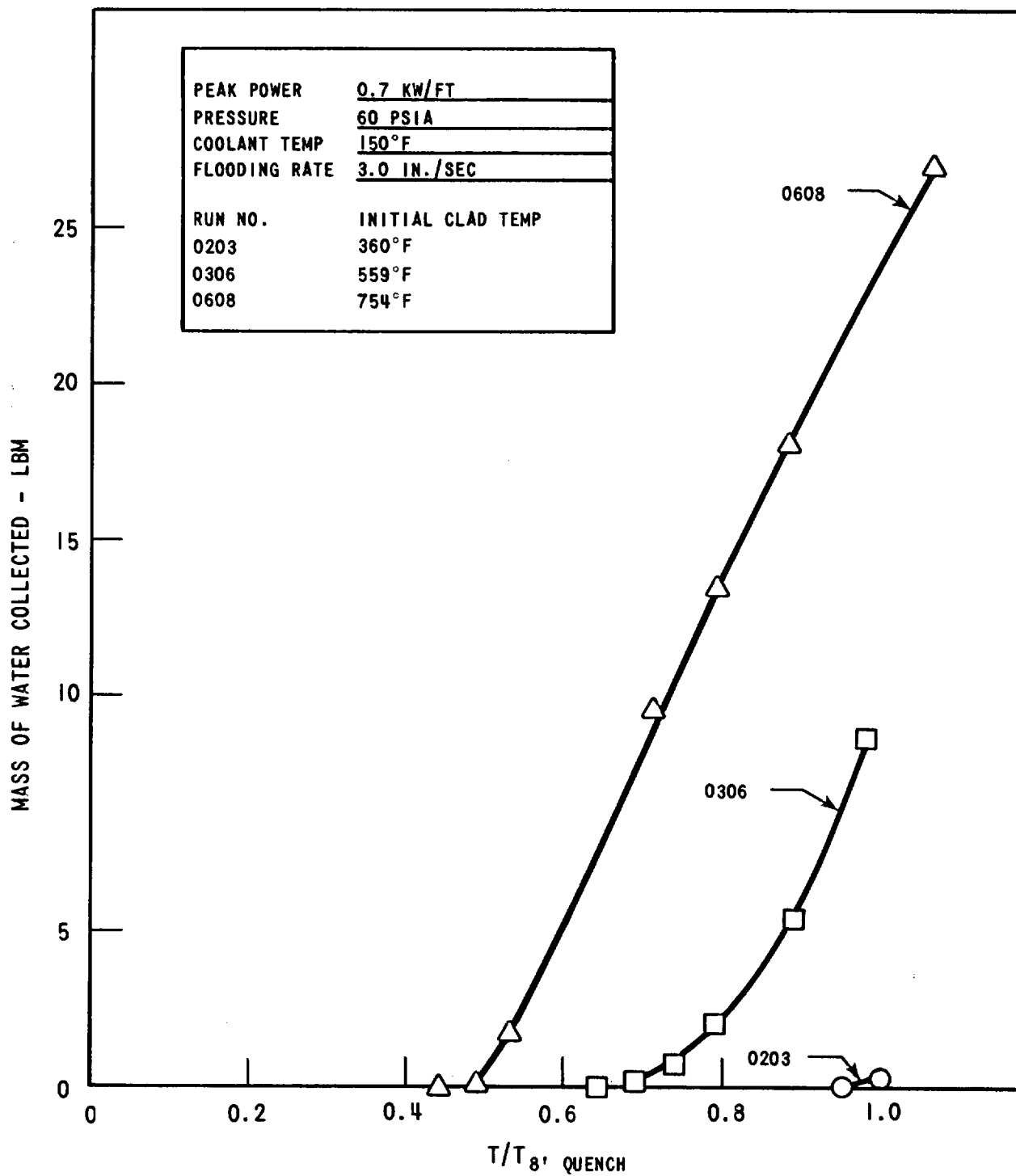


Figure B-21. Effect of Initial Clad Temperature on Entrainment

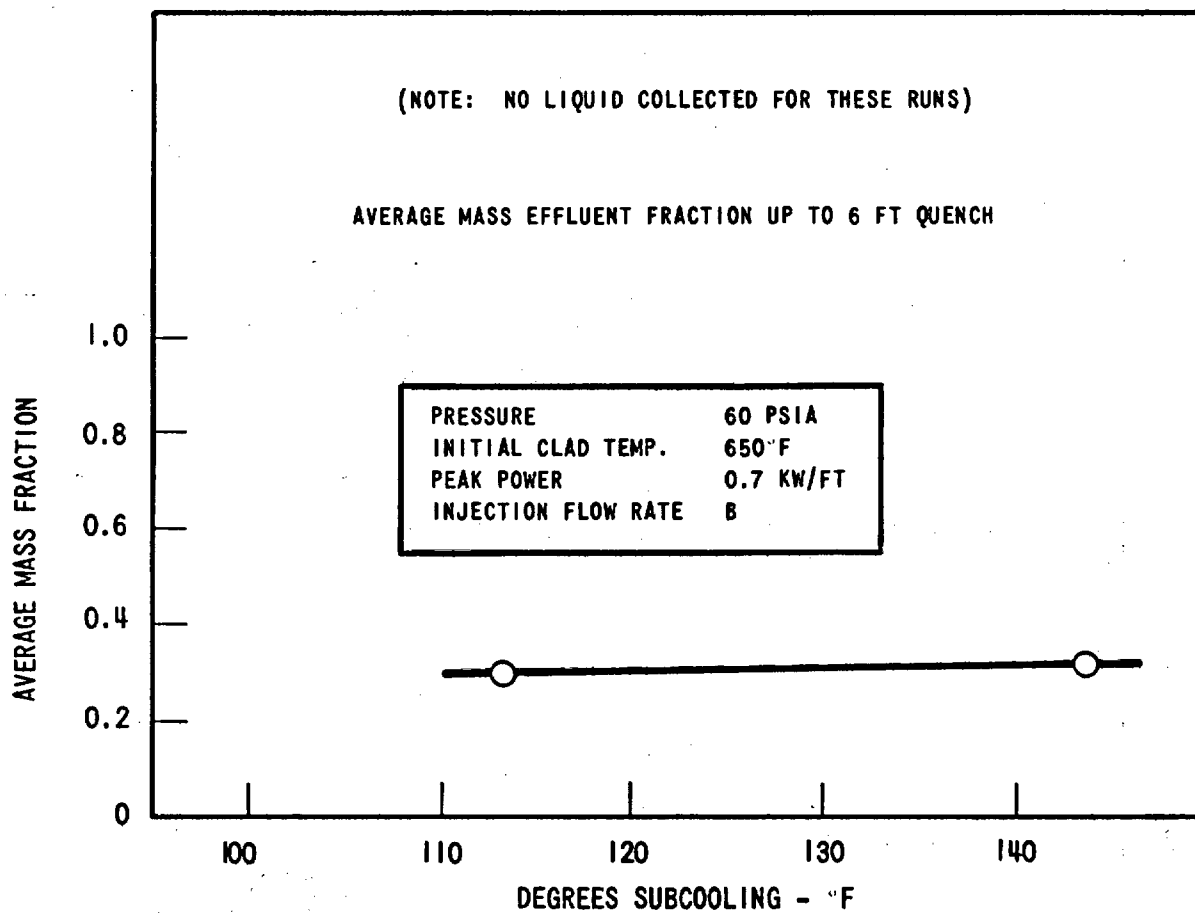


Figure B-22. Effect of Inlet Water Subcooling

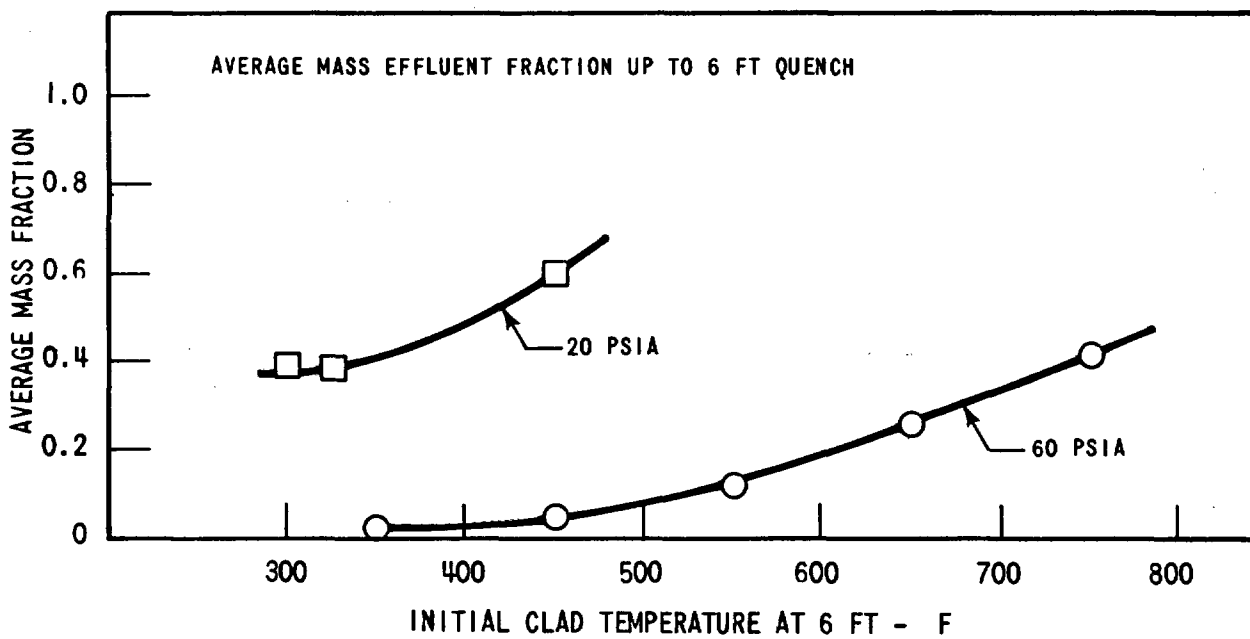
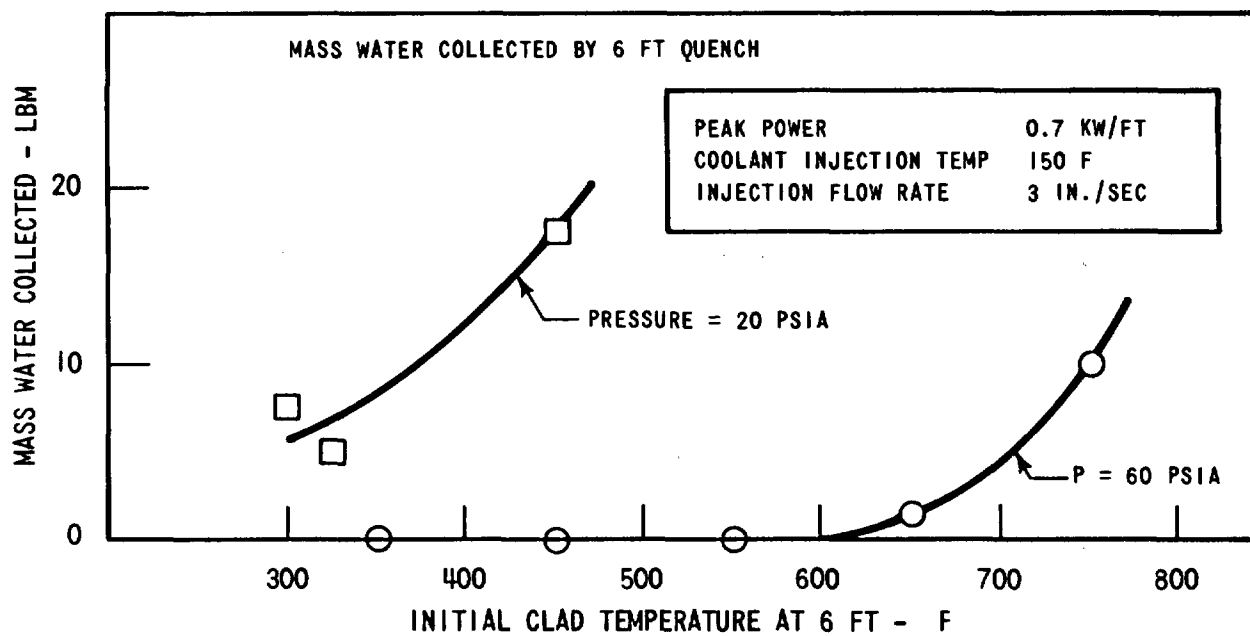


Figure B-23. Effect of Pressure

The increased mass effluent fraction and mass of liquid collected at lower pressure are consistent with the results presented in Reference 1 for higher temperature FLECHT runs. At 20 psia the specific volume of steam is about three times that at 60 psia. Thus, higher steam velocities will occur for the same rate of steam generation, resulting in more entrainment. Also, better heat transfer at higher pressure will tend to vaporize more of the entrained liquid, thus decreasing the amount of liquid collected.

The data presented do not show a constant amount of coolant subcooling, and thus do not reflect the effect of pressure alone. The results presented in Section B.5.2, however, indicate that the subcooling effect is negligible at 60 psia. Data were not taken for the subcooling effect at 20 psia.

B.5.4 Flooding Rate

The effect of flooding rate is shown in Figure B-24. Higher flooding rate results in lower amounts of entrained liquid and lower mass effluent fractions, if these quantities are referenced to a quench time. The higher flooding rate causes the point at which the inlet water reaches the saturation temperature to be higher in the bundle, and a faster rise of the quench level. The rate of steam generation is lower because more of the energy is used in raising the water temperature to saturation and also because the faster rise of the quench front results in lower clad temperatures. With less steam generation there is less entrainment.

B.5.5 Peak Power

The effect of peak power is shown in Figure B-25. This plot shows that as peak power increases the mass of liquid collected increases, as does the average mass effluent fraction. Higher peak power causes the rods to heat up faster resulting in higher clad temperatures. Consequently, there is more steam generation, and hence more entrainment, and a lower quench front velocity. Very low initial peak clad temperatures result in no effect of peak power on the amount of entrained water for the range of peak powers investigated.

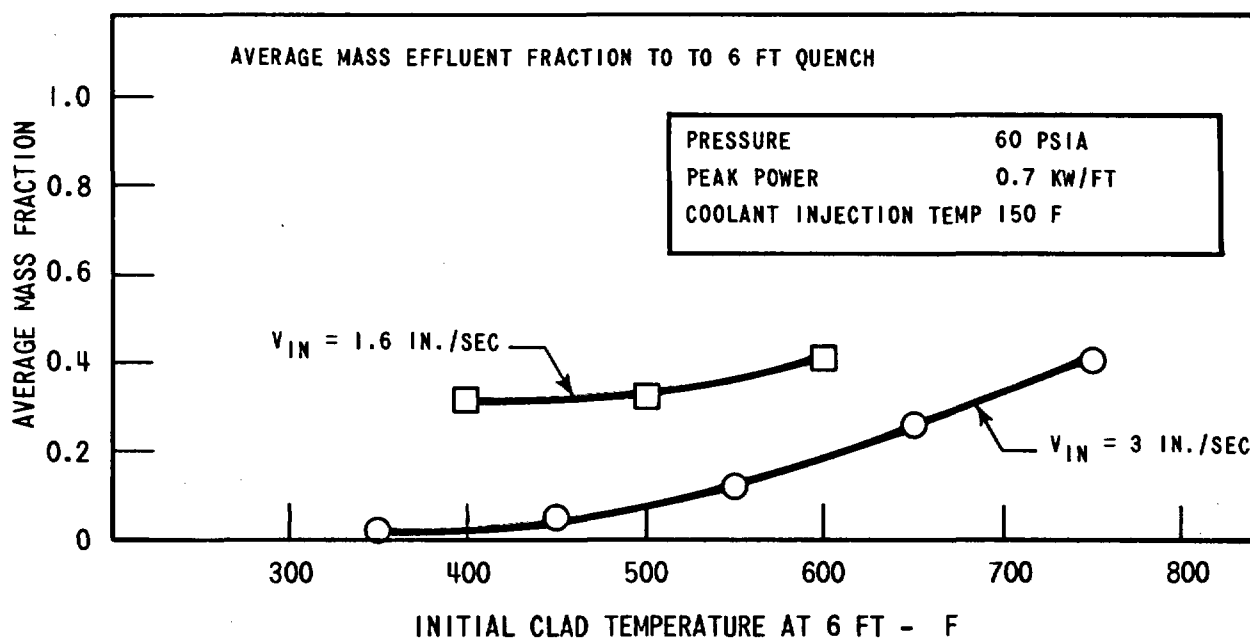
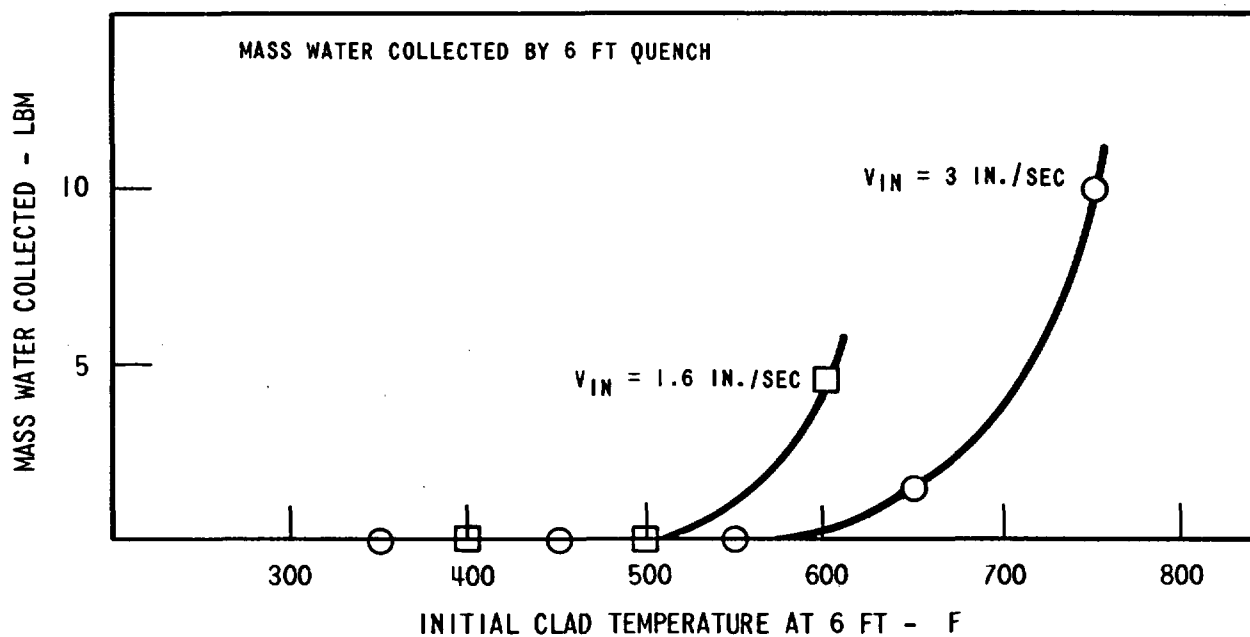


Figure B-24. Effect of Flooding Rate

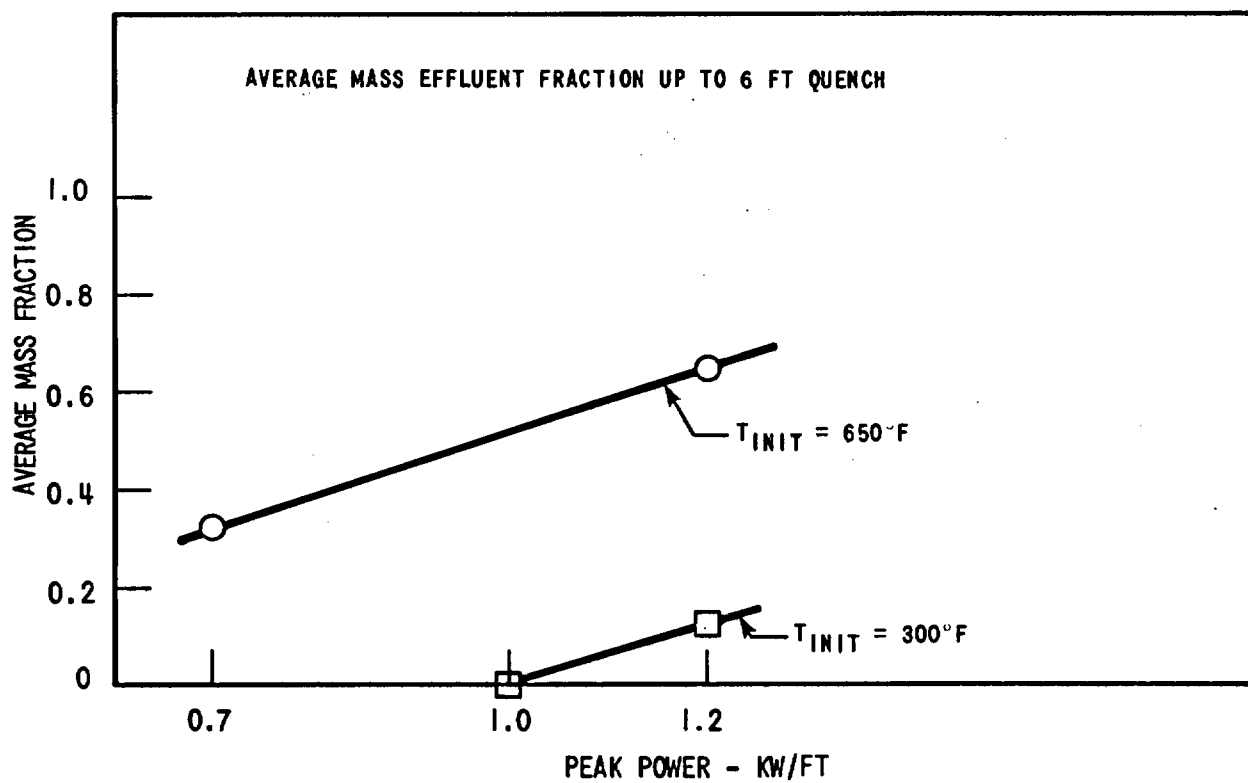
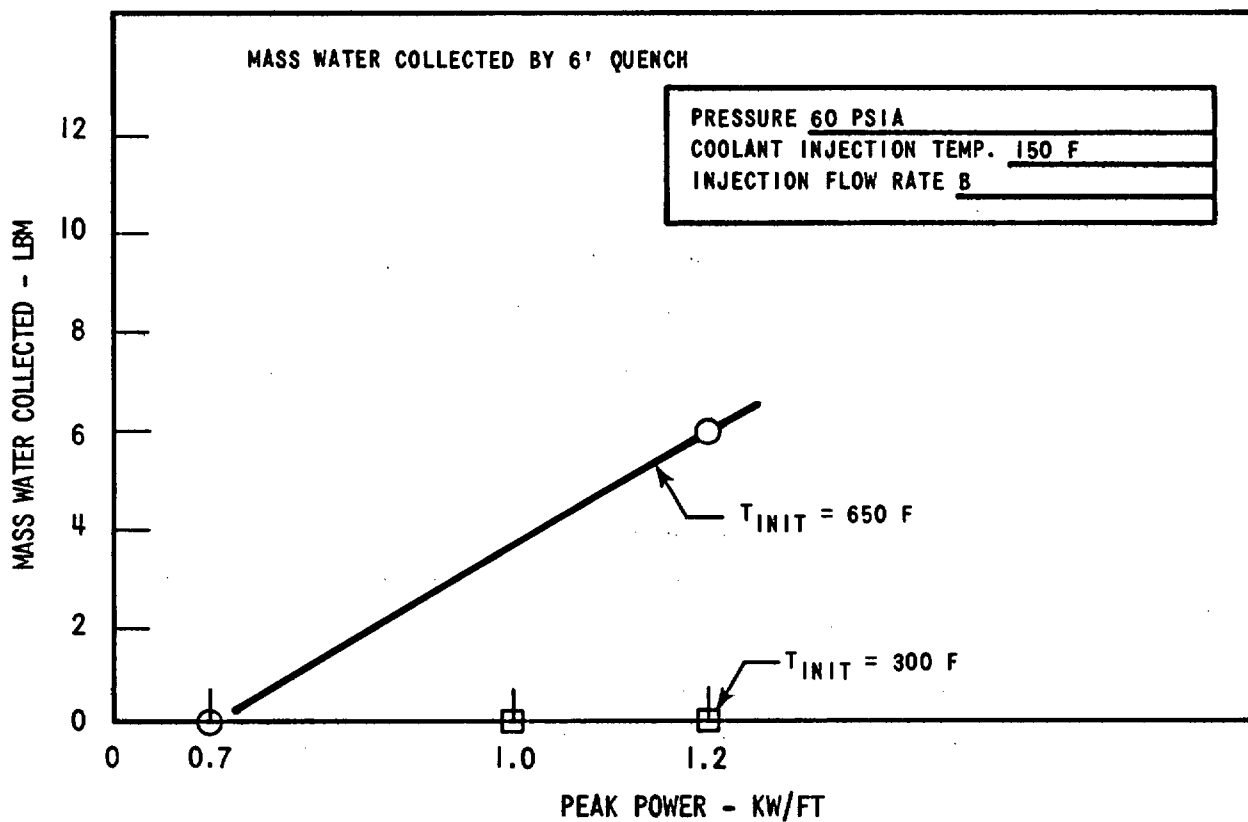


Figure B-25. Effect of Peak Power

B.6 CONCLUSIONS

These tests extend the range of the FLECHT conditions as closely as possible to the saturation temperature. Over the initial temperature range from 250°F to 750°F the following conclusions may be drawn:

1. Both the amount of liquid entrained and the average mass effluent fraction are significantly lower than in the high temperature FLECHT tests.
2. With initial clad temperatures very close to saturation temperature, the bundle quenches at nearly the cold fill rate with little or no liquid entrainment.
3. As the initial clad temperature increases, the temperature quench front diverges progressively further from the cold fill rate. This effect is greater at 20 psia than at 60 psia, but in both cases the 4 ft elevation is reached before significant mass effluent fractions are measured.
4. The mass of liquid collected and the average mass effluent fraction up to the time of the midplane quench increase as:
 - a. Flooding rate decreases
 - b. Initial clad temperature increases
 - c. Pressure decreases
 - d. Peak power increases

Coolant subcooling showed no significant effect.

APPENDIX B-1

**LOW CLAD TEMPERATURE FLECHT
RUN SUMMARY SHEETS**

1

2

3

4

LOW CLAD TEMPERATURE FLECHT RUN SUMMARY SHEET

RUN NO. 0104

DATE 11/8/72

A. RUN CONDITIONS

Pressure	57	psia
Initial Clad Temperature	459	°F
Peak Power	0.7	kw/ft
Coolant Temperature	143	°F
Flooding Rate	3.0 in./sec	for 0→end sec

B. INITIAL HOUSING TEMPERATURES

Elevation (ft)	Temperature (°F)
0	170
2	330
4	302
6	300
8	308
10	302
12	297
AVG.	301

LOW CLAD TEMPERATURE FLECHT RUN SUMMARY SHEET (Cont)

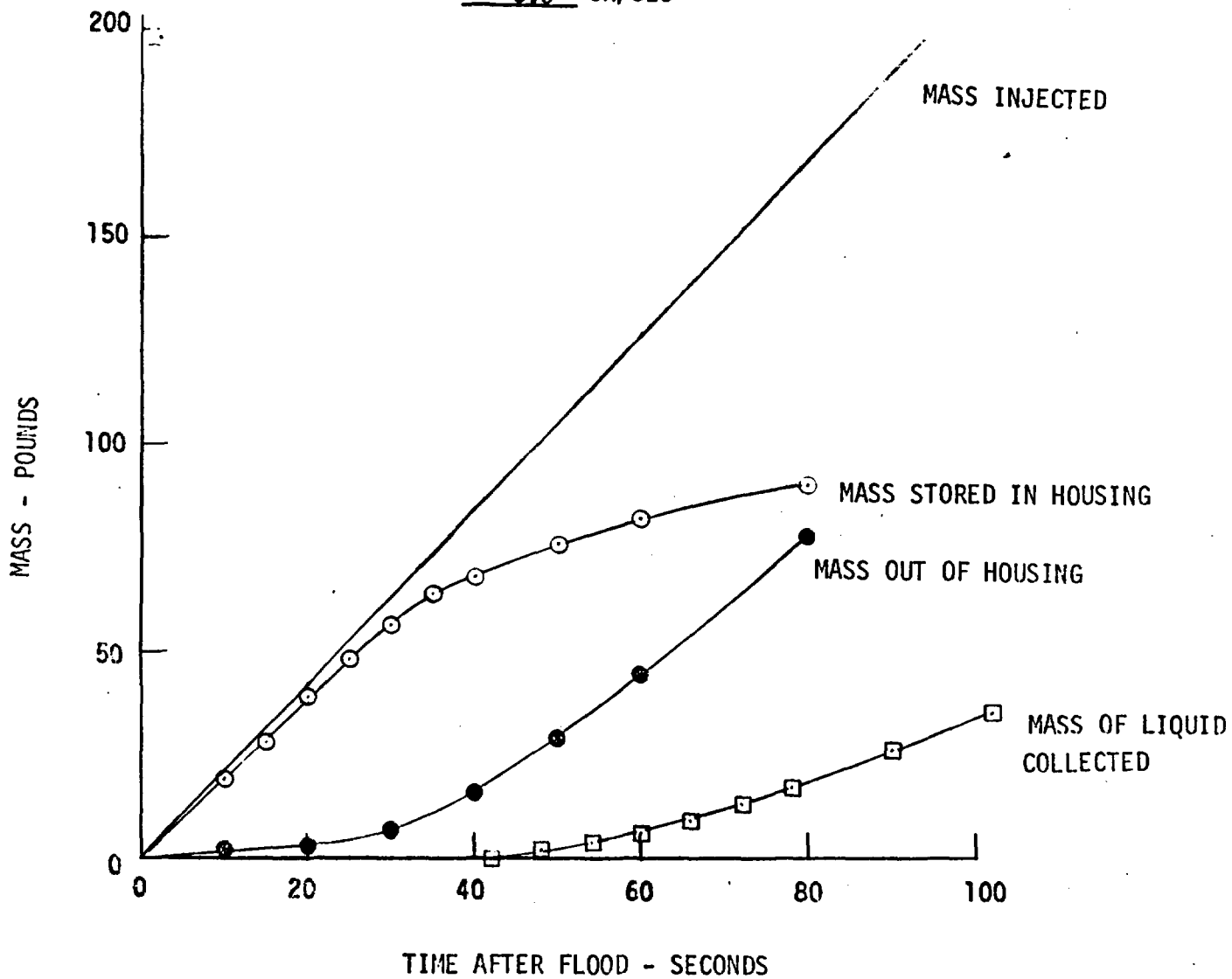
RUN NO. 0104

DATE 11/8/72

C. HEATER THERMOCOUPLE DATA

Rod/Elev.	Initial Temp. (°F)	Max. Temp. (°F)	Turnaround Time (Sec)	Quench Time (Sec)
5F/2'	352	372	10	10
5F/4'				
5F/6'				
5F/8'	418	677	27	29
5F/10'	378	556	32	34
5G/2'	347	368	8	8
5G/4'				
5G/6'	459	747	27	30
5G/8'	432	714	34	55
5G/10'	369	541	32	34
6G/2'	350	374	6	7
6G/4'	418	568	15	16
6G/6'				
6G/8'				
6G/10'	377	530	28	29
3H/2'				
3H/4'	411	553	13	14
3H/6'	453	730	24	26
3H/8'	402	658	28	30
3H/10'	366	537	37	40
4G/4'	450	630	16	19
4G/6'				
4G/10'	369	526	27	29
4H/4'	428	578	14	15
4H/6'				
4H/10'	365	525	29	34
7D/4'	418	569	14	16
7D/6'	445	685	23	25
7D/10'	367	536	30	32

RUN NO.: 0104
PEAK POWER: 0.7 KW/FT
PRESSURE: 57 PSIA
INITIAL CLAD TEMP.: 459 °F
COOLANT TEMP.: 143 °F
FLOODING RATE: 3.0 IN/SEC



1

2

3

4

LOW CLAD TEMPERATURE FLECHT RUN SUMMARY SHEET

RUN NO. 0203

DATE 11/14/72

A. RUN CONDITIONS

Pressure	60 psia
Initial Clad Temperature	360 °F
Peak Power	0.7 kw/ft
Coolant Temperature	144 °F
Flooding Rate	3.0 in./sec for 0→end sec

B. INITIAL HOUSING TEMPERATURES

Elevation (ft)	Temperature (°F)
0	178
2	352
4	320
6	340
8	312
10	309
12	289
AVG.	319

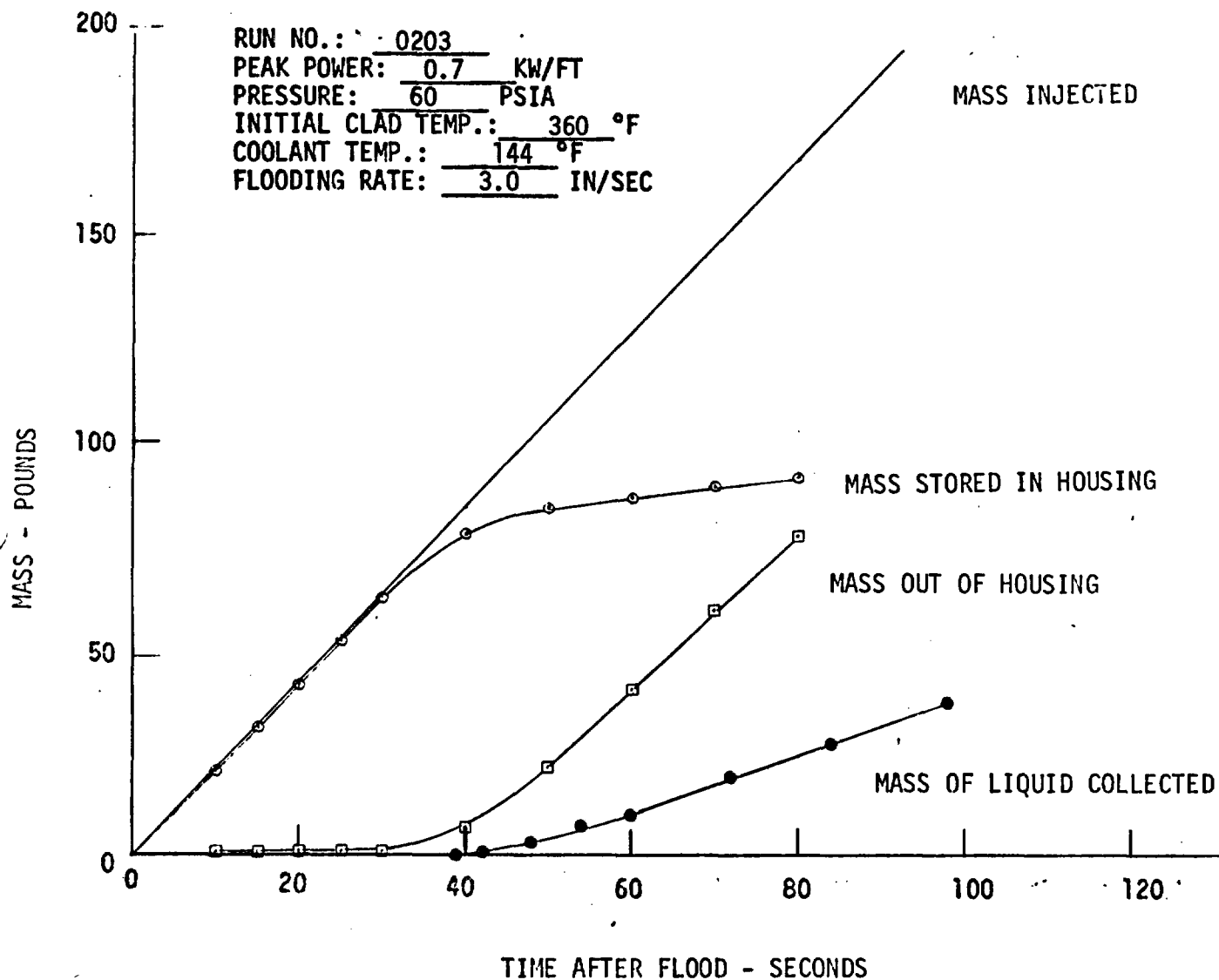
LOW CLAD TEMPERATURE FLECHT RUN SUMMARY SHEET (Cont)

RUN NO. 0203

DATE 11/14/72

C. HEATER THERMOCOUPLE DATA

Rod/Elev.	Initial Temp. (°F)	Max. Temp. (°F)	Turnaround Time (Sec)	Quench Time (Sec)
5F/2'	249	281	5	5
5F/4'				
5F/6'				
5F/8'	295	502	18	19
5F/10'	291	427	24	25
5G/2'	245	284	5	6
5G/4'				
5G/6'	360	664	27	28
5G/8'	294	646	40	40
5G/10'	290	427	28	29
6G/2'	245	284	5	6
6G/4'	318	442	11	12
6G/6'				
6G/8'				
6G/10'	291	430	24	25
3H/2'				
3H/4'	320	432	9	10
3H/6'				
3H/8'				
3H/10'	291	445	29	30
4G/4'	330	540	15	16
4G/6'				
4G/10'	291	427	24	24
4H/4'	337	456	10	11
4H/6'				
4H/10'	291	436	24	25
7D/4'	310	440	11	12
7D/6'	360	607	21	21
7D/10'	291	420	24	24



1

2

3

4

LOW CLAD TEMPERATURE FLECHT RUN SUMMARY SHEET

RUN NO. 0306

DATE 11/15/72

A. RUN CONDITIONS

Pressure	59 psia
Initial Clad Temperature	559 °F
Peak Power	0.7 kw/ft
Coolant Temperature	156 °F
Flooding Rate	3.0 in./sec for 0→endsec

B. INITIAL HOUSING TEMPERATURES

Elevation (ft)	Temperature (°F)
0	198
2	344
4	376
6	398
8	376
10	359
12	326
AVG.	357

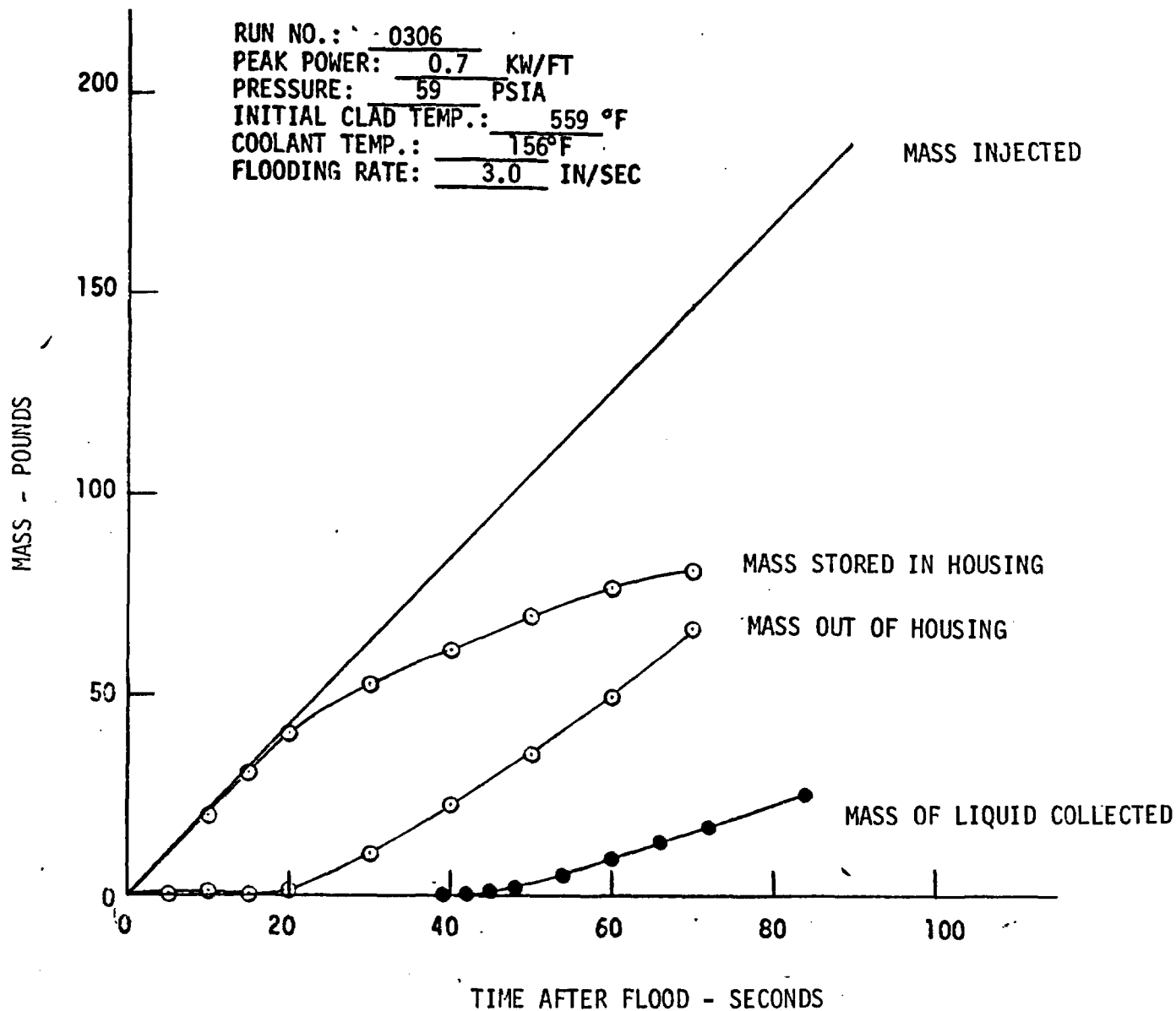
LOW CLAD TEMPERATURE FLECHT RUN SUMMARY SHEET (Cont)

RUN NO. 0306

DATE 11/15/72

C. HEATER THERMOCOUPLE DATA

Rod/Elev.	Initial Temp. (°F)	Max. Temp. (°F)	Turnaround Time (Sec)	Quench Time (Sec)
5F/2'	370	386	3	9
5F/4'				
5F/6'				
5F/8'	483	705	27	30
5F/10'	397	539	27	30
5G/2'	361	385	4	9
5G/4'				
5G/6'	559	800	26	36
5G/8'	502	748	38	60
5G/10'	392	515	24	29
6G/2'	368	392	5	10
6G/4'	478	603	14	16
6G/6'				
6G/8'				
6G/10'	389	518	22	24
3H/2'				
3H/4'	484	621	13	15
3H/6'	557	804	29	33
3H/8'				
3H/10'	392	535	32	35
4G/4'	522	695	14	15
4G/6'				
4G/10'	392	518	22	24
4H/4'	491	630	13	15
4H/6'				
4H/10'	395	525	23	24
7D/4'	477	585	11	13
7D/6'	545	755	25	30
7D/10'	386	528	26	29



1

2

3

4

5

LOW CLAD TEMPERATURE FLECHT RUN SUMMARY SHEET

RUN NO. 0405

DATE 11/15/72

A. RUN CONDITIONS

Pressure	59 psia
Initial Clad Temperature	449 °F
Peak Power	0.7 kw/ft
Coolant Temperature	144 °F
Flooding Rate	4.0 in./sec for 0→end sec

B. INITIAL HOUSING TEMPERATURES

Elevation (ft)	Temperature (°F)
0	226
2	355
4	350
6	413
8	383
10	324
12	297
AVG.	354

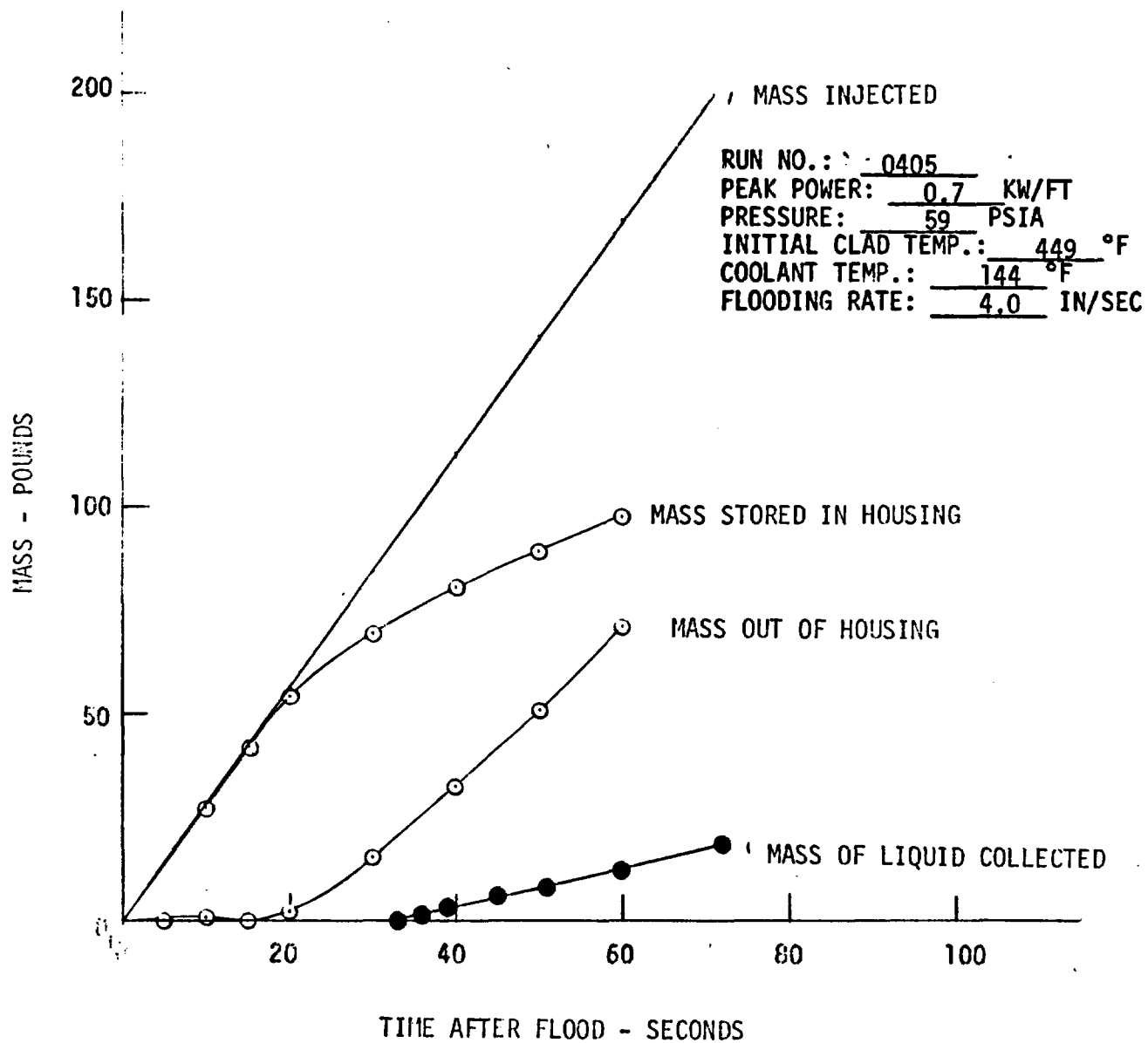
LOW CLAD TEMPERATURE FLECHT RUN SUMMARY SHEET (Cont)

RUN NO. 0405

DATE 11/15/72

C. HEATER THERMOCOUPLE DATA

Rod/Elev.	Initial Temp. (°F)	Max. Temp. (°F)	Turnaround Time (Sec)	Quench Time (Sec)
5F/2'	334	343	3	4
5F/4'				
5F/6'				
5F/8'	363	542	17	18
5F/10'	332	459	22	23
5G/2'	326	341	3	5
5G/4'				
5G/6'	444	627	14	15
5G/8'	381	599	22	24
5G/10'	330	452	22	23
6G/2'	322	342	14	5
6G/4'	363	471	10	11
6G/6'				
6G/8'				
6G/10'	323	447	22	23
3H/2'				
3H/4'	379	474	8	9
3H/6'				
3H/8'				
3H/10'	327	428	18	20
4G/4'	399	525	8	10
4G/6'				
4G/10'	327	449	22	23
4H/4'	379	479	9	10
4H/6'				
4H/10'	330	448	22	25
7D/4'	366	478	10	11
7D/6'	449	607	14	18
7D/10'	324	444	20	23



1

2

3

4

5

LOW CLAD TEMPERATURE FLECHT RUN SUMMARY SHEET

RUN NO. 0507

DATE 11/16/72

A. RUN CONDITIONS

Pressure	59	psia
Initial Clad Temperature	654	°F
Peak Power	0.7	kw/ft
Coolant Temperature	154	°F
Flooding Rate	3.0	in./sec for 0→end sec

B. INITIAL HOUSING TEMPERATURES

Elevation (ft)	Temperature (°F)
0	233
2	337
4	331
6	368
8	356
10	325
12	306
AVG.	335

LOW CLAD TEMPERATURE FLECHT RUN SUMMARY SHEET (Cont)

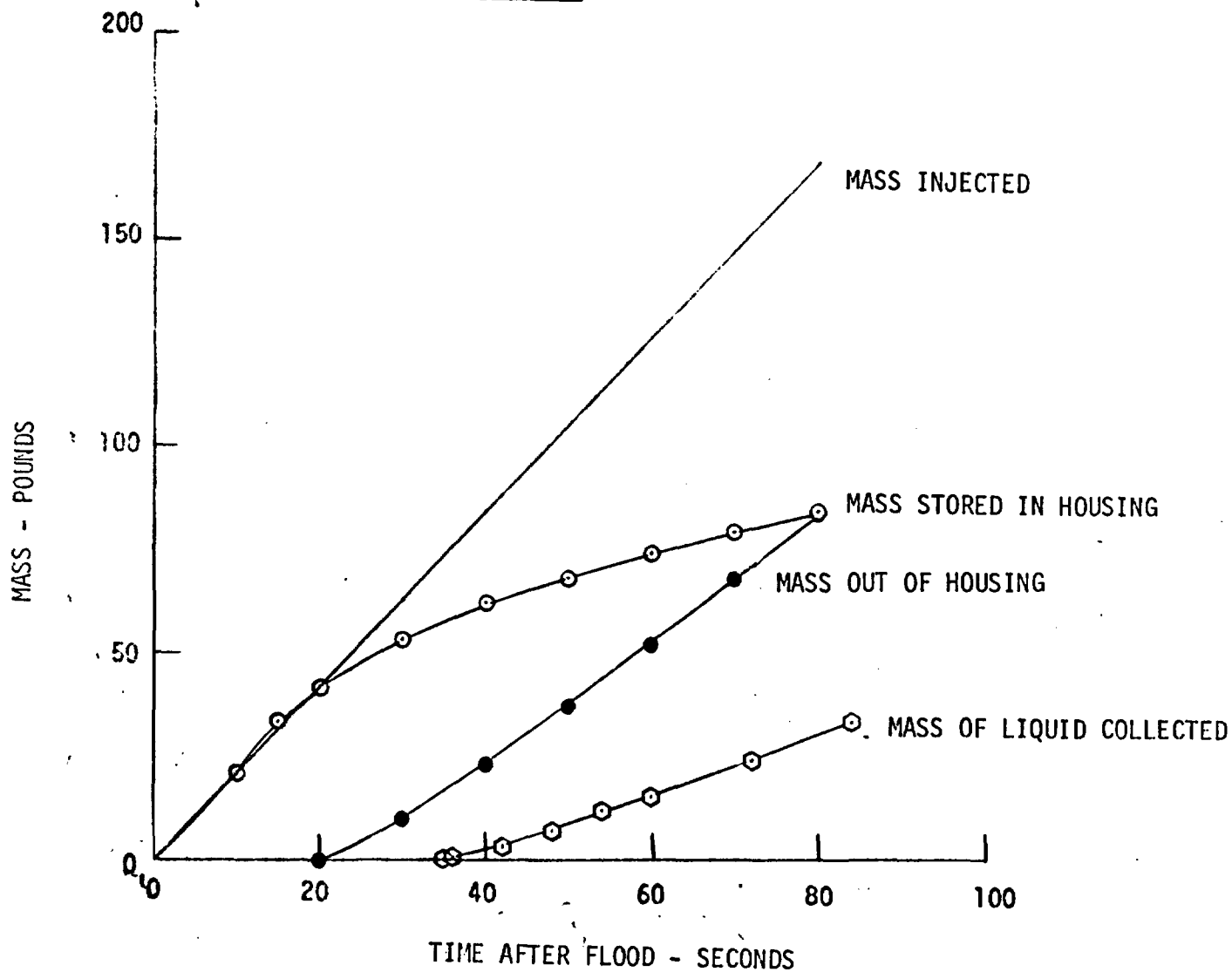
RUN NO. 0507

DATE 11/16/72

C. HEATER THERMOCOUPLE DATA

Rod/Elev.	Initial Temp. (°F)	Max. Temp. (°F)	Turnaround Time (Sec)	Quench Time (Sec)
5F/2'	420	453	6	8
5F/4'				
5F/6'				
5F/8'	551	746	24	27
5F/10'	422	566	30	33
5G/2'	412	417	2	5
5G/4'				
5G/6'	654	847	21	40
5G/8'	586	792	28	64
5G/10'	419	548	24	27
6G/2'	414	441	6	8
6G/4'	525	640	13	15
6G/6'				
6G/8'				
6G/10'	418	534	20	22
3H/2'				
3H/4'	539	645	11	13
3H/6'				
3H/8'				
3H/10'	421	559	30	33
4G/4'	600	741	15	19
4G/6'				
4G/10'	421	531	21	25
4H/4'	545	671	16	18
4H/6'				
4H/10'	427	541	21	24
7D/4'	525	645	12	14
7D/6'	628	801	20	38
7D/10'	415	543	24	26

RUN NO.: 0507
 PEAK POWER: 0.7 KW/FT
 PRESSURE: 59 PSIA
 INITIAL CLAD TEMP.: 654 °F
 COOLANT TEMP.: 154 °F
 FLOODING RATE: 3.0 IN/SEC



1

2

3

4

LOW CLAD TEMPERATURE FLECHT RUN SUMMARY SHEET

RUN NO. 0608

DATE 11/17/72

A. RUN CONDITIONS

Pressure	60 psia
Initial Clad Temperature	754 °F
Peak Power	0.7 kw/ft
Coolant Temperature	149 °F
Flooding Rate	3.0 in./sec for 0→end sec

B. INITIAL HOUSING TEMPERATURES

Elevation (ft)	Temperature (°F)
0	243
2	331
4	378
6	443
8	363
10	345
12	311
AVG.	339

LOW CLAD TEMPERATURE FLECHT RUN SUMMARY SHEET (Cont)

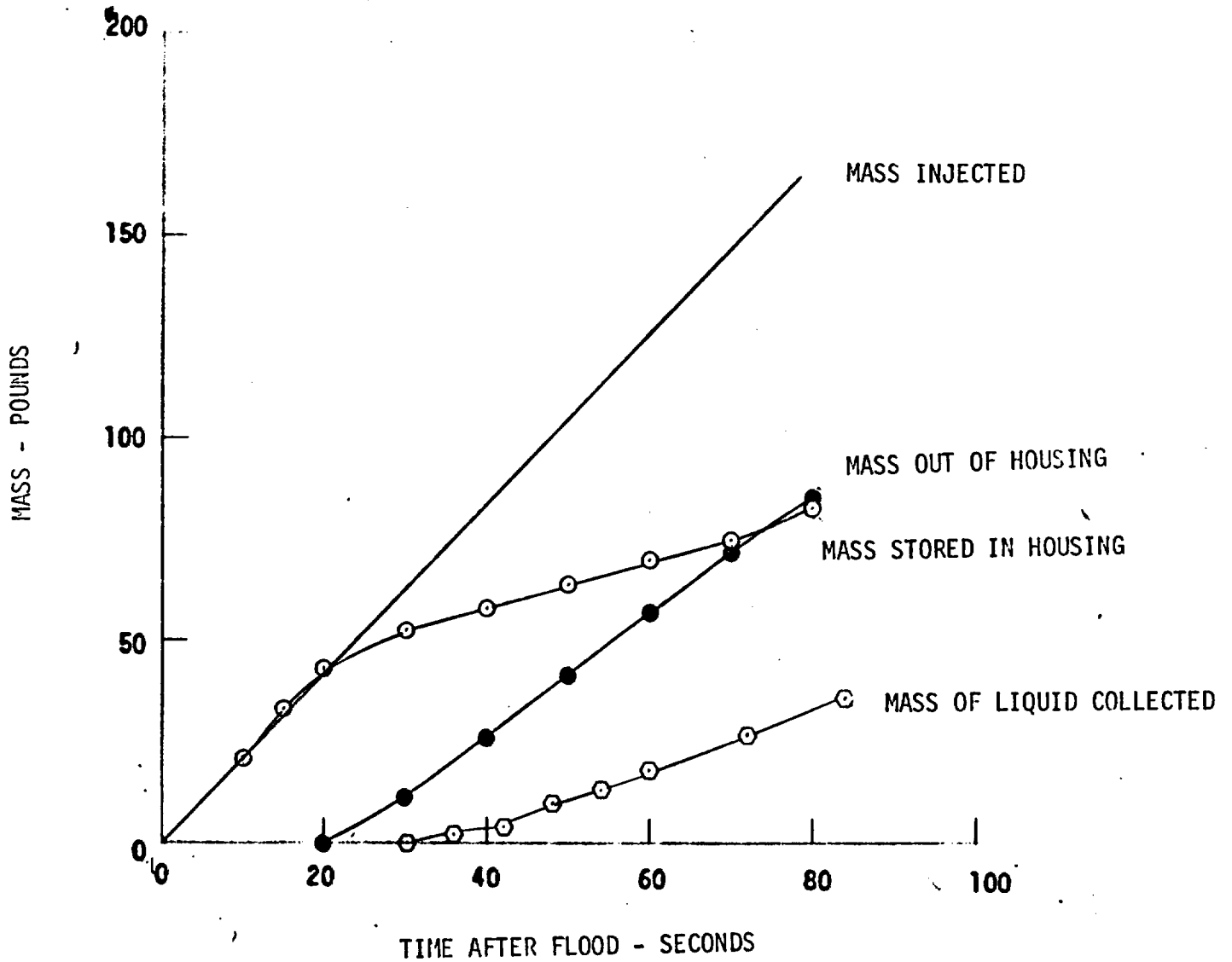
RUN NO. 0608

DATE 11/17/72

C. HEATER THERMOCOUPLE DATA

Rod/Elev.	Initial Temp. (°F)	Max. Temp. (°F)	Turnaround Time (Sec)	Quench Time (Sec)
5F/2'	460	484	4	5
5F/4'				
5F/6'				
5F/8'	630	803	28	30
5F/10'	480	620	33	36
5G/2'	448	479	5	6
5G/4'				
5G/6'	754	928	20	48
5G/8'	666	847	29	69
5G/10'	476	593	23	25
6G/2'	452	485	5	6
6G/4'	599	701	13	18
6G/6'				
6G/8'				
6G/10'	473	577	18	21
3H/2'				
3H/4'	616	726	14	16
3H/6'				
3H/8'				
3H/10'	474	606	34	39
4G/4'	692	809	13	21
4G/6'				
4G/10'	474	577	18	20
4H/4'	613	721	18	22
4H/6'				
4H/10'	480	584	19	22
7D/4'	598	715	15	18
7D/6'	716	873	18	43
7D/10'	468	605	38	41

RUN NO.: 0608
PEAK POWER: 0.7 KW/FT
PRESSURE: 60 PSIA
INITIAL CLAD TEMP.: 754 °F
COOLANT TEMP.: 149 °F
FLOODING RATE: 3.0 IN/SEC





LOW CLAD TEMPERATURE FLECHT RUN SUMMARY SHEET

RUN NO. 0701

DATE 11/21/72

A. RUN CONDITIONS

Pressure	23	psia
Initial Clad Temperature	375	°F
Peak Power	0.7	kw/ft
Coolant Temperature	23	°F
Flooding Rate	3.0	in./sec for 0→end sec

B. INITIAL HOUSING TEMPERATURES

Elevation (ft)	Temperature (°F)
0	197
2	285
4	313
6	347
8	326
10	278
12	248
AVG.	298

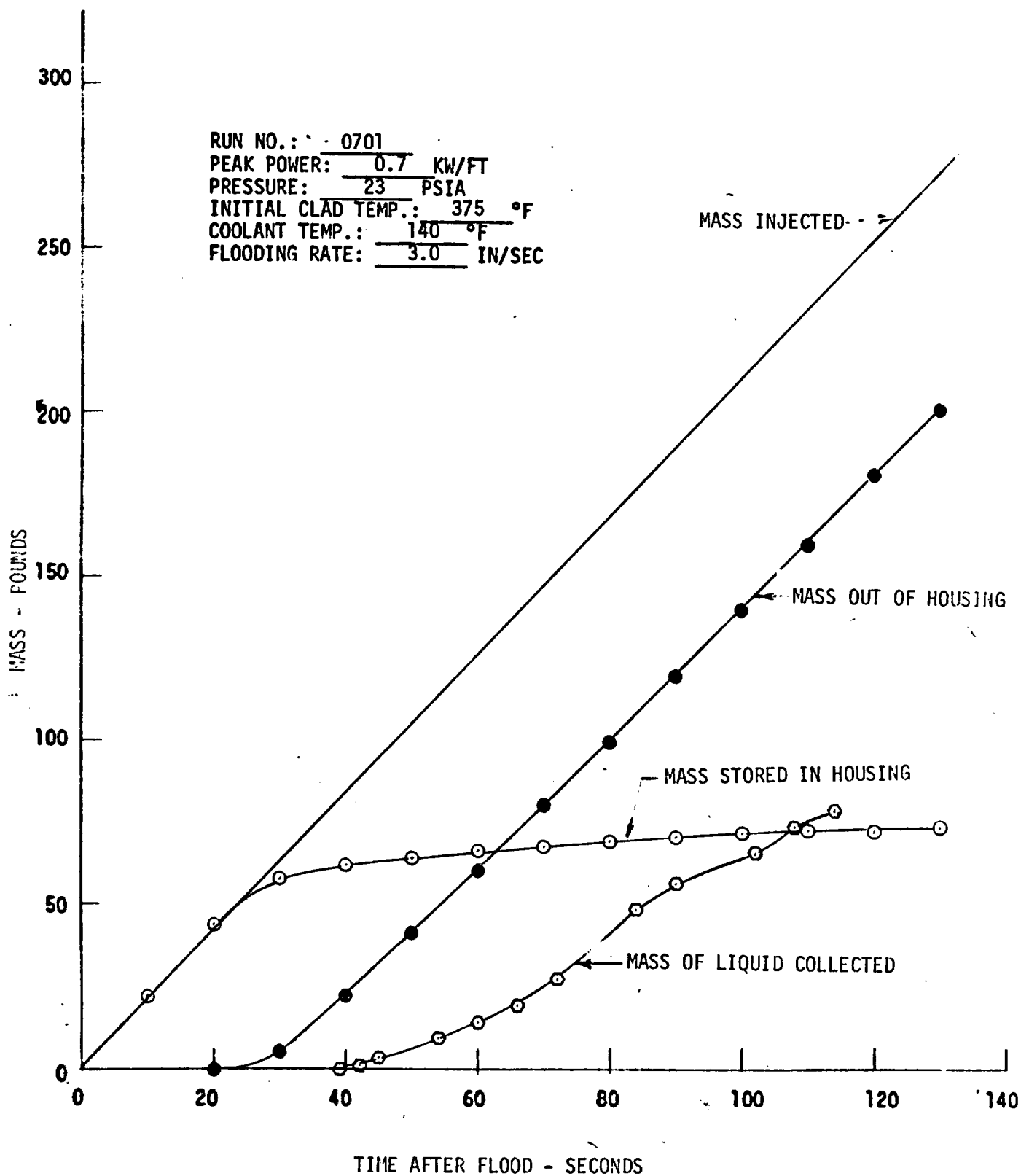
LOW CLAD TEMPERATURE FLECHT RUN SUMMARY SHEET (Cont)

RUN NO. 0701

DATE 11/21/72

C. HEATER THERMOCOUPLE DATA

Rod/Elev.	Initial Temp. (°F)	Max. Temp. (°F)	Turnaround Time (Sec)	Quench Time (Sec)
5F/2'	233	254	2	6
5F/4'				
5F/6'				
5F/8'	338	556	23	28
5F/10'	270	379	17	18
5G/2'	231	258	4	5
5G/4'				
5G/6'	375	690	47	49
5G/8'	349	686	60	121
5G/10'	271	371	17	19
6G/2'	233	264	4	6
6G/4'	276	393	10	12
6G/6'				
6G/8'				
6G/10'	257	366	17	19
3H/2'				
3H/4'	313	408	7	13
3H/6'				
3H/8'	339	597	30	58
3H/10'	274	389	24	25
4G/4'	317	504	13	15
4G/6'				
4G/10'	269	366	17	19
4H/4'	311	456	14	16
4H/6'				
4H/10'	266	371	18	20
7D/4'	289	400	10	12
7D/6'	381	610	24	38
7D/10'	267	379	22	23



1

2

3

LOW CLAD TEMPERATURE FLECHT RUN SUMMARY SHEET

RUN NO. 0802

DATE 11/21/72

A. RUN CONDITIONS

Pressure	20	psia
Initial Clad Temperature	453	°F
Peak Power	0.7	kw/ft
Coolant Temperature	142	°F
Flooding Rate	3.0	in./sec for 0→endsec

B. INITIAL HOUSING TEMPERATURES

Elevation (ft)	Temperature (°F)
0	181
2	284
4	301
6	303
8	298
10	259
12	234
AVG.	278

LOW CLAD TEMPERATURE FLECHT RUN SUMMARY SHEET (Cont)

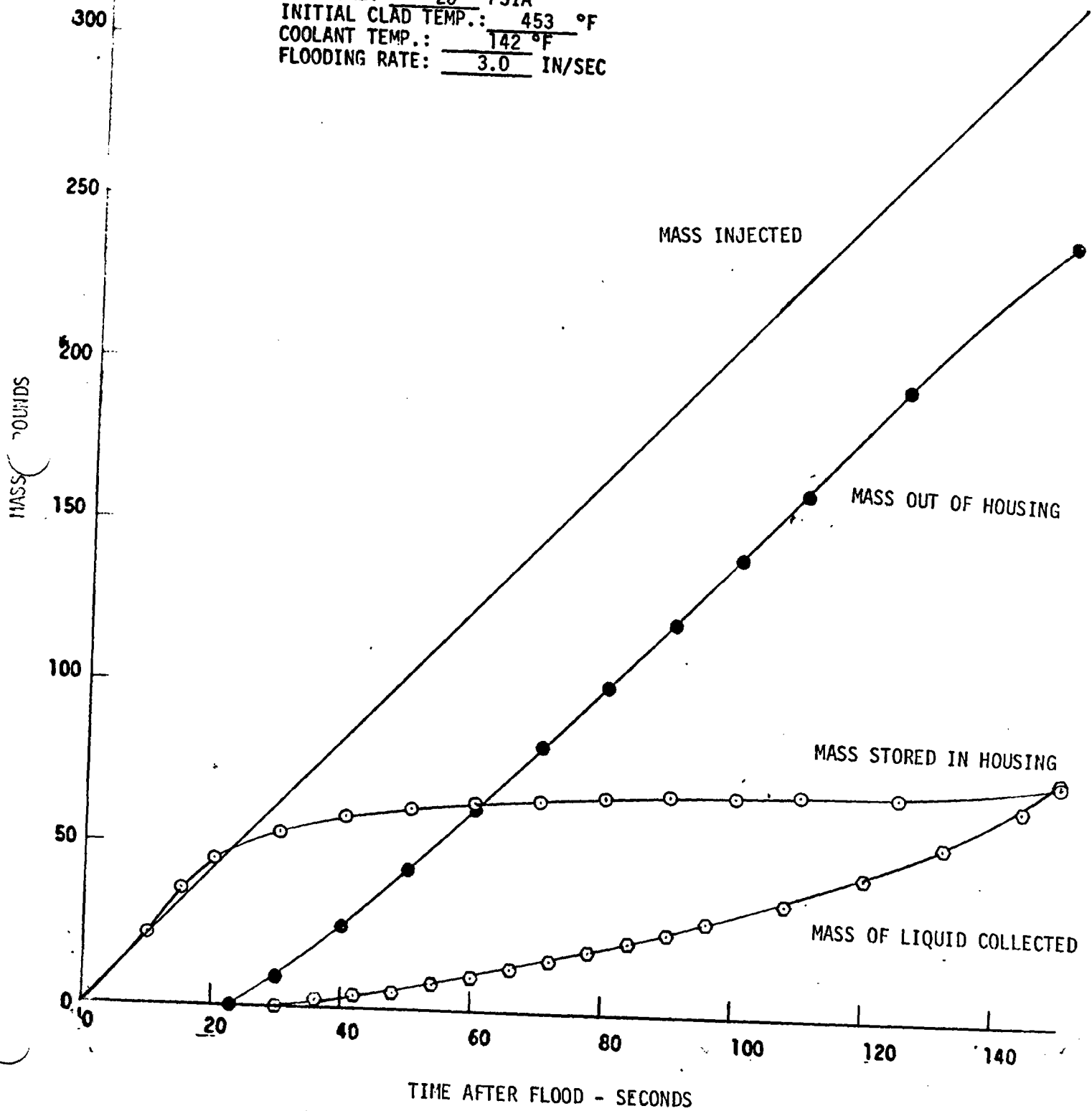
RUN NO. 0802

DATE 11/21/72

C. HEATER THERMOCOUPLE DATA

Rod/Elev.	Initial Temp. (°F)	Max. Temp. (°F)	Turnaround Time (Sec)	Quench Time (Sec)
5F/2'	294	325	5	7
5F/4'				
5F/6'				
5F/8'	397	617	30	32
5F/10'	313	424	19	22
5G/2'	287	323	5	6
5G/4'				
5G/6'	453	729	54	78
5G/8'	417	725	74	157
5G/10'	310	414	18	20
6G/2'	291	330	5	7
6G/4'	387	512	17	19
6G/6'				
6G/8'				
6G/10'	301	408	19	21
3H/2'				
3H/4'	418	547	16	23
3H/6'				
3H/8'	404	661	47	115
3H/10'	317	428	25	27
4G/4'	456	613	16	24
4G/6'				
4G/10'	311	391	13	18
4H/4'	415	543	16	20
4H/6'				
4H/10'	309	412	19	22
7D/4'	389	518	18	20
7D/6'	428	658	32	61
7D/10'	308	408	18	20

RUN NO.: 0802
 PEAK POWER: 0.7 KW/FT
 PRESSURE: 20 PSIA
 INITIAL CLAD TEMP.: 453 °F
 COOLANT TEMP.: 142 °F
 FLOODING RATE: 3.0 IN/SEC



1

2

3

LOW CLAD TEMPERATURE FLECHT RUN SUMMARY SHEET

RUN NO. 1109

DATE 11/29/72

A. RUN CONDITIONS

Pressure	20 psia
Initial Clad Temperature	311 °F
Peak Power	.70 kw/ft
Coolant Temperature	149 °F
Flooding Rate	3.0 in./sec for 0→end sec

B. INITIAL HOUSING TEMPERATURES

Elevation (ft)	Temperature (°F)
0	199
2	242
4	251
6	270
8	256
10	255
12	234
AVG.	237

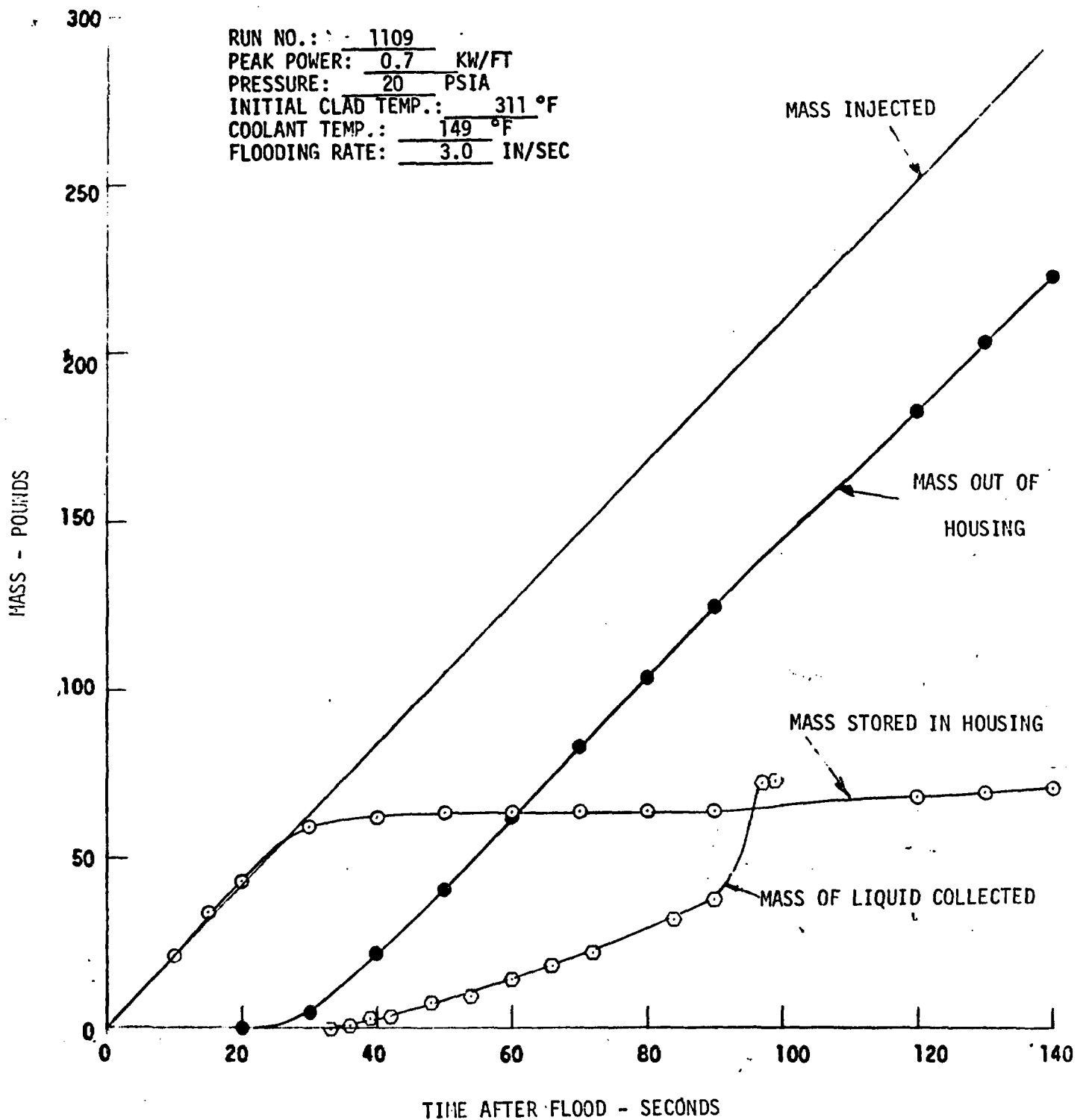
LOW CLAD TEMPERATURE FLECHT RUN SUMMARY SHEET (Cont)

RUN NO. 1109

DATE 11/29/72

C. HEATER THERMOCOUPLE DATA

Rod/Elev.	Initial Temp. (°F)	Max. Temp. (°F)	Turnaround Time (Sec)	Quench Time (Sec)
5F/2'	237	276	6	8
5F/4'				
5F/6'				
5F/8'	282	518	26	29
5F/10'	261	381	20	22
5G/2'	231	274	7	8
5G/4'				
5G/6'	311	668	50	52
5G/8'	301	673	97	
5G/10'	262	375	19	21
6G/2'	235	281	7	8
6G/4'	282	423	13	15
6G/6'				
6G/8'				
6G/10'	244	365	20	22
3H/2'				
3H/4'	297	424	11	13
3H/6'				
3H/8'	266	519	32	45
3H/10'	269	393	26	27
4G/4'	316	511	17	19
4G/6'				
4G/10'	262	371	20	22
4H/4'	303	433	12	14
4H/6'				
4H/10'	254	381	26	28
7D/4'	285	426	13	15
7D/6'	303	560	28	35
7D/10'	259	373	19	21



(

(

(

LOW CLAD TEMPERATURE FLECHT RUN SUMMARY SHEET

RUN NO. 1212

DATE 12/1/72

A. RUN CONDITIONS

Pressure	19	psia
Initial Clad Temperature	253	°F
Peak Power	0.7	kw/ft
Coolant Temperature	139	°F
Flooding Rate	6.5 in./sec for 0→3.4	sec
	.97 in./sec for 3.4→60	sec
	.96 in./sec for 60→end	sec

B. INITIAL HOUSING TEMPERATURES

Elevation (ft)	Temperature (°F)
0	169
2	173
4	183
6	181
8	175
10	190
12	210
AVG.	181

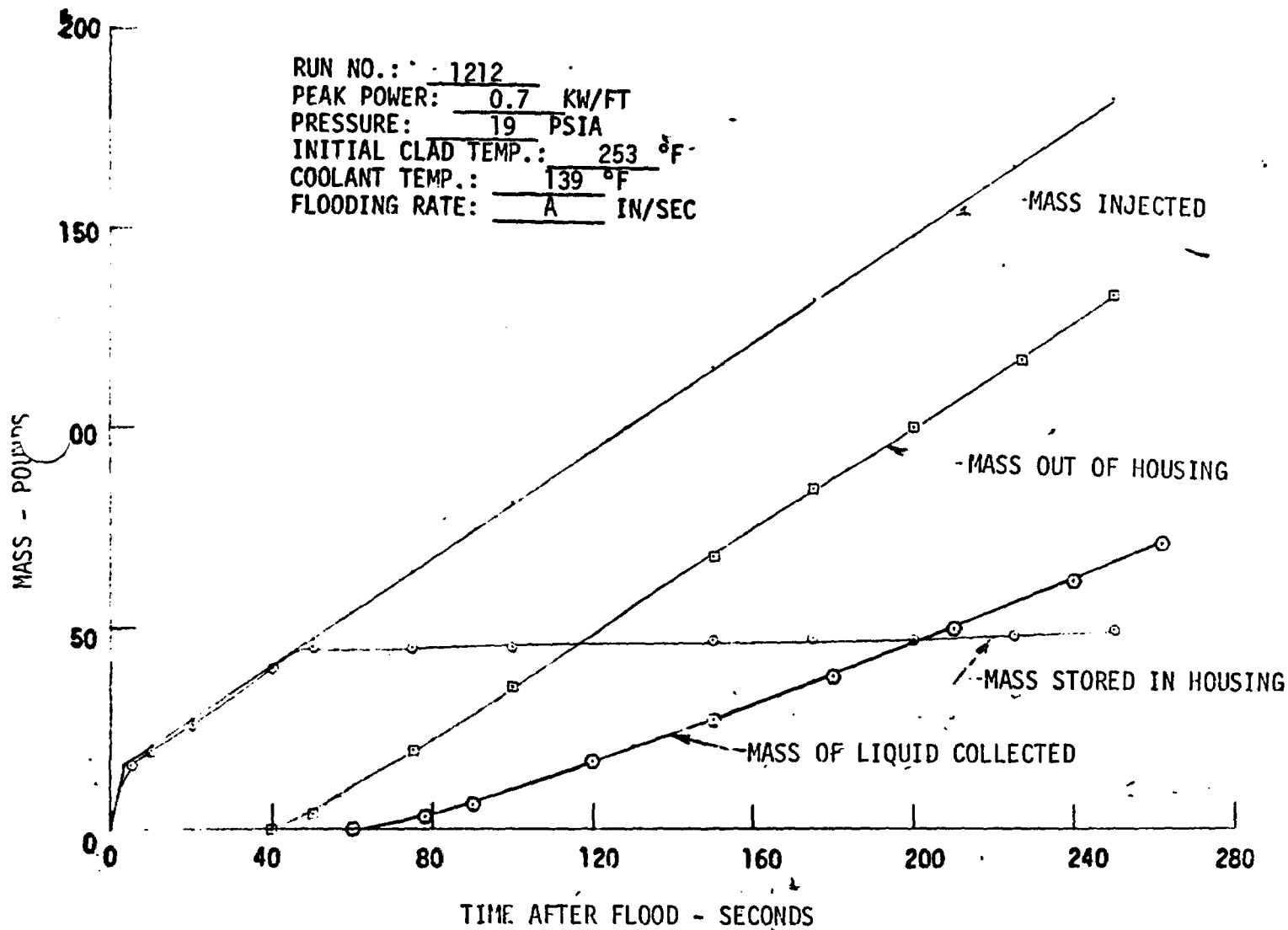
LOW CLAD TEMPERATURE FLECHT RUN SUMMARY SHEET (Cont)

RUN NO. 1212

DATE 12/1/72

C. HEATER THERMOCOUPLE DATA

Rod/Elev.	Initial Temp. (°F)	Max. Temp. (°F)	Turnaround Time (Sec)	Quench Time (Sec)
5F/2'	186	203	4	
5F/4'				
5F/6'				
5F/8'	229	795	127	203
5F/10'	213	562	85	88
5G/2'	181	209	47	
5G/4'				
5G/6'	253	825	74	125
5G/8'	240	863	127	258
5G/10'	212	495	52	56
6G/2'	183	207	4	
6G/4'	230	511	24	26
6G/6'				
6G/8'				
6G/10'	193	469	47	50
3H/2'				
3H/4'	235	505	24	29
3H/6'	258	813	76	96
3H/8'	205	849	132	221
3H/10'	215	565	138	514° @ 300 sec no quench
4G/4'	252	628	28	30
4G/6'				
4G/10'	210	466	42	44
4H/4'	242	542	28	30
4H/6'				
4H/10'	200	489	73	77
7D/4'	232	510	24	27
7D/6'	247	747	74	101
7D/10'	208	495	51	54



—

—

—

—

—

LOW CLAD TEMPERATURE FLECHT RUN SUMMARY SHEET

RUN NO. 1516

DATE 12/6/72

A. RUN CONDITIONS

Pressure	22	psia
Initial Clad Temperature	320	°F
Peak Power	1.0	kw/ft
Coolant Temperature	145	°F
Flooding Rate	6.1 in./sec for 0→3.4	sec
	3.1 in./sec for 3.4→15.5	sec
	1.0 in./sec for 15.5→end	sec

B. INITIAL HOUSING TEMPERATURES

Elevation (ft)	Temperature (°F)
0	181
2	254
4	274
6	296
8	274
10	243
12	220
AVG.	259

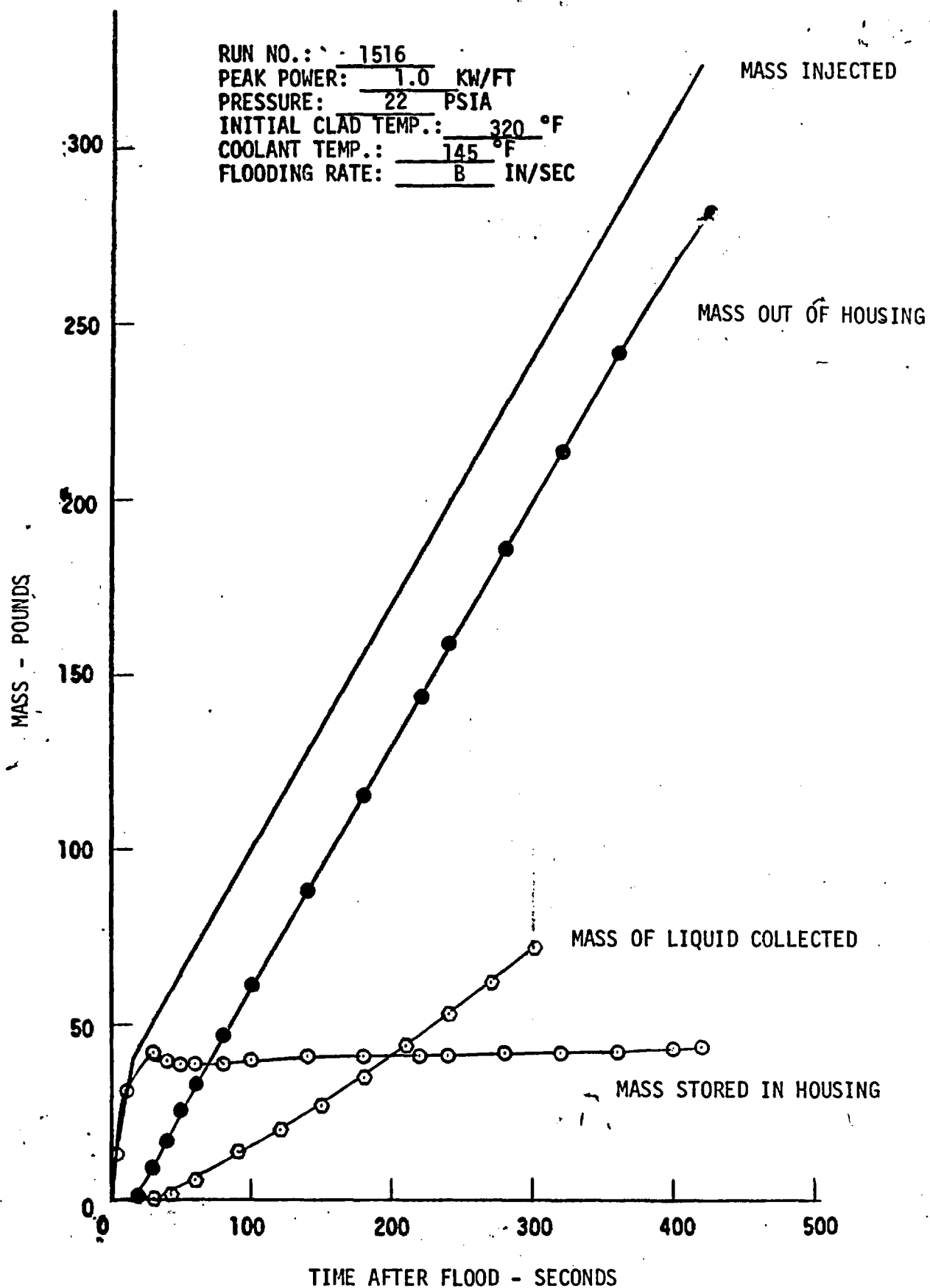
LOW CLAD TEMPERATURE FLECHT RUN SUMMARY SHEET (Cont)

RUN NO. 1516

DATE 12/6/72

C. HEATER THERMOCOUPLE DATA

Rod/Elev.	Initial Temp. (°F)	Max. Temp. (°F)	Turnaround Time (Sec)	Quench Time (Sec)
5F/2'	244	250	3	
5F/4'				
5F/6'				
5F/8'	279	663	30	32
5F/10'	270	403	14	16
5G/2'	246	254	3	6
5G/4'				
5G/6'	320		90	149
5G/8'				
5G/10'	300	1043	140	411
6G/2'	243	257	3	6
6G/4'	281	395	7	9
6G/6'				
6G/8'				
6G/10'	260	396	15	17
3H/2'				
3H/4'				
3H/6'	311	400	6	8
3H/8'	282	919	90	92
3H/10'	264	420	19	20
4G/4'	330	545	12	12
4G/6'				
4G/10'	267	295	14	16
4H/4'	326	495	12	13
4H/6'				
4H/10'	270	456	25	26
7D/4'	287	405	7	8
7D/6'	308	913	86	88
7D/10'	260	727	140	171



1

2

3

4

LOW CLAD TEMPERATURE FLECHT RUN SUMMARY SHEET

RUN NO. 1617

DATE 12/6/72

A. RUN CONDITIONS

Pressure	24 psia
Initial Clad Temperature	272 °F
Peak Power	1.2 kw/ft
Coolant Temperature	149 °F
Flooding Rate	6.2 in./sec for 0→3.4 sec
	3.1 in./sec for 3.4→15.7 sec
	.95 in./sec for 15.7→end sec

B. INITIAL HOUSING TEMPERATURES

Elevation (ft)	Temperature (°F)
0	178
2	245
4	244
6	240
8	230
10	232
12	223
AVG.	234

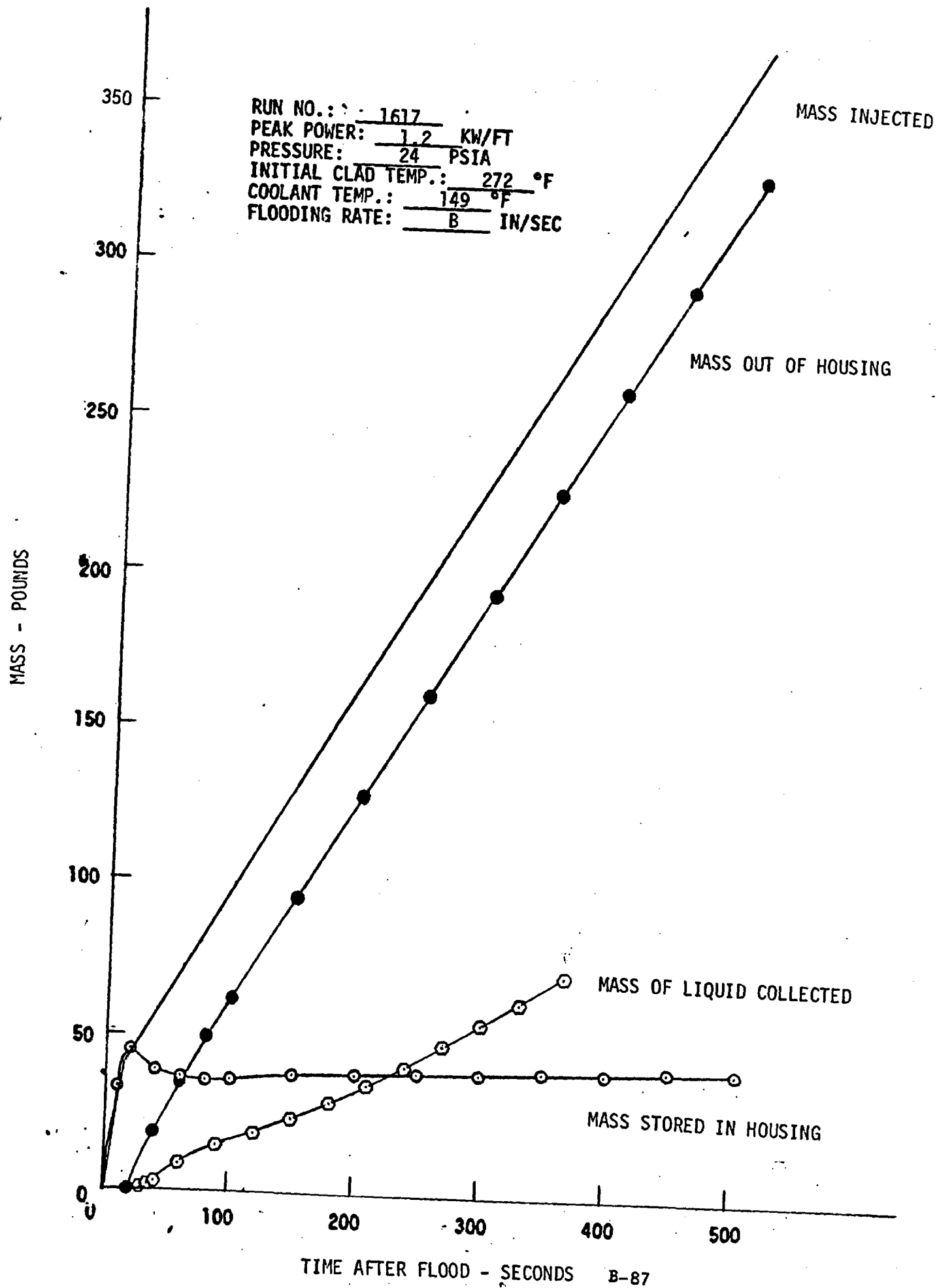
LOW CLAD TEMPERATURE FLECHT RUN SUMMARY SHEET (Cont)

RUN NO. 1617

DATE 12/6/72

C. HEATER THERMOCOUPLE DATA

Rod/Elev.	Initial Temp. (°F)	Max. Temp. (°F)	Turnaround Time (Sec)	Quench Time (Sec)
5F/2'	238	256	2	
5F/4'				
5F/6'				
5F/8'	242	970	102	116
5F/10'	240	414	16	18
5G/2'	231	256	3	5
5G/4'				
5G/6'	272	1114	96	153
5G/8'	250	1141	155	492
5G/10'	238	405	15	17
6G/2'	233	265	3	5
6G/4'	247	424	9	12
6G/6'				
6G/8'				
6G/10'	231	406	16	18
3H/2'				
3H/4'	260	406	7	9
3H/6'	267	1072	89	
3H/8'	252	948	70	73
3H/10'	246	508	32	34
4G/4'	264	464	8	12
4G/6'				
4G/10'	232	355	11	15
4H/4'	263	422	8	10
4H/6'				
4H/10'	247	417	16	19
7D/4'	247	432	9	12
7D/6'	270	1019	93	96
7D/10'	238	399	104	107



—

—

—

—

—

LOW CLAD TEMPERATURE FLECHT RUN SUMMARY SHEET

RUN NO. 1715

DATE 12/6/72

A. RUN CONDITIONS

Pressure	20 psia
Initial Clad Temperature	400 °F
Peak Power	0.7 kw/ft
Coolant Temperature	147 °F
Flooding Rate	6.2 in./sec for 0→3.4 sec 3.1 in./sec for 3.4→16.1 sec 1.01 in./sec for 16.1→end sec

B. INITIAL HOUSING TEMPERATURES

Elevation (ft)	Temperature (°F)
0	195
2	289
4	308
6	366
8	358
10	260
12	219
AVG.	300

LOW CLAD TEMPERATURE FLECHT RUN SUMMARY SHEET (Cont)

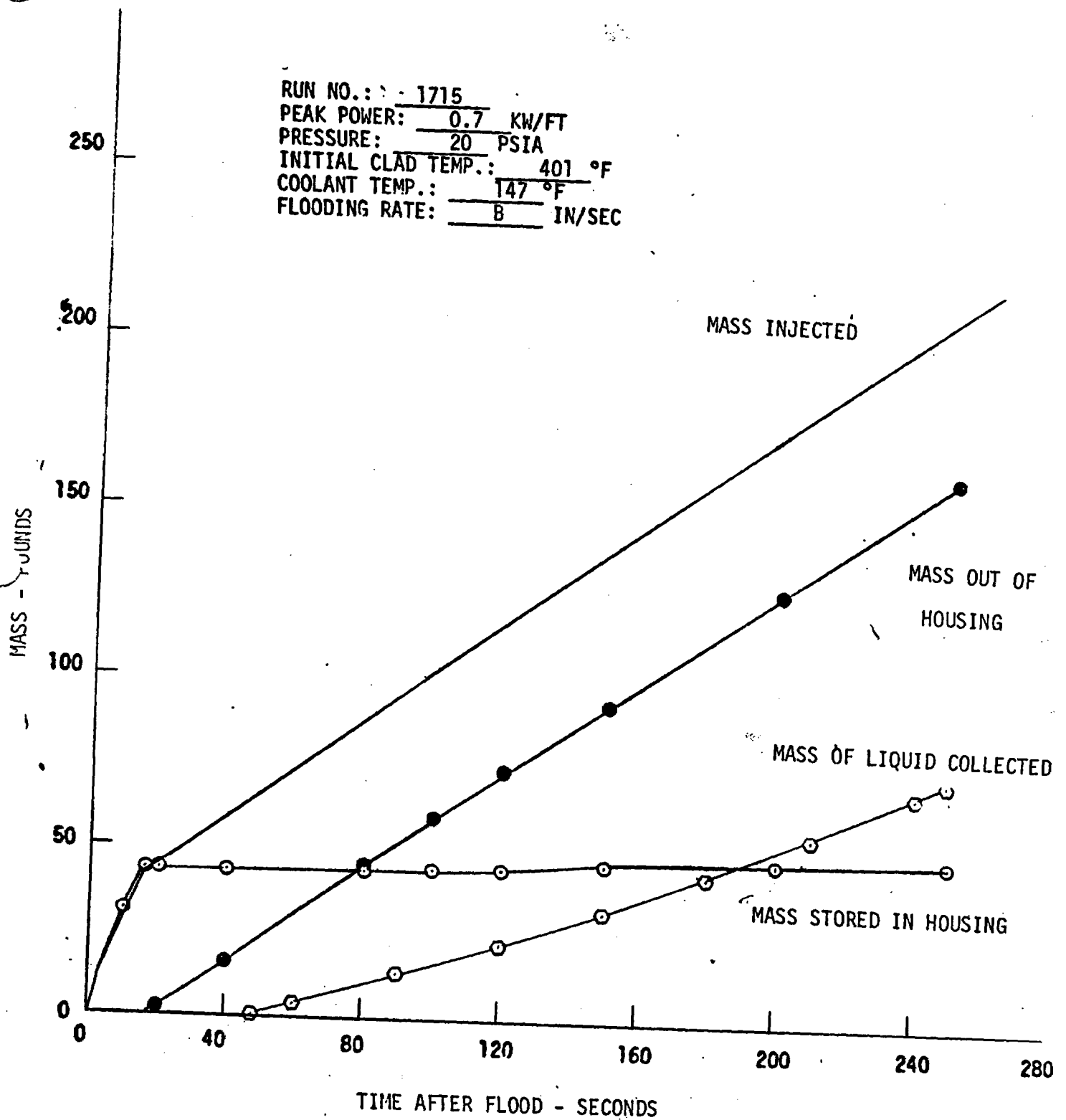
RUN NO. 1715

DATE 12/6/72

C. HEATER THERMOCOUPLE DATA

Rod/Elev.	Initial Temp. (°F)	Max. Temp. (°F)	Turnaround Time (Sec)	Quench Time (Sec)
5F/2'	265	266	1	
5F/4'				
5F/6'				
5F/8'	346	615	35	37
5F/10'	296	381	14	14
5G/2'	265	269	1	
5G/4'				
5G/6'	401	790	86	88
5G/8'	369	826	123	266
5G/10'	293	554	97	107
6G/2'	260	263	1	
6G/4'	347	419	6	7
6G/6'				
6G/8'				
6G/10'	289	359	12	14
3H/2'				
3H/4'	369	479	10	11
3H/6'				
3H/8'	360	851	120	220
3H/10'	292	394	18	20
4G/4'	407	544	11	12
4G/6'				
4G/10'	290	396	18	20
4H/4'	374	483	10	11
4H/6'				
4H/10'	297	420	24	25
7D/4'	348	420	6	7
7D/6'	378	701	58	60
7D/10'	293	591	105	108

RUN NO.: 1715
 PEAK POWER: 0.7 KW/FT
 PRESSURE: 20 PSIA
 INITIAL CLAD TEMP.: 401 °F
 COOLANT TEMP.: 147 °F
 FLOODING RATE: 8 IN/SEC



1

2

3

4

5

LOW CLAD TEMPERATURE FLECHT RUN SUMMARY SHEET

RUN NO. 1812

DATE 12/7/72

A. RUN CONDITIONS

Pressure	59 psia
Initial Clad Temperature	502 °F
Peak Power	0.7 kw/ft
Coolant Temperature	151 °F
Flooding Rate	6.4 in./sec for 0→3.4 sec
	3.3 in./sec for 3.4→15.4 sec
	.99 in./sec for 15.4→end sec

B. INITIAL HOUSING TEMPERATURES

Elevation (ft)	Temperature (°F)
0	197
2	333
4	375
6	392
8	384
10	301
12	283
AVG.	272

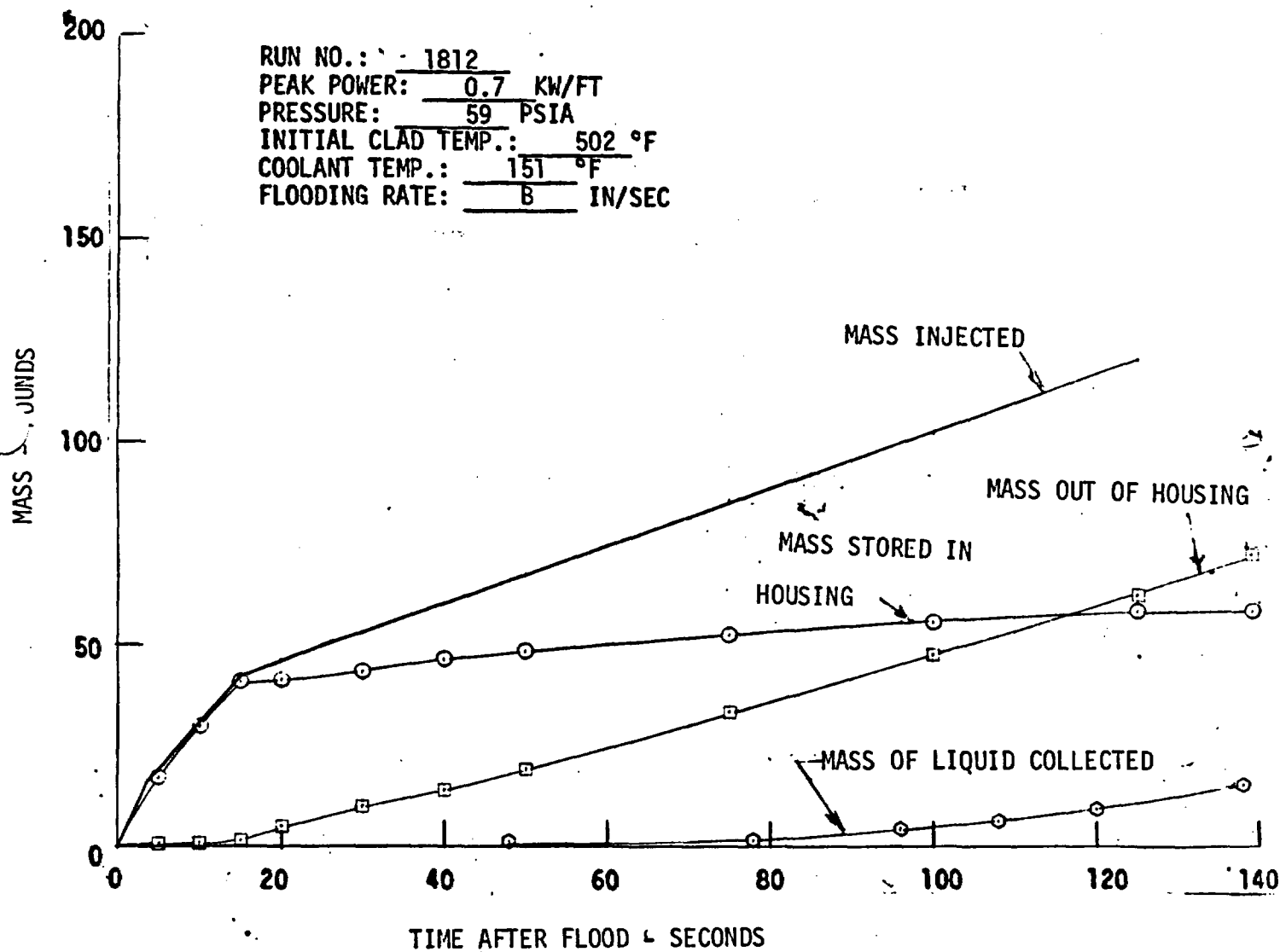
LOW CLAD TEMPERATURE FLECHT RUN SUMMARY SHEET (Cont)

RUN NO. 1812

DATE 12/7/72

C. HEATER THERMOCOUPLE DATA

Rod/Elev.	Initial Temp. (°F)	Max. Temp. (°F)	Turnaround Time (Sec)	Quench Time (Sec)
5F/2'	308	308	1	3
5F/4'				
5F/6'				
5F/8'	450	580	16	37
5F/10'	340	515	36	42
5G/2'	308	312	2	4
5G/4'				
5G/6'	502	780	42	49
5G/8'	470	770	48	80
5G/10'	335	540	46	47
6G/2'	312	318	2	3
6G/4'	435	515	7	8
6G/6'				
6G/8'				
6G/10'	320	500	36	42
3H/2'				
3H/4'	450	555	10	12
3H/6'	465	750	33	40
3H/8'	450	730	48	65
3H/10'	330	550	34	51
4G/4'	480	620	11	12
4G/6'				
4G/10'	330	535	46	49
4H/4'	460	570	11	43
4H/6'				
4H/10'	330	540	46	50
7D/4'	430	515	7	8
7D/6'	500	730	29	38
7D/10'				



1

2

3

4

LOW CLAD TEMPERATURE FLECHT RUN SUMMARY SHEET

RUN NO. 1913

DATE 12/7/72

A. RUN CONDITIONS

Pressure	58	psia
Initial Clad Temperature	310	°F
Peak Power	1.01	kw/ft
Coolant Temperature	156	°F
Flooding Rate	6.3	in./sec for 0→3.5 sec
	3.2	in./sec for 3.5→15.4 sec
	.99	in./sec for 15.4→end sec

B. INITIAL HOUSING TEMPERATURES

Elevation (ft)	Temperature (°F)
0	214
2	290
4	288
6	306
8	290
10	291
12	293
AVG.	289

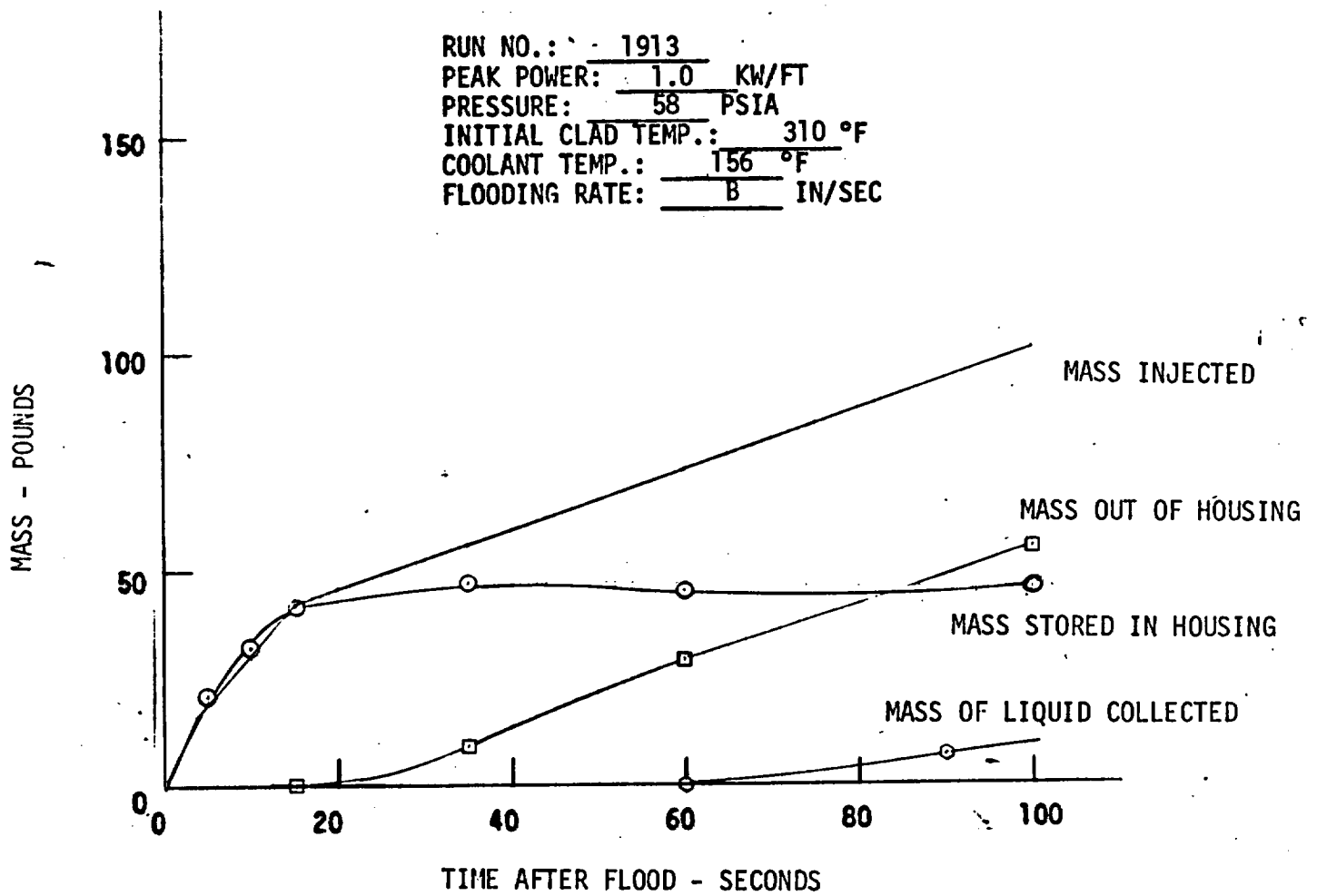
LOW CLAD TEMPERATURE FLECHT RUN SUMMARY SHEET (Cont)

RUN NO. 1913

DATE 12/7/72

C. HEATER THERMOCOUPLE DATA

Rod/Elev.	Initial Temp. (°F)	Max. Temp. (°F)	Turnaround Time (Sec)	Quench Time (Sec)
5F/2'	293	297	4	5
5F/4'				
5F/6'				
5F/8'	307	560	18	18
5F/10'	302	498	24	25
5G/2'	297	297	0	1
5G/4'				
5G/6'	310	597	15	15
5G/8'	318	755	13	15
5G/10'	302	490	23	24
6G/2'	298	298	0	1
6G/4'	302	393	6	6
6G/6'				
6G/8'				
6G/10'	296	485	24	26
3H/2'				
3H/4'	308	370	6	36
3H/6'				
3H/8'	300	600	24	25
3H/10'	300	520	34	36
4G/4'	303	410	7	7
4G/6'				
4G/10'	299	507	28	30
4H/4'	313	390	6	6
4H/6'				
4H/10'	299	489	25	26
7D/4'	301	399	7	7
7D/6'	310	555	14	15
7D/10'	295	485	23	24



1

2

3

4

5

LOW CLAD TEMPERATURE FLECHT RUN SUMMARY SHEET

RUN NO. 2014

DATE 12/8/72

A. RUN CONDITIONS

Pressure	60	psia
Initial Clad Temperature	312	°F
Peak Power	1.2	kw/ft
Coolant Temperature	150	°F
Flooding Rate	6.6	in./sec for 0→3.3 sec
	3.5	in./sec for 3.3→15.4 sec
	1.0	in./sec for 15.4→ sec

B. INITIAL HOUSING TEMPERATURES

Elevation (ft)	Temperature (°F)
0	279
2	305
4	299
6	289
8	291
10	292
12	295
AVG.	294

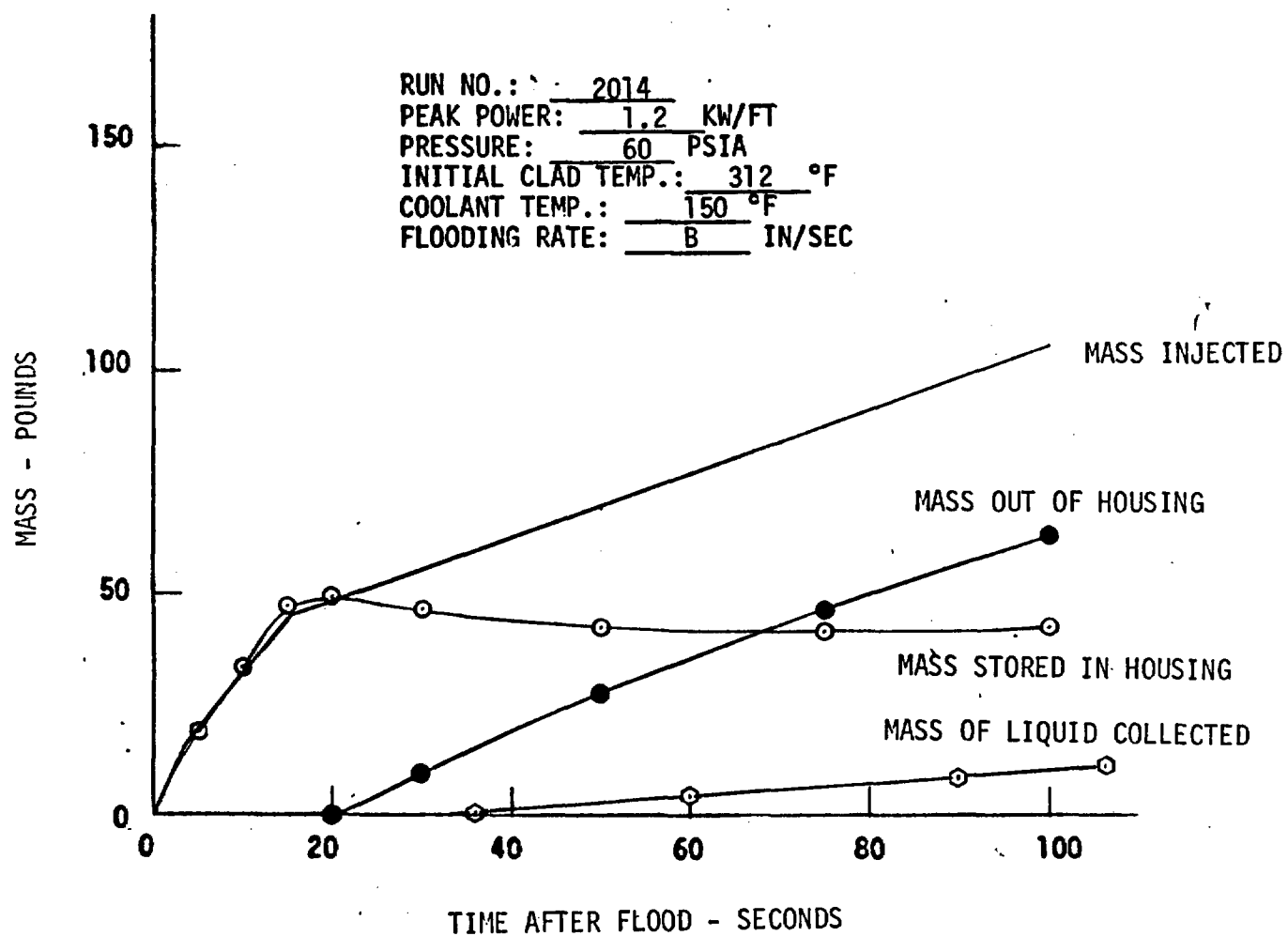
LOW CLAD TEMPERATURE FLECHT RUN SUMMARY SHEET (Cont)

RUN NO. 2014

DATE 12/8/72

C. HEATER THERMOCOUPLE DATA

Rod/Elev.	Initial Temp. (°F)	Max. Temp. (°F)	Turnaround Time (Sec)	Quench Time (Sec)
5F/2'	295	316	5	5
5F/4'				
5F/6'				
5F/8'	310	530	13	14
5F/10'	303	475	18	19
5G/2'	297	299	4	6
5G/4'				
5G/6'	312	760	25	26
5G/8'	320	898	66	68
5G/10'	303	480	18	19
6G/2'	299	299	0	0
6G/4'	302	416	7	8
6G/6'				
6G/8'				
6G/10'	295	477	18	19
3H/2'				
3H/4'	310	389	6	8
3H/6'				
3H/8'	303	645	25	26
3H/10'	300	501	23	24
4G/4'	310	425	6	7
4G/6'				
4G/10'	300	502	23	24
4H/4'	320	422	7	8
4H/6'				
4H/10'	300	480	19	20
7D/4'	305	425	7	8
7D/6'	310	599	15	16
7D/10'	298	501	23	24



LOW CLAD TEMPERATURE FLECHT RUN SUMMARY SHEET

RUN NO. 2122

DATE 12/8/72

A. RUN CONDITIONS

Pressure	59	psia
Initial Clad Temperature	498	°F
Peak Power	0.7	kw/ft
Coolant Temperature	149	°F
Flooding Rate	6.3	in./sec for 0→2.9 sec
	3.4	in./sec for 2.9→8.8 sec
	.92	in./sec for sec

B. INITIAL HOUSING TEMPERATURES

Elevation (ft)	Temperature (°F)
0	226
2	384
4	392
6	396
8	370
10	338
12	288
AVG.	361

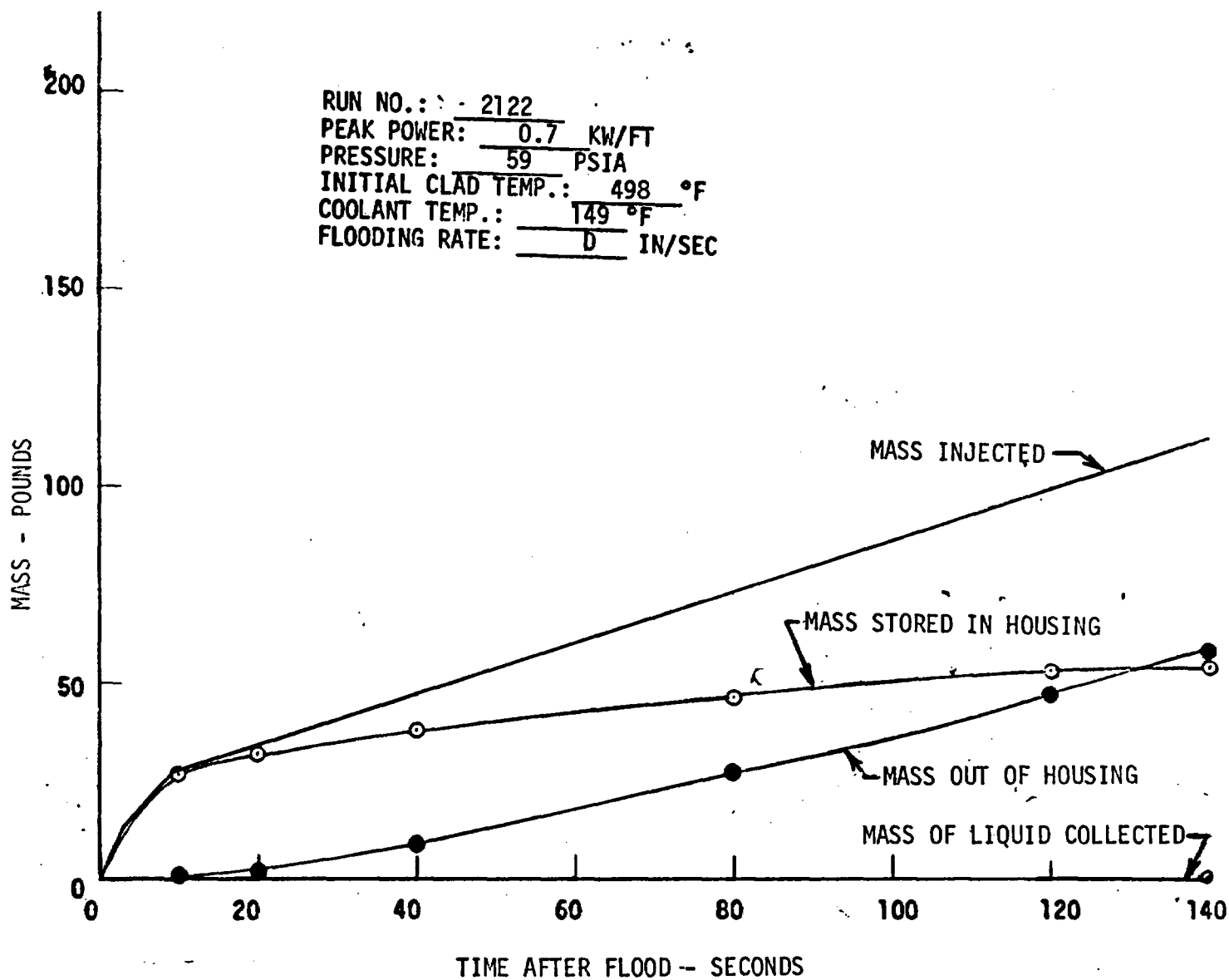
LOW CLAD TEMPERATURE FLECHT RUN SUMMARY SHEET (Cont)

RUN NO. 2122

DATE 12/8/72

C. HEATER THERMOCOUPLE DATA

Rod/Elev.	Initial Temp. (°F)	Max. Temp. (°F)	Turnaround Time (Sec)	Quench Time (Sec)
5F/2'	365	365	0	1
5F/4'				
5F/6'				
5F/8'	438	865	69	91
5F/10'	377	707	82	108
5G/2'	361	361	0	1
5G/4'				
5G/6'	498	845	38	60
5G/8'	463	926	69	120
5G/10'	376	700	87	113
6G/2'	365	365	0	1
6G/4'	442	549	11	14
6G/6'				
6G/8'				
6G/10'	366	708	89	92
3H/2'				
3H/4'	451	550	10	11
3H/6'	521	855	47	51
3H/8'	427	880	73	110
3H/10'	371	702	90	110
4G/4'	492	660	15	17
4G/6'				
4G/10'	371	688	67	70
4H/4'	463	565	10	13
4H/6'				
4H/10'	371	691	90	114
7D/4'	443	547	11	14
7D/6'	477	781	36	54
7D/10'	372	703	89	124



1

2

3

4

LOW CLAD TEMPERATURE FLECHT RUN SUMMARY SHEET

RUN NO. 2324

DATE 12/11/73

A. RUN CONDITIONS

Pressure	60	psia
Initial Clad Temperature	653	°F
Peak Power	1.2	kw/ft
Coolant Temperature	145	°F
Flooding Rate	6.3 in./sec for 0→3.1	sec
	3.7 in./sec for 3.1→14.8	sec
	.99 in./sec for 14.8→end	sec

B. INITIAL HOUSING TEMPERATURES

Elevation (ft)	Temperature (°F)
0	212
2	429
4	466
6	493
8	448
10	373
12	295
AVG.	417

LOW CLAD TEMPERATURE FLECHT RUN SUMMARY SHEET (Cont)

RUN NO. 2324

DATE 12/11/72

C. HEATER THERMOCOUPLE DATA

Rod/Elev.	Initial Temp. (°F)	Max. Temp. (°F)	Turnaround Time (Sec)	Quench Time (Sec)
5F/2'	429	436	1	2
5F/4'				
5F/6'				
5F/8'	550	1278	119	225
5F/10'	427	811	91	126
5G/2'	420	421	1	4
5G/4'				
5G/6'	653	1136	67	123
5G/8'	602	1254	119	252
5G/10'	429	562	14	16
6G/2'	427	444	3	6
6G/4'	555	716	11	14
6G/6'				
6G/8'				
6G/10'	392	498	10	13
3H/2'				
3H/4'	560	717	11	13
3H/6'	608	1185	68	119
3H/8'	542	1264	124	248
3H/10'	421	792	82	93
4G/4'	613	804	12	24
4G/6'				
4G/10'	425	689	52	64
4H/4'	587	775	21	25
4H/6'				
4H/10'	418	552	10	12
7D/4'	557	722	12	14
7D/6'	635	1060	53	112
7D/10'	391	930	141	252

250

RUN NO.: 2324
PEAK POWER: 1.2 KW/FT
PRESSURE: 60 PSIA
INITIAL CLAD TEMP.: 653 °F
COOLANT TEMP.: 145 °F
FLOODING RATE: B IN/SEC

200

MASS INJECTED

150

MASS OUT OF HOUSING

MASS - POUNDS

100

MASS STORED IN HOUSING

50

MASS OF LIQUID COLLECTED

0

40

80

120

160

200

240

280

TIME AFTER FLOOD - SECONDS

B-111

1

2

3

4

LOW CLAD TEMPERATURE FLECHT RUN SUMMARY SHEET

RUN NO. 2420

DATE 12/12/72

A. RUN CONDITIONS

Pressure	60 psia
Initial Clad Temperature	508 °F
Peak Power	.7 kw/ft
Coolant Temperature	146 °F
Flooding Rate	1.50 in./sec for 0→end sec

B. INITIAL HOUSING TEMPERATURES

Elevation (ft)	Temperature (°F)
0.	196
2	373
4	342
6	387
8	366
10	353
12	287
AVG.	352

LOW CLAD TEMPERATURE FLECHT RUN SUMMARY SHEET (Cont)

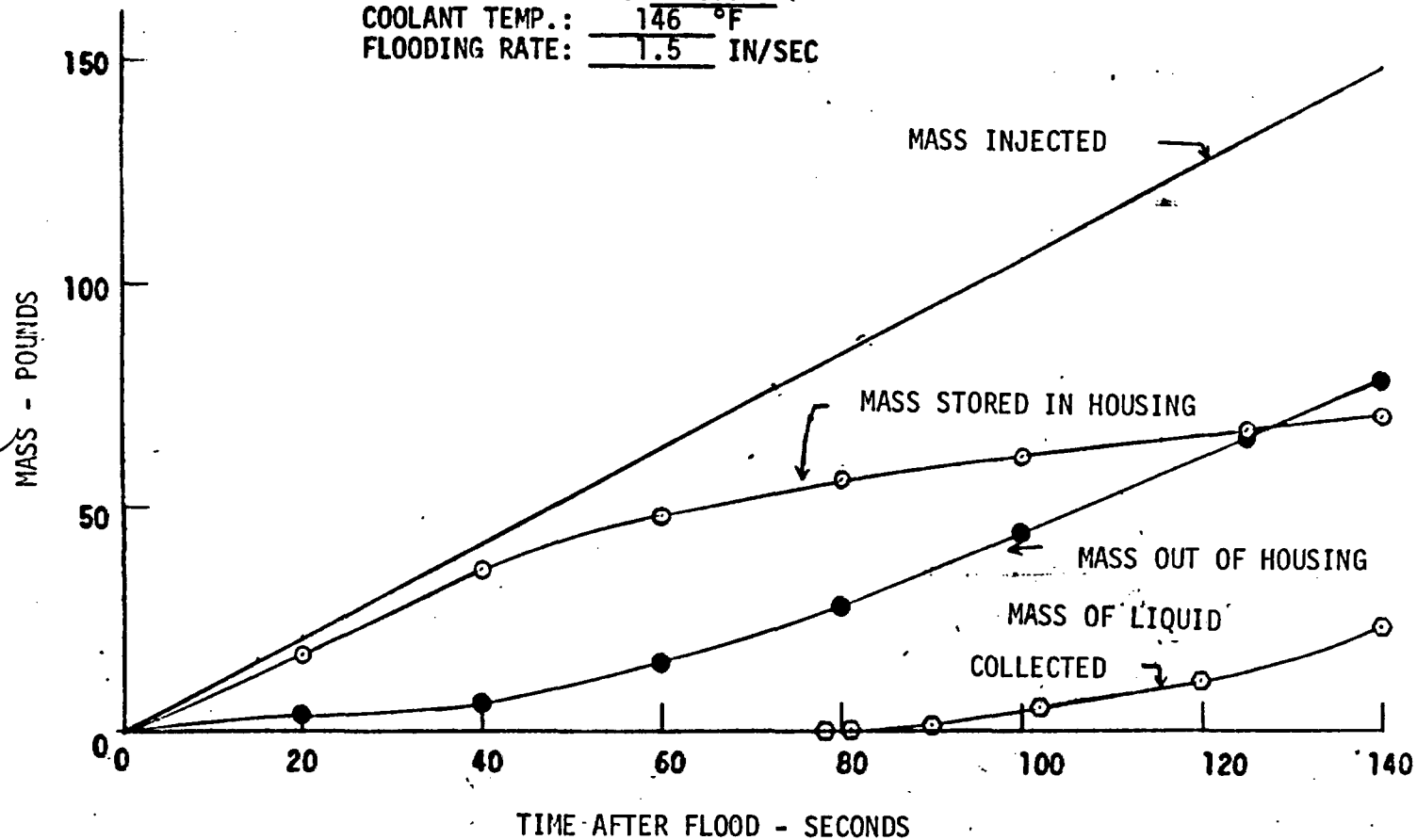
RUN NO. 2420

DATE 12/12/72

C. HEATER THERMOCOUPLE DATA

Rod/Elev.	Initial Temp. (°F)	Max. Temp. (°F)	Turnaround Time (Sec)	Quench Time (Sec)
5F/2'	326	404	13	14
5F/4'				
5F/6'				
5F/8'	406	860	67	98
5F/10'	360	680	80	83
5G/2'	319	397	14	15
5G/4'				
5G/6'	508	963	47	80
5G/8'	427	918	62	115
5G/10'	356	658	72	93
6G/2'	316	401	14	15
6G/4'	417	686	30	31
6G/6'				
6G/8'				
6G/10'	340	650	64	67
3H/2'				
3H/4'	424	710	32	34
3H/6'				
3H/8'	425	874	75	98
3H/10'	353	656	72	98
4G/4'	457	792	31	37
4G/6'				
4G/10'	354	646	62	66
4H/4'	434	723	33	35
4H/6'				
4H/10'	345	649	64	69
7D/4'	418	693	30	31
7D/6'	490	910	48	72
7D/10'	350	652	72	98

RUN NO.: 2420
 PEAK POWER: 0.7 KW/FT
 PRESSURE: 60 PSIA
 INITIAL CLAD TEMP.: 508 °F
 COOLANT TEMP.: 146 °F
 FLOODING RATE: 1.5 IN/SEC



1

2

3

LOW CLAD TEMPERATURE FLECHT RUN SUMMARY SHEET

RUN NO. 2519

DATE 12/12/72

A. RUN CONDITIONS

Pressure	61	psia
Initial Clad Temperature	603	°F
Peak Power	.7	kw/ft
Coolant Temperature	143	°F
Flooding Rate	1.52 in./sec	for 0 → end sec

B. INITIAL HOUSING TEMPERATURES

Elevation (ft)	Temperature (°F)
0	201
2	327
4	381
6	401
8	400
10	297
12	288
AVG.	341

LOW CLAD TEMPERATURE FLECHT RUN SUMMARY SHEET (Cont)

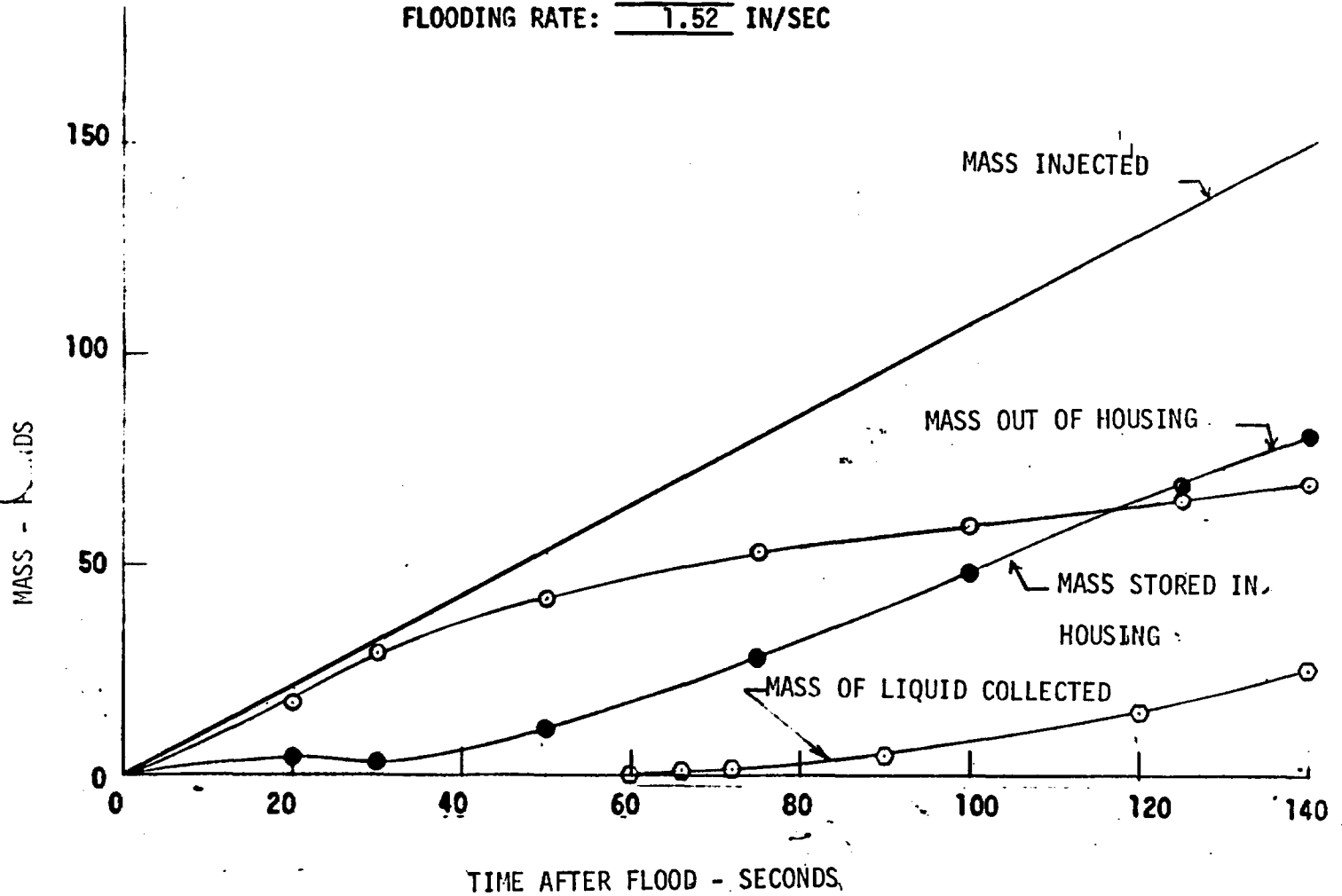
RUN NO. 2519

DATE 12/12/72

C. HEATER THERMOCOUPLE DATA

Rod/Elev.	Initial Temp. (°F)	Max. Temp. (°F)	Turnaround Time (Sec)	Quench Time (Sec)
5F/2'	363	460	16	17
5F/4'				
5F/6'				
5F/8'	537	937	60	108
5F/10'	385	723	74	77
5G/2'	359	435	14	16
5G/4'				
5G/6'	605	1039	48	90
5G/8'	559	996	62	127
5G/10'	380	677	76	98
6G/2'	359	458	17	18
6G/4'	506	757	30	39
6G/6'				
6G/8'				
6G/10'	364	668	63	66
3H/2'				
3H/4'	517	771	30	39
3H/6'				
3H/8'	512	919	73	114
3H/10'	374	676	77	114
4G/4'	568	878	30	43
4G/6'				
4G/10'	377	666	57	59
4H/4'	525	792	31	44
4H/6'				
4H/10'	369	657	71	87
7D/4'	504	762	30	40
7D/6'	581	979	48	31
7D/10'	380	688	75	98

RUN NO.: 2519
 PEAK POWER: 0.7 KW/FT
 PRESSURE: 61 PSIA
 INITIAL CLAD TEMP.: 603 °F
 COOLANT TEMP.: 143 °F
 FLOODING RATE: 1.52 IN/SEC



LOW CLAD TEMPERATURE FLECHT RUN SUMMARY SHEET

RUN NO. 2618

DATE 12/13/72

A. RUN CONDITIONS

Pressure	59	psia
Initial Clad Temperature	401	°F
Peak Power	.7	kw/ft
Coolant Temperature	146	°F
Flooding Rate	1.50	in./sec for 0→end sec

B. INITIAL HOUSING TEMPERATURES

Elevation (ft)	Temperature (°F)
0	223
2	313
4	347
6	371
8	369
10	319
12	282
AVG.	330

LOW CLAD TEMPERATURE FLECHT RUN SUMMARY SHEET (Cont)

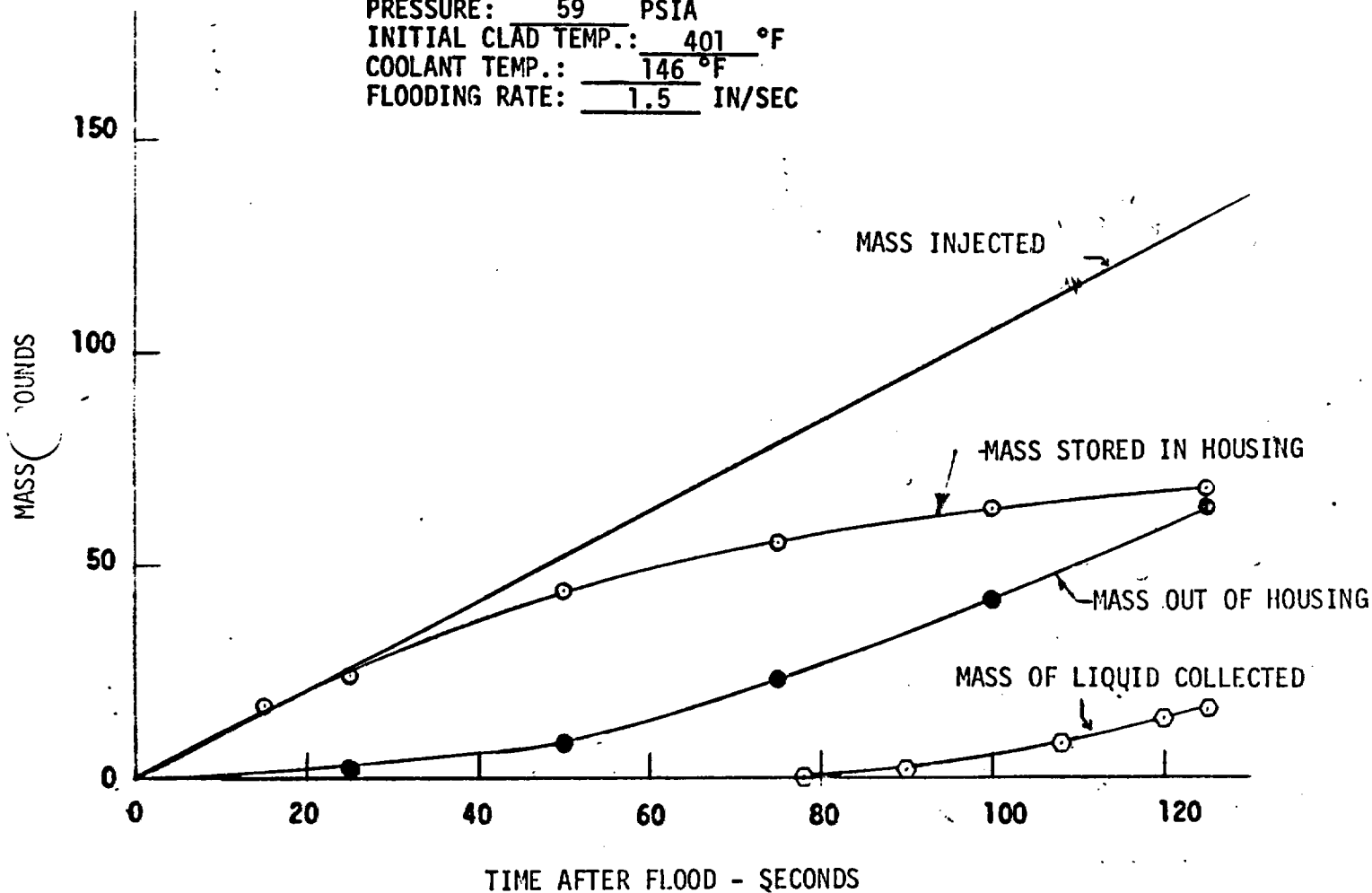
RUN NO. 2618

DATE 12/13/72

C. HEATER THERMOCOUPLE DATA

Rod/Elev.	Initial Temp. (°F)	Max. Temp. (°F)	Turnaround Time (Sec)	Quench Time (Sec)
5F/2'	280	370	15	16
5F/4'				
5F/6'				
5F/8'	340	835	64	84
5F/10'	316	640	67	79
5G/2'	273	359	16	17
5G/4'				
5G/6'	401	897	46	70
5G/8'	395	905	66	105
5G/10'	316	637	70	74
6G/2'	275	373	16	17
6G/4'	340	628	30	32
6G/6'				
6G/8'				
6G/10'	296	615	61	63
3H/2'				
3H/4'	353	650	29	31
3H/6'				
3H/8'	370	844	68	96
3H/10'	323	629	70	90
4G/4'	364	730	32	34
4G/6'				
4G/10'	311	623	60	62
4H/4'	357	670	30	32
4H/6'				
4H/10'	300	637	66	67
7D/4'	342	637	31	34
7D/6'	398	843	46	64
7D/10'	310	631	65	67

RUN NO.: 2618
PEAK POWER: 0.7 KW/FT
PRESSURE: 59 PSIA
INITIAL CLAD TEMP.: 401 °F
COOLANT TEMP.: 146 °F
FLOODING RATE: 1.5 IN/SEC



—

—

—

LOW CLAD TEMPERATURE FLECHT RUN SUMMARY SHEET

RUN NO. 2823

DATE 12/15/72

A. RUN CONDITIONS

Pressure	58	psia
Initial Clad Temperature	670	°F
Peak Power	.7	kw/ft
Coolant Temperature	147	°F
Flooding Rate	6.22 in./sec for 0→3.5	sec
	2.7 in./sec for 3.5→15.4	sec
	.95 in./sec for 15.4→end	sec

B. INITIAL HOUSING TEMPERATURES

Elevation (ft)	Temperature (°F)
0	224
2	364
4	399
6	409
8	400
10	366
12	309
AVG.	280

LOW CLAD TEMPERATURE FLECHT RUN SUMMARY SHEET (Cont)

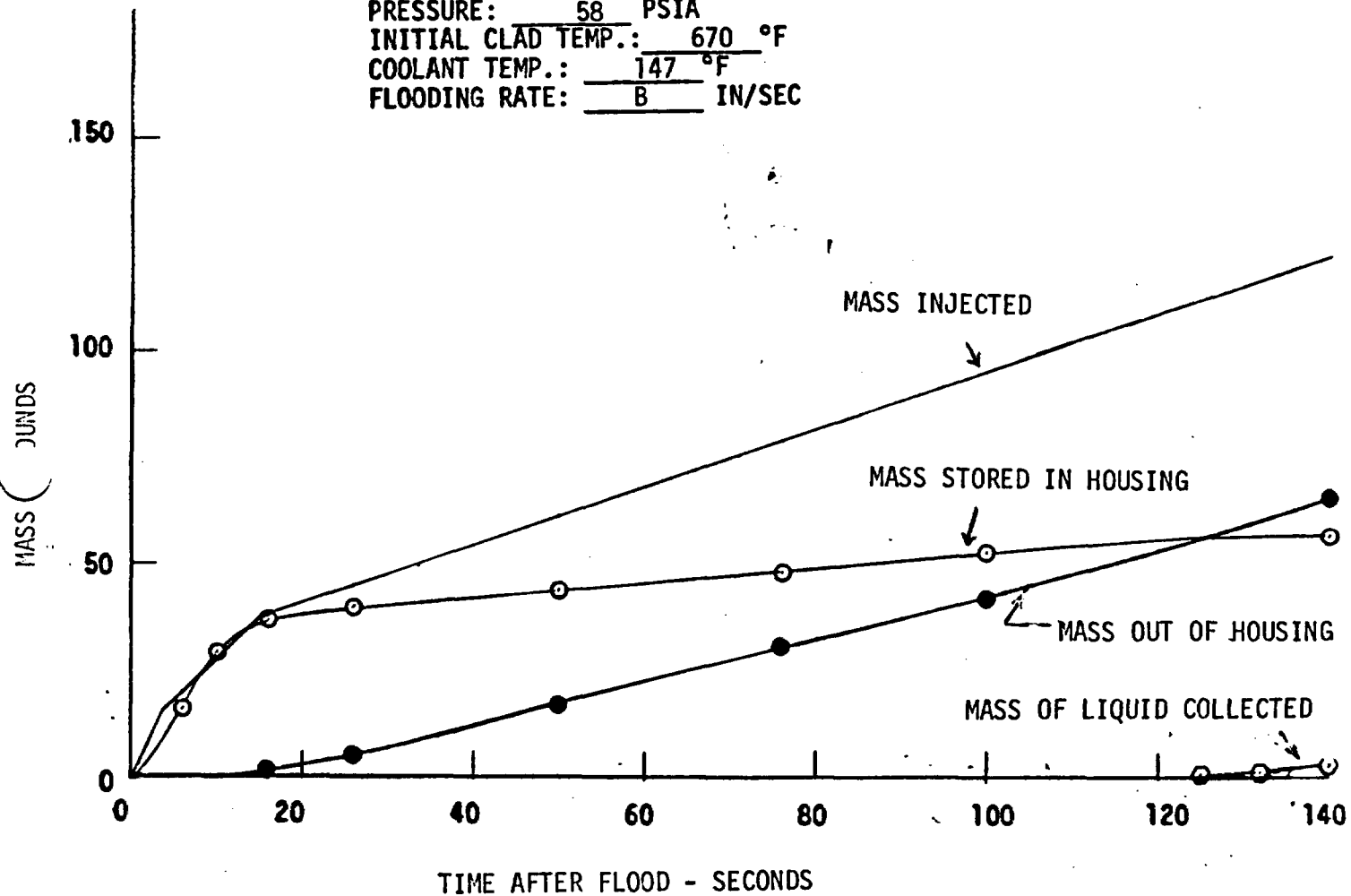
RUN NO. 2823

DATE 12/15/72

C. HEATER THERMOCOUPLE DATA

Rod/Elev.	Initial Temp. (°F)	Max. Temp. (°F)	Turnaround Time (Sec)	Quench Time (Sec)
5F/2'	468	468	0	0
5F/4'				
5F/6'				
5F/8'				
5F/10'	510	739	66	91
5G/2'	468	468	0	1
5G/4'				
5G/6'	670	887	28	60
5G/8'	630	952	56	114
5G/10'	497	727	68	119
6G/2'	480	480	1	2
6G/4'	605	683	11	13
6G/6'				
6G/8'				
6G/10'	481	719	79	81
3H/2'				
3H/4'				
3H/6'	650	880	33	44
3H/8'	565	874	63	77
3H/10'	470	701	79	82
4G/4'	652	748	11	16
4G/6'				
4G/10'	490	712	67	80
4H/4'	610	700	10	12
4H/6'				
4H/10'	473	686	68	86
7D/4'	605	690	11	13
7D/6'	640	833	30	55
7D/10'	490	730	70	114

RUN NO.: 2823
PEAK POWER: 0.7 KW/FT
PRESSURE: 58 PSIA
INITIAL CLAD TEMP.: 670 °F
COOLANT TEMP.: 147 °F
FLOODING RATE: B IN/SEC



1

2

3

LOW CLAD TEMPERATURE FLECHT RUN SUMMARY SHEET

RUN NO. 2921

DATE 12/15/72

A. RUN CONDITIONS

Pressure	59	psia
Initial Clad Temperature	660	°F
Peak Power	.7	kw/ft
Coolant Temperature	171	°F
Flooding Rate	5.4 in./sec for 0→3.8	sec
	2.5 in./sec for 3.8→7.3	sec
	.88 in./sec for 7.3→end	sec

B. INITIAL HOUSING TEMPERATURES

Elevation (ft)	Temperature (°F)
0	235
2	382
4	407
6	403
8	406
10	367
12	310
AVG.	376

LOW CLAD TEMPERATURE FLECHT RUN SUMMARY SHEET (Cont)

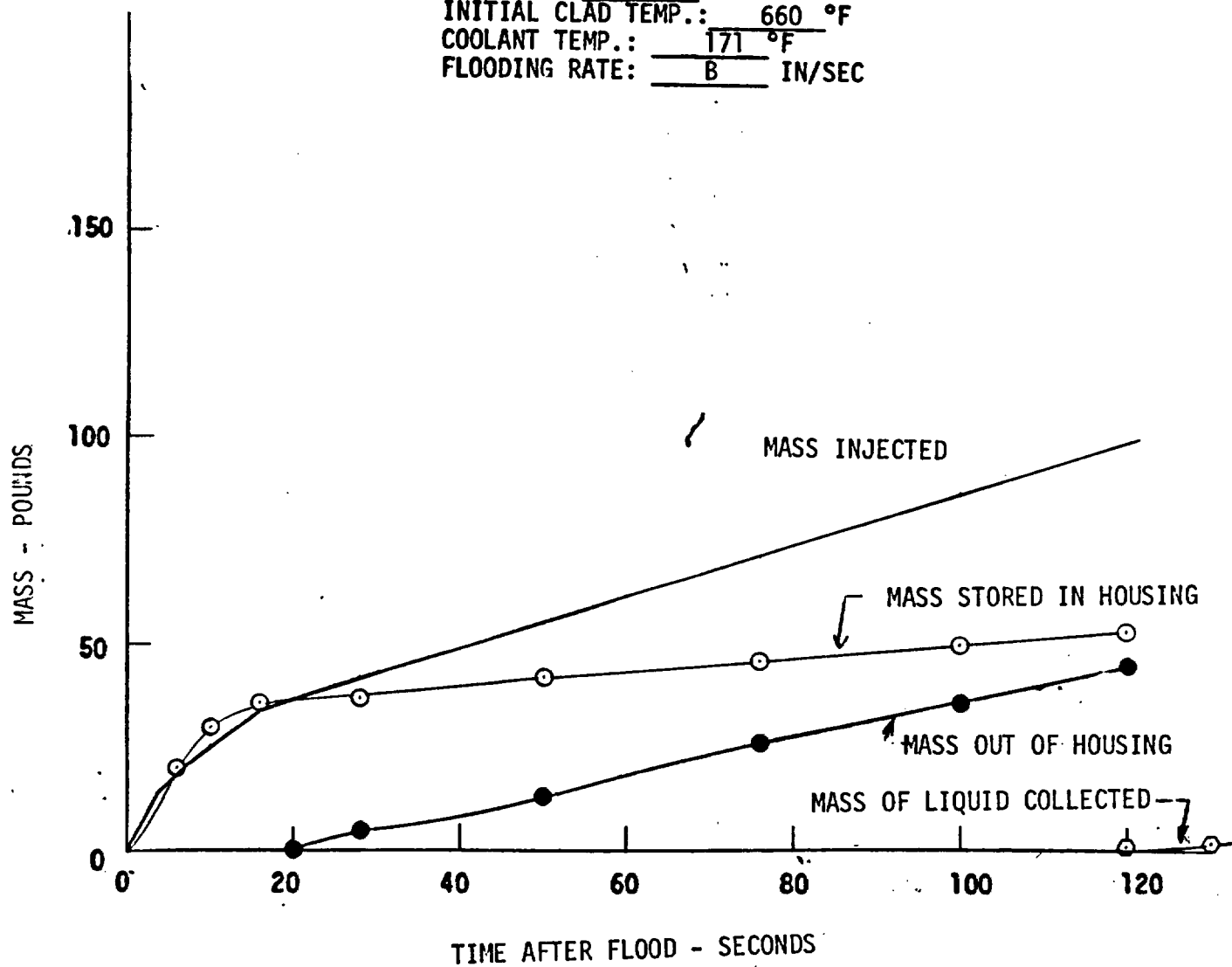
RUN NO. 2921

DATE 12/15/72

C. HEATER THERMOCOUPLE DATA

Rod/Elev.	Initial Temp. (°F)	Max. Temp. (°F)	Turnaround Time (Sec)	Quench Time (Sec)
5F/2'	537	537	0	3
5F/4'				
5F/6'				
5F/8'	476	574	28	40
5F/10'	503	729	63	83
5G/2'	537	537	0	3
5G/4'				
5G/6'	660	857	26	64
5G/8'	622	923	54	112
5G/10'	493	715	67	97
6G/2'	545	547	1	3
6G/4'	551	689	7	11
6G/6'				
6G/8'				
6G/10'	471	703	75	78
3H/2'				
3H/4'	510	587	12	14
3H/6'	640	854	31	41
3H/8'	556	851	57	95
3H/10'	461	695	80	83
4G/4'	648	746	11	13
4G/6'				
4G/10'	485	722	74	78
4H/4'	617	703	11	14
4H/6'				
4H/10'	465	680	69	90
7D/4'	609	676	12	16
7D/6'	631	794	26	52
7D/10'	478	709	65	133

RUN NO.: 2921
PEAK POWER: 0.7 KW/FT
PRESSURE: 59 PSIA
INITIAL CLAD TEMP.: 660 °F
COOLANT TEMP.: 171 °F
FLOODING RATE: B IN/SEC



—

—

—

—

—

APPENDIX C
TOP INJECTION TESTS

—

—

—

—

—

APPENDIX C

TOP INJECTION TESTS

C.1 INTRODUCTION

C.1.1 Purpose of Tests

Bottom flooding is the current mode of ECCS injection for most of the present generation of PWR designs and has been investigated in the PWR FLECHT program and elsewhere. Combined top and bottom injection has been investigated by Siemens in Germany. At a meeting held to discuss additional tests which might be performed as part of the FLECHT-SET program, the Consolidated Edison-ERC representative suggested that a series of top injection scoping tests be performed in the FLECHT-SET facility as a logical extension of the above investigations. The AEC, PWR vendors, and members of the Electrical Research Council agreed that the data obtained from these tests would be generally useful toward a further understanding of emergency core cooling system effectiveness and a series of top injection scoping tests was subsequently incorporated into the scope of work of the FLECHT-SET program.

C.2 TEST DESCRIPTION

C.2.1 Facility Layout

The top injection tests were conducted by injecting water into the FLECHT-SET upper plenum through the original FLECHT exit port as shown in Figure C-1. One specified ground rule used was that the injected water would not have a velocity component downward into the bundle. The injection pipe was positioned so that the injected water would penetrate at least three rows of rods into the bundle before falling down the heated rod length as shown in Figure C-2. Cold flow tests indicated the amount of penetration for the injection jet.

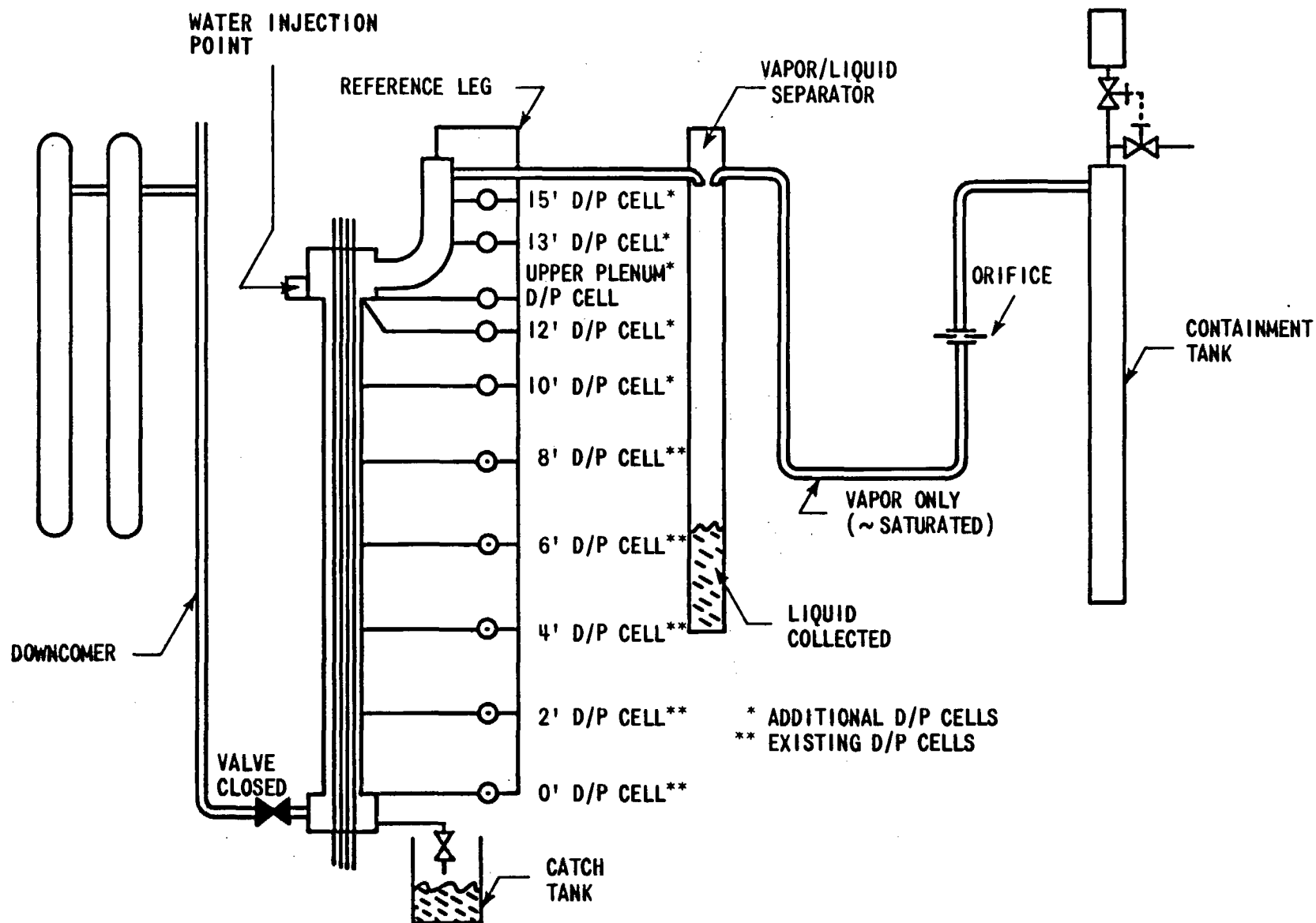


Figure C-1. Flecht-Set Configuration for Top Injection Tests

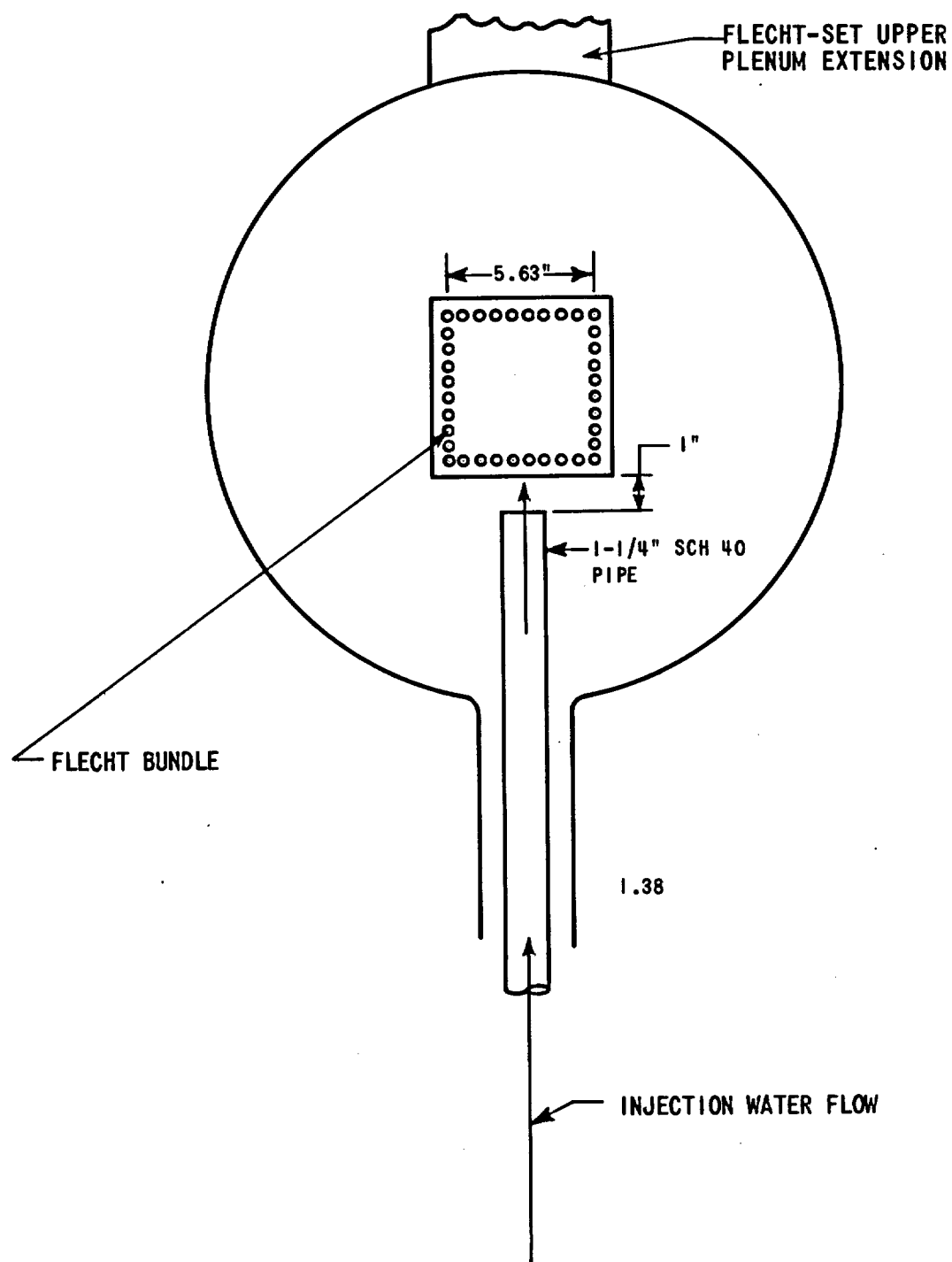


Figure C-2. Top Spray Injection Position

C.2.2 Instrumentation and Data Acquisition

The instrumentation used in these tests was the same as that used in the FLECHT-SET Phase A tests. However, by this time in the testing program less than one-half of the original bundle thermocouples were operating and no 8 ft. elevation thermocouples were functioning. The data acquisition system was the same as that used in the Phase A tests.

C.2.3 Test Procedure

The bundle and housing were heated to the required initial temperatures as required by the tests. The housing temperature distribution was controlled by pulsing the heater rod power and using the strip heaters mounted on the housing. The initial temperature of the housing was 800°F at the midplane and efforts were made to have the housing temperature as uniform as possible. The hot housing represented a fuel assembly channel wall in these tests. No water was in the FLECHT-SET system before or during heatup. The system was not pressurized for any of these tests and the downcomer was valved out of the system for all tests. The lower plenum of the bundle housing was open to the atmosphere and connected to a series of 55 gallon water collection drums. In this manner, no water could accumulate in the bundle during the test and would drain out of the housing into the collection drums. One test was conducted with the bundle drain closed so that water could accumulate in the bundle. At the conclusion of each test, the water was measured at all collection points in the FLECHT-SET system as well as the catch tanks at the bundle exit, and a crude mass balance was then performed on the system.

The test matrix for the top injection tests is given in Table C-1 and shows that the principal parameters investigated were initial temperature, peak power, subcooling, injection flow rate, and location of the system venting (i.e., was the bundle allowed to drain or not).

TABLE C-1

TOP INJECTION TEST MATRIX

Run No.	Initial Temp (°F)	Peak Power (kw/ft)	Injection Water Temp (°F)	Housing Temp (°F)	System Pressure (psia)	Injection Flow (gpm)	Remarks
5501	1100	0.4	150	800	14.7	15	System vented
5602	1100	0.6	150	800	14.7	15	System vented
5703	1100	0.7	150	800	14.7	15	System vented
5904	1400	0.7	150	800	14.7	15	System vented Initial temp effect
6007	1100	0.7	150	800	18.0	15	System not vented
6106	1100	0.7	82	800	14.7	15	System vented Subcooling effect
6205	1100	0.7	87	800	14.7	35	System vented Injection flow rate effect
6408	1100	0.7	180	800	14.7	15	System vented Subcooling effect

C.3 CALCULATIONS AND DATA REDUCTION

Since these were scoping tests to investigate a particular ECC injection concept, data reduction and analysis efforts were minimized and the effects of the system parameters given in Table C-1 were compared. DATAR was run for each top injection test, and local heat transfer coefficients and rod temperature histories were obtained. The housing temperature history and the water inventories at various locations in the system were also obtained and a rough mass balance for each test was attempted.

For the different parametric studies two quantities were examined:

1. The temperature distributions at different elevations in the bundle
2. The heat transfer history of selected rods within the bundle.

Both the heat transfer coefficients and rod temperatures were obtained directly from the DATAR computer program. The data sheets given in Appendix C-1 contain the rod temperature history in the same format as the Phase A test data. It should be noted that not all the rod temperatures quenched in these tests since the amount of cooling received by each rod was a strong function of its location within the bundle.

C.4 DISCUSSION OF TEST RESULTS

C.4.1 Run Summary Sheets

The run summary sheets for each test are given in Appendix C-1 along with the rod thermocouple initial temperature turnaround times, maximum temperatures, and quench times if the rod did quench. The run conditions, inlet flow, and amount of water collected in the system are also given in the run summary sheets for each test.

C.4.2 General Observations

The cold flow injection test which determined the location of the injection line with respect to the bundle indicated that the injection flow would penetrate some distance into the rod bundle. Examination of the

test data indicates that the injection water did not spread evenly over the bundle cross section, resulting in localized hot zones. The heat transfer in the hot zones, however, was sufficient to turn the temperature around and cool the rods. The only exception to this is Run 6106 in which there was a power scram when the rod temperature reached 2000°F.

All tests showed some net steam flow through the orifice downstream of the upper plenum, even though the bottom end of the bundle was vented to the atmosphere. This indicates that countercurrent steam/water flow may have existed to some extent in the bundle, preventing effective penetration of the water throughout the bundle. The largest orifice steam flow occurred in test 6007 when the bundle drain was closed and the injection water was allowed to accumulate. It should be noted that the orifice steam flow only accounted for 5-10 percent of the total mass injected into the system as shown in Table C-2 and does not account for generated steam which is condensed in the bundle.

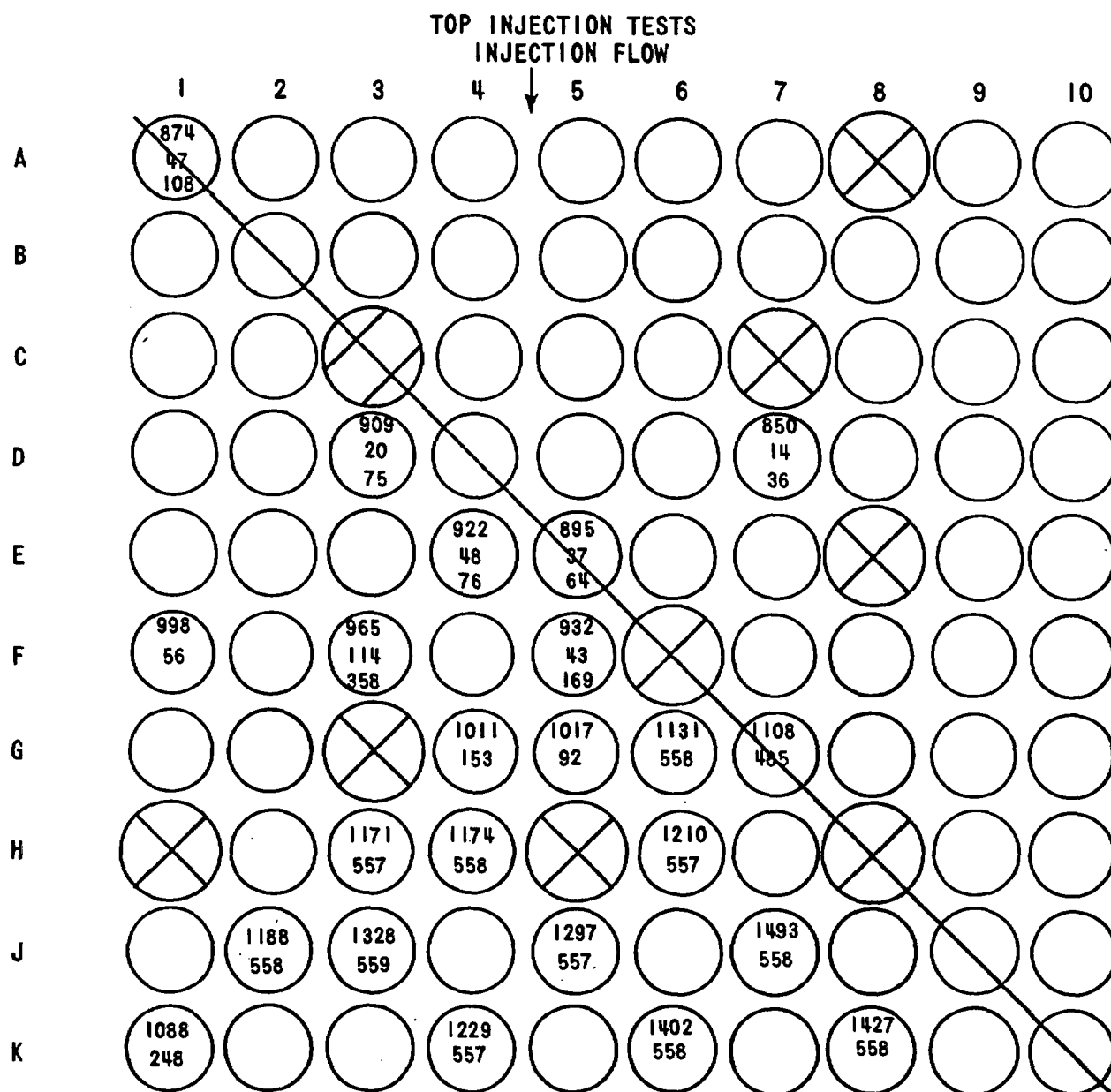
The rod temperature profiles indicate that, in general, the amount of cooling is just sufficient to remove the generated heat at some elevated temperature level. The rod temperature will tend to remain at a high value for extended periods of time and will slowly decrease as the rod power decreases. This thermal behavior indicates that the rod is in a steam cooling or extremely dispersed two-phase flow environment which provides low values of convective heat transport. The amount of entrained or splashing water which contacts a rod is very dependent on the location of that rod with respect to the upper plenum injection point. Rods closer to the injection point would quench at all elevations, while rods far away from the injection point did not quench even at the 10 ft elevation. The peak clad temperatures for the reference test, Run 5703, are shown in Figures C-3, C-4, C-5, and C-6 for the different thermocouple elevations. It should be noted that no 8 ft thermocouples were functioning in the bundle at this point in the test program. These figures show the sensitivity of the individual rod thermal behavior to its location in the bundle with respect to the injection point.

TABLE C-2

TOP INJECTION TESTS MASS COLLECTED

Run No.	Mass Collected in Barrels	Mass Collected in Carryover Tank	Mass Collected in Steam Probe	Mass Collected in Containment Tank	Mass Flow Through Orifice	Mass Collected in Upper Plenum	Total Mass Out	Total Mass In	Remarks
	(pounds)	(pounds)	(pounds)	(pounds)	(pounds)	(pounds)	(pounds)	(pounds)	
5501	1019.13	177.0	0	0	51.9	5.3	1253.33	1283.4	Time flow off at 743 sec
5602	1142.18	0	0	0	39.0	4.3	1185.48	1051.5	Time flow off at 600 sec
5703	1104.00	0	0	0	35.7	5.0	1144.7	1047.6	Stopped top flooding at 580 sec
5904	1056.00	0	0	0	45.5	0	1101.5	1001.1	Time flow off at 560 sec
6007	175.11	532.0	1.8	60.0	111.4	4.5	884.81	918.9	Time flow off at 558 sec
6106	524.00	1.3	123.0	0	27.6	6.3	682.2	716.9	Power scram at 180 sec Started bottom flooding
6205	--	--	--	--	--	--	--	--	Stopped flow at 549 sec Barrels overflowed onto floor
6408	1049.00	0	2.8	0	63.6	5.8	1121.2	1006.0	Stopped flow off at 588 sec

C-10



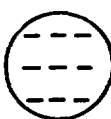
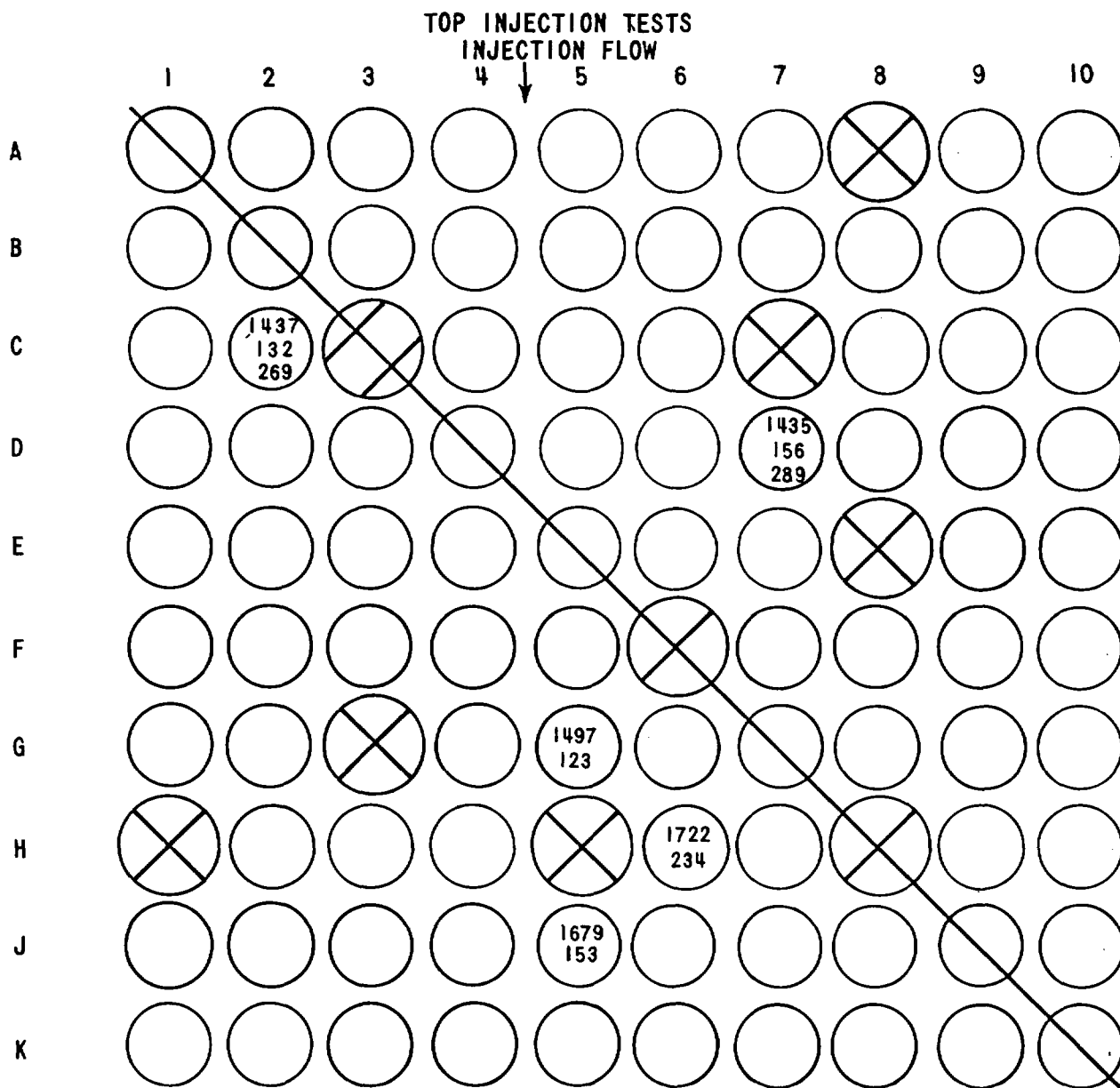
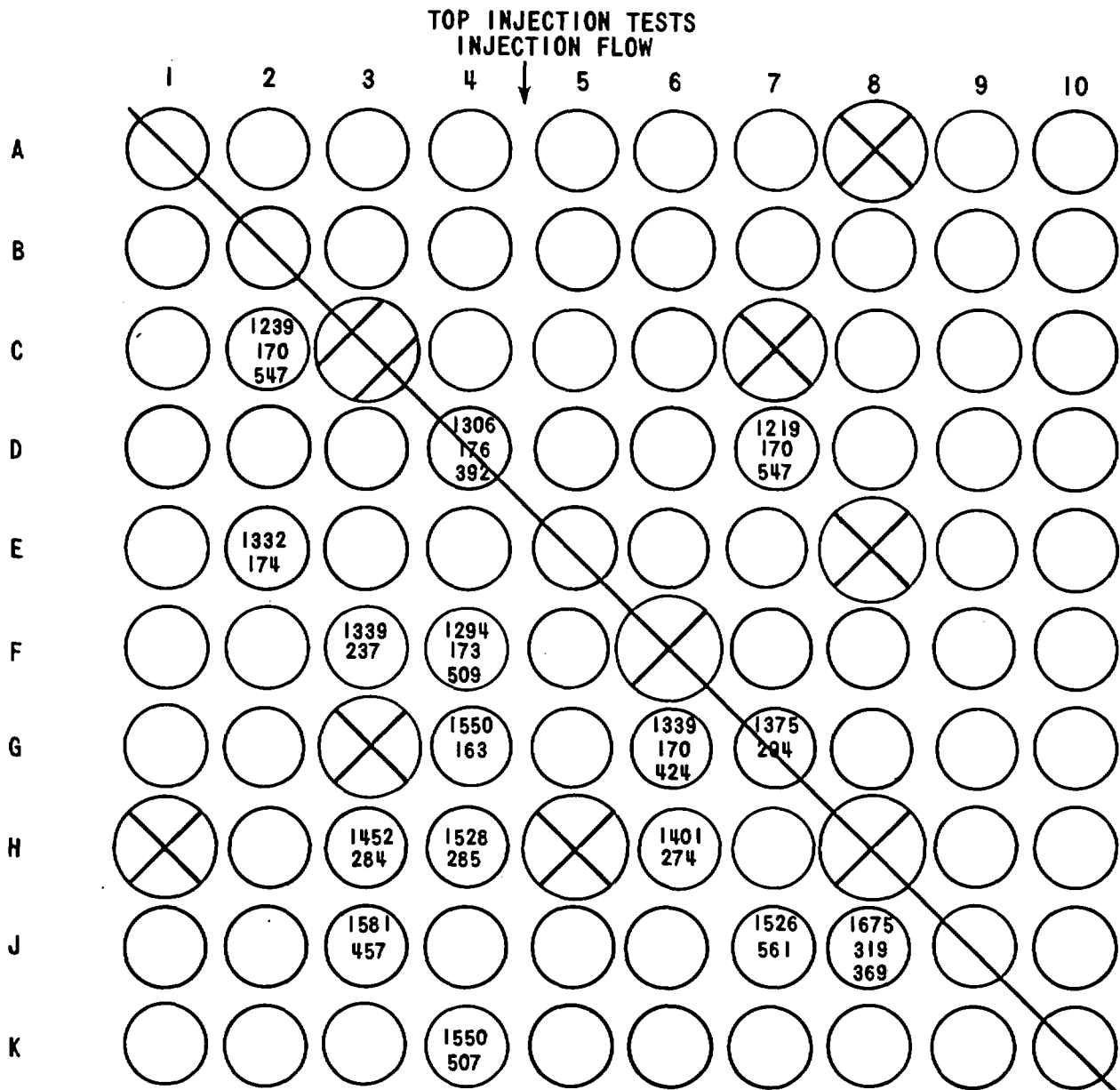
RUN NO. <u>5703</u>		KEY
ELEVATION <u>10'</u>		MAX TEMPERATURE
INITIAL TEMPERATURE <u>1100°F</u>		TURNAROUND TIME
PRESSURE <u>15 PSIA</u>		QUENCH TIME
T _{WATER} <u>150°F</u>		
POWER <u>0.7 KW/FT</u>		

Figure C-3. Run 5703, Ten-foot Cross-Sectional Bundle Maximum Temperatures, Turnaround Times, and Quench Times



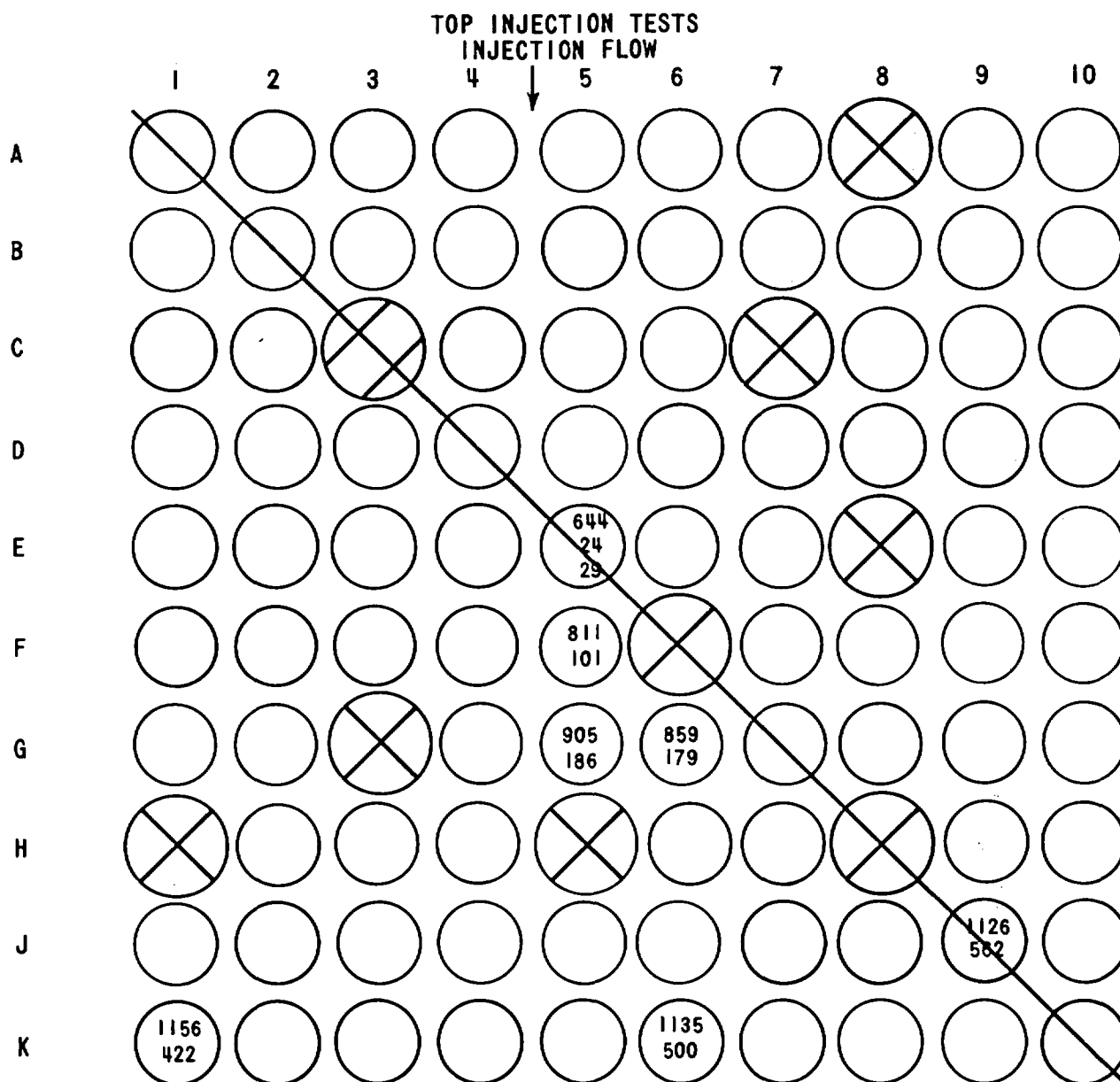
<p>RUN NO. <u>5703</u> ELEVATION <u>6'</u> INITIAL TEMPERATURE <u>1100°F</u> PRESSURE <u>15 PSIA</u> T_{WATER} <u>150°F</u> POWER <u>0.7 KW/FT</u></p>	<p>KEY --- MAX TEMPERATURE --- TURNAROUND TIME --- QUENCH TIME</p>
---	--

Figure C-4. Run 5703, Six-foot Cross-Sectional Bundle Maximum Temperatures, Turnaround Times, and Quench Times



<p>RUN NO. <u>5703</u></p> <p>ELEVATION <u>4'</u></p> <p>INITIAL TEMPERATURE <u>1100°F</u></p> <p>PRESSURE <u>15 PSIA</u></p> <p>T_{WATER} <u>150°F</u></p> <p>POWER <u>0.7 KW/FT</u></p>	<p>KEY</p> <div style="display: flex; align-items: center; justify-content: center;"> <div style="border: 1px solid black; border-radius: 50%; width: 40px; height: 40px; display: flex; flex-direction: column; align-items: center; justify-content: center;"> <div style="border-bottom: 1px dashed black; width: 100%; height: 100%;"></div> <div style="border-bottom: 1px dashed black; width: 100%; height: 100%;"></div> <div style="border-bottom: 1px dashed black; width: 100%; height: 100%;"></div> </div> <div style="margin-left: 10px;"> <p>MAX TEMPERATURE</p> <p>TURNAROUND TIME</p> <p>QUENCH TIME</p> </div> </div>
---	--

Figure C-5. Run 5703, Four-foot Cross-Sectional Bundle Maximum Temperatures, Turnaround Times, and Quench Times



RUN NO. <u>5703</u>		KEY
ELEVATION <u>2'</u>		MAX TEMPERATURE
INITIAL TEMPERATURE <u>1100°F</u>		TURNAROUND TIME
PRESSURE <u>15 PSIA</u>		QUENCH TIME
T _{WATER} <u>150°F</u>		
POWER <u>0.7 KW/FT</u>		

Figure C-6. Run 5703, Two-foot Cross-Sectional Bundle Maximum Temperatures, Turnaround Times, and Quench Times

C.4.3 Parameter Effects on Top Injection Performance

The effects of four different parameters were investigated in these tests: power (kw/ft peak), subcooling of the injection water, initial clad temperature, and injection flow rate. In characterizing the effects of these input parameters, the rod-to-rod maximum temperature, the peak temperature envelope, and the measured heat transfer coefficients will be examined. Since there was a flow distribution effect in these tests, picking a single rod which describes the bundle and test results is difficult. For purpose of comparison, Rod 5G will be used to characterize the 6 ft heat transfer in the bundle. In general, this particular rod was the hottest rod or one of the hottest rods in the test.

C.4.3.1 Peak Power Effects

Three peak power values were examined: 0.4 kw/ft, 0.6 kw/ft, and 0.7 kw/ft, as shown in Table C-3. The effect of power on the peak temperature envelope is shown in Figure C-7 and can be seen to have a relatively significant effect. The power effect on the rod temperature behavior and midplane heat transfer is shown in Figure C-8 and indicates that the increase in rod power increased the heat transfer coefficient.

One postulated reason for the increase in the heat transfer coefficient with increasing rod power is that the higher powered rods generate more steam in the upper and lower elevations in the bundle. This steam is then condensed by the incoming water, thereby raising the local water temperature. Increasing the water temperature has the effect of increasing the steam generation rate at the midplane, causing more uniform redistribution of the injected water. Unfortunately, insufficient instrumentation existed in the tests to verify this or other hypothesis.

The peak temperature distributions at the 6 ft elevation for these three cases are given in Figures C-4, C-9, and C-10, showing that as the rod power increased

TABLE C-3

TOP INJECTION TEST RESULTS

Run No.	Initial Temp (°F)	Peak Power (kw/ft)	Coolant Temp (°F)	Injection Flow (gpm)	Remarks	2 ft T _{max} (°F)	Elev Time (sec)	4 ft T _{max} (°F)	Elev Time (sec)	6 ft T _{max} (°F)	Elev Time (sec)	10 ft T _{max} (°F)	Elev Time (sec)
5501	1100	0.4	150	15	Drained	929 (5E)	160	1338	166	1480	560	1051	130
5602	1100	0.6	150	15	Drained	1129 (1K)	491	1546 (4J)	598	1594 (6H)	137	1347 (3J)	600
*5703	1100	0.7	150	15	Drained	1156 (1K)	422	1675 (9J)	319	1722 (6H)	234	1493 (7J)	558
5904	1400	0.7	150	15	Drained	1249 (1K)	498	1724 (9J)	308	1830 (6H)	171	1373 (6K)	241
6007	1100	0.7	150	15	Not Drained	943 (9J)	89	1327 (4G)	78	1423 (5J)	140	935 (4H)	20
**6106	1100	0.7	82	15	Drained	1145 (6K)	167	1775 (4H)	168	2010 (6H)	173	1463 (4H)	171
6205	1100	0.7	87	35	Drained	1276 (6K)	541	1698 (9J)	542	1901 (5J)	427	1393 (2J)	479
6408	1100	0.7	180	15	Drained	1182 (6K)	566	1804 (6K)	546	1705 (6H)	145	1459 (8K)	409

*Reference case.

**High temperature limit reached

NOTES:

- (1) All runs at 15 psia
- (2) Housing was heated to ~800°F for all runs

C-16

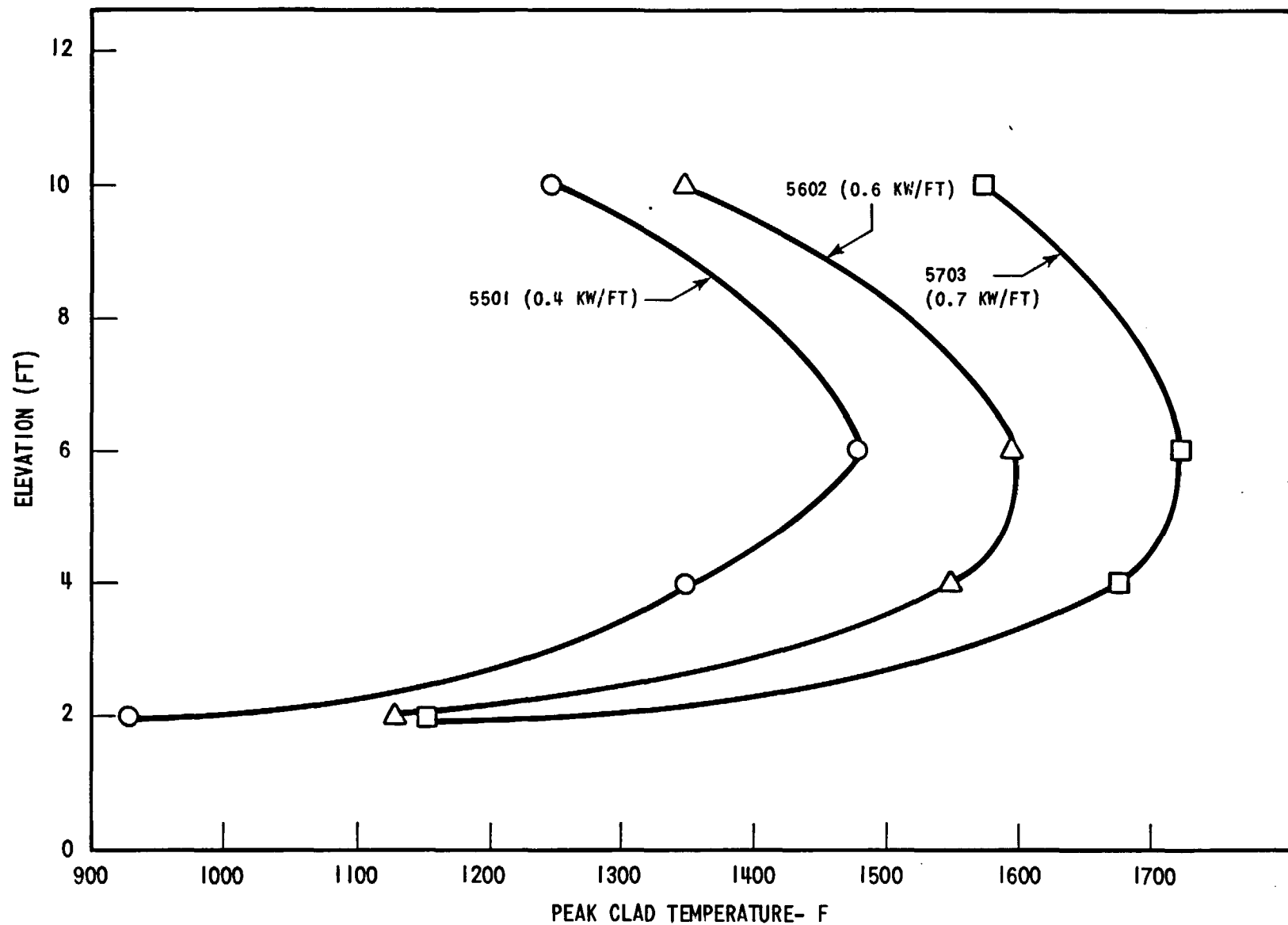


Figure C-7. Effect of Peak Power on Maximum Temperature Envelope

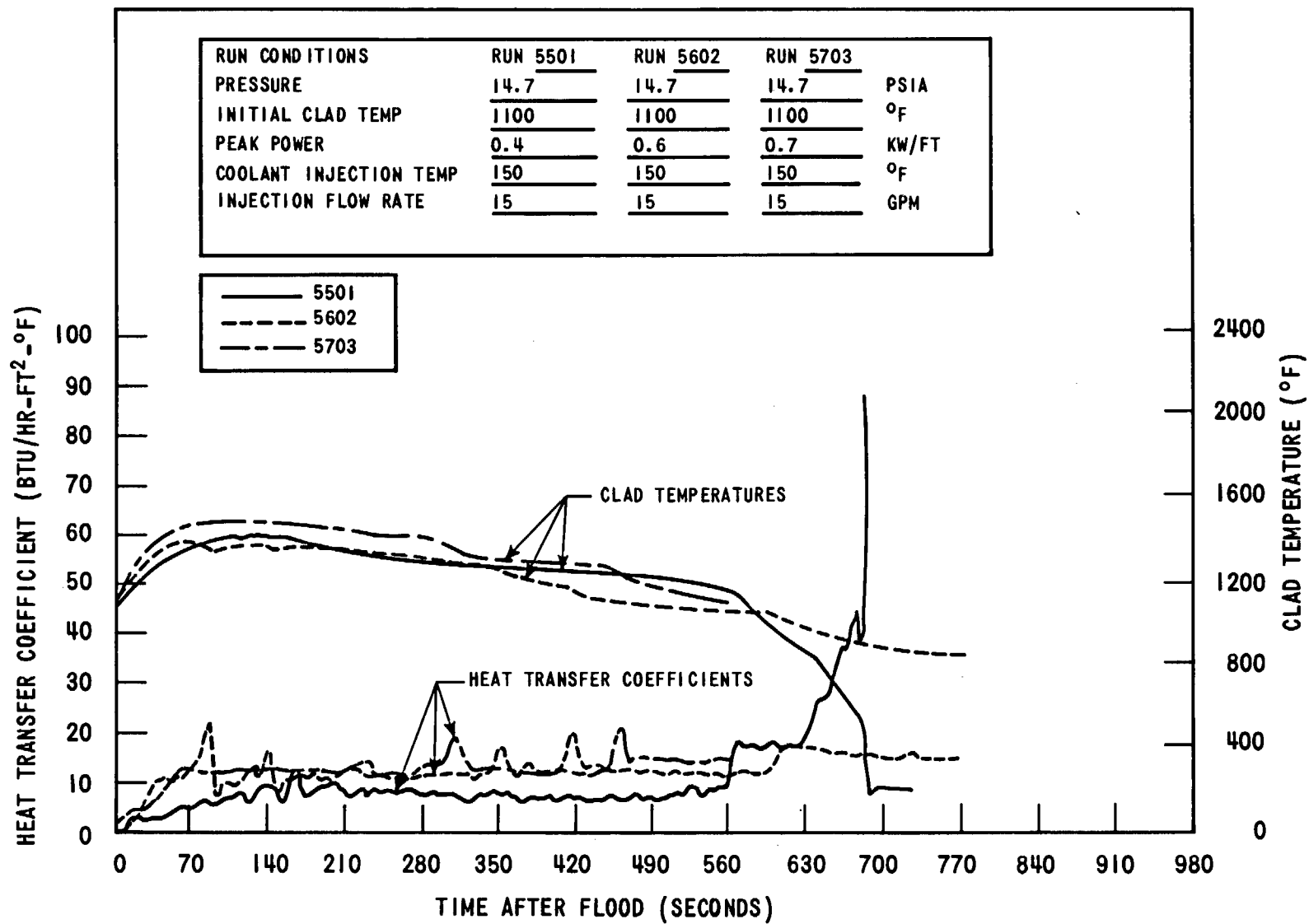


Figure C-8. Effect of Power on Rod 5G, Six-Foot Heat Transfer and Temperature

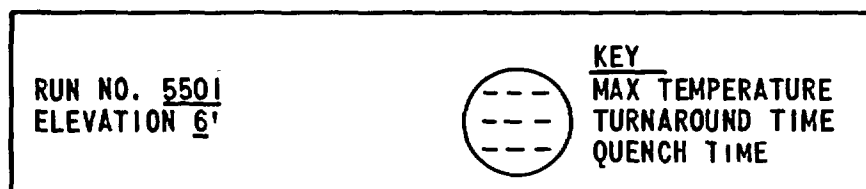
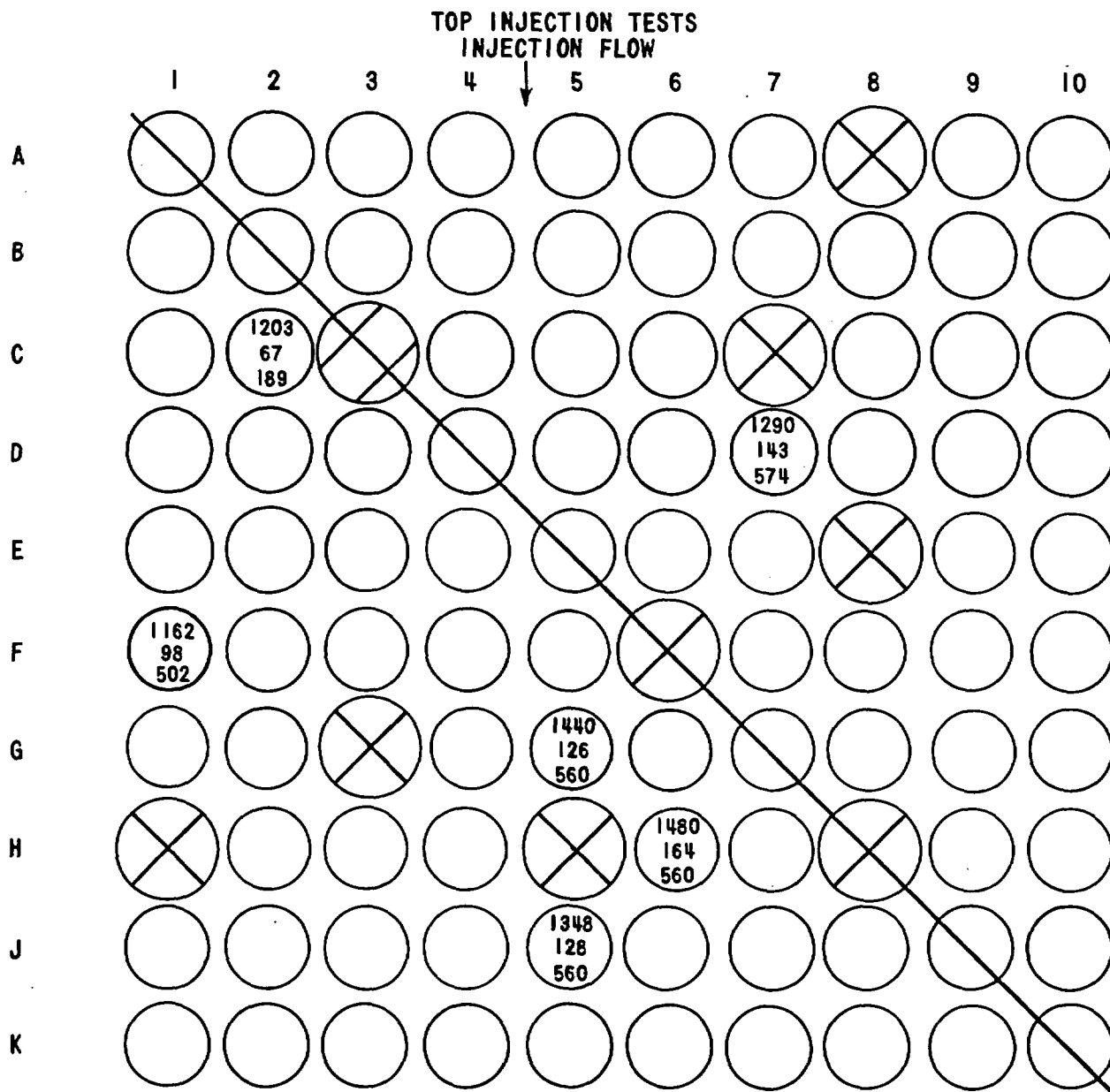
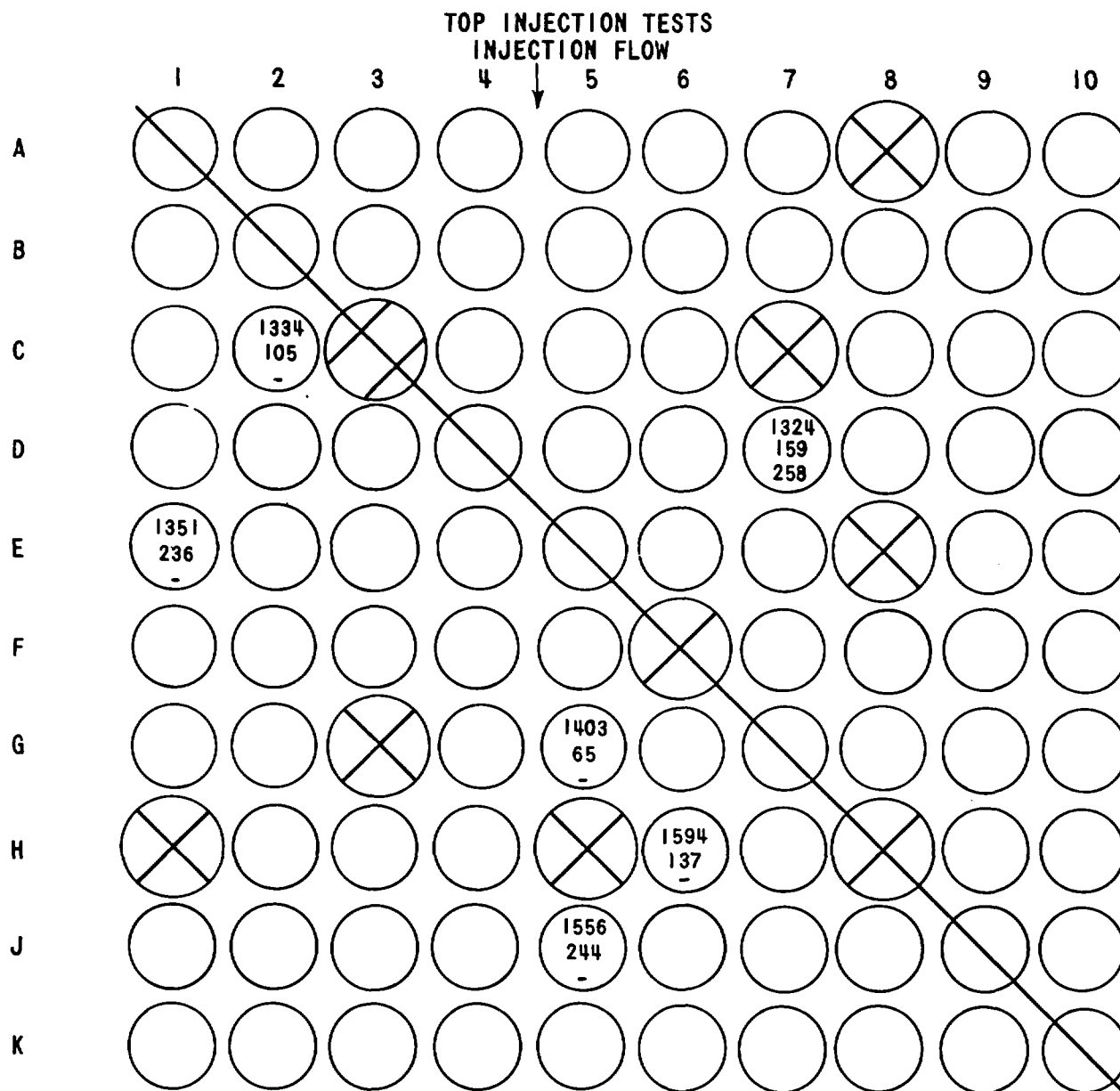


Figure C-9. Run 5501, Six-foot Cross-Sectional Bundle Maximum Temperatures, Turnaround Times, and Quench Times



RUN NO. 5602

ELEVATION 6'

KEY

MAX TEMPERATURE

TURNAROUND TIME

QUENCH TIME

Figure C-10. Run 5602, Six-foot Cross-Sectional Bundle Maximum Temperatures, Turnaround Times, and Quench Times

the peak rod temperature, turnaround times, and quench times all increased. These figures also indicate the amount of nonuniformity in the rod bundle temperatures due to the injection flow location.

C.4.3.2 Initial Temperature Effects

The effect of initial temperature on the maximum temperature envelope for Runs 5103 and 5904 is shown in Figure C-11. This figure indicates that increasing the initial temperature only increases the temperature at which the rod heat release rate equals the rod power generation rate. The measured heat transfer coefficients for these two runs are given in Figure C-12. As indicated in Figure C-13, the measured heat transfer coefficient is nearly the same for the first 300 seconds, after which time the lower initial temperature test had a larger film coefficient.

The rod-to-rod maximum temperature distribution is shown in Figures C-4 and C-14 for Runs 5703 and 5904 and indicates that nearly all of the instrumented rods are at a higher temperature for the higher initial temperature case.

C.4.3.3 Injection Water Temperature

The effect of injection water temperature was studied in more detail than the other parameters since it was found that the high subcooling test caused an over-temperature trip, resulting in a bundle power scram. The peak temperature envelopes for Runs 6106, 5703, and 6408, shown in Figure C-15, indicate that the water subcooling has a very pronounced effect on the bundle cooling performance. The measured heat transfer coefficient for rod 5G at the 6 ft elevation along with the measured rod temperature history is shown in Figures C-16 and C-17 for these runs. Figure C-16 shows that the heat transfer for the highly subcooled injection water case is very marginal, being less than $6 \text{ Btu/hr-ft}^2\text{-}^\circ\text{F}$ for most of the time, while the heat transfer for the higher

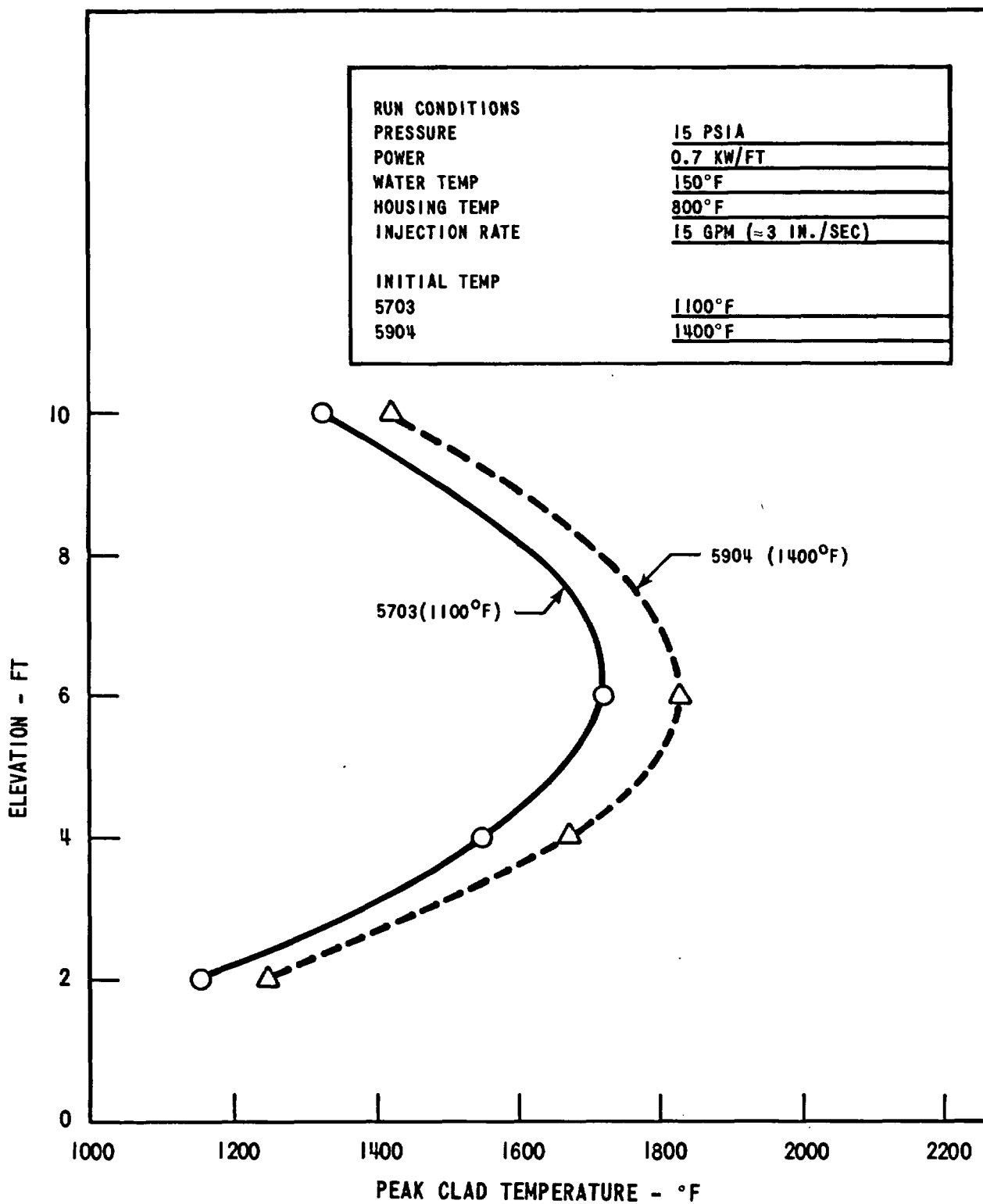


Figure C-11. Effect of Initial Temperature on Maximum Temperature Envelope

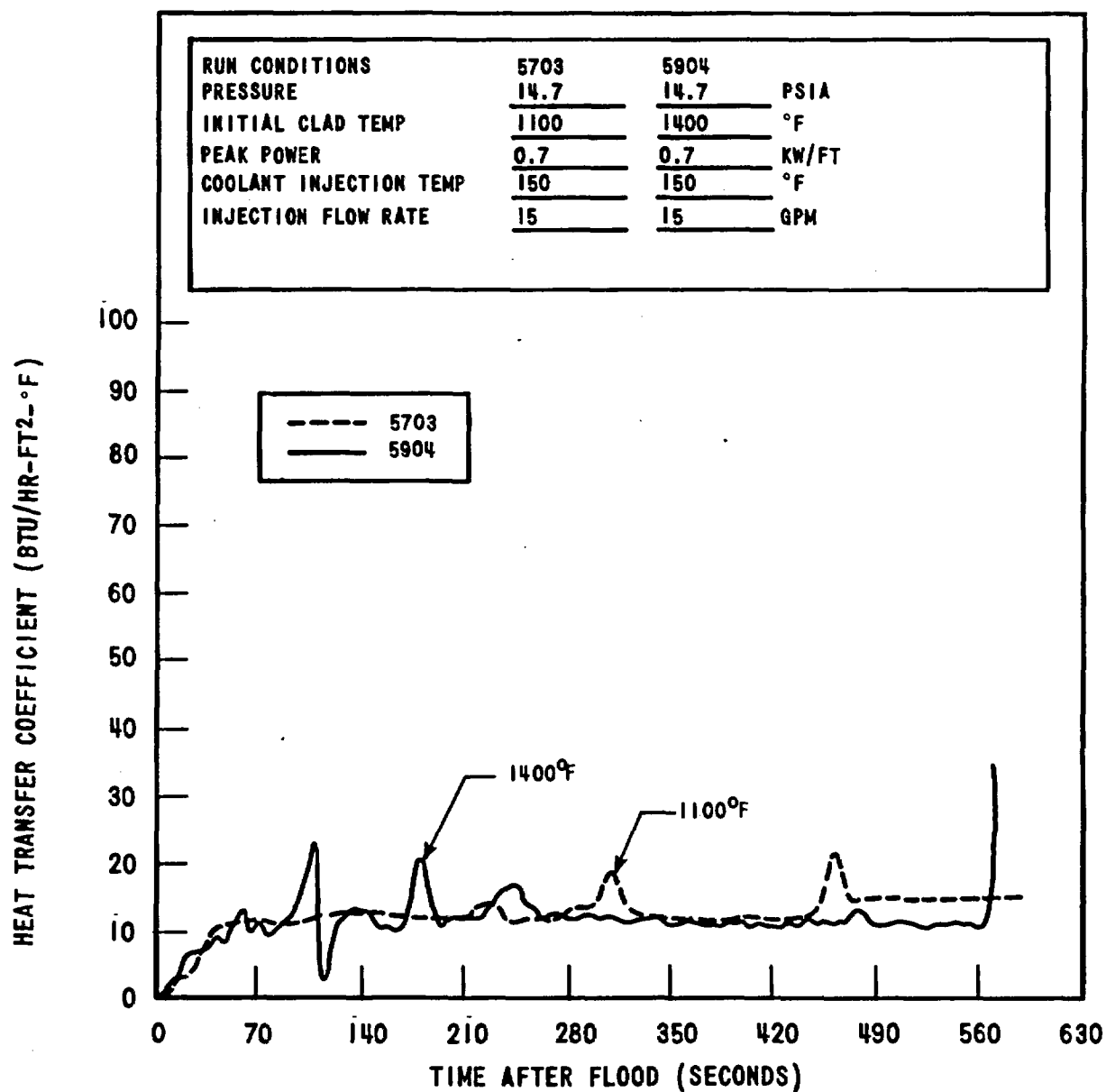


Figure C-12. Effect of Initial Temperature on Rod 5G, Six-foot Heat Transfer

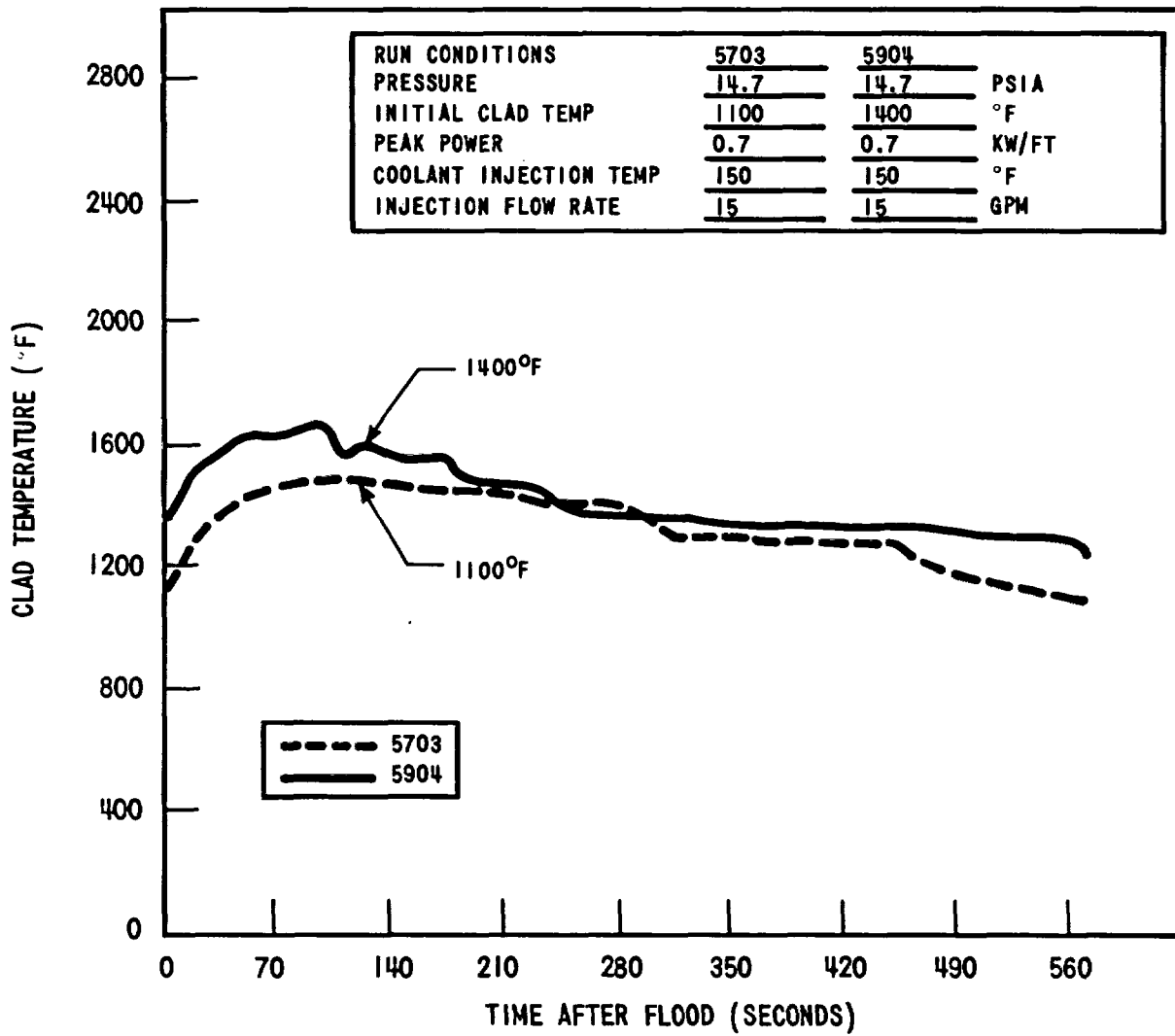


Figure C-13. Effect of Initial Temperature on Rod 5G Transient

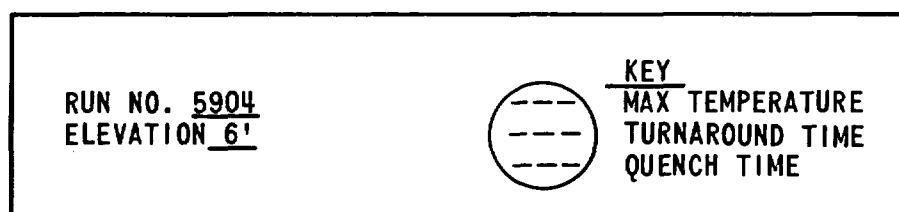
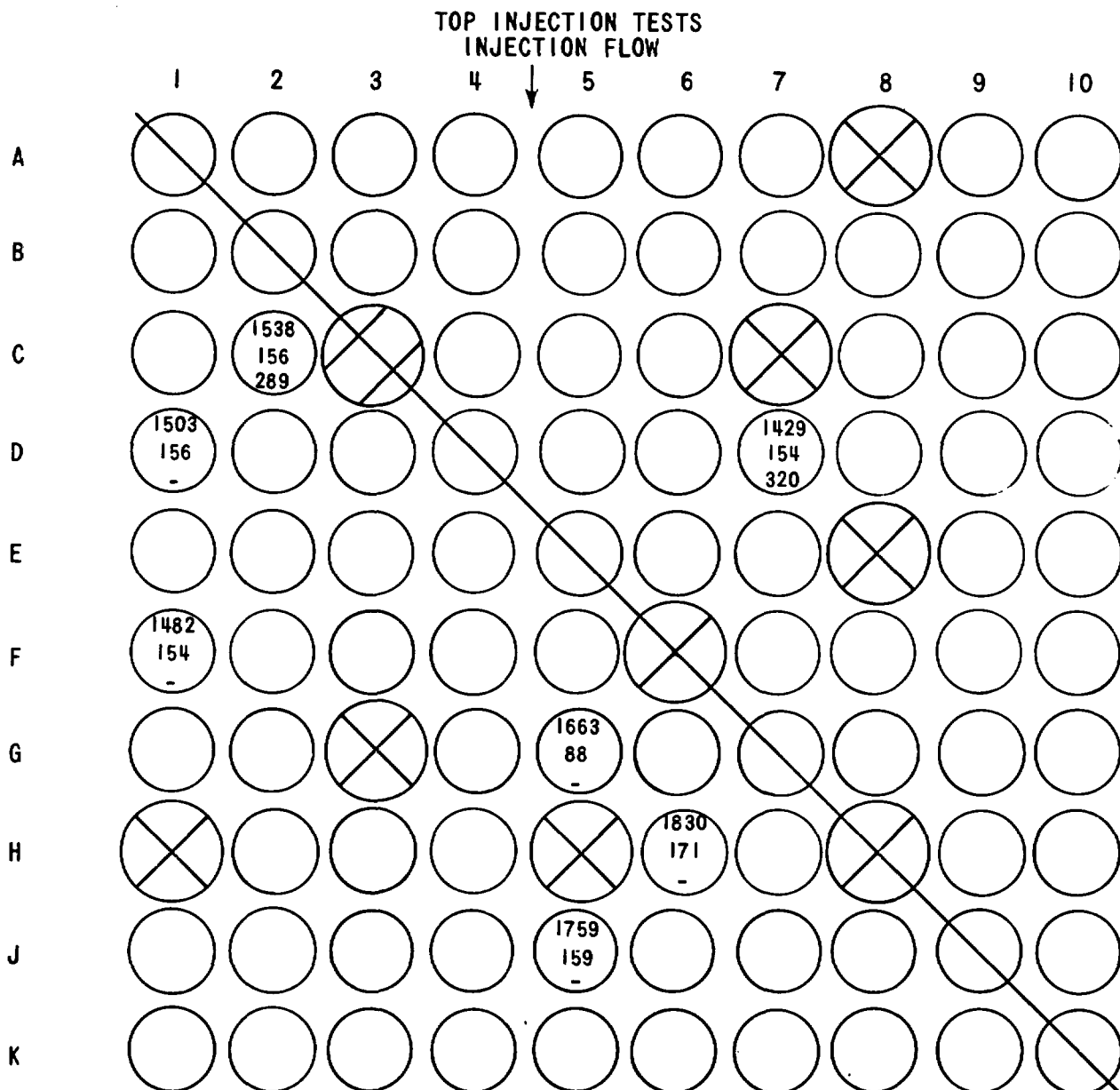


Figure C-14. Run 5904, Six-foot Cross-Sectional Bundle Maximum Temperatures, Turnaround Times, and Quench Times

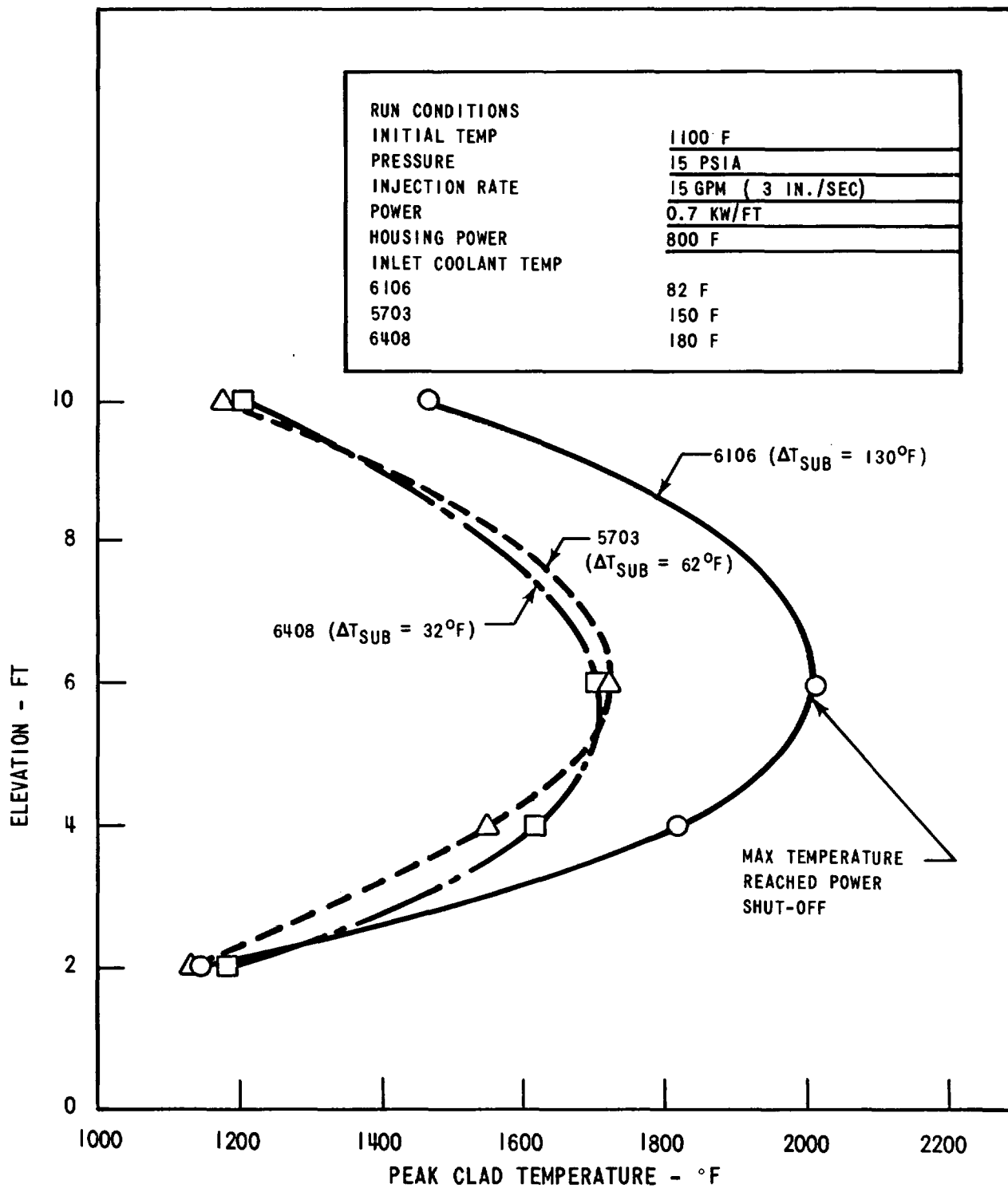


Figure C-15 Effect of Injection Water Temperature on Maximum Temperature Envelope

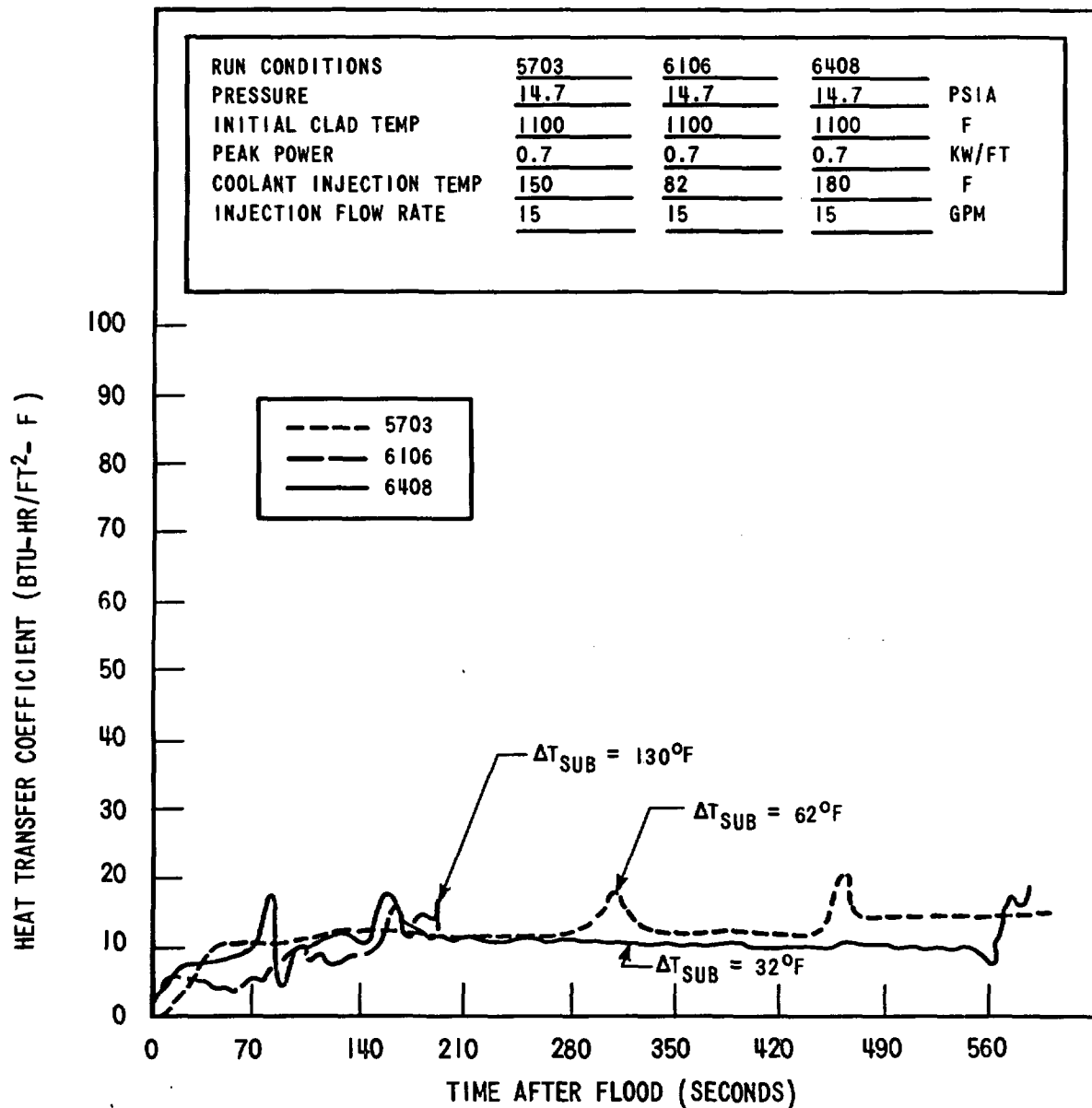


Figure C-16. Effect of Injection Water Temperature on Rod 5G Rod Heat Transfer

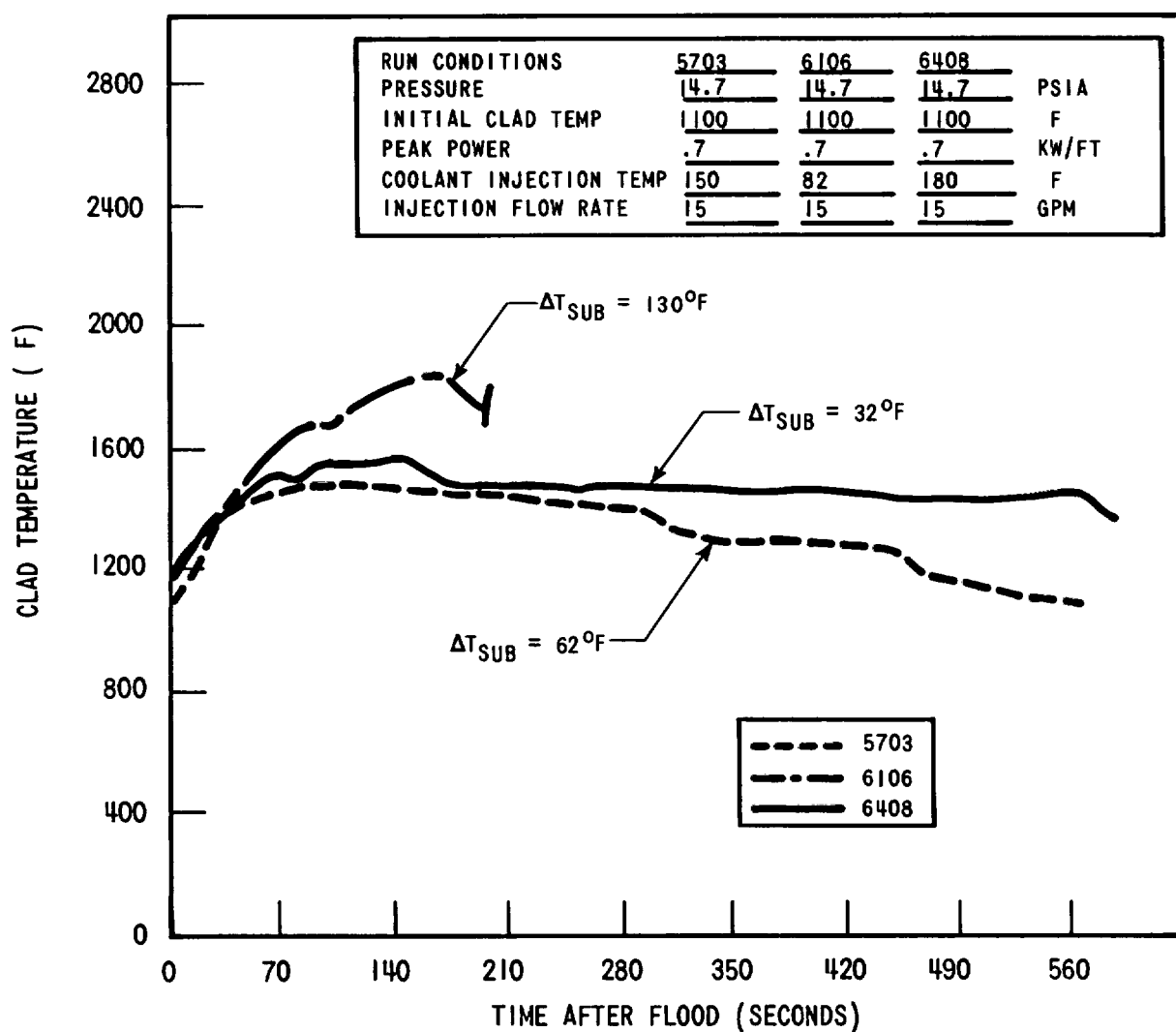


Figure C-17. Effect of Injection Water Temperature on Rod 5G Temperature

injection water temperatures is significantly larger. The larger heat transfer for the hotter injection water cases is believed to result from the increased steam generation within the bundle. By decreasing the injection water subcooling, the steaming rate is increased for the same water mass flow which acts to increase the turbulent steam/water mixing within the bundle. The increased mixing results in a more uniform and effective cooling of the bundle, since the transport of water droplets is increased by the additional steaming. The increased steam generation can be seen by comparing the orifice steam flow for these tests given in Table C-2. The steam flow out of the orifice for Run 6408 (high injection water temperature, 180°F) is over twice that for Run 6106 (low injection water temperature, 82°F).

The effects of the additional steaming can also be observed by comparing the rod-to-rod temperatures at the different elevations. The rod-to-rod temperatures were examined at 180 seconds, since this was the time that Run 6106 reached rod temperatures of 2000°F which then terminated the test. The rod-to-rod temperatures at the 6 ft elevation are shown in Figures C-4, C-18, and C-19.

C.4.3.4 Injection Flow Rate Effects

The effect of increasing the injection flow rate into the upper plenum was also studied to see if the rod heat transfer was sensitive to the flow rate. Since the top injection tests up to this time had run approximately 10 minutes in length, it was apparent that the 150 gallon FLECHT-SET accumulator was not large enough to run a higher flow test. Therefore, instead of using the accumulator for a water supply, the injection water was pumped into the upper plenum from the water storage supply. Using this water for injection resulted in a low injection water temperature (87°F) similar to that which caused Run 6106 to scram on peak temperature limit. However, by examining Figure C-20 it is apparent that if a sufficient amount of cold water is used it will provide sufficient cooling to maintain the bundle below 2000°F. It is also evident that the increased injection flow rate helped prevent channeling of the cold injection water down one side of the bundle.

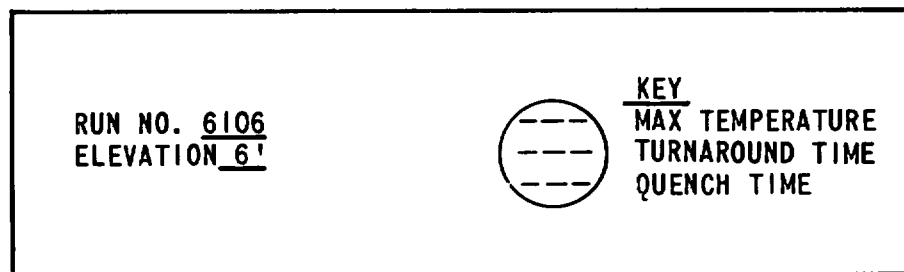
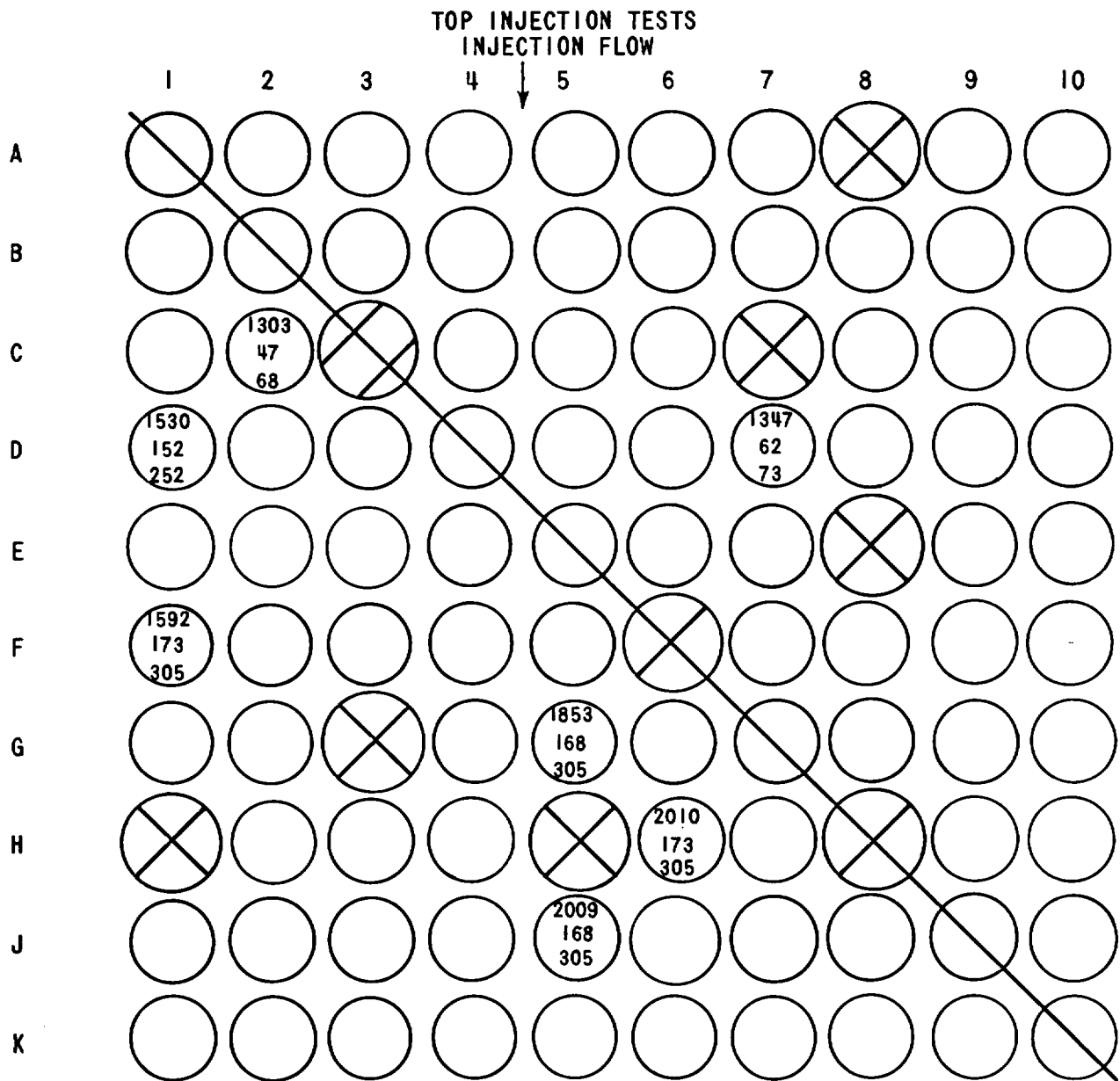


Figure C-18. Run 6106, Six-foot Cross-Sectional Bundle Maximum Temperatures, Turnaround Times, and Quench Times

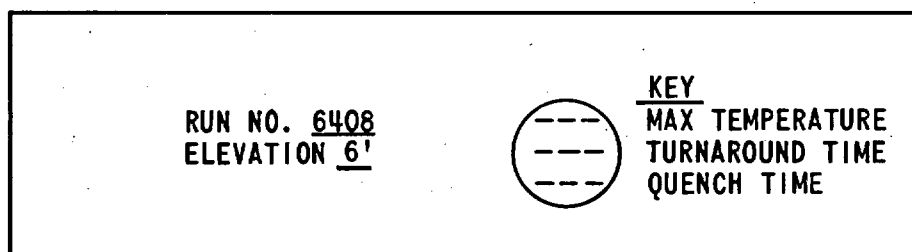
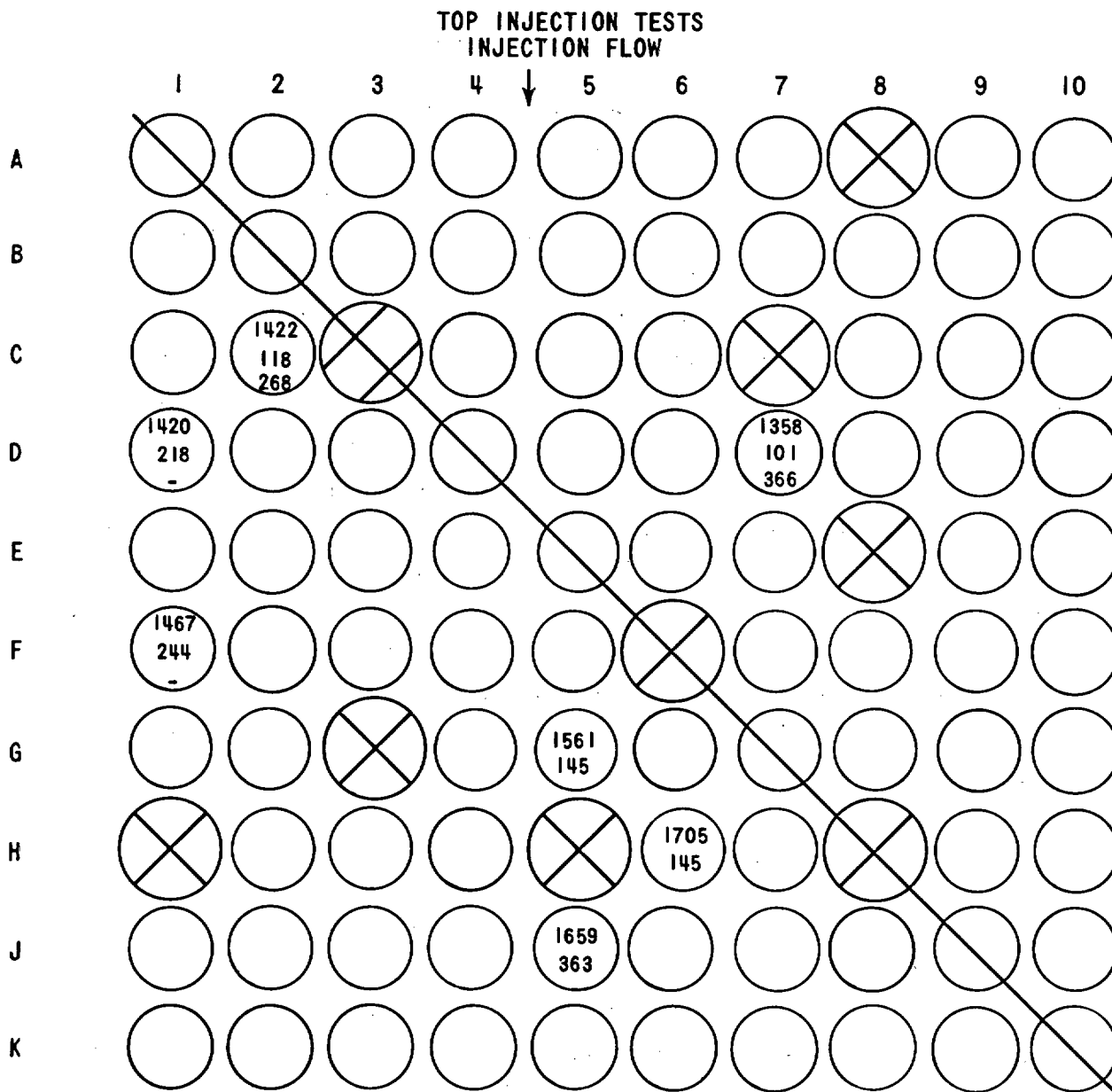


Figure C-19. Run 6408, Six-foot Cross-Sectional Bundle Maximum Temperatures, Turnaround Times, and Quench Times

The peak clad temperature envelope is shown in Figure C-20 and indicates that the maximum temperature reached was 1900°F, while the lower flow test (Run 6106) did exceed 2000°F, causing a high temperature power trip. The measured heat transfer coefficients and corresponding rod temperatures are given in Figures C-21 and C-22 and indicate that for Rod 5G at 6 ft there is an improvement in the rod cooling with increased injection flow rate. The radial rod-to-rod temperature distribution is given in Figure C-23 and can be compared to Figure C-18 to see the effect of increased injection flow rate on the individual rod temperatures. These two figures show the individual rod temperatures at 180 seconds, at which time Run 6106 reached 2000°F. As the figures show, more rods were cooled and quenched with the higher injection flow rate than with the lower flow rate. It is apparent that unless the top injection system designs result in a relatively uniform flow, very high injection flow rates must be used to achieve sufficient cooling with cold water. This flow distribution problem is relaxed somewhat when the water is hotter so that the increased bundle-generated steam helps distribute the flow more evenly.

C.4.3.5 Examination of the Bundle Venting Effect

All tests except Run 6007 allowed the injection water to drain out of the bundle so that no water inventory could accumulate in the bundle to cause a bottom flooding effect. Run 6007 was conducted with the bundle drain closed using the same system parameters as Run 5703 to obtain a comparison of the effect of not venting the system. The bundle vent path was now through the Phase A piping to the containment tank which was held at atmospheric pressure.

The peak clad temperature envelope for these two runs is shown in Figure C-24 and indicates that having the water accumulate in the bundle results in a significant rod temperature reduction. A flooding process is established which does prevent a significant portion of the injected water from reaching the rods. The mass collection in the Phase A carryover tank, shown in

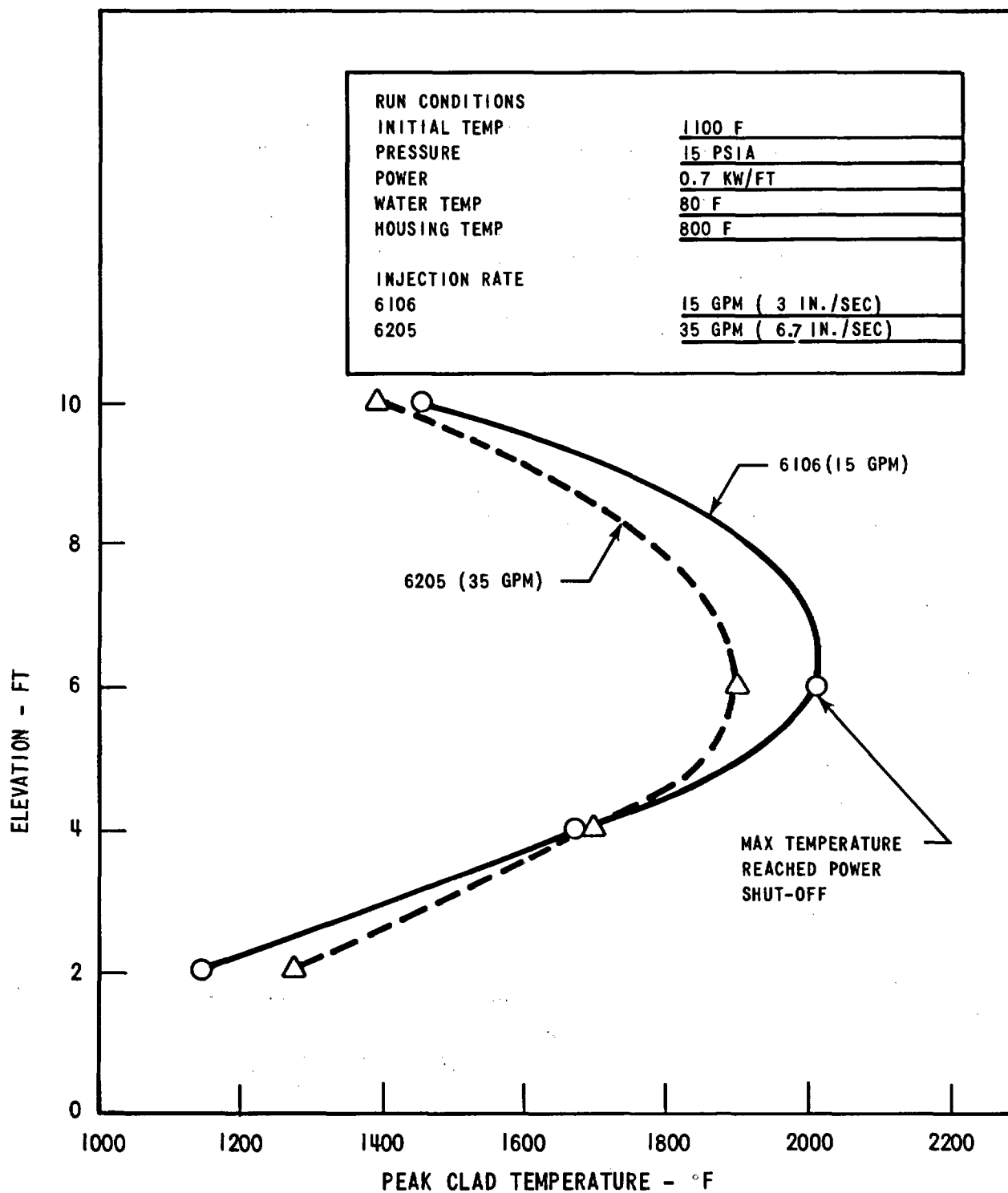


Figure C-20. Effect of Injection Water Flow Rate on Maximum Temperature Envelope

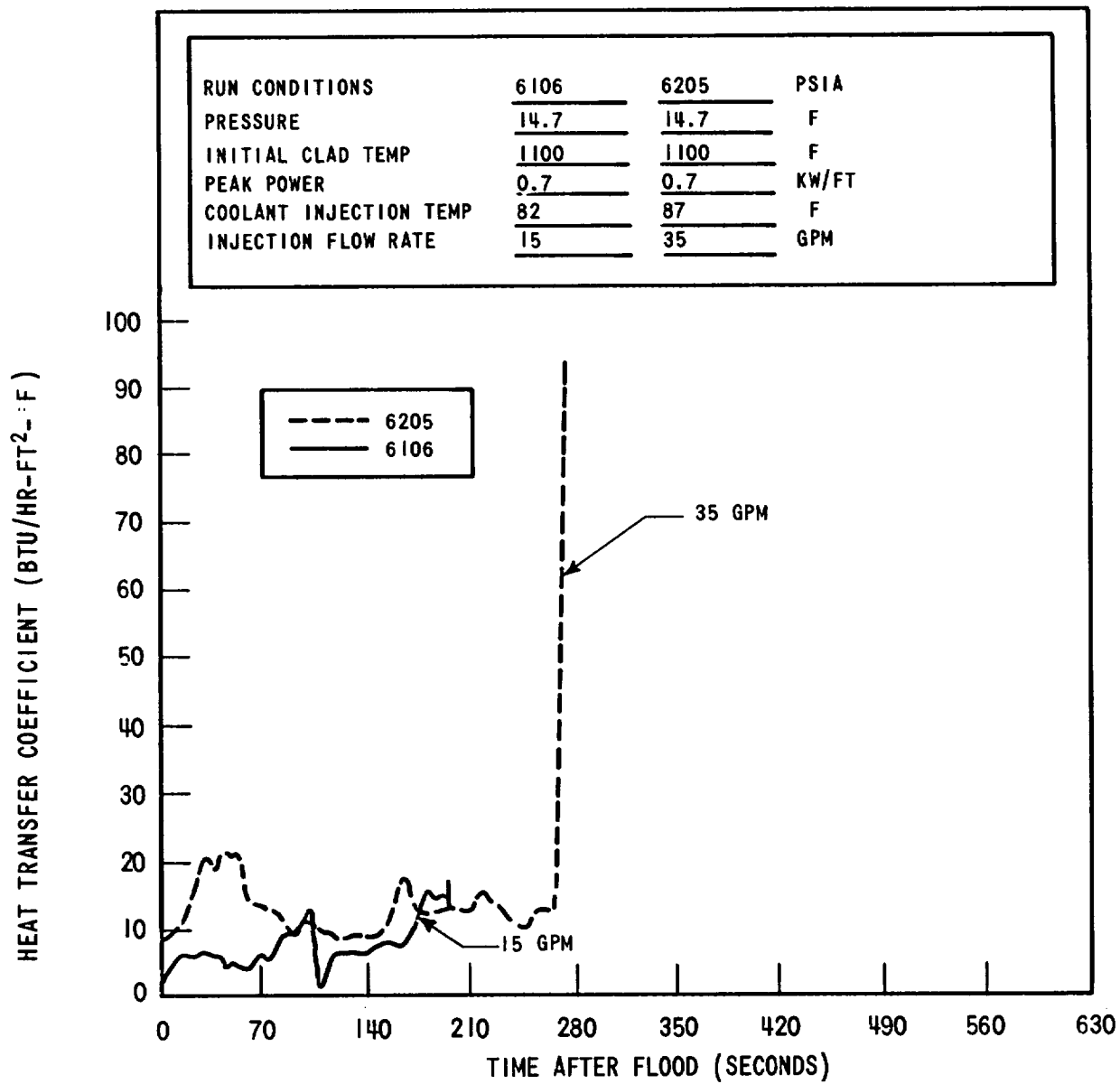


Figure C-21. Effect of Injection Water Flow Rate on Rod 5G Heat Transfer

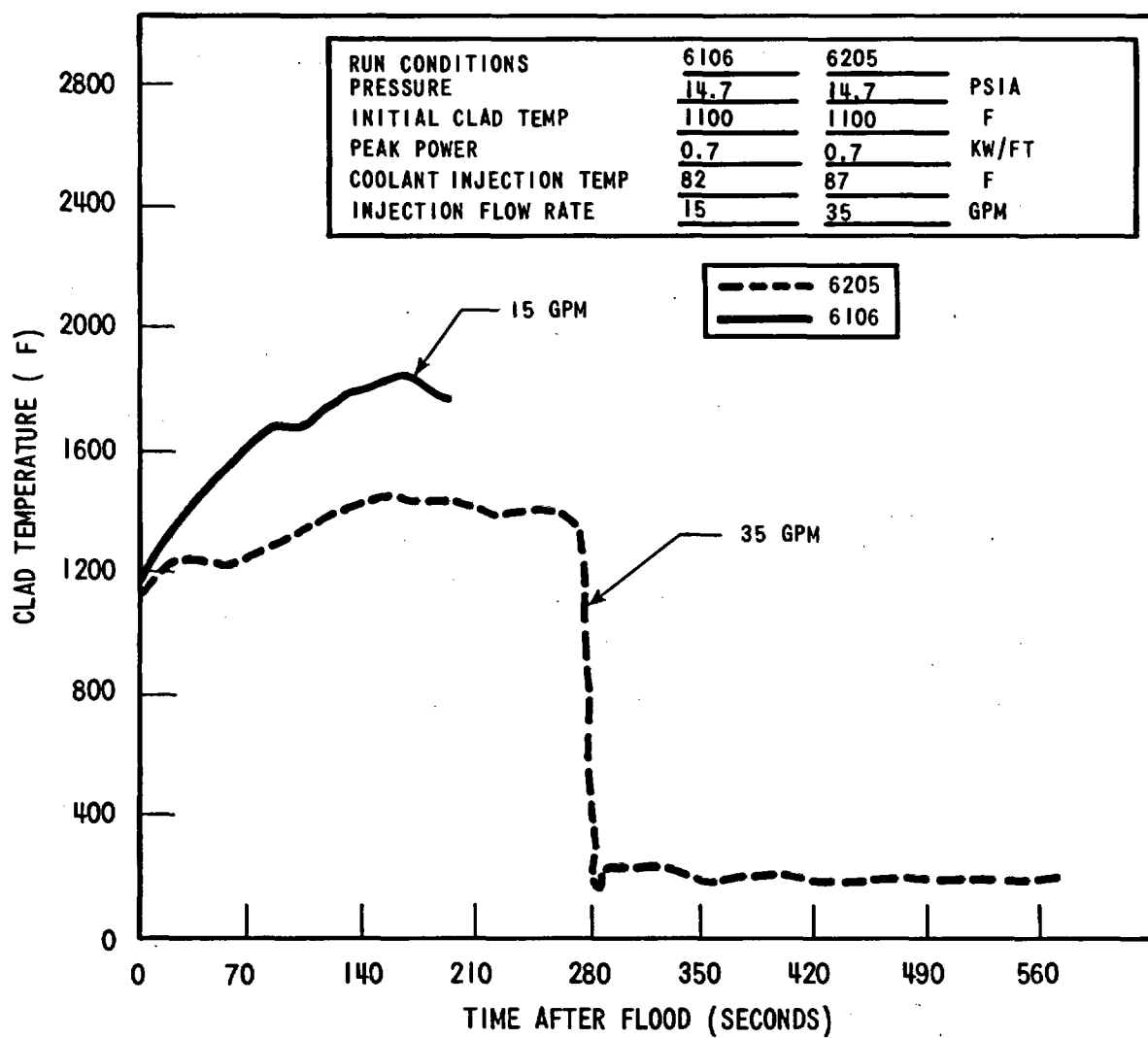


Figure C-22. Effect of Injection Water Flow Rate on Rod 5G Temperature Transient

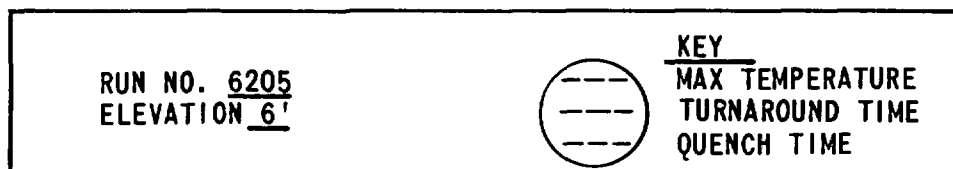
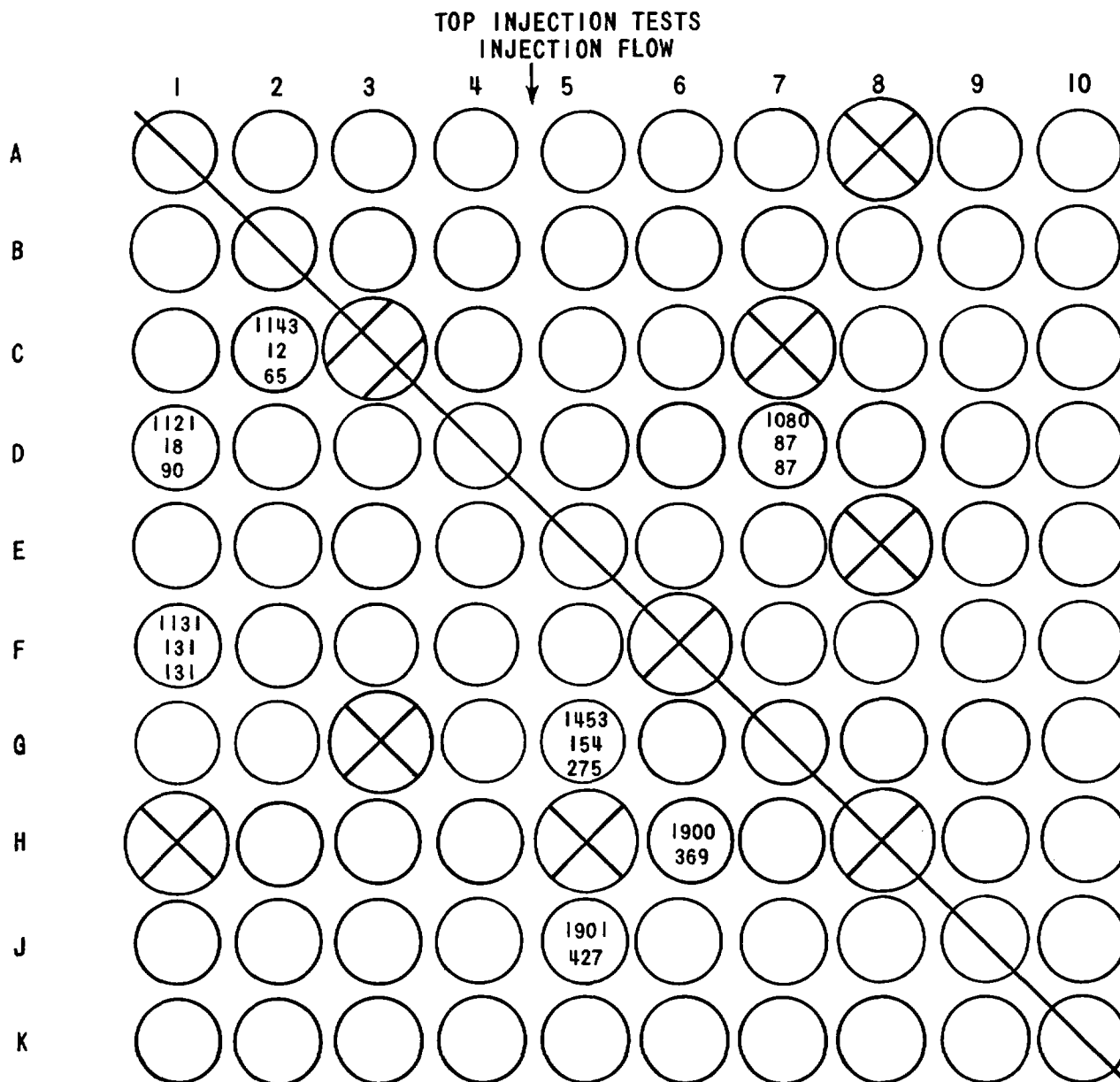


Figure C-23. Run 6205, Six-foot Cross-Sectional Bundle Maximum Temperatures, Turnaround Times, and Quench Times

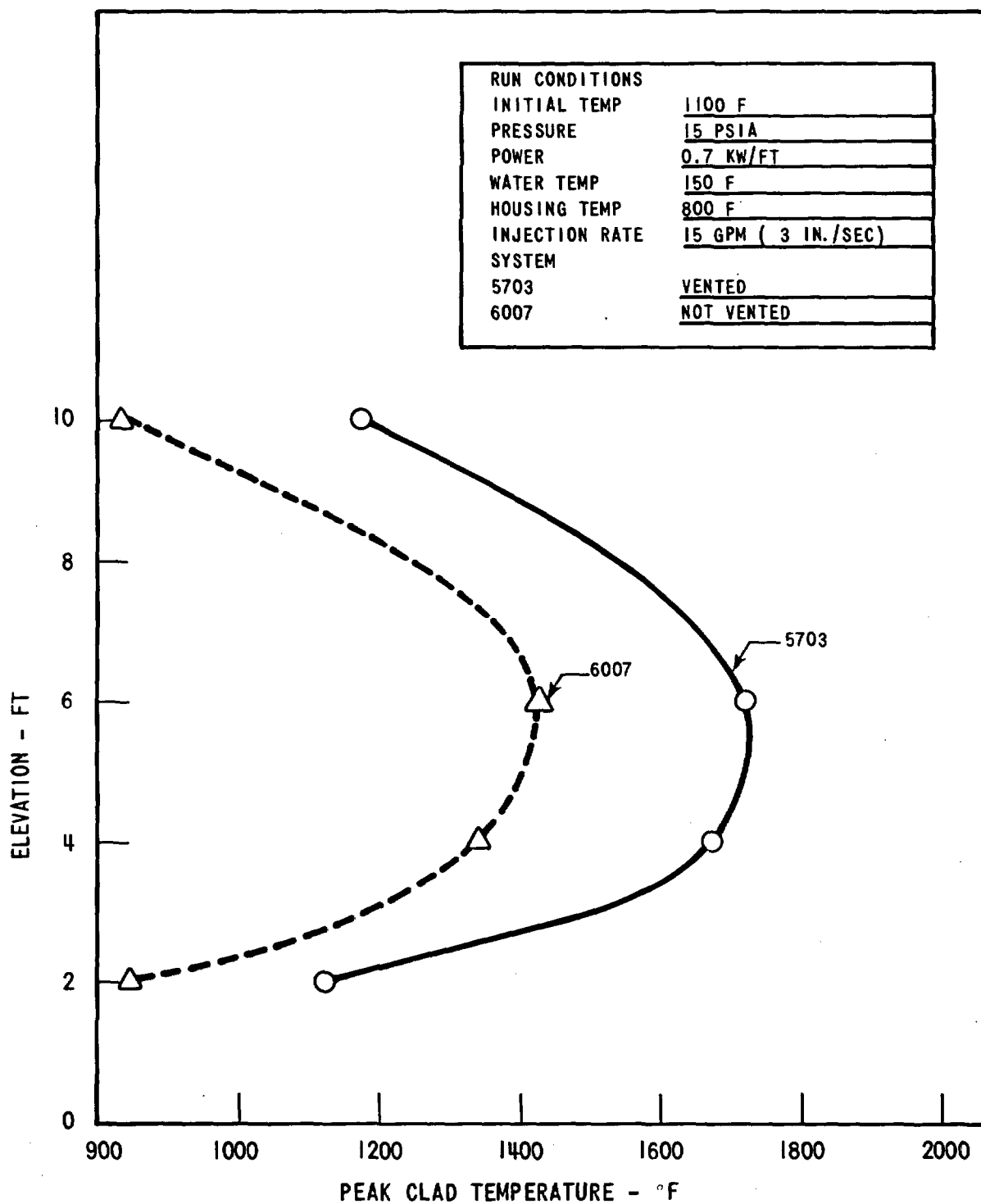


Figure C-24. Effect of Bundle Venting on Maximum Temperature Envelope

Table C-3, indicates that over one-half of the injected flow was carried to this tank by the bundle-generated steam flow. The total mass drained from the bundle and upper plenum extension was approximately 19 percent of the injected flow. However, the bundle flooding process is an effective mechanism to distribute that water which penetrates the steam upflow. The improved water distribution results in more uniform bundle temperatures and increased cooling. The axial pressure drop data indicate that there was approximately 3 ft of water in the bundle during the test. The rod temperature data indicate that all of the 2 ft and 4 ft thermocouples were quenched by 178 seconds and 395 seconds, respectively. The 6 ft heat transfer coefficient from Rod 5G is shown in Figure C-25 with its temperature history given in Figure C-26. It is apparent that the heat transfer is significantly improved in Run 6007 with the bundle drain closed. The heat transfer coefficients at different elevations is given in Figure C-27 and shows rod quenches similar to that in FLECHT. The 6 ft rod-to-rod temperature distribution is shown in Figure C-28 and indicates that all 6 ft rods quenched.

C.5 CONCLUSIONS

The top injection tests performed in FLECHT-SET Phase A indicate that core cooling can be obtained by this mode of ECC injection. It is also evident that the individual rod temperatures will remain at elevated temperatures for longer periods of time than a comparable bottom flooding FLECHT test with the same injection flow rate. The top flow distribution is a sensitive parameter in these tests and can result in only marginal cooling for rods which are removed from the coolant injection location.

The most significant parameters on the temperature history and rod heat transfer coefficient were the injection water subcooling, injection flow rate, and whether the water was allowed to accumulate in the bundle or not. The hot injection water resulted in more steam generation which helped to improve the flow distribution within the bundle so that better cooling was promoted. Cold injection water resulted in cold water channeling which created bundle hot spots.

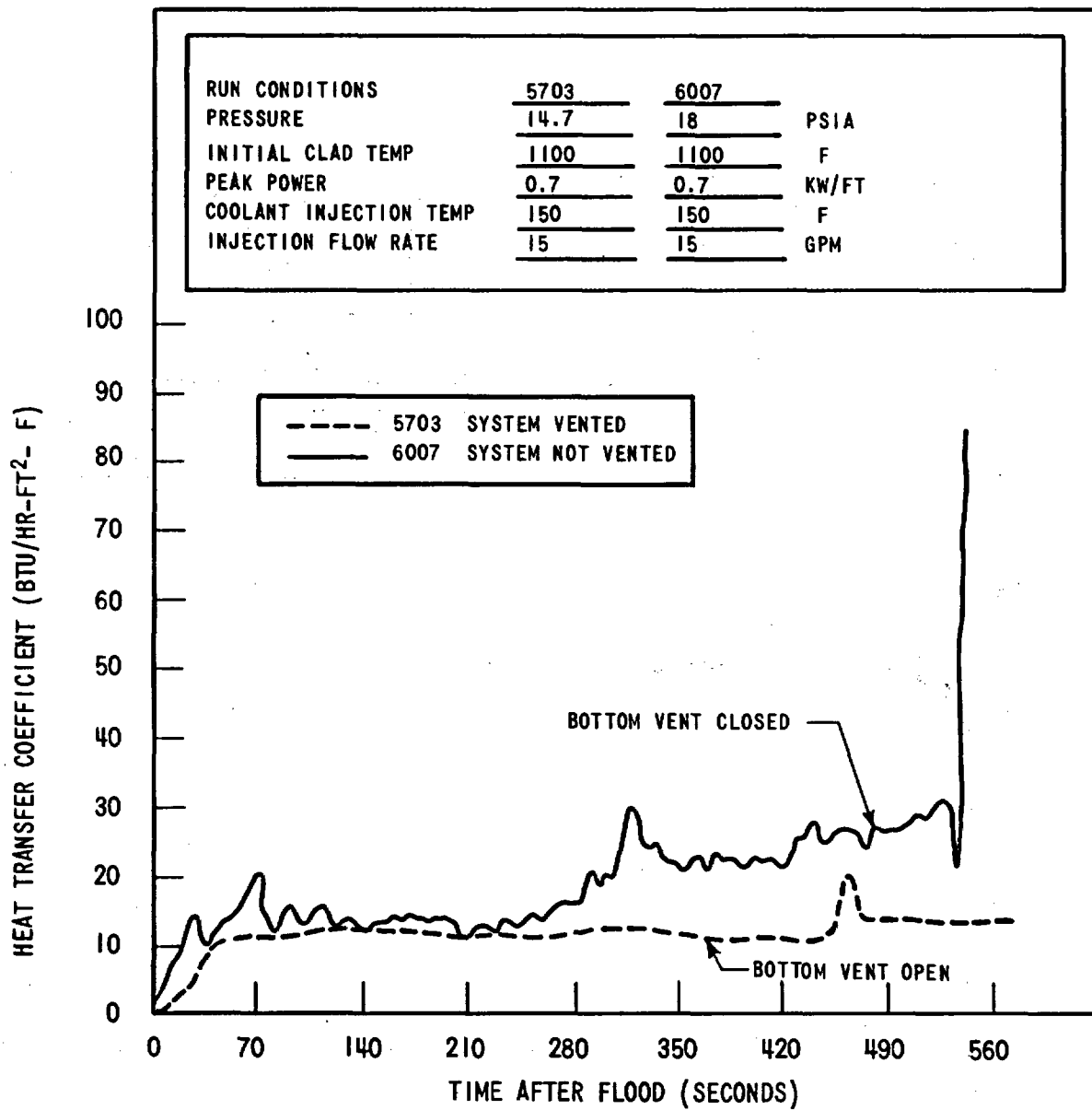


Figure C-25. Effect of Buxlle Venting on Rod 5G. Six-foot Heat Transfer

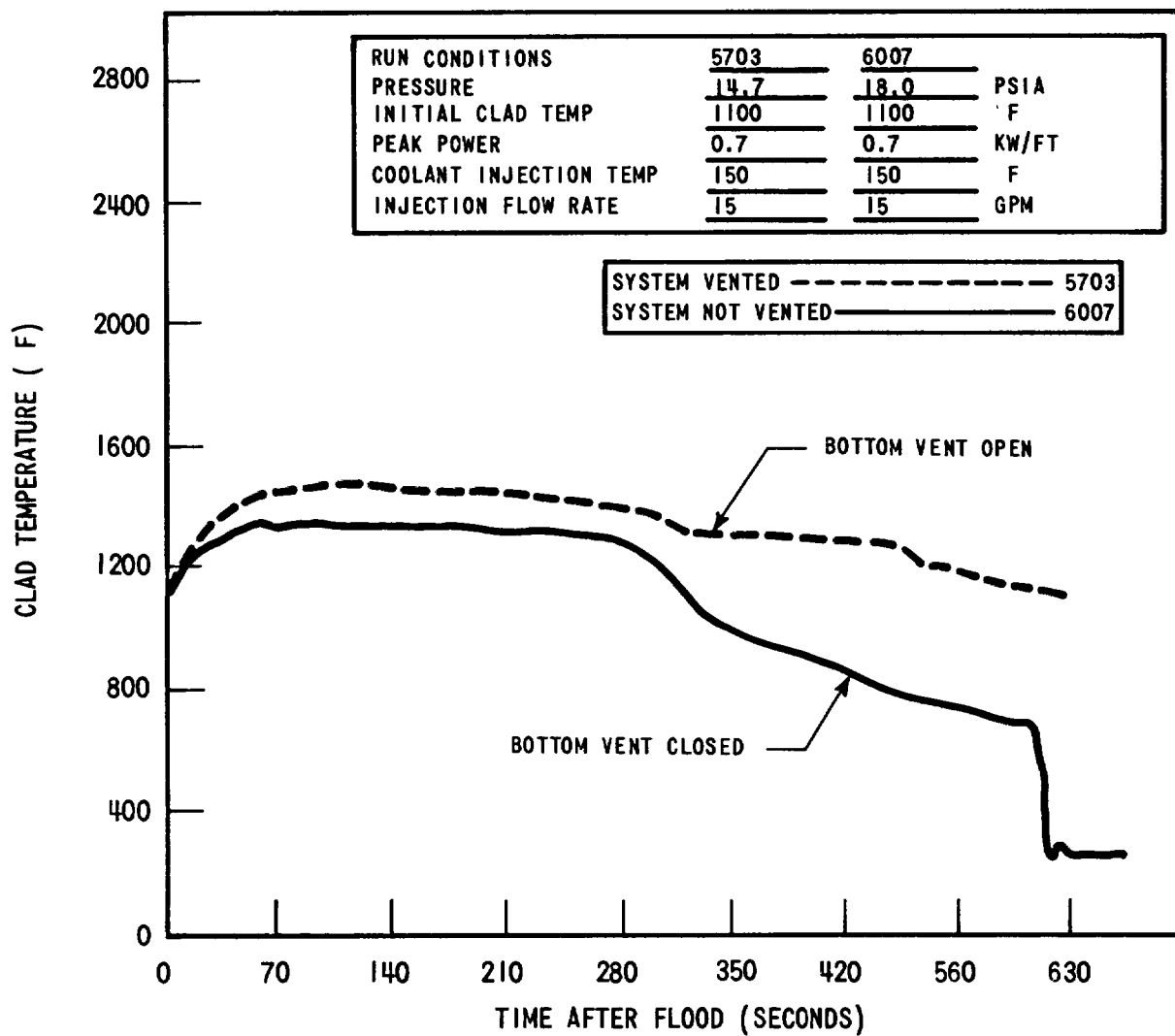


Figure C-26. Effect of Bundle Venting on Rod 5G, Six-foot Temperature

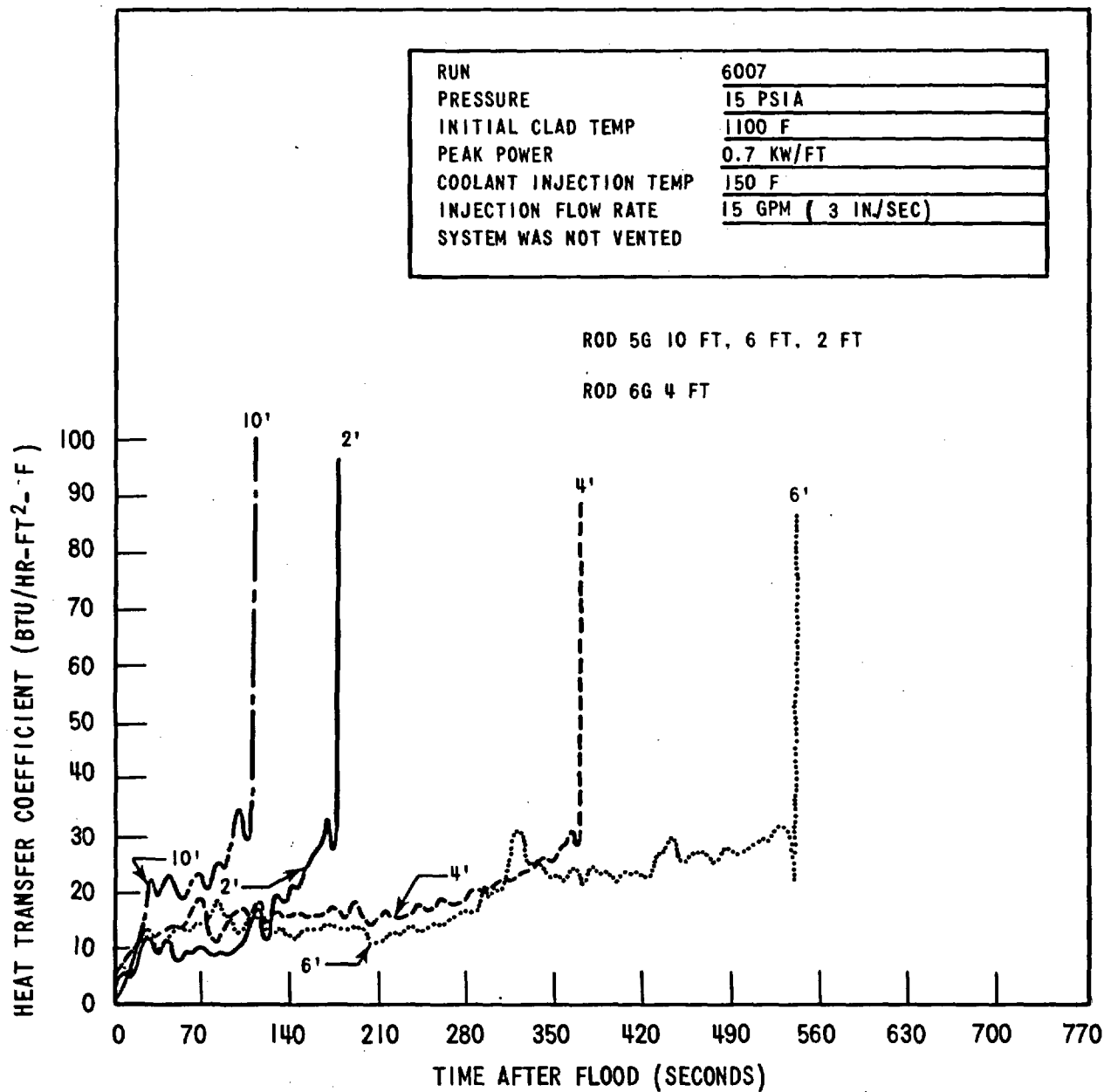
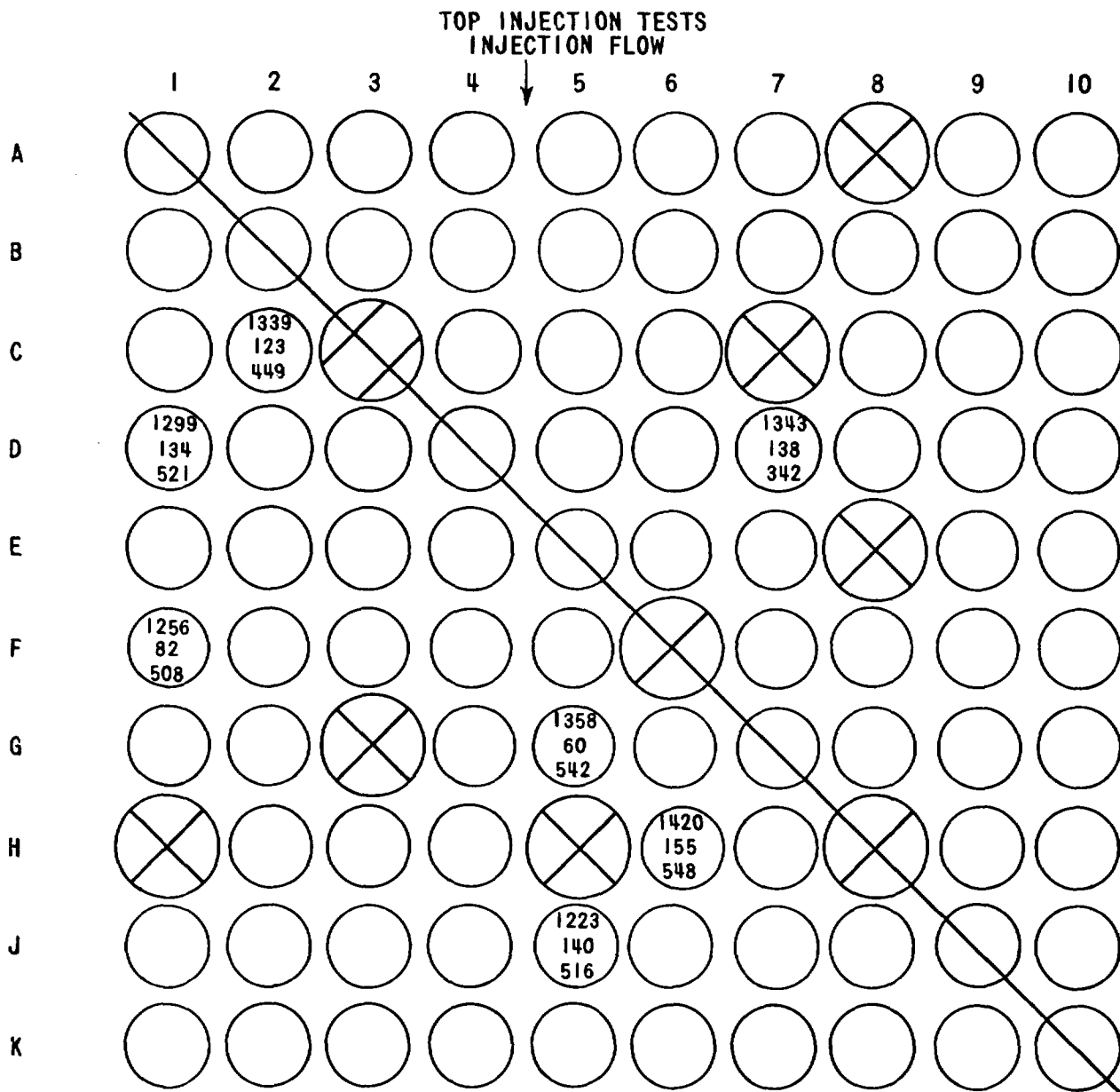
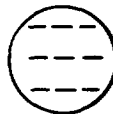


Figure C-27. Effect of Bundle Venting on Rod 5G Heat Transfer at All Elevations



RUN NO. 6007
ELEVATION 6'



KEY
MAX TEMPERATURE
TURNAROUND TIME
QUENCH TIME

Figure C-28. Run 6007, Six-foot Cross-Sectional Bundle Maximum Temperatures, Turnaround Times, and Quench Times

If a sufficient injection flow rate is used, the flow maldistribution effects are also minimized; however, it should be noted that the lower injection flow rate which was heated to 180°F provided better cooling than if increased cold flow was used. Therefore, the primary mechanism for mixing and promoting improved cooling appears to be the amount of steam generation in the bundle.

If the top injection water is allowed to accumulate in the bundle, the cooling performance of the bundle is significantly improved so that rod quenches typical of FLECHT occur. The maximum temperatures observed in this system configuration were lower than those observed in tests with similar system parameters but, in which no water was allowed to accumulate in the bundle.

APPENDIX C-1
TOP INJECTION TEST RUN SUMMARY SHEETS

1

2

3

4

5

6

TOP INJECTION TEST RUN SUMMARY SHEET

RUN NO. 5501

DATE 3/17/73

A. RUN CONDITIONS

Containment Pressure	14.7 psia
Initial Clad Temperature	1095 °F
Peak Power	0.4 kw/ft
Coolant Supply Temperature	151 °F
Injection Rate	15 gpm

B. INITIAL HOUSING TEMPERATURES

Elevation (ft)	Initial Temperature (°F)
0	389
2	674
4	798
6	847
8	804
10	803
12	465

C. WATER COLLECTED

FLECHT-SET Containment Tank	0	lbm at - °F
FLECHT-SET Separator Tank	177.75	lbm at 199°F
Steam Probe Tank	0	lbm at - °F
Upper Plenum	5.25	lbm at - °F
Collection Drums	(1) 101.39 lbm at 202°F	(3) 91.51 lbm at 198°F
	(2) 91.37 lbm at 202°F	(4) 89.0 lbm at 198°F

TOP INJECTION TEST SUMMARY SHEET (cont)

RUN NO. 5501

DATE 3/17/73

D. HEATER THERMOCOUPLE DATA

Rod/Elev.	Initial Temp. (°F)	Max. Temp. (°F)	Turnaround Time (sec)	Quench Time (sec)
5E/10'	849	951	74	439
5E/6'				
5E/2'	369	929	160	193
5F/10'	855	961	58	522
5F/2'	622	817	556	664
5G/10'	847	943	51	527
5G/6'	1098	1440	126	560
5G/4'				
5G/2'	629	864	468	659
6G/10'	920	1033	91	539
6G/4'				
6G/2'	638	865	515	665
7G/10'	824	970	123	582
7G/4'	931	1257	160	669
1K/10'				
1K/2'	719	757	256	649
3H/10'	848	892	46	262
3H/6'				
3H/4'				
6K/10'	899	1013	107	263
6K/4'				
6K/2'				
9J/10'				
9J/4'				
9J/2'				
1A/10'	837	863	23	51
1F/10'	913	945	36	108
1F/6'				
2C/10'				
2C/6'	1024	1203	67	189
2C/4'	921	1081	68	228
2E/10'				
2E/4'	910	1115	88	575

TOP INJECTION TEST SUMMARY SHEET (cont)

RUN NO. 5501

DATE 3/17/73

D. HEATER THERMOCOUPLE DATA (cont)

Rod/Elev.	Initial Temp. (°F)	Max. Temp. (°F)	Turnaround Time (sec)	Quench Time (sec)
2J/10'	835	895	35	140
2J/4'				
3D/10'				
3D/4'				
3F/10'	834	913	51	372
3F/6'				
3F/4'				
3J/10'	905	978	52	
3J/6'				
3J/4'	907	1248	305	676
4E/10'	846	931	56	390
4E/4'	926	1094	321	
4F/6'				
4F/4'	935	1192	88	575
4G/10'	846	935	51	383
4G/6'				
4G/4'	1037	1338	166	680
4H/10'	924	1005	51	384
4H/4'	977	1326	171	688
4K/10'	823	1248	305	676
4K/5'				
4K/4'	1026	1230	299	675
5J/10'	832	909	95	300
5J/6'	1019	1348	128	560
6H/10'	819	922	51	521
6H/6'	1034	1480	164	560
6H/4'	921	1229	166	680
7D/10'				
7D/6'	1063	1290	143	574
7D/6'	943	1132	176	676
7J/10'	903	1051	130	334
7J/6'				
7J/4'	904	1279	320	664
8K/10'	885	1003	108	273
8K/6'				

1

2

3

TOP INJECTION TEST RUN SUMMARY SHEET

RUN NO. 5602

DATE 3/21/73

A. RUN CONDITIONS

Containment Pressure	14.7 psia
Initial Clad Temperature	1100 °F
Peak Power	0.6 kw/ft
Coolant Supply Temperature	153 °F
Injection Rate	15 gpm

B. INITIAL HOUSING TEMPERATURES

Elevation (ft)	Initial Temperature (°F)
0	390
2	709
4	799
6	806
8	812
10	705
12	395

C. WATER COLLECTED

FLECHT-SET Containment Tank	0 lbm at - °F
FLECHT-SET Separator Tank	0 lbm at - °F
Steam Probe Tank	0 lbm at - °F
Upper Plenum	4.25 lbm at 158°F
Collection Drums	(1) 112.65 lbm at 202°F (3) 102.72 lbm at 200°F (2) 102.64 lbm at 202°F (4) 100.28 lbm at 198°F

TOP INJECTION TEST SUMMARY SHEET (cont)

RUN NO. 5602

DATE 3/21/73

D. HEATER THERMOCOUPLE DATA

Rod/Elev.	Initial Temp. (°F)	Max. Temp. (°F)	Turnaround Time (sec)	Quench Time (sec)
5E/10'	847	878	30	47
5E/6'				
5E/2'				
5F/10'	857	936	35	180
5F/2'	677	802	91	
5G/10'	849	1048	152	
5G/6'	1103	1403	65	
5G/4'				
5G/2'	674	839	162	
6G/10'	908	1083	140	
6G/4'				
6G/2'	689	825	94	553
7G/10'	821	1033	166	
7G/4'	951	1246	165	
1K/10'	806	1149	490	
1K/2'	775	1129	491	
3H/10'	825	1175	600	
3H/6'				
3H/4'	976	1357	164	
6K/10'				
6K/4'				
6K/2'	719	1071	601	
9J/10'				
9J/4'	971	1474	233	
9J/2'	691	1030	602	
1A/10'	817	881	53	115
1F/10'	887	1017	60	
1F/6'				
2C/10'				
2C/6'	1056	1334	105	
2C/4'	962	1168	161	166
2E/10'				
2E/4'	952	1226	165	

TOP INJECTION TEST SUMMARY SHEET (cont)

RUN NO. 5602

DATE 3/21/73

D. HEATER THERMOCOUPLE DATA (cont)

Rod/Elev.	Initial Temp. (°F)	Max. Temp. (°F)	Turnaround Time (sec)	Quench Time (sec)
2J/10'	825	1244	600	
2J/4'	712	1177	601	
3D/10'	859	863	17	59
3D/4'	899	1200	162	167
3F/10'	830	977	129	
3F/6'				
3F/4'	960	1235	162	548
3J/10'	883	1347	600	
3J/6'				
3J/4'	951	1548	598	
4E/10'	847	867	30	43
4E/4'	950	1111	159	331
4F/6'				
4F/4'	956	1215	159	518
4G/10'	847	1073	129	
4G/6'				
4G/4'	1075	1435	148	
4H/10'	912	1200	128	
4H/4'	1008	1461	154	
4K/10'	810	1242	599	
4K/6'				
4K/4'	948	1493	597	
5J/10'	824	1228	599	
5J/6'	1033	1556	244	
6H/10'	830	1112	599	
6H/6'	1028	1594	137	
6H/4'	945	1286	159	
7D/10'				
7D/6'	1056	1324	159	258
7D/4'	971	1155	161	476
7J/10'	884	1330	600	
7J/6'				
7J/4'	943	1339	602	
8K/10'	857	1276	600	
8K/6'				

TOP INJECTION TEST RUN SUMMARY SHEET

RUN NO. 5703

DATE 3/22/73

A. RUN CONDITIONS

Containment Pressure	14.7 psia
Initial Clad Temperature	1100 °F
Peak Power	0.7 kw/ft
Coolant Supply Temperature	150 °F
Injection Rate	15 gpm

B. INITIAL HOUSING TEMPERATURES

Elevation (ft)	Initial Temperature (°F)
0	372
2	643
4	818
6	779
8	782
10	544
12	342

C. WATER COLLECTED

FLECHT-SET Containment Tank	0 lbm at	°F
FLECHT-SET Separator Tank	0 lbm at	°F
Steam Probe Tank	0 lbm at	°F
Upper Plenum	5 lbm at	146°F
Collection Drums	(1) 106.81 lbm at - °F	(3) 98.85 lbm at - °F
	(2) 96.89 lbm at - °F	(4) 98.05 lbm at - °F

TOP INJECTION TEST SUMMARY SHEET (cont)

RUN NO. 5703

DATE 3/23/73

D. HEATER THERMOCOUPLE DATA

Rod/Elev.	Initial Temp. (°F)	Max. Temp. (°F)	Turnaround Time (sec)	Quench Time (sec)
5E10 (14)	810	895	37	68
6				
2 (67)	536	644	23	27
5F10 (21)	819	932	43	153
2 (70)	607	811	101	
5G10 (10)	812	1017	93	
6 (64)	1095	1497	122	
4				
2 (91)	875	905	183	
6G10 (27)	873	1133	558	
4 (98)	924	1338	172	428
2 (97)	615	859	179	
7G10 (11)	778	1108	484	
4 (77)	907	1376	170	
1K10 (19)	762	1106	392	
2 (68)	730	1156	422	
3H10 (24)	783	1574	342	
6				
4 (63)	958	1464	134	
6K10 (28)	836	1402	558	
4				
2 (60)	666	1135	500	
9J10				
4 (88)	962	1675	367	
2 (83)	635	1126	610	
1A10 (8)	772	874	48	113
1F10 (36)				
6 (58)				
2C10				
6 (94)	1043	1482	131	273
4 (103)	919	1238	218	550
2E10 (4)				
4 (75)	912	1331	221	

TOP INJECTION TEST SUMMARY SHEET (cont)

RUN NO. 5703

DATE 3/23/73

D. HEATER THERMOCOUPLE DATA

Rod/Elev.	Initial Temp. (°F)	Max. Temp. (°F)	Turnaround Time (sec)	Quench Time (sec)
2J10 (20)	786	1188	557	
4 (59)				
3D10 (12)	823	912	23	79
4 (105)	909	1302	322	396
3F10 (9)	791	965	114	
6				
4 (104)	910	1339	285	
3J10 (34)	852	1328	558	
6				
4 (100)	914	1581	494	
4E10 (16)	812	922	48	80
4 (73)	893	1183	155	371
4F06				
4 (62)	904	1294	255	528
4G10 (15)	808	1038	113	
6				
4 (74)	1058	1550	161	
4H10 (31)	879	1174	558	
4 (76)	980	1571	178	
4K10 (6)	768	1229	557	
6				
4 (84)	929	1550	504	
5J10 (5)	786	1297	556	
6 (99)	1011	1681	156	
6H10 (2)	792	1210	557	
6 (71)	1011	1722	236	
4 (78)	899	1401	173	
7D10 (3)	795	851	12	38
6 (61)	1043	1435	204	293
4 (102)	908	1219	220	599
7J10 (32)	851	1493	558	
6				
4 (72)	910	1526	609	

—

—

—

—

—

—

—

TOP INJECTION TEST RUN SUMMARY SHEET

RUN NO. 5904

DATE 3/23/73

A. RUN CONDITIONS

Containment Pressure	14.7 psia
Initial Clad Temperature	1400 °F
Peak Power	0.7 kw/ft
Coolant Supply Temperature	154 °F
Injection Rate	15 gpm

B. INITIAL HOUSING TEMPERATURES

Elevation (ft)	Initial Temperature (°F)
0	410
2	709
4	812
6	811
8	844
10	717
12	394

C. WATER COLLECTED

FLECHT-SET Containment Tank	0	lbm at	°F
FLECHT-SET Separator Tank	0	lbm at	°F
Steam Probe Tank	0	lbm at	°F
Upper Plenum	5.25	lbm at	153°F
Collection Drums	(1) 105.05	lbm at	204°F
	(2) 95.05	lbm at	204°F
	(3) 95.13	lbm at	202°F
	(4) 91.51	lbm at	198°F

TOP INJECTION TEST SUMMARY SHEET (cont)

RUN NO. 5904

DATE 3/23/73

D. HEATER THERMOCOUPLE DATA

Rod/Elev.	Initial Temp. (°F)	Max. Temp. (°F)	Turnaround Time (sec)	Quench Time (sec)
5E/10'	994	1061	30	102
5E/6'				
5E/2'	294	899	154	425
5F/10'	1002	1086	40	275
5F/2'	805	932	121	
5G/10'	985	1145	210	
5G/6'	1354	1663	88	
5G/4'				
5G/2'	800	953	178	
6G/10'	1041	1186	53	
6G/4'				
6G/2'	817	944	123	
7G/10'	946	1081	180	
7G/4'	1144	1462	116	
1K/10'	876	1258	329	
1K/2'	851	1249	498	
3H/10'	931	1259	210	
3H/6'				
3H/4'	1164	1532	198	
6K/10'	963	1373	241	
6K/4'				
6K/2'	811	1115	453	
9J/10'				
9J/4'	1112	1724	308	
9J/2'	786	1080	570	
1A/10'	890	946	35	124
1F/10'	981	1095	75	
1F/6'	1189	1482	154	
2C/10'				
2C/6'	1239	1538	156	289
2C/4'	1125	1274	156	
2E/10'	948	1032	40	355
2E/4'	974	1387	155	

TOP INJECTION TEST SUMMARY SHEET (cont)

RUN NO. 5904

DATE 3/23/73

D. HEATER THERMOCOUPLE DATA (cont)

Rod/Elev.	Initial Temp. (°F)	Max. Temp. (°F)	Turnaround Time (sec)	Quench Time (sec)
2J/10'	924	1329	240	
2J/4'	804	1263	569	
3D/10'	995	1035	10	47
3D/4'	1167	1401	156	411
3F/10'	951	1069	63	
3F/6'				
3F/4'	1147	1467	156	
3J/10'	988	1422	246	
3J/6'				
3J/4'	1108	1619	571	
4E/10'	987	1049	30	75
4E/4'	1159	1245	122	376
4F/6'				
4F/4'	1161	1390	154	
4G/10'	977	1169	213	
4G/6'				
4G/4'	1285	1673	155	
4H/10'	1036	1339	197	
4H/4'	1197	1719	155	
4K/10'	901	1324	240	
4K/6'				
4K/4'	1080	1550	155	
5J/10'	937	1319	235	
5J/6'	1228	1759	156	
6H/10'	957	1212	288	
6H/6'	1245	1830	171	
6H/4'	1133	1507	155	
7D/10'	969	1004	10	55
7D/6'	1288	1429	154	320
7D/4'	1173	1280	50	560
7J/10'	996	1394	236	
7J/6'				
7J/4'	1105	1573	155	
8K/10'	936	1326	357	
8K/6'				

—

—

—

—

—

—

TOP INJECTION TEST RUN SUMMARY SHEET

RUN NO. 6007

DATE 3/23/73

A. RUN CONDITIONS

Containment Pressure	18 psia
Initial Clad Temperature	1100 °F
Peak Power	0.7 kw/ft
Coolant Supply Temperature	150 °F
Injection Rate	15 gpm

B. INITIAL HOUSING TEMPERATURES

Elevation (ft)	Initial Temperature (°F)
0	452
2	709
4	776
6	803
8	758
10	690
12	324

C. WATER COLLECTED

FLECHT-SET Containment Tank	60	lbm at 186°F
FLECHT-SET Separator Tank	531.5	lbm at 198°F
Steam Probe Tank	1.75	lbm at 70°F
Upper Plenum	4.5	lbm at 151°F
Collection Drums	(1) 30.07 lbm at 200°F	(3) 17.71 lbm at 174°F
	(2) 16.39 lbm at 184°F	(4) 0 lbm at — °F

TOP INJECTION TEST RUN SUMMARY SHEET (cont)

RUN NO. 6007

DATE 3/23/73

D. HEATER THERMOCOUPLE DATA

Rod/Elev.	Initial Temp. (°F)	Max. Temp. (°F)	Turnaround Time (sec)	Quench Time (sec)
5E/10'	811	837	14	30
5E/6'				
5E/2'	728	887	94	160
5F/10'	817	856	19	47
5F/2'	767	903	94	171
5G/10'	802	856	19	131
5G/6'	1108	1359	60	542
5G/4'				
5G/2'	758	889	101	178
6G/10'	860	917	20	92
6G/4'				
6G/2'	769	905	95	178
7G/10'	760	814	19	157
7G/4'	979	1179	78	365
1K/10'	760	820	42	85
1K/2'	794	882	83	171
3H/10'	759	836	25	186
3H/6'				
3H/4'	992	1207	94	383
6K/10'	830	921	59	319
6K/4'				
6K/2'	763	942	93	168
9J/10'				
9J/4'	963	1342	95	371
9J/2'	742	943	89	167
1A/10'	785	795	2	21
1F/10'	849	887	20	109
1F/6'	1032	1256	82	508
2C/10'				
2C/6'	1050	1339	123	449
2C/4'	967	1092	85	350
2E/10'	794	833	19	91
2E/4'	961	1102	83	349

TOP INJECTION TEST RUN SUMMARY SHEET (cont)

RUN NO. 6007

DATE 3/23/73

D. HEATER THERMOCOUPLE DATA (cont)

Rod/Elev.	Initial Temp. (°F)	Max. Temp. (°F)	Turnaround Time (sec)	Quench Time (sec)
2J/10'	789	860	30	440
2J/4'	758	931	88	165
3D/10'	817	840	13	30
3D/4'	989	1123	90	350
3F/10'	783	823	19	102
3F/6'				
3F/4'	981	1127	62	361
3J/10'	855	927	26	490
3J/6'				
3J/4'				
4E/10'	813	842	14	36
4E/4'	979	1048	83	304
4F/6'				
4F/4'	984	1092	60	359
4G/10'	796	856	19	102
4G/6'				
4G/4'	1079	1327	78	365
4H/10'	862	935	20	153
4H/4'	1012	1284	94	383
4K/10'	758	840	35	420
4K/6'				
4K/4'	939	1200	93	349
5J/10'	789	862	20	151
5J/6'	1032	1423	140	516
6H/10'	782	841	18	190
6H/6'	1035	1420	155	548
6H/4'	968	1171	78	365
7D/10'	788	808	13	30
7D/6'	1062	1343	138	342
7D/4'	991	1137	79	383
7J/10'	849	933	26	252
7J/6'				
7J/4'	954	1215	84	372
8K/10'	809	919	75	357
8K/6'				

TOP INJECTION TEST RUN SUMMARY SHEET

RUN NO. 6106

DATE 3/24/73

A. RUN CONDITIONS

Containment Pressure	14.7 psia
Initial Clad Temperature	1100 °F
Peak Power	0.7 kw/ft
Coolant Supply Temperature	82 °F
Injection Rate	15 gpm

B. INITIAL HOUSING TEMPERATURES

Elevation (ft)	Initial Temperature (°F)
0	468
2	716
4	742
6	785
8	833
10	715
12	326

C. WATER COLLECTED

FLECHT SET Containment Tank	0	lbm at - °F
FLECHT SET Separator Tank	122.75	lbm at 200°F
Steam Probe Tank	1.25	lbm at 80°F
Upper Plenum	6.25	lbm at 141°F
Collection Drums	(1) 56.06 lbm at 152°F	(3) 46.77 lbm at 176°F
	(2) 45.60 lbm at 170°F	(4) 43.58 lbm at 178°F

TOP INJECTION TEST RUN SUMMARY SHEET

RUN NO. 6106

DATE 3/24/73

D. HEATER THERMOCOUPLE DATA

Rod/Elev.	Initial Temp. (°F)	Max. Temp. (°F)	Turnaround Time (sec)	Quench Time (sec)
5E/10'	911	963	65	65
5E/6'				
5E/2'	675	735	46	46
5F/10'	922	1085	171	305
5F/2'	724	994	168	339
5G/10'	912	1332	170	305
5G/6'	1177	1853	168	305
5G/4'				
5G/2'	721	1014	168	340
6G/10'	974	1351	171	305
6G/4'	1013	1450	169	368
6G/2'	735	1023	169	335
7G/10'	876	1271	170	305
7G/4'	986	1445	168	362
1K/10'	838	1195	171	305
1K/2'	816	1100	168	339
3H/10'	873	1356	171	305
3H/6'				
3H/4'	1013	1668	167	383
6K/10'	917	1350	171	305
6K/4'				
6K/2'	761	1145	167	339
9J/10'				
9J/4'	976	1670	169	390
9J/2'	729	1113	168	345
1A/10'	846	1015	159	235
1F/10'	934	1296	166	305
1F/6'	1071	1592	173	305
2C/10'				
2C/6'	1112	1303	47	68
2C/4'	972	1257	158	203
2E/10'	885	1124	155	210
2E/4'	979	1344	168	345

TOP INJECTION TEST RUN SUMMARY SHEET (cont)

RUN NO. 6106

DATE 3/24/73

D. HEATER THERMOCOUPLE DATA (cont)

Rod/Elev.	Initial Temp. (°F)	Max. Temp. (°F)	Turnaround Time (sec)	Quench Time (sec)
2J/10'	869	1363	171	305
2J/4'	770	1149	167	326
3D/10'	910	935	10	49
3D/4'	999	1259	142	153
3F/10'	886	1243	170	305
3F/6'				
3F/4'	990	1427	169	363
3J/10'	937	1454	171	305
3J/6'				
3J/4'	971	1691	169	
4E/10'	905	941	16	43
4E/4'	983	1169	148	334
4F/6'				
4F/4'	996	1384	167	366
4G/10'	906	1342	170	305
4G/6'				
4G/4'	1108	1816	168	366
4H/10'	973	1463	171	305
4H/4'	1036	1775	168	384
4K/10'	849	1307	170	
4K/6'				
4K/4'	956	1586	168	384
5J/10'	876	1372	170	308
5J/6'	1080	1209	169	305
6H/10'	886	1365	170	300
6H/6'	1082	2010	173	305
6H/4'	797	1555	168	384
7D/10'	885	882	0	5
7D/6'	1109	1347	62	73
7D/4'	1000	1088	53	81
7J/10'	940	1443	171	305
7J/6'				
7J/4'	964	1615	168	454
8K/10'	894	1309	171	305
8K/6'				

TOP INJECTION TEST RUN SUMMARY SHEET

RUN NO. 6205

DATE 3/25/73

A. RUN CONDITIONS

Containment Pressure	14.7 psia
Initial Clad Temperature	1100 °F
Peak Power	0.7 kw/ft
Coolant Supply Temperature	86 °F
Injection Rate	35 gpm

B. INITIAL HOUSING TEMPERATURES

Elevation (ft)	Initial Temperature (°F)
0	471
2	733
4	800
6	752
8	801
10	773
12	374

C. WATER COLLECTED

FLECHT-SET Containment Tank	0 lbm at - °F
FLECHT-SET Separator Tank	0 lbm at - °F
Steam Probe Tank	0 lbm at - °F
Upper Plenum	7.25 lbm at 152°F
Collection Drums	Filled and overflowed.

TOP INJECTION TEST SUMMARY SHEET (cont)

RUN NO. 6205

DATE 3/25/73

D. HEATER THERMOCOUPLE DATA

Rod/Elev.	Initial Temp. (°F)	Max. Temp. (°F)	Turnaround Time (sec)	Quench Time (sec)
5E/10'	908	908	2	50
5E/6'				
5E/2'	649	666	10	10
5F/10'	926	933	2	90
5F/2'	706	794	54	110
5G/10'	916	1001	229	240
5G/6'	1119	1453	154	275
5G/4'				
5G/2'	715	933	349	470
6G/10'	972	1080	146	152
6G/4'	1017	1236	277	299
6G/2'	734	881	122	216
7G/10'	879	1105	283	
7G/4'				
1K/10'	869	920	18	100
1K/2'				
3H/10'	884	1183	345	
3H/6'				
3H/4'				
6K/10'	935	1378	517	
6K/4'				
6K/2'				
9J/10'				
9J/4'				
9J/2'	743	1221	574	
1A/10'	878	888	12	12
1F/10'	953	974	14	75
1F/6'	1009	1131	131	131
2C/10'				
2C/6'	1035	1143	12	65
2C/4'				
2E/10'	911	917	12	45
2E/4'				

TOP INJECTION TEST SUMMARY SHEET (cont)

RUN NO. 6025

DATE 3/25/73

D. HEATER THERMOCOUPLE DATA (cont)

Rod/Elev.	Initial Te Temp. (°F)	Max. Temp. (°F)	Turnaround Time (sec)	Quench Time (sec)
2J/10'	895	1237	544	
2J/4'	759	1312	541	
3D/10'	929	936	5	37
3D/4'	999	1048	23	74
3F/10'	901	917	12	95
3F/6'				
3F/4'	994	108		
3J/10'	961	1393	479	
3J/6'				
3J/4'	979	1687	521	
4E/10'	922	930	7	45
4E/4'	990	1000	16	82
4F/6'				
4F/4'	996	1115	236	303
4G/10'	914	1027	300	320
4G/6'				
4G/4'	1102	1459	171	508
4H/10'	977	1232	307	
4H/4'	1035	1569	447	
4K/10'	875	1258	543	
4K/6'				
4K/4'	963	1601	542	
5J/10'	894	1303	527	
5J/6'	1024	1901	427	
6H/10'	894	1220	305	
6H/6'	1034	1900	369	
6H/4'	983	1404	542	
7D/10'	886	876	0	2
7D/6'	1059	1080	87	87
7D/4'	992	1008	34	100
7D/10	956	1374	500	
7J/6'				
7J/4'	970	1666	541	
8K/10'				
8K/6'				

TOP INJECTION TEST RUN SUMMARY SHEET

RUN NO. 6408

DATE 3/26/73

A. RUN CONDITIONS

Containment Pressure	14.7 psia
Initial Clad Temperature	1100 °F
Peak Power	0.7 kw/ft
Coolant Supply Temperature	172 °F
Injection Rate	15 gpm

B. INITIAL HOUSING TEMPERATURES

Elevation (ft)	Initial Temperature (°F)
0	418
2	686
4	731
6	769
8	820
10	931
12	380

C. WATER COLLECTED

FLECHT-SET Containment Tank	0	lbm at - °F
FLECHT-SET Separator Tank	0	lbm at - °F
Steam Probe Tank	2.75	lbm at 70°F
Upper Plenum	5.75	lbm at 156°F
Collection Drums	(1) 105.02 lbm at 205°F	(3) 93.95 lbm at 200°F
	(2) 93.83 lbm at 203°F	(4) 91.11 lbm at 194°F

TOP INJECTION TEST SUMMARY SHEET (cont)

RUN NO. 6408

DATE 3/26/73

D. HEATER THERMOCOUPLE DATA

Rod/Elev.	Initial Temp. (°F)	Max. Temp. (°F)	Turnaround Time (sec)	Quench Time (sec)
5E/10'	950	978	21	86
5E/6'				
5E/2'	690	893	212	284
5F/10'	958	1018	37	
5F/2'	738	888	96	
5G/10'	951	1087	130	
5G/6'	1182	1561	145	
5G/4'				
5G/2'	737	957	485	
6G/10'	1002	1125	182	
6G/4'				
6G/2'	753	917	281	
7G/10'	904	1109	214	
7G/4'	1003	1405	545	
1K/10'	987	1223	248	
1K/2'	805	1092	362	
3H/10'	936	1154	248	
3H/6'				
3H/4'	1018	1462	162	
6K/10'	1030	1407	387	
6K/4'				
6K/2'	766	1182	566	
9J/10'				
9J/4'	1005	1804	546	
9J/2'	952	1113	451	
1A/10'	1026	1083	37	192
1F/10'	1057	1110	193	
1F/6'	1071	1467	244	
2C/10'				
2C/6'	1096	1422	118	268
2C/4'	974	1181	159	
2E/10'	986	1077	42	441
2E/4'	977	1231	158	

TOP INJECTION TEST SUMMARY SHEET (cont)

RUN NO. 6408

DATE 3/26/73

D. HEATER THERMOCOUPLE DATA (cont)

Rod/Elev.	Initial Temp. (°F)	Max. Temp. (°F)	Turnaround Time (sec)	Quench Time (sec)
2J/10'	1012	1243	248	
2J/4'	764	1179	367	
3D/10'	993	1035	26	87
3D/4'	1007	1233	154	
3F/10'	950	1066	59	
3F/6'				
3F/4'	999	1300	153	
3J/10'	1057	1340	248	
3J/6'				
3J/4'	977	1578	397	
4E/10'	967	1017	32	81
4E/4'	970	1028	97	191
4F/6'				
4F/4'	1004	1224	151	
4G/10'	953	1098	120	
4G/6'				
4G/4'	1113	1619	180	
4H/10'	1026	1203	99	
4H/4'	1035	1558	191	
4K/10'	970	1297	358	
4K/6'				
4K/4'	962	1534	446	
5J/10'	991	1250	363	
5J/6'	1093	1659	363	
6H/10'	950	1128	241	
6H/6'	1096	1705	145	
6H/4'	992	1373	163	
7D/10'				
7D/6'	1110	1358	101	366
7D/4'	992	1103	281	
7J/10'	1038	1431	398	
7J/6'				
7J/4'	974	1581	567	
8K/10'	1014	1459	409	
8K/6'				

